THE UNIVERSITY
of EDINBURGH

Differential roles for dendritic cell subsets during *Schistosoma mansoni* infection

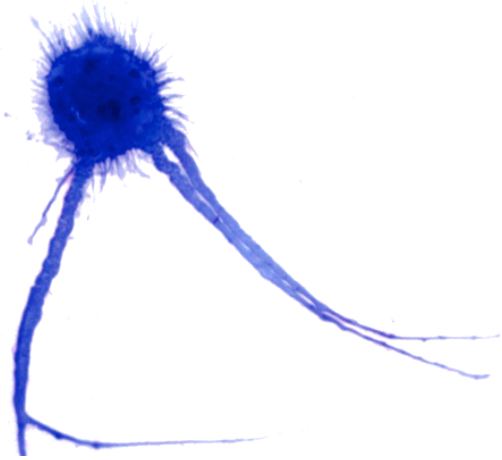

Angela Kerstin Marley

A thesis submitted for the degree of Doctor of Philosophy

University of Edinburgh

2015

DECLARATION

I, the undersigned, hereby declare that the contents of this thesis have been composed by myself and that the work described herein is entirely my own unless acknowledged otherwise.

Angela Kerstin Marley

ACKNOWLEDGEMENTS

I would like to thank Andrew for giving me the opportunity to do my PhD in a very exciting field. Your continuous enthusiasm inspired me to do the best I can and kept me motivated when (assuredly on rare occasions…) the science didn't. Thank you for always being supportive and positive, even from afar.

A special thanks also to Alex for giving me a smooth start to my PhD and for the continuous help and support throughout. Those long experiment days wouldn't have been half as much fun or as successful without you.

A major thank you to everyone from the MacDonald team over the years. Thank you Lucy, Lauren, Pete, Gareth, Rachel, Sheila and Rinku for all of your help and for always being a source of ideas.

Thanks to everyone in IIIR for making the institute such an amazing and happy place, and for endless advice and support. Martin, your FACS wizardry was invaluable. A huge thank you also to Rick Maizels and his lab for adopting me.

I am so lucky to have an amazing family and many cherished friends (near and far) who gave me never-ending support, love and understanding. You know who you are. Thank you, Dad, for being my rock and for reading this "mystery novel" again and again… and again. Mum, thank you for being here when I was too busy to be there, and for always making sure I had a stock of my much loved German food. Caroline and Georgina, I would not have enjoyed my PhD as much without you, thank you for being a constant source of smiles, hugs, chocolate, and accidental snorts and squeaks that made me laugh so much from day one.

Danke Oma, dass du mich immer blind unterstützt hast. Deine Worte waren mir so wichtig in dieser Zeit und werden mir immer in Erinnerung bleiben. Damit widme ich dir diese Doktorarbeit. Ich vermisse dich sehr.

Finally, thank you Miguel. I have no words except I love you.

EXPERIMENTAL CONTRIBUTIONS

The D28-D105 *S. mansoni* infection time-course experiment in chapter 3 was developed and conducted in collaboration with Dr. Alexander Phythian-Adams and Dr. Jess Borger.

Dr. Tim Kendall at the Western General Hospital in Edinburgh provided invaluable assistance and support in the development of hepatic granuloma quantification methods in chapter 3 and 4. Tim also kindly provided an algorithm template to be used for histological analysis in these experiments.

Dr. Alexander Phythian-Adams undertook the CD11c.DOG depletion experiments and kindly provided liver samples from these experiments for histological analysis in chapter 3.

The *Batf3* project was developed in collaboration with Dr. Alexander Phythian-Adams.

Dr. Peter Cook, Dr. Lucy Jones, Dr. Lauren Webb, Gareth-Rhys Jones and Prof. Andrew MacDonald provided technical assistance in the *S. mansoni* infection experiments in chapter 3 and 4. Sheila Brown performed and analysed serum isotype antibody assays detailed in chapter 4.

Prof. Mark Arends at the Western General Hospital in Edinburgh provided invaluable training and support for pathology scoring systems developed for ileal granulomatous inflammation and muscle injury analysis in chapter 4.

Aoibheann Mullan performed pathological scoring analysis for granulomatous inflammation in the intestines at D52 of *S. mansoni* infection in chapter 4.

The *ex vivo* OT-II culture system for the assessment of dendritic cell function was developed in collaboration with Dr. Rachel Lundie. Dr. Martin Waterfall performed all of the DC FACS sorting in chapter 5.

LAY SUMMARY

Parasitic infection often evokes disgust, outrage and horror, as the idea of a worm nesting inside us and eating our food makes us feel uneasy to say the least. But becoming infected with a parasite constitutes a risk mainly on travels to tropical areas of the world, and this generally gives us at other times a sense of security that life-threatening worms are far, far away.

However, anyone who suffers from allergic reactions, such as hay fever, already has a lot in common with a parasite-infested individual; the type of immune response is on many levels identical. To elucidate further: the immune system has evolved a form of response that is essential for controlling long-term parasitic infection. However, it is this type of immune response that goes wrong in allergic and some autoimmune disorders. So why can we mount a protective immune response against parasites, but not control such a similar response in allergies?

The answer to this question remains very unclear. In contrast to immune responses against the common cold, the flu and other viral and bacterial infections, immune responses vital for our defences against parasites are still largely a mystery.

As a model for parasitic infection we have been using a blood fluke called *Schistosoma mansoni*. Schistosomiasis is a devastating disease in sub-Saharan Africa causing about 200,000 deaths per year, and in 2012 249 million infections were recorded. Infection with the parasite occurs when freshwater sources are contaminated with the excreta of infected individuals. Once inside the host, mature worms live in the blood vessels and, rather romantically, male and female worms pair for life. Fertile females produce up to 300 eggs per day, and it is the release of these eggs which triggers strong immune responses causing most of the symptoms experienced during infection.

Most eggs find their way out of the body through the faeces. However some eggs get carried to the liver by the blood stream, or get stuck in intestinal tissue. This causes dramatic damage to the tissue in these areas. As a response immune cells gather

around the egg to protect the surrounding tissue from toxins release by the egg, forming a so-called “granuloma”.

Dendritic cells (DCs) play an essential role in stimulating this immune response. They are professionals at identifying a potential threat and travel around the body to alert and activate other immune cells, such as T cells. However, the exact mechanisms for the direction of T cell responses by DCs during *S. mansoni* infection remains unclear. Furthermore, distinct DC subsets are present within different tissue sites. Thus we have studied the importance of DC subsets for the induction of T cell responses and the formation of granulomas during *S. mansoni* infection.

A greater understanding of the anti-parasite immune cocktail will provide further essential clues on how we fight worms. Furthermore, this will ultimately help piece together why and how the immune response goes haywire in allergies, opening doors for therapies in all of those areas.

ABSTRACT

Schistosoma mansoni infection leads to chronic inflammation and detrimental granulomatous pathology mediated largely by Th2 immune responses. Dendritic cells (DCs) provide an essential link between the innate and the adaptive immune response, and are critical for Th2 induction during *S. mansoni* infection. But the function of DCs in this process and the specific mechanisms they employ are not yet fully understood. Indeed, the role for individual DC subsets during the induction of Th2 responses is also unclear. Furthermore, the importance of DCs during the formation of granulomatous legions, and whether they interact with T cells at this site, is yet to be determined.

The formation of granulomatous pathology is initiated by the onset of *S. mansoni* egg production, as eggs get stuck in the intestine and the liver. In the first part of this thesis the formation of granulomas in the liver during *S. mansoni* infection is studied. Novel methods for quantification of histological data are used to examine the kinetics of granuloma development and the location of $CD11c^+$ DCs throughout infection. Additionally, CD11c-diphtheria toxin receptor mice are used to investigate the importance of DCs during granuloma formation. Depletion of $CD11c^+$ DCs resulted in a striking reduction in granuloma formation at the time-point for initial egg arrival in the liver. Two weeks later, depletion of $CD11c^+$ DCs did not impede granuloma formation, however led to altered structural arrangement of the granuloma. These data highlight the importance of DCs during the initial granuloma formation process, so as to prevent the toxic damage to hepatocytes by the *S. mansoni* egg.

DC subsets display unique functions in infection settings. The function of $CD8\alpha^+$ cDCs during the induction of Th1 responses is well understood, however their role during Th2 induction is yet to be determined. In the second part of this thesis the importance of one of these subsets, $CD8\alpha^+$ cDCs, during Th2 induction is assessed using *Batf3*$^{-/-}$ mice. Lacking $CD8\alpha^+$ cDCs and migratory $CD103^+$ cDCs, *Batf3*$^{-/-}$ mice displayed dysregulated induction of immune responses during *S. mansoni* infection. This altered the immunological balance to an enhanced Th2 and impaired Th1

response ultimately leading to fatality of *Batf3*$^{-/-}$ mice. This underlines that CD8α^{+} cDCs are not fundamentally required for the induction of Th2 immune responses, yet they play a role either directly or indirectly for the induction of appropriate immune responses during *S. mansoni* infection.

As implied DCs are capable of inducing very strong Th2 immune responses, however *S. mansoni* does not classically activate DCs. To elucidate further, the expression of activation markers is muted in response to SEA compared to bacterial or viral stimuli. In the final part of this thesis a co-culture system is used to address whether *S. mansoni* infection alters the function of DCs in the liver during infection. More specifically, the ability of DCs to take up, process and present antigen to CD4^{+} T cells and thereby induce T cell proliferation and cytokine production was assessed. Comparing cDCs to pDCs revealed that cDC are more efficient inducers of CD4^{+} T cell responses, however no major changes were found after *S. mansoni* infection. In contrast, co-culture with specific DC subsets illuminated that only CD8α^{-} cDCs have enhanced capabilities to induce CD4^{+} T cell responses during *S. mansoni* infection. These data demonstrate that distinct DC subsets may hold the key for unravelling the mechanisms for Th2 induction.

ABBREVIATIONS

AAMΦ	Alternatively activated macrophage
ALT	Alanine transaminase
AP	Alkaline phosphatase
AP-1	Activator protein 1
APC	Antigen presenting cell
Arg-1	Arginase 1
BAC	Bacterial artificial chromosome
Batf3	Basic leucine zipper transcription factor ATF-like 3
BCR	B cell receptor
BF	Bright field
BM	Bone marrow
BMDC	Bone marrow dendritic cell
CAMΦ	Classically activated macrophage
cDC	Conventional dendritic cell
CDP	Common dendritic cell progenitors
CLR	C-type lectin receptor
CTL	Cytotoxic T Lymphocyte
CTLA-4	cytotoxic T-lymphocyte-associated protein 4
DAMPS	Danger-associated molecular patterns
DC	Dendritic cell
DC-SIGN	Dendritic cell-specific ICAM-3 grabbing nonintegrin
dLN	Draining lymph node
DTR	Diphtheria toxin receptor
DTx	Diphtheria toxin
ELISA	Enzyme linked immune sorbent assay
ERK	Extracellular signal-related kinase
FACS	Fluorescent activated cell sorting
FCS	Foetal calf serum
Foxp3	Forkhead Box P3
FRC	Fibroblastic reticular cells
FTL3L	FMS-like tyrosine kinase 3

GMFI	Geometric mean fluorescence intensity
GRAIL	Gene related to anergy in lymphocytes
HDM	House dust mite
HEV	High endothelial venules
HSB	Hepatic stellate cell
HSD	Honest significant difference
ICC	Intracellular cytokine
Id2	Inhibitor of DNA binding 2
IFN	Interferon
IgSF	Immunoglobulin superfamily
IL	Interleukin
ILC	Innate lymphoid cell
iLN	Inguinal lymph node
IRF	Interferon regulatory factor
iTreg	Inducible Treg
LCMV	Lymphocytic choriomeningitis virus
LN	Lymph node
LNFPIII	Lacto-N-fucopentaose III
LP	Lamina propria
LPS	Lipopolysaccharide
MAPK	Mitogen-activated protein kinase
MBP	Major basic protein
MDP	Common macrophage-DC progenitors
MGL	Macrophage galactose-type lectin
MHC	Major histocompatibility complex
MHC-I	MHC class I
MHC-II	MHC class II
mLN	Mesenteric lymph node
MMP	Matrix metalloproteinases
mRNA	Messenger ribonucleic acid
MT	Masson's trichrome
MyD88	Myeloid differentiation primary response 88

MΦ	Macrophage
ndLN	Non draining lymph node
NFκB	Nuclear factor kappa B
NK	Natural killer cell
NLR	Nod-like receptor
NO	Nitric oxide
nTreg	Natural Treg
o/n	Overnight
OCT	Optimum cutting temperature formulation
OVA	Ovalbumin
PALT	Portal tract-associated lymphoid tissue
PAMPS	Pathogen-associated Molecular Pattern
PBS	Phosphate buffer solution
PD-1	Programmed cell death 1
pDC	Plasmacytoid dendritic cell
pLN	Popliteal lymph node
pOVA	OVA peptide
PP	Peyer's patches
PRR	Pattern recognition receptor
PSR	Picrosirius red
RA	Retinoic acid
RLR	Rig-I-like receptor
ROI	Reactive oxygen intermediates
ROS	Reactive oxygen species
rRNA	Ribosomal ribonucleic acid
RT	Room temperature
SCID	Severe combined immunodeficiency
SEA	Soluble egg antigen
SOM	Somatostatin
SP	Substance P
SPF	Specific pathogen-free
SSC	Side scatter

STAT	Signal transducer and activator of transcription
TAP	Transporter associated with antigen processing
TCR	T cell receptor
Tfh	T follicular helper cell
TGF	Transforming growth factor
Th	T helper cell
Tip-DC	TNF- and inducible NO synthase producing inflammatory DC
TLR	Toll Like Receptor
TNF	Tumour necrosis factor
TNFRSF	Tumour necrosis factor receptor superfamily
Treg	T regulatory cell
TSLP	Thymic stromal-derived lymphopoietin
VAP-1	Vascular adhesion protein 1
WT	Wild Type
YFP	Yellow fluorescent protein

TABLE OF CONTENTS

1 General Introduction

On encountering a pathogen the host relies heavily on its immune system for the recognition and neutralization of the threat, thereby guarding the host's health and survival. Various complex mechanisms and many molecular components are essential for a fast and specific immune response, and the interplay between all constituents must be regulated for a successful elimination of the pathogenic agent. The first-line of defence is the innate immune system, comprising many different immune cells that act broadly using anti-pathogenic strategies to combat the threat whilst also educating adaptive immune cells to induce specific immune responses (Janeway, 1989). The extensive coordination and communication between these two systems showcases the intricacy of this highly evolved and sophisticated immune system so vital for host survival.

1.1 Innate immune responses

If skin or mucosal barriers are broken, innate cells including neutrophils, macrophages (MΦs), basophils, mast cells, eosinophils and dendritic cells (DCs) rapidly migrate to the site of infection (Janeway, 1989; Janeway and Medzhitov, 2002). Antimicrobial activities kill the pathogen, such as the release of reactive oxygen species (ROS) and nitric oxide (NO) by classically activated MΦs (CAMΦs), and the expression of cytokines including tumour necrosis factor-α (TNF-α), interleukin (IL) 12p70 and IL-6 to attract and activate other immune cells (Janeway, 1992).

The detection of a pathogenic threat is initiated by the recognition of components that are non-self and conserved among microbial species, termed pathogen-associated molecular patterns (PAMPs) (Janeway, 1989; Janeway and Medzhitov, 2002). A large number of innate immune cells express pattern recognition receptors (PRRs) encoded by the host's germline (Takeuchi and Akira, 2010). It was initially thought that PRRs exclusively recognise non-self antigens, but they can also bind to endogenous ligands such as nucleic acids and heat shock proteins released by

damaged or necrotic cells termed danger-associated molecules (DAMPs) (Bianchi, 2007; Matzinger, 1994). In the mid 1990's, Toll-like receptors (TLRs) were the first PRRs to be identified (Belvin and Anderson, 1996), and were subsequently found to signal via an intracellular adaptor protein myeloid differentiation primary response 88 (MyD88) to induce specific immune responses towards microbes (Kawai and Akira, 2010). TLRs can be grouped depending on their location in the cell and the type of microbial ligands they recognise; TLR1, TLR2, TLR4, TLR5, TLR6, and TLR11 are expressed on the cell surface and predominantly bind microbial membrane components including lipids, lipoproteins and proteins, whereas TLR3, TLR7, TLR8 and TLR9 are found within intracellular vesicles such as endosomes, lysosomes, endolysosomes and the endoplasmic reticulum, where they are exposed to and recognise pathogen derived nucleic acids (Kawai and Akira, 2010). The discovery of TLR4 proved to be significant, as this particular TLR recognises bacterial lipopolysaccharide (LPS), which is found on the outer membrane of gram-negative bacteria that can cause septic shock (Poltorak et al., 1998). Following the discovery of TLRs, various cytosolic PRRs such as RIG-I-like receptors (RLRs) and Nod-like receptors (NLRs) were identified (Kawai and Akira, 2010). These PRRs can share ligands with TLRs and together perform critical roles in innate immune responses, including the induction of proinflammatory responses.

Although one of the main functions of the innate immune system is to detect microorganisms and mount a first-line defence against the pathogenic threat, innate immunity must also efficiently regulate inflammation and maintain immunological homeostasis (Janeway and Medzhitov, 2002). Many innate immune cells have dual functional roles in initiating immune responses whilst also controlling the extent of this response. For example, MΦs exhibit potent antimicrobial activities including the production of NO and ROS, but when the infection clears MΦs produce anti-inflammatory cytokines such as IL-10 and transforming growth factor-β (TGF-β) to tune down immune responses (Murray and Wynn, 2011). In addition, a crucial part of the innate immune system is carried out by antigen presenting cells (APCs) such as DCs and MΦs, which communicate specific information about the microbial invasion to the adaptive immune response.

1.2 Dendritic cells

In 1973, DCs were first identified as APCs by Ralph Steinman in the mouse spleen due to their unique dendritic morphology compared with MΦs (Steinman and Cohn, 1973). Since this discovery it has become clear that, although other immune cells can act as APCs, DCs are the most potent immune cells in this regard (Mildner and Jung, 2014; Steinman, 2012). Their location in peripheral tissues, such as the skin or mucosal tissues, as well as lymph nodes (LNs), places DCs in ideal positions for pathogen encounter at body barriers or entries to organs (Banchereau and Steinman, 1998). DCs efficiently take up antigen in the periphery and migrate to lymphoid organs, where they present processed antigen to different subsets of naive T lymphocytes, including $CD4^+$ and $CD8^+$ αβ T cells that are part of the adaptive immune response (Bonasio and Andrian, 2006). Presenting a pathogen-derived peptide to adaptive T cells conveys specific information about the particular pathogenic threat that the DC has encountered. Thus, as part of the innate immune system DCs provide a rapid non-specific response upon activation following recognition of microbial product, and induce a second-line defence that is antigen-specific by T cells (Janeway and Medzhitov, 2002).

1.2.1 Dendritic cell activation and function

1.2.1.1 Dendritic cell activation

Conventional DC activation occurs through interaction with PAMPs or DAMPs from a pathogen via PRRs expressed on the cell surface (Janeway, 1989; Kapsenberg, 2003; Matzinger, 2002). Upon stimulation with antigen, DC expression of various surface molecules including the chemokine receptor CCR7 is increased (Förster et al., 1999), which enables DCs to migrate to the peripheral T cell zones within LNs via the afferent lymph (MartIn-Fontecha et al., 2003; Saeki et al., 1999). CCR7 recognises chemokines CCL19, produced by stromal cells and DCs in the T cell zone, and CCL21, expressed by endothelial cells of lymphatic vessels and high endothelial venules (HEV) (Gunn et al., 1998; Kriehuber et al., 2001; Ngo et al., 1998; Willimann et al., 1998). Recognition and uptake of antigen results in substantial upregulation in a range of surface markers and cytokines, which are required for efficient communication with T cells (Banchereau et al., 2000). This

enhanced ability to migrate to LNs and upregulate surface markers and cytokine expression after encountering a pathogen distinguishes DCs from other APCs (Banchereau and Steinman, 1998; Förster et al., 2012; Geissmann et al., 2010).

1.2.1.2 Antigen uptake, processing and presentation by DCs

Unactivated DCs, sometimes termed 'immature' DCs, are scavengers that sample the tissue environment for harmful pathogenic agents by various mechanisms including receptor mediated endocytosis, phagocytosis and macropinocytosis (Guermonprez et al., 2002). The first two uptake pathways require receptor recognition for internalisation of macromolecules and particulate antigen respectively (Guermonprez et al., 2002). Macropinocytosis is the main antigen uptake mechanism that DC utilise to take up soluble antigen, and this process is critical for non-specific and rapid sampling of a large amount of surrounding fluid in the environment (Guermonprez et al., 2002). Notably, macropinocytosis can be induced transiently in MΦs (Racoosin and Swanson, 1989; 1992) and epithelial cells (West et al., 1989) by growth factors, but this process is constitutive in unactivated DCs (Sallusto et al., 1995). Thus, continuous and effective sampling of the environment further distinguishes DCs from other APCs.

Once inside DCs, antigen is processed and degraded by DC machinery, which produces a short peptide that is loaded on major histocompatibility complex (MHC) molecules (Mellman and Steinman, 2001). The effectiveness of antigen processing is dependent on the activation status of DCs, as interaction with microbial components that potently activate DCs, such as LPS, substantially enhances lysosomal acidification and antigen proteolysis (Trombetta et al., 2003). Uniquely, regulation of lysosomal acidity allows for efficient preservation of antigen within DCs for subsequent presentation to T cells, and it is thought that the ability of DCs to take up and process antigen is unrivalled by other APCs that also express MHC, including MΦs (Mildner and Jung, 2014).

Effective presentation of antigen to naive T cells by DCs in lymphoid tissue is promoted by high level MHC expression, which further implicates DCs as the main APC for T cell activation (Steinman et al., 1979). It is generally thought that antigen

peptides derived from the external environment are loaded onto class II MHC molecules (MHC-II) in endocytic organelles, and that peptide loaded on MHC-II is recognised by $CD4^+$ T cells (Neefjes et al., 2011). In contrast, endogenously derived antigen is recognised by $CD8^+$ T cells, and is loaded onto class I MHC (MHC-I) molecules after translocation into the endoplasmic reticulum by transporter associated with antigen processing (TAP) (Neefjes et al., 2011). However, cross-presentation pathways exist that allow for the presentation of exogenous antigen on MHC-I (Joffre et al., 2012; Villadangos and Schnorrer, 2007) (Diagram. 1.1). Cross-presentation of peptides enables the induction of immune responses by healthy APCs via presentation of intracellular antigen derived from damaged cells such as tumour cells or those infected with a virus (Heath et al., 2004). Thus, some flexibility in antigen presentation pathways via MHC molecules exists, which extends their capacity to activate different T cell subsets.

1.2.2 The diversity of murine DCs

Although all DCs exhibit similar functions in antigen recognition, uptake and processing, DCs are a heterogeneous population of professional APCs that can be broadly divided into two main groups: conventional or classical DCs (cDCs) and plasmacytoid DCs (pDCs) (Merad and Manz, 2009). cDCs play a major role in the induction of adaptive immune responses against pathogens, but are also important in the maintenance of immune tolerance against self antigens (Merad et al., 2013). pDCs on the other hand are primarily involved in anti-viral responses and produce copious amounts of type I interferons (IFNs), which aid in eliminating virus infected cells (Reizis et al., 2011).

1.2.2.1 Conventional dendritic cell subsets

cDCs represent a small group of haematopoietic cells that reside in most lymphoid and non-lymphoid tissues (Merad et al., 2013). This group of DCs displays an enhanced ability compared with pDCs in tissue injury detection, the capture of both exogenous and endogenous antigens, and the processing and presentation of antigen to T cells (Mildner and Jung, 2014; Villadangos and Young, 2008). LN resident cDCs differentiate from cDC precursors formed in the bone marrow (BM), and reside in the LN from then on (Diagram. 1.2) (Merad et al., 2013). Lymphoid cDCs

are frequently divided into two main subsets; $CD8\alpha^+$ cDCs and $CD11b^+$ cDCs (Merad et al., 2013). Tissue resident cDC subsets on the other hand are commonly referred to as $CD103^+$ and $CD11b^+$ cDCs, and together these subsets account for approximately 1-5% of all cells in peripheral tissue (Merad et al., 2013). Tissue resident $CD11b^+$ cDCs closely resemble their counterparts in the LNs, whereas $CD103^+$ cDCs represent the migratory non-lymphoid equivalent of lymphoid $CD8\alpha^+$ cDCs and express low levels of CD8α (Bursch et al., 2007; Ginhoux et al., 2007; Poulin et al., 2007). Indeed migratory $CD103^+$ cDCs and lymphoid $CD8\alpha^+$ cDCs are thought to be both developmentally and functionally equivalent (Bedoui et al., 2009; Edelson et al., 2010; Ginhoux et al., 2009). Notably, migratory $CD103^+$ cDCs should not be confused with intestinal $CD103^+$ cDCs that are located in Peyer's patches (PPs) and the lamina propria (LP) (Coombes et al., 2007), as intestinal $CD103^+$ cDCs are thought to be functionally specialised due to their distinct location in the gut (Denning et al., 2011). Intestinal $CD103^+$ cDCs traffic to the mLNs, where interaction with T cells leads to upregulation of gut-homing markers CCR9 and $a_4\beta_7$ (Jaensson et al., 2008; Johansson-Lindbom et al., 2005). This process is dependent on the ability of intestinal $CD103^+$ cDCs to metabolise dietary retinoids to retinoic acid (RA) (Iwata et al., 2004).

Lymphoid $CD8\alpha^+$ cDCs and migratory $CD103^+$ cDCs are FMS-like tyrosine kinase 3 ligand (Flt3L) dependent and are phenotypically immature in the steady state (Shortman and Heath, 2010). In accordance with their name $CD8\alpha^+$ cDCs express CD8α homodimers, but not CD8αβ heterodimers as seen on T cells (Vremec et al., 2000). However, the term "$CD8\alpha^+$ cDCs" is a somewhat inappropriate name for this subset since CD8α itself is only expressed in later stages of development, and can be found on certain migratory cDCs as well as on pDCs (Shortman and Heath, 2010). Thus, other markers including the glycoprotein CD24 (Askew and Harding, 2008) and C-type lectins CD205 (DEC205) (Jiang et al., 1995) and Clec9a (Sancho et al., 2008) are currently used to distinguish CD8α-lineage cDCs. In recent years a chemokine receptor, XCR1, has been identified as a more specific marker since it is found on both $CD8\alpha^+$ and $CD8\alpha^-$ cDCs belonging to the CD8α cDC lineage, including peripheral $CD103^+$ cDCs (Annabell Bachem, 2012). As such, XCR1 will

perhaps replace the current name for CD8α$^+$ cDCs in future. Clearly cDC subsets are still confusing in terms of their surface marker expression, and the nomenclature has not yet been universally adopted. For the purpose of this thesis, DC subset names outlined in table 1.1 will be used, as in most tissues these are still commonly accepted names for each subset.

In early reports, *ex vivo* CD8α$^+$ cDCs were shown to be proficient in cross-presentation of cell-associated antigen to CD8$^+$ T cells via MHC-I, indicating that they are important for cytotoxic lymphoid (CTL) responses (Haan et al., 2000). CD8α$^+$ cDCs are also known to produce high levels of the inflammatory cytokine IL-12 upon stimulation *in vitro* and *in vivo* (Maldonado-López et al., 1999; Reis e Sousa et al., 1997). By measuring CD4$^+$ and CD8$^+$ T cell proliferation to targeted antigen *in vivo* it was shown that CD8α$^+$ cDCs are superior antigen cross-presenters, whereas CD11b$^+$ cDCs are proficient in the uptake of exogenous antigen and display an enhanced capacity to present peptide to CD4$^+$ T cells via MHC-II (Dudziak et al., 2007). This is due to different machinery within these subsets: CD8α$^+$ cDCs contain enhanced levels of TAP proteins required for the loading of processed peptide on MHC-I, whereas CD11b$^+$ cDCs are enriched in components such as cathepsins and proteases required for antigen processing to peptide ligands and subsequent loading onto MHC-II (Dudziak et al., 2007; Joffre et al., 2012). However, CD8α$^+$ cDCs are capable of presenting antigen and activating CD4$^+$ T cells, even though this occurs at a lower level relative to CD11b$^+$ cDCs (Shortman and Heath, 2010).

Similar to CD8α$^+$ cDCs, CD11b$^+$ cDCs rely on Flt3L and are reduced in Flt3L deficient mice, albeit to a lesser extent than CD8α$^+$ cDCs (McKenna et al., 2000; Waskow et al., 2008). Lymphoid CD11b$^+$ cDCs represent a more heterogeneous population in comparison with CD8α$^+$ cDCs, and remain less well characterised. CD11b$^+$ cDCs do not express CD8α and are often found to be the dominant subset in the lymphoid resident cDC population (Merad et al., 2013). CD11b is also expressed on a group of monocytes that are recruited during inflammation via CCR2 (Robays et al., 2007). These monocytes express CD64 and FcεRIα, which can be used to distinguish monocytes from CD11b$^+$ cDCs (Plantinga et al., 2013). On the other

hand, $CD11b^+$ cDCs can be further distinguished by their high level of CD172a (Sirp-α) expression (Lahoud et al., 2006). Preferential antigen presentation to $CD4^+$ T cells by $CD11b^+$ cDCs via MHC-II described above extends to responses against viral infection with influenza, when $CD8\alpha^+$ cDC induce CTL responses (Kim and Braciale, 2009). Recently, a role for $CD11b^+$ cDCs during the induction of $CD4^+$ T cell responses against helminth infection and allergic inflammation has been proposed, and this will be discussed in more detail in section 1.9.3 (Plantinga et al., 2013; Williams et al., 2013).

Models depleting DCs have been used to uncover the importance of distinct DC subsets in the steady state and immune responses during infection with a pathogen. Depletion of $CD11c^+$ DCs has been achieved by using a model in which CD11c-expressing cells also express the transgene for the diphtheria toxin receptor (DTR) (Hochweller et al., 2008; Jung et al., 2002). Treatment with Diphtheria toxin (DTx) efficiently depletes CD11c-expressing cells by terminating protein synthesis and causing cells to die by apoptosis (Diagram 1.3) (Bar-On and Jung, 2010). An early CD11c.DTR model used a primate DTR transgene and enabled short-term depletion of cDCs without side-effects (Jung et al., 2002). However, from around 5 days after initial treatment, DTx mediated side effects are caused by the expression of DTR on non-haematopoietic cells resulting in the death of the animal. A more recent system using CD11c.DOG mice has a human DTR inserted into a bacterial artificial chromosome (BAC) construct, and this can be used for long-term depletion of CD11c-expressing cells lasting 11-12 days (Hochweller et al., 2008). Within 12 hours of DTx treatment 80% depletion is achieved, but after 72 hours $CD11c^{high}$ cells begin to repopulate the mouse and consistent DTx administration is required to maintain depletion (Hochweller et al., 2008). The depletion of DC subsets in this model extends to both cDCs and pDCs, whereas in CD11c.DTR mice pDCs are not depleted in every tissue site (Sapoznikov et al., 2007). Although high level expression of the integrin CD11c in addition to MHC-II (Metlay et al., 1990) is frequently used to distinguish DCs from other immune cells, CD11c is also expressed by other immune cells including MΦs (Jakubzick et al., 2006; Lloyd et al., 2008; Niess et al., 2005). As such, $CD11c^+$ MΦs are likely also depleted in both

CD11c.DTR and CD11c.DOG mice, and this is an important factor to consider when using this model (van Blijswijk et al., 2013).

In recent years transcription factors unique to cDC differentiation and developmental stages have been discovered, and this research has delivered some clarity on cDC ontogeny and also provided a platform for the identification of novel depletion models (Satpathy et al., 2012a). For example, transcription factor Zbtb46 is specific to cDCs and can be used to distinguish cDCs from other myeloid populations (Meredith et al., 2012a; Satpathy et al., 2012a). Zbtb46 is expressed by committed cDC progenitors as well as lymphoid resident and peripheral cDC subsets (Meredith et al., 2012a; Satpathy et al., 2012a). It is also notable that Zbtb46 is expressed by erythroid cells and endothelial cells, but its expression in haematopoietic cells is limited to cDCs (Satpathy et al., 2012a). For this reason models such as zDC-DTR mice, which can be used to deplete all cells expressing Zbtb46 in the steady state (Meredith et al., 2012a), and $Zbtb46^{+/gfp}$ mice that label these cells (Satpathy et al., 2012a), have been proposed as more specific tools for investigating cDC function compared with inducible CD11c depletion models (Hochweller et al., 2008; Jung et al., 2002). However, zDC protein is downregulated in splenic $CD11c^{+}$ populations after treatment with PRR ligands such as poly I:C (a synthetic analogue of double-stranded RNA) *in vivo*, which suggests that these models cannot be used to examine cDC function during immune responses against pathogens (Meredith et al., 2012b).

Recently, Schraml *et al.,* (2013) described a model to genetically trace cDCs by labelling them with yellow fluorescent protein (YFP) based on the expression of C-type lectin Clec9a (DNGR1). This model was generated by crossing mice expressing Cre recombinase under control of the *Clec9a* locus (Clec9a-Cre) with Rosa26-$stop^{flox}$-enhanced YFP reporter mice, referred to as $Clec9a^{+/cre}Rosa^{+/EYFP}$ mice. Detection of YFP identifies cDC precursors and cDCs, but not common MΦ-DC progenitors (MDPs) in $Clec9a^{+/cre}Rosa^{+/EYFP}$ mice. Specifically, $Clec9a^{+/cre}Rosa^{+/EYFP}$ mice enable the genetic labelling and tracing of cDC precursors and cDCs that have historically expressed Clec9a, and the authors propose that this model can be used to examine the location and proportion of cDCs during

inflammation (Schraml et al., 2013). In a subsequent study, an inducible cDC depletion model was generated by crossing Rosa26-lox-stop-lox(LSL)-DTR mice with Clec9a-Cre mice and administrating DTx to deplete cDCs (van Blijswijk et al., 2014). These mice are referred to as *Clec9a*$^{+/Cre}$*ROSA*^{iDTR} mice, and allow for efficient cDC depletion following DTx administration. Notably, the use of these animals revealed that *Clec9a*$^{+/Cre}$*ROSA*^{iDTR} mice develop LN hypocellularity and reduced DC frequency even when DTx was not injected, and the authors suggest that this phenotype is a feature common to other murine models that express DTR on DCs (van Blijswijk et al., 2014). This finding underlines the importance of using appropriate controls when utilising DTR based models (i.e. PBS injected DTR expressing mice as well as wild type (WT) mice), and caution should be taken when interpreting the data obtained from these mice as the naïve setting is different. Although current models for cDC depletion exhibit various caveats, they provide a valuable tool for the examination of the role of this large DC group during the steady state and inflammatory conditions.

Similar to "bulk" cDCs, differential dependence on transcription factors by distinct cDC subsets has helped understanding of CD8α$^+$ and CD11b$^+$ cDC ontogeny and function. CD11b$^+$ cDCs rely on IFN regulatory factor 4 (IRF4) (Suzuki et al., 2004) and Notch2 (Lewis et al., 2011) for their development, whilst CD8α$^+$ cDCs are dependent on IRF8, inhibitor of DNA binding 2 (Id2) and Basic leucine zipper transcription factor ATF-like 3 (*Batf3*) (Jackson et al., 2011). In fact, transcription factors IRF8, Id2 and *Batf3* are required sequentially during the development of CD8α$^+$ cDCs, which was established using Id2-GFP reporter mice (Jackson et al., 2011). Jackson *et al.,* (2011) showed that IRF8 is required for the development of all Id2 expressing cDC progenitors (as well as pDCs (Becker et al., 2012; Schiavoni et al., 2002)), but *Batf3* is necessary specifically during later developmental stages of CD8α$^+$ cDCs. *Batf3* is an activator protein 1 (AP-1) transcription factor (Murphy et al., 2013), which forms a heterodimer with Jun before binding AP-1 (Iacobelli et al., 2000). AP-1 regulates gene expression involved in cell proliferation, cytokine expression and apoptosis (Wagner and Eferl, 2005). Notably, *Batf3* is related to Batf and Batf2 (Murphy et al., 2013), and these transcription factors have been reported to

be important for the development of Th17 cells (Schraml et al., 2009) or a subset of lung resident DCs and MΦs (Tussiwand et al., 2012) respectively.

In 2008, a transgenic mouse deficient in the transcription factor *Batf3* was shown to specifically lack splenic CD8α$^+$ cDCs and the equivalent migratory CD103$^+$ cDC subset (Hildner et al., 2008). This study showed that *Batf3*$^{-/-}$ mice exhibit impaired CTL responses against West Nile virus (Hildner et al., 2008) and display reduced protection against tumourogenesis (Fuertes et al., 2011; Hildner et al., 2008). Further studies using the *Batf3* model have since shown that CD8α$^+$ cDCs are required for the induction of CD8$^+$ T cell responses against infection with Sendai virus (Edelson et al., 2010), influenza virus (Waithman et al., 2013), and cytomegalovirus (Torti et al., 2011). *Batf3* dependent DCs are also essential for intact CD4$^+$ T cell responses during *Toxoplasma gondii* (Mashayekhi et al., 2011) and *Leishmania major* (Ashok et al., 2014) infection. Thus, research using *Batf3*$^{-/-}$ mice has elevated our understanding on the important role of CD8α$^+$ cDCs during antigen cross-presentation to CD8$^+$ T cells and the induction of CD4$^+$ T cell responses *in vivo* against acute viral and bacterial infections. However, the role of CD8α$^+$ cDCs in chronic infections remains unclear, including infection with helminths (Pearce and MacDonald, 2002). Taken together, the identification of transcription factor dependence by distinct cDC subsets has enabled the generation of mouse models for the investigation of the function of different DC types during immune responses against pathogens.

1.2.2.2 Plasmacytoid dendritic cells

pDCs display distinct life cycles and functions compared with cDC (Reizis, 2010; Villadangos and Young, 2008). Although pDCs share a similar origin to cDCs, as both develop from a common DC progenitor (CDP), cDCs require additional development to pre-cDCs in the blood whilst pDCs fully differentiate in the BM (Naik et al., 2007) (Diagram 1.2). pDCs rely on the transcription factor E2-2 for their development in the BM (Cisse et al., 2008) and maintenance in the periphery (Ghosh et al., 2010). In addition, pDCs rely on both IRF4 (Schiavoni et al., 2002) and IRF8 (Tsujimura et al., 2003) for their development. In the steady state, pDCs are commonly found in the blood from where they enter lymphoid tissue (Cella et al.,

1999). Murine pDCs can be distinguished by their low level expression of MHC-II and CD11c, as well as their expression of CD45R (B220), PDCA-1, Ly6C, Siglec-H and Ly49Q (Reizis et al., 2011).

pDCs are generally thought to be poorer APCs than cDCs (Villadangos and Young, 2008). Young *et al.*, (2008) showed that purified pDCs capture fluorescently labelled OVA protein more slowly than cDCs *in vitro*, but pDCs generate degradation products of OVA at a similar rate. This indicates that pDC endocytic vesicles are more degenerative preventing effective preservation of antigen. On the other hand, slow degradation in cDCs enables sufficient preservation of exogenous antigen for subsequent processing and presentation to $CD4^+$ T cells (Savina et al., 2006). Furthermore, persistent turn over of antigen complexed MHC-II on the cell surface of pDCs as well as low expression of MHC-II generally renders interaction with T cells ineffective (Villadangos and Young, 2008). Instead, pDCs are well known for their enhanced ability relative to cDCs to produce type I IFNs in response to TLR7 or TLR9 detection of viruses (Satpathy et al., 2012b; Swiecki et al., 2010; Wang et al., 2008). During viral infection, pDCs are rapidly recruited to infection sites (Baldwin et al., 2004; Smit et al., 2006) and contribute to natural killer (NK) cell and $CD8^+$ T cell recruitment and activation (Pinto et al., 2011; Swiecki et al., 2010). A study that administered an antibody depleting pDCs (120G8) showed that pDCs drastically limit replication of respiratory syncytial virus and also reduce pulmonary inflammation and airway hyperresponsiveness (Wang et al., 2006). Further, depletion models using the BDCA2-DTR transgenic mouse model (Table 1.2) indicated that pDCs induce early activation of NK cells during infection with murine cytomegalovirus and promote the survival of $CD8^+$ T cells in vesicular stomatitis viral infection (Swiecki et al., 2010). These studies have placed pDCs as a dominant DC subset for limiting viral replication by the production of type I IFNs and enhancing viral clearance (Satpathy et al., 2012b).

1.2.2.3 Monocyte derived dendritic cells

Similar to pDCs, monocytes circulate in the blood in the steady state and develop from BM precursors (Diagram 1.2) (Domínguez and Ardavín, 2010). Blood derived monocytes can differentiate into either MΦs or DCs (Satpathy et al., 2012b). Two

distinct monocyte subsets have been identified: Ly6C^{low} CX3CR1^{high} CCR2^{low} and Ly6C^{high} CX3CR1^{low} CCR2^{high} monocytes (Geissmann et al., 2008; Satpathy et al., 2012b). The former constitute patrolling monocytes that migrate along the blood endothelium, and this process facilitates rapid recruitment to sites of inflammation. Within inflamed tissue, these monocytes are thought to be responsible for the secretion of inflammatory cytokines or for contributing to wound healing (Auffray et al., 2007; Geissmann et al., 2008). Instead, the latter subset is termed "inflammatory monocytes" and arrives later at the site of inflammation compared with patrolling monocytes. These monocytes have been reported to differentiate into cells sometimes termed TNF- and inducible nitric oxide synthase- producing inflammatory DCs (Tip-DCs) (Merad et al., 2013), which represent a dominant cell type during inflammation (Geissmann et al., 2003; Serbina et al., 2003). Although frequently named DCs, these cells do not express Zbtb46, the transcription factor expressed by cDCs (Meredith et al., 2012a; Satpathy et al., 2012a). This indicates that "Tip-DCs" may be inflammatory MΦs or monocytes rather than DCs. Furthermore, MΦs and DCs can originate from MDPs in the BM, whereas a distinct pathway leads to monocyte development (Geissmann et al., 2010) (Diagram 1.2). Additionally, recent studies have highlighted that the development and maintenance of cDCs and most tissue resident MΦs is independent of monocytes (Ginhoux and Jung, 2014). For example, it is now known that in particular some tissue resident MΦs have an embryonic origin (Davies et al., 2013). However, monocyte derived cells have been reported as being capable of antigen presentation in some settings including during allergic responses (Hammad et al., 2010; Plantinga et al., 2013), and these monocytes express CD64 and MAR-1 (Plantinga et al., 2013). Taken together, "Tip-DCs" are not strictly DCs when defined by their transcription factor usage and ontogeny, but they can exhibit some DC similarity in their function during immune responses. Thus, monocytes have emerged as a distinct cellular system that is highly dynamic and plastic, and is capable of acquiring both DC and MΦ-like functions in certain immune settings (Ginhoux and Jung, 2014).

1.2.2.4 Human dendritic cells

In 2012, Ralph Steinman was awarded the Nobel prize in Physiology or Medicine for his discovery of DCs in 1973, and their role in adaptive immunity. Thus, it has long

been known that DCs are critical for the immune system (Steinman, 2012), but only recently has it become clear that DCs are crucial for human health and disease (Collin et al., 2011; Steinman, 2012). Spontaneous DC deficiency in humans has been identified surprisingly late, which explains the relative paucity of data describing human DC subsets (Collin et al., 2011; Steinman, 2012). However, recent research has highlighted the importance of DCs for human health, as mutations in GATA binding protein 2 (GATA2) or IRF8 lead to DC deficiency resulting in severe immunodeficiency (Dickinson et al., 2011; Hambleton et al., 2011). Most knowledge arises from studies on human circulating blood DCs, with both cDCs and pDCs identified (Merad and Manz, 2009). To date, it is unclear whether CDPs exist in human BM or in the blood, but there is some evidence that tissue derived human DC subsets require continuous replenishment from blood–borne pre-cursors (Collin et al., 2013). A human equivalent of murine LN resident CD8α$^+$ cDCs and migratory CD103$^+$ cDCs has been described as expressing Clec9a and XCR1 similar to the murine counterpart, but uniquely expresses the integral membrane protein CD141 and intracellular adhesion protein Necl2, and does not express CD8α (Diagram. 1.4) (Collin et al., 2013; Villadangos and Shortman, 2010). CD141$^+$ DCs have been identified among resident LN, spleen, tonsil and BM resident DCs (Collin et al., 2013), as well as in peripheral tissues such as the skin, liver and lung (Haniffa et al., 2012). Both human and murine CD8α$^+$ cDCs rely on *Batf3* and IRF8 for their development and each expresses TLR3 (Jongbloed et al., 2010; Poulin et al., 2010). In addition human CD8α$^+$ DC counterparts are functionally similar to murine DCs, since they take up dead cells and cross-present antigen to CD8$^+$ T cells (Collin et al., 2013; Villadangos and Shortman, 2010). The human counterparts for CD11b$^+$ cDCs are thought to be CD1c$^+$ DCs, which represent the major population of human myeloid DCs in the blood (Collin et al., 2013). CD1c$^+$ DCs are efficient activators of naive CD4$^+$ T cells, but are less effective at cross-presenting antigen to CD8$^+$ T cells compared with CD141$^+$ DCs (Collin et al., 2013). Thus, recent advances have improved our understanding on DC heterogeneity in humans, but many open questions remain about DC origin and the generation of immune responses by human DCs.

1.3 T cell activation by dendritic cells

Although DC diversity underlines the heterogeneity of this innate immune cell population, one of the key roles for all DCs is the activation of T cells via the presentation of antigen (Kapsenberg, 2003). T cell activation by peptide loaded DCs requires the interaction of various cellular components, and the recognition of MHC-peptide complex via the T cell receptor (TCR) is the first stimulatory signal that T cells receive (Kapsenberg, 2003). Indeed, the activation of $CD4^+$ T cells is dependent on MHC-II and their antigen recognition ability is restricted to MHC-II presentation. Following signal 1, which determines antigen specificity, signal 2 comprises co-stimulatory or co-inhibitory mechanisms that direct T cell function and fate (Kapsenberg, 2003). Signal 2 is critical for this process, given that the provision of signal 1 in the absence of an appropriate signal 2 results in T cell unresponsiveness to antigen, sometimes termed T cell anergy (this will be discussed in section 1.8.2) (Bour-Jordan and Bluestone, 2009). The provision of signal 1 and 2 is dependent on upregulation of MHC and co-stimulatory molecule expression such as CD40, CD80, CD86 and OX40-L by the DC, which are required for efficient communication with T cells (Banchereau et al., 2000). Thus, these molecules are often used as markers for DC activation. Co-stimulatory/-inhibitory molecules are present on the cell surface of DCs and bind to the corresponding receptor or ligand on the T cell surface, frequently co-localising with the TCR (Chen and Flies, 2013). Further, these molecules synergise with TCR signals to promote or inhibit T cell function and activation, often controlling signals for the survival and proliferation of the cell (Saito et al., 2010). Notably, co-stimulation is also important for effective APC function mediated by DCs (Kobayashi et al., 2004). For example, CD40 engagement activates intracellular signalling pathways that are implicated in the promotion of cytokine production and upregulation of CD80 and CD86 surface marker expression by DCs (Kobayashi et al., 2004).

Signal 3 is delivered mainly in the form of cytokines provided by DCs and probably also from other APCs, which determine T cell polarisation (Kapsenberg, 2003). Thus, signal 3 is thought to provide qualitative information determined by the interaction of the DC with the pathogen at the site of inflammation (Kaliński et al.,

1999). For instance, the production of cytokines such as IL-6, IL-12p70 and TNF-α by DCs is substantially increased upon TLR ligation during conventional DC activation (Morelli et al., 2001), and these cytokines are thought to induce a potent inflammatory immune response. In fact, $CD8\alpha^+$ cDCs have been identified as the main producers of IL-12 in *T. gondii* and *L. major* infection (Ashok et al., 2014; Mashayekhi et al., 2011). However, in some cases (i.e. certain helminth infections) the polarisation of T cells is largely independent of TLR stimulation (Layland et al., 2005), and this will be described in more detail in section 1.9.

There are two main groups of co-stimulatory/-inhibitory molecules: immunoglobulin superfamily (IgSF) and the TNF receptor superfamily (TNFRSF). One of the main surface molecules expressed by T cells that is important for co-stimulation/-inhibition is CD28, which belongs to the IgSF (Linsley and Ledbetter, 1993). The B7 family ligands CD80 and CD86, both of which are often expressed by APCs (Greenwald et al., 2005; Linsley and Ledbetter, 1993), provide co-stimulatory signals to the T cell when bound to CD28. Another receptor member of the IgSF expressed by T cells is ICOS, which is bound by its activatory ligand ICOS-L on APCs (Hutloff et al., 1999). Receptor-ligand pairs CD40-CD154 (CD40L) (Caux et al., 1994), OX40-OX40-L (Fillatreau and Gray, 2003; Ohshima et al., 1997) and RANK-RANK-L (Anderson et al., 1997) are members of the TNFRSF that orchestrate co-stimulatory mechanisms and are important for activated T cell survival, differentiation and proliferation, such as the promotion of IL-2 production by T cells (Chen and Flies, 2013). To ensure optimal T cell activation via these processes, co-stimulatory ligands expressed by DCs are upregulated following activation as mentioned above, and naïve T cells consistently express CD28 on their cell surface (Chen and Flies, 2013; Kapsenberg, 2003). Thus, naïve T cells are dependent on interaction with DCs for efficient primary activation (Boyman et al., 2009).

During DC:T cell interaction, co-inhibitory mechanisms are in place to regulate the activatory mechanisms described above (Chen and Flies, 2013). One molecule belonging to the IgSF performing this task is cytotoxic T-lymphocyte-associated

protein 4 (CTLA-4), which is released from intracellular compartments and transported to the site of ligation on the T cell surface when TCR molecules have bound MHC on the APC (Egen and Allison, 2002; Linsley et al., 1996). Similar to CD28, CTLA-4 binds to CD80 and CD86 (Linsley et al., 1996) leading to the transduction of inhibitory signals as well as the endocytosis and degradation of CD28 (Berg and Zavazava, 2008). Further inhibition can occur through capture and degradation of CD80 and CD86 by CTLA-4, removing the ligands from the surface of the APC (Qureshi et al., 2011). IgSF member programmed cell death 1 (PD-1) is another inhibitory receptor on T cells (Ishida et al., 1992), and is most known for driving $CD8^+$ T cell anergy (Chikuma et al., 2009; Tsushima et al., 2007). Moreover, DCs have been shown to be responsible for upregulation of PD-1 on antigen-specific $CD4^+$ T cells in experimental autoimmune encephalomyelitis (Yogev et al., 2012). Thus, DCs are important for the provision of a cohort of co-signals to T cells for their activation, polarisation and function, and the interaction with CD28 is thought to be the key primary process that determines T cell fate (Chen and Flies, 2013).

1.4 Homeostasis of naïve, effector and memory T cells

DC: T cell interaction is not only a process that is critical for T cell activation, but is also a fundamental requirement for T cell homeostasis in the steady state and during immune responses (Boyman et al., 2009). T cell homeostasis is thought to refer to the maintenance of a consistent number of T cells within the T cell pool. T lymphocyte homeostasis varies depending on the type of T cells; the main groups are thought to be αβ and γδ T cells, and little is known about the survival of γδ T cells in comparison with αβ T cells (Marrack and Kappler, 2004). Thus, for the purpose of this thesis only αβ T cells will be discussed. A pool of mature naïve T cells exists in secondary lymphoid organs and is consistently replenished by T cells generated in the thymus (Surh and Sprent, 2008; Takada and Jameson, 2009). Stringent thymic homeostatic processes control *de novo* T cell generation; immature double positive $CD4^+$ $CD8^+$ T cells that display high avidity to self peptides bound to MHC molecules are deleted during negative selection, whereas positive selection occurs when T cells that receive weak but significant TCR signals during this process

survive and differentiate into $CD4^+$ $CD8^-$ or $CD4^-$ $CD8^+$ single positive T cells via contact with self peptide bound MHC-II or MHC-I respectively (Sprent and Surh, 2011). Approximately 98% of double positive T cells die rapidly due to a lack of a TCR signal, i.e. these T cells die from "neglect" rather than targeted deletion (Sprent and Surh, 2011).

Differentiated single positive naïve $CD4^+$ or $CD8^+$ T cells that have migrated from the thymus to secondary lymphoid organs are long-lived, and express low levels of CD44 and CD69 (Sprent and Surh, 2011). Instead, naïve T cells express the selectin CD62L (L-Selectin) (Giblin et al., 1997) and chemokine receptor CCR7 (Miyasaka and Tanaka, 2004). These molecules aid migration of T cells to LNs and PPs, which express the appropriate ligands for these molecules (CD34 and glycam-1 for CD62L, CCL19 and CCL21 for CCR7). Naïve T cells consistently recirculate secondary lymphoid organs and do not enter tissue sites directly. In the LN, CCR7 expression enables naïve T cells to enter through the HEV into the T cell zone, and exit through sinuses into the efferent lymph (Takada and Jameson, 2009). A fibroblastic reticular cell (FRC) network expressing CCL19 and CCL21 facilitates T cell motility and confinement within the T cell zone. In addition, FRCs produce the survival cytokine IL-7 and thereby promote the metabolism and survival of naïve T cells in the LN (Takada and Jameson, 2009). The expression of IL-7Rα (CD127) on naïve T cells is induced by transcription factor FoxO1, which also induces CD62L and CCR7 expression (Link et al., 2007). Together with survival cytokines, DC mediated self peptide MHC stimulation can upregulate the expression of anti-apoptotic proteins including Bcl-2 and Bcl-XL in T cells (McKinstry et al., 2010a). It is currently thought that the dependence on consistent low level TCR signalling for survival of naïve T cells that have left the thymus is set by positive selection within the thymus during T cell development (Garbi et al., 2010; Surh and Sprent, 2008).

Cell death is an essential component during T cell homeostasis, allowing for the maintenance of the naïve T cell pool size by counteracting the remarkable proliferative capacity of T cells (Marrack and Kappler, 2004). The fairly constant number of naïve T cells as well as the fact that T cells in the pool divide only at low

levels in the steady state indicates that competition for resources, such as IL-7 or MHC stimulation, may be limiting the size of the naïve T cell pool (Marrack and Kappler, 2004). Thus, T cell apoptosis is thought to occur due to a lack of survival signals, which increases the expression of pro-apoptotic proteins and caspases, such as Bim, that mediate the breakdown of mitochondrial pathways (McKinstry et al., 2010b).

T cell responses are initiated within the T cell zone of the LN, where antigen loaded DCs activate naïve T cells via antigen-peptide MHC stimulation and co-stimulation including CD28 ligation (Jenkins et al., 2001; Takada and Jameson, 2009). Proliferation of activated T effector cells is characteristic of a T cell response against a pathogen, and this results in upregulation of CD44 and CD69 on the T cell surface (Sprent and Surh, 2011). T cell activation also increases the expression of IL-2 by T cells, which signals through both autocrine and paracrine pathways (Boyman et al., 2009). IL-2 signalling via ligation with CD25 (the IL-2R) promotes metabolic processes, the expression of anti-apoptotic survival factors and proliferation of T cells (Boyman et al., 2009). T cell proliferation is followed by a contraction phase, which is controlled by distinct processes (Dutton et al., 1998). A small population of antigen-specific T cells survive T cell contraction and express high levels of CD44; these cells are termed memory T cells (Sprent and Surh, 2011).

Homeostatic mechanisms that control the effector and memory T cell pool are currently under active research, and are less well understood compared with naïve T cell homeostasis. The mechanisms identified to date which regulate effector/memory T cell reactivation, proliferation, cytokine production and survival are thought to be similar, but not identical, to homeostatic regulation of naïve T cells. For example, naïve, effector and memory $CD4^+$ T cells require MCH-II:TCR signalling for activation and IL-7 for prolonged survival, whereas co-stimulation via CD28 is only essential in initial priming events of naïve $CD4^+$ T cells (Boyman et al., 2009). Rather, activated $CD4^+$ T cells require co-stimulation through various members of the TNFRSF, including OX40 (Redmond et al., 2009) or ICOS (Simpson et al., 2010) for their differentiation, effector function, survival and the formation of

memory $CD4^+$ T cells (Chen and Flies, 2013). Nevertheless, the cytokine response by activated $CD4^+$ T cells is at least in part dependent on CD28 interaction (Harris and Ronchese, 1999). For example, Rulifson *et al.,* (1997) showed that in particular the production of cytokines IL-4 and IL-5 by effector $CD4^+$ T cells is promoted by CD28 ligation upon restimulation of $CD4^+$ T cells with immobilised αCD3 (a T cell co-receptor).

The type of survival factors involved in the promotion of T cell proliferation also varies slightly depending on the activation state of the T cell. Administration of IL-7/αIL-7 mAb complexes *in vivo* can induce low level naïve T cell proliferation in steady state conditions, whereas cytokines IL-2 (and to a lesser extent IL-15) normally lead to rapid proliferation and differentiation into effector/memory $CD4^+$ T cells (Boyman et al., 2009). Responsiveness to IL-2 is enhanced following activation of $CD4^+$ T cells, as activated $CD4^+$ T cells have upregulated the expression of CD25 (Boyman et al., 2009). Taken together, the mechanisms that drive T cell homeostasis are thought to vary depending on the activation state of the lymphocyte, but the factors mediating these processes are similar.

1.5 $CD4^+$ T cell subsets

Activation of $CD4^+$ T cells by APCs during immune responses results in rapid proliferation and the secretion of cytokines that activate and recruit other immune cells, as well as inducing humoral responses orchestrated by B cells and cytotoxic responses by $CD8^+$ T cells (Broere et al., 2011). Particularly, their ability to help B cell antibody class-switching via CD40-L provision has given $CD4^+$ T cells the name "T helper" (Th) cells (Wykes, 2003). Th cells can differentiate into distinct subsets, which can be identified based on the cocktail of cytokines that they secrete following successful activation. In 1986, two main Th subsets were identified: Th1 and Th2 cells (Mosmann et al., 1986). Since then other T helper subsets including IL-17 producing Th17 cells, T regulatory cells (Treg) and T follicular helper (Tfh) cells have been identified, all of which will be discussed in this section.

The main factor determining T cell subset fate is the type of signal (signal 3) provided by the APC, which depends on the type of DAMPs or PAMPS that the PRRs on the APC recognise (Kapsenberg, 2003). Typically, viruses, bacteria and protozoa induce IL-12 production by APCs, particularly by DCs, which is a central mechanism for polarising $CD4^+$ T cells towards a Th1 immune response (Hilkens et al., 1997; Macatonia et al., 1995) (Diagram. 1.5). IL-12 leads to downstream signalling through signal transducer and activator of transcription protein 4 (STAT4) (Thierfelder et al., 1996), and induces the transcription factor T-bet (Lazarevic et al., 2013). T-bet activates IFN-γ production, which is a typical hallmark of $CD4^+$ T cell differentiation into Th1 cells (Szabo et al., 2000). IFN-γ is a potent mediator of CAMΦ activation resulting in NO and ROS production that aids intracellular pathogen killing (Young and Hardy, 1995). Additionally, IFN-γ activates CTL responses by $CD8^+$ T cells against viral infection (Walsh and Mills, 2013). Th1 cells also activate B cell humoral responses and induce antibody class-switching predominantly to IgG2a (Stevens et al., 1988) and IgG2c (Barr et al., 2009) in mice. These particular antibody isotypes in the mouse orchestrate opsonisation, complement fixation and neutralisation of viruses (Bluestone et al., 2009). Although initial priming of Th1 subsets requires interaction with APCs, IFN-γ produced by NK cells or differentiated Th1 cells can also help determine T cell polarisation (Boehm et al., 1997).

Th17 responses were discovered when it became clear that many autoimmune diseases are not mediated by IFN-γ, but by $CD4^+$ T cells producing IL-17 (Harrington et al., 2005; Langrish et al., 2005). Since then, Th17 cells have been viewed as a distinct subset to Th1 and Th2 cells, and their development is negatively regulated by IFN-γ (Harrington et al., 2005). In addition, IL-12 mediates the suppression of IL-17 and induces IFN-γ production by human $CD4^+$ T cells *in vitro* (Hoeve et al., 2006). Th17 differentiation is dependent on signalling through transcription factors STAT3 (Egwuagu, 2009) and RORγt (Ivanov et al., 2006). Th17 responses are now thought to be responsible for the development of pathology during autoimmune diseases (Ivanov et al., 2006; Langrish et al., 2005) as well as asthma (Cosmi et al., 2011), colitis and psoriasis (Weaver et al., 2013). Functions of Th17

cells during immune responses are focused mainly in the gastrointestinal tract, airway, lungs and the skin and act against extracellular bacteria and fungi (Khader et al., 2009). Thus, Th17 cells are predominantly found at mucosal sites including the LP of the intestine (Ivanov et al., 2006). Th17 cells produce IL-22 as well as a large amount of IL-17, and both cytokines are taken up by surrounding epithelial cells (Khader et al., 2009). Subsequently, the release of antimicrobial peptides and chemokines by epithelial cells recruits granulocytes including neutrophils and induces inflammation, which aids in the clearance of fungal and bacterial pathogens (Singh et al., 2014).

Similar to Th1 development, signal 3 for Th17 is now fairly well understood; cytokines TGF-β and IL-6 are important for Th17 differentiation (Singh et al., 2014). Th17 induction in response to *Propionibacterium acnes* (a gram-positive bacterium) and *Salmonella typhimurium* (a gram-negative bacterium) is dependent on DC derived CD40 expression and IL-6 production (Perona-Wright et al., 2009). An alternative pathway for Th17 induction involves the production of IL-21, which suppresses the induction of Tregs and together with TGF-β induces IL-17 production by naïve $CD4^+$ T cells (Korn et al., 2007). $CD4^+$ T cells are likely sources for both TGF-β and IL-21, the latter of which may act in an autocrine feedback loop (Nurieva et al., 2007). IL-23 (Hoeve et al., 2006) and IL-1β (Ikeda et al., 2014), which are likely DC derived, further promote Th17 development and activity (Walsh and Mills, 2013).

Th2 immune responses are active mainly during parasitic infection with helminths, and are less well understood compared with Th1/17 responses (Kool et al., 2012). Although Th2 immune responses provide protection against helminth infection, they can also be detrimental to the host in allergic or fibrotic diseases (MacDonald and Maizels, 2008). Unlike Th1/17 responses, the identity of signal 3 provided by APCs for the direction of Th2 differentiation remains unknown. Despite insufficient understanding of the initiation mechanism governing Th2 responses, major advances have been made in characterising this distinct adaptive response. As such, it has been reported that a low TCR signal and co-stimulation via CD28, OX40 and ICOS are

implicated in Th2 induction, resulting in transcription factor GATA3 expression (Kapsenberg, 2003). Th2 differentiation is thus determined by the stabilisation of GATA3 in a $CD4^+$ T cell, triggering activation of the *il4* gene locus and subsequent production of IL-4 (Lee and Rao, 2004).

In addition to IL-4 production, stabilisation of GATA3 in $CD4^+$ T cells induces production of IL-5, IL-9, IL-10 and IL-13 by Th2 cells (Pulendran and Artis, 2012) (Diagram. 1.5). IL-4 and IL-13 enhance smooth muscle contraction and epithelial cell turnover, which can help in the expulsion of parasites particularly in the intestine (Anthony et al., 2007) (Diagram 1.6). IL-4 drives antibody class-switching by B cells towards the production of IgE, which is a potent stimulator of mast cell and basophil degranulation resulting in the release of antimicrobial components including histamine and proteoglycans (Kool et al., 2012). IL-5 drives the differentiation of eosinophils (Takatsu and Nakajima, 2008), which harbour granules containing various cytokines, chemokines, enzymes and growth factors including major basic protein (MBP) that can mediate anti-pathogenic responses and trigger histamine release by mast cells (Rothenberg and Hogan, 2006). Th2 cytokines, in particular IL-4, promote alternatively activated MΦs (AAMΦ), which are involved in anti-inflammatory processes important in wound healing and resolution of inflammation (Murray and Wynn, 2011; Sica et al., 2014). Thus, type 2 immune responses are often characterised by the activation of eosinophils, AAMΦs, basophils and mast cells as well as goblet cell hyperplasia, but the exact mechanisms that induce Th2 immune responses remain unknown (Allen and Sutherland, 2014; Kool et al., 2012; Licona-Limón et al., 2013) (Diagram. 1.6).

To better understand the mechanisms and key cytokines that may be involved in the induction of Th2 responses, the involvement of IL-4 during Th2 priming has been extensively studied. Exogenous IL-4 triggers STAT6 signalling, which further promotes TCR mediated *gata3* expression (Cote-Sierra et al., 2004). TCR interaction also causes IL-2 production that activates STAT5 via an autocrine feedback system, lowering the requirement for exogenous IL-4 at later stages of Th2 development (Yamane et al., 2005). It has been suggested that basophils can provide an early IL-4

signal (Perrigoue et al., 2009; Sokol et al., 2009; Yoshimoto et al., 2009) and that they can present antigen and prime Th2 responses (Perrigoue et al., 2009; Yoshimoto et al., 2009). However, some experiments depleting basophils may also have depleted a subset of DCs, thus a specific requirement for basophils in Th2 differentiation has not yet been confirmed (Hammad et al., 2010; Okoye and Wilson, 2011; Sokol et al., 2008). Indeed, various studies have found basophils to be redundant during Th2 priming *in vivo* (Hammad et al., 2010; Ohnmacht et al., 2010; Phythian-Adams et al., 2010; Smith et al., 2012). While basophils can interact with antigen-specific T cells in the periphery, they do not interact with naïve T cells within the LNs and production of IL-4 by basophils is T cell dependent (Sullivan et al., 2011). Critically, basophils do not possess the cellular machinery that is required for efficient uptake and processing of antigen described in section 1.2.1 (Otsuka et al., 2013). Thus, their potent ability to process and present complex antigens and high MHC-II expression levels makes DCs a more likely APC for Th2 induction compared with basophils (Lambrecht et al., 2009; Paul and Zhu, 2010; Voehringer, 2009). In support of this various studies using DC depletion models have shown DCs to be necessary for the induction of Th2 responses in various settings (Kool et al., 2008; Phythian-Adams et al., 2010; van Rijt et al., 2005).

Recently, a group of lineage negative cells, innate lymphoid cells 2 (ILC2s), was identified as a further possible innate source of Th2 cytokines in type 2 immunity (Halim et al., 2014). ILC2 are found in the mLNs and intestines of mice infected with gastrointestinal helminths (Fallon et al., 2006; Neill et al., 2010; Saenz et al., 2010) and in the lungs of mice during allergic airway responses (Halim et al., 2012). ILC2s produce Th2 cytokines and a pathway has been described by which ILC2 IL-13 production promotes DC migration from the periphery to LNs, where they prime Th2 immune responses (Halim et al., 2014). MHC-II dependent interaction between T cells and ILCs has been shown to occur during type 2 responses to the gastrointestinal nematode *Nippostrongylus brasiliensis* (Oliphant et al., 2014). In addition, ILC2s express CD80 and CD86 indicating that they are capable of providing co-stimulatory signals to T cells (Oliphant et al., 2014). Thus, ILC2s may play a previously unappreciated role in the orchestration of Th2 immune responses.

However, a recent study shows that although ILC2s may play a critical role in the induction of local immune responses when antigen is delivered through mucosal routes, they are not required for responses against systemically delivered antigens (Gold et al., 2014). This highlights that the initiation of Th2 responses during systemic infection likely requires antigen loaded DC migration to the draining LN (dLN), and this cannot be replaced by ILC2s. These findings further underline the important role for DCs during the induction of Th2 responses, and this will be described in more detail in section 1.9.

An additional $CD4^+$ T cell subset that has been implicated in the production of Th2 cytokines, in particular IL-4, is the Tfh group. Tfh cells are a subset of $CD4^+$ T cells that specialise in the provision of B cell help and the formation of germinal centres in the spleen and LNs (Crotty, 2011). Upon antigen binding via the B cell receptor (BCR), B cells migrate from the marginal zone to the edge of the T cell zone in the spleen or LN enabling them to receive help from activated $CD4^+$ T cells (Vinuesa et al., 2005). Activated B cells then differentiate either into short-lived, low-affinity plasma cells and localise to the LN medullary chords (red pulp in the case of the spleen), or seed follicles to form germinal centres for the development of high-affinity memory B cells and long-lived plasma cells (Vinuesa et al., 2005). Tfh cells form an integral part of the germinal centre by inducing antibody class-switching and plasma cell formation, and have been found to contribute to various human health problems including autoimmunity, immunodeficiency and lymphomas (Tangye et al., 2013). Tfh cells were initially described in human tonsils, where high level expression of CXCR5 was found on a large proportion of $CD4^+$ T cells (Breitfeld et al., 2000; Schaerli et al., 2000). CXCR5 is a chemokine receptor that uniquely enables Tfh cells to enter the B cell zone in the germinal centre (Crotty, 2011). Recently, it has been shown that the transcription factor Ascl2 initiates Tfh development by upregulating CXCR5 and downregulating CCR7 expression (Liu et al., 2014). Tfh differentiation can be induced by IL-6 and IL-21, most likely provided by DCs, B cells or T cells (Eto et al., 2011), and relies on ICOS to activate transcription factor Bcl6 expression (Choi et al., 2011). The expression of Bcl6 is currently thought to be the defining transcription factor for Thf differentiation

(Crotty, 2011). Similar to Th17 cells, Tfh cells secrete IL-21 but can be distinguished by their surface expression of ICOS, PD-1 and CXCR5 (Crotty, 2011). Notably, Tfh development is normal in both IL-6 and IL-21 deficient mice, probably due to redundancy in signalling pathways (Crotty, 2011). Thus, Tfh developmental pathways remain unclear and ongoing research aims to further understand this follicular $CD4^+$ T cell subset and to develop novel therapies targeted to Tfh cells.

The above $CD4^+$ T cell responses are critical for the orchestration of distinct immune responses against a pathogenic threat, but the regulation of these subsets by Tregs is essential to prevent detrimental pathology driven by overt inflammation. The induction of Tregs is hallmarked by the expression of the transcription factor forkhead box P3 (foxp3) as well as CD25 and CD4 (Fontenot et al., 2003; Hori et al., 2003). Similar to $CD4^+$ $Foxp3^-$ T cells, IL-2 is crucial for the survival and function of differentiated Tregs (Fontenot et al., 2003; Zheng et al., 2008; 2007). There are two principal types of Treg cells: natural Tregs (nTregs) that develop in the thymus and regulate immunity against self peptides, and inducible Tregs (iTregs) which are generated within peripheral organs and regulate immunity mainly against commensal bacteria (Horwitz et al., 2008; Larkin, 2013). TGF-β (Chen, 2003; Cobbold et al., 2004) and RA (Coombes et al., 2007) are involved in the differentiation and promotion of Treg cells, and DCs are capable of inducing Treg responses (Coombes et al., 2007; Yamazaki et al., 2008). Tregs are thought to produce substantial amounts of TGF-β and IL-10, which are principal cytokines involved in the downmodulation of effector/memory $CD4^+$ T cell responses (Sakaguchi et al., 2009). Microscopy techniques have also depicted direct interaction between DCs and Tregs through the expression of neuronal guidance protein neurophili-1 by Tregs (Sarris et al., 2008; Tang et al., 2006), which is important for Treg mediated suppression (Solomon et al., 2011). These studies underline the importance of DCs during Treg function and activity *in vivo.*

1.5.1 Transcriptional control of T cell subset development and plasticity

The $CD4^+$ T cell nomenclature described above suggests that the $CD4^+$ T cell subsets are completely distinct from each other, and this was believed to be the case for numerous years. However, studies have since shown that a degree of flexibility exists during T cell differentiation, allowing for T cell plasticity *in vivo* (Bluestone et al., 2009). It is likely that plasticity in Th2 populations in particular exists due to the rather large cohort of cytokines that they produce. In support of this, T cells producing IL-4 but not IL-13 or IL-5 are located in the B cell zone within the dLN (Liang et al., 2011). Furthermore, Tfh cells have been shown to differentiate from IL-4 producing Th2 cells within the LN during helminth infection (Glatman Zaretsky et al., 2009). In fact, it has been suggested that Tfh cells are the primary cell type responsible for IL-4, but not IL-13, production in lymphoid tissue in response to helminth antigen (Liang et al., 2011).

Additional evidence for T cell plasticity is provided by the discovery of $GATA3^+$ T-bet^+ T cells in helminth infection with *Schistosoma mansoni* (Peine et al., 2013). This cell type expresses both IL-4 and IFN-γ, and it has been suggested that the presence of IL-4/IFN-γ double producers prevents severe immunopathology by maintaining a critical balance between Th1 and Th2 immune responses during infection (Peine et al., 2013). Recently it has been shown that IL-4/IFN-γ double positive cells generated during *S. mansoni* infection display a distinct DNA methylation signature at key cytokine genes as well as *gata3*, which indicates that DNA methylation processes may be important for the co-existence of Th1 and Th2 characteristics (Deaton et al., 2014).

Although $CD4^+$ T cell plasticity evidently occurs during differentiation, key processes are equally important to maintain and balance distinct $CD4^+$ T cell responses. This is achieved by various counter-regulatory and antagonistic mechanisms between the molecular components driving $CD4^+$ T cell differentiation. For example, IL-6 inhibits the generation of iTregs and favours the generation of Th17 cells (Veldhoen et al., 2006). Transcription factor T-bet expression inhibits

transcription of genes encoding IL-4 and IL-5 (Szabo et al., 2000), whereas GATA3 expression suppresses IL-12 signalling (Ouyang et al., 1998). Furthermore, numerous reports have outlined reciprocal antagonisation between IL-4 and IFN-γ during $CD4^+$ T cell differentiation (Paludan, 1998). IFN-γ represses IL-4 secretion by Th2 cells (Gajewski et al., 1988) and inhibits IL-4 mediated induction of the IgE receptor, FcεRII (Rousset et al., 1988). It has been shown that IFN-γ directly suppresses the transcription of the *il4* gene via IRF-1 and IRF-2, which bind IL-4 promotor sites (Elser et al., 2002). In contrast, IL-4 inhibits Th1 polarisation by activating STAT6, which has been reported to bind to the same DNA oligonucleotide as STAT4 (Schindler et al., 2001). Indeed, IL-4/IFN-γ cross-regulation is thought to occur predominantly through competition for transcription signalling pathways (Paludan, 1998).

1.6 Schistosomiasis

The initiation of $CD4^+$ Th2 cell responses has been extensively studied during infection with helminths that are potent inducers of Th2 responses, such as *S. mansoni* (Pearce and MacDonald, 2002). At least 200 million people are thought to be chronically infected with schistosomiasis worldwide (Gryseels et al., 2006). Primarily sub-Saharan regions of Africa are affected, but the disease is classed as endemic in over 74 countries (Ross et al., 2002). Five species of schistosomes are responsible for human infections: *S. mansoni, S. japonicum, S. haematobium, S. intercalatum and S. mekongi.* The first three are the most extensively studied in clinical research. An estimated 280,000 deaths occur every year as a consequence of *S. mansoni* or *S. haematobium* infection in sub-Saharan Africa alone (van der Werf et al., 2003). With the exception of *S. haematobium*, all species cause hepatosplenic and intestinal schistosomiasis, whereby the adult worms reside in the mesenteric vasculature and produce eggs. *S. haematobium* resides in the blood supply surrounding the bladder and causes urogenital schistosomiasis (Ross et al., 2002). Currently, therapeutics for the disease rely on the anti-parasitic activity of praziquantal, but the distribution of praziquantal to populations at risk is challenging (Doenhoff et al., 2009; Fenwick et al., 2003). Furthermore, there is a danger that with increases in mass

treatment resistance to praziquantal could begin to develop (Fallon and Doenhoff, 1994). An effective vaccine would be greatly beneficial for the control of the disease in endemic areas, and an open question in schistosome biology revolves around how immune mechanisms in individuals that have acquired resistance to reinfection mediate protection. Unravelling the immune responses that govern disease progression upon *S. mansoni* infection will aid the design of new vaccines and therapies against schistosomiasis (Pearce and MacDonald, 2002).

1.6.1 The life cycle of Schistosoma mansoni

Schistosomes are rather unusual in several respects when one compares their biology with that of other digenian parasites. As such *S. mansoni* displays unique features that include the following: schistosomes only infect two rather than three hosts; reproduction in the mammalian host occurs through pairing of separate male and female schistosomes as opposed to hermaphrodite or asexual reproduction; infection with schistosomes occurs through the skin rather than by ingestion; they reside in the intravascular system of the host (Pearce and MacDonald, 2002). The life cycle of *S. mansoni* begins with asexual reproduction within the intermediate host, the *Biomphalaria glabrata* fresh water snail, from which microscopic *Schistosoma* cercariae are shed by the snails and released into the water at which point this free living aquatic stage of the parasite can survive for up to 72h (Gryseels et al., 2006; Pearce and MacDonald, 2002) (Diagram. 1.7). Infection of the definitive (mammalian) host occurs through direct contact with contaminated water, when highly motile cercariae burrow through the skin and transform into schistosomula. Immature schistosomula then enter the vasculature and migrate through the body until settling in the portal vasculature where they mature into adult worms (Pearce and MacDonald, 2002).

After approximately 28 days of infection, established worm pairs produce up to 300 eggs per day (Gryseels et al., 2006). *S. mansoni* eggs normally migrate through the intestinal tissue into the lumen, and consequently become excreted in the faeces. However, a proportion of the *S. mansoni* eggs are also swept in the

bloodstream to the liver, where they enter through the sinusoids and become lodged in the parenchyma (Pearce and MacDonald, 2002). Upon arrival of eggs in intestinal or liver tissue, the immune system responds by enveloping the egg in collagen rich granulomas, which protect the surrounding tissue from toxins released by the egg. It is thought that granuloma formation is required for efficient egg migration through the tissue, as eggs themselves are not motile (Doenhoff et al., 1981). Immunocompromised hosts such as HIV infected patients display impaired *S. mansoni* egg migration, which highlights that an intact immune system is essential for efficient *S. mansoni* egg transit (Karanja et al., 1997). Granuloma mediated protection has also been reported as a critical process for the progression of bacterial infection with *Mycobacterium tuberculosis* (Doenhoff, 1998). Although initially protective to the host, chronic accumulation of granulomas causes fibrotic legions to form, and much of the pathology associated with *S. mansoni* infection is caused by eggs lodged within the intestine and the liver (Pearce and MacDonald, 2002). Fibrosis in the liver leads to high blood pressure and subsequent enlargement of the portal vessel. The poor blood flow into the organ then results in the formation of new but fragile blood vessels that bypass the fibrotic liver, leading to portal shunting (Pearce and MacDonald, 2002). This dramatically increases the risk of haemorrhages in the peritoneum, which ultimately leads to fatality (Pearce and MacDonald, 2002). Thus, the regulation of the host's immune responses is essential to control the outcome of the disease.

1.7 Structural arrangement of the granuloma

Given that the occurrence of granulomatous inflammation is a key mediator of pathology during *S. mansoni* infection, the formation and development of granulomas has been a central area of research associated with schistosomiasis. The structure of *S. mansoni* granulomas has been well characterised using electron microscopy and other histology methods to show two major stages in granuloma development: the pre-granulomatous or exudative phase, and the mature granuloma or exudative-productive phase (Lenzi et al., 1998). Much like a beehive, the granuloma forms an entity that is organised and intricate. Early

stages of development involve innate immune cells that form an initial barrier around the egg (Lenzi et al., 2006; Weinstock et al., 1999). Only a few lymphocytes are found at this initial stage (Almadi et al., 2011; Chuah et al., 2014). The production of fibrous and extracellular material gradually transforms these loose clusters of innate immune cells into a more organised network (Lenzi et al., 2006; 1999). Extracellular matrix components, such as fibronectin and tenascin, are located predominantly but not exclusively in the central zone of the developing exudative granuloma (Lenzi et al., 2006; Silva et al., 2000). Fibre radiation centres (collagen anchorage points) shape this collagen mesh, whereas fibres in the peripheral zone are mostly thin and loosely arranged (Lenzi et al., 1999; 2006; Silva et al., 2000). The granuloma architecture is thus determined by an irregular collagenic topology, enabling cells to move bidirectionally from the periphery to the egg (Lenzi et al., 2006; Steinberg, 1996).

Myofibroblasts derived from hepatic stellate cells (HSCs) are thought to be the main source of collagen in the liver (Wynn, 2008). During early stages of granuloma development in murine *S. mansoni* infection collagen type III (thick fibres) is more frequent. However, this is replaced by collagen type I (thin fibres) in later stages (Grimaud et al., 1987; Silva et al., 2000). This transition from type III to type I collagen during granuloma development also occurs during human *S. mansoni* infection (Adnani, 1985). Other types of collagen (e.g. type IV) have also been found in granulomas, but these are thought to be less abundant in comparison with type I and III collagen (Grimaud et al., 1987; Silva et al., 2000).

As the granuloma matures, the fibrous framework creates a scaffold for a compact and spherical shape displaying three distinct layers: the internal or peri-ovular layer, the medial or paracentral layer and the external layer (Lenzi et al., 1998). By isolating cells from granulomas, Lenzi *et al.*, (2006) reported that mature exudative-productive granulomas contain more than 40,000 cells, highlighting the importance of an organised extracellular matrix. The mature granuloma contains a cohort of adaptive immune cells including T cells and B

cells, as well as the established innate cell network (Jacobs et al., 1999; Lenzi et al., 1998; Weinstock and Boros, 1983). The outer layer of cells appears to flatten (Bentley et al., 1982), forming a boundary between granulomatous tissue and the liver parenchyma (Hams et al., 2013). Such cellular morphology has been described in granulomas formed *in vitro* by co-culturing isolated spleen cells from *S. mansoni* infected mice with live eggs obtained from adult worm pairs (Bentley et al., 1982). This closure of the granuloma is created by intimate cell connections through pan-cadherins, occludin and connexin-43 (Lenzi et al., 2006). The granuloma persists around the *S. mansoni* egg until inflammatory processes are downmodulated and collagen is degraded (Lenzi et al., 1998), but often a fibrotic plaque or scarring remains (Pearce and MacDonald, 2002). The exact processes that allow granulomas to resolve are not yet fully understood, but a role for MΦ collagen degradation has been suggested (Barron and Wynn, 2011; Duffield et al., 2005; Herbert et al., 2004; Silva et al., 2000; Wynn and Barron, 2010). Many fundamental open questions remain about granuloma formation and development, including what the exact functional roles are that distinct immune cells play, and which cells interact with each other, during this important process (this will be described in more detail in chapter 3, when granuloma formation during *S. mansoni* infection will be investigated).

1.8 The development of immune responses against *S. mansoni* infection

The formation of granulomas is highly dependent on the type of immune response induced against the *S. mansoni* egg (Wynn, 2004). Schistosomes have evolved to co-exist with their hosts for many years, and this relationship can even last for decades in some cases (Pearce and MacDonald, 2002). In the course of chronic infection with *S. mansoni,* the immune response progresses through at least three stages, which are intimately linked to the development of the parasite (Pearce and MacDonald, 2002). Initial immune responses in the first 21 to 35 days are induced against migrating parasite larval schistosomes, and these are characterised by a fine-tuned balance, or mix, of Th1 and Th2 immune responses (Grzych et al., 1991; Pearce and MacDonald, 2002). The different

developmental stages of schistosomes that are present in mammals are known to produce cross-reactive antigens, and immune responses formed against larval forms of the parasite likely exhibit cross-reactivity against *S. mansoni* eggs later on in infection (Lukacs and Boros, 1991). When egg production begins 28-42 days after infection, a shift to a dominant Th2 immune response occurs and granulomatous inflammation as well as collagen deposition becomes apparent (Grzych et al., 1991; Pearce et al., 1991). Downmodulation of Th1 responses at this time-point also correlates with an increase in IL-10 production (Sher et al., 1991). Given that the parasite is long-lived and worm pairs continue to produce hundreds of eggs per day (Gryseels et al., 2006; Pearce and MacDonald, 2002), Th2 responses and granuloma development continue to increase until approximately day 56, when the strength of the Th2 response reaches its peak (Pearce and MacDonald, 2002). At this time-point fibrotic pathology is prevalent, and Th2 cytokines are implicated in the promotion of collagen formation (Fallon et al., 2000a). Subsequently, it is thought that consistent egg antigen exposure leads to Th2 response modulation, resulting in a decline of the Th2 response and an increase in regulatory responses between days 70 to 105 (Lundy and Lukacs, 2013; Pearce and MacDonald, 2002). During this time-frame effector/memory $CD4^+$ T cells are thought to be unresponsive, or hyporesponsive, and this will be described in more detail in section 1.8.2. As a result of Th2 hyporesponsiveness, granulomatous inflammation is downmodulated but fibrosis around newly deposited eggs is increased, and this persists throughout the remainder of the infection.

1.8.1 Consequences of dysregulated $CD4^+$ T cell responses against *S. mansoni* eggs

The development of immune responses during *S. mansoni* infection underlines that the induction of $CD4^+$ Th2 immune responses and fibrotic mechanisms is intricately linked to the pathological outcome of the disease (Grzych et al., 1991; Pearce et al., 1991; Pearce and MacDonald, 2002; Vella and Pearce, 1992). In fact, the balance or mix between Th1 and Th2 responses throughout *S. mansoni* infection is critical to prevent overt pathology, morbidity and mortality that is

associated with skewed Th1 or Th2 responses (Hoffmann et al., 2000; Wynn, 2004). The importance of T cells during granuloma pathology was first shown by several groups using severe combined immunodeficiency (SCID) or nude mice, which revealed that T cell deficiency leads to severely impaired granuloma formation during infection (Amiri et al., 1992; Boros, 1989; Byram and Lichtenberg, 1977; Cheever et al., 1993; 1999; Doenhoff et al., 1981; Dunne and Doenhoff, 1983). A dominant role of $CD4^+$ αβ T cells in hepatic granuloma formation was established by the use of depleting antibodies (Mathew and Boros, 1986), whilst γδ T cells are not required for initial granulomatous processes (Iacomini et al., 1995). These findings led to the investigation of the requirement for intact Th2 responses during granuloma formation, and studies using MHC-$II^{-/-}$ (Hernandez et al., 1997) or $STAT6^{-/-}$ (Kaplan et al., 1998) mice showed that impaired Th2 mechanisms result in reduced or even absent granuloma formation in the liver during *S. mansoni* infection. An impairment in granuloma formation leads to tissue exposure to egg derived toxins, including Omega-1, which can lead to tissue necrosis in the liver (Dunne et al., 1991). Subsequent death of animals that lack Th2 immune responses has also been linked to changes in the intestines, as severe damage caused by egg transit through the tissue when granuloma formation is reduced can lead to haemorrhages that are thought to allow entry of bacteria and endotoxins into the blood circulation (Fallon et al., 2000b).

The importance of Th2 responses for granulomatous inflammation promoted the investigation of the role of individual cytokines during *S. mansoni* granuloma formation. IL-$4^{-/-}$ mice develop acute cachexia mediated by TNF-α resulting in increased mortality, but overall granuloma size and eosinophilia within the liver is unchanged compared with WT controls (Brunet et al., 1997). This finding led to the hypothesis that, although animals in Th2 deprived environments can succumb to septic shock and die, individual Th2 cytokines are not a fundamental requirement for granuloma formation (Wynn et al., 2004). Jankovic *et al.,* (1999) showed that both IL-4 and IL-4R deficient mice, the latter of which cannot respond to IL-13 as well as IL-4, remain able to develop a Th2 immune

response during infection, albeit to a lesser extent compared with WT mice. The same study showed that IL-4, but not IL-4R knockout mice, can form granulomatous tissue around the egg in the liver (Jankovic et al., 1999a). This observation suggests that cells capable of responding to IL-4 and IL-13 including AAMΦs, DCs, endothelial cells and/or fibroblasts are important for granuloma formation (Jankovic et al., 1999a). Indeed, when IL-4/IL-13 double deficient mice were examined, overall granuloma formation is reduced in the lung following intravenous injection of *S. mansoni* eggs (McKenzie et al., 1999). A similar trend is seen in the liver when residual IL-13 is depleted from IL-$4^{-/-}$ mice using an αIL-13 antibody (Chiaramonte et al., 1999), or when using IL-4/IL-13 deficient mice (Fallon et al., 2000a). This suggests that IL-4 and IL-13 largely compensate for each other during the formation of granulomatous inflammation. In addition, a critical feature of Th2 responses is enhanced eosinophilia, which is thought to be induced by IL-5 (Takatsu and Nakajima, 2008). IL-$5^{-/-}$ mice develop significantly smaller granulomas devoid of eosinophils that appear less fibrotic and contain larger populations of MΦs and fibroblasts (Reiman et al., 2006). Thus, we know that intact Th2 immune responses and IL-4R signalling pathways are important for the formation of granulomas during *S. mansoni* infection, thereby protecting host tissues from toxins produced by the egg.

Although it is clear that intact Th2 immune responses are required for granuloma formation, initial granulomas are in fact formed in a mixed Th1/Th2 environment (Hams et al., 2013), which raises the possibility that Th1 immune cells may also play a role. It has been shown that Th1 impairment in mice deficient in IFN-γ or $CD8^{+}$ T cells does not alter granulomatous inflammation in the liver at D56 or D112 post *S. mansoni* infection (Yap et al., 1997). Furthermore, STAT4 deficient mice, which have defects in the signal transduction pathways affecting Th1 development, also form normal granulomatous legions during *S. mansoni* infection in comparison with WT mice (Kaplan et al., 1998). Notably, smaller and more fibrotic granulomas have been reported in Th1 deficient MyD$88^{-/-}$ mice, and the authors suggest that TLR-

mediated antigen-specific Th1 responses could be important indirectly for the suppression of Treg responses during granuloma formation (Layland et al., 2005). Overall, these reports indicate that the formation of granulomas during *S. mansoni* infection is largely independent of Th1 elements, but TLR-mediated antigen-specific Th1 responses may be important indirectly for this process.

Although the induction of Th1 responses is not critical for granuloma formation, there is some evidence to suggest that Th1 components are crucial for the regulation of Th2 mediated pathology. For example, enhancement of Th1 responses achieved by IFN-γ administration to *S. mansoni* infected mice suppresses liver granuloma size and hepatic fibrosis (Czaja et al., 1989; Lukacs and Boros, 1993). This suggests that Th1 responses may be involved in the downregulation of granulomatous inflammation by regulating Th2 immune responses, due to cross-regulatory activity between IL-4 and IFN-γ described in section 1.5.1. $CD8^+$ T cells have been reported as important players for the downmodulation of granuloma size, but their presence *in vivo* is not critical for this process (Chensue et al., 1993; 1981; Yap et al., 1997). Although desirable for alleviating Th2 mediated pathology, enhanced Th1 responses are often associated with elevated levels of TNF-α resulting in more severe disease (Boros and Whitfield, 2006; Brunet et al., 1997; Fallon and Dunne, 1999; Fallon et al., 2000b; Hoffmann et al., 2000). For example, IL-10/IL-4 double cytokine deficient mice develop elevated Th1 responses, but not Th2 responses, 56 days post infection marked by increased IFN-γ (Hoffmann et al., 2000). These mice form granulomas that appear normal in size, but are less fibrotic, and contain fewer eosinophils. Hoffmann *et al.*, (2000) additionally showed that IL-10/IL-4 deficient mice display elevated levels of TNF-α in the serum compared with WT mice, and cannot survive acute *S. mansoni* infection. TNF-α has been shown to promote liver fibrosis and hepatomegaly (Joseph and Boros, 1993; Mwatha et al., 1998) and increases hepatic granuloma area of chronically infected mice (Joseph and Boros, 1993). Thus, it seems likely that the granulomas forming in IL-10/IL-4 deficient mice are driven at least in part by TNF-α. However, TNF-α is dispensable during granuloma formation (Davies et al., 2004) and instead may

play a more important role in parasite survival or fecundity (Amiri et al., 1992; Oliveira et al., 2009). Closer investigation of Th1 mediated granulomatous inflammation in IL-10/IL-4 deficient mice revealed a significant influx of neutrophils in these granulomas, and this may contribute to increased morbidity experienced by IL-10/IL-4 deficient mice during *S. mansoni* infection (Hoffmann et al., 2001). This highlights the absolute necessity of balanced Th1 and Th2 responses during *S. mansoni* infection to prevent severe pathology and morbidity, when neither Th1 or Th2 elements of the immune response against the parasite are extreme (Wynn et al., 2004).

During chronic stages of *S. mansoni* infection Th2 immune responses are gradually downmodulated and granulomatous lesions resolve (Boros et al., 1975; Chensue et al., 1992; Henderson et al., 1992; Lundy and Lukacs, 2013). It is probable that these two processes are linked, as repeated administration of rIL-4 or rIL-2 to chronically infected mice restores granuloma size to that generated during peak growth (Mathew et al., 1990; Yamashita and Boros, 1992). A role for IL-10 in immune response suppression has been reported, as IL-10 deficient mice do not downregulate immune responses in the mLN and the spleen or granulomatous inflammation in the liver during chronic stages of infection (D105) (Sadler et al., 2003). However, multiple cell types including B cells, Tregs, DCs, MΦs and $CD4^+$ T cells produce IL-10, which complicates investigation of regulatory responses during *S. mansoni* infection (Stadecker, 1999; Wilson et al., 2007).

Treg responses are also known to regulate Th1 and Th2 immune responses during *S. mansoni* infection, but the role for IL-10 in this process is disputed as suppression of IL-4 and IFN-γ can be IL-10 independent (Wilson et al., 2007). Treg activity during helminth infections was initially described in patients infected with filarial or schistosome parasites, who displayed a hyporesponsive T cell response (Wilson et al., 2007). Tregs expand in unison with Th2 responses during *S. mansoni* infection and maximum numbers in the liver are observed at D112 when modulatory processes are prevalent (Singh et al., 2005; Taylor et al.,

2006). Taylor *et al.,* (2006) additionally showed that a single dose of *S. mansoni* eggs is sufficient to induce a Treg response in the dLN. This indicates that *S. mansoni* eggs are potent inducers of Treg responses as well as effectors of Th2 immune responses. Treg mediated modulation during *S. mansoni* infection has been reported for intestinal granulomas, where $CD4^+$ $CD25^+$ $Foxp3^+$ Tregs downregulate the development of granulomas in the colon via TGF-β as well as the production of collagen (Turner et al., 2011). In the liver, severe pathology is also prevented by Tregs (Layland et al., 2007) via both IL-10 dependent and independent mechanisms (Dewals et al., 2010; Hesse et al., 2004).

In addition to Tregs, a role for B cells in T cell downmodulatory processes has been identified, as B cell deficient mice fail to downmodulate $CD4^+$ T cell mediated granulomas during chronic stages of infection (Jankovic et al., 1998). Notably, Jankovic *et al.,* (1998) showed that granulomatous responses were downmodulated via Fc receptor signalling independent of IL-10. Suppression of Th2 responses during *S. mansoni* infection by AAMΦs expressing arginase 1 (Arg-1) is also thought to be IL-10 independent, and the mechanism that orchestrates this process will be described in more detail in chapter 3 (Pesce et al., 2009). Taken together, Tregs, B cells and AAMΦs are implicated in the downmodulation of $CD4^+$ T cell responses during *S. mansoni* infection, and the mechanisms beyond the secretion of IL-10 are under active research (Wilson et al., 2007).

1.8.2 T cell anergy/hyporesponsiveness during *S. mansoni* infection

During $CD4^+$ T cell downmodulation in later stages of *S. mansoni* infection, $CD4^+$ T cells are thought to become anergic or hyporesponsive, and a decrease in splenic Th2 cell activity is first observed around D56 of murine infection (Taylor et al., 2009). Anergic T cells are antigen experienced T cells that do not become fully activated, but survive for an extended period of time in this unresponsive state (Kuklina, 2013; Schwartz, 2003). There are two distinct types of T cell anergy: clonal anergy and adaptive tolerance (Chiodetti et al., 2006).

Clonal anergy principally occurs through growth arrest and can be overcome by IL-2 administration (Chiodetti et al., 2006). Adaptive tolerance, also termed *in vivo* anergy, is characterised by inhibition of proliferative and effector functions frequently initiated by CTLA-4 ligation (Schwartz, 2003). In contrast to clonal anergy, adaptive tolerance cannot be overcome by IL-2 (Chiodetti et al., 2006). An E3 ubiquitin ligase termed gene related to anergy in lymphocytes (GRAIL) has been reported as being expressed by hyporesponsive/anergic T cells, which provides a cell intrinsic mechanism for the induction of anergy (Anandasabapathy et al., 2003; Seroogy et al., 2004). Taylor *et al.,* (2009) showed that chronic hyporesponsive $CD4^+$ T cells from D105 of *S. mansoni* infection which express GRAIL did not revert to a proliferative state when transferred into D49 infected mice (Taylor et al., 2009). The fundamental role of GRAIL in this process was shown by suppressing GRAIL, which prevented the development of hyporesponsiveness in $CD4^+$ T cells (Taylor et al., 2009).

In addition to cell intrinsic processes, extracellular mechanisms have been reported to orchestrate T cell hyporesponsiveness during *S. mansoni* infection: repeated antigen stimulation leads to elevated expression of inhibitory CD200-CD200R ligand-receptor pairs on Th2 cells, eventually resulting in the loss of proliferative capacity (Caserta et al., 2012; Gorczynski, 2012). However, whether this extrinsic mechanism represents clonal anergy or *in vivo* adaptive tolerance remains unclear.

T cell anergy, or hyporesponsiveness, is dissimilar to cell extrinsic PD-1 mediated T cell exhaustion mechanisms classically described during chronic viral infections (Morou et al., 2014; Shin and Wherry, 2007; Yi et al., 2010). Loss of T cell function during exhaustion is accompanied by the expression of PD-1, which was first identified on virus-specific $CD8^+$ T cells during chronic lymphocytic choriomeningitis (LCMV) (Barber et al., 2006). During T cell exhaustion GRAIL and other anergy related genes are not expressed by T cells (Kim and Ahmed, 2010; Wherry et al., 2007). Increased expression of PD-1L on MΦs has been reported in *S. mansoni* infection when animals are infected with

single sex worms resulting in infection lacking egg production (Smith et al., 2004). However, PD-1L is predominantly recognised by Th1 cells (Loke and Allison, 2003), and the observation that PD-1L is upregulated may not hold relevant implications for the downmodulation of Th2 responses against *S. mansoni* eggs. Thus, it is highly probable that immune downregulation during *S. mansoni* infection is mechanistically distinct from PD-1 mediated T cell exhaustion described above, although the possibility that PD-1-dependent mechanisms play a role cannot be dismissed (Smith et al., 2004).

1.9 The importance of dendritic cells during *S. mansoni* infection

1.9.1 Dendritic cell activation for Th2 polarisation in response to *S. mansoni* egg antigens

Although the character and development of $CD4^+$ T cell responses during *S. mansoni* infection are well understood, little is known in comparison of how schistosome antigens activate APCs including DCs to drive Th2 polarisation. Several studies have investigated the capacity of schistosome experienced DCs to induce Th2 immune responses following recognition of the parasite, and most have used *S. mansoni* soluble egg antigen (SEA) to assess this process (Perona-Wright et al., 2006). SEA represents a soluble extract obtained from isolated *S. mansoni* eggs (MacDonald et al., 2001) (section 2.3.4, chapter 2), and is predominantly composed of hundreds of proteins as well as some sugars and lipids (Mathieson and Wilson, 2010; Meevissen et al., 2011). Stimulation with SEA is sufficient to induce murine Th2 immune responses *in vivo* (Okano et al., 1999). This effect can be replicated *in vitro* with BMDCs or purified splenic DCs stimulated with SEA, which efficiently prime $CD4^+$ T cell responses towards a Th2 phenotype *in vivo* and *in vitro* (Jankovic et al., 2004; MacDonald et al., 2001). In addition, human DCs stimulated with SEA polarise Th2 immune responses effectively *in vitro* (de Jong et al., 2002). Yet, SEA-pulsed BMDCs, splenic or human DCs exhibit only minor upregulation of activation markers including MHC-II, CD40, CD80, CD86 and OX40-L in comparison with

bacterial antigens (Agrawal et al., 2003; de Jong et al., 2002; Jankovic et al., 2004; MacDonald et al., 2001). In addition, SEA-pulsed BMDCs do not produce substantial amounts of inflammatory cytokines including IL-6 and IL-12p70 or cytokines associated with Th2 responses such as IL-4 or IL-10 *in vitro* (MacDonald et al., 2001). Indeed, DCs do not produce IL-4 (MacDonald et al., 2001) or require to produce IL-4 for efficient Th2 induction (Jankovic et al., 2004; MacDonald and Pearce, 2002). In line with these findings, some reports have indicated that exogenous IL-4 may not be critical for Th2 induction: Th2 responses can be induced both *in vitro* and *in vivo* when $CD4^+$ T cells are not able to respond to IL-4 (i.e. T cells that lack the IL-4R), albeit at a lower level compared with WT T cells (Jankovic et al., 2000; Yamane et al., 2005). Microarray analysis of BMDCs exposed to SEA revealed that less than 30 out of 12,000 mouse genes were significantly altered in the array compared with unstimulated DCs, which emphasises the low level changes in the DC phenotype that occur in response to SEA on a mRNA level (Kane et al., 2004). Thus, the activation phenotype of schistosome experienced DCs is distinct from conventional activation status of DCs that mediate Th1/17 responses, yet enables the induction of potent Th2 responses (Perona-Wright et al., 2006).

The potency of SEA to influence DC activation has been outlined by studies that have reported SEA mediated inhibition of BMDC cytokine production and surface marker expression following bacterial stimulation or TLR ligation with ligands including LPS, which results in dampened upregulation of MHC-II, co-stimulatory molecules and IL-12 production (Cervi et al., 2004; Kane et al., 2004; Perona-Wright et al., 2012). It has been suggested that suppression of classical DC activation may occur through downmodulation of signalling pathways such as nuclear factor kappa B (NFκB) and extracellular signal-regulated kinase (ERK) by SEA (Kane et al., 2004). However, SEA has also been reported to activate c-Fos in human monocyte DCs via ERK signalling, which directly represses the transcription of IL-12 (Agrawal et al., 2003). Recently, the impact of SEA on the mTOR signalling pathway in human monocyte derived DCs was examined (Hussaarts et al., 2013). The mTOR

signalling pathway represents a key metabolic pathway that incorporates signals from growth factors and nutrients, which is involved in DC differentiation and function including antigen presentation to T cells (Salmond and Zamoyska, 2011). Hussaarts *et al.,* (2013) reported that although mTOR inhibitors dampen DC maturation and promote Th2 induction, neither SEA or omega-1 altered signalling through the mTOR pathway. Taken together, the activation phenotype of DCs stimulated with SEA differs from classically activated DCs, but the exact mechanisms that mediate schistosome experienced DC activation are largely unclear.

1.9.2 Recognition of *S. mansoni* antigens by DCs

Numerous SEA components have been closely examined to clarify how the egg stage of the parasite may interact with DCs for the polarisation of Th2 immune responses. In particular, two glycoproteins IPSE/α-1 (or SmEP25) (Schramm et al., 2006) and omega-1 (Dunne et al., 1991) are major constituents of SEA. IPSE/α-1 activates various immune cells such as mast cells, basophils, eosinophils and MΦs (Abdulla et al., 2011; Donnelly et al., 2008; Sabin et al., 1996; Schramm et al., 2003; Williams et al., 2005). For example, IPSE/α-1 activates basophil IL-4 production (Schramm et al., 2006), which is dependent on the production of IgE *in vivo* (Schramm et al., 2007). This suggests that efficient induction of Th2 immune responses likely requires activation of multiple accessory cell types (Allen and Sutherland, 2014).

Omega-1 is a T2 ribonuclease that is highly toxic to host cells including hepatocytes (Fitzsimmons et al., 2005), which underlines the importance of granuloma formation around the *S. mansoni* egg in the liver for efficient protection of the surrounding parenchyma. Omega-1 is a more recently discovered Th2 inducing glycoprotein present in SEA, yet omega-1 depleted SEA retains its Th2 induction ability (Everts et al., 2009; Steinfelder et al., 2009). Once inside the cell, Omega-1 acts as an RNase and degrades both messenger and ribosomal RNA (mRNA and rRNA), which ultimately halts protein synthesis (Everts et al., 2012). The same study showed that omega-1 is taken up by DCs via the mannose C-type lectin receptor (CLR) (Everts et al.,

2012). Indeed, the examination of various Th2 inducing components within SEA has aided the identification of the PRRs which recognise these antigens. Various other glycoproteins present in SEA have been shown to bind to CLRs, including DC-specific intercellular adhesion molecule-3-grabbing non-integrin (DC-SIGN) and the MΦ galactose-type lectin (MGL) (Meevissen et al., 2011; van Liempt et al., 2007). On the other hand, numerous studies have shown that Th2 induction during *S. mansoni* infection is MyD88 independent, which is a classical signalling pathway following TLR stimulation (Layland et al., 2005). Further understanding of how *S. mansoni* Th2 inducing antigens are recognised and how they activate DCs will help investigation into the mechanisms required for Th2 induction.

Isolated glycan moieties from SEA have been suggested to be sufficient to stimulate DCs to induce Th2 responses, which underlines the potential importance of SEA glycosylation for its antigenicity (Faveeuw et al., 2002; Okano et al., 1999). One such glycan is lacto-N-fucopentaose III (LNFPIII) (Okano et al., 2001), which binds TLR4 on BMDCs (Thomas et al., 2003). Following TLR4 ligation LNFPIII activates ERK consistently (Thomas et al., 2003) and NFκB transiently (Thomas et al., 2005). In contrast, LPS ligation with TLR4 results in the stimulation of mitogen-activated protein kinases (MAPK) kinases p39, JNK and ERK, as well as prolonged activation of NFκB (Thomas et al., 2005). However, expression of TLR4 and various other TLRs is not essential for the induction of Th2 immune responses against *S. mansoni* (Jankovic et al., 2004; Kane et al., 2004; Layland et al., 2005; Vanhoutte et al., 2008). Therefore, it is plausible that additional co-receptors such as certain CLRs may contribute to determining the downstream intracellular signalling events that succeed TLR4 binding of LNFPIII (Hokke and Yazdanbakhsh, 2005). Further investigation of the signalling pathways that are activated after SEA recognition by DCs will help in understanding the activatory phenotype required for Th2 polarisation.

1.9.3 Dendritic cells are necessary for the induction of Th2 immune responses against *S. mansoni*

Although the mechanisms DCs employ for the induction of Th2 immune responses remain elusive, extensive progress has been made in understanding the fundamental components orchestrating the interaction between DCs and $CD4^+$ T cells during Th2 initiation. Studies using BMDCs have shown that although upregulation of activation markers is subtle, co-stimulatory molecules OX40-L (Jenkins et al., 2007) and MHC-II (MacDonald et al., 2001) on the cell surface of BMDCs are necessary for the optimal induction of Th2 immune responses against *S. mansoni* antigen. CD40:CD154 interaction is also essential for DC mediated Th2 induction *in vivo*, as CD40 deficient mice develop impaired Th2 responses during *S. mansoni* infection (MacDonald et al., 2002a; 2002b). In addition, splenic DCs from $CD154^{-/-}$ *S. mansoni* infected animals are not activated even at a low level (Straw et al., 2003). These findings highlight that even though the activation level of DCs in Th2 settings is low in comparison with bacterial stimuli, this activation phenotype is indeed an important feature during Th2 induction. In addition to DC surface markers, DC cell intrinsic expression of NFkB is also a crucial component for this process, as NFκB deficient BMDCs show a reduced ability to induce Th2 responses in culture with $CD4^+$ T cells (Artis et al., 2005).

Investigation into the contribution of tissue factors produced in response to Th2 inducing antigens has provided further insight into DC activation in a Th2 setting. Infection with parasites including *Heligmosomoides polygyrus, N. brasiliensis* and *S. mansoni,* or exposure to allergens, triggers the release of multiple tissue factors including thymic stromal-derived lymphopoietin (TSLP), IL-25 and IL-33, which have been shown to promote Th2 responses and worm expulsion (Kool et al., 2012). TSLP is thought to induce the expression of OX40-L by DCs during allergic responses (Ito et al., 2005), and activate human DCs to produce cytokines such as CCL17 and CCL22 (Fontenot et al., 2009; Ito et al., 2005). The expression of these chemokines recruits Th2 cells in particular, as their receptor (CCR4) is thought to be expressed preferentially by Th2 cells

(Bonecchi et al., 1998; D'Ambrosio et al., 1998; Sallusto et al., 1998). This provides a mechanism by which DCs may recruit Th2 cells to the tissue site during helminth infection or allergic responses. However, the role for TSLP in this process is not critical, as TSLP deficient animals induce intact Th2 responses during *S. mansoni* infection (Massacand et al., 2009). Taken together, numerous studies highlight the importance of core DC functions for $CD4^+$ T cell priming towards a dominant Th2 immune response during *S. mansoni* infection.

To date, the best evidence for the requirement of DCs during the induction of Th2 responses has recently been provided through use of cell specific DC depletion models, such as CD11c.DOG mice. In 2010 our laboratory reported that $CD11c^+$ DC depletion in CD11c.DOG mice impairs the induction of Th2 immune responses either after injection of *S. mansoni* eggs or during active *S. mansoni* infection at D42 (Phythian-Adams et al., 2010). This identified DCs as the major cell type that is required for the induction of Th2 responses against *S. mansoni* infection. Although a cohort of *S. mansoni* stimulated innate immune cells including ILC2s, basophils and MΦs is likely required for optimal Th2 induction, the requirement for DCs to induce Th2 immune responses during *S. mansoni* infection makes them key to identifying the exact mechanisms that govern this process. Indeed, the requirement for DCs in the induction of Th2 responses has also been established in non-schistosome Th2 settings such as allergic asthma (Kool et al., 2008; van Rijt et al., 2005).

Given that DCs are necessary for the induction of Th2 responses in various settings, the involvement of specific DC subsets during the induction of Th2 responses is currently an area of active research. Recently, IRF4 dependent $CD11b^+$ cDCs have been shown to represent the main subset for the induction of Th2 responses in the lung to house dust mite allergen (HDM) (Plantinga et al., 2013). Plantinga *et al.,* (2013) used *Flt3l*-deficient mice, which lack $CD103^+$ cDCs and $CD11b^+$ cDCs but not monocyte derived $CD11b^+$ cDCs, and exposed these animals to HDM. They showed that *Flt3l*-deficient animals display significantly less eosinophil and lymphocytic infiltration in the lung compared

with WT mice, indicating impaired Th2 induction in response to HDM allergen. To exclude the requirement of $CD103^+$ cDCs for Th2 induction in this model, langerin-DTR mice were used (Plantinga et al., 2013), which lack $CD103^+$ cDCs in the lung (Kissenpfennig et al., 2005). Thus, $CD11b^+$, but not $CD103^+$ cDCs, appear to be the main DC subset required for the induction of allergic airway Th2 responses in the lung (Plantinga et al., 2013).

Additional evidence implicating IRF4 dependent DCs in the induction of Th2 responses has been obtained by using another model for the specific depletion of $CD11b^+$ cDCs; mice with CD11c restricted deficiency in the *Irf4* gene (CD11c-cre^{pos} $IRF4^{flox}$) lack $CD11b^+$ cDCs in the spleen, skin and gut LNs (Vander Lugt et al., 2014). However, Gao *et al.,* (2013) used CD11c-cre^{pos} $IRF4^{flox}$ mice and showed that IRF4 controls the function and differentiation of a distinct DC subset in the skin expressing CD301b and PDL2. The authors reported that depletion of dermal $CD301b^+$ $PDL2^+$ DCs results in impaired induction of Th2 responses *in vivo* during allergic inflammation and infection with the helminth *N. brasiliensis* (Gao et al., 2013). This finding is in line with another study that used an alternative model (Mgl2DTR mice) to deplete dermal $CD301b^+$ DCs, which shows that these DCs are required for antigen presentation to $CD4^+$ T cells *in vitro* and the development of Th2 responses during *N. brasiliensis* infection (Kumamoto et al., 2013). Thus, the type of DCs that are depleted using IRF4 deficient mice remains controversial, and this may be due to differential developmental requirements for IRF4 of DCs within different tissues, which further underlines the vast heterogeneity within the $CD11b^+$ cDC group (Mildner and Jung, 2014). Nevertheless, the transcription factor IRF4 appears to be a key mediator of Th2 differentiation induced by DCs, as IFR4 deficient GM-CSF differentiated BM derived DCs (BMDCs) show an impaired ability to induce Th2 responses *in vitro* and *in vivo* (Gao et al., 2013; Williams et al., 2013). It has been proposed that IRF4 is required for effective antigen presentation by $CD11b^+$ cDCs to $CD4^+$ T cells (Vander Lugt et al., 2014) or the production of cytokines by DCs that are associated with Th2 responses (i.e. IL-10 and IL-33) (Gao et al., 2013). Yet, it is likely that multiple mechanisms are important for

effective initiation of Th2 responses, and further research is necessary to delineate the mechanisms that are mediated by IFR4 (Tjota and Sperling, 2014). Taken together, emerging evidence implicating IRF4 dependent DCs during the induction of Th2 responses in various disease settings suggests that this DC subset may also be the critical DC for this process during *S. mansoni* infection.

1.10 Thesis aims

The work detailed in this thesis broadly aims to better understand the role of distinct DC subsets during the induction of Th2 immune responses and the formation of Th2-mediated pathology.

The first aim of this thesis was to determine whether DCs are critical for the formation and development of granulomatous inflammation during parasitic *S. mansoni* infection.

The second aim was to assess whether deficiency in a distinct DC subset, $CD8\alpha^+$ cDCs, alters the initiation of Th2 immune responses and subsequent pathology during later stages of *S. mansoni* infection.

The final aim of this thesis was to examine whether *S. mansoni* infection alters core functions exhibited by different DC subsets.

1.10 Figures and tables

Table 1.1

Phentypic marker	pDCs	CD8α⁺ cDCs		CD11b⁺ cDCs		CD103⁺ CD11b⁺ intestinal cDCs
		Lymphoid	Peripheral	Lymphoid	Peripheral	Peripheral
B220	+	–	–	–	–	–
CD103	–	+/–	++	–	–	++
CD11b	–	–	–	+	+	+
CD11c	+	+++	++	+++	++	++
CD172 (Sirpα)	+	–	–	++	++	–
CD205 (DEC205)	–	++	++	+	ND	ND
CD24	ND	++	++	+	+/–	++
CD4	+	–	–	+/–	–	–
CD64	–	–	–	–	++	–
CD8α	subset	+	+/–	–	–	–
Clec9a	+	++	++	–	–	–
CX3CR1	–	subset	–	–	++	–
Ly6C	++	–	–	–	+/–	–
MHC-II	+	++	++	++	++	++
PDCA-1	+	-	-	-	-	-
XCR1	–	+	+	–	–	–

This table showing the surface marker expression by mouse lymphoid or peripheral DC subsets is adapted from Merad *et al.,* (2013) and Mildner *et al.,* (2014) (+ = expressed by DC, − = not expressed, subset = expressed by some DCs belonging to a distinct group, ND = not determined).

Table 1.2

Mouse model	Cell types depleted	Ref
Constitutive Deficiency		
Batf3$^{-/-}$	CD8α^{+} and migratory CD103^{+} cDCs	Hilder *et al.,* 2008
CD11c.DTA	cDCs, pDCs, LCs, and possibly certain macrophages, plasmablasts, activated T cells, NK cells, and Ly-6Clow monocytes	Ohnmacht *et al.,* 2009
Irf4$^{-/-}$	pDCs, CD11b^{+} cDCs, plasma cells	Suzuki *et al.,* 2004
Irf8$^{-/-}$	CD8α^{+} and migratory CD103^{+} cDCs, pDCs, Langerhans cells	Schiavoni *et al.,* 2002
Inducible depletion		
CD11c.DTR	cDCs and to a lesser extent pDCs, but also certain macrophages, plasmablasts, activated T cells, NK cells, and Ly-6Clow monocytes	Jung *et al.,* 2002
CD11c.DOG	cDCs, pDCs, but also certain macrophages, plasmablasts, activated T cells, NK cells, and Ly-6Clow monocytes	Hochweller *et al.,* 2008
zDC.DTR	cDCs and probably certain activated monocytes	Meredith *et al.,* 2012
BDCA.DTR / SiglecH.DTR	pDCs	Swiecki *et al.,* 2010, Takagi *et al.,* 2011
Clec9a.DTR	CD8α^{+} DCs and, likely, nonlymphoid tissue CD103^{+} CD11b^{-} DCs. Partial depletion of pDCs.	Piva *et al.,* 2012
CD205.DTR	CD8α^{+} DCs, dermal DCs,and LCs	Fukaya *et al.,* 2012

This table is adapted from Merad *et al.,* (2013) and Van Blijswijk *et al.,* (2013).

Diagram 1.1

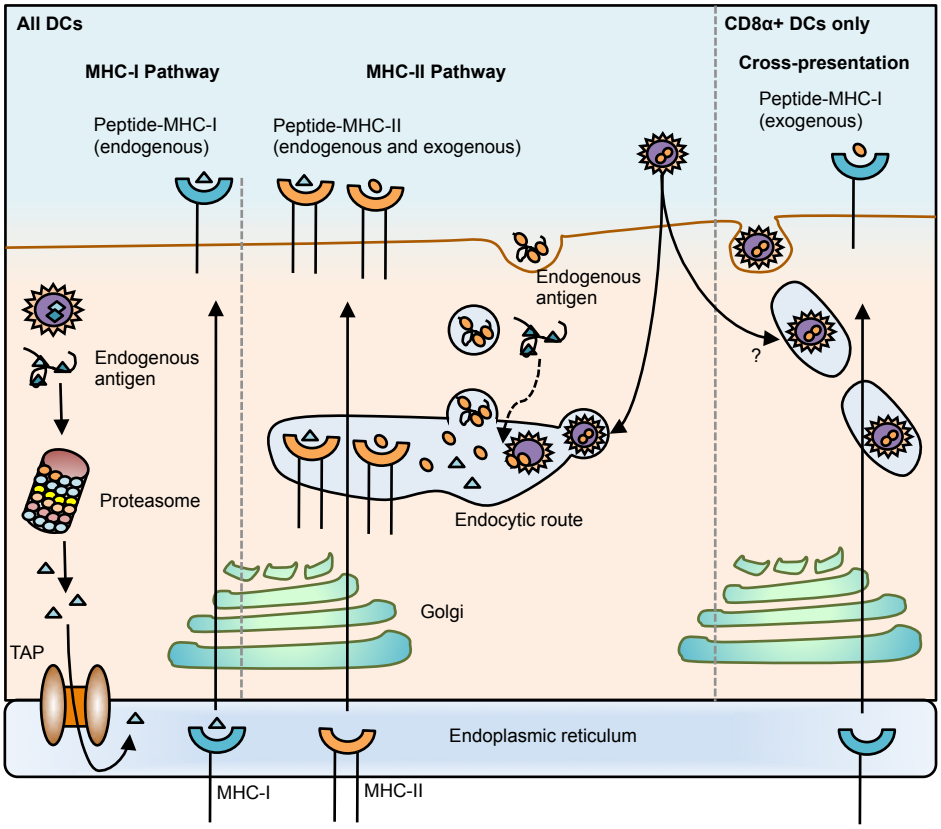

Diagram 1.1 Cross-presentation of antigen by DCs

All DCs are capable of presenting antigen via MHC-I and MHC-II presentation pathways. Antigen derived from proteins degraded in the cytosol comprise almost exclusively endogenous peptides synthesised by the cell and are presented mainly by MHC-I molecules. Exogenous antigen is taken up and degraded in endosomes, and is typically presented on MHC-II molecules. Notably, endogenous components including plasma membrane proteins, components of the endocytic pathway and cytosolic proteins can access endosomes by autophagy, and are also presented on MHC-II molecules. $CD8\alpha^{+}$ cDCs uniquely deliver exogenous antigens to the MHC class I pathway, which is termed cross-presentation. The mechanisms involved in this pathway are still poorly understood. TAP = transporter associated with antigen processing. This figure is adapted from Villadangos and Schnorrer *et al.,* (2007).

Diagram 1.2

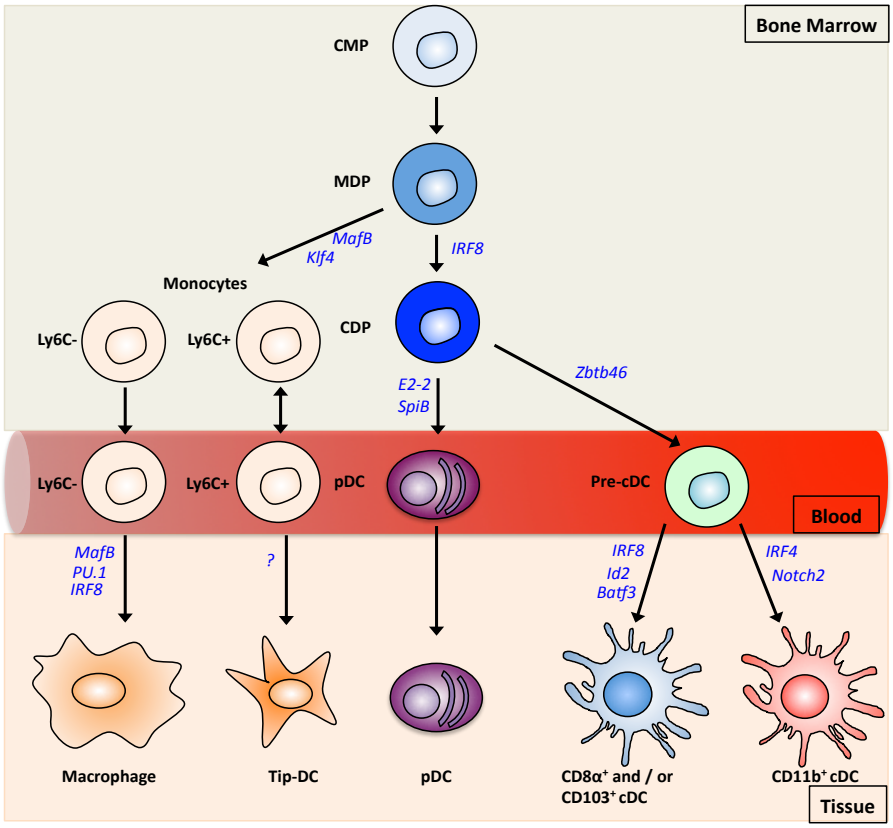

Diagram 1.2 The development of myeloid populations from the bone marrow

This figure summarises developmental stages of myeloid populations and the transcription factors (blue) involved. The first developmental events occur in the BM, where granulocyte-MΦ progenitors (GMP) give rise to macrophage-DC progenitors (MDP). MDPs differentiate into common myeloid progenitors (CMP) and monocytes. CDPs can give rise to pDCs or pre-cDCs. pDCs fully differentiate in the BM and circulate in the blood, whereas pre-cDCs migrate via the blood to differentiate into cDC subsets in the periphery. MΦs can be derived from monocytes that have migrated from the blood to peripheral tissues. During inflammation, monocytes can also give rise to a DC-like population, which are referred to as Tip-DCs. This figure is adapted from Satpathy *et al.,* (2012), Merad *et al.,* (2013) and Mildner *et al.,* (2014).

Diagram 1.3

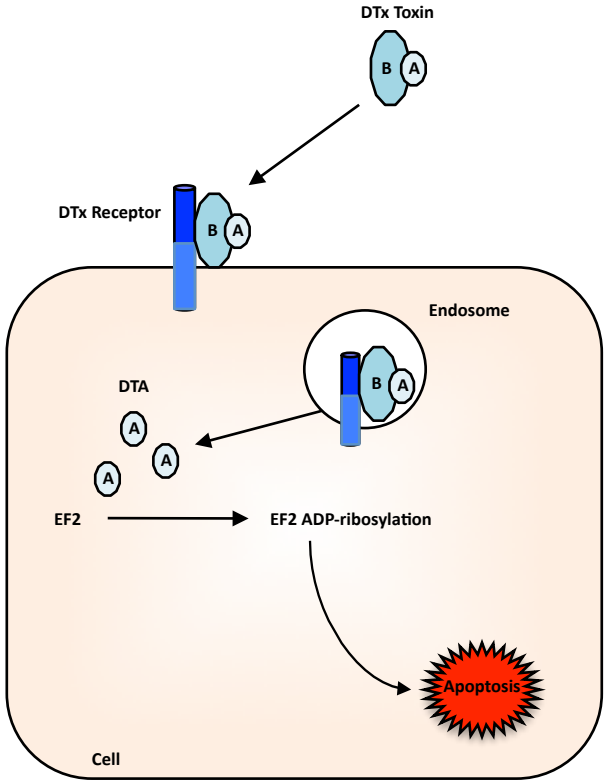

Diagram 1.3 DTx mediated CD11c depletion in CD11c.DOG mice
This figure illustrates the receptor mediated Diphtheria Toxin (DTx) endocytosis in cells expressing high affinity DTx receptor (DTR). The DTR binds the B subunit of the DTx, which initiates the uptake of the DTR-DTx complex. Endocytic release of the DT A subunit inhibits protein synthesis in the cell by catalysing an inactivating ADP-ribosylation of elongation factor 2, which leads to apoptosis. This figure is adapted from Bar-On *et al.,* (2010).

Diagram 1.4

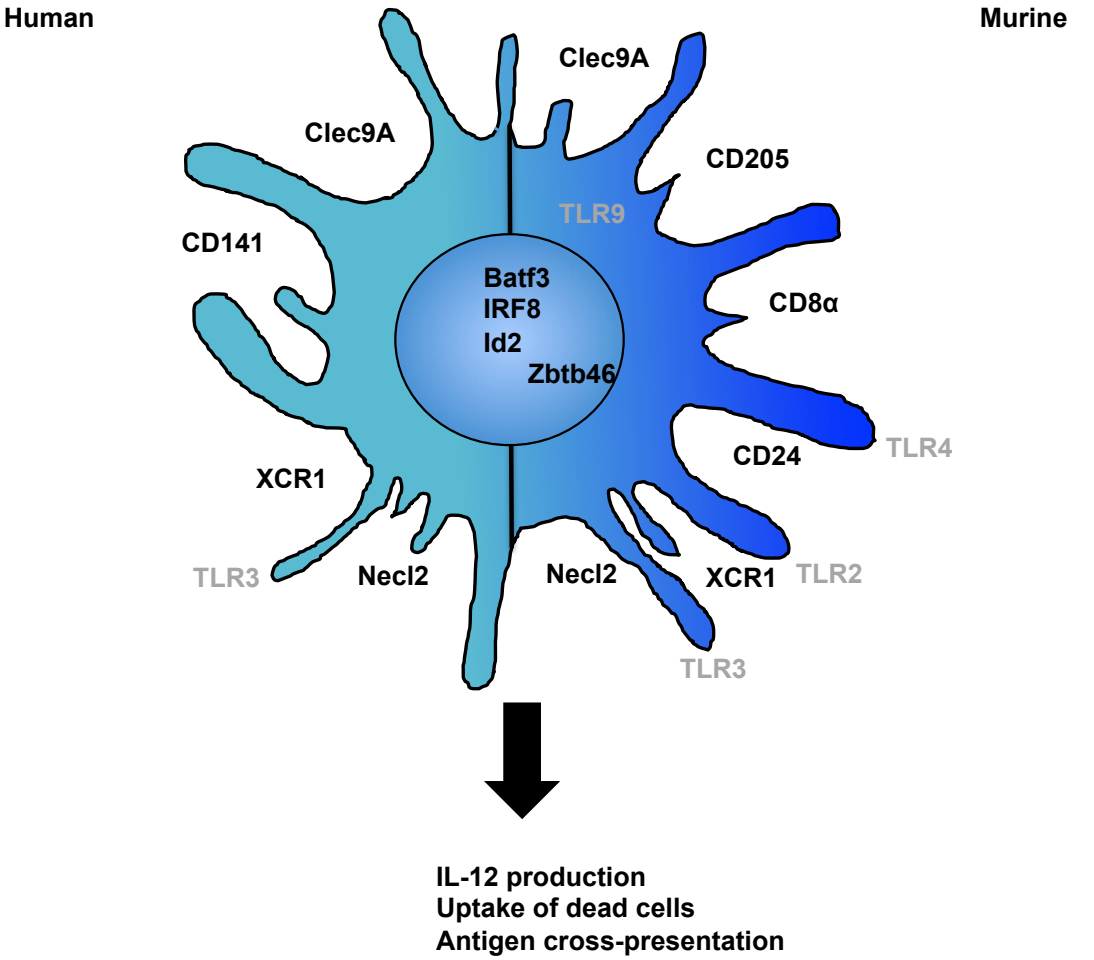

Diagram 1.4 *Batf3* dependent dendritic cells in human and mouse

This figure compares surface markers, transcription factor expression and main functions of *Batf3* dependent DCs in the human and mouse. Notably, the human counterpart does not express CD8α and is commonly referred to as $CD141^+$ DCs. *Batf3*, Id2 and IRF8 have been shown to be expressed in both human and murine $CD141^+/CD8\alpha^+$ cDCs (Villadangos and Shortman, 2010), whereas Zbtb46 has only been identified in the murine counterpart (Satpathy et al., 2012b). This figure was adapted from Collin *et al.* (2011).

Diagram 1.5

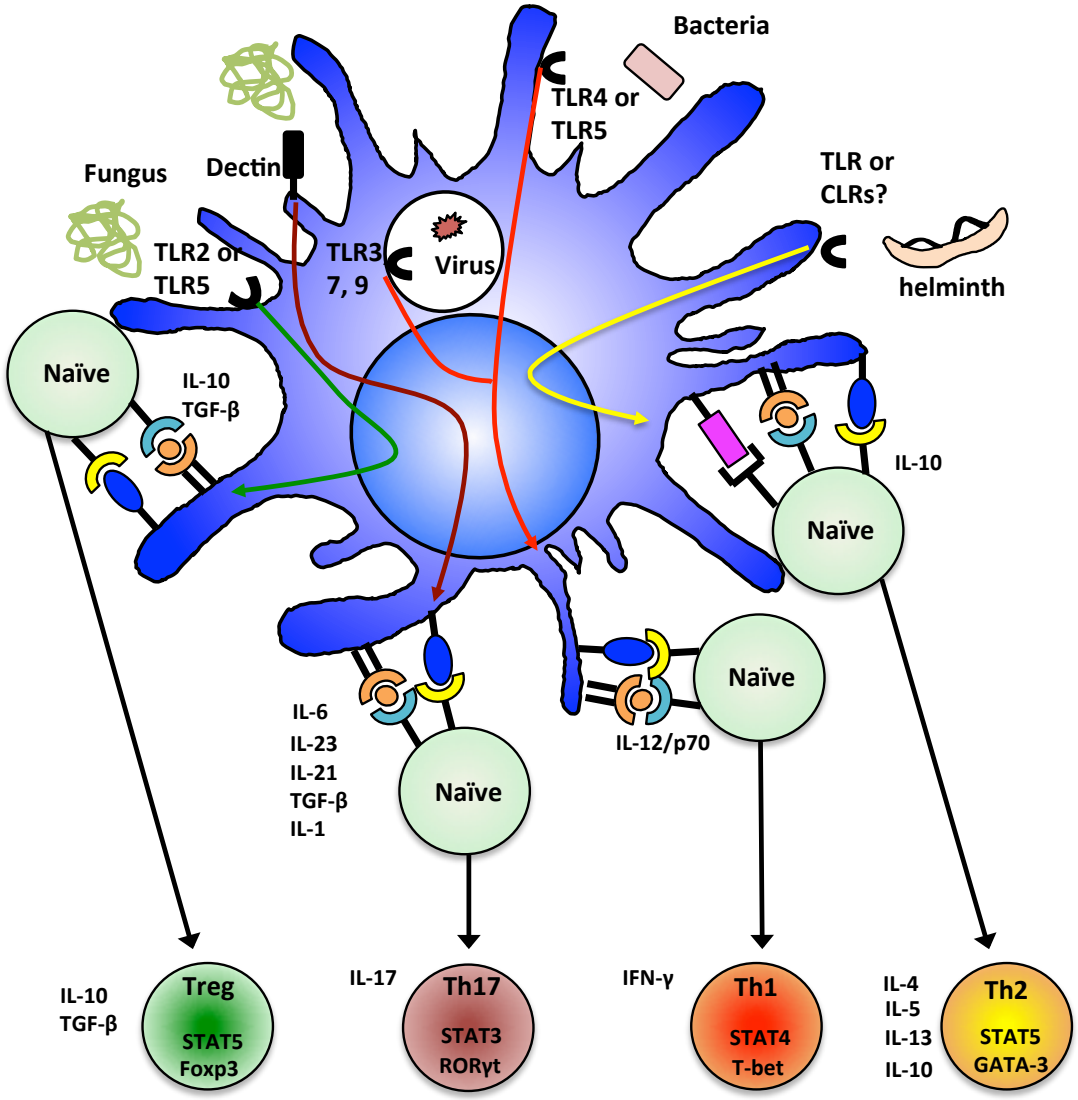

Diagram 1.5 T helper cell polarisation by dendritic cells
DCs are activated through stimulation by PAMPS (or in some cases DAMPS) via PRRs, and subsequently take up and process antigen for presentation on MHC molecules (signal 1). Upon activation DCs upregulate the expression of co-stimulatory molecules required for efficient interaction with $CD4^+$ T cells (signal 2). The type of pathogen the DC encounters determines the type of signalling pathway that leads to the production of a polarising factor often in the form of a cytokine (signal 3). This figure is adapted from Pulendran *et al.,* (2010).

Diagram 1.6

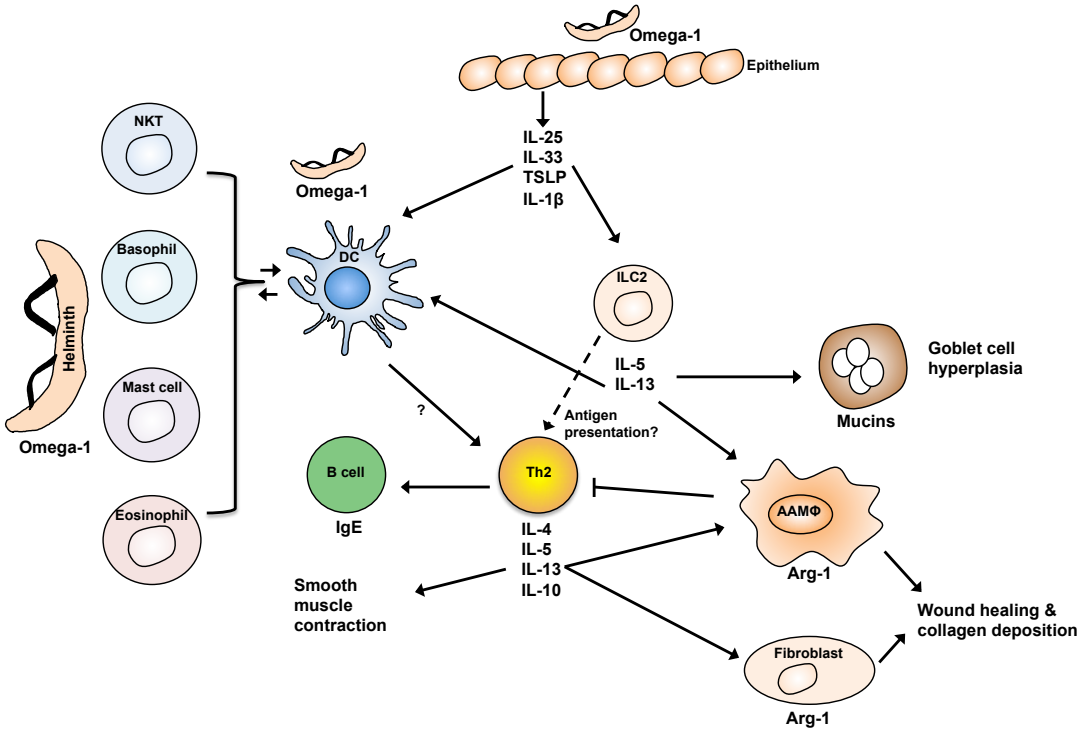

Diagram 1.6 The induction and promotion of type 2 responses during helminth infection

Type 2 responses are initiated by helminths that damage the epithelium, which induces the secretion of IL-25, IL-33, TSLP and IL-1β. Those cytokines derived from epithelial cells activate ILC2 cells that subsequently secrete type 2 cytokines. The secretion of type 2 cytokines by ILC2 cells induces mucus secretion by goblet cells and contributes to alternative activation of MΦs (IL-13). Secretion of IL-5 by ILC2 cells results in the recruitment and activation of mast cells and eosinophils. In addition, certain antigens such as omega-1 from the helminth *S. mansoni* and cytokines released by other innate immune cells likely prime DCs to induce Th2 responses in lymphoid tissue, which further amplifies the secretion of type 2 cytokines in the microenvironment. The production of IL-4 by Th2 cells leads to the antibody class-switching to IgE by B cells in lymphoid organs, and IL-13 production induces wound healing and collagen deposition orchestrated by AAMΦs and fibroblasts. This diagram is adapted from Allen *et al.,* (2011), Pulendran *et al.,* (2010) and Licona-Limon *et al.,* (2013).

Diagram 1.7

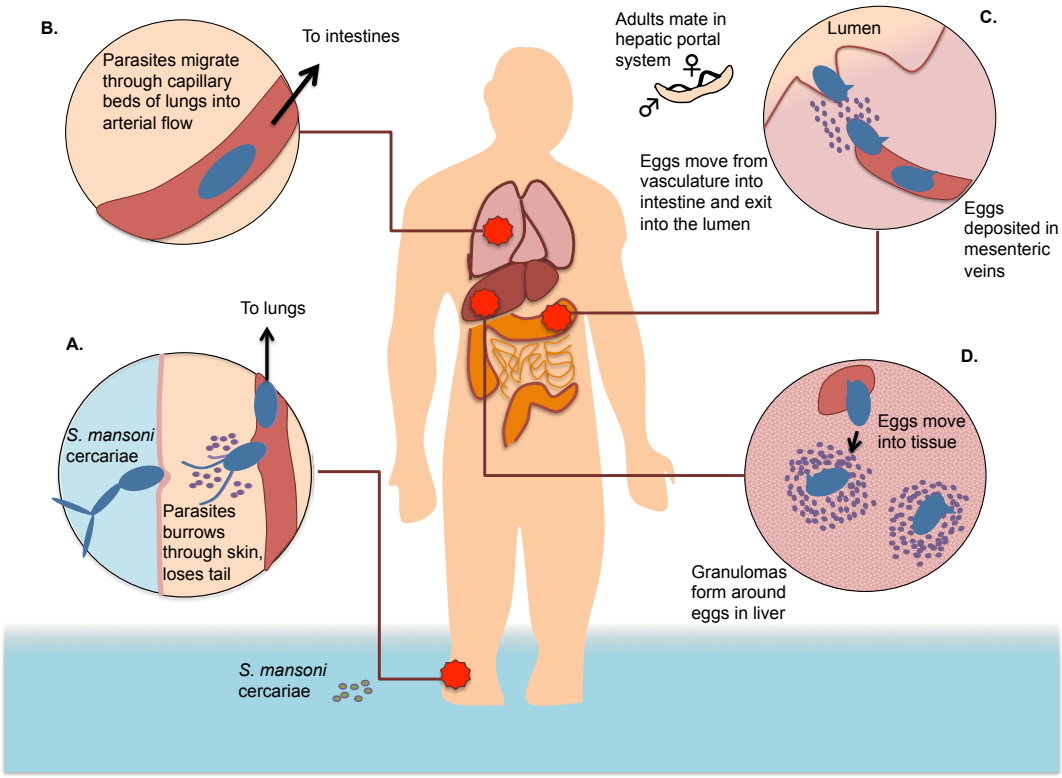

Diagram 1.7 The life cycle of *Schistosoma mansoni*

The *S. mansoni* life cycle is complex and involves the infection of multiple hosts. **A.** The intermediate host, an infected *biomphalaria glabrata* fresh water snail, releases infectious highly motile cercariae into the water that are attracted to lipids found on human skin (the definitive host). The cercariae often enter the epidermis through hair follicles, where they shed their tails and become schistosomulae. In the skin, schistosomulae secrete proteases and degrade basement membranes to aid transit from the skin into the blood. **B.** Once in the vasculature, immature schistosomulae begin to mature and are swept though the blood circulation into the heart and become lodged in the lungs, where they must cross capillary beds to enter the arterial blood flow. **C.** Mature adult schistosomes settle in mesenteric veins, where female and male worms pair and begin laying eggs. The eggs normally transverse from the vasculature through intestinal tissue, where granulomatous inflammation occurs, and are excreted through in the faeces of the infected host. **D.** Some eggs are swept by the blood flow into the liver, where they are trapped in small sinusoidal vessels. This initiates the formation of hepatic granulomas around the egg. Notably, parasite migration through the body causes significant tissue damage and haemorrhaging in the mammalian host at almost every stage. This figure was adapted from Allen and Wynn, 2011 (Allen and Wynn, 2011).

2 Materials and Methods

2.1 Use of animals

Experiments were performed using 8–12 week old mice. C57BL/6 *Batf3*$^{-/-}$ mice were kindly provided by Ken Murphy (Washington University), and OT-IIxLy5.1 mice by David Gray (The University of Edinburgh). All mice were kept under specific pathogen–free (SPF) conditions at the University of Edinburgh Animal Facilities. The fewest number of animals possible were used in all experiments, whilst achieving statistical significance. All experiments were approved under a Project Licence granted by the Home Office (U.K.) and conducted in accordance with local guidelines.

2.2 Maintenance of the *S. mansoni* life cycle

S. mansoni infected fresh water *Biomphalaria glabrata* snails were obtained from Dr. Fred Lewis (Biomedical Research Institute, Rockville, MD). At delivery, snails were pre-patent (2 weeks post-infection) and maintained in aerated tanks containing carbon filtered water. This water was chlorine free and pre-warmed, and the tanks were cleaned periodically. Little gem or romaine lettuce, rinsed in carbon filtered water, was given to the snails 3 times per week. The room was maintained at 26-27°C.

Infected snails become patent between 4 and 5 weeks after infection. To prevent infection when handling the snails, two layers of nitrile gloves, a face-mask and lab coat were worn. In preparation for infection approximately 30-40 snails were transferred from the tank to a beaker containing a small amount of carbon filtered water. The beaker containing the infectious snails was placed under a heat lamp for 50 min to encourage cercarial 'shedding'. The carbon filtered water containing the cercariae was then poured into a 50 ml Falcon tube and the snails were returned to their tanks. Once shed, the cercariae swim to the top of the tube, and so the cercarial

water was gently stirred with a figure of eight motion using a 1 ml/gilson (blue tip, with the end removed with scissors to reduce shear forces) to collect a 200 µl aliquot for counting to calculate accurate concentrations. 200 µl of Lugol's iodine solution was added to the aliquot, which killed the cercariae and stained them for counting with a dissection microscope. The average of three counts was taken to determine the concentration of cercariae. Carbon filtered water was then added to dilute the cercariae to the appropriate concentration for infection. For transfer to the animal facility, the tube containing the cercariae was sealed securely and carried in secondary containment to reduce risk of exposure.

2.3 *S. mansoni* infection procedure

The infection procedure was the same for experimental and egg harvest infections. Egg harvest infections were conducted to isolate *S. mansoni* eggs from the liver, which could be used in egg injection experiments (section 2.3.3). To avoid possible complications associated with lower susceptibility to infection with older male mice (Nakazawa et al., 1997), female animals were used exclusively for infection. Female mice were anaesthetised with a mix of medatomidine (domitor) and ketamine (vetalar) diluted in sterile PBS (e.g. 0.25 ml domitor and 0.19 ml vetalar diluted in 2.6 ml PBS; injected i.p. 0.01 ml/g per female mouse). The abdomen of the anaesthetised animals was shaved. The mice were then placed onto a heat-mat with a 1 cm diameter steel ring securely taped over the shaved region. 200 µl of the previously prepared cercarial water was transferred into the ring with a Gilson pipette, and a further 200 µl of pond water was added to cover the entire exposed skin with water. This water was carefully removed after 30 min and added to a tube containing ethanol to kill any remaining cercariae. The animals were then revived with atipamezole (antisedan) diluted in PBS (0.04 ml of antisedan and 0.96 ml of PBS; injected s.c. 0.1 ml per female mouse). While the animals were coming round, they were placed into a heat chamber and observed.

2.3.1 Immunisation with Diphtheria toxin for CD11c$^+$ cell depletion

Mice were injected i.p. daily for a period of 9 to 12 days with 8 ng/g diphtheria toxin (DTx) (Sigma D0564) in PBS, or with PBS alone (Phythian-Adams et al., 2010). The dose was based on previous optimisation in the MacDonald lab. Solid DTx, which is highly toxic to humans, was dissolved by injecting sterile tissue culture grade ddH_20 through the lid of the vial. Once dissolved to a final concentration of 0.5 mg/ml, 10 µl aliquots were stored at -80°C.

2.3.2 Preparation of serum

For analysis of antibody isotypes present in the blood, blood samples were collected 1 day before the harvest date of infection experiments. A maximum of 270 µl blood was collected per 25g mouse into eppendorf tubes, and the samples were stored at 4°C for 10 min to allow the blood to clot. Then the samples were centrifuged for 10 min at 8°C, which collects the coagulated blood in the pellet of the tube below a layer of serum. The serum was carefully transferred into fresh eppendorf tubes. Serum aliquots were stored at -80°C.

2.3.3 Isolation of eggs

Livers of mice infected with ~180 cercariae were harvested on D49 (2-3 weeks following the onset of egg production) of infection, and transferred into tubes containing PBS and penicillin/streptomycin (pen/strep) (Gibco - Invitrogen). Eggs were purified exclusively from livers to limit the amount of endotoxin contamination that may occur from using intestinal tissues from mice, as the high bacterial load of the intestines likely presents a greater risk for endotoxin contamination than does the liver. The livers were then rinsed with 70% ethanol and washed three times with sterile PBS before being minced under aseptic conditions using sterile razor blades in Petri dishes. Minced livers were digested overnight (o/n) at 37°C with filter-sterilised 1.47 U/ml solution of collagenase D in the presence of Polymyxin B sulfate (Sigma Aldrich) and pen/strep to ensure the breakdown of collagen whilst limiting bacterial contamination. Following o/n digestion, the liver fragments were washed with PBS and resuspended in PBS before being layered onto a 33% percoll gradient to separate the eggs from hepatocytes. After centrifugation at 420 xg the upper layers were

removed gently to leave the eggs in a pellet at the bottom of the tube. The eggs were collected and washed with PBS. Freshly isolated eggs were then counted and stored at -80°C.

2.3.4 Production of SEA

Endotoxin-free soluble egg antigen (SEA) was prepared in-house as previously described (MacDonald et al., 2001). After thawing, *S. mansoni* eggs were transferred to a Tenbroeck 7 ml tissue grinder to which sterile PBS was added. The eggs were then carefully homogenised using a twisting and grinding motion. After ~20 rotations the eggs were checked for disruption. This was repeated ~15 times on ice until 95% of the eggs were disrupted. The resulting homogenate was then transferred to a 15 ml tube and centrifuged at 2800 xg for 15 min at 4°C. The supernatants were transferred to 1 ml micro-centrifuge tubes and spun at 16,000 xg for 10 min. The pooled supernatants were filter sterilised through a 0.45 μm filter. The isolated SEA protein concentration was determined using a Bradford (coomassie) protein assay and a known BSA standard. The SEA was aliquoted before storage at -80°C.

2.4 Parasitology of *S. mansoni* infected mice

2.4.1 Tissue for egg counts

A caudate liver lobe and gut tissue (the small intestine) were harvested and stored at -80°C to preserve the tissue for egg counting. After thawing, each sample was removed from the tube and weighed. 15 ml/g of liver tissue or 7.5 ml/g of gut tissue of 4% KOH dissolved in ddH_20 was added to each sample and digested o/n at 37°C. The next day, 100 μl of digested tissue was transferred to a gridded Petri dish and each sample was counted 3 times using a dissection microscope. The average egg count per sample, the weight of the tissue taken before digestion and the total tissue weight taken on the harvest date were used to calculate the total number of eggs per liver or intestine.

2.4.2 Collection of worms

Animals were perfused immediately after schedule 1 killing using sterile-filtered cell isotonic citrate saline solution (15 g/ml sodium citrate and 8.5 g/ml sodium chloride,

Sigma). The hepatic portal vein was careful severed, avoiding damage to the intestines, and approximately 25-30 ml saline solution slowly injected into the heart, using constant pressure and a 30 ml syringe, enabling the collection of worms perfused out of the mesenteric veins. The perfused blood and buffer containing the worms was collected into a Petri dish and then transferred to a 50 ml Falcon tube. Collected worms were stored in perfusion buffer for up to 48h at 4°C prior to counting.

Settled blood was resuspended by inverting the Falcon tubes and spun at 400 xg for 5 min. Excess perfusion buffer was removed and the pellet resuspended. 3 ml of 1x BD FACS fix/lysis solution was added per sample and incubated for 2-5 min. The worm/fix/lysis solution was poured through a 100 μm cell strainer and washed with PBS to collect the worms in the cell strainer. Collected worms were washed onto a gridded Petri dish with 10 ml PBS. All worms were counted using a dissection microscope, and numbers of identified female, male and immature worms were recorded.

2.5 Immunisation with *S. mansoni* eggs

For egg injections, mice were immunised s.c. in the top of each hind foot with 2,500 eggs in 50 μl PBS, or PBS alone for controls, as described previously (Phythian-Adams et al., 2010).

2.6 Preparation of tissue for histology

For histological analysis by light microscopy, the median liver lobe and approximately 1.5 cm of the ileum were harvested and gently transferred to 10% NBF for at least 24h for fixation. The fixed tissue was then transferred to 20% ethanol at room temperature (RT) for storage prior to processing. The tissues were sent to a Histology department (QMRI, Edinburgh), where they were processed, embedded in paraffin, cut into 5 μm thick sections and stained with either Masson's Trichrome (MT) to stain granulomatous inflammation including type III collagen deposition, or Picrosirius Red (PSR) to measure type I and III collagen more specifically. The median liver lobe was cut from the top in such a way that the

maximum surface area was available for analysis. Tissue from the ileum was mounted to give longitudinal cross sections. To enable the comparison of subsequent sections for each stain, two consecutive sections were mounted (one per slide). To maximise the number of unique granulomas in each section per stain on each slide, a minimum distance of 50 μM was cut away between sections after two consecutive sections were taken. The eggs are approximately 60 μM wide and 140 μM long (Ross et al., 2002). Every slide was blinded before subsequent analysis to avoid misinterpretation of the results.

For immunohistochemical analysis by confocal microscopy, a protocol was used that was previously optimised in the MacDonald laboratory. Approximately 0.5 cm tissue sections from the left liver lobe were cut and placed into optimum cutting temperature formulation (OCT) for storage at -80°C. 20 μm cryosections were cut using a cryostat set to -21°C and laid onto microscope slides (C.A.Hendley). Freshly cut tissue sections were placed into a box to avoid dust particle deposition on the slides, and left at RT to dry o/n. Dried tissue sections were then fixed in ice-cold acetone for 5 min before storage at -20°C.

For confocal staining, frozen cryosections were thawed and rehydrated with 1x PBS for 5 min at RT, with washes repeated 3 times. To avoid high background staining (i.e. through dust particles), sections were kept in a humidifying chamber throughout the rest of the staining procedure. Slides were then washed once in PBS-T (Tween20 diluted 1:1,000 in PBS). FcR-Block (2.4G2) was added to a 10% block solution (1% BSA, 10% FCS in PBS-T) at 0.005 μg/μl, and this blocking solution was added to the sections and incubated for 1h at RT to prevent non-specific staining. Blocked sections were then stained o/n at 4°C with fluorescently labelled monoclonal antibodies in 2% block solution (0.2% BSA, 2% FCS in PBS-T) (Table 2.1). Stained cryosections were washed once with PBS-T followed by 2 washes with PBS, and then stained with 1 μg/ml DAPI dissolved in PBS for 15 min at RT. Finally, cryosections were allowed to dry and were mounted in ProLong Gold antifade reagent (LifeTechnologies) with coverslips (thickness n1), which preserves the

signals of the fluorescently labelled target cells for long-term storage and suppresses photobleaching.

2.6.1 Quantification of histological analysis.

2.6.1.1 Quantification of granulomatous inflammation or fibrosis

To determine the proportion of granulomatous inflammation in liver sections objectively, a novel quantification method was developed. For median liver lobe sections stained with MT or PSR, a dotslide digital slide scanner (Olympus BX51, VS-ASW FL Software) was used to scan the sections creating bright field (BF) overview images of the whole slide (see Fig. 2.1). Staining with MT results in differential colouring of granulomas and inflammatory infiltrate (blue) compared with the liver parenchyma (purple), and this is an essential feature for effective quantification of granulomatous inflammation by this method. Specifically, MT is described as staining type III collagen, as well as nuclei of immune cells, blue (Amin and Mahmoud-Ghoneim, 2011; Calvi et al., 2012; Diaz Encarnacion et al., 2004; Whittaker et al., 1994). Using FIJI imaging analysis software (ImageJ 1.48r) individual liver sections were cropped to obtain an image consisting solely of the liver section with all background removed. The colour threshold was then set using hue, saturation and brightness (HSB) settings to select either granulomas alone (only blue staining) or the whole liver section. These HSB threshold settings were introduced into an algorithm developed by Dr. Tim Kendall (Western General Hospital, Edinburgh), which enabled the quantification of the number of pixels for the region of interest. Two algorithms were used for the analysis of each image: one containing HSB settings for the selection of granulomatous inflammation (blue pixels only), and the other containing HSB settings for the selection of the whole tissue (all pixels). The algorithm essentially enabled the automatic application of the HSB settings to each sample, and then produced a new black and white image for the quantification step. In each new black and white image the black pixels represent the region of interest (i.e. either granulomatous inflammation or whole tissue), and the number of black pixels was quantified by the algorithm. The number of black pixels calculated by the algorithm for each image was then used to determine the proportion of granulomatous inflammation per tissue section (i.e. proportion of granulomatous

inflammation = (n of pixels for granulomatous inflammation / n of pixels for whole tissue section) x 100.). Thus, this novel technique allows for efficient and objective quantification of the proportion of granulomatous inflammation in livers of *S. mansoni* infected mice.

For more precise measurement of fibrosis, liver sections were stained with PSR. The slides were scanned and images cropped as described above. PSR stains type I and type III collagen red, whereas the rest of the tissue is stained yellow (Calvi et al., 2012). Although MT stains type III collagen and is frequently used as a measure of fibrosis (Calvi et al., 2012), other components within the tissue, as mentioned above, are also stained by MT (Amin and Mahmoud-Ghoneim, 2011; Diaz Encarnacion et al., 2004; Whittaker et al., 1994). Thus, PSR was used for more specific analysis of collagen deposition, and the HSB threshold was set to select for red pixels. The proportion of collagen per liver section was then quantified using the algorithm as explained above.

All tissue samples in each experiment were stained on the same day to avoid different staining levels. Notably, variation in staining intensity was often evident between experiments that were processed and stained on separate days.

2.6.1.2 Granuloma and muscle scoring of intestinal tissue

Due to the complex structure of the ileum and the lack of ability to distinguish between granulomatous inflammation and the surrounding gut tissue when using MT staining, granulomatous legions in the intestine were instead quantified using a scoring system. Similar scoring systems are standard methods for the assessment of intestinal inflammation in other systems, such as colitis (Horino et al., 2008). Ileal sections stained with MT were analysed using a light microscope at x20 or x40 magnification (Leica DM2000 camera). Single egg granulomas were scored for their intensity and severity of inflammation using a scoring system ($0,^{+},^{++},^{+++}$) developed together with Dr. Mark Arends (Western General Hospital, Edinburgh) (See Fig. 2.2). Scoring was determined as a measure of numerous features: the approximate number of the immune cells around the egg, the type of immune cells present (eosinophils, MΦs, lymphocytes etc), the size of the granuloma, the density of

immune cells, and the level of damaged ileal tissue surrounding the granuloma (i.e. crypt architecture, goblet cell size and collagen deposition). A score of 0 represents no inflammation visible around the egg with no or mild damage to the surrounding tissue, whereas a score of $^{+++}$ indicates severe inflammation due to large granulomas densely packed with immune cells such as eosinophils, structural damage to adjacent ileal crypts, and increased goblet cell size and collagen deposition. The level of inflammation in the granulomatous legion likely correlates with the number of eggs trapped in the granuloma, thus only single egg granulomas were analysed to enable comparison across experiments.

Damage to the circular muscle in the ileum found in infected mice was scored for each sample in a similar way as above ($0,^{+},^{++},^{+++}$) based on scoring techniques developed previously for different kinds of pathology (Horino et al., 2008). This specific scoring system for muscle injury was developed together with Dr. Mark Arends (Western General Hospital). Higher scores indicate architectural damage to the muscle, a large number vacuole-like structures formed in the muscle, and increased collagen deposition between the muscle and the submucosa compared with muscle in naïve mice (see Fig. 2.3).

2.6.1.3 Confocal microscopy analysis

Cryosections stained with fluorescently labelled antibodies (section 2.6) were analysed using a Leica Confocal SP5 microscope. The offset (the minimal signal intensity detected by the sensor), gain (signal amplification at the camera sensor) and laser power (light intensity) were adjusted for each experiment using isotype and single stained controls, to obtain optimum detection of the fluorochromes. Cross-section photographs of granulomas were approximately 5 μm thick, and consisted of individual Z-stacked images each 0.25 μm thick (400Hz, 1024x1024, 8-16bit, x20 or x40 magnification). These were overlaid using extended focus for subsequent analysis. As in section 2.6.1.2, only single egg granulomas were photographed to enable comparison across experiments.

Analysis of confocal photographs was carried out using Volocity imaging software (PerkinElmer). For each photograph, the contrast was enhanced to remove

background staining, which was determined by analysing images of unstained and isotype control samples. The egg was then cropped out of the image to exclude possible autofluorescence during subsequent quantification steps. Snapshots of cropped images were captured separately for each fluorochrome used (i.e. a separate image was captured for CD11c, Siglec-F and TCR-β staining). For each snapshot, the surface area of positive staining around the egg was then measured by the software, which detects positive staining of the fluorochromes above a fixed intensity. The intensity was set using isotype controls for each fluorochrome labelled antibody used. Therefore, this technique enables the quantification of staining for specific immune cells in cross-sections of granulomas in the liver.

2.7 Preparation of samples for cell culture

2.7.1 Use of antibiotics

To prevent bacterial contamination during culture, pen/step was added to DC:T cell co-culture assays, cell isolations, egg isolations and wash media. Although this could have an inhibitory effect on cell growth in culture, antibiotics were necessary to prevent erroneous results obtained due to variation in bacterial contamination. This is particularly important when culturing DCs, as LPS contamination by gram-negative bacteria can have a dramatic impact on DC activation and function (Granucci et al., 1999).

2.7.2 Heat-inactivation of FCS

The foetal calf serum (FCS) used in BMDC medium and other media was inactivated through heat treatment at 58°C for 50 min. Heat inactivation was used to denature the components of the complement cascade in the serum that could damage the cells being cultured or prepared (Rahman et al., 2011).

2.8 Preparation of tissue for cell culture

Popliteal (pLN) and inguinal (iLN) LNs were harvested at D5, D7 or D9 after egg injection in immunisation experiments. Tissue samples of livers and mesenteric LNs (mLN) were obtained from both naïve and *S. mansoni* infected mice, which were

killed by CO_2 asphyxiation between D28 and D105 of infection, according to licence regulations.

2.8.1 Cell isolation methods for culture

In preparation for single cell suspensions, tissues were first enzymatically digested to obtain maximum numbers of rare cell types. Whole LNs were digested at 37°C for 30 min with 1.75 Wunsch Units/ml Liberase TL (Roche) and 80 Kunitz Units/ml DNase I type VI (Sigma-Aldrich) in HBSS (Sigma-Aldrich) containing 50 U/ml penicillin and 50 µg/ml streptomycin (Invitrogen) based on previous optimisation in the MacDonald laboratory. To stop the digestion, 10 µl 0.1M, pH 7.3, EDTA (Ambion) stop solution/ml was added, the tube was topped up with DMEM containing 50 U/ml penicillin and 50 µg/ml streptomycin, then contents filtered using a 70 µm cell strainer to obtain single-cell suspensions. Livers were digested using the same method, following perfusion and dicing of the tissue. A syringe plunger was used to pass the digested liver through a 100 µm cell strainer. The resulting suspension was then resuspended in 33% isotonic Percoll (GE Healthcare) and centrifuged at 700 xg in order to separate leukocytes from other liver cells. Isolated leukocytes were then resuspended and passed through a 40 µm cell strainer to remove *S. mansoni* eggs. The single cell suspension was treated with RBC lysis solution. Cell suspensions from all tissues were counted using trypan blue to distinguish live and dead cells, and resuspended for use.

2.8.2 Cell culture for cytokine analysis

LN cells or isolated liver leukocytes ($1x10^6$ – $2x10^6$ cells/ml) were cultured in X-vivo 15 medium (BioWhittaker) containing 2mM L-Glutamine and 50µM 2-ME (Invitrogen) in 96-well plates at 37°C in a humidified atmosphere of 5% CO_2 with or without 15 µg/ml SEA for antigen-specific restimulation. For polyclonal restimulation with αCD3 culture plates were incubated for 24h with 16.7µg/ml αCD3 at 4°C. Before culture, the αCD3 was removed and the wells were washed with PBS prior to transfer of the cells into the well.

In preparation for intracellular cytokine staining (ICC), LN cells or liver leukocytes were restimulated o/n in αCD3 coated plates for polyclonal restimulation as above,

with the addition of 2 μg/ml soluble αCD28. αCD3/CD28 was chosen for restimulation, as this is thought to be a physiologically relevant stimulation for T cells in culture, and is less cytotoxic in comparison with other components commonly used *in vitro* or *ex vivo* including PMA/Ionomycin (Olsen and Sollid, 2013). After o/n incubation, 2 μg/ml Monesin (Golgistop, BD) was added to all cultures for 6h to block the transport and thus secretion of cytokines prior to cell harvest and staining (Mascher et al., 1999; Mollenhauer et al., 1990).

2.8.3 Liver dendritic cell purification

DC: T cell co-culture experiments were conducted to examine the capacity of DC subsets to process and present antigen to T cells (Schnorrer et al., 2006; Wilson et al., 2003; Young et al., 2007). Liver DCs were enriched from 12-36 naïve C57BL/6 mice and 4-8 *S. mansoni* infected C56BL/6 mice using a Dynabeads® Mouse DC Enrichment kit (Invitrogen, 11429D) following the manufacturer's protocol. Pooled enriched DCs were counted and stored in complete media o/n at 4°C at a concentration of $2x10^6$ cells/ml. This step was necessary for practical reasons due to the length of the protocol, and an optimisation experiment was carried out to compare the functionality of enriched DCs before and after o/n resting. This experiment confirmed that DCs retain antigen presentation and processing abilities after o/n storage at 4°C. The following day, the enriched DCs were counted again, centrifuged at 300 xg for 5 min and resuspended at $10x10^6$ cells/ml in flow buffer (0.5% FCS/PBS). Enriched DCs were then stained with fluorescently labelled antibodies for 15 min at 4°C. After staining, DCs were washed with flow buffer and resuspended to $2.5x10^7$ cells/ml for fluorescence activated cell sorting (FACS). 5 μl 7-AAD (BD Pharmingen) was added to 1 ml of enriched DCs to determine the proportion of live cells within the cell preparation. To distinguish cDC and pDC subsets in the DC enriched population and to prevent contamination with MΦs (expressing F4/80) or NK cells (expressing NK1.1), cDCs were sorted as $CD11c^{high}$ $PDCA\text{-}1^-$ $F4/80^-$ $NK1.1^-$ cells and pDCs as $CD11c^{int}$ $PDCA\text{-}1^+$ $F4/80^-$ $NK1.1^-$ cells using a BD FACS Aria II cytometer (see table 2.1) (Rahman and Aloman, 2013). cDCs and pDCs were sorted into 15 ml tubes containing 1 ml pure FCS with 1% PenStrep, and sorted samples were kept at RT until culture.

For cDC subset purification, enriched DCs were stained additionally with CD8α and CD205 fluorescent antibodies. This allowed for sorting of $CD8\alpha^+$ $CD205^+$ $CD11c^{high}$ $PDCA^-$ 1^- $F4/80^-$ $NK1.1^-$ cDCs ($CD8\alpha^+$ cDCs) and $CD8\alpha^-$ $CD205^-$ $CD11c^{high}$ PDCA-1^- $F4/80^-$ $NK1.1^-$ cDCs ($CD8\alpha^-$ cDCs) (Hildner et al., 2008; Pillarisetty et al., 2004).

2.8.4 Purification of *ex-vivo* naïve $CD4^+$ T cells

To obtain pure $CD4^+$ T cell populations, the spleen and LNs were harvested from 1-2 female OT-IIxLy5.1 mice and a single cell suspension prepared by crushing through gauze to release the cells, with the resulting suspension then being centrifuged at 300 xg for 5 min. For the spleen, RBC lysis buffer (Sigma) was used to lyse RBCs, following which cells were washed and pooled with isolated LN cells. Naïve $CD4^+$ (OT-II) T cells were enriched using a Dynabeads® Untouched™ Mouse CD4 Cells Kit (Invitrogen, 11415D) following the manufacturer's protocol. Enriched naïve $CD4^+$ T cells were washed and resuspended in DMEM for CFSE labelling.

To ascertain the purity of $CD4^+$ T cells that express the TCR V alpha 2 chain specific for class II OVA peptide (pOVA) (Barnden et al., 1998), the proportion of naïve $CD4^+$ $V\alpha2^+$ T cells was assessed by flow cytometry using a FACS LSR II. In addition, the activation status of naïve $CD4^+$ $V\alpha2^+$ T cells was confirmed by analysing the expression of CD44 and CD69; naïve T cells only express very low levels of CD44 and CD69 compared with effector/ memory T cells (Sprent and Surh, 2011).

2.8.5 Purification of *in vitro* activated $CD4^+$ T cells

For *in vitro* activation of $CD4^+$ T cells, the spleen was harvested from an OT-IIxLy5.1 female mouse, and a single cell suspension obtained using the method described in section 2.8.4. Freshly isolated spleen cells were cultured in a flask in the presence of 1 mg/ml sterile-filtered endotoxin-free OVA protein (Sigma, A5503) for 7 days at 37°C in a humidified atmosphere of 5% CO_2. Endotoxin was removed from OVA protein in-house to avoid activation of DCs by LPS (Granucci et al., 1999); sterile-filtered 20 mg/ml OVA protein dissolved in ddH_20 was passed through a HiTrap Q Sepharose FF column using an AKTA Prime liquid chromatography

system. At day 3 of culture, 2 ng/ml IL-2, 10 ng/ml IL-7 and 10 ng/ml IL-15 were added to the culture flask containing spleen cells and OVA protein to promote effector/memory $CD4^+$ T cell differentiation (Caserta et al., 2010; Van Belle et al., 2012). At day 5, cultured spleen cells were split 1:1 and transferred to new culture flasks containing fresh media with cytokines as above. After 7 days of culture the cells were harvested, centrifuged at 300 xg for 5 min, and resuspended in DMEM for CFSE labelling.

The purity (CD4 and Vα2 expression) and activation status (CD44 and CD69 expression) of *in vitro* activated $CD4^+$ T cells after 7 days of culture with OVA was assessed by flow cytometry as described in section 2.8.4.

2.8.6 CFSE labelling of $CD4^+$ T cells

To measure the proliferation of $CD4^+$ T cells in culture, freshly isolated enriched naïve and *in vitro* activated $CD4^+$ T cells were labelled with 5 μM CFSE (Invitrogen) for 15 min at 37°C (Cook et al., 2012). Excess CFSE was allowed to leach from the cells for 45 min at 37°C. CFSE-labelled $CD4^+$ T cells were washed and counted before culture with DCs. To calculate final numbers of $CD4^+$ T cells the trypan blue cell count of $CD4^+$ T cells was multiplied by the % purity obtained from flow cytometry analysis.

2.8.7 DC : T cell co-culture

The protocol conducted to set up DC:T cell co-cultures is summarised in figure 2.4. For assays with class II pOVA, purified liver DCs from naïve or *S. mansoni* infected mice were pulsed with 10μM, 1μM or 0.01μM $OVA_{323-339}$ (08503-5mg, Cambridge Bioscience) in 15 ml Falcon tubes for 45 min at 37°C following a protocol previously optimised in the MacDonald laboratory (Cook et al., 2012). Before co-culture with $CD4^+$ T cells, pOVA pulsed DCs were washed to remove free peptide. For assays with OVA protein, 500μg/ml, 50μg/ml or 0.5μg/ml endotoxin-free soluble OVA protein was added to sorted liver DCs from naïve or *S. mansoni* infected mice in 15 ml Falcon tubes. The dose of OVA protein for the addition to the culture, as well as the length of the culture (3 vs. 4 days) was tested and optimised in the MacDonald laboratory. 5000 $OVA_{323-339}$ pulsed DCs or DCs in the presence of

soluble OVA protein were then cultured with 50,000 CFSE-labelled naïve or *in vitro* activated OT-II TCR transgenic $CD4^+$ T cells in 96-well plates (U-bottom) for 68-72h (Schnorrer et al., 2006; Wilson et al., 2003; Young et al., 2007). Cells were harvested to assess CFSE dilution by flow cytometry as a measure for cell proliferation, and supernatants were stored at -20°C for subsequent cytokine analysis by enzyme linked immune sorbent assay (ELISA).

2.9 Cell staining by flow cytometry

2.9.1 Cell surface staining

For cells isolated from liver and LNs and for purified naïve or *in vitro* activated $CD4^+$ T cells, cell staining was commenced directly after tissue preparation was completed to ascertain the viability of the cells. After incubation with FcR-Block (2.4G2 produced in-house) for 15 min at 4°C, cells were stained for 30 min at 4°C with cell surface markers for several different cell populations (see Table 2.1). Appropriate isotype controls were used to identify cell populations of interest. All antibodies for flow cytometry were purchased from BD, eBioscience, or BioLegend. Samples were acquired using a FACS LSR II or FACSCanto II flow cytometer using BD FACSDiva software and analysed with FlowJo v.9.5.2 software (Tree Star, Inc.).

For enriched hepatic DCs, staining was conducted after o/n resting at 4°C as described in section 2.8.3. Enriched DCs were stained for 15 min with antibodies in the presence of FcR-Block at 4°C. Stained DCs were then washed and resuspended in flow buffer for FACS sorting.

2.9.2 Intracellular cytokine staining

After restimulation (section 2.8.2) and surface staining, liver leukocytes or LN cells were fixed with 1% isotonic formaldehyde. BD Perm/Wash buffer (BD) was then used to permeabilise the cells, which were then stained with antibodies for intracellular cytokines in BD Perm/Wash buffer (Table 2.1).

2.10 ELISA

2.10.1 Cytokine analysis of culture supernatants

For cytokine analysis, protocols were used that were previously optimised in the MacDonald laboratory. Paired capture and detection antibodies (produced from hybridomas in-house or purchased from R&D Systems, BD, or eBioscience, Table 2.2) were used for analysis of murine IL-4, IL-5, IL-10, IL-13, IL-17, IFN-γ and TNF-α. Plates (NUNC Maxisorp) were washed with 0.05% Tween20 in PBS and blocked with 10% NCS/PBS. Recombinant cytokine standards (Peprotech or BD) were used to determine the quantity using a standard curve. Plates were developed by incubation with 50 µl 1:1,000 HR-peroxidase–labelled streptavidin (KPL), and the addition of 100 µl TMB substrate solution (Sigma-Aldrich). The reaction was stopped with 100 µl 0.18M H_2SO_4 and the absorbance was read at 450 nm using a Laboratory Systems Multiskan Ascent plate reader.

2.10.2 Analysis of serum antibodies

Serum was collected 1 day before the end of infection experiments (section 2.3.2) and the antibody isotypes present were measured using previously optimised protocols in the MacDonald laboratory. Total IgE was measured using paired capture and detection antibodies (BD Pharmingen) and murine IgEκ (BD Pharmingen) to assess quantity using a standard curve. Plates were blocked with 10% NCS/PBS, washed, developed and read as above. SEA-specific total Ig, IgG1, IgG2b, IgG2c, IgG3 and IgM antibody titres were determined using endpoint dilutions measured by ELISA. Plates were coated with 0.25 µg per well of SEA in 0.1M pH 9.6 Carbonate/Bicarbonate buffer, washed as above and blocked with 1% BSA/PBS. Serum samples were analysed using serial 2-fold dilutions. SEA-specific isotypes were detected using Alkaline Phosphatase (AP) conjugated anti-mouse total Ig, IgG1, IgG2b, IgG2c, IgG3 and IgM antibodies (SouthernBiotech). Absorbance at 405nm was determined as above after addition of 50µl PNPP substrate (SouthernBiotech). All antibodies for ELISA were purchased from BD Pharmingen, eBioscience, Biolegend or SouthernBiotech (Table 2.2).

2.11 Statistical analysis of results

Statistical analyses were performed using GraphPad Prism 5.0d software or JMP 11 (Statistal Discovery™, SAS). Student's t tests were used to determine if there were significant differences between two sample groups. One-way ANOVA was used for more than 2 sample groups and two-way ANOVA if there was more than one independent variable. Analysis of pooled data from experimental repeats conducted on different days was carried out using a mixed model analysis, labelling the day of the experiment as a random factor. Subsequently, a Tukey's honest significant difference (HSD) test was performed to determine significance between groups. *, $P < 0.05$; **, $P < 0.01$; ***, $P < 0.001$, ****, $P < 0.0001$.

Table 2.1 Flow cytometry and confocal microscopy antibodies

Antigen	Clone	Isotype	Host	Conjugate	Flow: Titration	Confocal: Titration	Manufacturer
B220	RA3-6B2	IgG2a, κ	Rat	BV605	1:200	-	BioLegend
CD103	2E7	IgG	Ar Ham	PerCP/Cy5.5	1:50	-	eBioscience
CD11b	M1/70	IgG2b, κ	Rat	BV711	1:300	-	BioLegend
CD11c	N418	IgG	Ar Ham	BV421	1:50	-	BioLegend
CD11c	N418	IgG	Ar Ham	AF647	-	1:250	eBioscience
CD19	1D3	IgG2a, κ	Rat	PE/CF594	1:400	-	BioLegend
CD205	NLDC-145	IgG2a, k	Rat	APC	1:200	-	BioLegend
CD24	M1/69	IgG2b, κ	Rat	PE/Cy7	1:800	-	BioLegend
CD25	7D4	IgM κ	Rat	PerCP/Cy5.5,	1:100	-	BioLegend
CD3	17A2	IgG2b	Rat	APC/eFluor780	1:100	-	eBioscience
CD4	RM4-5	IgG2a, κ	Rat	AF700	1:400	-	eBioscience
CD4	RM4-5	IgG2a, κ	Rat	BV650	1:200	-	BioLegend
CD40	3/23	IgG2a, κ	Rat	FITC	1:200	-	BioLegend
CD44	IM7	IgG2b, κ	Rat	BV570	1:100	-	BioLegend
CD49b	DX5	IgM, κ	Rat	APC/eFluor780	1:200	-	eBioscience
CD69	H1.2F3	IgG	Ar Ham	FITC	1:100	-	BioLegend
CD80	16-10A1	IgG2, κ	Ar Ham	PerCP/Cy5.5	1:200	-	BD Pharmingen
CD8α	53-6.7	IgG2a, κ	Rat	PE/CF594	1:300	-	BD Pharmingen
CD8α	53-6.7	IgG2a, κ	Rat	PE/Cy7	1:800	-	BioLegend
CD8α	53-6.7	IgG2a, κ	Rat	PerCP/Cy5.5	1:200	-	BioLegend
F4/80	BM8	IgG2a	Rat	PE/Cy7	1:200	-	BioLegend
F4/80	BM8	IgG2a	Rat	PE	1:150	-	BioLegend
FoxP3 (intranuclear)	FJK-16s	IgG2a, κ	Rat	eF450	1:200	-	eBioscience
IFN-γ (intracellular)	XMG1.1	IgG1, κ	Rat	eF450	1:200	-	eBioscience
IgM	RMM-1	IgG2a κ	Rat	APC/eFluor780	1:200	-	BioLegend
IL-10 (intracellular)	JES5-16E3	IgG2b	Rat	PE	1:200	-	eBioscience
IL-13 (intracellular)	eBio13A	IgG1, κ	Rat	AF488	1:200	-	eBioscience
IL-17 (intracellular)	TC11-18H10.1	IgG1	Rat	PE/Cy7	1:200	-	eBioscience
IL-4 (intracellular)	11B11	IgG1	Rat	APC,	1:200	-	eBioscience
Ly6C	AL-21	IgM, κ	Rat	BV570	1:100	-	BioLegend
Ly6G	1A8	IgG2a, κ	Rat	APC/eFluor780	1:200	-	BD Pharmingen
MHCII	M5114	IgG2b	Rat	AF700	1:800	-	eBioscience
MHCII	M5114	IgG2b	Rat	eF450	1:800	-	eBioscience
MHCII	M5114	IgG2b	Rat	PerCP/Cy5.5	1:800	-	eBioscience
NK1.1	PK136	IgG2a, κ	Ms	APC/780	1:100	-	eBioscience
PDCA1	JF05-1C2.4.1	IgG2b	Rat	PE	1:25	-	Miltenyi Biotec
SiglecF	E50-2440	IgG2a, κ	Rat	PE	-	1:100	eBioscience
TCR-β	H57-597	IgG2, λ	Ar Ham	APC/eFluor780	1:200	-	eBioscience
TCR-β	H57-597	IgG	Ar Ham	AF488	-	1:50	BioLegend
Terr119	TER-119	IgG2b, κ	Rat	AF700	1:100	-	eBioscience
Va2	B20.1	IgG2a, λ	Rat	PE	1:400	-	BD Pharmingen

Table 2.2 ELISA antibodies

Primary					
Antigen	**Clone**	**Host**	**Conjugate**	**Concentration**	**Manufacturer**
IL-4	11B11	Rat	Purified	2ug/ml	Homegrown
IL-5	TRFK5	Rat	Purified	2ug/ml	Homegrown
IL-10	JES16-E3	Rat	Purified	1ug/ml	eBioscience
IL-13	Ebio13A	Rat	Purified	2ug/ml	eBioscience
IL-17	TC11-18H0	Rat	Purified	0.5ug/ml	BD Pharmingen
IFN-y	R4-6A2	Rat	Purified	2ug/ml	eBioscience
TNF-a	Duoset DY410	Rat	Purified	0.8ug/ml	R&D
IgE	R35-72	Rat	Purified	1ug/ml	BD Pharmingen
Standard					
IL-4			Recombinant	20ng/ml	Peprotech
IL-5			Recombinant	20ng/ml	Peprotech
IL-10			Recombinant	20ng/ml	BD Pharmingen
IL-13			Recombinant	50ng/ml	Peprotech
IL-17			Recombinant	20ng/ml	eBioscience
IFN-y			Recombinant	50ng/ml	Peprotech
TNF-a			Recombinant	0.4ng/ml	R&D
IgE	C48-2		Purified	2ug/ml	BD Pharmingen
Detection antibody					
IL-4	BVD6-24G2	Rat	Biotin	0.25ug/ml	BD Pharmingen
IL-5	TRFK4	Rat	Biotin	0.3ug/ml	eBioscience
IL-10	SXC-1	Rat	Biotin	0.2ug/ml	BD Pharmingen
IL-13	Polyclonal sera	Rabbit	Biotin	0,1ug/ml	Peprotech
IL-17	TC11-8H4.1	Rat	Biotin	0.25ug/ml	BD Pharmingen
IFN-y	XMG1.2	Rat	Biotin	0.2ug/ml	BD Pharmingen
TNF-a	Duoset Dy410		Biotin	0.2ug/ml	R&D
IgE	R35-118	Rat	Biotin	0.5ug/ml	BD Pharmingen
				Dilution	
IgM	Alkaline Phosphatase Polyclonal Sera	Goat		1:2000	Southern Biotech
IgG1	Alkaline Phosphatase Polyclonal Sera	Goat		1:2000	Southern Biotech
IgG2b	Alkaline Phosphatase Polyclonal Sera	Goat		1:2500	Southern Biotech
IgG2c	Alkaline Phosphatase Polyclonal Sera	Goat		1:1000	Southern Biotech
IgG3	Alkaline Phosphatase Polyclonal Sera	Goat		1:1000	Southern Biotech
Total Ig	Alkaline Phosphatase Polyclonal Sera	Goat		1:2500	Southern Biotech

Figure 2.1

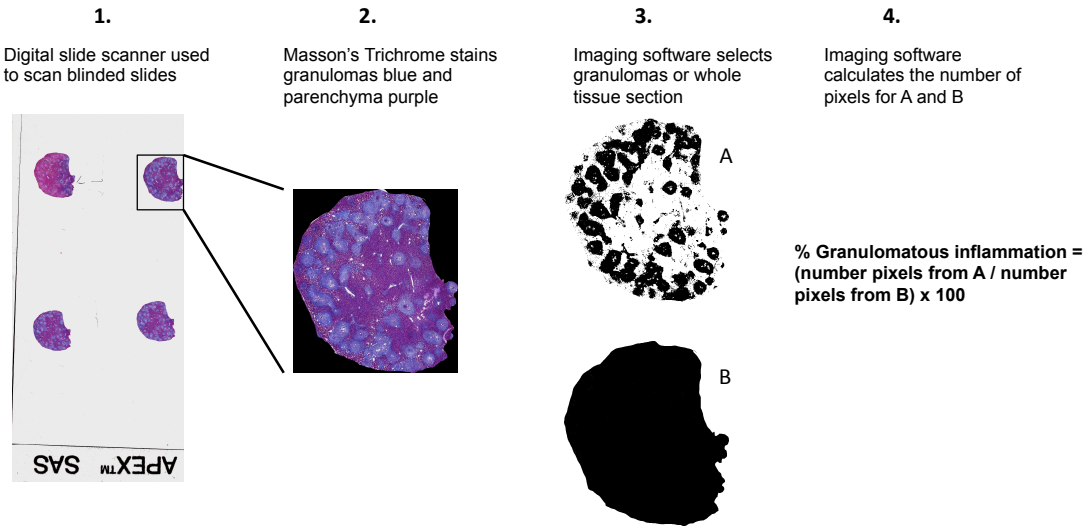

Figure 2.1 Histological quantification of hepatic granulomatous inflammation

1. Microscope slides containing sections of the median liver lobe were stained with MT, blinded and scanned with a dotslide digital slide scanner (Olympus BX51, VS-ASW FL Software) to create a BF image of the whole slide. 2. FIJI imaging analysis software (ImageJ 1.48r) was used to crop individual liver sections and create an image consisting solely of the liver section with all background removed. 3. The colour threshold was set using HSB settings to select for granulomatous inflammation (blue) or the whole tissue section. These HSB threshold settings were inserted into an algorithm developed by Dr. Tim Kendall. The algorithm was then run on each image twice, creating one image with black pixels representing granulomatous inflammation (A) and a second image where black pixels represent the whole of the tissue section (B). 4. After black and white images of the tissue section were created, the number of black pixels in each image was calculated by the algorithm. These numbers were used to determine the total proportion of granulomatous inflammation present in the liver section, providing an objective measurement of the total burden of granulomatous inflammation in the liver.

Figure 2.2

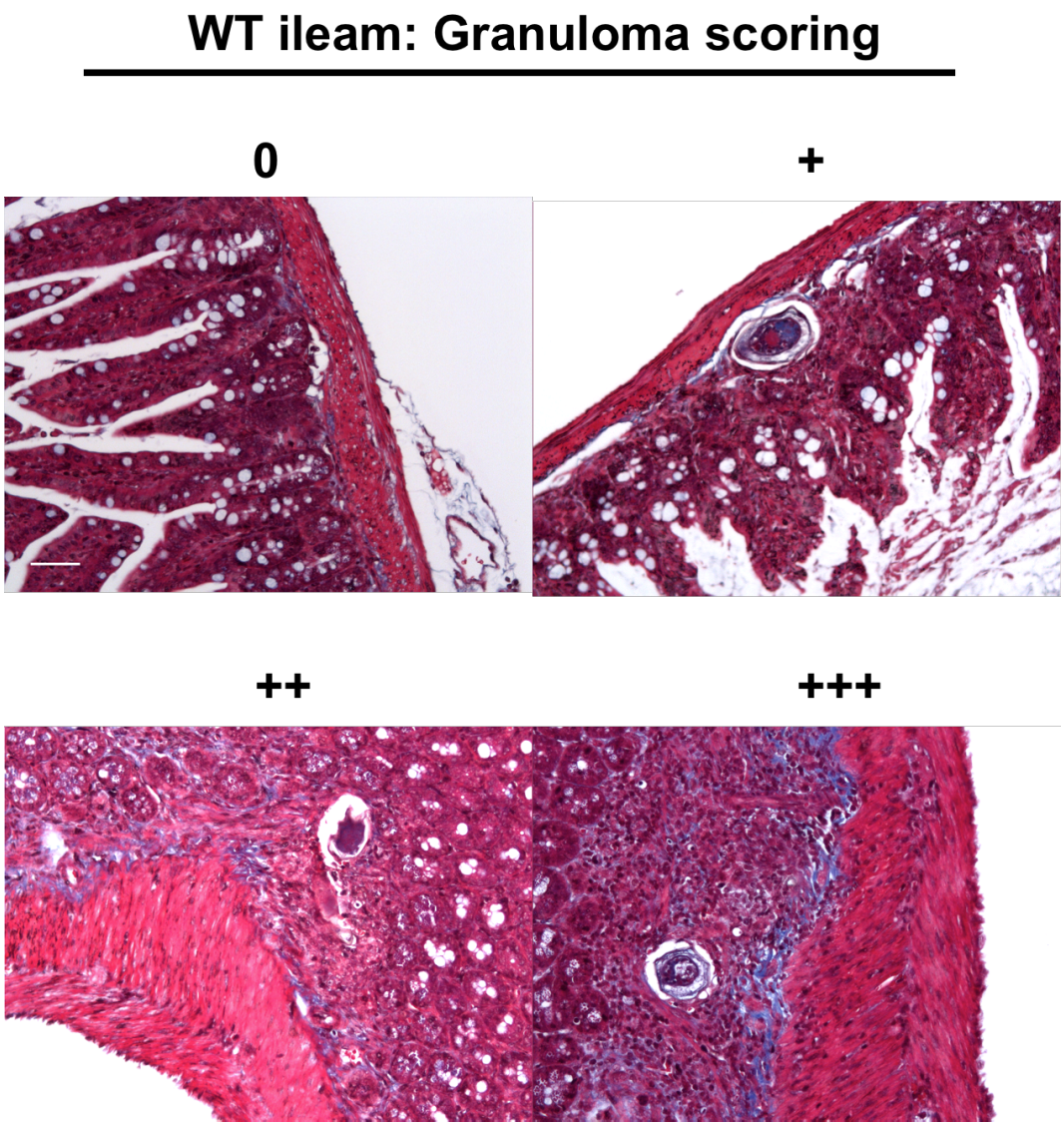

Figure 2.2 Scoring system for ileal granulomas
Median liver lobe sections were stained with MT, blinded and analysed using a light microscope. Representative BF images are shown from D42 of infection for scored granulomas in the ileum. Single egg granulomas present in the ileum were scored for their intensity and density of immune cells, and the amount of damage visible in the surrounding tissue (including crypt architecture, goblet cell size and collagen deposition). Score 0 represents absent granuloma formation around the egg, and score $^{+++}$ represents the highest pathological score. No statistics can be performed on scores.

Figure 2.3

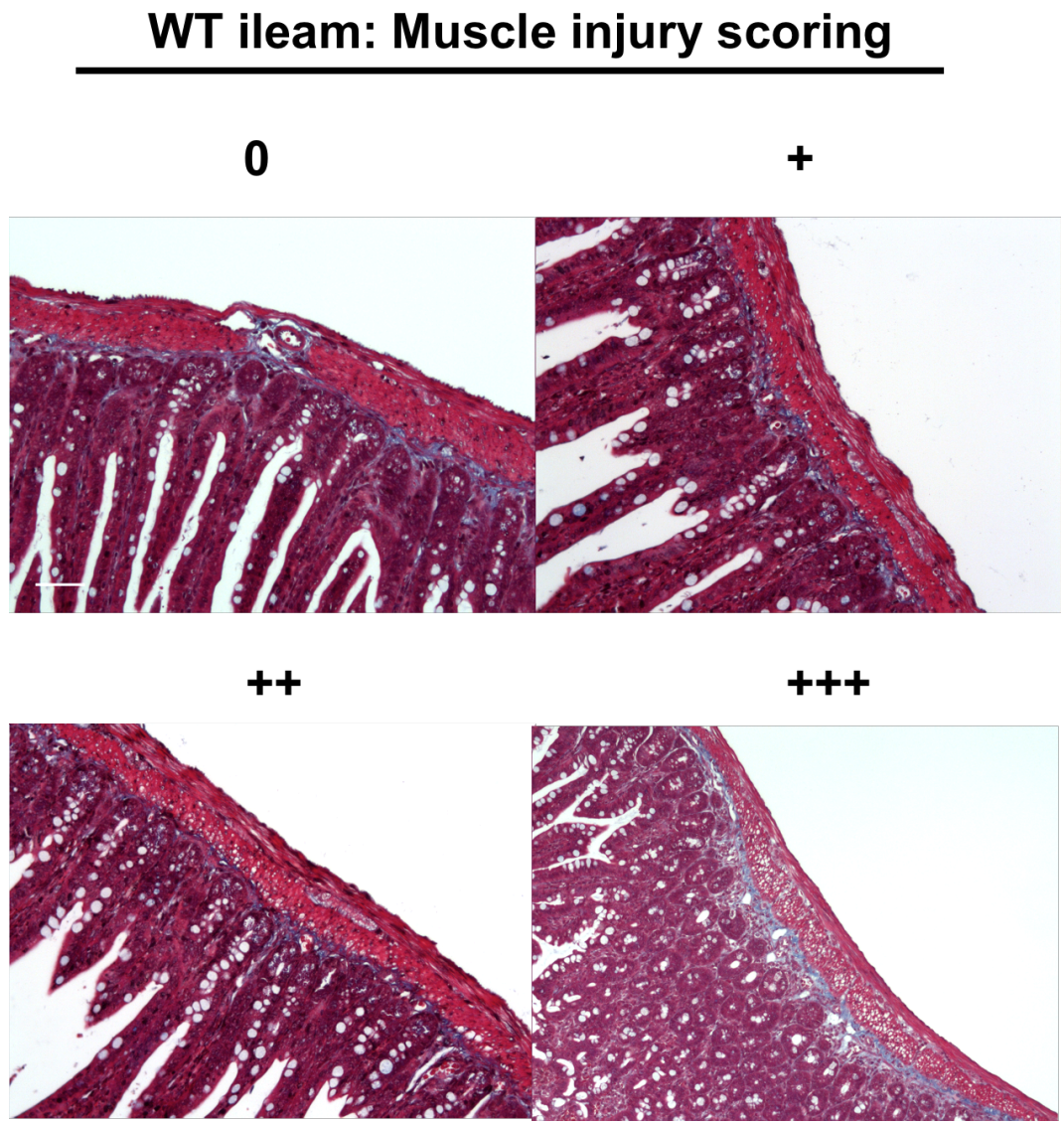

Figure 2.3 Scoring system for ileal circular muscle injury
Median liver lobe sections were stained with MT, blinded and analysed using a light microscope. Representative BF images are shown from D42 of infection for scored muscle injury in the ileum. Score 0 represents absent muscle injury (i.e. comparable muscle structure with that of naïve animals), and score $^{+++}$ represents the highest pathological score, representing damage to muscle architecture, substantial vacuole deposition in the muscle (identified as white and round features in the muscle) and collagen formation (blue) in between the muscle and the submucosa.

Figure 2.4

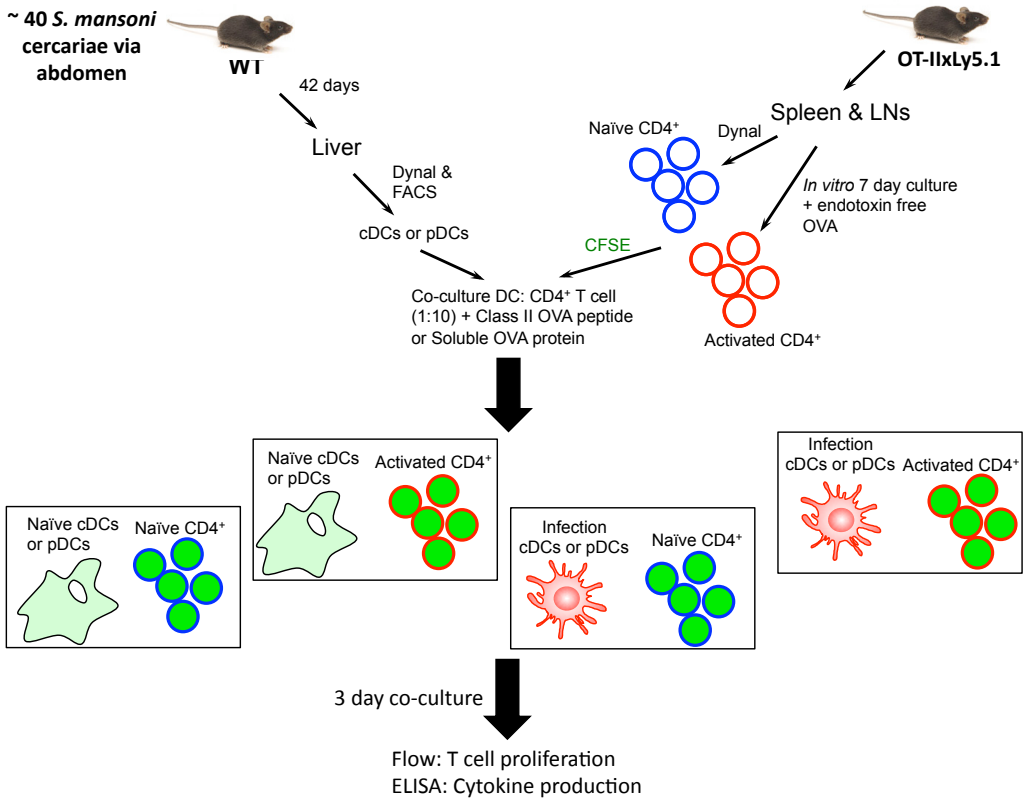

Figure 2.4 DC:T cell co-culture assay method
This figure summarises the protocol used for the set up of DC:T cell co-culture assays used in chapter 5 to investigate hepatic DC function during *S. mansoni* infection. 1. Liver leukocytes were isolated from naïve or D42 infected WT mice and enriched for DCs by negative selection (Dynabeads). Enriched DCs were then further purified by FACS to obtain pure populations of live DC subsets (i.e. cDCs and pDCs), and assessed for activation status by flow cytometry. 2. Naïve splenic and lymphoid $CD4^+$ T cells were enriched from OT-IIxLy5.1 mice by negative selection (Dynabeads). 3. Splenic $CD4^+$ T cells were activated *in vitro* in the presence of OVA protein 7 days prior to culture with DCs. 4. Naïve and *in vitro* activated $CD4^+$ T cells were assessed for purity and activation status by flow cytometry, and labelled with CFSE. 5. For pOVA assays, FACS sorted DCs were pulsed with pOVA (323-339) prior to culture. This assay was done to investigate the ability of DCs to present antigen to naïve or previously activated $CD4^+$ T cells. For soluble protein assays, soluble OVA protein was added to FACS sorted DCs and was present throughout the culture period. In this case the ability of DCs to take up, process and present antigen was examined. 5,000 FACS sorted DCs (either pulsed with OVA for 45 min or in the presence of soluble OVA protein) were co-cultured with 50,000 naive or *in vitro* activated $CD4^+$ T cells for 3 days. After culture, T cell proliferation was analysed by flow cytometry and cytokines present in the supernatant were measured by ELISA.

3 The importance of dendritic cells in the formation of granulomatous inflammation during *S. mansoni* infection

3.1 Abstract

Although granuloma formation during *S. mansoni* infection forms a pathological pillar of the disease, the underlying cellular mechanisms for initial granuloma development are not well-defined. We have conducted a detailed study investigating changes in granulomatous tissue during the entire course of infection, from acute to chronic stages. DCs were found to be present within the granuloma throughout its development, and close positioning with T cells provided a further indication of their behaviour in the dynamic granuloma. Using CD11c-diphtheria toxin receptor mice we could show that DC depletion reduces granuloma formation. In contrast, granuloma formation was unimpaired in *Batf3*$^{-/-}$ mice, which lacked a specific subset of DCs called CD8α^{+} cDCs. These data highlight the critical role of CD8α^{-} cDCs during granuloma formation thus providing further insight into the granulomatous processes that govern the disease.

3.2 Introduction

S. mansoni associated pathology and the polarisation of $CD4^+$ T cell immune responses are intimately linked to parasite egg production by mature worm pairs in the mesentery (Grzych et al., 1991; Pearce et al., 1991; 1998; Vella and Pearce, 1992) (section 1.8, chapter 1). A female worm will produce around 300 eggs per day, which then transit from the mesentery through intestinal tissue into the lumen (Gryseels et al., 2006). Consequent excretion of the eggs completes the mammalian section of the life cycle, which then resumes in fresh water snails that are infected with miracidia that hatch from the egg when it contacts fresh water (Pearce and MacDonald, 2002) (see diagram 1.7). Yet, in murine *S. mansoni* infection approximately 70% of eggs are swept away by the bloodstream, eventually becoming lodged in liver sinusoids (Cheever, 1987). This makes the liver a major site for egg accumulation as arrival in the parenchyma is a dead end for the parasite, and thus hepatic granulomatous inflammation contributes greatly to the overall disease burden for the host (Pearce and MacDonald, 2002). The exact mechanisms and immune cells that are important for hepatic granuloma formation and development remain unclear. Thus, work in this chapter aims to investigate granuloma development in the liver during *S. mansoni* infection, and to better understand the role of the immune response during this process. Additionally, work in this chapter aims to overcome some of the technical challenges associated with granuloma research.

Most early reports used a pulmonary model of granuloma formation developed by Von Lichtenberg (Lichtenberg, 1962). Persistent egg delivery into the liver during natural *S. mansoni* infection challenges granuloma research, as new and old granulomas will be present at every time-point. Thus, the inspiration for Von Lichtenberg's pulmonary model was based on synchronous egg delivery into the tissue, creating a more controlled time-frame for study of granuloma formation and development. However, egg injection models have been shown to result in less intense granulomas and fewer fibrotic responses (Cheever et al., 2002; Edungbola and Schiller, 1979; Eltoum et al., 1995; Mansy, 1998) possibly due to a lack of cross-reactive memory T cells established during prepatent infection, which aid the generation of granulomas at the onset of egg laying (Lukacs and Boros, 1991). The

use of eggs that have been kept *in vitro* for 2 to 3 days prior to egg injection in some studies may also contribute to a reduced granulomatous response as a result of weaker antigenic secretions by the egg (Eltoum et al., 1995). Therefore, the investigation of hepatic granulomas during natural infection is beneficial towards understanding the type of immune cells and mechanisms that are required for their formation and development.

3.2.1 The location and function of immune cells in the granuloma

Granuloma development in the liver is determined by various different cell types and an intricate network of extracellular components, as described in chapter 1 (Lenzi et al., 2006). These components work together to form a stable and efficient entity protecting the host against toxic and damaging properties secreted by the egg (Hams et al., 2013). Given that the granuloma forms such an organised structure, we hypothesized that investigation into the location of immune cells will provide an essential insight into their behaviour and function within the granuloma.

Due to various technical challenges associated with the investigation of immune cell location within the granuloma, the location of cells easily recognised by morphology, such as MΦs and eosinophils, has been most extensively studied. Eosinophils are easily distinguishable from other immune cells using eosin dyes, such as H&E, which stain the characteristic granules within the cells (Lugo-Villarino et al., 2010). Initial recruitment of eosinophils to the liver most likely occurs before substantial egg deposition, when they are located diffusely in the parenchyma presumably responding to hepatocyte injury (Hams et al., 2013; Moore et al., 1977; Wynn et al., 2004). As such eosinophils are one of the first responders after *S. mansoni* egg arrival in the liver (Lenzi et al., 1998). Eosinophil interaction with the egg has previously been investigated using *in vitro* granulomas, which are formed by co-culturing spleen cells from *S. mansoni* infected mice with live eggs obtained from adult worm pairs (Bentley et al., 1982; Doughty and Phillips, 1982). Bentley *et al.,* (1982) showed that initial eosinophil contact with the egg during the formation of *in vitro* granulomas occurs at the spine. After granuloma formation eosinophils have been observed to occupy most parts of the granuloma although they also uniquely locate close to the *S. mansoni* egg (Lenzi et al., 2006). Degranulation and death of eosinophils on the egg

shell surface has been described and is termed the Splendore-Hoeppli phenomenon, which indicates that eosinophils are involved in the killing of the egg (Kephart et al., 1988).

Efficient recruitment of eosinophils to the liver requires Th2 cytokines such as IL-5 and IL-13 (Reiman et al., 2006; Sher et al., 1990), and eosinophils have been shown to enhance IL-5 production by $CD4^+$ T cells in the granuloma, thereby promoting Th2 responses (Metwali et al., 1993). To show this, Metwali *et al.,* (1993) isolated hepatic *S. mansoni* granulomas by liver homogenisation and sedimentation of granulomas, followed by digestion for characterisation of granuloma specific immune cells. Although eosinophil infiltration is a well established feature of granulomatous inflammation, eosinophil deficiency does not alter granuloma formation or pathology, which suggests that other immune cells compensate for eosinophils in their absence (Swartz et al., 2006).

MΦs have typically been found close to eosinophils and are also present in initial granuloma formation (Geuskens et al., 1991). Due to their large size MΦs are also distinguishable from other cell types using most dyes. *In vitro* granuloma studies have described MΦs surrounding and covering the egg shell surface by exhibiting a flattened morphology (Bentley et al., 1982). As part of the innate first-line defence against a pathogen, it is likely that hepatic MΦs are involved in the recruitment and activation of immune cells for granuloma formation during schistosomiasis (Sica et al., 2014). For example, in early pulmonary granulomas CAMΦs have been shown to produce large amounts of TNF-α and IL-1β (Chensue et al., 1989), and together with IL-6 these cytokines are thought to be the main primary inducers of cellular aggregation during granuloma formation (Boros, 1994). In addition, CAMΦs may be involved in egg killing similar to eosinophils, as they exhibit a microbicidal activity against the parasite through the production of NO (Gazzinelli et al., 1992; Oswald et al., 1992).

As the granuloma develops, MΦs are thought to be influenced by the dominant Th2 cytokine milieu and become alternatively activated (Metwali et al., 1996; Sandler et al., 2003). This hypothesis is supported by high expression of proteins associated with alternative activation such as Arg-1, FIZZ-1 and YM-1 by granulomatous tissue

(Hesse et al., 2001). Recent studies have shown that AAMΦs in the liver differentiate primarily from blood circulating monocytes during *S. mansoni* infection (Girgis et al., 2014; Nascimento et al., 2014). The fundamental importance of AAMΦs during *S. mansoni* infection was elucidated in a study using $LysM^{cre}IL\text{-}4R\alpha^{-/flox}$ mice, which are deficient in AAMΦs marked by a reduction in Arg-1 and an inability to mediate normal wound healing (Herbert et al., 2004). Herbert *et al.,* (2004) showed that mice deficient in AAMΦs are unable to survive acute *S. mansoni* infection. This is linked to hepatic damage caused by egg toxins leaking from the granuloma and entry of endotoxins into the blood circulation ultimately leading to critical weight loss and sepsis. In addition, AAMΦs expressing Arg-1 are thought to act as Th2 suppressor cells in more chronic stages of *S. mansoni* infection (Pesce et al., 2009). Arg-1 is an enzyme that catalyses the hydrolysis of arginine to urea and ornithine (Mills, 2001), and arginine is a critical resource for $CD4^+$ T cell function (Rodriguez et al., 2007). Pesce *et al.,* (2009) showed that Th2 suppression by Arg-1^+ MΦs is independent of TGF-β and IL-10 production, and the authors suggest that MΦs deplete arginine in the environment instead. Thus, AAMΦs are currently thought to contribute to the suppression of Th2 immune responses and fibrotic processes particularly during later stages of infection (Herbert et al., 2004; Pesce et al., 2009). This is in line with current thinking in the literature that a switch from parasite killing functions to wound repair by MΦs is likely critical in the face of chronic helminth infection (Barron and Wynn, 2011). Notably, Nascimento *et al.,* (2014) show that CAMΦs likely remain present after the induction of Th2 responses, as expression of iNOS and TNF persists in the liver (Nascimento et al., 2014). This suggests that MΦ heterogeneity exists in the granuloma throughout *S. mansoni* infection. Indeed, the type and role of MΦs in the *S. mansoni* granuloma are areas of active research, and it is likely that their functions change depending on the immune environment and the stage of granuloma maturity (Barron and Wynn, 2011).

The largest cells within the granuloma are the giant cells, which have been described in the granuloma after about 45 days of infection (Lenzi et al., 1998). Two different types of giant cells have been described in both human and murine infection (el-Shoura, 1994; Lenzi et al., 1998). One appears randomly and typically locates distant to the egg (Lenzi et al., 1998). Its cytoplasm is rich with schistosome pigment suggesting they may have similar phagocytic roles compared with MΦs (Lenzi et al.,

1998). The second type of giant cell is more frequent and found on the surface of the egg shell (Lenzi et al., 1998). It is conceivable that giant cells are in fact formed by MΦs merging together, and this may be induced by IL-4 (Helming and Gordon, 2007). However, whether this is the case or what specific role giant cells play in the granuloma remains unclear.

Other innate immune cells such as mast cells, DCs, NK cells, NKT cells and neutrophils also populate the granuloma although less is known about their location and interaction with other cell types compared with eosinophils and MΦs (Hams et al., 2013; Weinstock and Boros, 1983). Interestingly, an electron microscopy study in 1982 using the *in vitro* granuloma model observed cellular extensions into the egg shell pores (Bentley et al., 1982). Although these cells appeared to have a similar morphology to MΦs, it is possible that they were in fact DCs, especially as some of them were markedly smaller in comparison with MΦs and giant cells, and given that DC research was at that time in its infancy. This hypothesis clearly requires further investigation, but these early studies may have depicted for the first time DC interaction with the *S. mansoni* egg. The proportion of neutrophils in *S. mansoni* granulomas induced by egg injection was found to be around 10% compared with 70% eosinophilia (Moore et al., 1977), whereas neutrophils are more frequent in *S. japonicum* granulomas (Hsü et al., 1972; Lichtenberg et al., 1973). Pronounced neutrophilia accompanied by increased apoptotic cell populations in the *S. mansoni* granuloma has been reported in Th1 polarised mice (IL-10/IL-4$^{-/-}$), and these mice do not survive acute infection (Hoffmann et al., 2000; 2001). Thus, changes in neutrophilia in *S. mansoni* granulomas may provide an indication of the type of immune response orchestrating granulomatous inflammation, which can substantially impact the progression of the disease.

Although innate immune responses are clearly involved in the initial formation of granulomas, the adaptive immune response including T and B cells forms a major constituent of the established granuloma (Lenzi et al., 1998; Weinstock and Boros, 1983). It has been reported that B cells locate to all regions of the granuloma (Jacobs et al., 1999). Although B cells are not required for granuloma formation, they play a role in downregulating CD4^{+} T cell responses during granuloma development (Jankovic et al., 1998) (section 1.8.1, chapter 1). T cells have been described mostly

in the periphery of the granuloma, but some can be found dispersed throughout every zone (Bentley et al., 1982; Chuah et al., 2014; Hams et al., 2013). $CD4^+$ T cells are thought to be the main T cell subset present within the granuloma, and the majority of $CD4^+$ T cells exhibit an effector/memory phenotype that is *S. mansoni* egg-specific (Hogan et al., 2002; Rumbley and Phillips, 1999). Indeed, $CD4^+$ T cells are required for granuloma development during *S. mansoni* infection, as in their absence granuloma formation is impaired resulting in severe hepatotoxicity and accumulation of damaged and necrotic cells around the egg (Amiri et al., 1992; Byram and Lichtenberg, 1977; Cheever et al., 1999; Doenhoff et al., 1981; Dunne and Doenhoff, 1983; Mathew and Boros, 1986) (section 1.8.1, chapter 1), whilst $CD8^+$ T cells and γδ T cell deficient animals form expected granulomatous inflammation in the liver (Iacomini et al., 1995; Yap et al., 1997). In fact, $CD4^+$ T cells are the only key cell type that is known to date to be an absolute requirement for hepatic granuloma formation during *S. mansoni* infection. Numerous reports have since pointed to a dominant role for Th2 cells and IL-4R signalling for granuloma development, as granulomas are often reduced or absent when these processes are impaired (Chiaramonte et al., 1999; Fallon et al., 2000a; 2000b; Hernandez et al., 1997; Jankovic et al., 1999b; Kaplan et al., 1998; MacDonald and Pearce, 2002; MacDonald et al., 2002a; McKenzie et al., 1999) (described in section 1.8.1, chapter 1). These findings highlight the importance of Th2 associated mechanisms for appropriate granuloma formation that protects the surrounding tissue from *S. mansoni* egg derived toxins (Doenhoff et al., 1981; Dunne et al., 1991; Fallon et al., 2000a). This raises the question whether DCs play an important role in granuloma formation, as $CD11c^+$ DCs are necessary for the induction of Th2 responses during *S. mansoni* infection (Phythian-Adams et al., 2010).

3.2.1.1 How might dendritic cells be involved in granuloma formation during *S. mansoni* infection?

Previous research into the activation and function of DCs during *S. mansoni* infection has essentially focused on early priming of Th2 cells in secondary lymphoid tissue (Baumgart et al., 2006; Grzych et al., 1991; McKee and Pearce, 2004; Pearce et al., 1991; Taylor et al., 2009) (section 1.9, chapter 1), whereas the lack of specific DC surface markers and their overall scarcity have discouraged investigation into their role during granuloma formation. Given that $CD11c^+$ DCs are required for Th2

induction during *S. mansoni* infection (Phythian-Adams et al., 2010), it is plausible that DCs may be required for granuloma formation indirectly (Banchereau and Steinman, 1998). This mechanism would involve the polarisation of naïve $CD4^+$ T cells towards a Th2 type in lymphoid tissues by *S. mansoni* egg experienced DCs, and subsequent migration of antigen-specific $CD4^+$ T cells to the tissue site (Banchereau and Steinman, 1998). In support of this hypothesis, DC co-stimulation has been shown to be important for hepatic granuloma formation, as granulomas are reduced in size in $CD154^{-/-}$ mice, where DC co-stimulation and Th2 induction are impaired (MacDonald et al., 2002a).

Although it can be postulated that DCs are activating naïve $CD4^+$ T cells in the granuloma, this is unlikely as the majority of $CD4^+$ T cells within the granuloma are effector/memory cells (Rumbley and Phillips, 1999), and naïve T cells are not thought to enter the site of inflammation directly and instead recirculate secondary lymphoid organs (Girard et al., 2012). However, a growing body of evidence supports the concept that the liver is a secondary lymphoid organ (Crispe, 2009). For example, hepatic DCs have been reported to mature within the granuloma during *P. acnes* induced granulomatous liver disease and then migrate to the portal tract-associated lymphoid tissue (PALT) where they activate naïve T cells (Yoneyama et al., 2001). Blood-LN translocation via the hepatic sinusoids has been reported in the rat, creating a potential important niche for circulating DCs in the liver (Kudo et al., 1997). Therefore, primary T cell activation by DCs in the liver is possible, but it is unlikely that this process is occurring locally in the granuloma. This stipulates that DCs interact with effector/memory $CD4^+$ T cells in the granuloma (Hogan et al., 2002; Rumbley and Phillips, 1999), which could be important for the local maintenance of $CD4^+$ T cell responses. Yet, it remains unknown whether DCs interact with effector/memory $CD4^+$ T cells within the hepatic granuloma, and little is known about DC function in more chronic infection settings when granulomas are well established (Pearce and MacDonald, 2002). Effector/memory $CD4^+$ T cells can interact with other APCs that express MHC-II, such as B cells (Croft et al., 1994), which are activated at the onset of egg production and undergo clonal proliferation during *S. mansoni* infection (Hernandez et al., 1997). Thus, antigen-specific B cells should provide another source of TCR stimulation during *S. mansoni* infection, indicating that DCs may not be a fundamental requirement for the maintenance of antigen-specific $CD4^+$

T cell responses. Work in this chapter seeks to better understand DC contribution to the development of granulomas during *S. mansoni* infection, and to determine whether DCs are interacting with T cells within the granuloma.

DC subsets perform distinct functions during immune responses against a pathogen, and various studies have proposed a dominant role for IRF4 dependent cDCs in the induction of Th2 immune responses during allergic inflammation and parasitic infection with *N. brasiliensis* (Gao et al., 2013; Kumamoto et al., 2013; Plantinga et al., 2013; Williams et al., 2013) (section 1.9.3, chapter 1). The best example of this was shown recently by Plantinga *et al.,* (2013), who used various transgenic mouse models to delineate that $CD11b^+$ cDCs are required for the induction of Th2 responses against the HDM allergen in the lung. On the other hand, $CD8\alpha^+$ cDCs that are dependent on *Batf3* have emerged as essential players in the promotion of Th1 and CTL responses against acute viral and bacterial infection (Edelson et al., 2010; Hildner et al., 2008; Torti et al., 2011; Waithman et al., 2013), and are the main producers of IL-12 during *T. gondii* and *L. major* infection (Ashok et al., 2014; Mashayekhi et al., 2011). The importance of $CD8\alpha^+$ cDCs during chronic infection and in Th2 settings has not previously been addressed. Given that mixed/balanced Th1/Th2 immune responses are crucial to prevent severe pathology during *S. mansoni* infection (section 1.8.1, chapter 1) (Hoffmann et al., 2000; Wynn et al., 2004), we reasoned that the absence of $CD8\alpha^+$ cDCs could alter granuloma formation if Th1 responses are impaired. Thus, we investigated the role of *Batf3* dependent cDCs in granuloma formation during *S. mansoni* infection. Subsequently, the impact of *Batf3* deficiency on the induction of Th1 and Th2 immune responses against *S. mansoni* will be investigated in chapter 4.

3.3 Study Rationale

In this chapter, the role of $CD11c^+$ DCs in hepatic granuloma formation and the development of the immune response during the course of murine *S. mansoni* infection were investigated using flow cytometry and microscopy techniques. To increase fundamental understanding of how granulomas are generated during infection, novel microscopy techniques were developed to determine the total burden of granulomatous inflammation (immune cell aggregation and collagen deposition) on the liver and the extent of fibrosis over a defined time-course following the initiation of egg laying by the parasite. To complement this approach, confocal microscopy was used to better define the immune cells present and their location in the granuloma over the same time-course, focusing on DCs, MΦs, eosinophils and T cells.

To directly assess the importance of DCs during granuloma formation, the CD11c.DOG model was used to enable inducible depletion of cDCs and pDCs expressing high levels of CD11c for a window of up to 12 days (section 1.2.2, chapter 1) (Hochweller et al., 2008). Granuloma formation was examined at D42 (early stage granuloma development, with low Th2 responses and minimal hepatic pathology) or D52 (later stage granuloma development, with high Th2 responses and more evident hepatic pathology) post *S. mansoni* infection of mice in which $CD11c^+$ DCs had been depleted (Pearce and MacDonald, 2002).

To refine our understanding of the relative importance of DC subsets, *Batf3*$^{-/-}$ mice, which specifically lack $CD8\alpha^+$ and migratory $CD103^+$ cDCs (described in section 1.2.2, chapter 1) (Hildner et al., 2008), were used to determine the role of this conventional DC subset in granuloma development during *S. mansoni* infection.

3.4 Results

3.4.1 Granuloma development during *S. mansoni* infection

Granulomatous inflammation in the liver was examined during a time-course experiment from D28 to D105 to assess how granuloma area changes during the course of infection. This time-frame encompasses various stages in parasite development including the pairing of mature *S. mansoni* adult worms in the mesentery (approximately D28) and the onset of egg production (D28-D42), which induces a dominant Th2 immune response by the host that becomes downmodulated in more chronic stages of infection (approximately D56 to D105) (Pearce and MacDonald, 2002). As expected, analysis of the parasitology during this time-course revealed no major changes in worm burden over time, but a significant increase in the number of eggs that accumulated in the liver from D42 onwards (Fig. 3.1A-B). In previous literature, hepatic and pulmonary granuloma area has been estimated using various different techniques, often subjective and involving time-consuming analysis of individual granulomas, typically excluding multiple egg granulomas or those containing eggs of certain maturity states from the analysis (Colley, 1975; Domingo and Warren, 1968; Hoffmann et al., 1999; Kaplan et al., 1998; Layland et al., 2005; Lichtenberg, 1962). Commonly, such techniques would only focus on single egg granulomas in a clear cross-section. To objectively quantify the total area of granulomatous inflammation in liver sections a novel method was developed (Fig. 3.1C-D) (this method is described in section 2.6.1, chapter 2). Liver sections (5 μM thick) from the median lobe (or left medial lobe (Fiebig et al., 2012)) were stained with Masson's Trichrome (MT), which differentially stains the granuloma as well as vascular tissue compared with the surrounding liver parenchyma (Amin and Mahmoud-Ghoneim, 2011; Krishna, 2013). An algorithm was used to identify stained granulomas or whole tissue, and the number of pixels in the region of interest was measured to calculate the total proportion of granulomatous inflammation per liver section. The staining of vascular tissue accounts for background values measured in naïve animals. Using this novel technique, the total area of granulomatous inflammation was observed to increase significantly from D42 until it reached a plateau at D84 (Fig. 3.1C). Granulomatous inflammation accounted for up to 50% of the total tissue section area from D84 to D105. Eggs continued to accumulate in the

liver in this time-frame, suggesting ongoing arrival and deposition of new eggs in these more chronic stages of infection (Fig. 3.1B).

3.4.2 Th2 development during *S. mansoni* infection

The type of immune response induced during *S. mansoni* infection ultimately determines the cellular composition of granulomas, and therefore plays an important role in the formation of granulomatous inflammation as discussed in section 1.8.1. Previous literature investigating T cell responses in the spleen during *S. mansoni* infection have shown that $CD4^+$ T cell responses shift from mixed Th1/Th2 responses to a dominant Th2 responses at the onset of egg production (Baumgart et al., 2006; Grzych et al., 1991; McKee and Pearce, 2004; Pearce et al., 1991; Taylor et al., 2009), but to the best of our knowledge detailed analysis of immune responses in the liver has not yet been conducted. To assess how T cell populations change during the course of the infection in the liver, *ex vivo* $CD4^+$ and $CD8^+$ T cell populations were examined by flow cytometry (Fig. 3.2A-C). The proportion of hepatic TCR-β^+ cells stayed at a consistent level during infection until D105 when values were similar to naïve levels (Fig. 3.2A-B & D). Analysis of T cell subsets in the liver at D42 of infection showed that approximately 52% of TCR-β^+ cells were $CD4^+$ T cells and 35% were $CD8^+$ T cells, and that these proportions were comparable at all the time-points measured (Fig 3.2A & D). The fold change of numbers of TCR-β^+ cells and $CD4^+$/$CD8^+$ T cell subsets from infected animals increased between D28 and D42 and remained above the naïve baseline throughout infection (Fig. 3.2C).

The character of the hepatic immune response during the course of murine infection was assessed by determining the cytokine profile of isolated liver leukocytes in response to restimulation with SEA in culture. Supernatants were harvested and analysed by ELISA to measure SEA-specific cytokine production. At D28, the level of IFN-γ produced by liver leukocytes from infection after restimulation with SEA was significantly increased compared with naïve animals (Fig. 3.3A). At D42, there was a significant increase in the amount of antigen-specific IL-4, IL-5, IL-10 and IL-13 produced by liver leukocytes when compared with naïve controls (Fig. 3.3A). The level of IL-5 and IL-13 remained significantly increased compared with the amounts produced in the antigen-specific restimulation assay by naïve animals at all the time-points measured (Fig. 3.3A). Although there was a trend for increased levels of IL-4

production by liver leukocytes at each time-point compared with naïve controls, the absolute amount of IL-4 detected was lower than that of either IL-5 or IL-13. However, there was a significant increase in antigen-specific IL-4 at D42 and D84 (Fig. 3.3A). The amount of IL-10, which is known to be produced by Tregs, Th2 cells, DCs, B cells and MΦs during *S. mansoni* infection (Hesse et al., 2004; Sher et al., 1991; Stadecker, 1999), was increased significantly from D42 to D105 during infection (Fig. 3.3A). The highest fold changes of IL-10 relative to uninfected controls were evident at D28 and D105 (Fig. 3.3B). In contrast, there was a striking reduction in the fold change of IFN-γ produced by liver leukocytes from infected mice compared with naïve mice at D42 until D84 (Fig. 3.3B), consistent with the prevailing view in the literature that it is between D42 and D52 of infection that the Th2 response begins to dominate in this infection (Grzych et al., 1991; Pearce and MacDonald, 2002). These dramatic changes in SEA-specific cytokine production coincided with egg production and their accumulation in the liver (Fig. 3.1B), and are in keeping with previous descriptions of the changes in cytokine environment in the spleen over the course of murine *S. mansoni* infection (Grzych et al., 1991; Pearce et al., 1991; Pearce and MacDonald, 2002; Sher et al., 1991).

To determine whether the trend in SEA-specific cytokine levels reflects T cell cytokine production, liver leukocytes were cultured with αCD3/CD28 and assessed by flow cytometry after ICC. Cells from the livers were restimulated with αCD3/CD28, as this is thought to be a physiologically relevant stimulation for T cells in culture, and is less cytotoxic in comparison with other reagents commonly used *in vitro* or *ex vivo* including PMA/Ionomycin (Olsen and Sollid, 2013) (section 2.8.2, chapter 2). An increase in IL-4^+ and IL-13^+ $CD4^+$ T cell populations in response to polyclonal activation was comparable in trend with total cytokine production after SEA restimulation measured by ELISA (Fig. 3.3C-D). Furthermore, liver leukocytes from infected animals produced more IL-10 relative to cells from naïve animals at all time-points (Fig. 3.3C). IFN-γ^+ $CD4^+$ T cells were detected at relatively high levels in naïve animals, and thus the fold change for IFN-γ production during infection did not increase much above naïve controls in early stages of infection (Fig. 3.3C-D). However, the fold change of IFN-γ expressed by $CD4^+$ T cells in this assay was below the naïve baseline from D42-D105 (Fig. 3.3C). A similar trend was seen for IFN-γ produced by $CD8^+$ T cells after polyclonal restimulation (Appendix Fig. 7.1B).

Thus, ICC analysis of cytokine positive T cells followed the same overall trend as cytokines produced by total liver leukocytes in response to SEA.

3.4.3 High levels of CD11c expression on cDCs and MΦs

The need for lineage negative markers to distinguish hepatic DCs from other cells provides an additional challenge for visualisation of DCs by confocal microscopy, as CD11c is also expressed by various immune cells including MΦs and eosinophils (Huh et al., 2014; Jakubzick et al., 2006; Lloyd et al., 2008; Niess et al., 2005; Throsby et al., 2000). The overall proportion of CD11c expression in the liver was unchanged compared with naïve mice from D28 to D84, but was significantly increased at D105 (Fig. 3.4A). To assess whether CD11c can be used as a marker for hepatic DCs, the expression of CD11c by DCs, MΦs and eosinophils was investigated by flow cytometry at D42 of *S. mansoni* infection when Th2 immune responses are induced (Pearce and MacDonald, 2002). Notably, the staining panel used for this analysis was originally designed to enable the analysis of the maximum number of different immune cells, including T cells and various different DC subsets. Given that eosinophils can be identified by their granularity (side scatter, SSC) and low level MHC-II expression (van Rijt et al., 2002), the eosinophil marker Siglec-F was not used in this case to allow for the use of other monoclonal antibodies (Zhang et al., 2004). The analysis of different immune cell populations expressing CD11c at D42 showed that mainly MΦs and cDCs expressed CD11c in naïve mice, whereas few eosinophils and pDCs expressed CD11c at D42 of *S. mansoni* infection (Fig. 3.4B). The geometric mean fluorescence intensity (GMFI) of CD11c expression was also analysed by flow cytometry and showed that both naïve and infection derived cDCs and CD11c-expressing MΦs expressed high levels of CD11c compared with other cell types, whereas the expression level was lower for eosinophils and pDCs (Fig. 3.4C).

3.4.4 Similar CD11c and TCR-β staining in the granuloma

The location of $CD11c^+$ cells was investigated during granuloma formation using confocal microscopy to further understand their behaviour during infection (Fig. 3.5). To assess the location of $CD11c^+$ cells relative to other immune cells, the presence of eosinophils and T cells in hepatic granulomas was also examined. In the liver Siglec-F is expressed exclusively by eosinophils and thus was used to identify these cells in

the granuloma (Zhang et al., 2004). TCR-β was used to detect $CD4^+$ and $CD8^+$ T lymphocytes, but TCR-β is also expressed by NKT cells (MacDonald, 1995). Yet, less than 10% of total liver *ex vivo* TCR-β^+ cells analysed by flow cytometry were $NK1.1^+$, which is a surface marker expressed by NKT cells (Koo and Peppard, 1984) (Appendix Fig. 7.2). Thus, it was postulated that the majority of TCR-β^+ cells in the granuloma were T cells as opposed to NKT cells.

Representative confocal photographs of cross-sections from the left liver lobe stained for CD11c, TCR-β and Siglec-F are shown for each time-point, which portrayed different stages of granuloma formation (Fig. 3.5A). At D28 no eggs were found in the tissue (Fig. 3.1B), but disorganised clusters of immune cells, mostly Siglec-F^+, were observed (Fig. 3.5A). From D42 onwards granulomas gradually matured as indicated by the more compact and spherical organisation of TCR-β^+ and $CD11c^+$ cells (section 1.7, chapter 1). $CD11c^+$ and TCR-β^+ cells were found in close proximity to each other throughout infection, but due to the high density of immune cells within the granuloma accurate co-localisation analysis was not possible (Fig. 3.5A D28-D105). The location of Siglec-F^+ cells in the granuloma appeared to be distinct from both TCR-β^+ and $CD11c^+$ staining; Siglec-F^+ cells were often seen very close to the *S. mansoni* egg as well as occupying more peripheral areas of the granuloma. Thus, confocal analysis of $CD11c^+$, TCR-β^+ and Siglec-F^+ staining in the *S. mansoni* granuloma provided valuable information about the approximate locations of cells expressing these markers, even though co-localisation analysis could not be conducted.

Measuring the surface area of positive staining around the egg in each confocal image enabled quantification of TCR-β^+, Siglec-F^+ and $CD11c^+$ cells in each granuloma in terms of total surface area (Fig. 3.5B) (this method is described in detail in section 2.6.1, chapter 2). The mean values from figure 3.5B were used to determine the representative confocal images shown in figure 3.5A. Siglec-F^+ and $CD11c^+$ staining around the egg increased from D42 to D56 (Fig. 3.5B), and the area measured was higher than values obtained from TCR-β^+ staining. After D42, the level of Siglec-F^+ staining decreased, whereas $CD11c^+$ staining around the egg remained constant until D105. TCR-β^+ staining around the egg increased from D42 to D56 and then remained

constant until D84. After D84, TCR-β^+ staining decreased again to similar levels detected at D42. The kinetics of $CD11c^+$, TCR-β^+ and Siglec-F^+ positive staining during the time-course determined by confocal microscopy were similar to absolute cell numbers in the liver assessed by *ex vivo* flow cytometry (Fig. 3.5C-D). Interestingly, the main difference between confocal microscopy and *ex vivo* flow cytometry data was observed when analysing $CD11c^+$ cells. As mentioned, $CD11c^+$ cell staining by confocal microscopy remained at a constant level from D56-D105, whereas absolute numbers as assessed by flow cytometry on isolated/mixed liver leukocytes decreased from D56 to D84 to similar levels seen at D42 (Fig. 3.5B-D). Thus, quantification of positive staining around the egg for certain immune markers enabled quantification for kinetic analysis of the presence of those cell types specifically in the granuloma throughout infection.

3.4.5 The proportion of granulomas in the liver strikingly increases over the course of several days during *S. mansoni* infection

All of the data thus far indicated that many immunological and pathological changes occur suddenly at some time between D42 and D56 of infection. To better define the timing of this pivotal step in the initial formation of granulomatous inflammation in more detail at early stages of infection, liver sections from the median lobe were taken every 3 days from D36 to D51. Analysis of the total proportion of granulomas revealed a dramatic increase after D45 resulting in 20% granulomatous inflammation in liver sections by D51 (Fig. 3.6A-B). This increase in hepatic granulomas correlated with an increase in the number of eggs measured in the liver during the same time-frame (Fig. 3.6A).

Confocal analysis of sections from the liver showed that granulomas appeared small and disorganised at D36 and D39 (Fig.3.7A), even though some eggs were detected in the liver during these time-points (Fig.3.6A). However, by D42 the small number of granulomas identified had already started to adopt a more spherical shape and increased visibly in size (Fig.3.7A). This is supported by confocal measurements of cell types within the granuloma, as TCR-β, Siglec-F and CD11c positive staining increased gradually from D36 to D48 (Fig. 3.7B). The area of Siglec-F^+ and $CD11c^+$ staining around the egg increased further until D51, whereas levels of TCR-β^+

staining markedly decreased again. Thus, analysis of immune cell presence in the granuloma shows that these cells are present within a few days of initial egg deposition (Fig. 3.7).

3.4.6 Collagen formation in the granuloma at early stages of development

Collagen formation in the granuloma provides structure and support, creating the typical spherical shape of a mature granuloma as described in section 1.7, chapter 1. Although this transformation was visible by confocal microscopy on sections stained for immune cell markers, collagen itself could not be identified. Both MT and PSR stains have been previously used in the literature to detect collagen deposition in tissue sections, but the two dyes differentially stain collagen: PSR stains type I (thick fibres) and type III (thin fibres) collagen, whereas MT stains only type III collagen (Calvi et al., 2012). MT often produces variable results in terms of collagen measurements, and it has been suggested that the quality of collagen staining with MT is dependent on the structural arrangement and density of collagen fibres (i.e. more densely packed collagen may prevent the blue dye from entering the structure efficiently) (Whittaker et al., 1994). Comparison between liver sections stained with MT and PSR revealed slightly different patterns; MT stained the total area of granulomatous inflammation including the accumulation of immune cells and initiation of fibrosis, whereas PSR highlighted mainly the periphery of the granuloma (Fig. 3.8A). Thus MT, but not PSR, stains other features of the granuloma as well as collagen including nuclei of immune cells and other basophilic structures (components that take up basic dyes) (Amin and Mahmoud-Ghoneim, 2011; Diaz Encarnacion et al., 2004; Whittaker et al., 1994). For these reasons MT was used to measure overall granulomatous inflammation, whereas PSR staining was used to more accurately quantify collagen as a measure of fibrosis.

Collagen deposition in PSR stained median liver lobe sections was measured with the same novel technique used previously for MT stained sections (Fig 3.8B-C). The level of collagen detected by PSR was only marginally above naïve values until D45 post infection, after which it significantly increased to approximately 15% of total liver area by D51 (Fig. 3.8B) (MT data reproduced from figure 3.6B for ease of direct comparison with PSR).

3.4.7 TCR-β$^+$ staining around the *S. mansoni* egg is reduced in the absence of CD11c$^+$ DCs at D42

Having shown that CD11c$^+$ cells are present in the granuloma at early stages of formation (Fig. 3.5 & Fig. 3.7), we next investigated the total proportion of granulomatous inflammation and immune cell presence in hepatic granulomas following targeted depletion of CD11c$^+$ cells. Phythian-Adams *et al.,* (2010) reported that CD11c$^+$ DCs are necessary for the induction of Th2 responses during *S. mansoni* infection, which raised the possibility that granuloma formation would also be reduced in the absence of these cells. CD11c.DOG mice were used to deplete CD11c$^{+/high}$ cells from *S. mansoni* infected mice by administration of DTx 12 days before harvest (from D29 to D40), whereas control animals were treated with PBS. Granulomatous inflammation was quantified using liver sections stained with MT as before. As shown previously (Fig. 3.1C) the proportion of granulomas as measured by MT staining at D42 post infection was very low (<0.4% of tissue), and not significantly greater in infected mice relative to naïve controls (Fig. 3.9A). In addition, CD11c depletion had little impact on the proportion of granulomatous inflammation at this early stage of granuloma formation (Fig. 3.9A). However, granuloma specific measurements by confocal microscopy confirmed that depletion with DTx significantly reduced levels of CD11c$^+$ and TCR-β$^+$ staining in granulomas compared with PBS controls (Fig 3.9B). The variation between the results following CD11c depletion suggests that histological quantification of total granulomatous inflammation and confocal measurements of immune cells within the granuloma are complementary but not directly comparable. As such, confocal microscopy provides a method for detailed analysis of specific immune cells as opposed to total granulomatous inflammation. Siglec-F staining was not addressed, as the staining for this marker had not yet been optimised at the time of the experiment.

3.4.8 The structure and composition of granulomas is altered in the absence of CD11c$^+$ DCs at D52

I have shown that the proportion of granulomatous inflammation increased substantially between D42 and D51 of *S. mansoni* infection (Fig. 3.6B), which suggests that the impact of CD11c depletion may be more dramatic at D51 compared with D42. To understand better the role for CD11c$^+$ DCs at later stages of granuloma

formation, $CD11c^+$ cells were depleted from D42 to D51 of infection (Fig. 3.10). Measuring granuloma area at D52 following depletion indicated no change in total granulomatous inflammation comparing infected DTx treated with PBS control animals (Fig. 3.10A). Again, $CD11c^+$ staining in the granuloma was significantly decreased in DTx treated mice compared with controls, confirming depletion of this cell type in these animals (Fig. 3.10B). Interestingly, Siglec-F^+ staining around the egg was also decreased significantly in DTx treated compared with control mice, whereas the apparent reduction in TCR-β^+ staining was not significant. This indicates that although granulomas developed in CD11c depleted animals, the cellular composition of their hepatic granulomas was altered as compared with control animals. Although confocal images revealed that granulomas formed in DTx treated mice, the majority of positive staining for immune cells located to the periphery of the granuloma, depicting a different structure compared with granulomas in control mice (Fig. 3.10C). In particular, the location of TCR-β^+ staining was focused at the periphery rather than throughout every region of the granuloma as in undepleted controls.

3.4.9 The composition of granulomas is altered in *Batf3*$^{-/-}$ mice at D42

To investigate more specifically which DC subsets are important for granuloma formation, we used *Batf3*$^{-/-}$ mice to address the role of $CD8\alpha^+$ cDCs relative to total $CD11c^+$ DCs at D42 of infection. The *Batf3* deficient phenotype will be addressed comprehensively in chapter 4, when the ability of these animals to induce Th2 immune responses will be assessed. Although *Batf3*$^{-/-}$ mice showed no significant alterations in total granulomatous inflammation at this time-point (Fig. 3.11A), a trend for increased fibrosis compared with infected WT mice was observed (Fig. 3.11B). Notably, the proportion of granulomatous inflammation detected in this experiment was higher than in CD11c.DOG control mice at D42 (Fig. 3.9A), and this may be due to variability in the onset of egg production during the infection (i.e. earlier egg production in WT mice shown in figure 3.11 compared with control mice in figure 3.9 would result in advanced granuloma development). The levels of total $CD11c^+$ cells in granulomas were significantly decreased, even though only one subset of DCs was depleted (Fig. 3.11C). As opposed to the global $CD11c^+$ depletion model at D42 (Fig 3.9B), TCR-β^+ staining was unchanged in *Batf3*$^{-/-}$ mice compared

with WT mice as was Siglec-F $^{+}$ staining (Fig. 3.11C). Finally, confocal images of granulomas did not depict obvious differences in granuloma composition when CD8α^{+} cDCs were reduced (Fig. 3.11D), which underlines the value of quantifying the presence of specific immune cells in the granuloma.

3.5 Summary of main results

- The induction of Th2 immune responses in the liver correlated with the arrival of *S. mansoni* eggs and the formation of granulomatous inflammation (Fig. 3.1 & Fig. 3.3).
- The total proportion of granulomatous inflammation did not decrease in parallel with Th2 downmodulation in chronic stages of infection (Fig. 3.1 & Fig. 3.3).
- Granulomatous inflammation, collagen deposition and the arrival of $CD11c^+$, Siglec-F^+ and TCR-β^+ cells in the liver occurred rapidly within a few days around D45 of infection following the onset of egg production (Fig. 3.6 & Fig. 3.7 & Fig. 3.8).
- $CD11c^+$ and TCR-β^+ cells localised in close proximity to each other in the granuloma throughout infection (Fig. 3.5).
- TCR-β^+ staining around the egg in the liver decreased in CD11c depleted mice (CD11c.DOG mice) at D42 (Fig. 3.9), but not D52 (Fig. 3.10).
- The location of TCR-β^+ staining around the egg was focused at more peripheral areas of the granuloma in CD11c deficient mice at D52 of infection (Fig. 3.10).
- The total proportion of granulomatous inflammation in the liver was unchanged in DTx treated CD11c.DOG mice at D42 and D52 (Fig. 3.9 & Fig. 3.10).
- The total proportion of granulomatous inflammation, fibrosis and Siglec-F^+ and TCR-β^+ staining in the liver was unchanged in *Batf3*$^{-/-}$ mice at D42 of infection, but staining for CD11c was reduced (Fig. 3.11).

3.6 Discussion

The work presented in this chapter provides further insight into the intimate relationship between how long the mammalian host has been infected, immune response development and granuloma formation during *S. mansoni* infection. Investigating the role of DCs in these processes revealed that the presence of T cells in the granuloma during *S. mansoni* infection is severely reduced following depletion of $CD11c^+$ cells prior to egg arrival in the liver. Furthermore, the location of T cells was found to be different when $CD11c^+$ cells were depleted a few weeks later and granulomatous processes were already established. In contrast, the absence of $CD11c^+$ $CD8\alpha^+$ cDCs alone did not reduce T cell populations in the granuloma at D42, but decreased the presence of $CD11c^+$ cells substantially. These novel data elevate current understanding of which immune cells are important for granuloma formation, suggesting that DCs are critical for normal T cell presence, and that $CD11c^+$ $CD8\alpha^-$ DCs may play a dominant role in this process.

3.6.1 Granuloma formation during *S. mansoni* infection

The development of $CD4^+$ T cell responses during *S. mansoni* infection is best characterised in the spleen (and to a lesser extent mLNs), and is hallmarked by a switch from mixed Th1/Th2 responses to dominant Th2 responses against the eggs at approximately D42 of infection (Baumgart et al., 2006; Grzych et al., 1991; McKee and Pearce, 2004; Pearce et al., 1991; Taylor et al., 2009) (section 1.8, chapter 1). We have shown for the first time that a similar immune response kinetic occurs in the liver, an important site for egg deposition and pathology during *S. mansoni* infection (Cheever, 1987)*;* analysis of cytokines produced by liver leukocytes from D42 to D56 in response to SEA showed that strong Th2 responses were induced during this time-frame, whereas Th1 responses decreased (Fig. 3.3). In addition, our data indicate that the amount of antigen-specific IL-10 produced by liver leukocytes increased in parallel with Th2 cytokine production. As might have been expected from the ELISA results, qualitative analysis of $CD4^+$ T cell cytokine expression following polyclonal restimulation showed that the ratio of $CD4^+$ T cells from infection that stained positive for Th2 cytokines and IL-10 increased compared with naïve mice from D42 to D56, whereas the fold change of IFN-γ^+ $CD4^+$ T cells decreased. In line with these results, IL-10 production by SEA-restimulated splenocytes has been reported to

increase when Th1 responses decrease during *S. mansoni* infection (Sher et al., 1991). Enhanced IL-10 production is thought to represent increases in Th2 as well as iTreg responses, since these cell types are the main producers of IL-10 during *S. mansoni* infection (Baumgart et al., 2006; McKee and Pearce, 2004). Thus, we have shown that the induction of dominant Th2 and regulatory responses correlates with downmodulation of Th1 responses in the liver, which is in line with the previous literature that has described this type of immune response development in secondary lymphoid organs (Pearce and MacDonald, 2002).

Th2 cytokine production and proliferation in the spleen and liver is downmodulated in more chronic stages of infection (after D56) (Wilson et al., 2007), which is associated with upregulation of GRAIL expression by hyporesponsive $CD4^+$ T cells (Taylor et al., 2009) (section 1.8.2, chapter 1). Th2 downmodulation is an area of active research and is currently thought to be mediated by immune cells including Tregs, B cells and AAMΦs via IL-10 dependent and/or independent pathways (section 1.8.1, chapter 1) (Lundy and Lukacs, 2013; Wilson et al., 2007). Failure to suppress Th2 responses during more chronic *S. mansoni* infection is linked with overt pathology and increased mortality due to uncontrolled Th2 mediated fibrosis and granulomatous inflammation in both human and murine schistosomiasis (Hoffmann et al., 2000; Wynn et al., 2004). Although Taylor *et al.,* (2009) reported a decrease in IL-4 production by hepatic $CD4^+$ T cells at D112 compared with D56, no reports have conducted a detailed kinetic analysis of Th2 cytokine production in the liver during this time-frame. We show that antigen-specific Th2 responses gradually decreased from D56 to D105, whereas IL-10 production relative to naïve animals increased (Fig. 3.3B). As such our data is in line with previously published reports that have described downmodulation of Th2 responses and increased regulatory responses in later stages of infection (Lundy and Lukacs, 2013; Wilson et al., 2007), and we have additionally conducted a more comprehensive analysis of the immune response kinetics in the liver.

Notably, non $CD4^+$ T cell cytokine production plays an important role during the course of *S. mansoni* infection and should not be underestimated (Herbert et al., 2004; Oliphant et al., 2014; Rumbley et al., 1999). For example, $CD8^+$ T cells also produce IFN-γ, and innate immune cells such as NK cells and ILCs are likely to be

contributing to the cytokine pool during infection (Czaja et al., 1989; Frucht et al., 2001; Fuchs et al., 2013; Pedras-Vasconcelos and Pearce, 1996; Shang et al., 2000). Yet, our data as well as previous literature suggest that $CD4^+$ T cells are the main producers of Th1 and Th2 cytokines in response to *S. mansoni* eggs (Fig. 3.3C compared with Appendix Fig. 7.1) (Baumgart et al., 2006; Grzych et al., 1991; McKee and Pearce, 2004; Pearce et al., 1991; Taylor et al., 2009).

By developing a novel technique to objectively determine the proportion of granulomatous tissue within whole liver sections, we were able to assess changes in granulomatous inflammation as $CD4^+$ T cell immune responses develop during the course of *S. mansoni* infection (Fig. 3.1). To our knowledge, this new approach is the first to enable objective quantification of the total burden of granulomatous inflammation and collagen deposition in the liver during *S. mansoni* infection. When investigating hepatic granulomas it is important to consider that new eggs continuously arrive in the tissue (Gryseels et al., 2006; Pearce and MacDonald, 2002), which means that individual granulomas are likely to be at different stages of maturation. Furthermore, multiple eggs in a cluster could pose more of a threat compared with those containing a single egg, and may induce larger and more intense granulomas that take longer to mature and control. Previous techniques that have selected individual granulomas and estimated area or volume based on manually identifying their perimeter potentially bias the readout. In fact, our results show that early granulomas are often irregular (Fig. 3.7A). The technique described in this thesis largely overcomes these caveats, and provides an efficient method for the objective quantification of total granulomatous inflammation at every time-point. Additionally, this quantification method can be utilised in future to measure other tissue components (i.e. lipid accumulation) as long as the feature of interest can be efficiently distinguished from the liver parenchyma.

Using conventional methods for granuloma measurements, various previous studies have reported an increase in granuloma volume or area in the liver when Th2 responses are induced during *S. mansoni* infection (Boros et al., 1975; Haseeb et al., 2001). We have shown that the total proportion of granulomatous inflammation, including the accumulation of inflammatory immune cells and the initiation of fibrosis, increased dramatically from D42 to D56 (Fig. 3.1). This increase in

granulomatous inflammation correlated with the detection of *S. mansoni* eggs in the liver (D42). Together these results indicate that initial granuloma formation in the liver begins at a time-point when there is a mixed Th1 and Th2 immune response (Fig. 3.3), and this supports the literature view that significant increases in the size of granulomas is associated with dominance of Th2 responses (Grzych et al., 1991; Pearce et al., 1991; Pearce and MacDonald, 2002; Vella and Pearce, 1992).

Following the initial formation of granulomas, we have identified that the total proportion of granulomatous inflammation present in the liver markedly increased from D56 to D84 post infection, when a plateau is reached (Fig. 3.1). This suggests that total granulomatous inflammation continues to increase until regulatory responses are well established and Th2 cytokine responses are reduced to levels similar to D28 prior to egg production (Fig. 3.3B) (Lundy and Lukacs, 2013; Pearce and MacDonald, 2002). Moreover, granulomatous inflammation persists following Th2 downmodulation until at least D105. In support of these findings, Hasseeb *et al.,* (2001) report that the volume of individual newly formed hepatic granulomas during *S. mansoni* infection increases from D56 to D70 (later time-points were not analysed). However, other studies have proposed that the size of newly formed granulomas in the lung following egg injection and in the liver during active infection decreases from D56 to approximately D140 (8-20 weeks) (Boros et al., 1975; Colley, 1975). Indeed, it is frequently thought that granuloma size decreases in correlation with the downmodulation of Th2 immune responses during more chronic stages of infection (Lundy and Lukacs, 2013; Wilson et al., 2007). The discrepancies between these studies may reflect the subjectivity in identifying newly formed granulomas for analysis, which are generally determined by pronounced eosinophilia and an intact *S. mansoni* egg (Colley, 1975). This highlights that the kind of quantification method used and the types of granulomas included in the analysis are important factors to consider when measuring granulomatous inflammation.

Our analysis of granulomatous inflammation during later stages of *S. mansoni* infection suggests that a decrease in Th2 responses does not lead to immediate resolution of established granulomas (i.e. collagen degradation) or prevent the formation of new granulomas. Indeed, the formation of new granulomas is required throughout *S. mansoni* infection to protect surrounding hepatocytes from toxins

produced by the egg, as new eggs continuously arrive in the liver (Fig. 3.1) (Gryseels et al., 2006; Pearce and MacDonald, 2002). It is possible that granulomas formed against newly arrived eggs in more chronic stages are smaller than those formed during peak Th2 responses, which is likely due to reduced immune cell aggregation following Th2 downmodulation (Lundy and Lukacs, 2013). Yet, hyporesponsive Th2 cells are detected in the liver at least until D112, which suggests that these cells remain a constituent of the granuloma even though Th2 effector functions are suppressed (Taylor et al., 2009). Moreover, granulomas are thought to exhibit a more fibrotic phenotype containing predominantly thick type I collagen fibres during more chronic stages of infection (Silva et al., 2000), as collagen fibres, fibroblasts and numerous innate immune cells including MΦs remain present in hepatic granulomas when Th2 responses are downmodulated (Lenzi et al., 1998; Silva et al., 2000). Taken together, regulation of Th2 responses in later stages of infection is critical for the prevention of overt Th2 dependent pathology (Hoffmann et al., 2000; Wynn et al., 2004), but granulomas must persist at some level to allow for sufficient protection against egg derived toxins (Dunne et al., 1991; Fitzsimmons et al., 2005). Thus, investigating the development and resolution of the granulomatous response through measurement of total area as performed in this chapter may be a more accurate description of egg-induced pathology in the liver during *S. mansoni* infection compared with the analysis of individual granulomas. This has important implications for understanding the progression of the disease, as inflammatory and fibrotic responses against *S. mansoni* eggs in the liver are responsible for most of the severe pathology experienced by the host (Wynn et al., 2004).

3.6.2 The presence and location of CD11c$^+$ cells during granuloma development

Once the kinetics of the development of granulomatous pathology throughout *S. mansoni* infection was established, we were able to assess the location of specific immune cells within granulomas during the course of infection. Previous studies investigating immune cell location during granuloma formation *in vivo* or *in vitro* have predominantly used light or electron microscopy, which enables analysis of cellular size and morphology (Bentley et al., 1982; Lenzi et al., 1998). By using confocal microscopy and quantifying the positive staining for cell surface markers, we were able to analyse the location and presence of specific immune cells that may

be involved locally in granuloma development during infection. Our data show that clusters of immune cells (including $CD11c^+$ cells) and disorganisation of the parenchyma are visible in the liver before egg arrival (Fig. 3.5A D28). Maturing larval schistosomes are carried by the blood flow through the body before settling in the mesentery and developing to adulthood (Pearce and MacDonald, 2002). Thus, the release of larval and adult antigens into systemic circulation could lead to hepatocyte damage and immune activation in affected areas prior to egg deposition (Hams et al., 2013).

When egg production begins between D28-D42 (Pearce and MacDonald, 2002) (Fig. 3.1B), it is likely that egg-derived antigens are carried in the bloodstream to the liver before the eggs themselves arrive. Additional mechanical injury to the tissue as well as toxic damage is then caused when eggs enter the liver through sinusoids (Doenhoff et al., 1981; Dunne et al., 1991). At this stage immune cell aggregates become more defined and start enveloping the egg (Fig. 3.5A, D42), whilst also creating more space by destroying surrounding damaged hepatocytes (Lenzi et al., 2006) (section 1.7, chapter 1). The kinetic trend for the presence of $CD11c^+$ cells during granuloma formation observed by quantification of surface marker staining detected around the egg by confocal microscopy was similar compared with data from *ex vivo* flow cytometry, and provided an indication of the presence of DCs in the granuloma. Both techniques showed that CD11c expression drastically increased from D42 to D56 (Fig. 3.5), when Th2 cytokine production by liver leukocytes and granulomatous inflammation in the liver were induced (Fig. 3.3). An interesting deviation in the trend observed with flow cytometry and confocal microscopy was found during more chronic stages of infection; $CD11c^+$ cells remained in the granuloma at high levels, as assessed by confocal analysis focusing on granulomas, whereas flow cytometry showed an overall decrease in the number of $CD11c^+$ cells in the liver (Fig. 3.5, D56 – D105). These data highlight one of the advantages of using confocal microscopy quantification techniques over flow cytometry, as the ability to focus on granulomas specifically has raised the possibility that $CD11c^+$ cells remain involved in the granuloma during resolution in chronic stages of infection, even though flow cytometry indicates that their proportions decrease in the whole tissue at these time-points. Overall, our data suggest that DCs play a role in granuloma development

throughout infection, including the progression to more mature and fibrotic granulomas and possibly subsequent resolution of granulomatous inflammation.

The period of infection between D36 and D51 is crucial during *S. mansoni* infection, as this time-frame encompasses the arrival of eggs into the liver and the induction of dominant Th2 immune responses and granuloma formation (Grzych et al., 1991; Pearce and MacDonald, 2002). Thus, this time-course experiment enabled a more detailed analysis of which immune cells are present during initial stages of granuloma development. Eosinophils and MΦs are thought to be the first innate immune cells to arrive in the liver when eggs become lodged in the parenchyma (Lenzi et al., 1998), but the presence of DCs during this process has not been directly addressed. Using confocal microscopy we have shown that $CD11c^+$ cells are present at early stages of granuloma formation (Fig. 3.7, D36), which suggests DCs are possibly amongst the first responders to arrive around the *S. mansoni* egg lodged in the liver parenchyma.

One disadvantage associated with using CD11c as a marker for DCs in the granuloma for analysis by confocal microscopy is that other immune cells express CD11c (Huh et al., 2014; Jakubzick et al., 2006; Niess et al., 2005) (Fig. 3.4). Although CD11c has infrequently been used to identify hepatic MΦs (Davies et al., 2013), high levels of CD11c expression is common by MΦs present in the LP (Niess et al., 2005) and in the lung (Jakubzick et al., 2006). Eosinophils express low levels of CD11c (Huh et al., 2014), but higher levels are found on some thymic eosinophils (Throsby et al., 2000). Thus, we investigated the level of CD11c expression by hepatic MΦs, eosinophils, and DC subsets by flow cytometry to better understand which immune cells are likely detected when using this marker for confocal microscopy analysis. These data indicate that cDCs expressed high levels of CD11c, whereas pDCs and eosinophils expressed only low levels of this integrin. In support of this, previous literature has shown pDCs (Merad et al., 2013) and eosinophils (Huh et al., 2014) to express low levels of CD11c compared with cDCs. Notably, some hepatic MΦs, either monocyte-derived or resident Kupffer cells (Davies et al., 2013), expressed CD11c at similar levels compared with cDCs at D42 of *S. mansoni* infection. Indeed, it has been reported that MΦs detected by confocal microscopy upregulate CD11c in the liver during steatohepatitis, which is a model for liver inflammation (Lloyd et al., 2008). The authors suggested that CD11c is upregulated on resident hepatic $F4/80^+$ $CD11b^-$

MΦs during inflammation, but the possibility that some of these cells may represent a subset of DCs was not addressed. Recently, it has also been shown that hepatic F4/80^{+} CD11c^{high} MΦs can be detected in high frequencies by flow cytometry in *S. mansoni* infected mice (Nascimento et al., 2014). Taken together, CD11c positive staining in the granuloma assessed by confocal microscopy most probably identifies CD11c^{high} cDCs and MΦs, whereas pDCs and eosinophils are not detected with this marker. Given that it is not possible to definitively distinguish cDCs from MΦs by confocal microscopy using CD11c alone, it is conceivable that CD11c expression in the granuloma reflects the presence of both of these cell types throughout granuloma development.

3.6.2.1 Functions of dendritic cells and macrophages in the *S. mansoni* granuloma

Hepatic cDCs and MΦs may exhibit various different functions as the immune response and the granuloma develops during *S. mansoni* infection. Given that DCs are thought to be superior APCs (Steinman, 2012), we hypothesised that DCs play a dual role in directing T cell responses during granuloma formation: DCs may be important indirectly via the priming of CD4^{+} T cells towards a Th2 phenotype in secondary lymphoid tissue, whilst DCs in the liver may support the maintenance of effector/memory CD4^{+} T cells locally (section 3.2.1.1). On the other hand, AAMΦs have been reported to mediate the suppression of Th2 responses in the liver during *S. mansoni* infection via the depletion of Arg-1 (Pesce et al., 2009). This suggests that AAMΦs are not major players in the maintenance of Th2 responses in established granulomas, and instead they exert a level of regulation on effector/memory CD4^{+} T cells indirectly by depleting nutrients that are important for the survival of CD4^{+} T cells (Pesce et al., 2009). Notably, some functions displayed by DCs and MΦs in granuloma formation may overlap. For example, the initial recruitment of inflammatory cells via the production of cytokines to peripheral sites of inflammation is generally a function attributed to CAMΦs (Soehnlein and Lindbom, 2010), but DCs also secrete cytokines including TNF-α and IL-6 in response to LPS (Lacy and Stow, 2011; Morelli et al., 2001). Therefore, it is plausible that in the presence of TSLP and/or *S. mansoni* egg derived antigen cDCs become activated in the liver and recruit inflammatory cells to the granuloma (Paul and Zhu, 2010).

Another aspect of granuloma formation that may be at least in part orchestrated by cDCs and/or MΦs is the synthesis and degradation of collagen. Granuloma formation during *S. mansoni* infection is marked by substantial collagen deposition by HSCs and myofibroblasts (Hams et al., 2013; Wilson et al., 2007), which is thought to provide an organised extracellular network for the bidirectional movement of immune cells from the parenchyma to the egg (Lenzi et al., 2006). It is unlikely that DCs direct collagen synthesis during *S. mansoni* infection, as they have been shown to be inefficient activators of myofibroblasts during experimental liver fibrosis (Pradere et al., 2013). In contrast, the same study reported that MΦs effectively activate the NF-κB pathway in HSCs, which increases HSC survival *in vitro* and *in vivo* and promotes progression into a myofibroblastic phenotype (Pradere et al., 2013). The authors propose that both CAMΦs and AAMΦs may contribute to the promotion of collagen synthesis during experimental fibrosis in the liver. Therefore, MΦs, but not cDCs, may be important to drive initial fibrosis during granuloma formation in *S. mansoni* infection.

During later and more chronic stages of infection, granuloma resolution requires the degradation of fibrotic material and the clearance of dead cells when Th2 immune responses are downmodulated (Lundy and Lukacs, 2013), which is also a function often attributed to MΦs (Wynn and Barron, 2010). In particular AAMΦs are known to be important in wound healing processes in the liver as well as the intestine to prevent sepsis (Herbert et al., 2004) (section 3.2.1). Notably, a role for DCs in collagen degradation has been proposed; DCs mediate the regression of experimental hepatic fibrosis via a matrix metallopeptidase (MMP9) dependent mechanism (MMPs are enzymes that degrade extracellular matrix components) (Jiao et al., 2012). This suggests that cDCs may contribute to collagen degradation during later stages of granuloma development in *S. mansoni* infection. Therefore, $CD11c^+$ cells that were present in later stages of infection as shown by confocal microscopy (Fig. 3.5 D56-D105) may represent both MΦs and cDCs that are involved in granuloma resolution, but a role for DCs in this process during *S. mansoni* infection remains to be established.

In summary, MΦs in *S. mansoni* granulomas are likely important for the initiation and regulation of Th2 dependent fibrosis, and the latter may be orchestrated in part by

indirect suppression of Th2 immune responses (Pesce et al., 2009; Pradere et al., 2013). On the other hand, DCs generally possess an unrivalled ability to present antigen to T cells particularly during T cell priming events (Mildner and Jung, 2014), which suggests that direct interaction with effector/memory T cells is perhaps a more likely function performed by DCs locally in the granuloma.

3.6.3 The kinetics of T cell presence and location in *S. mansoni* granulomas

When eosinophils, MΦs and likely DCs form the initial barrier around the egg during early granuloma formation, the presence of lymphocytes is rare (Lenzi et al., 1998). In agreement with this, confocal analysis of TCR-β^+ staining in this chapter indicates that few T cells are present in the granuloma at this stage compared with $CD11c^+$ cells and Siglec-F^+ cells (Fig. 3.7 D36 - D45). A delay in T cell ingress to the granuloma relative to cDCs, MΦs and eosinophils is likely due to the difference in the core functions of innate and adaptive immune cells during characteristic immune responses against a pathogen: the adaptive immune response is antigen-specific and requires activation mediated by APCs, predominantly DCs, in secondary lymphoid tissues (Janeway and Medzhitov, 2002). As such, DC activation and migration to the LN must occur prior to the arrival of egg antigen-specific $CD4^+$ T cell arrival in the granuloma. The small proportion of T cells present prior to substantial egg antigen-specific effector $CD4^+$ T cell arrival may represent cross-reactive effector/memory T cells responding to antigen from previous parasite life cycle stages (Lukacs and Boros, 1991). Overall, we have provided detailed analysis of the timing of T cell arrival and distribution in the granuloma, which is in line with expectations from previous literature that has shown innate immune cells including eosinophils to surround the egg prior to the detection of lymphocytes (Lenzi et al., 1998).

Confocal data showing the presence of T cells from D45 to D51 suggest that at early time-points relative to granuloma formation antigen primed T cell populations may arrive sequentially into the granuloma, as positive staining for TCR-β increases from D45 to D48, but then rapidly decreases again at D51 (Fig. 3.7B). This kinetic has been previously described *in vivo* during repeated antigen exposure with OVA, when primary antigen stimulation leads to a first "wave" antigen-specific T cell response that is followed by a stronger and faster T cell response when a second antigen dose is

administered (Hutchison et al., 2009). However, this hypothesis seems improbable as continuous antigen exposure in the liver after the onset of egg production likely results in uninterrupted recruitment of T cells to the granuloma. To investigate whether T cell recruitment to the granuloma is in fact staggered, a repeat of this time-course including later time-points could be conducted, and flow cytometric analysis of T cell numbers present in the liver or isolated granulomas during this time-frame would compliment confocal microscopy data.

3.6.4 Eosinophil presence and distribution throughout granuloma development in *S. mansoni* infection

Eosinophils are known to be amongst the first responders in the liver, most likely induced by increased IL-5 production as the Th2 immune response is generated (Chiaramonte et al., 1999; Fallon, 2000; Reiman et al., 2006; Sher et al., 1990). We have also shown that eosinophils were present during initial stages of granuloma formation by using confocal microscopy. Close positioning of eosinophils to the egg suggests a role for this cell type in egg killing, sequestration of toxic components or the formation of an early physical barrier between the egg and surrounding host cells (Olds and Mahmoud, 1980) (James and Colley, 1978) (Fig. 3.5 & 3.7). These functions are probably not specific to eosinophils, however, as eosinophil ablation does not impair granuloma formation (Swartz et al., 2006).

In summary, our data support the concept that granulomatous inflammation against *S. mansoni* eggs lodged in the tissue takes only a few days to initiate (Bentley et al., 1982). The surprisingly rapid accumulation of immune cells and initiation of fibrosis emphasises that pathology during *S. mansoni* infection is induced promptly when the immune response shifts to a dominant Th2 response against the eggs (Grzych et al., 1991). In addition, the data provide depth to current understanding of the kinetics and location of initial immune cell arrival at the egg during *S. mansoni* infection. Although our data implicate D45 specifically as a tipping point in this transition, the exact timing may vary between infections since it likely depends on the maturation of the parasite, the onset of egg deposition, and the consequent initiation and development of a Th2 dominated immune response (Pearce and MacDonald, 2002).

3.6.5 Collagen formation during granuloma development

In addition to the rapid recruitment of immune cells to the granuloma, we have shown that collagen type I and III deposition begins to increase substantially within a short period of time after the onset of egg production at approximately D45 (Fig. 3.8). In support of this finding, a study from 1982 using the *in vitro* granuloma model described in section 3.2.1 has reported the presence of fibroblasts 3 days following initiation of culture, and significant collagen deposition was visible after 9 days (Bentley et al., 1982). The collagen isotype in granulomas is known to change from predominantly type III to type I during murine (Grimaud et al., 1987; Silva et al., 2000) and human (Adnani, 1985) *S. mansoni* infection. Type IV collagen, which is not detected with PSR staining, has also been found in *S. mansoni* granulomas (Silva et al., 2000), but this isotype is less prevalent compared with type I and III collagen (Grimaud et al., 1987). Analysis of PSR stained sections using a microscope polarising filter would allow for differentiation of type I and type III collagen in future, which is observed red and green respectively (Hoffmann et al., 2000; Junqueira et al., 1978; Pauschinger et al., 1999). Furthermore, the analysis of profibrotic genes for α-SMA or collagen type I by PCR, measurement of hydroxyproline content in liver tissue or determining hepatic injury by ALT measurement would provide additional support for fibrotic measurements (Loebermann et al., 2009). This data further underlines the rapid onset of granulomatous inflammation during *S. mansoni* infection.

3.6.6 Are dendritic cells and T cells interacting in the hepatic *S. mansoni* granuloma?

Having established the presence and kinetics of DCs/MΦs, T cells and eosinophils during granuloma development, we assessed the relative location of these cell types. Comparison of $CD11c^+$ cell location with other immune cells by confocal microscopy showed that they were present in close proximity to TCR-β^+ cells at every time-point measured (Fig. 3.5A D28 - D105). This lends support to our working hypothesis that $CD11c^+$ cells are directly interacting with T cells in the granuloma, whereas direct interaction with eosinophils is less likely because Siglec-F^+ cells were found in different locations. Close positioning of $CD11c^+$ and effector/memory T cells may promote the maintenance of Th2 responses in the granuloma during *S. mansoni* infection. Given that MΦs are known to suppress effector/memory Th2 responses

during *S. mansoni* infection, the promotion of $CD4^+$ T cell responses is perhaps more likely performed by DCs (Pesce et al., 2009).

If DCs play a role in the maintenance of effector/memory $CD4^+$ T cells during the initiation of granuloma formation, this could involve recruitment, retention and/or reactivation of antigen-specific T cells. It has been reported that Th2 cells preferentially express the receptor CCR4 compared with Th1 cells *in vitro* (Bonecchi et al., 1998; D'Ambrosio et al., 1998; Sallusto et al., 1998), and human DCs upregulate the expression of CCL17 and CCL22 (ligands for CCR4) upon interaction with TSLP (Fontenot et al., 2009; Ito et al., 2005) (section 1.9.3, chapter 1). A key role for CCR4 expression by human effector/memory $CD4^+$ T cells has been identified *ex vivo* and *in vivo* for the accumulation of effector/memory Th2 cells in allergic airway inflammation during asthma (Yoshie and Matsushima, 2015). Furthermore, it has been proposed that DC derived CCL17 and CCL22 play a critical role in the recruitment of Th2 cells (Perros et al., 2009; Medoff et al., 2009), whereas MΦs have not yet been implicated in this process. It has also been shown that CCL17 or CCL22 depletion reduces the size of pulmonary granulomas during *S. mansoni* infection (Jakubzick et al., 2004). Thus, the expression of CCR4 ligands by DCs may be important for the recruitment of effector/memory Th2 cells to the egg. In support of this hypothesis, the presence of T cells increased in parallel with $CD11c^+$ cells from D45 to D48, whereas Siglec-F^+ cells gradually increased from D36 to D51 (Fig. 3.7B). In addition, this mechanism would also promote close proximity of these cell types within granulomatous inflammation, which may be important for the retention and reactivation of Th2 cells.

A major role of DCs in the homeostasis of $CD4^+$ T cells is thought to be the provision of TCR signalling via peptide loaded MHC-II; naïve $CD4^+$ T cells require peptide complexed MHC-II:TCR interaction for antigen-specific activation, and this type of interaction promotes efficient effector/memory $CD4^+$ T cell reactivation (Boyman et al., 2009) (section 1.4, chapter 1). This suggests that DCs may reactivate effector/memory $CD4^+$ T cells in the granuloma through persistent antigen-specific MHC:TCR stimulation. The level of MHC-II expression on naïve IL-$7R\alpha^+$ DCs is thought to be controlled by the availability of survival cytokine IL-7 (Guimond et al., 2009). An increase in IL-7 leads to decreased expression of MHC-II by IL-$7R\alpha^+$ DCs,

which thereby limits the number of $CD4^+$ T cells that undergo homeostatic proliferation. Indeed, enhanced proliferation of $CD4^+$ T cells in the absence of antigen stimulation occurs *in vivo* when the number of DCs in the system is increased through treatment with Flt3L (Guimond et al., 2009). This process links the number of DCs to the size of $CD4^+$ T cell populations. Thus, continuous MHC:TCR interaction within the granuloma may be required for optimal reactivation as well as regulation of effector/memory $CD4^+$ T cell responses.

In addition to stimulation via the TCR, increasing evidence in the literature points to an important role for co-stimulation in the maintenance of effector/memory $CD4^+$ T cell responses. For example, consistent CD28 ligation *in vitro* maintains IL-4 and IL-5 production by activated $CD4^+$ T cells (Rulifson et al., 1997). Furthermore, ICOS and OX40 interaction promotes $CD4^+$ T cell differentiation, effector function, proliferation, survival and the formation of memory cells (Chen and Flies, 2013). On the other hand, DCs may be involved in the provision of survival cytokines including IL-7, IL-15 and IL-2 to prevent effector T cell apoptosis in the granuloma, as a decrease in the availability of these factors is thought to promote T cell contraction (McKinstry et al., 2010a) (section 1.4, chapter 1). Thus, consistent DC mediated co-stimulation via numerous molecules and the provision of survival cytokines may contribute to the maintenance of Th2 cytokine production and proliferation in the granuloma during *S. mansoni* infection.

In summary, the data in this chapter so far improve our understanding of the possible functions of DCs in the liver during *S. mansoni* infection, as the location of $CD11c^+$ cells support our hypothesis that DCs interact with effector/memory $CD4^+$ T cells in the granuloma, and there are multiple different possible mechanisms that DCs may employ to mediate T cell presence and function in the granuloma. Given that $CD4^+$ T cells are necessary for granuloma formation during *S. mansoni* infection (Amiri et al., 1992; Byram and Lichtenberg, 1977; Cheever et al., 1999; Doenhoff et al., 1981; Dunne and Doenhoff, 1983; Mathew and Boros, 1986), we reasoned that DC mediated effector/memory $CD4^+$ T cell maintenance might be a fundamental requirement for appropriate granuloma development.

3.6.7 The importance of dendritic cells in granuloma formation

To investigate whether DCs are required for the initiation of granulomatous inflammation, we used CD11c.DOG mice to deplete $CD11c^+$ cells and investigate granuloma formation at D42 of infection. Measuring the total proportion of granulomatous inflammation in *S. mansoni* infected CD11c depleted animals did not identify a significant difference compared with control animals (Fig. 3.9A), which indicates that $CD11c^+$ cells are not required for the overall recruitment of granuloma inflammatory cells and the initiation of collagen synthesis. However, there was no significant difference in the proportion of granulomatous inflammation recorded comparing naïve with *S. mansoni* infected animals, which may be due to insufficient granuloma formation in this experiment relative to vascular collagen in naïve animals. This is most likely attributable to the early time-point analysed, as the specific timing of egg production by the parasite can vary in experimental infections. Thus, caution should be taken when drawing conclusions from this result, as changes in the total proportion of granulomatous inflammation may become more evident when granuloma formation is increased.

Given that $CD11c^+$ cells are found in close proximity to T cells in the granuloma during *S. mansoni* infection (Fig. 3.5), we quantified the presence of T cells at D42 by confocal microscopy when $CD11c^+$ cells were depleted. These data show that fewer T cells were present in depleted compared with control animals, which lends further support to our hypothesis that DCs recruit or retain effector/memory $CD4^+$ T cells locally to the granuloma, possibly via DC expression of CCL17 and CCL22 (Jakubzick et al., 2004; Perros et al., 2009; Medoff et al., 2009). To test whether this scenario occurs during granuloma formation, the expression of CCR4 by $CD4^+$ T cells and CCL17/CCL22 by DCs (i.e. in comparison with MΦs) from the liver or preferably from isolated granulomas could be assessed by flow cytometry. Transgenic murine models deficient in CCR4, CCL17 or CCL22, or the administration of αCCR4 or αCCL17/CCL22 antibodies could also be used to test the importance of this interaction for Th2 migration to the granuloma during *S. mansoni* infection *in vivo* (Belperio et al., 2004; Perros et al., 2009; Schuh et al., 2002).

To elucidate whether the requirement for $CD11c^+$ to recruit or retain T cells in the granuloma extends to later stages of development when granulomas are well established, we investigated the impact of CD11c depletion at D52. Given that Th2 responses are induced approximately 10 days earlier, analysis at D52 also represents a relevant time-frame for the assessment of local DC mediated effector/memory Th2 maintenance. The data from this experiment show that neither the proportion of granulomatous inflammation nor T cell presence in the granuloma were altered significantly in depleted animals (Fig. 3.10), indicating that $CD11c^+$ cells are not essential for T cell recruitment or retention at this time-point. However, the location of T cells was focused at more peripheral areas of the granuloma in CD11c deficient animals compared with controls (Fig. 3.10C), which suggests that $CD11c^+$ cells are important to recruit T cells to normal locations in established granulomas. Indeed, CCR4:CCL22 interaction may be important for T cell location, as this type of interaction results in firm binding between $CD4^+$ T cells and DCs using an *in vitro* flow arrest assay described in Wu *et al.,* (2001).

If DCs control the location of T cells within the granuloma, this process would perhaps promote engagement with activated $CD4^+$ T cells to enable effector/memory Th2 reactivation (Wu et al., 2001). This hypothesis is supported by ongoing work in the lab which shows that hepatic T cells displayed impaired Th2 cytokine production in CD11c depleted animals compared with controls at D52 of infection (Dr. Alexander Phythian-Adams, unpublished data). Analysis of $CD4^+$ T cell cytokine expression isolated from granulomas specifically would provide more accurate information on whether Th2 responses are reduced when CD11c cells are depleted. Decreased IL-5 production may explain the reduction of eosinophils observed at D52 (Sher et al., 1990), although the possibility that the administration of DTx has a direct effect on eosinophil populations cannot be dismissed. To exclude this eosinophils in DTx treated wild type animals could be examined (Isaksson et al., 2012). Taken together, the data from CD11c depletion experiments have provided evidence that DCs may be important for the initial recruitment and retention of effector/memory $CD4^+$ T cells to the granuloma, and the ability to do so possibly promotes reactivation or maintenance of Th2 responses in established granulomas. The capacity of DCs to maintain effector/memory $CD4^+$ T cell cytokine production and proliferation will be addressed in chapter 5 by using an OT-II co-culture system.

To extend our understanding of which specific DC subsets may be involved in T cell interactions in the granuloma outlined above, we asked whether CD8α$^+$ cDCs are important for this process. We used *Batf3*$^{-/-}$ mice that specifically lack CD8α$^+$ and migratory equivalent CD103$^+$ cDCs to examine granuloma formation employing the same techniques as before (Hildner et al., 2008). Investigation of the presence of T cells showed that this was not significantly changed in *Batf3* deficient mice at D42 of infection (Fig. 3.11), which points to a more dominant role for other CD11c$^+$ DCs depleted in the CD11c.DOG model including pDCs and CD11b$^+$ cDCs (or CD11c^{high} MΦs) during the recruitment or retention of T cells at this time-point. In addition, eosinophil presence was unchanged in *Batf3* deficient granulomas, which suggests that Th2 responses in these mice are intact and this will be addressed further in chapter 4. However, the presence of CD11c$^+$ cells was significantly reduced in granulomas formed in *Batf3*$^{-/-}$ mice. This decrease in granuloma CD11c expression may reflect the absence of CD8α$^+$ cDCs in the granuloma, indicating that this subset may normally be present at this time-point. However, it is more plausible that CD8α$^+$ cDCs mediate the recruitment or retention of other CD11c$^+$ cells including different DC subsets or MΦs, as CD8α$^+$ cDCs represent a small proportion (approximately 10%) of total CD11c$^+$ cDCs in the spleen and LNs (Hildner et al., 2008). Such a scenario has not been addressed previously in the literature, but recruitment of CD11c$^+$ cells could occur via the soluble factors CD8α$^+$ cDCs are known to produce including IL-12, IFN-α, TNF-α, IL-10 and TGF-β (Bamboat et al., 2010; Hochrein et al., 2001; Martínez-López et al., 2014; Mashayekhi et al., 2011; Pillarisetty et al., 2004; Shortman and Heath, 2010; Yamazaki et al., 2008). A role for TNF-α in the recruitment of inflammatory cells to *S. mansoni* granulomas has been proposed previously, as neutralisation of TNF-α results in decreased granuloma volume at D56 of infection (Hoffmann et al., 1998). Flow cytometric analysis of isolated granulomas from liver would enable the identification of the CD11c$^+$ cell type(s) that is reduced in *Batf3* deficient granulomas in future. Subsequently, the migration capacity of such CD11c$^+$ cells in response to TNF-α or other CD8α$^+$ cDC derived cytokines could be tested *in vitro* using a migration transwell assay (Bertho, 2005).

Taken together, we have provided evidence that the location of CD11c$^+$ cells and T cells may promote direct interaction between these cells types in the granuloma, and

that normal presence of T cells is dependent on $CD11c^+$ cells in early stages of granuloma development. Although the possibility that $CD11c^{high}$ MΦs play a role cannot be dismissed, our data support the hypothesis that DCs may be important for the initial recruitment or retention of T cells to the granuloma. Moreover, we have determined that the involvement of a small subset of DCs, $CD8\alpha^+$ cDCs, is not essential for the recruitment or retention of T cells, which significantly elevates our understanding of which DC subsets are likely interacting with T cells in the granuloma and mediate T cell presence and location.

3.6.8 Limitations of the techniques used and future directions

The use of microscopy for the investigation of granuloma formation in this chapter has provided invaluable insight into the location and presence of immune cells in the liver throughout *S. mansoni* infection, which has furthered our understanding of local immune cell interactions and the importance of $CD11c^+$ cells during granuloma formation. Although microscopy along with the development of novel objective quantification methods in this chapter has proved both powerful and beautiful, various limitations associated with these techniques should be considered.

First, the median and left liver lobe was used to examine granulomatous inflammation in the liver by histology and confocal microscopy respectively, and it was assumed that *S. mansoni* eggs induce comparable granulomatous responses in all liver lobes (left, right, median and caudate lobes). Each liver lobe is thought to perform similar functions including uptake of amino acids, carbohydrates, bile acids, cholesterol, proteins, lipids and vitamins for storage and metabolism (Malarkey et al., 2005). In addition every liver lobe receives blood from the portal vein (Malarkey et al., 2005), which drains the intestines where mature worm pairs produce eggs (Pearce and MacDonald, 2002). This indicates that eggs are delivered into every liver lobe from the portal vein. However, possible variation in the timing of egg arrival or the distribution of eggs cannot be dismissed. Thus, analysis of granuloma formation and development in the right and caudate liver lobes would be advantageous in future to determine how representative granulomatous inflammation in the lobes used in this chapter are of the whole liver. Second, co-localisation analysis (i.e. for CD11c and TCR-β positive staining) was not possible with our confocal photographs due to the

high density of immune cells present in each granuloma, and so we cannot definitively state that these cells are interacting. Live imaging of granulomas in *S. mansoni* infected mice by multiphoton microscopy would enable the observation of cellular movement in the granulomas, which provides a potential tool in future to better understand which cells are in direct contact with each other in the granuloma. In addition, this method could be used to visualise immune cell interaction with the egg in the liver and other potential cellular interactions that we have not addressed.

One disadvantage associated with the use of CD11c.DOG mice is that depletion likely results in a loss of hepatic $CD11c^{high}$ MΦs as well as DCs (van Blijswijk et al., 2013). Therefore, a possible role for MΦs in the mechanisms proposed above in mediating T cell recruitment, retention or reactivation in the granuloma cannot be dismissed. However, CAMΦs are predominantly associated with Th1 responses and are thought to be involved in the recruitment of inflammatory immune cells and in parasite killing (Chensue et al., 1989; Gazzinelli et al., 1992; Oswald et al., 1992), whilst AAMΦs play a role in suppressing Th2 responses and regulating fibrosis during *S. mansoni* infection as mentioned previously (Herbert et al., 2004; Pesce et al., 2009). In agreement with the latter, the loss of hepatic $CD11c^{high}$ MΦs when monocytes are ablated (CCR2-DTR mice) results in enhanced Th2 cytokine production by spleen cells stimulated *ex vivo* with SEA (Nascimento et al., 2014). Thus, it is plausible that DCs are more likely candidates for the induction and maintenance of Th2 immune responses during *S. mansoni* infection. Nevertheless, future work that assesses the distinct functions of DCs and MΦs is required to confirm this hypothesis. To better distinguish DCs from MΦs in the *S. mansoni* granuloma by confocal microscopy in future $Clec9a^{+/cre}Rosa^{+/EYFP}$ mice could be used, which should enable the specific detection of cDC precursor derived cells that constitutively express YFP (Schraml et al., 2013). Although only the $CD8\alpha^{+}$ cDC subset expresses high levels of Clec9a on their surface (see table 1.1), this Cro-loxP system enables the labelling of all cDCs including $CD11b^{+}$ cDCs, that have historically expressed Clec9a (Schraml et al., 2013) (see section 1.2.2.1, chapter 1). Therefore, investigation of YFP expression during granuloma development would further our understanding of the presence and location of DCs specifically during *S. mansoni* infection in future.

Recently, it has been demonstrated that DCs are important for neutrophil homeostasis by regulating the release of neutrophils from the BM (Jiao et al., 2014). The exact mechanism for this was not described, but it is possible that an increase in G-CSF production triggers neutrophil release from the BM after DC depletion (Jiao et al., 2014). This mechanism highlights another potential drawback using the CD11c depletion model, as uncontrolled neutrophil accumulation in hepatic granulomas may impact the formation and immune cell composition of granulomas directly (van Blijswijk et al., 2013). Indeed, neutrophils release ROIs and other cytotoxic factors upon activation, and their presence in hepatic granulomas during *S. mansoni* infection has been associated with severe egg induced immunopathology possibly due to the formation of proinflammatory necrotic lesions (Fallon et al., 2000b; Hirata et al., 2002). To test whether CD11c depletion leads to enhanced neutrophil recruitment to the granuloma during *S. mansoni* infection, the expression Ly-6G in the granuloma could be assessed by confocal microscopy or flow cytometry to identify neutrophils (Daley et al., 2007). Herbert *et al.,* (2004) depleted neutrophils in *S. mansoni* infected mice by administrating a RB6-8C5 monoclonal antibody, which revealed that neutrophils do not play an essential role in mediating the survival of the host. If neutrophilia is increased in CD11c ablated mice, the depletion of neutrophils with RB6-8C5 in this system would help delineate whether neutrophils contribute to impaired Th2 responses and T cell presence and location in CD11c deficient granulomas.

Finally, given that we have identified $CD8\alpha^{+}$ cDCs as non essential players in granuloma formation, the use of transgenic mouse models that are deficient in other DC subsets such as pDCs (i.e. BDCA2-DTR mice or 120G8 antibody administration) or $CD11b^{+}$ cDCs (i.e. CD11c-cre^{pos} $IRF4^{flox}$ or $Flt3L^{-/-}$ mice) would be beneficial in future to dissect which specific DC type is important for effector/memory T cell recruitment/retention/reactivation in the granuloma (Plantinga et al., 2013; Swiecki et al., 2010; Vander Lugt et al., 2014; Wang et al., 2006).

3.7 Conclusion

We have conducted a detailed analysis of the immune response development (Th1 vs. Th2) in the liver throughout *S. mansoni* infection, and found that hepatic granuloma formation increases in parallel with Th2 immune responses upon the onset of egg production by the parasite in this tissue (Pearce and MacDonald, 2002). These data complement previous literature that has outlined the type of immune response induced during *S. mansoni* infection in the spleen (Baumgart et al., 2006; Grzych et al., 1991; McKee and Pearce, 2004; Pearce et al., 1991; Taylor et al., 2009). Our investigation of granulomatous inflammation in more chronic stages of infection revealed that a decrease in granulomatous processes does not occur immediately when Th2 responses are downmodulated. Thus, by developing novel quantification methods for the examination of the total burden of granulomatous inflammation on the liver we have shown that granulomatous processes persist during later stages of infection, which is likely critical for the prevention of damage to the surrounding parenchyma caused by continuous egg arrival in the tissue (Hams et al., 2013).

Visualisation of the presence and location of certain immune cells within the granuloma indicated that $CD11c^+$ cells and T cells reside in close proximity to each other, which provide initial indications that these cells are interacting in the granuloma. Moreover, we show that cDCs and/or CD11c-expressing MΦs play a key role in the recruitment or retention of T cells in the granuloma, as their depletion results in remarkably reduced T cell presence. This was apparent despite incomplete depletion of $CD11c^+$ cells, suggesting that other APCs are unable to substitute for them during granuloma formation. Interestingly, CD11c depletion at later stages of infection did not impair T cell presence but instead altered the location of T cells and the composition of the granuloma, suggesting that cDCs or CD11c-expressing MΦs may be involved in granuloma maintenance after initial formation. Finally, by analysing the impact of *Batf3* deficiency, we could show that $CD8\alpha^+$ cDCs are not important for T cell presence in granulomas, but this subset is required for the appropriate immune cell composition of *S. mansoni* granulomas.

3.8 Figures and tables

Figure 3.1

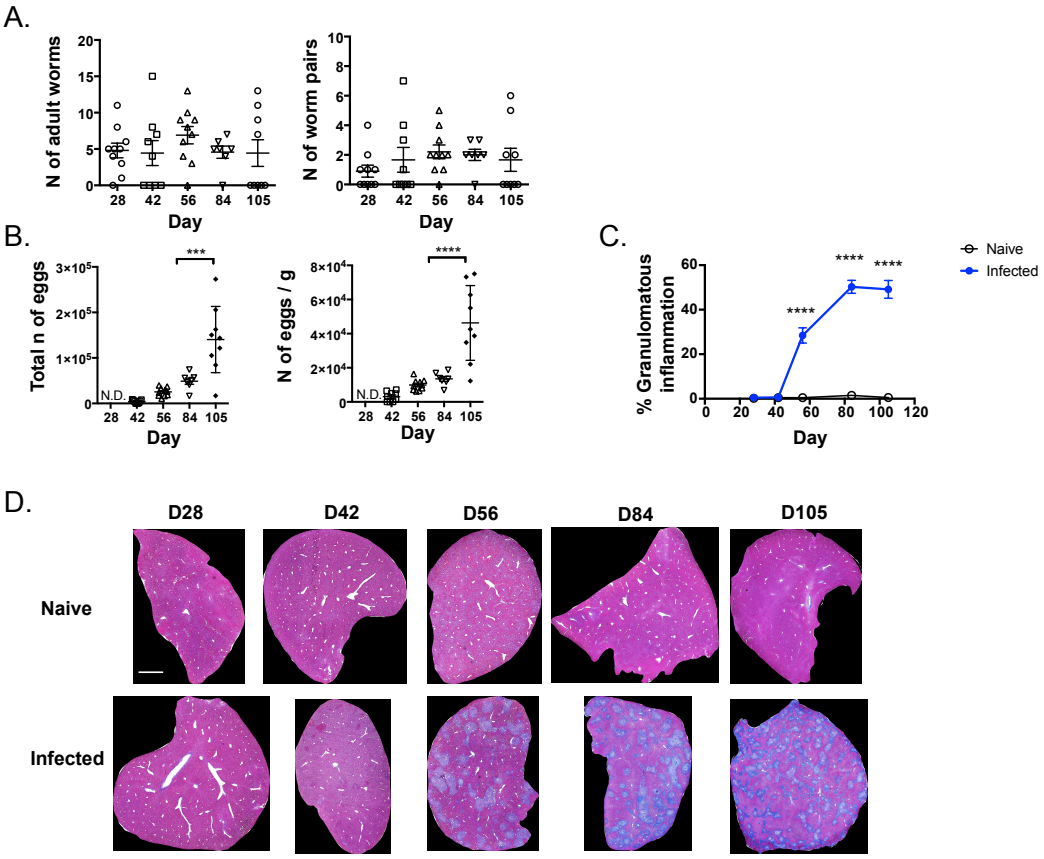

Figure 3.1 Granuloma formation during *S. mansoni* infection is initiated at D42

A. Animals were perfused via the left heart ventricle and exiting the hepatic portal vein to collect adult worms prior to dissection. The number of adult worms and worm pairs was counted using a dissection microscope. **B.** Liver tissue was digested with 4% KOH o/n and schistosome eggs counted. The number of eggs per liver and eggs per gram of liver was determined. N.D. = not detected **C.** The median liver lobe was fixed with 10% NBF and cut into 5 µM sections for staining with MT. The proportion of total granulomatous inflammation represents granulomatous inflammatory cells and type I collagen deposition, which was determined by using an algorithm for objective quantification. **D.** Representative images of liver sections stained with MT used for calculation of total proportion of granulomas per liver section. 1 of 1 (A to D) experiments. Two-way ANOVA (* $P \leq 0.05$, ** $P \leq 0.01$, *** $P \leq 0.001$, ****$P \leq 0.0001$). Bars are SEM of 7-10 mice/group (A-B) and 5 infected and 2 naïve mice/group (C-D).

Figure 3.2

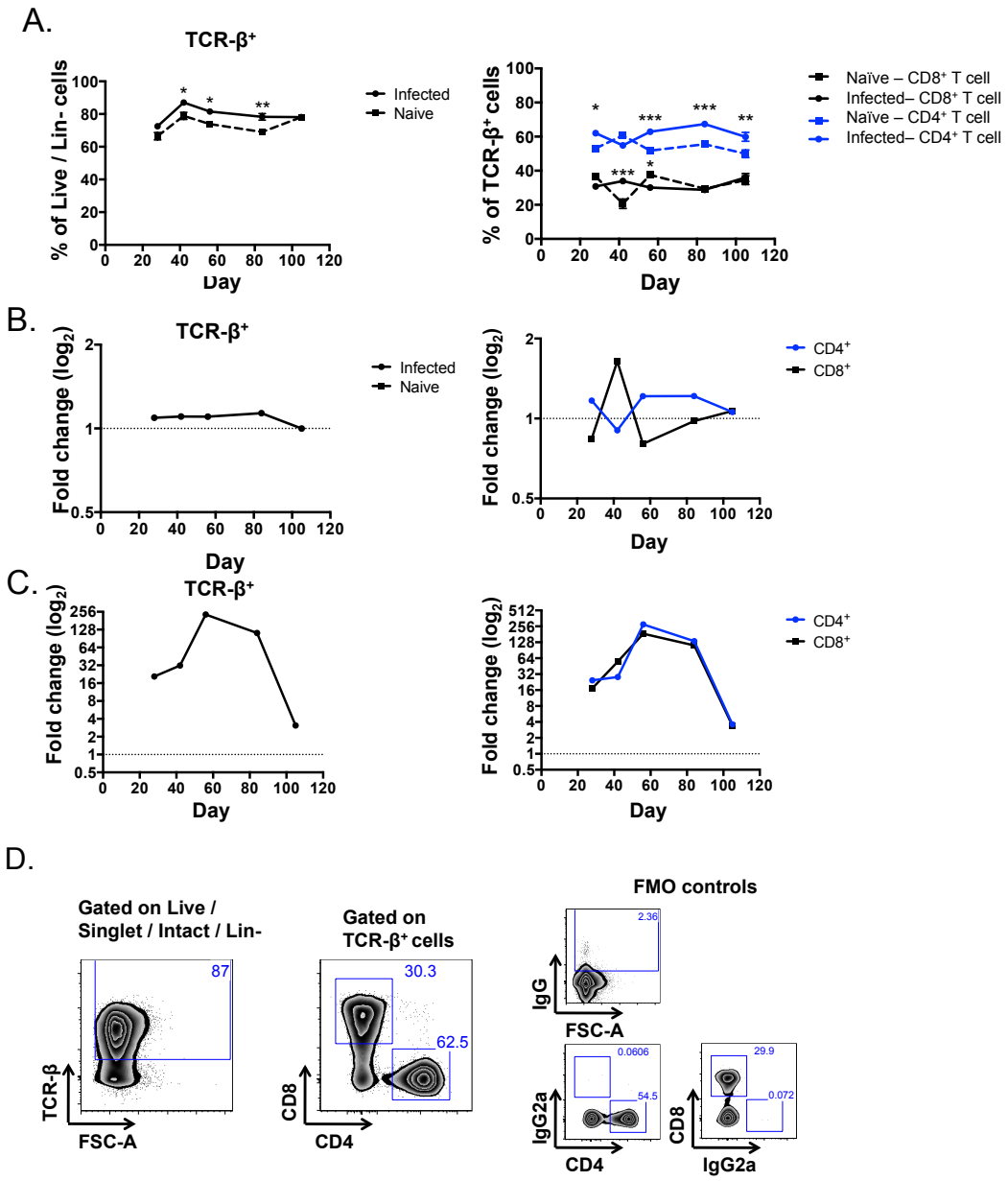

Figure 3.2 T cell populations in the liver at D42 of *S. mansoni* infection

Liver leukocytes from naïve or *S. mansoni* infected mice were isolated. **A.** Liver leukocytes were assessed by flow cytometry for the proportions of total TCR-β^+ of lineage negative cells (Live / Singlet / Intact / Siglec-F^- MHC-II^- $B220^-$ $CD19^-$ $NK1.1^-$ $GR\text{-}1^-$ $CD11b^-$ $PDCA\text{-}1^-$ cells), and $CD4^+$ and $CD8^+$ T cells of TCR-β^+ cells at each time-point. **B-C.** The fold change for the proportion of T cells **(B)** and the numbers of T cells **(C)** was calculated relative to the naïve baseline (dotted line). **D.** Representative flow plots from D56 are shown for *ex vivo* T cell populations per time-point. Gates were set using FMO controls. 1 of 1 (A to D) experiments. Two-way ANOVA (* $P \leq 0.05$, ** $P \leq 0.01$, *** $P \leq 0.001$, ****$P \leq 0.0001$). Statistics were used to compare naïve with infected values. Bars are SEM of 3-4 samples per group. Cells from 2-3 mice were pooled per sample.

Figure 3.3

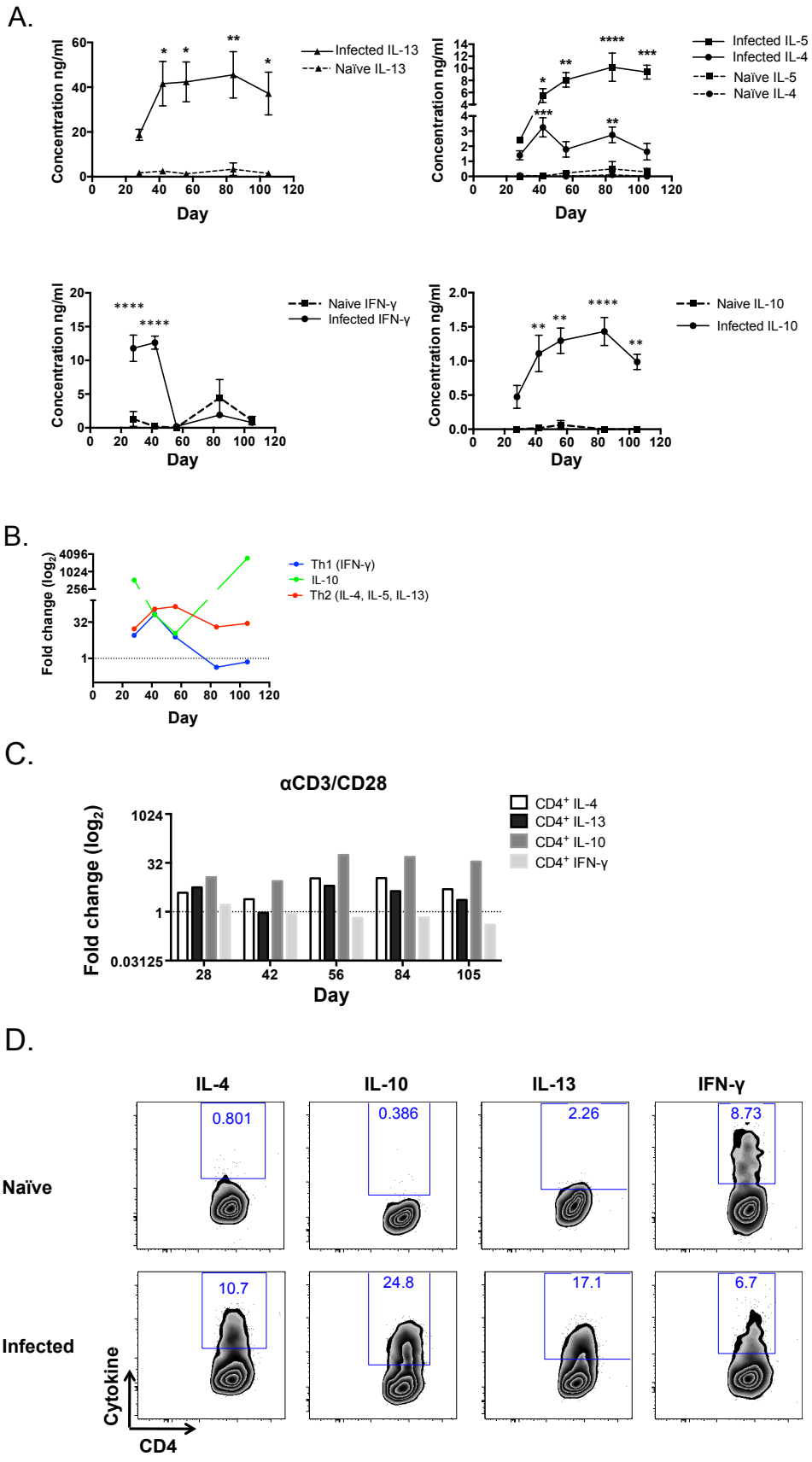
A.
Concentration ng/ml
Day
Infected IL-13
Naïve IL-13
Infected IL-5
Infected IL-4
Naïve IL-5
Naïve IL-4
Naive IFN-γ
Infected IFN-γ
Naive IL-10
Infected IL-10
B.
Fold change (log2)
Th1 (IFN-γ)
IL-10
Th2 (IL-4, IL-5, IL-13)
C.
αCD3/CD28
CD4+ IL-4
CD4+ IL-13
CD4+ IL-10
CD4+ IFN-γ
D.
IL-4
IL-10
IL-13
IFN-γ
Naïve
Infected
0.801
0.386
2.26
8.73
10.7
24.8
17.1
6.7
Cytokine
CD4

Figure 3.3 Th2 responses are induced at D42 of *S. mansoni* infection
Liver leukocytes from naïve or *S. mansoni* infected mice were isolated. **A.** Liver leukocytes were restimulated with SEA in culture for 72h before supernatant harvest and assessment of cytokine levels by ELISA. Background cytokine production detected in samples with medium alone was subtracted from SEA-restimulated values. **B.** As naïve levels of cytokine production varied over the time-course, the fold change compared with the naïve baseline (dotted line) levels was determined to show trends for cytokine production more clearly. The fold change was plotted for Th2, IFN-γ and IL-10 cytokines produced in infection. **C.** Liver leukocytes were restimulated o/n with αCD3/CD28, or medium alone for controls. $CD4^+$ T cell intracellular cytokine production was assessed by flow cytometry, and the fold change was determined as in (B). **D.** Representative flow plots from D56 of ICC are shown for each cytokine. Gates were set using FMO controls. 1 of 1 (A to D) experiments. Two-way ANOVA (* $P \leq 0.05$, ** $P \leq 0.01$, *** $P \leq 0.001$, ****$P \leq 0.0001$). Statistics were used to compare naïve to infected values. Bars are SEM of 3-4 samples per group. Cells from 2-3 mice were pooled per sample.

Figure 3.4

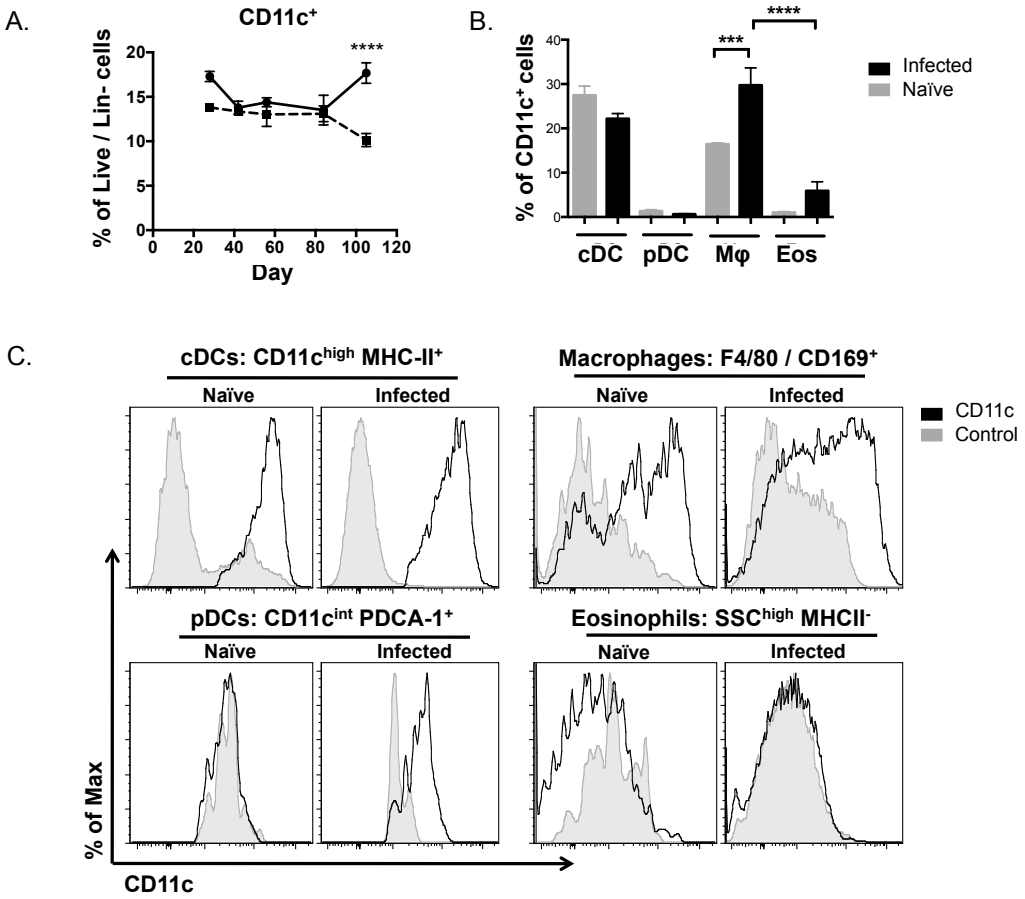

Figure 3.4 Differential CD11c expression on innate immune cells at D42
Livers from naïve or *S. mansoni* infected mice were harvested at D42 and liver leukocytes were isolated. **A.** The proportion of total $CD11c^+$ cells in the liver during *S. mansoni* infection was determined *ex vivo* by flow cytometry. **B**. The proportion of cDCs, pDCs, macrophages (MΦ) and eosinophils (Eos) expressing CD11c is shown for D42 of infection. **C**. Flow plots are shown for the GMFI for CD11c expression at D42 of infection by the cell types analysed in (B). The FMO control for each group is shown in grey. 1 of 1 (A to C) experiments. One-way ANOVA (* $P \leq 0.05$, ** $P \leq 0.01$, *** $P \leq 0.001$, ****$P \leq 0.0001$). Bars are SEM of 3-4 samples per group. Cells from 2-3 mice were pooled per sample.

Figure 3.5

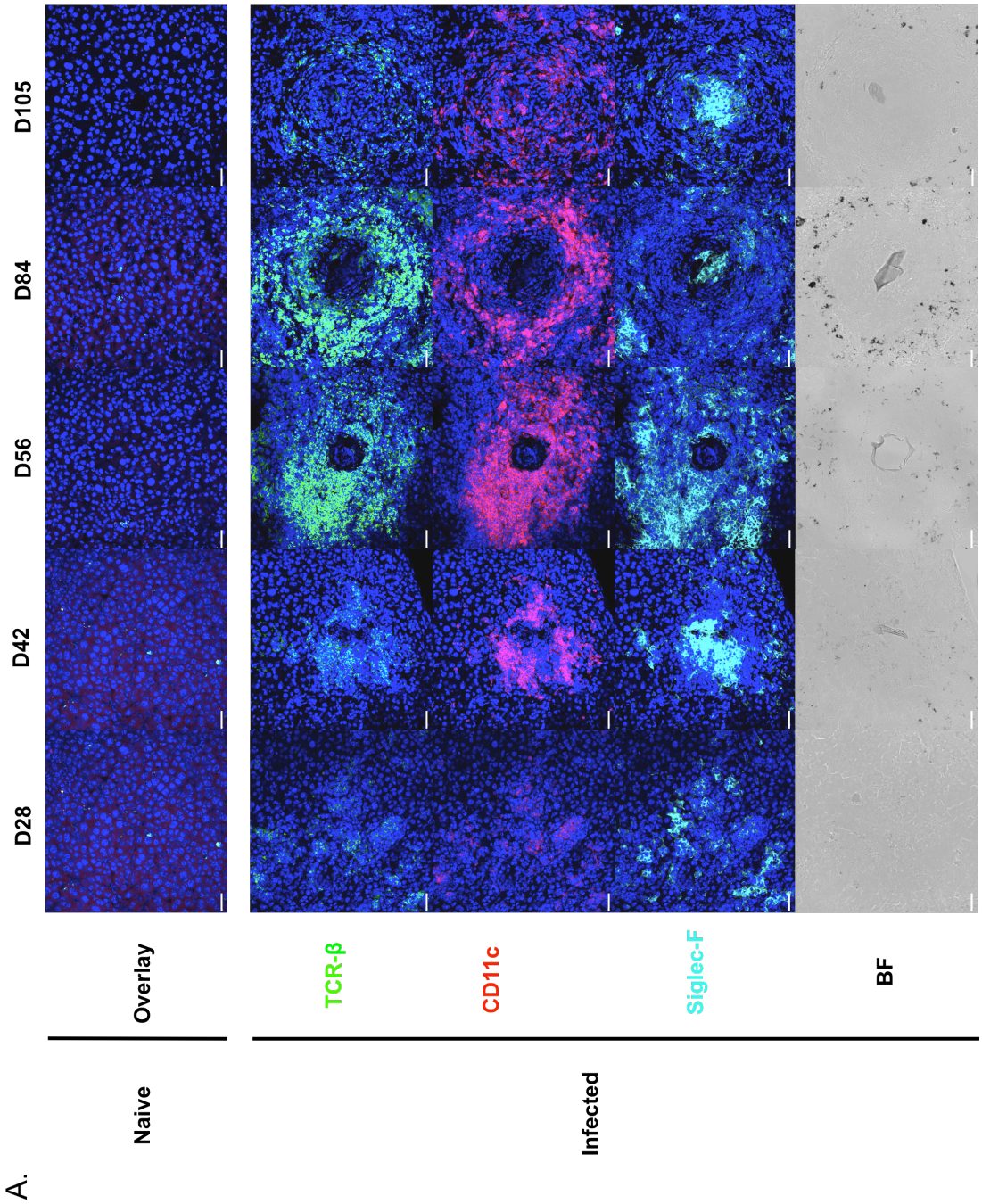
A.
Naive
Infected
Overlay
TCR-β
CD11c
Siglec-F
BF
D28
D42
D56
D84
D105

Figure 3.5

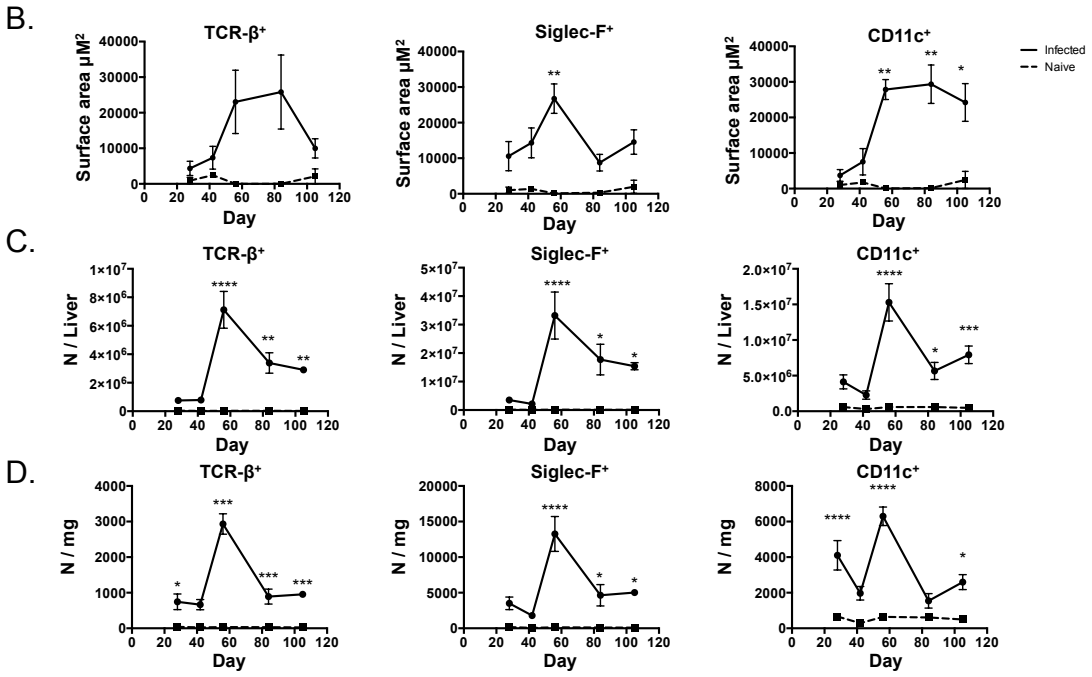

Figure 3.5 CD11c$^+$ and TCR-β$^+$ cells locate to similar areas in the granuloma

Liver tissue from the left liver lobe was embedded in OCT and cut into 20 µM sections. Cryosections were fixed in acetone and stained for confocal microscopy. **A.** Representative confocal microscopy images depict granuloma development throughout the infection. Scale = 39µM. **B.** To quantify the data, the surface area of positive staining around the egg was measured for TCR-β, CD11c and Siglec-F using Volocity imaging software. Only single egg granulomas were photographed. **C - D.** Using values acquired by flow cytometry, the total numbers and numbers / mg of tissue for TCR-β$^+$, Siglec-F$^+$ and CD11c$^+$ cells were calculated for each time-point. 1 of 2 (A) and 1 of 1 (B - D) experiments. Two-way ANOVA (* $P \leq 0.05$, ** $P \leq 0.01$, *** $P \leq 0.001$, ****$P \leq 0.0001$). Bars are SEM of 3 granulomas for naïve and 10 granulomas for infected tissue samples per group. Photos were taken from 3 naïve and 5 *S. mansoni* infected mice.

Figure 3.6

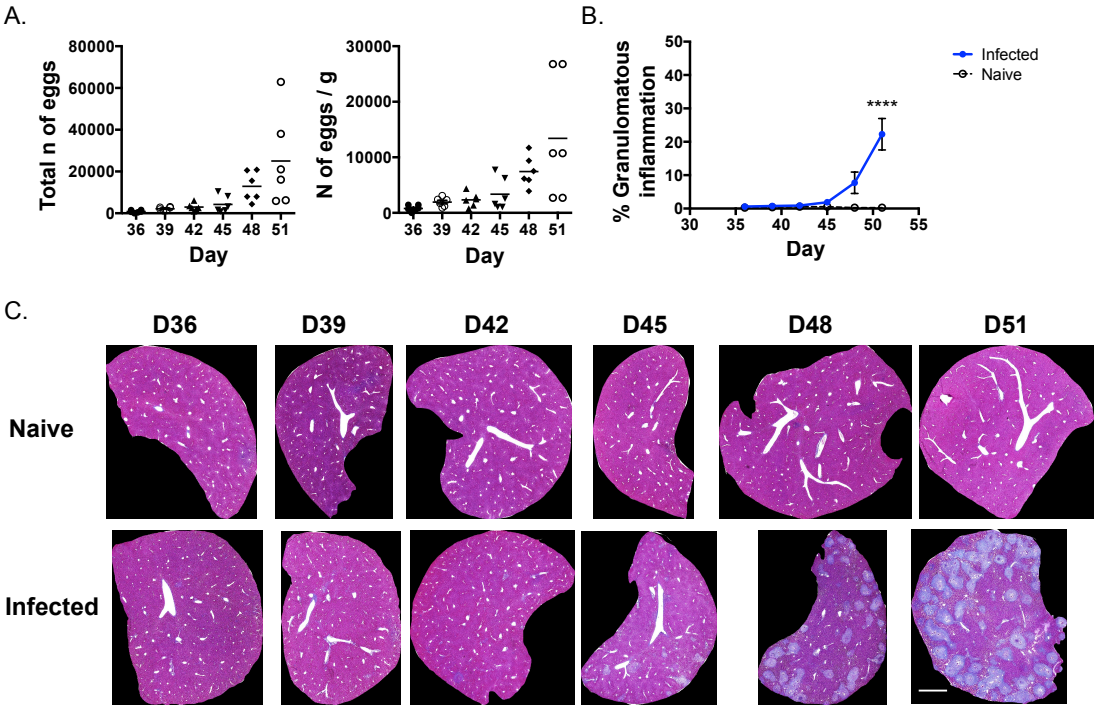

Figure 3.6 Granulomatous pathology increases rapidly during infection
Livers from *S. mansoni* infected mice were harvested at D36, D39, D42, D45, D48 and D51. **A.** The total number of eggs deposited in the caudate liver lobe were counted and used to determine the number of eggs per gram of tissue **B.** The proportion of granulomatous inflammation in the median liver lobe was measured for each time-point **C.** Representative images of liver sections stained with MT are shown for naïve and *S. mansoni* infected mice. Scale = 1 mm. Two-way ANOVA (* $P \leq 0.05$, ** $P \leq 0.01$, *** $P \leq 0.001$, ****$P \leq 0.0001$). Bars are SEM of 3 naïve and 6 infected mice per group. 1 of 2 (A) and 1 of 1 (B to C) experiments.

Figure 3.7

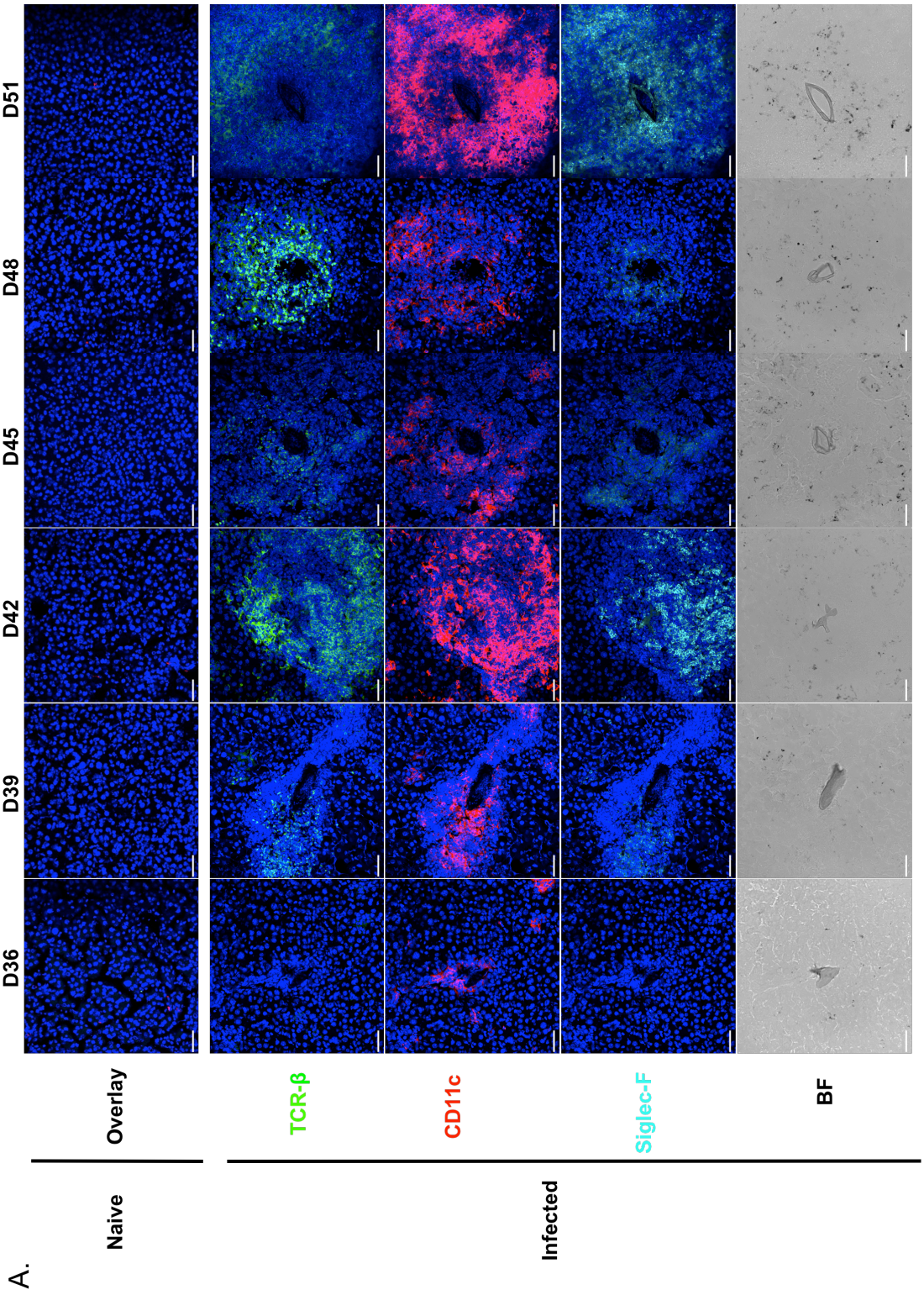
A.
Naive
Infected
Overlay
TCR-β
CD11c
Siglec-F
BF
D36
D39
D42
D45
D48
D51

Figure 3.7

B.

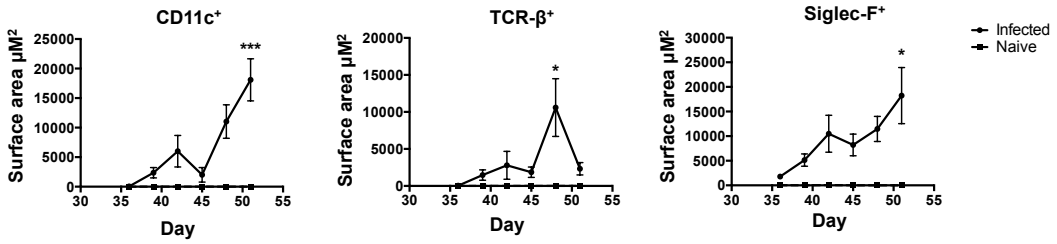

Figure 3.7 Visualisation and quantification of immune cells during granuloma formation

At the time-point of granuloma formation, confocal microscopy was used to investigate the presence and location of TCR-β^+, CD11c$^+$ and Siglec-F$^+$ cells every 3 days from D36-D51 in the left liver lobe. **A.** Representative confocal microscopy images are shown for liver sections from naïve and infected animals. Scale = 48µM. **B.** Quantification of positive staining on confocal images displays the kinetics of TCR-β^+, Siglec-F$^+$ and CD11c$^+$ staining during initial granuloma development. 1 of 1 (A to B) experiments. Two-way ANOVA (* $P \leq 0.05$, ** $P \leq 0.01$, *** $P \leq 0.001$, ****$P \leq 0.0001$). Bars are SEM of 3 granulomas from naïve mice and 10 granulomas from infected mice per group. Photos of granulomas were taken from 3 naïve and 6 infected animals.

Figure 3.8

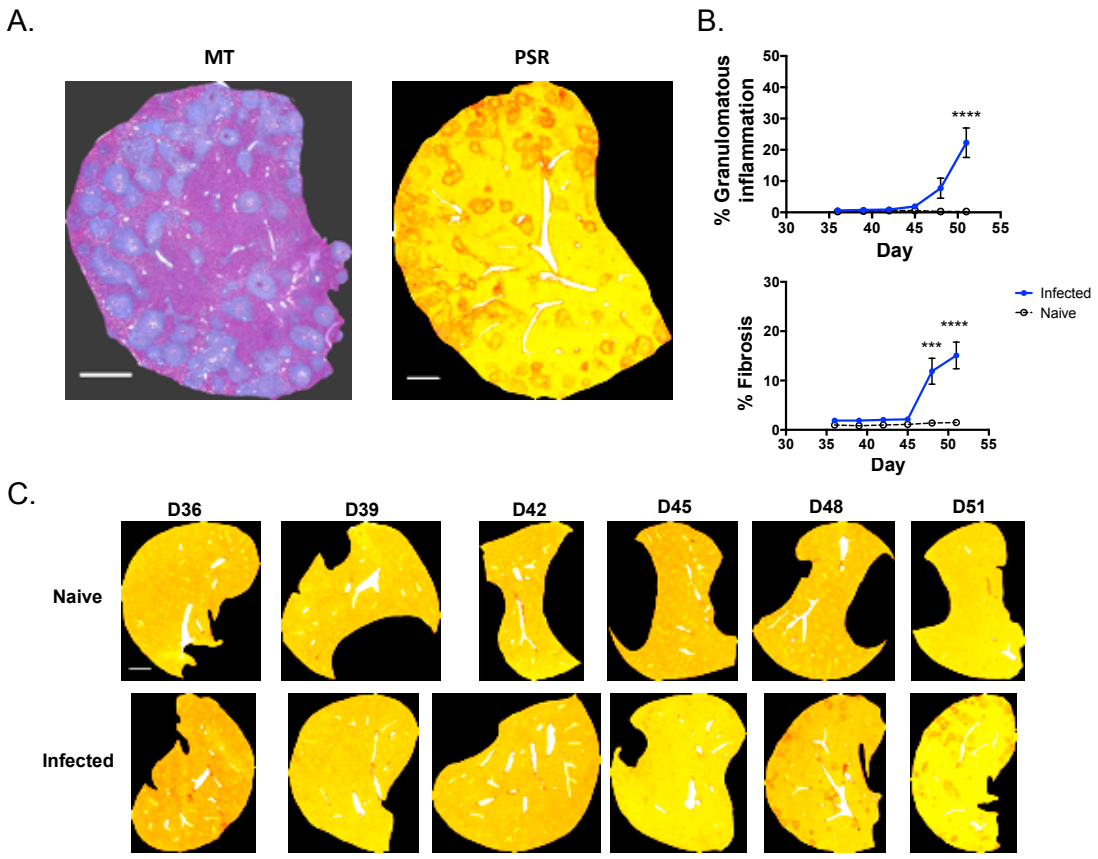

Figure 3.8 Collagen deposition begins in early stages of granuloma formation

A. Representative BF images are shown of tissue sections from the same median liver lobe stained with MT and PSR to compare total granuloma area staining (blue) with collagen deposition staining (red) respectively. Granulomas stained with MT appear as different shades of blue, bright blue staining most likely depicting type III collagen and pale blue highlighting other features of the granuloma. Scale = 1mm. **B.** Collagen deposition on PSR stained slides was measured using imaging software to provide an objective measurement of fibrosis. This showed a comparable trend compared with granulomatous inflammation (granulomatous inflammation graph previously shown in Figure 3.6). **C.** Representative images are shown for PSR stained liver sections from naïve and infected animals. Scale = 1mm. 1 of 2 (A to C) experiments. Two-way ANOVA (* $P \leq 0.05$, ** $P \leq 0.01$, *** $P \leq 0.001$, ****$P \leq 0.0001$). Bars are SEM of 3 naïve and 6 infected mice per group.

Figure 3.9

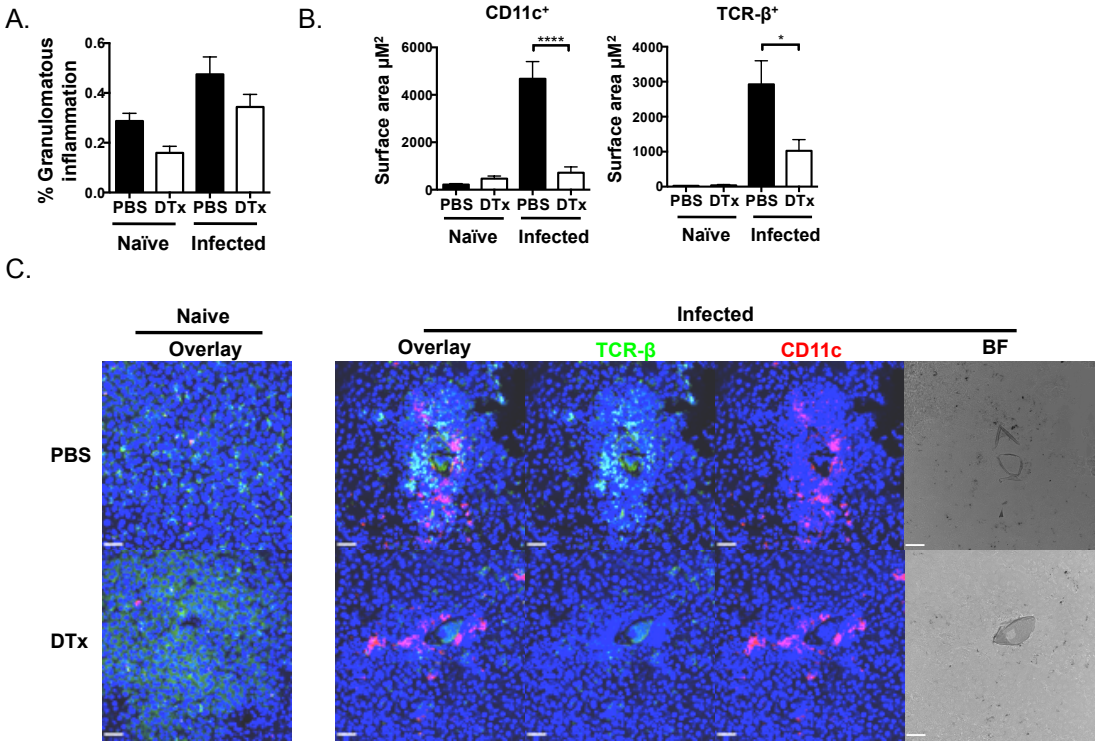

Figure 3.9 T cell presence in granulomas is reduced in the absence of CD11c$^+$ DCs at D42

CD11c.DOG mice were treated daily with DTx for CD11c depletion or PBS for controls from D29 to D40 of *S. mansoni* infection. Livers were harvested at D42 of infection. **A.** The total proportion of granulomatous inflammation from MT stained median liver lobe sections was determined. Very few granulomas were present in the tissue resulting in unchanged granuloma area in infection compared with background values. **B.** The surface area of CD11c and TCR-β staining around the egg in left liver lobe sections was measured to compare the presence of CD11c$^+$ cells and T cells in the granuloma of WT vs. CD11c depleted mice. **C.** Representative confocal overlay and BF images are shown for naïve and infected animals treated with either PBS or DTx. Scale = 39 µM. 1 of 1 (A to B) and 1 of 2 (C) experiments. Two-way ANOVA (* $P \leq 0.05$, ** $P \leq 0.01$, *** $P \leq 0.001$, ****$P \leq 0.0001$). Bars are SEM of 25 granulomas per group. Photos were taken from 2 naïve mice or 5 infected mice.

Figure 3.10

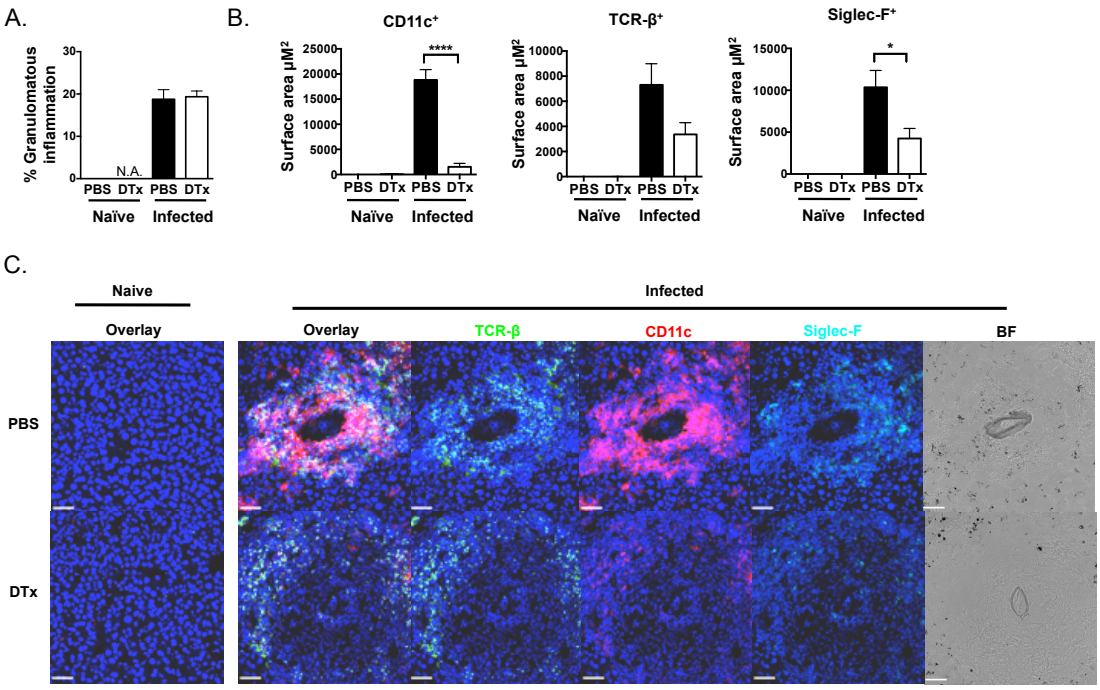

Figure 3.10 Depletion of CD11c$^+$ cells alters granuloma composition at D52

CD11c.DOG mice were treated daily with DTx for CD11c depletion or PBS for controls from D42 to D51 of *S. mansoni* infection. **A.** The total proportion of granulomatous inflammation in WT and depleted animals was determined using MT stained median liver lobe sections. **B.** Quantification of CD11c, Siglec-F and TCR-β staining enabled the comparison of these cell types in granulomas in the left liver lobe formed in WT and depleted animals. **C.** Representative confocal overlay and BF images are shown for naïve and infected animals treated with either PBS or DTx. Granulomas of DTx treated animals appear structurally distinct from PBS controls. Scale = 48 µM. 1 of 1 (A to C) experiments. Two-way ANOVA (* $P \leq 0.05$, ** $P \leq 0.01$, *** $P \leq 0.001$, ****$P \leq 0.0001$). Bars are SEM of 20 granulomas per group. Photos were taken from 3 naïve mice or 4 infected mice. N.A. = Not available.

Figure 3.11

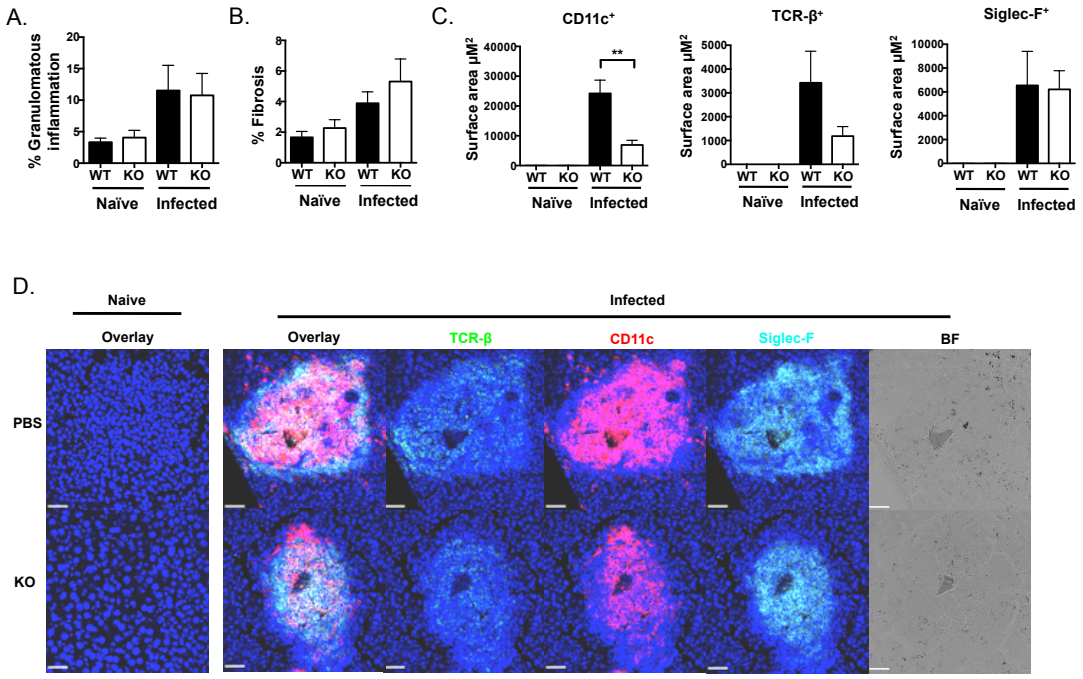

Figure 3.11 Granuloma formation in the absence of CD8α^{+} DCs at D42
A. The total area of granulomatous inflammation was measured using MT stained median liver lobe sections in WT and *Batf3*$^{-/-}$ mice at D42 post infection with *S. mansoni.* **B.** The level of fibrosis in WT and *Batf3*$^{-/-}$ mice were examined using PSR stained median liver lobe sections. **C.** Granulomas were assessed for the surface area of positive staining for TCR-β, CD11c and Siglec-F in the left liver lobe using imaging software. **D.** Representative confocal overlay and BF images are shown for naïve and infected WT and *Batf3*$^{-/-}$ animals. Scale = 48 µM. 1 of 1 (A to D) experiments. Two-way ANOVA (* $P \leq 0.05$, ** $P \leq 0.01$, *** $P \leq 0.001$, ****$P \leq 0.0001$). Bars are SEM of 20 granulomas per group. Photos were taken from 3 naïve or infected mice.

4 CD8α$^+$ cDCs are not required for the induction of Th2 immune responses during *S. mansoni* infection

4.1 Abstract

In helminth infection DCs direct T cell responses towards a Th2 phenotype, providing an essential link between innate and adaptive immunity. However, the specific cDC subsets involved, and the precise mechanisms they use to induce a Th2 response, remain unclear. Using a murine model of *Schistosoma mansoni* infection we have previously shown that CD11c$^+$ DCs are required for Th2 induction (Phythian-Adams et al., 2010). To improve our understanding as to which CD11c$^+$ DC subsets are important for this process we have used *Batf3*$^{-/-}$ mice, which are deficient in CD8α$^+$ and migratory CD103$^+$ CD11b$^-$ cDCs (Hildner et al., 2008). CD8α$^+$ DCs have emerged as essential APCs for antigen cross-presentation and in the generation of Th1 immunity, but their function in a Th2 setting is currently unknown. *S. mansoni* egg injection and infection of *Batf3*$^{-/-}$ mice suggests that immune responses against the eggs were dysregulated in the absence of CD8α$^+$ cDCs; Th2 immune responses were enhanced and Th1 responses impaired. The data indicated that CD8α$^+$ cDCs are not a fundamental requirement for Th2 induction, although they are required for the induction of balanced immune responses against *S. mansoni*.

4.2 Introduction

It has been shown that DCs are sufficient to induce Th2 immune responses *in vivo* (Perona-Wright et al., 2006), and our laboratory published that $CD11c^+$ DCs are necessary for the induction of a Th2 response during *S. mansoni* infection (Phythian-Adams et al., 2010). However, it remains unclear which specific $CD11c^+$ DC subsets are essential for appropriate Th2 induction, and whether the type of DC required changes depending on the stage of infection. One of these candidates is the $CD8\alpha^+$ cDC subset, and the role of this particular DC during the induction of immune responses to *S. mansoni* infection will be investigated in this chapter. $CD8\alpha^+$ cDCs (and their $CD103^+$ migratory counterparts) have emerged as important players in cross-presentation to $CD8^+$ T cells and Th1 responses against acute viral or bacterial infections (Edelson et al., 2010; Hildner et al., 2008; Mashayekhi et al., 2011; Torti et al., 2011; Waithman et al., 2013) (Diagram 4.1). In addition, there is some evidence to suggest that $CD8\alpha^+$ cDCs are involved in the induction of Tregs in the steady state through endogenous production of TGF-β (Scott et al., 2011; Yamazaki et al., 2008). However, the role of $CD8\alpha^+$ cDCs during the induction of Th2 immune responses in an infection setting, i.e. whether this subset promotes, inhibits or regulates Th2 responses, remains largely unknown (see diagram 4.1).

In chapter 3, we have shown that the proportion of hepatic granulomatous inflammation was unchanged in *Batf3*$^{-/-}$ mice at D42 of *S. mansoni* infection (Fig. 3.11). This result suggests that Th2 immune responses were not impaired in *Batf3*$^{-/-}$ mice, as impairment in the Th2 response such as in MHC-$II^{-/-}$ (Hernandez et al., 1997) and $STAT6^{-/-}$ (Kaplan et al., 1998) mice often correlates with reduced granuloma formation. Given the importance of $CD8\alpha^+$ cDCs during the induction of Th1 immune responses against viral and bacterial infection, it is perhaps more likely that $CD8\alpha^+$ cDCs play a critical role during the induction of Th1 responses in *S. mansoni* infection, particularly during early stages of infection when there is a mixed Th1/Th2 immune response (Pearce and MacDonald, 2002). Thus, we hypothesised that $CD8\alpha^+$ cDCs might not be required for the induction of Th2 responses per se, but may play a role in the development of appropriately mixed Th1 and Th2 immune responses to *S. mansoni* infection. In support of this hypothesis, recent publications investigating

allergic Th2 responses (Engler et al., 2014) and immune responses against *L. major* (Ashok et al., 2014) have provided initial insight into the possible functions of CD8α$^+$ cDCs during the induction of Th2 responses. For instance, *Batf3*$^{-/-}$ mice display decreased Th1 responses against infection with *L. major*, rendering these mice more susceptible to the disease, which is controlled in particular by IFN-γ and IL-12 (Ashok et al., 2014). The authors also reported that Th2 and Th17 responses, as well as levels of the antibody isotype IgE in the serum, are enhanced in *L. major* infected *Batf3*$^{-/-}$ mice (Ashok et al., 2014). Furthermore, it has been shown that CD8α$^+$ cDCs play a role in the modulation or regulation of Th2 immune responses during allergic airway inflammation with *H. pylori* (Engler et al., 2014). Yet, the exact mechanisms that CD8α$^+$ cDCs may employ to regulate or inhibit Th2 responses in this setting, and whether CD8α$^+$ cDCs are important during the induction of Th2 responses during chronic helminth infection, have not yet been addressed.

4.2.1 The *Batf3*$^{-/-}$ mouse – advantages and disadvantages

Batf3 is an AP-1 transcription factor (Murphy et al., 2013), which forms a heterodimer with Jun before binding AP-1 (Iacobelli et al., 2000). *Batf3* is essential for the development of CD8α$^+$ cDCs (Hildner et al., 2008), and *Batf3*$^{-/-}$ mice are an excellent tool for investigating the role of this subset in infection settings. Aspects of CD8α$^+$ cDC biology have been ably demonstrated in studies using *Batf3* deficient animals, including those mentioned above (Ashok et al., 2014; Engler et al., 2014) and others discussed in section 1.2.2.1 in chapter 1, but as with any biological model it is important to understand the potential drawbacks when using the model in order to draw the correct conclusion from the results.

Firstly, the initial study using *Batf3*$^{-/-}$ mice on a 129SV genetic background showed complete deficiency of CD8α$^+$ cDCs (Hildner et al., 2008), but it has since been reported that this subset is absent in the spleen and mediastinal LNs but not skin draining iLNs of C57BL/6 *Batf3*$^{-/-}$ mice (Edelson et al., 2011; Waithman et al., 2013). Secondly, *Batf3*-independent mechanisms through non-AP-1 factors, such as IRF4 and IRF8, can induce reconstitution CD8α$^+$ cDCs in a Th1 infection setting (Tussiwand et al., 2012). These compensatory mechanisms are driven by cytokines IL-12 and IFN-γ that induce the expression of transcription factors *Batf* and *Batf2*, which are related to *Batf3* and are important for the development of Th17 (Schraml et

al., 2009) or a subset of lung resident DCs and MΦs (Tussiwand et al., 2012) respectively. *Batf* and *Batf2* compensate for the loss of *Batf3* by binding to non-AP1 factors through shared leucine-zipper domains that function as a leucine rich dimerisation domain (Tussiwand et al., 2012). It would not be unreasonable to hypothesize that the low level of the Th1 relative to Th2 responses in *S. mansoni* infection is insufficient to cause the reconstitution of $CD8\alpha^+$ cDCs (Pearce and MacDonald, 2002), unlike scenarios where robust Th1 responses are present, such as during viral or bacterial infections (Murphy et al., 2013; Tussiwand et al., 2012). Yet, confirming the loss of $CD8\alpha^+$ cDCs in *Batf3*$^{-/-}$ mice in our system and verifying the level of this subset in the tissues of interest after infection with *S. mansoni* is essential.

Overall, *Batf3*$^{-/-}$ mice remain a powerful tool for investigating the function of $CD8\alpha^+$ cDCs, as the specificity for the loss of this subset is unrivalled by other models such Clec9a.DTR (Piva et al., 2012) and CD205.DTR (Fukaya et al., 2012) inducible systems (see table 1.2). Therefore, the *Batf3*$^{-/-}$ model does not suffer from typical limitations including deficiency of additional cell types or the requirement to use radiation BM chimera mice (i.e. mice that have been heavily irradiated and reconstituted with cells from a genetically different mouse). Thus, we felt that *Batf3*$^{-/-}$ mice were an excellent model to use in the investigation of the specific functional role of $CD8\alpha^+$ cDCs during the induction of Th2 responses against *S. mansoni* infection.

4.3 Study rationale

In this chapter the induction of Th2 immune responses against *S. mansoni* eggs using an egg injection model was examined in C57BL/6 *Batf3*$^{-/-}$ mice, which constitutively lack CD8α^{+} cDCs (Hildner et al., 2008). This provided a tool to assess the immune responses in these mice in an acute model of Th2 induction in the absence of cross-reactive antigens normally found in infection, which is representative of a primary response to *S. mansoni* eggs *in vivo*. The importance of CD8α^{+} cDCs during Th2 induction was investigated, revealing whether they inhibit, promote or regulate Th2 responses. In addition, the role of CD8α^{+} cDCs for Th1 induction against *S. mansoni* eggs was addressed. The kinetics of the response to injected *S. mansoni* eggs were examined to investigate whether the lack of CD8α^{+} cDCs shifts the timing of immune responses in *Batf3*$^{-/-}$ mice. Thus, this experimental egg injection model granted analysis of the importance of CD8α^{+} cDCs during Th2 induction prior to assessing their role during *S. mansoni* infection.

To ascertain the importance of CD8α^{+} cDCs in the initiation of Th2 responses during chronic natural infection, *Batf3*$^{-/-}$ mice were infected with *S. mansoni,* and the development of the immune response was analysed at D42 of infection. *S. mansoni* induces a strong Th2 immune response against the eggs at this time-point (Pearce and MacDonald, 2002), which makes this parasite an excellent tool to investigate Th2 priming in an infection setting. The deposition of eggs and formation of granulomas in the liver and intestine leads to severe detrimental pathology during the progression of the *S. mansoni* infection (Wynn et al., 2004) (section 1.6 & 1.7, chapter 1). To elucidate whether CD8α^{+} cDCs play a role during pathological processes associated with egg deposition, granulomatous inflammation was investigated in the liver and intestine of *Batf3*$^{-/-}$ mice *S. mansoni* infection. The analysis of pathology was conducted at D42 as well as D52, as the latter represents a time-point when granulomatous inflammation is more prevalent (Pearce and MacDonald, 2002).

4.4 Results

4.4.1 CD8α$^+$ cDCs are reduced in the popliteal lymph nodes of *S. mansoni* egg-injected *Batf3*$^{-/-}$ mice

To model an acute Th2 immune response an egg injection experiment was carried out to determine the impact of CD8α$^+$ cDC deficiency on the Th2 response normally generated against *S. mansoni* eggs in the popliteal LNs (pLNs) (i.e. the dLN). iLNs (i.e. non draining LNs (ndLN)) were additionally harvested and analysed in the same way as the pLNs to control for responses primed against *S. mansoni* eggs in the pLN. The proportion of CD11c$^+$ MHC-II$^+$ cDCs that was also CD8α$^+$ in the pLNs and iLNs of WT mice was assessed by flow cytometry (Fig. 4.1A). To distinguish the CD8α$^+$ cDC subset from other cDCs expressing high levels of CD11c and MHC-II, CD205 was used as an additional marker (Hildner et al., 2008). To further ascertain the identity of CD8α$^+$ cDCs in the LNs analysed, CD8α$^+$ CD205$^+$ cDCs from WT mice were shown to be CD11b^{low}, CD103$^+$ and CD24^{high} based on work shown in Hildner *et al.*, (2008) (see table. 1.1). In addition to CD8α$^+$ CD205$^+$ cDCs, a population of CD8α$^-$ CD205$^+$ cDCs was found to be present in pLNs and iLNs of WT mice. This CD8α$^-$ CD205$^+$ cDC population in the LNs expressed higher levels of CD11b, but lower levels of CD24 and CD103 compared with CD8α$^+$ CD205$^+$ cDCs (Fig. 4.1A). Based on the literature, it is possible that this population represents cDC precursors that are unable to differentiate further in the absence of *Batf3* and this will be discussed in detail in section 4.6.1 of this chapter (Caminschi et al., 2012; Naik et al., 2006). Flow cytometric analysis of the pLNs from *Batf3*$^{-/-}$ mice revealed a significant decrease in CD8α$^+$ CD205$^+$ cDCs as a percentage of CD11c$^+$ MHC-II$^+$ cells in this system compared with WT mice (Fig. 4.1B). In contrast to pLNs, the proportion of CD8α$^+$ CD205$^+$ cDCs was unchanged in iLNs of *Batf3*$^{-/-}$ mice. Given that migratory CD103$^+$ cDCs, which are functionally equivalent to CD8α$^+$ cDCs, are dependent on *Batf3* for their development (Hildner et al., 2008), cDC populations expressing CD103 vs. CD11b were also examined (Fig. 4.1C). The proportions of cDCs expressing CD103 were significantly decreased in both the pLNs and iLNs of *Batf3*$^{-/-}$ compared with WT mice. Once the expected *Batf3*$^{-/-}$ phenotype was confirmed it was possible to go on to ask what impact this deficiency has on immune responses initiated by parasite eggs.

4.4.2 Th2 immune responses are induced in *Batf3*$^{-/-}$ mice against *S. mansoni* eggs

The cytokine expression profile of cells from pLNs was examined in order to directly assess whether *Batf3*$^{-/-}$ mice lacking CD8α^{+} cDCs are able to generate Th2 responses against *S. mansoni* eggs injected into the foot. We first assessed whether *Batf3* deficiency impacts the proportion and number of immune cells within LNs following *S. mansoni* egg injection. The total number of live cells present in the dLN after egg injection was calculated using the proportions of live cells present in the pLN determined by flow cytometric analysis and total numbers of trypan blue negative cells counted with a microscope (Fig. 4.2A). This revealed that the total number of live cells in the pLNs was not significantly altered in the absence of CD8α^{+} cDCs compared with WT controls. To investigate T cell populations in *Batf3*$^{-/-}$ mice after egg injection, CD4^{+} and CD8^{+} T cell subset proportions were examined by flow cytometry, and total numbers of these T cell subsets in pLNs were calculated from numbers of total live cells in figure 4.2A. A marginal decrease in the proportion of CD8^{+} T cells as a percentage of live cells was observed at D5 in *Batf3*$^{-/-}$ mice compared with WT mice, whereas proportions of both CD4^{+} and CD8^{+} T cells were unchanged at D7 but increased at D9 (Fig. 4.2B). The total number of CD4^{+} and CD8^{+} T cells was unchanged in *Batf3*$^{-/-}$ mice at all time-points measured in comparison with WT animals (Fig. 4.2C).

The immune response was examined by measuring egg antigen-specific cytokine production by pLN cells after egg injection, following *in vitro* culture with SEA for 72h. The samples in this assay represent pooled pLN cells from 4-5 animals, as insufficient cells were available for the analysis of individual samples (Fig. 4.3A). This type of analysis was carried out on D5, D7 and D9 post egg injection to assess the immune response kinetics in *Batf3*$^{-/-}$ mice. *Batf3*$^{-/-}$ mice displayed increased pLN cell production of IL-4, IL-5, IL-13, IL-10 and IL-17 compared with WT egg-injected mice at every time-point measured. On the other hand, IFN-γ and TNF-α production in egg-injected *Batf3*$^{-/-}$ mice was reduced compared with WT mice at every time-point measured (Fig. 4.3A). This phenotype of decreased TNF-α and IFN-γ and increased IL-4, IL-5, IL-13, IL-10 and IL-17 production in *Batf3*$^{-/-}$ mice was also apparent in

iLNs, but the amount of each cytokine detected from this tissue was generally lower compared with pLNs (with the exception of IL-17) (Fig. 4.3A).

Given that the amount of IL-4 production by pLN cells in response to SEA restimulation was significantly increased in *Batf3*$^{-/-}$ mice and that this could not be explained by a substantial increase in the proportion of CD4^{+} T cells in culture, ICC was conducted in order to specifically address cytokine production by T cell subsets *ex vivo* (Fig. 4.3B). For this assay, WT or *Batf3*$^{-/-}$ pLN or iLN cells were restimulated with αCD3/CD28 o/n resulting in polyclonal activation of T cells. T cell specific cytokine expression in the LNs was assessed by flow cytometry after ICC. In egg-injected WT mice, ICC staining showed that the proportions of cytokine positive CD4^{+} T cells were increased in the pLNs compared with the iLNs for every cytokine analysed (Fig. 4.3B). When comparing these populations with those present in *Batf3*$^{-/-}$ mice, IL-4^{+} CD4^{+} and IL-10^{+} CD4^{+} T cell populations in pLNs followed a similar trend as the ELISA results described above for these cytokines: the proportion of IL-4^{+} CD4^{+} T cells was significantly increased at D7 and D9 in *Batf3*$^{-/-}$ compared with WT mice, and the proportion of IL-10^{+} CD4^{+} T cells was significantly increased at D5 and D7. The proportion of IL-13^{+} CD4^{+} T cells was unchanged when comparing *Batf3*$^{-/-}$ with WT mice (Fig. 4.3B). In line with lower levels of antigen-specific IFN-γ, the proportion of IFN-γ^{+} CD4^{+} T cells was reduced in the pLNs of *Batf3*$^{-/-}$ compared with WT mice at D9 (Fig. 4.3B). The proportion of IL-17^{+} CD4^{+} T cells was also decreased in *Batf3*$^{-/-}$ mice at D9 compared with WT mice (Fig. 4.3B), which contradicts the trend for IL-17 production produced by ELISA analysis (Fig. 4.3A). The discrepancies within the results may be due to differences in the assays used i.e. antigen-specific restimulation for 72h compared with polyclonal restimulation o/n, and the details on this will be discussed in section 4.6.5 of this chapter. To assess the level of cytokine expression by T cell subsets, the GMFI for cytokine staining was measured (Fig. 4.3C). No major differences in *Batf3*$^{-/-}$ mice were found when assessing the GMFI of IL-4, IL-10, or IL-17 staining on CD4^{+} T cells compared with WT mice, with the exception of a marginally lower level of IL-4 expression by *Batf3*$^{-/-}$ CD4^{+} T cells on D5 (Fig. 4.3C-D). Analysing the GMFI of IL-13 staining on CD4^{+} T cells revealed an increase of IL-13 expression at D7 and D9 in the absence of CD8α^{+} cDCs, whereas the GMFI of IFN-γ was significantly reduced in *Batf3*$^{-/-}$ CD4^{+} T cells compared with WT controls (Fig. 4.3C-D). Together, these data indicated that

Th2 immune responses were enhanced, and Th1 responses impaired, following subcutaneous injection of *Batf3*$^{-/-}$ mice with *S. mansoni* eggs.

4.4.3 CD8α^{+} cDCs are reduced during *S. mansoni* infection at D42 in the mLN and the liver

Since our results from the *S. mansoni* egg model of acute Th2 induction indicated that *Batf3*$^{-/-}$ mice mounted Th2 responses that appeared enhanced, but failed to develop normal Th1 responses, we next addressed whether this phenotype was also evident in an infection setting. *Batf3*$^{-/-}$ mice were infected with *S. mansoni* and the development of the immune response was analysed in the mLN and the liver. These tissue sites are of particular interest when studying the immune response developed against *S. mansoni* eggs during infection; the mLN is a priming/restimulation site that drains the intestine, and the liver is an effector site where granulomatous legions form around the eggs (described in section 1.6 and 1.7, chapter 1). Given that CD8α^{+} cDCs have been shown to reconstitute in Th1 immune environments (Tussiwand et al., 2012), the proportion of CD8α^{+} cDCs in *Batf3*$^{-/-}$ mice was assessed by flow cytometry at D42 post *S. mansoni* infection, when the immune response shifts from a mixed Th1/Th2 to a dominant Th2 response (Pearce and MacDonald, 2002). Several markers were used to distinguish CD8α^{+} cDCs including CD205, as previously conducted for the egg injection experiment (section 4.4.1, Fig. 4.1). CD8α^{+} cDCs in the mLNs and livers of naïve WT mice were CD103^{+} CD24^{+} and CD11b^{low} (Fig. 4.4A). A population of CD8α^{-} CD205^{+} cells was observed in the mLNs and livers of WT mice, which may be similar to a population also observed in the pLN of egg-injected mice (section 4.4.1, Fig 4.1A). In line with what has been described in the literature (Hildner et al., 2008), naïve *Batf3*$^{-/-}$ mice displayed a significant reduction in CD8α^{+} cDC populations compared with WT mice, although this was more complete in the liver than the mLN (Fig. 4.4B).

To investigate whether *S. mansoni* infection impacts the *Batf3*$^{-/-}$ phenotype, the proportion of this subset was assessed in infected *Batf3*$^{-/-}$ mice, which showed a similar reduction in the proportion of CD8α^{+} cDCs compared with naïve mice, confirming that CD8α^{+} cDC populations are significantly reduced in these tissues at D42 of infection (Fig. 4.4B). In both livers and mLNs, a population of CD8α^{-} CD205^{+} and CD8α^{+} CD205^{-} cDCs was additionally apparent after flow cytometric

analysis in *Batf3*$^{-/-}$ and WT mice. When CD103^{+} CD11b^{low} migratory cDCs were analysed, they were significantly reduced in naïve and *S. mansoni* infected *Batf3*$^{-/-}$ mice compared with WT controls (Fig. 4.4C). Deficiency in CD8α^{+} and migratory CD103^{+} cDCs in livers and mLNs of *Batf3*$^{-/-}$ mice confirmed the use of this model to investigate the impact this has on the immune response during *S. mansoni* infection.

4.4.4 Th2 immune responses against *S. mansoni* infection are enhanced at D42 in *Batf3*$^{-/-}$ mice

The impact of *Batf3* deficiency on immune response development was investigated at D42 of *S. mansoni* infection. Increased numbers of cells in the mLN indicate priming/restimulation in *Batf3*$^{-/-}$ mice resulting in larger adaptive immune cell populations, including T cells (Fig. 4.5A). Flow cytometry analysis of T cell subsets in the mLN at D42 of infection showed that the proportion of CD4^{+} TCR-β^{+} T cells was unchanged in *Batf3*$^{-/-}$ compared with WT mice, whereas the proportion of CD8^{+} TCR-β^{+} T cells was decreased in *Batf3*$^{-/-}$ mice (Fig. 4.5B). Total numbers of both T cell subsets increased almost 2-fold in *Batf3*$^{-/-}$ compared with WT mice (Fig. 4.5C). Together these data suggest enhanced proliferation of effector T cells in the mLN of *Batf3*$^{-/-}$ mice.

To analyse the character of the immune response, isolated mLN cells were cultured with SEA for 72h and cytokine production was measured by ELISA (Fig. 4.5D). It should be noted that in some cases (i.e. as stated in figure legends for ELISA measurements of antigen-specific cytokine production in figure 4.5 and 4.6 and serum antibody in figure 4.8) data were pooled from infection experiments at D40 and D42, as these time-points both represent the induction phase of Th2 responses to *S. mansoni* eggs during infection (Pearce and MacDonald, 2002). Although there may be subtle differences in the development of the immune response between D40 and D42 during infection, the use of a mixed model statistical analysis software enabled analysis of these data by adding the day as a random factor, thereby compensating for any significant differences in the data between D40 and D42. In aid of clarity, I will refer to pooled D40/D42 data as D42 data in this chapter from here on. The results from the SEA restimulation assay showed that the amount of IL-4, IL-5, IL-10, IL-13 and IL-17 production by mLN cells followed the trend set in the egg injection experiment; the amount of each cytokine was significantly increased in infected *Batf3*$^{-}$

$^{-/-}$ compared with WT mice (Fig. 4.5D). On the other hand, the amount of IFN-γ as well as TNF-α production was significantly reduced in *Batf3*$^{-/-}$ mice in comparison with infected WT controls.

Qualitative analysis of T cell cytokine production using ICC after o/n αCD3/CD28 restimulation revealed a significant increase in the proportion of *Batf3*$^{-/-}$ CD4^{+} T cells that were IL-4^{+} and IL-10^{+} in comparison with WT mice, whereas the proportion of IL-13^{+} CD4^{+} and IL-17^{+} CD4^{+} T cells appeared unchanged (Fig. 4.5E). The proportion of IFN-γ^{+} CD4^{+} T cells measured by ICC after polyclonal restimulation was decreased in the mLN of *S. mansoni* infected *Batf3*$^{-/-}$ compared with WT mice (Fig. 4.5E). Assessing the GMFI of CD4^{+} T cells producing Th2 cytokines showed that the level of IL-4 production by CD4^{+} T cells was significantly increased in mLNs of *S. mansoni* infected *Batf3*$^{-/-}$ compared with WT mice, whereas levels of IL-10 and IL-13 were unchanged (Fig. 4.5F-G). In contrast, the level of IFN-γ expressed by both CD4^{+} and CD8^{+} T cells was reduced in *Batf3*$^{-/-}$ mice (Fig. 4.5F-G). This indicated that although CD4^{+} and CD8^{+} T cell numbers were increased, fewer T cells were polarised to become IFN-γ producing cells and those cells that are activated are less able to make IFN-γ. Overall the results from the mLN of *Batf3*$^{-/-}$ mice infected with *S. mansoni* follow the trends predicted from the egg injection experiment, as the production of Th2 cytokines is increased whilst Th1 responses are decreased.

To compare immune responses occurring in the mLN with an effector site, where primed T cells mediate mixed Th1 and Th2 responses against *S. mansoni* eggs (Pearce and MacDonald, 2002), the liver was analysed for T cell populations and cytokine production utilising the same methods. The total number of live liver leukocytes present in *Batf3*$^{-/-}$ mice was similar to the numbers present in WT controls (Fig. 4.6A). When T cell populations were assessed, a significant decrease in the proportion of CD8^{+} T cells was seen in *Batf3*$^{-/-}$ compared with WT mice, whereas the proportion of *Batf3*$^{-/-}$ CD4^{+} T cells remained unchanged (Fig. 4.6B). Although a trend for reduced hepatic CD8^{+} T cell numbers was found in *Batf3*$^{-/-}$ mice, total numbers of both T cell subsets were not significantly different compared with WT animals (Fig. 4.6C).

Overall, cytokine production in response to SEA by isolated liver leukocytes from *Batf3*$^{-/-}$ mice followed similar trends compared with the results described for the mLN above. Liver leukocytes produced increased amounts of IL-4, IL-5 and IL-10 compared with WT mice (Fig. 4.6D). The amount of IFN-γ produced by liver leukocytes was decreased in *Batf3*$^{-/-}$ mice following SEA restimulation. There were no major changes apparent in the proportions of *Batf3*$^{-/-}$ CD4^{+} T cells expressing IL-4, and IL-13 measured by ICC compared with WT mice, but *Batf3*$^{-/-}$ mice displayed increased proportions of CD4^{+} T cells that were IL-10^{+} after restimulation with αCD3/CD28 (Fig. 4.6E). CD4^{+} IFN-γ^{+} T cells were reduced in *Batf3*$^{-/-}$ mice compared with WT controls. GMFI measurements showed a trend for increased IL-4 and significantly increased IL-10, IL-13 and IL-17 expression by hepatic *Batf3*$^{-/-}$ CD4^{+} T cells (Fig. 4.6F-G). Taken together, the data obtained for the mLN and liver at D42 post *S. mansoni* infection indicated that the production of Th2 cytokines was enhanced, whereas Th1 cytokines, in particular IFN-γ, were reduced in *Batf3*$^{-/-}$ mice in both priming and effector sites when compared with WT animals.

Given that Th2 immune responses appeared enhanced in *Batf3*$^{-/-}$ mice, we next investigated the activation status of T cells by flow cytometry to determine the proportion of effector T cell populations present in *Batf3*$^{-/-}$ mice. Proportions and numbers of CD4^{+} TCR-β^{+} T cells expressing the IL-2 receptor and activation marker CD25 were significantly increased in *S. mansoni* infected *Batf3*$^{-/-}$ mice compared with WT controls, and this was the case in both the mLN and the liver (Fig. 4.7A-B & E). To assess whether increases in Th2 cytokine production and effector CD4^{+} T cells found in *Batf3*$^{-/-}$ mice may be due to altered regulation, Treg cell populations were also examined by flow cytometry for the expression of Foxp3 and CD25. This analysis showed that the proportion of Foxp3^{+} Treg cells of CD4^{+} TCR-β^{+} cells was significantly increased in the mLNs and livers of *Batf3*$^{-/-}$ mice in comparison with WT animals (Fig. 4.7C & E), whereas the absolute number of Foxp3^{+} Tregs was increased significantly in the mLN but not the liver (Fig. 4.7D). Given that both effector T cell and Treg populations were increased in *Batf3*$^{-/-}$ mice, the ratio between effector T cells and Treg cells was calculated for infected mice to provide an indication as to whether Treg populations increased in unison with effector T cells. In the mLNs of infected animals the effector T:Treg ratio was approximately 1:14 for WT mice and 1:7 for *Batf3*$^{-/-}$ mice, and in the liver the ratio was 1:1.5 and 1:0.5 in WT and *Batf3*$^{-/-}$

mice respectively. These calculations show that the ratio of Treg cells per effector T cell was decreased in *Batf3*$^{-/-}$ mice compared with WT mice infected with *S. mansoni*.

To examine another adaptive immune arm during the responses against *S. mansoni* infection at D42 in *Batf3*$^{-/-}$ mice, B cell populations were analysed by flow cytometry. Specifically, increased Th2 cytokine production by T cells and larger populations of T effector cells may impact the development of B cell responses that rely on T cell help (Cerutti et al., 2012). Numbers of CD19^{+} cells were significantly increased in the mLN of infected *Batf3*$^{-/-}$ mice compared with WT mice, whilst the proportion CD19^{+} cells (of total live cells) was unchanged (Fig. 4.8A). In the effector site, the analysis of hepatic CD19^{+} B cell populations showed that there were no major differences in the proportion and total numbers of CD19^{+} cells in *Batf3*$^{-/-}$ mice relative to WT controls (Fig. 4.8A). This shows that the expansion of CD19^{+} B cells was increased in the priming site in *Batf3*$^{-/-}$ mice, but not in the effector site.

Ashok *et al.,* (2012) show that levels of serum IgE and antigen-specific IgG1 antibody responses are increased in *Batf3*$^{-/-}$ mice during *L. major* infection. IL-4 has been reported to drive antibody class-switching to IgE and IgG1, which is associated with a dominant Th2 response (Walsh and Mills, 2013). To investigate whether humoral responses were altered in a *Batf3* deficient environment during *S. mansoni* infection, antibody responses were measured by assessing the isotypes present in the serum collected at D41 post infection. *Batf3*$^{-/-}$ mice displayed significantly increased amounts of total IgE in the serum during infection compared with WT animals (Fig. 4.8B). SEA-specific IgG1 as well as IgG2b, IgM and total Ig were not significantly altered in *Batf3*$^{-/-}$ mice, whereas levels of IgG2c and IgG3 were significantly decreased (Fig. 4.8C). These data show that the quality of B cell responses is altered in infected *Batf3*$^{-/-}$ mice at D42 resulting in increased antibody class switching to IgE responses, but decreased production of SEA-specific IgG2c and IgG3 compared with infected WT mice.

4.4.5 Critical weight loss and increased fatality in *S. mansoni* infected *Batf3*$^{-/-}$ mice

A significant factor contributing to the phenotype of *S. mansoni* infected *Batf3*$^{-/-}$ mice from D46 was a substantial weight loss experienced by *Batf3*$^{-/-}$ mice, whereas WT

mice maintained their body weight (Fig. 4.9A). We hypothesised that the greater weight loss observed in *Batf3*$^{-/-}$ mice might be due to a greater number of parasite larvae surviving to adulthood leading to a greater egg burden. When we analysed the number of worm pairs and adult worms (Fig. 4.9B), we found that there were no significant differences at D42 of infection comparing *Batf3*$^{-/-}$ with WT mice. Moreover, measurement of egg burdens at D42 in the liver (Fig. 4.9C) and intestine (Fig. 4.9D) indicated that these were not significantly different in *Batf3*$^{-/-}$ mice.

Given that *S. mansoni* infection frequently causes substantial enlargement of the spleen and liver of the host, we assessed whether hepatosplenomegaly was altered when CD8α^{+} cDCs are reduced. Hepatomegaly was unchanged at D42, suggesting that immune processes associated with egg deposition in the liver, including granulomatous inflammation, did not significantly alter the size of this organ at this time-point (Fig. 4.9E). Taken together, at D42 *Batf3*$^{-/-}$ mice exhibit similar infection levels compared with WT mice. However, *Batf3*$^{-/-}$ mice lost a critical amount of weight from D46 post infection, which granted investigation into the pathology in more chronic stages of *S. mansoni* infection.

4.4.6 *Batf3*$^{-/-}$ mice exhibit more severe pathology during *S. mansoni* infection

Th2 immune response are strongly implicated in the development of pathology during *S. mansoni* infection (Wilson et al., 2007; Wynn, 2004), and thus we reasoned that an increase in Th2 cytokine production in *Batf3*$^{-/-}$ mice may alter granulomatous pathology. To assess the total burden of granulomas in the liver, total granulomatous inflammation present in sections from the median liver lobe stained with MT was quantified using the algorithm described in chapter 3 (this method is described in chapter 2 section 2.6.1). Given that pathology associated with *S. mansoni* infection is established in more chronic stages of infection (Pearce and MacDonald, 2002), we reasoned that any changes in pathology may be more evident a few weeks after the onset of egg production. Therefore, we assessed granulomatous inflammation at D42 and D52 of *S. mansoni* infection, which also encompasses the time-frame during which *Batf3*$^{-/-}$ mice lose a critical amount of weight. Notably, the time-points analysed (D42 and D52) were from two separate experiments rather than a contiguous time-course, making it difficult to draw direct comparisons between D42 and D52 data sets

regarding the proportion of granulomatous inflammation and fibrosis, due to likely variation in the initial infective exposure. With this in mind, both time-points will be described together from here on in an attempt to better understand the pathology in *Batf3*$^{-/-}$ mice.

The data revealed that total granulomatous inflammation including collagen deposition and cellular aggregation at D42 and D52 was unchanged in *Batf3*$^{-/-}$ compared with WT mice (Fig. 4.10A). Although MT stains type III collagen, collagen deposition was more accurately measured in the liver using PSR stained sections from the median liver lobe, as PSR stains collagen more specifically than MT (as described in section 3.4.6, chapter 3). Thus, the deposition of type I and III collagen was measured in a similar way to granulomatous inflammation using PSR stained median liver lobe sections to measure the level of fibrosis in the tissue (Fig. 4.10B-C). The proportion of fibrosis in the liver was not markedly different at D42 (data repeated from Fig. 3.11A, chapter 3 for ease of comparison with D52), but was significantly greater at D52 in infected *Batf3*$^{-/-}$ compared with WT controls (Fig. 4.10B-C). Given that granulomas present in the liver appeared more fibrotic, granulomas forming in the intestine were also examined to identify whether this phenotype was specific to the liver.

Histological analysis of ileal sections was conducted to investigate granulomatous inflammation that formed as a result of egg transit through the intestinal tissue from the mesentery into the lumen. We hypothesised that enhanced Th2 responses and impaired Th1 responses in the mLN may alter the granulomatous response in the intestines. Due to the more complex architecture of the gut, the novel granuloma area analysis method used for the liver could not be used in this tissue. Instead, granulomas in the ileum were scored for their intensity and size to compare the pathology associated with granulomatous inflammation in *Batf3*$^{-/-}$ mice with WT controls (Fig. 4.10D). This method is described in more detail in section 2.6.1 chapter 2. WT mice displayed varying severity scores of granulomatous inflammation, but when compared with *Batf3*$^{-/-}$ mice this analysis revealed interesting pathological indications. First, high scores were more frequent in infected *Batf3*$^{-/-}$ than in WT mice at D42 post *S. mansoni* infection (Fig. 4.10D). A similar result was found when analysing granulomas in the ileum from D52 infected *Batf3*$^{-/-}$ and WT mice. Second,

some areas of the circular (inner) intestinal muscle of infected mice displayed an accumulation of vacuole-like features at D42, which in some cases severely disrupted the structure of the muscle indicating damage (Fig. 2.3, chapter 2). This type of vacuole formation in the muscle has not yet been described, but may indicate muscle injury (Prof. Mark Arends, Western General Hospital). Nevertheless, comparison of WT with *Batf3*$^{-/-}$ mice at D42 of infection revealed that this type of muscle injury was increased in the absence of CD8α^{+} cDCs (Fig. 4.10E). Taken together, initial investigations into pathology in the intestines at D42 indicate that the response to eggs in this tissue may be aggravated in *Batf3*$^{-/-}$ mice, though additional analysis is required to determine whether this similarly occurs at D52.

4.5 Summary of Results

S. mansoni egg injection

- *Batf3*$^{-/-}$ mice developed early and enhanced Th2 but impaired Th1 cytokine production in the pLN compared with WT mice after s.c. injection of *S. mansoni* eggs (Fig. 4.3).

S. mansoni infection

- At D42 of *S. mansoni* infection, *Batf3*$^{-/-}$ mice developed elevated Th2 and impaired Th1 cytokine responses in the mLN (Fig. 4.5) and the liver (Fig. 4.6).
- The proportion and number of effector $CD4^+$ T cell and $CD25^+$ $Foxp3^+$ Treg populations were increased in *Batf3*$^{-/-}$ mice compared with WT mice (Fig. 4.7).
    - Approximate effector T:Treg ratios during infection:
        - mLN = 1:14 for WT mice and 1:7 for *Batf3*$^{-/-}$ mice.
        - Liver = 1:1.5 for WT mice and 1:0.5 for *Batf3*$^{-/-}$ mice
- $CD19^+$ B cell numbers were increased in the mLN, but not the liver, of *Batf3*$^{-/-}$ mice compared with WT mice (Fig. 4.8).
- Antibody class-switching to IgE was increased, whereas antigen-specific isotypes IgG2c and IgG3 were decreased in the serum of *Batf3*$^{-/-}$ mice compared with WT mice at D42 of infection (Fig. 4.8).
- *Batf3*$^{-/-}$ mice lost a critical amount of weight from D46 to D52 of infection (Fig 4.9).
- The proportion of granulomatous inflammation and fibrosis was unchanged in *Batf3*$^{-/-}$ mice, but intestinal granulomas were more severe at D42 of infection (Fig. 4.10).
- At D52, the proportion of granulomatous inflammation was unchanged whereas hepatic fibrosis and intestinal granulomas were more severe in *S. mansoni* infected *Batf3*$^{-/-}$ mice compared with WT controls (Fig. 4.10).

4.6 Discussion

The work presented in this chapter shows that CD8α$^+$ cDCs are not required for the induction of Th2 responses after *S. mansoni* egg injection or at D42 during natural infection. Investigating the role of CD8α$^+$ cDCs during *S. mansoni* infection using *Batf3*$^{-/-}$ mice revealed that a substantial reduction in this subset results in enhanced Th2 immune responses in the mLN and the liver, whilst Th1 responses are impaired at D42. However, there is some evidence to suggest that CD8α$^+$ cDCs are important for the regulation of Th2 responses to ensure the development of "appropriate" immune responses and granulomatous pathology during later stages of infection (D52). These data provide novel insight into the role of CD8α$^+$ cDCs during chronic infection with a parasite, which improves our understanding on the importance of this rare DC type during infectious disease.

4.6.1 CD8α$^+$ cDC lineage cells in *Batf3*$^{-/-}$ mice

Since it has become evident that DC subsets fulfil distinct functional roles during infectious disease (section 1.2.2, chapter 1) (Mildner and Jung, 2014), specific gene deficient or depletion models are essential to unravel the role of DCs in different infection settings *in vivo*. When *Batf3*$^{-/-}$ mice were generated in 2008 by Hildner *et al.,* they provided a promising tool for investigating the role of CD8α$^+$ cDCs during infection. However, as the level of deficiency in *Batf3*$^{-/-}$ mice on the C57BL/6 genetic background is variable depending on the tissue analysed (Edelson et al., 2011; Tussiwand et al., 2012), it was essential to first examine CD8α$^+$ cDC levels in each tissue of interest and in the experimental model used.

In this chapter differential levels of CD8α$^+$ cDC deficiency in *Batf3*$^{-/-}$ mice were revealed in pLNs, iLNs, mLNs and livers using a cocktail of surface markers including CD205, CD24 and CD103 to distinguish this subset from other cDCs. In the liver the proportion of CD8α$^+$ cDCs in naïve or *S. mansoni* infected *Batf3*$^{-/-}$ mice was drastically reduced thereby exhibiting the most marked deficiency of this subset compared with the other sites examined (Fig. 4.4). On the other hand, residual CD8α$^+$ cDCs that express CD8α, CD205 and CD24 were present in pLNs and iLNs of *Batf3*$^{-/-}$ mice after egg injection and in mLNs of naïve or *S. mansoni* infected *Batf3*$^{-/-}$ mice (Fig. 4.1B & Fig. 4.4B). CD103$^+$ cDCs were decreased by a higher percentage in all

tissues examined compared with CD8α$^+$ cDCs, which indicates that migratory CD103$^+$ cDC deficiency is more complete compared with CD8α$^+$ cDCs in these tissues. These findings are in line with the literature, as populations of CD8α$^+$ cDCs have been reported in iLNs of naive *Batf3*$^{-/-}$ mice on a C57BL/6 background (Edelson et al., 2011; Waithman et al., 2013). In addition, Waithman *et al.,* (2013) showed that CD103$^+$ cDCs are absent in iLNs in C57BL/6 *Batf3*$^{-/-}$ mice. Thus, incomplete deficiency of CD8α$^+$ cDCs in C57BL/6 *Batf3*$^{-/-}$ mice is likely due to differences in the genetic background of these mice compared with 129S6/SvEv *Batf3*$^{-/-}$ mice, which results in differential requirement for *Batf3* by CD8α lineage cDCs in these mice.

The D42 time-point is critical during *S. mansoni* infection for it is at this point that the switch from a mixed Th1/Th2 to a dominant Th2 immune response occurs (Pearce and MacDonald, 2002). Levels of Th1 cytokines are still abundant at D42, as shown by the high levels of IFN-y presented in this chapter (Fig. 4.5) and in chapter 3 (Fig. 3.3). It is well established that Th1 cytokines, in particular IFN-γ and IL-12, can trigger *Batf3* independent reconstitution of CD8α$^+$ cDCs (Tussiwand et al., 2012), and we investigated this phenomenon during *S. mansoni* infection. Our data indicate that infection with *S. mansoni* does not induce sufficient IFN-γ and IL-12 to trigger significant *Batf3* independent mechanisms for reconstitution of CD8α$^+$ cDCs at D42, as the proportion of CD8α$^+$ cDCs in *Batf3*$^{-/-}$ mice was unaltered compared with naïve levels (Fig. 4.4). However, the possibility that CD8α$^+$ cDCs are reconstituted temporarily at earlier stages of *S. mansoni* infection when Th1 responses are more prevalent cannot be dismissed and a time-course covering the period D0 to D42 would address this. Reconstitution of CD8α$^+$ cDCs during later stages of infection (i.e. at D52) is unlikely as Th1 responses are normally downmodulated upon the onset of egg production (Pearce et al., 1991), but the proportion of CD8α$^+$ cDCs should also be examined at those time-points to exclude this possibility. It has been shown that IL-12 and IFN-γ mRNA levels are increased in the lungs at D1 and D3 following intravenous egg injection, and thereafter the expression of these cytokines decreases (Wynn et al., 1994). A time-course experiment (i.e. D1 to D14) would enable us to determine whether *S. mansoni* egg injection induces the reappearance of CD8α$^+$ cDCs in the LNs examined in this chapter, and WT animals could be injected with PBS to control for egg injection. Nevertheless, our data indicate that CD8α$^+$ cDCs are not reconstituted in *Batf3*$^{-/-}$ animals at a time-point during infection when Th1 responses

are apparent, which argues that immune responses to *S. mansoni* eggs are not sufficient to induce this process.

Given that the deficiency of CD8α$^+$ cDCs was less complete compared with CD103$^+$ cDCs, CD8α lineage cDC subtypes were investigated in more detail to better understand the *Batf3*$^{-/-}$ phenotype. In the work detailed in this chapter, closer examination of CD8α$^+$ cDCs and various subtypes that belong to this lineage revealed that CD8α$^-$ CD205$^+$ cDCs remained present in the LNs of *Batf3*$^{-/-}$ mice (Fig. 4.1 & 4.4). Splenic immature pre-cursors have been previously reported in naïve *Batf3*$^{-/-}$ mice, expressing CD205, CD24 and Clec9A but not CD8α (Caminschi et al., 2012). Therefore, the population of CD8α$^-$ CD205$^+$ cDCs found in naïve and *S. mansoni* infected *Batf3*$^{-/-}$ mice may represent immature pre-cursors of the CD8α$^+$ cDC subset lineage, which have not yet reached the developmental stage that requires *Batf3* expression. In addition to CD8α$^-$ CD205$^+$ cDCs, a small population of CD8α$^+$ CD205$^-$ cDCs was evident in the liver and LNs of both WT and *Batf3*$^{-/-}$ mice. While CD8α$^+$ CD205$^-$ cDCs may also be pre-cursors to CD8α$^+$ cDCs, it is seems more likely that this population represents pDC-related CX3CR1$^+$ CD8α$^+$ DCs (Bar-On et al., 2010). In support of this finding, CX3CR1$^+$ CD8α$^+$ DCs do not depend on *Batf3* for their development (Bar-On et al., 2010).

One notable feature of both CD8α$^+$ CD205$^+$ cDCs and CD8α$^-$ CD205$^+$ cDCs present in the mLNs and the livers of *Batf3*$^{-/-}$ mice was that they expressed higher levels of CD11b and lower levels of CD103 compared with those from WT mice (Appendix Fig. 7.3). In line with this finding, Edelson *et al.,* (2011) also showed that residual CD8α lineage cDCs in C57BL/6 *Batf3*$^{-/-}$ mice express lower levels of CD103 compared with WT mice. This might suggest that residual CD8α lineage cDCs in *Batf3*$^{-/-}$ mice are functionally distinct from their WT counterparts. Supporting this hypothesis, Caminischi *et al*., (2012) have shown that C57BL/6 mice reconstituted with BM from 129S6/SvEv *Batf3*$^{-/-}$ mice are not capable of MHC-I presentation to OT-I T cells *in vivo* compared with the control group, whereas they are able to present pOVA via MHC-II to OT-II T cells. Furthermore, it has recently been reported that the capacity to cross-present occurs at later stages of CD8α$^+$ cDC development (Sathe et al., 2011). MHC-I and MHC-II presentation by CD8α cDC lineage pre-cursors could be tested in future by purifying residual cDC subsets from *Batf3*$^{-/-}$ mice for

culture with $CD4^+$ or $CD8^+$ T cells (e.g. from OT-II and OT-I transgenic mice respectively) *ex vivo* to examine their ability to present antigen and induce T cell proliferation and cytokine production. In addition the production of cytotoxic components such as Granzyme B by $CD8^+$ T cells could be measured to determine the cytotoxic capacity of $CD8^+$ T cells in the presence of CD8α lineage cDC subtypes. Taken together, our data and previous work in the literature suggest that *Batf3*$^{-/-}$ mice are deficient in mature CD8α lineage cDCs efficient in antigen cross-presentation upon stimulation, whereas residual pre-cursor cDCs of this lineage remain present and are likely functionally distinct (Caminschi et al., 2012).

4.6.2 *Batf3*$^{-/-}$ mice display enhanced Th2 immune responses against *S. mansoni* eggs

S. mansoni egg injection subcutaneously into the top of the feet of WT mice induces an acute Th2 immune response in the pLNs, which can be examined without the additional complexities of systemic *S. mansoni* infection (Phythian-Adams et al., 2010). The data in this chapter have shown that, as expected, egg injection into WT mice induced antigen-specific IL-4 in the pLN from D5 to D9, correlating with decreased IFN-γ during this time-frame (Fig. 4.3). Increased antigen-specific IL-4 as well as consistent IL-5, IL-13 and IL-10 production against *S. mansoni* eggs occurred in *Batf3*$^{-/-}$ mice, which reflects unimpaired induction of Th2 immune responses. This suggests that $CD8\alpha^+$ cDCs are not required for the induction of Th2 responses to *S. mansoni* eggs *in vivo*. Furthermore, *Batf3*$^{-/-}$ mice displayed elevated Th2 immune responses even at D5 when WT levels were still low, which might indicate that the kinetics of Th2 induction could be altered in these animals. Analysis of D3 responses in this type of experiment would provide additional information as to whether Th2 induction occurs earlier in *Batf3*$^{-/-}$ compared with WT mice. Thus, *Batf3*$^{-/-}$ mice were not only capable of inducing Th2 responses, they displayed strikingly increased SEA-specific IL-4 production compared with WT mice. Given that IL-10 is also produced by Treg cells (particularly iTregs) during *S. mansoni* infection (Baumgart et al., 2006; McKee and Pearce, 2004), the intact production of this cytokine may also reflect unimpaired regulatory processes in *Batf3*$^{-/-}$ mice, and this concept will be addressed later on.

Unlike Th2 responses, *Batf3*$^{-/-}$ mice failed to generate equivalent Th1 responses compared with WT mice (Fig 4.3). IFN-γ production by pLN cells was reduced in *Batf3*$^{-/-}$ mice, and this is in line with previous literature that describes CD8α^{+} cDCs as important players in Th1 and antigen cross-presentation responses (Ashok et al., 2014; Edelson et al., 2010; Haan et al., 2000; Hildner et al., 2008; Mashayekhi et al., 2011; Torti et al., 2011; Waithman et al., 2013). Further repeats of this egg injection/pLN assay need to be undertaken before firm conclusions can be drawn, as this time-course has only been carried out once and some samples had to be pooled for SEA-specific restimulation due to low numbers of cells (Fig. 4.3). However, the same overall trend was found in *Batf3*$^{-/-}$ mice at D7 alone after SEA restimulation when individual samples were analysed by ELISA (Appendix Fig. 7.4). Overall, the data underline that although CD8α lineage cDCs were not completely absent in pLNs of *Batf3*$^{-/-}$ mice, the comparison of immune responses generated by *Batf3*$^{-/-}$ and WT mice uncovered dramatically altered cytokine production in response to *S. mansoni* eggs in the absence of *Batf3*.

Cytokine responses in the iLNs of egg-injected *Batf3*$^{-/-}$ mice, which did not exhibit as significant a decrease in CD8α^{+} cDCs as pLNs (Fig. 4.1), followed a similar trend to responses in the pLN, with higher levels of Th2 cytokines, and lower levels of IFN-γ, in the absence of *Batf3*. We initially selected iLNs on the understanding that these were ndLNs for s.c. administration of antigen to the foot (Hebel and Stromberg, 1976; Tilney, 1971), as they have been predominantly described as dLNs for the skin (Byrne et al., 2008; Edelson et al., 2010; Henri et al., 2001). However, to our surprise, after we had carried out these experiments and could detect a low level egg-specific response in the iLNs, we found evidence in the literature that iLNs can in fact drain the foot site (Harrell et al., 2008). Thus, lower antigen-specific Th2 responses in the iLNs compared with the pLNs raises the question of whether *S. mansoni* egg stimulated DCs migrate more efficiently to pLNs compared with iLNs from the foot, which has not yet been addressed in the literature. On the other hand, low level responses could also occur through recirculation of T cells responding to antigen from another site i.e. the pLN or the spleen. Lymphocyte recirculation is an established feature of naïve antigen-specific T cells, which migrate through specialised endothelium of secondary lymphoid organs (Marelli-Berg et al., 2008). This process is critical for immune surveillance of the immune system, but antigen recognition and

co-stimulation provided by APCs usually prevent recirculation and promote migration of the antigen primed T cell to the site of inflammation (Marelli-Berg et al., 2008) (discussed in 1.4, chapter 1). For example, it has been suggested that the co-stimulatory molecule CD28 is required for efficient T cell localisation to the CNS *in vivo* during experimental encephalomyelitis (Chang et al., 1999; Girvin et al., 2000), which perhaps occurs through upregulation of integrin-mediated cell adhesion. Although the exact mechanisms that mediate efficient T cell migration to the correct tissue site remain unclear, ineffective co-stimulation and/or enhanced co-inhibition provided by cDCs within the pLNs could conceivably result in inefficient migratory cues from the site of T cell priming, and thus lead to low level systemic recirculation of antigen primed T cells in both WT and *Batf3*$^{-/-}$ mice. In any case, the low level responses in the iLN support our line of thinking that Th2 responses are increased in *Batf3* deficient animals.

One limitation of the bulk culture of LN cells is that the cytokine profiles measured may not solely be attributable to T cells, as other lymphoid cells including DCs, B cells, FRCs and some MΦs will also be present in culture (Andrian and Mempel, 2003). To more directly address the impact of *Batf3* deficiency on T cell cytokine production in the dLN following egg injection, *ex vivo* intracellular staining of pLN T cells was conducted. This approach showed that a larger proportion of CD4^{+} T cells produced IL-4 and IL-10 in *Batf3*$^{-/-}$ mice, with CD4^{+} T cells also expressing higher amounts of IL-13 per cell (Fig. 4.3). These results strongly support the ELISA data from bulk LN cultures after SEA restimulation, indicating that Th2 immune responses in *Batf3*$^{-/-}$ mice following egg injection are not only intact, but enhanced, relative to WT mice. In contrast to this enhanced Th2 profile, the ICC data showed that CD4^{+} and CD8^{+} T cells from *Batf3*$^{-/-}$ mice were significantly less able to produce IFN-γ after polyclonal restimulation. This is in line with our hypothesis that Th1 immune responses against *S. mansoni* eggs are impaired in *Batf3*$^{-/-}$ mice, and is consistent with previous studies in non Th2 systems, which have shown that in the absence of mature CD8α^{+} cDCs, CD4^{+} and CD8^{+} T cells produce lower levels of IFN-γ (Ashok et al., 2014; Mashayekhi et al., 2011). Thus, using an egg injection model we were able to show that *Batf3*$^{-/-}$ mice induce dysregulated immune responses *in vivo* against *S. mansoni* eggs.

4.6.3 Immune responses in *Batf3*$^{-/-}$ mice at D42 of *S. mansoni* infection

4.6.3.1 *Batf3*$^{-/-}$ mice display enhanced Th2 and impaired Th1 immune responses against *S. mansoni* infection

Having identified that *Batf3* dependent DCs were not required for the induction of Th2 responses following schistosome egg injection, we next addressed whether *Batf3*$^{-/-}$ mice were capable of developing Th2 immunity during active infection. The immune phenotype in *Batf3*$^{-/-}$ mice was examined at D42 of infection after the onset of egg production, which consequently induces a dominant Th2 immune response in WT animals (Pearce and MacDonald, 2002) (Fig. 3.3, chapter 3). Thus, this is an early time-point in immune response development against the egg during *S. mansoni* infection, which can be considered as the early phase of Th2 priming (Phythian-Adams et al., 2010). The mLNs are of particular interest as a site of Th2 initiation by intestinal and LN resident DCs, including CD103^{+} cDCs (Scott, 2011), against antigens from eggs produced by adult worms in the mesenteric vessels which transit across the intestine wall and into the lumen (Pearce and MacDonald, 2002). The type of immune response in the liver was also investigated, as a large proportion of the eggs produced by the parasite are swept through the bloodstream into this effector site (Cheever, 1987).

Cytokine production by mLN and liver leukocytes from infected *Batf3*$^{-/-}$ mice was in line with the results from the egg injection experiments, as the amount of antigen-specific Th2 cytokines were enhanced (Fig. 4.5 & 4.6). Cytokine expression by T cells detected by ICC after αCD3/CD28 stimulation indicate that mLN CD4^{+} T cells in *Batf3*$^{-/-}$ mice consist of a larger population of primed polyclonal CD4^{+} T cells producing Th2 cytokines with an enhanced capacity for per cell production of IL-4. In the liver, ICC analysis showed that the per cell production of IL-13 and IL-10 by hepatic CD4^{+} T cells was increased, but the proportions of Th2 cytokine positive T cells in *Batf3*$^{-/-}$ mice were unchanged. Thus, the data obtained from the SEA stimulation of bulk LN or liver leukocytes in culture generally showed a more distinct increase in Th2 responses in *Batf3*$^{-/-}$ mice during infection, particularly in terms of increased IL-4 production, compared with qualitative analysis of T cell cytokine production with ICC. Possible explanations for this discrepancy between ICC and

ELISA analysis of cytokine production by liver leukocytes will be discussed in more detail in section 4.6.5. Nevertheless, in answer to our original question we have shown that CD8α$^+$ cDCs are not required for the induction of Th2 responses against *S. mansoni* eggs following egg injection or during natural infection. This is in line with our hypothesis and current thinking in the literature that IRF4 dependent cDCs (i.e. CD11b$^+$ cDCs) are the principle subset involved in the induction of Th2 responses to a pathogen (Gao et al., 2013; Kumamoto et al., 2013; Plantinga et al., 2013; Williams et al., 2013).

In contrast to Th2 responses, antigen-specific Th1 responses were decreased in *Batf3*$^{-/-}$ mice at D42 of *S. mansoni* infection in both the mLN and the liver (Fig. 4.5 & 4.6). Further, flow cytometric analysis of CD4$^+$ and CD8$^+$ T cell populations in the mLN and cytokine production assessed by ICC indicated that, even though the absolute numbers of CD4$^+$ and CD8$^+$ T cells were increased in the mLNs of *Batf3*$^{-/-}$ mice, the proportion of IFN-γ$^+$ T cells was decreased. This suggests that priming of CD4$^+$ and CD8$^+$ T cells in the mLN renders them unable to produce IFN-γ efficiently in the absence of CD8α$^+$ cDCs. Liver investigations revealed that a similar impairment in Th1 responses during *S. mansoni* infection occurred in the effector site, where T cell numbers were not drastically changed. Thus, our data build on previous literature investigating the role of CD8α$^+$ cDCs in acute bacterial and parasite infection (Ashok et al., 2014; Mashayekhi et al., 2011), as we have shown that *Batf3*$^{-/-}$ mice display impaired Th1 responses in a helminth infection setting, where Th2 responses are central for the development of the disease (Pearce and MacDonald, 2002).

Given that *Batf3* dependent cDCs are known as the main source of IL-12 during *T. gondii* infection (Mashayekhi et al., 2011) and *L. major* infection (Martínez-López et al., 2014), impaired Th1 immune responses in *Batf3*$^{-/-}$ mice during *S. mansoni* infection shown in this chapter may also be due to reduced levels of IL-12 needed for efficient Th1 induction and downstream IFN-γ production (Mashayekhi et al., 2011), as well as impaired cytotoxic responses (Hildner et al., 2008). In support of this hypothesis, administration of recombinant IL-12 induces IFN-γ mRNA expression in the lung following intravenous *S. mansoni* egg injection, whilst IL-12 neutralisation with an αIL-12 antibody impairs IFN-γ expression (Wynn et al., 1994). In addition, it has been shown that the maintenance of effector Th1 function in the lung during

chronic infection with tuberculosis requires IL-12, as effective Th1 responses in IL-12p40$^{-/-}$ mice were achieved only through continuous IL-12 administration (Feng et al., 2005). The requirement for CD8α^{+} cDCs in the induction and maintenance of Th1 responses could in theory be validated by the administration of recombinant IL-12 to *Batf3*$^{-/-}$ mice, as this may lead to reconstitution of CD8α^{+} cDCs via *Batf3* independent mechanisms *in vivo* (Tussiwand et al., 2012). In this experiment, we would expect reconstitution of CD8α^{+} cDCs and IL-12 to restore Th1 responses during *S. mansoni* infection. A specific role for IL-12 could then be assessed in an *ex vivo* culture system where CD4^{+} T cells and CD8α^{+} cDCs isolated from *S. mansoni* infected mice are cultured in the presence or absence of recombinant IL-12 or αIL-12 antibody. Indeed, the production of IL-12 by CD8α^{+} cDCs may be a key pathway for the induction of appropriately balanced or mixed Th1 and Th2 immune responses during *S. mansoni* infection.

4.6.3.2 Possible mechanisms that CD8α^{+} cDCs employ during *S. mansoni* infection

Having established that Th2 immune responses are enhanced in *Batf3*$^{-/-}$ mice infected with *S. mansoni* at D42 or following egg injection, it is plausible that CD8α^{+} cDCs either directly or indirectly regulate the induction of Th2 responses. To better understand the mechanism responsible for Th2 response regulation by CD8α^{+} cDCs, the impact of cytokines produced by this cDC subset including IL-12, IFN-α, TNF-α, IL-10 and TGF-β on T cell function could be investigated in future (Bamboat et al., 2010; Hochrein et al., 2001; Martínez-López et al., 2014; Mashayekhi et al., 2011; Pillarisetty et al., 2004; Shortman and Heath, 2010; Yamazaki et al., 2008).

Direct modulation of Th2 responses in *S. mansoni* infection by CD8α^{+} cDCs may occur via the production of soluble molecules that are implicated in Th1 immunity, such as IL-12 (Schroder, 2003). A reduction in CD8α^{+} cDCs and Th1 induction via IL-12 signalling in *Batf3*$^{-/-}$ mice during *S. mansoni* conceivably results in larger pool of CD4^{+} T cells that differentiate into Th2 cells. In fact, it is likely that IL-12 produced by CD8α^{+} cDCs is also important for controlling the plasticity of IFN-γ/IL-4 double-positive T cells present during *S. mansoni* infection (Deaton et al., 2014; Peine et al., 2013) (introduced in section 1.5.1, chapter 1). Thus, a lack of Th1 polarisation signals may abrogate the development of IFN-γ/IL-4 double-positive T

cells in *Batf3*$^{-/-}$ mice in infection, resulting in a larger population of IL-4 single-positive T cells.

In addition to skewing naïve CD4$^+$ T cell polarisation, IL-12 may impact the function of effector/memory CD4$^+$ T cell populations directly. Various studies have reported that IL-12 administration during parasitic infection including *S. mansoni* infection causes a switch from a Th2 to a Th1 response *in vivo* (Bancroft et al., 1997; Nabors et al., 1995; Wynn et al., 1994). Another study reported that committed Th2 cells generated *in vitro* produce less IL-4 and IL-5 and more IFN-γ in response to recombinant IL-12, which is thought to be due to retained responsiveness to IL-12 (Moriggl et al., 1998). Similarly, various studies have shown that administration of IL-12 can revert allergen-specific human polarised Th2 cells to a Th0/Th1 phenotype *in vitro* (Kaliński et al., 2000; Smits et al., 2001b; Sornasse et al., 1996). Yet, long-term stimulated murine Th2 cells are thought to become more resistant to a reversal in their phenotype (Murphy et al., 1996), and as such it is thought that the level of responsiveness to IL-12 by Th2 cells (i.e. expression of the IL-12 receptor) seems to be critical for this process (Szabo et al., 1995). Thus, the impact of IL-12 during *S. mansoni* infection may be dependent on the proportion of IL-12 responsive Th2 cells in the primed/effector/memory Th2 cell pool. However, a possible role for IFN-γ or other Th1 cytokines in the regulation of Th2 responses particularly during parasitic infection cannot yet be dismissed, and the direct affects of IL-12 on established Th2 cells remain poorly characterised. Indeed, downstream signalling events following IL-12 stimulation may be key to understanding the impact this cytokine has on CD4$^+$ T cell responses (Murphy and Stockinger, 2010), and this will be discussed in more detail in chapter 5 when the function of CD8α$^+$ cDCs at D42 of *S. mansoni* infection is investigated.

In addition to IL-12, IFN-α may contribute to direct Th2 immune response suppression, as IFN-α has been shown to promote IL-10 production and inhibit IL-4 production by human CD4$^+$ T cells that were previously activated by CD3/CD28 stimulation *in vitro* (Aman et al., 1996). In fact, splenic CD8α$^+$ cDCs are major producers of IFN-α compared with other cDC subsets (Hochrein et al., 2001), and FLT3L CD24$^+$ cDCs, which are the *in vitro* equivalent of CD8α$^+$ cDCs (Naik et al., 2005), produce type I IFNs in response to SEA (work conducted by Dr. Lauren

Webb). Yet, the role of type I IFNs during Th2 response setting remain unclear to date, and it is possible that IFN-α is positively involved in Th2 induction during *S. mansoni* infection.

Alternative to inflammatory cytokines, TGF-β or IL-10 produced by $CD8\alpha^+$ cDCs could directly suppress Th2 responses, as these cytokines are well known for their regulatory effects on effector $CD4^+$ T cell responses (Couper et al., 2008; Gorelik and Flavell, 2002). Indeed, $CD8\alpha^+$ cDCs, but not $CD8\alpha^-$ cDCs, have been shown to modulate Th2 responses and reverse airway hyperresponsiveness and eosinophilia in an asthma model (Gordon et al., 2005). The production of IL-10 and TGF-β by $CD8\alpha^+$ cDCs was necessary for downregulation of Th2 cytokine levels and IgE responses *in vitro* by splenocytes isolated from mice that had been sensitised for asthma-like disease (Gordon et al., 2005). Interestingly, modulation of allergic responses in the asthma model was most efficient when cDCs were in direct contact with T cells, but the nature of this interaction i.e. co-stimulatory/-inhibitory signals was not addressed (Gordon et al., 2005). While the production of TGF-β was not examined in our work, $CD8\alpha^+$ cDCs may produce this cytokine during *S. mansoni* infection as DCs are not conventionally activated (MacDonald et al., 2001). The production of TGF-β and IL-10 by $CD8\alpha^+$ cDCs from *S. mansoni* infection compared with naïve or Th1-challenged mice could be tested by PCR, and a bioassay for the detection of TGF-β could be used to complement the measurement of gene expression (Khan et al., 2012; Tesseur et al., 2006). However, although studies investigating $CD8\alpha^+$ cDC function in the steady state or allergic Th2 responses (i.e. in the absence of substantial Th1 responses) suggest that Th2 regulation mediated by $CD8\alpha^+$ cDCs may involve cytokines that exhibit established functions in the suppression of $CD4^+$ T cell responses, the potent capacity of $CD8\alpha^+$ cDCs to induce Th1 and CTL responses perhaps argues against this hypothesis when Th1 inflammation is apparent, including during *S. mansoni* infection (Hildner et al., 2008; Maldonado-López et al., 1999; Mashayekhi et al., 2011; Pulendran et al., 1999).

The induction of Th1 responses by $CD8\alpha^+$ cDCs may in fact represent an indirect mechanism for the regulation of Th2 responses induced by other cDC subsets (Seder et al., 1993). Given the established literature on cross-regulation between IL-4 and IFN-γ (Paludan, 1998) (section 1.5.1, chapter 1), IFN-γ produced by $CD4^+$ T cells

may then indirectly regulate/inhibit Th2 cell differentiation and proliferation (Gajewski et al., 1988), and suppress IL-4 production by activated $CD4^+$ T cells (Elser et al., 2002; Oswald et al., 1994; S W Chensue, 1994; Trinchieri, 2003). However, the impairment of Th1 responses does not automatically equal enhanced Th2 responses and certainly does not always result in increased weight loss during *S. mansoni* infection, as found for *Batf3*$^{-/-}$ mice in this chapter (Fig. 4.9). For example, mice deficient in MyD88 that lack antigen-specific Th1 responses develop a marginally increased Th2 response, but are able to maintain their body weight (Layland et al., 2005). Furthermore, IFN-$\gamma^{-/-}$ mice do not exhibit increased mortality or significant increases in IL-4 production by splenocytes *in vivo* (Yap et al., 1997). This suggests that decreased IFN-γ alone is unlikely to be the sole factor contributing to the regulation or inhibition of Th2 responses in WT animals during *S. mansoni* infection, which points to a specific role for $CD8\alpha^+$ cDCs. Thus, the combination of numerous soluble factors including IL-12 and IFN-α perhaps determines the efficiency of Th2 downmodulation by $CD8\alpha^+$ cDCs. Indeed, IFN-α has been shown to augment IL-12 mediated IFN-γ production by $CD4^+$ T cells *in vitro* (Wenner et al., 1996).

One additional functional aspect that may be altered in *Batf3*$^{-/-}$ mice is the phenotype of $CD8\alpha^-$ cDCs during *S. mansoni* infection. $CD8\alpha^-$ cDCs may be more activated in the absence of $CD8\alpha^+$ cDCs, and activation markers (e.g. CD80/86 or CD40) (Banchereau et al., 2000; Perona-Wright et al., 2006) on $CD8\alpha^-$ cDCs in *Batf3*$^{-/-}$ mice could be examined by flow cytometry to provide an insight into the status of these cDCs. Although it is not yet known how/if cytokines secreted by $CD8\alpha^+$ cDCs, such as IL-12, impact on other cDC subsets, the hypothesis can be made that $CD8\alpha^+$ cDCs are directly inhibiting or regulating the capacity of $CD8\alpha^-$ cDCs to induce Th2 responses against *S. mansoni* infection. Thus, the combination of reduced $CD8\alpha^+$ cDC mediated regulation and altered $CD8\alpha^-$ DC activity may result in a breakdown in regulatory processes leading to increased Th2 immune responses in *Batf3*$^{-/-}$ mice responding to *S. mansoni* egg antigens.

To address whether $CD8\alpha^+$ cDCs regulate or inhibit Th2 responses primed by other DCs, the capacity of sorted $CD8\alpha^-$ (i.e. $CD11b^+$) cDCs to polarise Th2 responses to SEA could be tested in a culture system with $CD4^+$ T cells, where $CD8\alpha^+$ cDCs are

either absent or present in the culture. The number of CD8α$^+$ cDCs added to the culture should be titrated to assess whether regulation/inhibition of CD8α$^-$ cDCs is dependent on the number of CD8α$^+$ cDCs added. If CD8α$^+$ cDCs regulate Th2 polarisation by CD8α$^-$ cDCs we would expect that decreased Th2 cytokine production, including IL-4, would correlate with increased numbers of CD8α$^+$ cDCs in the culture. Following experiments could then specifically examine the impact of soluble factors secreted by CD8α$^+$ cDCs on Th2 cytokine production. This scenario can be tested by adding recombinant cytokine (i.e. rIL-12) to either *ex vivo* or *in vitro* FLT3L CD11b$^+$ cDCs after sorting and during stimulation in culture with SEA. The activation phenotype of these cells could then be analysed, and their potential to prime Th2 responses could be examined either *in vivo* by cell transfer into mice or *in vitro* by culture with CD4$^+$ T cells. Thus, in the process of investigating why CD8α$^+$ cDCs are important for balanced immune responses during *S. mansoni* infection, we would aim to delineate key soluble factors involved in orchestrating Th2 cell responses. Once identified, the impact of such mediators on multiple aspects of CD8α$^-$ cDC activation including antigen uptake, processing and presentation and cytokine production could then also be interrogated.

4.6.3.3 The activation status of CD4$^+$ T cells in *Batf3*$^{-/-}$ mice is increased at D42 of *S. mansoni* infection

Given that Th2 responses were increased in *Batf3*$^{-/-}$ mice, we asked whether the activation status of CD4$^+$ T cells was altered in the face of reduced CD8α$^+$ cDCs. Proportions of CD4$^+$ T cells expressing CD25, but not Foxp3, were analysed to gain an insight into whether increased Th2 responses correlated with increased proliferation of effector CD4$^+$ T cells. This revealed that the numbers and proportions of effector CD25$^+$ Foxp3$^-$ CD4$^+$ TCR-β$^+$ T cell populations were increased in both the mLNs and livers compared with those observed in WT mice (Fig. 4.7). Thus, increased Th2 immune responses in *Batf3*$^{-/-}$ mice were accompanied by activation and expansion of a larger population of effector CD4$^+$ TCR-β$^+$ T cells than is evident in WT mice, even in the liver where total CD4$^+$ T cell numbers were unchanged (Fig. 4.6). To further assess the impact of enhanced effector Th2 cytokine production on the adaptive immune response during *S. mansoni* infection in *Batf3*$^{-/-}$ mice, B cell and Treg populations were next examined.

4.6.3.4 B cell populations and antibody class-switching in *Batf3*$^{-/-}$ mice during *S. mansoni* infection

Flow cytometric analysis of B cells during *S. mansoni* infection when CD8α^{+} cDCs were reduced showed that the number of B cells was increased in mLNs of *Batf3* deficient mice (Fig. 4.8), which may be a direct effect of increased numbers of CD4^{+} T helper cells present in this tissue (Cerutti et al., 2012; Parker, 1993). CD4^{+} T cells activate B cells via CD40L stimulation and cytokine expression including IL-4, and this kind of interaction is required for efficient B cell proliferation and Ig class switching (Cerutti et al., 2012; Parker, 1993). Thus, enhanced numbers of CD4^{+} T cells and IL-4 production in the mLN conceivably result in larger numbers of B cells in *Batf3*$^{-/-}$ mice due to increased availability of activatory signals.

To assess whether the function of B cells in *Batf3*$^{-/-}$ mice was altered, antibody isotypes present in the serum were examined. This analysis revealed elevated levels of Ig class switching to IgE in *Batf3*$^{-/-}$ mice, which further underlines that Th2 immune responses were systemically increased in the absence of CD8α^{+} cDCs (Fig. 4.8). A greater systemic abundance of IgE likely results in increased mast cell and basophil degranulation in *Batf3*$^{-/-}$ mice, which could be examined in future by measuring the amount of histamine present in the serum. Increased class-switching to IgE is probably a direct result of enhanced IL-4 production in *Batf3*$^{-/-}$ mice, as IL-4 has been shown to mediate IgE class-switching via nuclear factor NFIL3 induction (Kashiwada et al., 2010). Thus, enhanced levels of IL-4 may act as a powerful amplifier of B cell help provided by T cells as well as IgE production. A role for CD8α^{+} cDCs in regulating IgE production by B cells via the production of IFN-α is possible, as IFN-α has been shown to suppress IL-4 induced IgE production by B cells *in vitro* (Pene et al., 1988). In addition, IFN-γ inhibits class-switching to IgE, and has been reported to limit B cell proliferation and expansion by IL-4 (Hasbold et al., 1999). Thus, a reduction of IFN-γ levels in *Batf3*$^{-/-}$ mice likely contributes to elevated/less controlled levels of antibody class-switching to IgE and increased proportions of B cell populations. This lends further support to our hypothesis that CD8α^{+} cDC derived cytokines may regulate or inhibit type 2 immune responses during *S. mansoni* infection.

Th2 cytokines IL-4 (Siebenkotten et al., 1992) and IL-5 (Mizoguchi et al., 1999) have been described to induce murine Ig class switching in B cells to antibody isotype IgG1 *in vitro*. Yet unlike IgE, levels of SEA-specific IgG1 were not significantly enhanced at D42 in the serum of *Batf3*$^{-/-}$ mice (Fig. 4.8). This indicates that the mechanisms for IgE and IgG1 induction are in some way distinct. Indeed, it has been reported that high levels of IL-4 can inhibit IgG1 production by B cells, whereas IL-4 consistently drives IgE class-switching (Snapper et al., 1988). Further, IFN-γ mediated inhibition of IL-4 induced class-switching affects IgE more drastically than IgG1 (Hasbold et al., 1999), which suggests that levels of IgG1 would be less affected by the reduced levels of IFN-γ in *Batf3*$^{-/-}$ mice. IFN-γ has also been shown to induce the production of IgG2c (Barr et al., 2009) and IgG3 (Snapper et al., 1992) in mice, and so the reduced levels of IFN-γ most likely explain the reduction in SEA-specific antibody isotypes IgG2c and IgG3 in *Batf3*$^{-/-}$ mice at D42.

Taken together, these results show that B cell antibody production is altered in the absence of CD8α^{+} cDCs, which is likely a direct effect of impaired Th1 and enhanced Th2 responses at D42 of *S. mansoni* infection. To test this hypothesis, sorted CD4^{+} T cells from *S. mansoni* infected mice could be co-cultured with isolated B cells for the examination of antibody isotypes produced in the assay. Activation of B cell subsets, including marginal zone and follicular B cells, could also be assessed more thoroughly by flow cytometry using surface markers including IgD, IgM, CD19, B220 and CD23 (Pillai and Cariappa, 2009). In addition, it can be postulated that germinal centre formation in *Batf3*$^{-/-}$ mice may be enhanced, which could be addressed by immunofluorescent staining of mLN or spleen tissue sections for fluorescent microscopic analysis. Peanut agglutinin and IgD are commonly used to stain B cells in the germinal centre and the mantel (layer of naïve B cells surrounding the germinal centre) respectively (Schwickert et al., 2007), and CD3 could be used to stain for T cells (Mack and Sokol, 2005). This technique would provide information about the size of germinal centres formed, and the location of B and T cells in the germinal centre. Along the same lines, it would be of interest to investigate Tfh populations in *Batf3*$^{-/-}$ mice by flow cytometry using cell markers ICOS, PD-1 and CXCR5 (Crotty, 2011), as these cells specialise in the provision of B cell help and the formation of germinal centres (Crotty, 2011) (section 1.5, chapter 1). Indeed, enhanced numbers of CD4^{+} T cells in the mLN but not the liver may indicate an

increase specifically in the Tfh population in the mLN, and this may additionally account for increased antibody production by B cells (Crotty, 2011).

4.6.3.5 Treg populations in *Batf3*$^{-/-}$ mice during *S. mansoni* infection increase in parallel with Th2 responses

Dysregulated adaptive immune responses in *Batf3*$^{-/-}$ mice raised the question whether regulatory processes were also altered in these mice, and thus analysis of Treg cell populations and IL-10 production by flow cytometry was conducted. The data show that the proportion of Treg populations was increased in infected *Batf3*$^{-/-}$ mice compared with WT controls. This correlates with previous literature, which reports that Treg populations increase in parallel with Th2 responses during *S. mansoni* infection (Taylor et al., 2006), and contribute towards the regulation of Th2 responses (Baumgart et al., 2006). Treg cells also expand during Th1 mediated infection, such as *Mycobacterium tuberculosis* (Arram et al., 2014; Shafiani et al., 2013). Therefore, Treg populations may increase as a direct result of enhanced Th2 populations in *Batf3*$^{-/-}$ mice, in an attempt to exert a level of control on the exaggerated Th2 response during *S. mansoni* infection.

Notably, the comparison of effector T cell with Treg cell populations revealed that in relation to effector T cells the ratio of Treg cells was decreased in *Batf3* deficient mice compared with WT controls. An altered ratio suggests that the number of Tregs per effector CD4$^+$ T cell is reduced in *Batf3*$^{-/-}$ animals at D42 of *S. mansoni* infection, which argues that enhanced Th2 responses in *Batf3*$^{-/-}$ mice may not be efficiently regulated. This raises the question whether the quality of Treg responses is altered in *Batf3*$^{-/-}$ mice. Therefore, the possibility that CD8α$^+$ cDCs are involved in the differentiation of Tregs that suppress Th2 responses cannot be dismissed. Indeed, splenic naïve CD8α$^+$ cDCs have been reported to induce iTreg cells via TGF-β both *in vitro* and *in vivo* following CD4$^+$ T cell stimulation with low antigen doses (Yamazaki et al., 2008). Yet, increased antigen-specific IL-10 and proportions of IL-10$^+$ CD4$^+$ T cells in infected *Batf3*$^{-/-}$ mice (Fig. 4.5 & 4.6) suggest that enhanced IL-10 production may at least be partially due to increased Treg function as well as enhanced Th2 immune responses. Further experiments determining the source of IL-10 are necessary for full interpretation of this result and to clarify whether the function of regulatory responses is sufficient to compensate for a reduced number of Tregs per

effector T cell in *Batf3*$^{-/-}$ mice. For more specific qualitative analysis to determine both the source of IL-10 and the functionality of Tregs during *S. mansoni* infection in *Batf3* deficient environments, IL-10 cytokine reporter mice could be infected with *S. mansoni* to examine IL-10 producing populations by flow cytometry. Nevertheless, the data indicate that the CD8α^{+} cDCs are not required for the induction of Treg populations during *S. mansoni* infection, which is in line with the current literature that reports CD8α^{+} cDCs as key players for the induction of Th1 responses during infectious diseases (Ashok et al., 2014; Mashayekhi et al., 2011).

4.6.3.6 Th17 responses in *Batf3*$^{-/-}$ mice during *S. mansoni* infection

IL-17 is commonly found at only very low levels in *S. mansoni* infected C57BL/6 mice (Perona-Wright et al., 2012). This likely explains why IL-17 production was generally observed only marginally above the detection limit when measured both by ELISA and ICC in the work detailed in this thesis, increasing the possibility of technical error (Fig 4.5 & 4.6). Although close to the detection limit, antigen-specific IL-17 was increased in *Batf3*$^{-/-}$ mice at D42 post infection in the mLN, which is similar to pLN IL-17 production observed following *Batf3*$^{-/-}$ egg injection (Fig 4.3). This raises the possibility that CD8α^{+} cDCs are important for regulating the expression of IL-17 by CD4^{+} T cells. In support of our data, it has been reported that *S. mansoni* infected IFN-γ deficient mice (Rutitzky and Stadecker, 2011) and *L. major* infected *Batf3*$^{-/-}$ mice (Ashok et al., 2014) display enhanced Th17 responses. IFN-γ inhibits IL-17 production (Harrington et al., 2005; Hoeve et al., 2006; Park et al., 2005) and so a lack of IFN-γ produced by T cells in *Batf3*$^{-/-}$ mice may also be contributing to the modest increase in Th17 responses observed in our experiments (Harrington et al., 2005; Park et al., 2005). Thus in our work, a reduction in CD8α^{+} cDCs may result in reduced IL-12 levels in *Batf3*$^{-/-}$ mice, leading to decreased regulation of IL-17 production mediated by IFN-γ. This is a noteworthy point to consider, as elevated IL-17 is associated with increased pathology in schistosome infection (Rutitzky and Stadecker, 2006), Measurement of IL-12 levels in the serum or administration of recombinant IL-12 or IFN-γ to *Batf3*$^{-/-}$ mice and analysis of Th17 responses would address this scenario following egg injection or during *S. mansoni* infection. Notably, IL-17 detected by ICC in *Batf3*$^{-/-}$ was not significantly increased in the mLN or the pLN (Fig. 4.5 & 4.3 respectively), which could suggest a non- αβ T cell IL-17 source, such as γδ T cells, may be dysregulated in these animals (O'Brien et

al., 2009). Alternatively, the discrepancy between IL-17 production measured by ELISA and ICC may reflect the limits of detection of these assays.

In summary, the absence of $CD8\alpha^+$ cDCs in our system results in impaired Th1 immune responses, and likely a reduction in direct and/or indirect Th2 regulation by $CD8\alpha^+$ cDCs at D42 of *S. mansoni* infection. Consequently, defective Th2 regulation may increase the available help for B cell activation in lymphoid tissues, resulting in enhanced B cell proliferation and increased antigen-specific antibody production. Treg populations increased in parallel with Th2 populations to regulate the exaggerated response against *S. mansoni* eggs, but regulation per antigen primed $CD4^+$ T cell may be decreased. Furthermore, $CD8\alpha^+$ cDCs may be involved in the regulation of Th17 responses against *S. mansoni* eggs. Thus, these data underline that systemic immune responses to *S. mansoni* are dysregulated in *Batf3*$^{-/-}$ mice resulting in increased Th2 responses, compared with WT animals.

4.6.4 Increased pathology in *Batf3*$^{-/-}$ mice during *S. mansoni* infection

We have shown that the removal of a rare cDC subset results in substantially increased mortality during *S. mansoni* infection as well as dysregulated $CD4^+$ T cell responses (Fig. 4.5 & 4.6). Knowing that Th2 responses peak around D56 during murine *S. mansoni* infection (Pearce and MacDonald, 2002) (Fig. 3.3 Chapter 3), it was hypothesised that *Batf3*$^{-/-}$ Th2 responses would remain higher than WT at later stages of infection. The assessment of $CD4^+$ T cell responses in the mLN and the liver at D52 was unsuccessful due to limited numbers of cells in the *Batf3*$^{-/-}$ group for this analysis, and this is an aspect to pursue in future. Nevertheless, it was possible to examine the pathology in *Batf3*$^{-/-}$ mice at D52, which provided an initial insight into the possible reasons for the extreme weight loss exhibited by these animals in this time-frame.

The data obtained from analysing the parasitemia and hepatosplenomegaly at D42 suggest that increased weight loss in *Batf3*$^{-/-}$ mice is not due to altered parasite burdens. TNF-α mediated cachexia and mortality have been previously described in IL-4$^{-/-}$ mice infected with *S. mansoni* (Brunet et al., 1997). Our laboratory has observed a similar weight loss phenotype during an equivalent time-frame when bulk

$CD11c^+$ DCs were depleted, resulting in impaired Th2 immune induction during *S. mansoni* (Dr. Alexander Phythian-Adams, unpublished data). However, in the current *Batf3*$^{-/-}$ model the induction of Th2 responses was unimpaired and TNF-α production reduced (Fig. 4.5 & 4.6), suggesting alternative reasons for the death of these animals. Given that Th2 cytokines are important for fibrotic mechanisms in both murine and human schistosomiasis (de Jesus et al., 2004; Fallon et al., 2000a; Wynn, 2004), we assessed whether pathology in liver and intestinal tissue of *Batf3*$^{-/-}$ mice was altered following *S. mansoni* infection.

We investigated granulomatous pathology in the liver and small intestine in *Batf3*$^{-/-}$ mice both at D42 and D52 to address whether changes in pathology contribute to increased mortality in later stages of infection. In the liver, granulomatous inflammation and fibrosis were measured using the novel quantification method developed for chapter 3 (Fig. 3.1). Although the proportion of total granulomatous inflammation in the liver was not altered in *Batf3*$^{-/-}$ mice compared with WT mice, type I and III collagen deposition around the granuloma appeared increased, particularly by D52 post infection (Fig 4.10). IL-13 is thought to be a key Th2 cytokine for the induction and promotion of fibrosis, as IL-13 but not IL-4 deficient mice display decreased hepatic collagen deposition during *S. mansoni* infection (Fallon et al., 2000b). IL-13 is thought to mediate fibrosis through promoting alternative activation of MΦs, thereby increasing L-ornithine and L-proline production by MΦs, which in turn promotes fibroblast activation and collagen production (Hesse et al., 2001). On the other hand, IL-13 may directly activate fibroblasts, as these express the IL-13 receptor (Chiaramonte et al., 1999). Thus, it is conceivable that increased Th2 responses in *Batf3*$^{-/-}$ mice at D42 enhanced fibrotic processes directly, which results in exacerbated pathology at D52. This is a critical point to consider, as uncontrolled fibrosis is detrimental to the host during *S. mansoni* infection and often results in increased mortality due to multiple organ failure (Wynn, 2004). As such, increased fibrosis in *Batf3*$^{-/-}$ mice may lead to portal shunting (section 1.6.1, chapter 1), which causes the blood supply to bypass the liver and prevents T cells from entering the granuloma. This may lead to decreased T cell responses against the egg in the liver, possibly increasing exposure to egg derived toxins by hepatocytes. Thus, an increase in fibrotic processes in *Batf3*$^{-/-}$ mice may lead to liver failure due to a lack of blood supply, which would contribute to the ultimate death of

the animal. Liver function could be tested by measuring alanine transaminase (ALT) levels, which would provide an indication of the level of hepatocellular damage in the tissue (Hoffmann et al., 2000). Furthermore, these results underline that the analysis of Th2 responses in *Batf3*$^{-/-}$ mice at D52 as done in this thesis for D42 would be beneficial to better understand the changes in pathology observed in these animals.

In the ileum, single egg granulomas were more severe in *Batf3*$^{-/-}$ mice at both D42 and D52 post infection, resulting in additional damage to the surrounding tissue (Fig. 4.10). The blind scoring system used to assess this pathology was developed to provide an objective measurement of the burden of granulomatous inflammation in the gut, where the complex nature of the tissue architecture prevented quantification with the slide scanning method developed for use in the liver (Fig. 2.1, chapter 2). As an alternative, granuloma size in the small intestine could be measured by selecting a range of example granulomas in cross-section manually and using image analysis software to estimate area and volume, as has been commonly done in the past (Cheever et al., 1984; Hoffmann et al., 2000; Souza et al., 2011; Warren and Domingo, 1970; Yap et al., 1997). However, calculating granuloma size by this method is quite subjective, and heavily influenced by the particular example and cross-section photographed, which could lead to misinterpretation of the results. Thus, it was felt that blind scoring the granulomas provided a more objective and accurate read out of the severity of granulomatous inflammation in the gut, as this technique takes into account the density of the granuloma, damage to the surrounding tissue, collagen deposition and the type of immune cells present as well as the size of the granuloma.

Our identification of elevated pathological scores for ileal granulomas in *Batf3*$^{-/-}$ mice (Fig. 4.10) leads to interesting questions concerning the role of intestinal CD103^{+} cDCs and RA production during *S. mansoni* infection. Intestinal CD103^{+} cDCs originate in the LP and migrate to the mLNs where they induce iTreg responses and provide signals for iTreg migration to the intestine (Jaensson et al., 2008; Strauch et al., 2001). This process could be abrogated in *Batf3*$^{-/-}$ mice, resulting in uncontrolled Th2 responses in the mLN as well as more severe intestinal granulomatous inflammation due to a lack of iTreg mediated regulation. To address this hypothesis, an *ex vivo* functional assay could be conducted by culturing sorted cDC subsets from

S. mansoni infected WT or *Batf3*$^{-/-}$ mice with CD4^{+} T cells to examine the expansion of CD25^{+} Foxp3^{+} Tregs. However, a role for DC mediated induction of Treg responses including intestinal RA producing CD103^{+} cDCs, or whether their function to promote Treg differentiation changes during helminth infection, has not yet been shown in the literature. Indeed, the function of intestinal CD103^{+} cDCs is likely to change following helminth infection considering recent findings that have implicated these cells in the induction of Th17 responses against pathogenic bacteria (Persson et al., 2013; Satpathy et al., 2013). Therefore, severe intestinal granulomatous inflammation is perhaps more likely a consequence of increased Th2 immune responses leading to enhanced immune cell recruitment and collagen deposition mediated by IL-13 in the granuloma (Fallon et al., 2000a). Future studies investigating the type of immune response in the small intestine through analysing cytokine production by CD4^{+} T cells and the proportion of intestinal CD103^{+} cDCs and Tregs would address this hypothesis.

During the analysis of ileal granulomas, vacuole-like structures present in the circular muscle of the intestine were observed in *S. mansoni* infected mice. Vacuole formation can occur due to hydropic damage during colitis (Perše and Cerar, 2012) or due to lipid accumulation in non-alcoholic fatty liver disease (also known as steatosis) (Yeh and Brunt, 2014), but this type of vacuole formation in the muscle has not to our knowledge been documented during *S. mansoni* infection previously. The presence of lipids in the muscle could be assessed by histology in future by using Oil Red O or sudan black stains (Boyle et al., 2012). Irrespective of the nature of muscle vacuoles in *S. mansoni* infected mice, the presence of vacuoles is likely an indication of muscle damage, as a severe breakdown in the muscle structure due to large and multiple vacuoles was observed in some cases (Fig. 2.3, chapter 2). Exacerbated muscle injury was found in *Batf3*$^{-/-}$ mice, which may inhibit efficient functioning of the intestine (Fig 4.10). Whether this is also the case at D52 needs to be determined, yet this could indicate that disrupted intestinal muscle tissue may contribute to the weight loss shown in figure 4.9.

Given that *Batf3*$^{-/-}$ mice display impaired Th1 and CTL responses (Edelson et al., 2010; Hildner et al., 2008; Mashayekhi et al., 2011; Torti et al., 2011; Waithman et al., 2013), it is possible that *Batf3*$^{-/-}$ mice are more susceptible to certain bacterial or

viral infections or commensals normally found in SPF facilities that are not immunogenic in WT mice, or are less able to maintain a protective barrier in the intestine. For example, "co-infection" with *S. mansoni* in such circumstances could lead to altered activation phenotype of DCs and induction of helminth-specific Th17 responses (Perona-Wright et al., 2012). However, the intestinal architecture shown in figure 2.2 and figure 2.3 does not suggest significant bacterial infiltration compared with the intestinal architecture following experimental colitis (Laroui et al., 2012), and together with increased fibrosis (Fig. 4.10) this argues against the breakdown of the mucosa in the intestine. Nevertheless, the occurrence of sepsis in *Batf3*$^{-/-}$ mice could be assessed more accurately by measuring levels of IL-6, TNF-α and IL-12 in the serum.

In summary, increased granulomatous inflammation in the intestine and fibrosis in the liver, as well as severe injury to the circular intestinal muscle in *Batf3*$^{-/-}$ mice due to early and enhanced Th2 responses conceivably deteriorate the health of the animal during *S. mansoni* infection. This highlights the importance of the induction of Th1 responses during infection to counter-regulate Th2 mediated pathology (Hoffmann et al., 2000; Wynn et al., 1997), placing CD8α^{+} cDCs as a key cell type for maintaining balanced immune responses during *S. mansoni* infection.

4.6.5 Limitations and future directions

Although the techniques used in this chapter provided an excellent overview of the induction and character of immune responses as well as the extent of pathology in *Batf3*$^{-/-}$ mice during *S. mansoni* infection, understanding the limitations associated with the approach used is critical. The discrepancy between ELISA and ICC techniques observed in some cases (e.g. the liver at D42, Fig. 4.6) may suggest that the production of Th2 cytokines measured by ELISA is not solely T cell derived. Innate cells including MΦs, ILCs, NK or NKT cells could be contributing to the cytokine pool detected in bulk culture supernatants by ELISA. Notably, the innate immune system is located primarily in peripheral tissues rather than priming sites (Murphy et al., 2014), which indicates that contribution by innate immune cells is more likely in the liver compared with the mLNs. In particular, investigation of NKT cell populations in our model would be interesting, as CD8α^{+} cDCs have been reported to determine the NKT cell cytokine production profile in response to

glycolipid antigens (Arora et al., 2014). Therefore, a deficiency in CD8α$^+$ DCs may alter NKT cell cytokine production in the liver, perhaps leading to decreases in IFN-γ and increases in IL-4 production, which may contribute to increased Th2 responses in *Batf3*$^{-/-}$ mice. Unfortunately analysis of NKT cell cytokine production using our current ICC assay is not ideal as NKT cells lose expression of NK1.1 *in vitro* (Chen et al., 1997). Cytokine reporter mice would be beneficial for the analysis of NKT cell cytokine production in future. However, analysis of total TCR-β$^-$ cell populations after restimulation with αCD3/CD28 did not suggest a significant contribution from non-conventional T cells to the cytokine pool (Appendix, Fig. 7.1C). This is in line with the expectation and αCD3/CD28 preferentially stimulates conventional T cells compared with other immune cells (Trickett and Kwan, 2003).

Discrepancies between ELISA and ICC results could alternatively reflect technical differences between the assays. Analysis by ICC provides more specific information about T cell cytokine production, but unsatisfactory results were obtained by SEA restimulation for ICC with which very few cytokine positive cells could be detected by flow cytometry (Dr. Alexander Phythian-Adams & Angela Marley, unpublished data). Therefore, although not antigen-specific, polyclonal stimulation with αCD3/CD28 was necessary to detect sufficient cytokine positive T cells by flow cytometry. Thus, it can be postulated that differences in SEA-specific responses are somewhat muted by measuring total antigen independent T cell cytokine production.

In addition to affecting immune cell development, differences in the types of APC present from birth may also affect parasite development, as it has been shown that CD4$^+$ T cell help mediated by innate immune cells including DCs or MΦs facilitates the development of male worms and egg production by worm pairs (Lamb et al., 2010). Furthermore, cross-reactive antigens are produced during early stages of the *S. mansoni* infection (Lukacs and Boros, 1991), which may initiate immune responses that are key to later regulation of immune responses to the egg (Pearce and MacDonald, 2002). Thus, to assess the specific role of CD8α$^+$ cDCs at particular stages of infection would require an inducible depletion model. The first inducible depletion model for *Batf3* deficiency was developed recently by Ashok *et al.,* (2014) by creating mixed BM chimeras (CD11c-DTR x *Batf3*$^{-/-}$*)* to investigate the impact of depletion in early and later stages of *L. major* infection. Such an approach would be

advantageous in future studies to confirm the importance of $CD8\alpha^+$ cDCs during specific stages of infection and immune response development, which would build on the understanding gained by the data in this chapter that this DC subset is likely involved in the regulation of Th2 responses during *S. mansoni* infection.

4.7 Conclusion

In conclusion, we have shown that the immune response against *S. mansoni* eggs or during active infection in *Batf3*$^{-/-}$ mice is dysregulated, and that the outcome of this seems to be dependent on the time-point analysed. The field of DC subsets is expanding, and it is becoming increasingly clear that distinct DC types are important for functional and appropriate immune responses to pathogenic agents. The data described in this chapter indicate that early and enhanced Th2 as well as impaired Th1 responses may lead to exacerbated pathology in *Batf3*$^{-/-}$ mice, ultimately resulting in critical weight loss and death of *Batf3*$^{-/-}$ mice during *S. mansoni* infection. The imbalance in the immune response may be a direct result of the loss of CD8α^{+} cDCs, and/or indirectly due to the lack of Th1 responses. Therefore, the data shown in this chapter improve our understanding of the type of DCs involved during schistosome infection by showing that CD8α^{+} cDCs are not a fundamental requirement for Th2 induction, but they contribute to the induction of an "appropriate" immune response to *S. mansoni*.

Excluding CD8α^{+} cDCs as the most important subset for Th2 induction narrows the potential subsets that are involved in this process to CD8α^{-} cDCs. It is tempting to suggest that CD11b^{+} cDCs may be the more likely candidates due to their enhanced ability to present antigen compared with pDCs (Merad et al., 2013). Indeed, CD11b^{+} cDCs have been described as the main subset for Th2 induction in various settings such as allergy (Kumamoto et al., 2013; Plantinga et al., 2013; Williams et al., 2013). Further investigation into the role of CD11b^{+} cDCs during *S. mansoni* will help in unravelling the mechanisms responsible for inducing Th2 immune responses, and better understanding of this will assist in the development of therapeutics for Th2 mediated disease.

4.8 Figures and tables

Diagram 4.1

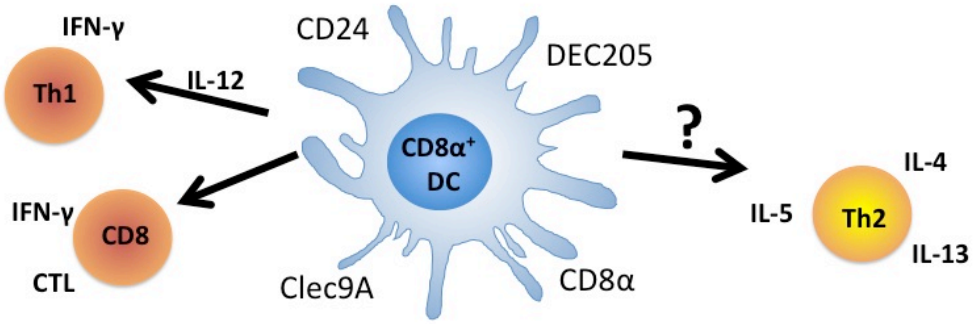

Diagram 4.1 CD8α$^+$ cDCs function in immunity
The role of CD8α$^+$ cDCs in the induction of Th1 responses and CTL immunity against viral and bacterial infection is well established (Ashok et al., 2014; Edelson et al., 2011; Hildner et al., 2008; Mashayekhi et al., 2011; Torti et al., 2011; Waithman et al., 2013). However, the role of CD8α$^+$ cDCs during Th2 responses, in particular in chronic helminth infection is largely unknown. We used *Batf3*$^{-/-}$ mice, which specifically lack this subset, to investigate the function of CD8α$^+$ cDCs during infection with *S. mansoni.*

Figure 4.1

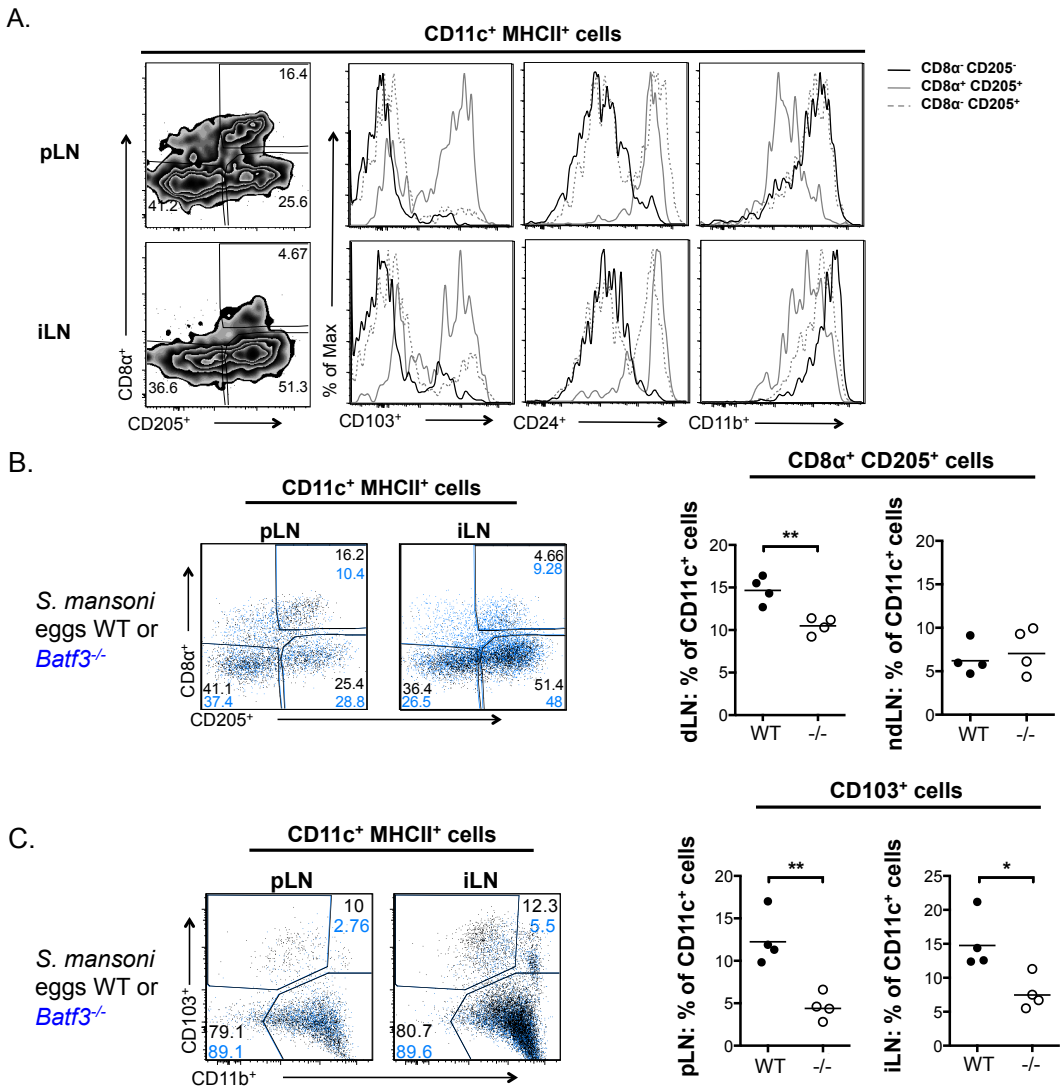

Figure 4.1 CD8α$^+$ cDCs are reduced in the popliteal LNs in *Batf3*$^{-/-}$ mice
S. mansoni eggs were injected s.c. into WT or *Batf3*$^{-/-}$ mice. Popliteal LNs (pLNs) and inguinal LNs (iLNs) were harvested 7 days later for flow cytometric analysis. **A.** DCs present in pLNs and iLNs from WT mice were assessed for CD8α and CD205 expression. Relative expression of CD103, CD24 and CD11b is shown for CD8α$^+$ CD205$^+$, CD8α$^-$ CD205$^+$ and CD8α$^-$ CD205$^-$ cDC populations. **B.** The proportion of CD8α$^+$ CD205$^+$ cDCs of the CD11c$^+$ MHC-II$^+$ cDC population is shown for *S. mansoni* egg-injected WT and *Batf3*$^{-/-}$ mice. *Batf3*$^{-/-}$ cells are shown in blue and WT cells in black. **C.** CD103$^+$ cDCs and CD11b$^+$ cDCs were examined, and proportions of CD103$^+$ DCs in WT and *Batf3*$^{-/-}$ mice are shown. 1 of 3 experiments (A to C). One-way ANOVA (*, $P < 0.05$; **, $P < 0.01$; ***, $P < 0.001$, ****, $P < 0.0001$). SEM is shown for 4 mice per group.

Figure 4.2

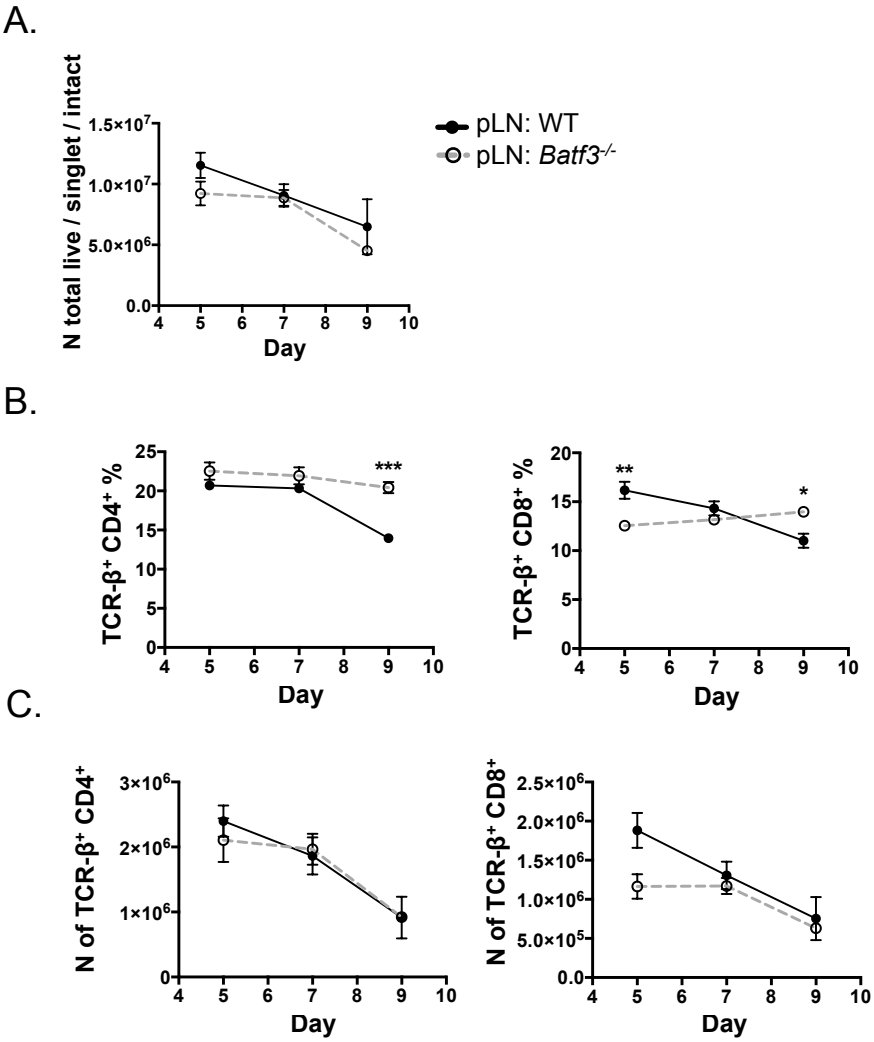

Figure 4.2 T cell populations in *S. mansoni* egg-injected *Batf3*$^{-/-}$ mice
S. mansoni eggs were injected s.c. into WT or *Batf3*$^{-/-}$ mice. 5, 7, and 9 days later pLNs were harvested for flow cytometric analysis. **A.** Total cell numbers for pLNs of WT and *Batf3*$^{-/-}$ mice were determined using trypan blue counts. **B.** pLN cells from egg-injected WT and *Batf3*$^{-/-}$ mice were analysed by flow staining for TCR-β^{+} T cells to examine CD4^{+} and CD8^{+} T cell proportions as a percentage of live/single/intact cells. **C.** Trypan blue counts from (A) were used to calculate the absolute numbers of CD4^{+} and CD8^{+} T cells per pLN pair per mouse. Data are 1 of 1 experiment (A to C). Two-way ANOVA (*, $P < 0.05$; **, $P < 0.01$; ***, $P < 0.001$, ****, $P < 0.0001$). Mean values ± SEM are shown for 4-5 mice/group.

Figure 4.3

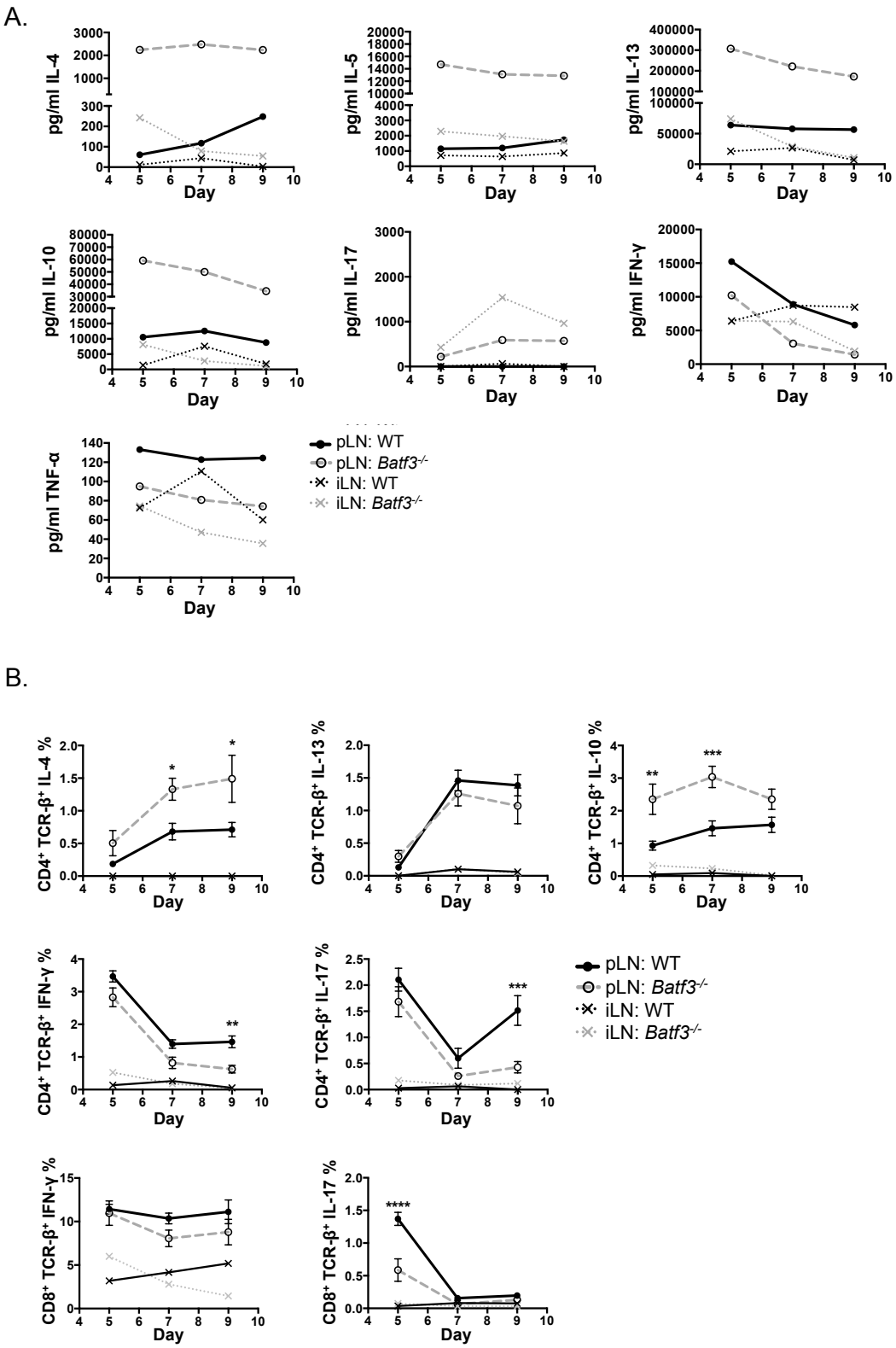
A.
pg/ml IL-4
pg/ml IL-5
pg/ml IL-13
pg/ml IL-10
pg/ml IL-17
pg/ml IFN-γ
pg/ml TNF-α
Day
pLN: WT
pLN: Batf3-/-
iLN: WT
iLN: Batf3-/-
B.
CD4+ TCR-β+ IL-4 %
CD4+ TCR-β+ IL-13 %
CD4+ TCR-β+ IL-10 %
CD4+ TCR-β+ IFN-γ %
CD4+ TCR-β+ IL-17 %
CD8+ TCR-β+ IFN-γ %
CD8+ TCR-β+ IL-17 %
Day
pLN: WT
pLN: Batf3-/-
iLN: WT
iLN: Batf3-/-

Figure 4.3

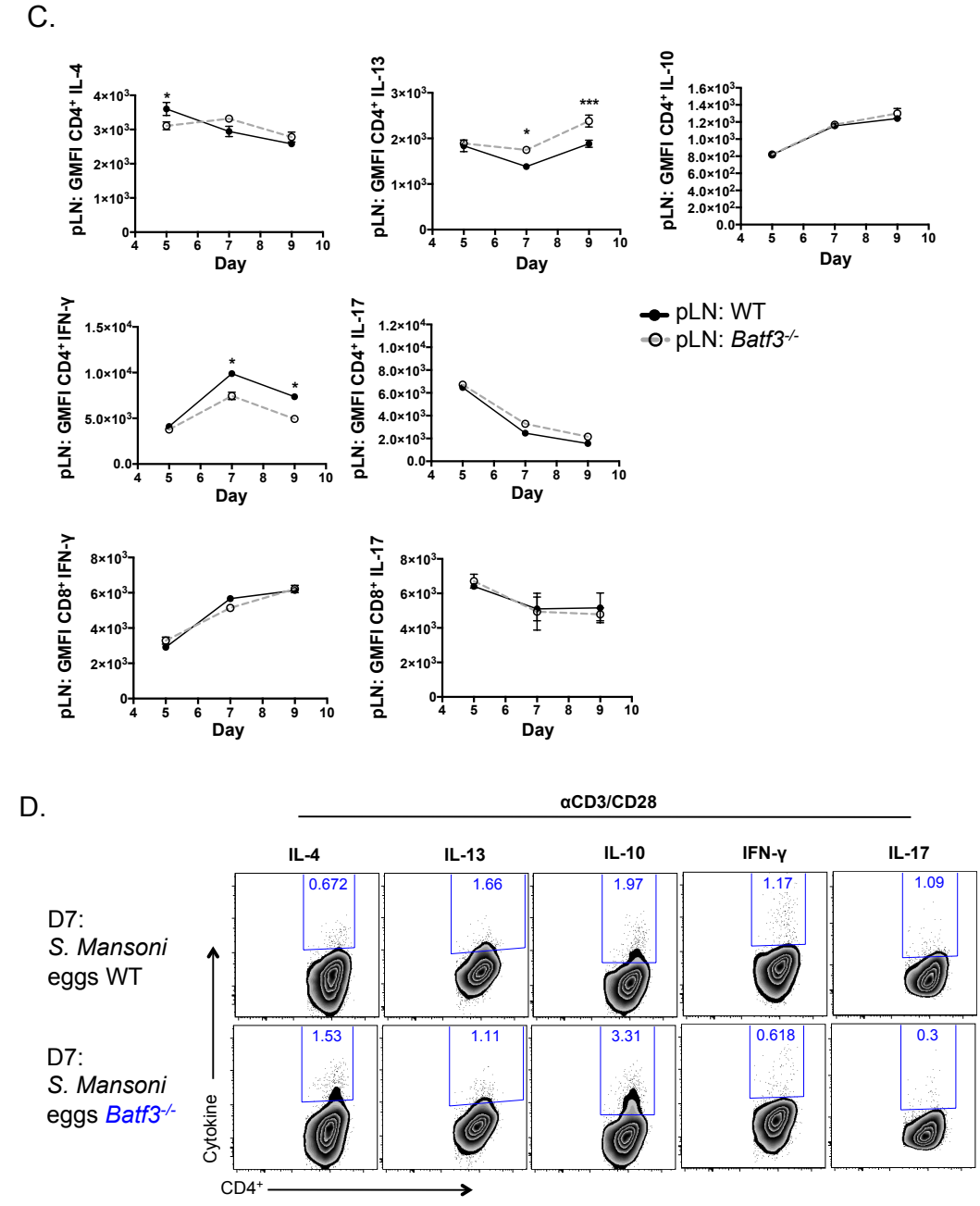

Figure 4.3 Th2 induction against *S. mansoni* eggs is unimpaired in *Batf3*$^{-/-}$ mice

S. mansoni eggs were injected into WT or *Batf3*$^{-/-}$ mice. 5, 7, and 9 days later pLNs and iLNs were harvested for analysis of cytokine production *in vitro* in response to SEA **A.** Cells from pLNs or iLNs of WT or *Batf3*$^{-/-}$ mice were pooled and cultured for 72h with 15 μg/ml SEA or media alone. Supernatants were collected to assess cytokine production by ELISA (data presented with medium alone background

subtracted). N = 1 (pools of 4-5 mice). **B.** Cells from pLNs and iLNs were restimulated with αCD3/CD28 o/n and assessed for ICC by flow cytometry. $CD4^+$ TCR-β^+ and $CD8^+$ TCR-β^+ T cells were analysed for cytokine expression. **C.** The GMFI was determined to assess the level of cytokine expression by $CD4^+$ and $CD8^+$ T cells. **D.** Representative flow cytometry plots are shown for $CD4^+$ T cell cytokine expression at D7. Gates were set using FMO controls. Data are 1 of 1 experiment (A to D). Two-way ANOVA (*, $P < 0.05$; **, $P < 0.01$; ***, $P < 0.001$, ****, $P < 0.0001$). Mean values ± SEM are shown for 4-5 mice/group.

Figure 4.4

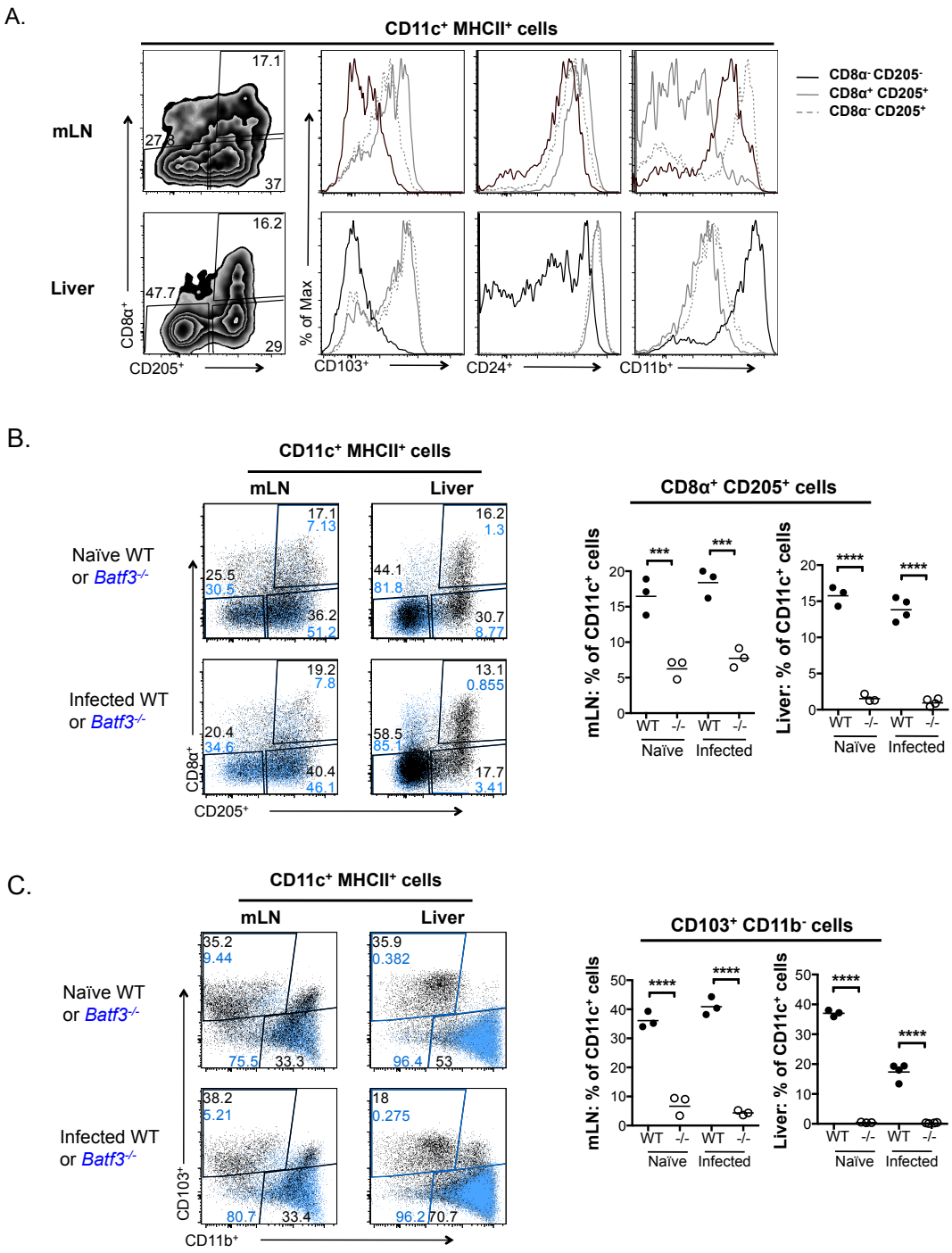

Figure 4.4 The proportion of CD8α$^+$ DCs is reduced in the mLN and the liver of *Batf3*$^{-/-}$ mice at D42

The mLNs and livers from naïve or D42 *S. mansoni* infected WT or *Batf3*$^{-/-}$ mice were harvested and isolated. mLN and liver leukocytes were analysed by flow cytometry for the presence of CD8α$^+$ cDCs **A.** CD8α$^+$ CD205$^+$, CD8α$^-$ CD205$^+$ and CD8α$^-$ CD205$^-$ cDCs in the mLN and the liver from naïve WT mice were assessed for their expression of CD103, CD24 and CD11b. **B.** Representative flow plots for CD11c$^+$ MHC-II$^+$ cDC subsets are shown to display expression of CD8α and CD205 in the

mLN and liver leukocytes from naïve and infected animals. *Batf3*$^{-/-}$ cells are shown in blue and WT cells in black and the proportion of CD8α^{+} cDCs in WT compared with *Batf3*$^{-/-}$ mice is shown graphically. **C.** In both tissues the proportion of *Batf3*-dependent migratory CD103^{+} cDCs was analysed in WT and *Batf3*$^{-/-}$ mice as for CD8α^{+} cDCs in (B). Representative flow plots and the proportions of CD103^{+} cDCs for WT and *Batf3*$^{-/-}$ mice are shown. Gates were set using FMO controls. 1 of 2 experiments (A to C). Two-way ANOVA (*, $P < 0.05$; **, $P < 0.01$; ***, $P < 0.001$, ****, $P < 0.0001$). Bars are SEM of 3-4 mice per group.

Figure 4.5

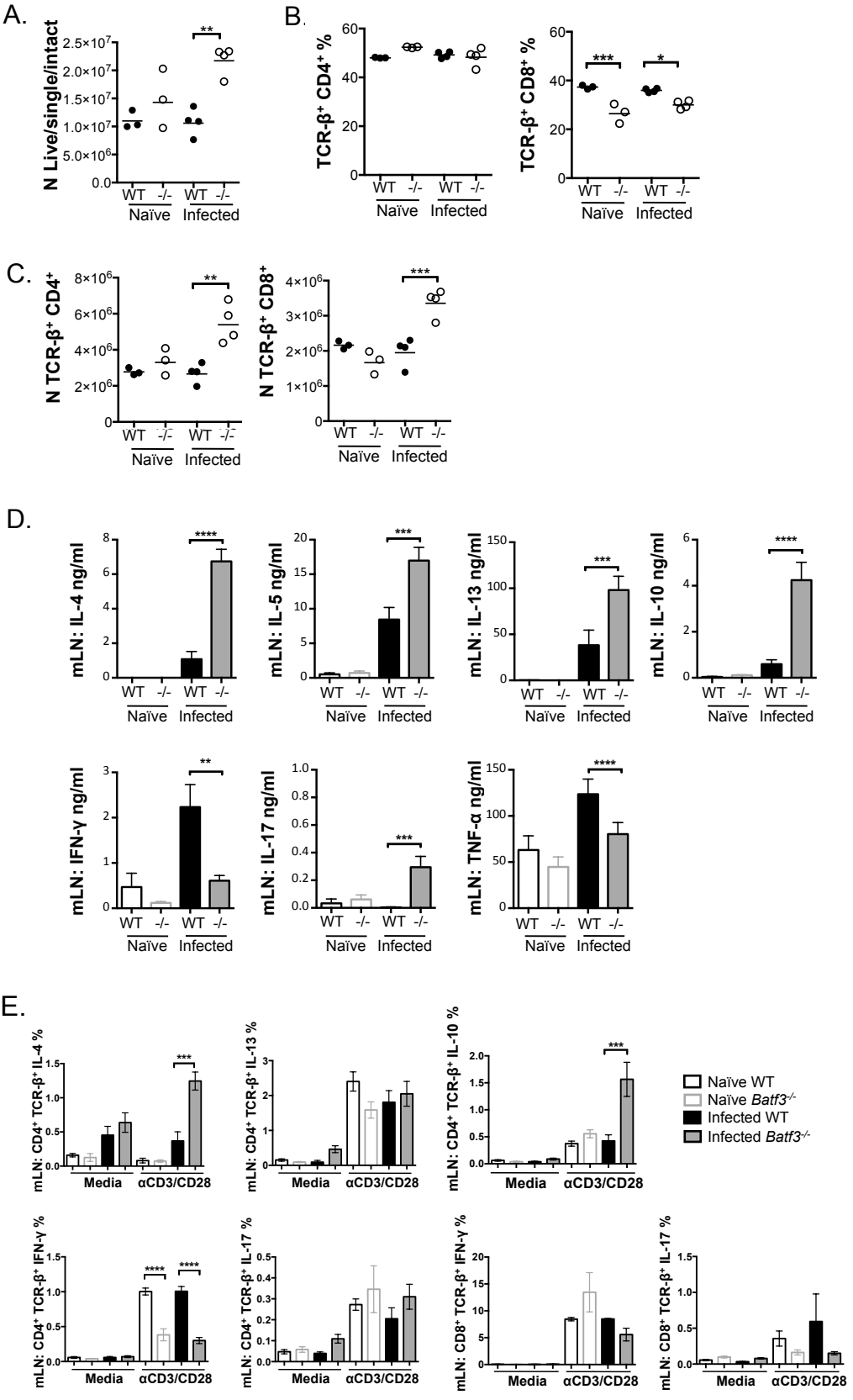
A.
N Live/single/intact
B.
TCR-β+ CD4+ %
TCR-β+ CD8+ %
C.
N TCR-β+ CD4+
N TCR-β+ CD8+
D.
mLN: IL-4 ng/ml
mLN: IL-5 ng/ml
mLN: IL-13 ng/ml
mLN: IL-10 ng/ml
mLN: IFN-γ ng/ml
mLN: IL-17 ng/ml
mLN: TNF-α ng/ml
WT -/- WT -/-
Naïve Infected
E.
mLN: CD4+ TCR-β+ IL-4 %
mLN: CD4+ TCR-β+ IL-13 %
mLN: CD4+ TCR-β+ IL-10 %
mLN: CD4+ TCR-β+ IFN-γ %
mLN: CD4+ TCR-β+ IL-17 %
mLN: CD8+ TCR-β+ IFN-γ %
mLN: CD8+ TCR-β+ IL-17 %
Media αCD3/CD28
Naïve WT
Naïve Batf3-/-
Infected WT
Infected Batf3-/-

Figure 4.5

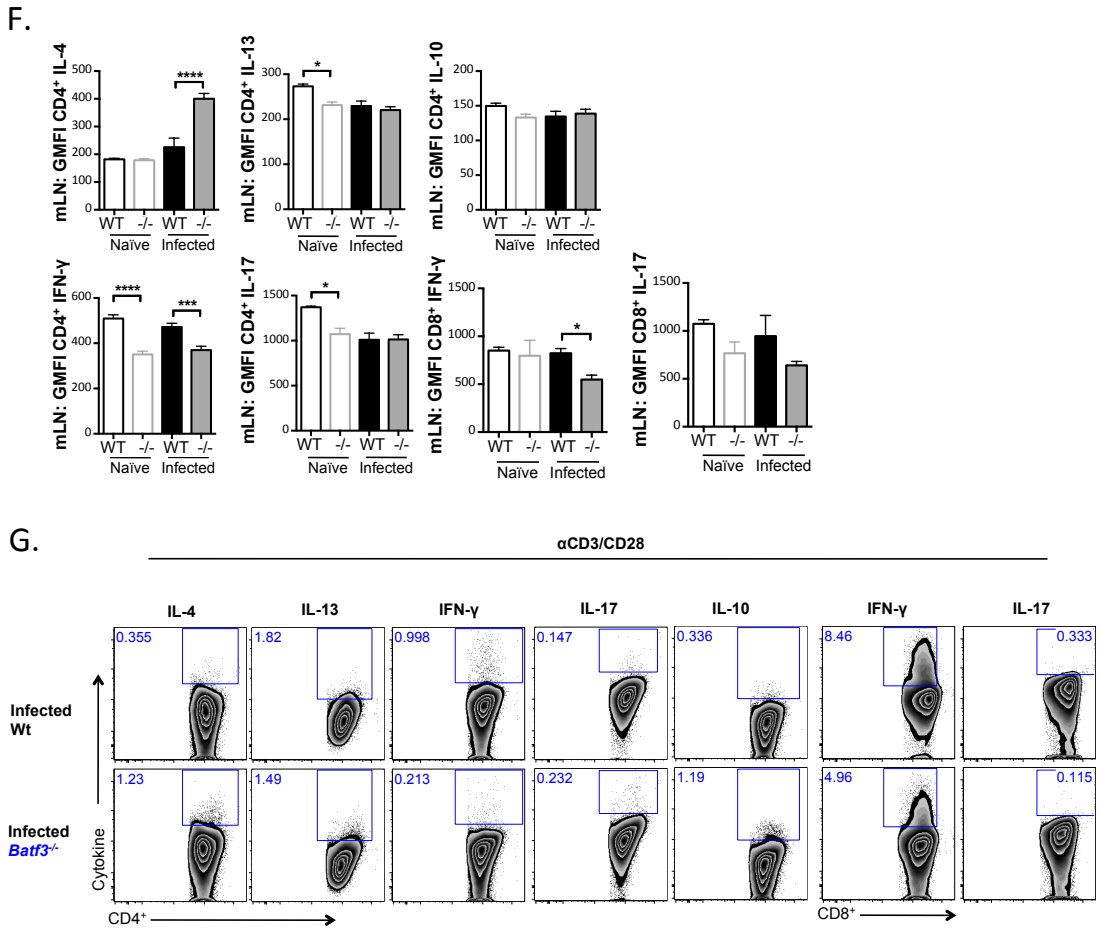

Figure 4.5 In priming sites the induction of Th2 responses at D42 during *S. mansoni* infection does not require CD8α$^+$ DCs

mLNs from naïve or *S. mansoni* infected mice were harvested on D42 of infection. **A.** Trypan blue counts were used to calculate the number of total live cells present in the mLN. **B-C.** Flow cytometry analysis of T cell populations expressing CD4 or CD8 are shown as total numbers and percentage of live/intact/single TCR-β$^+$ cells. **D**. Cells from naïve or infected WT and *Batf3*$^{-/-}$ mice were cultured with 15 μg/ml SEA or media alone for 72h and supernatants were collected for ELISA analysis of cytokine production (data presented with medium alone background subtracted). **E.** Intracellular T cell cytokine staining was assessed by flow cytometry. CD8$^+$ T cells did not produce detectable IL-4, IL-13 or IL-10. **F.** The GMFI of T cell cytokine expression was determined by flow cytometry. **G**. Representative flow plots for T cell cytokine production are shown in response to αCD3/CD28 restimulation. Gates were set using FMO controls. 1 of 2 experiments (A to C) or 1 of 1 experiments (E to G), two-way ANOVA. Data in (D) are from 2 experiments (from D40 and D42 experiments as described in section 4.4.4) and were analysed by mixed model statistics blocking the day of experiment. (*, $P < 0.05$; **, $P < 0.01$; ***, $P < 0.001$, ****, $P < 0.0001$). Error bars are SEM of 3-4 mice per group.

Figure 4.6

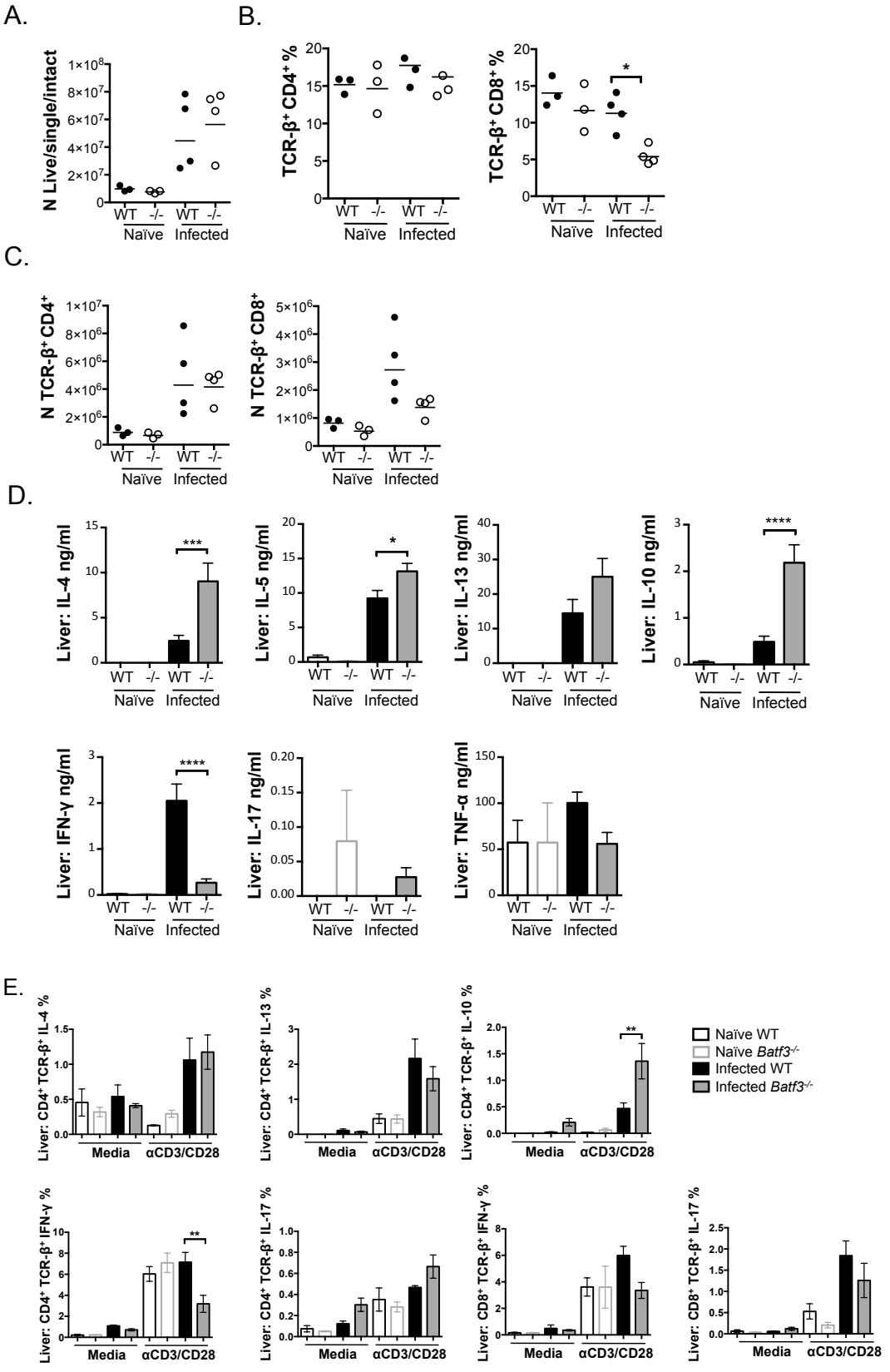
A.
B.
C.
D.
E.
N Live/single/intact
TCR-β+ CD4+ %
TCR-β+ CD8+ %
N TCR-β+ CD4+
N TCR-β+ CD8+
Liver: IL-4 ng/ml
Liver: IL-5 ng/ml
Liver: IL-13 ng/ml
Liver: IL-10 ng/ml
Liver: IFN-γ ng/ml
Liver: IL-17 ng/ml
Liver: TNF-α ng/ml
Liver: CD4+ TCR-β+ IL-4 %
Liver: CD4+ TCR-β+ IL-13 %
Liver: CD4+ TCR-β+ IL-10 %
Liver: CD4+ TCR-β+ IFN-γ %
Liver: CD4+ TCR-β+ IL-17 %
Liver: CD8+ TCR-β+ IFN-γ %
Liver: CD8+ TCR-β+ IL-17 %
WT
-/-
Naïve
Infected
Media
αCD3/CD28
Naïve WT
Naïve Batf3-/-
Infected WT
Infected Batf3-/-

Figure 4.6

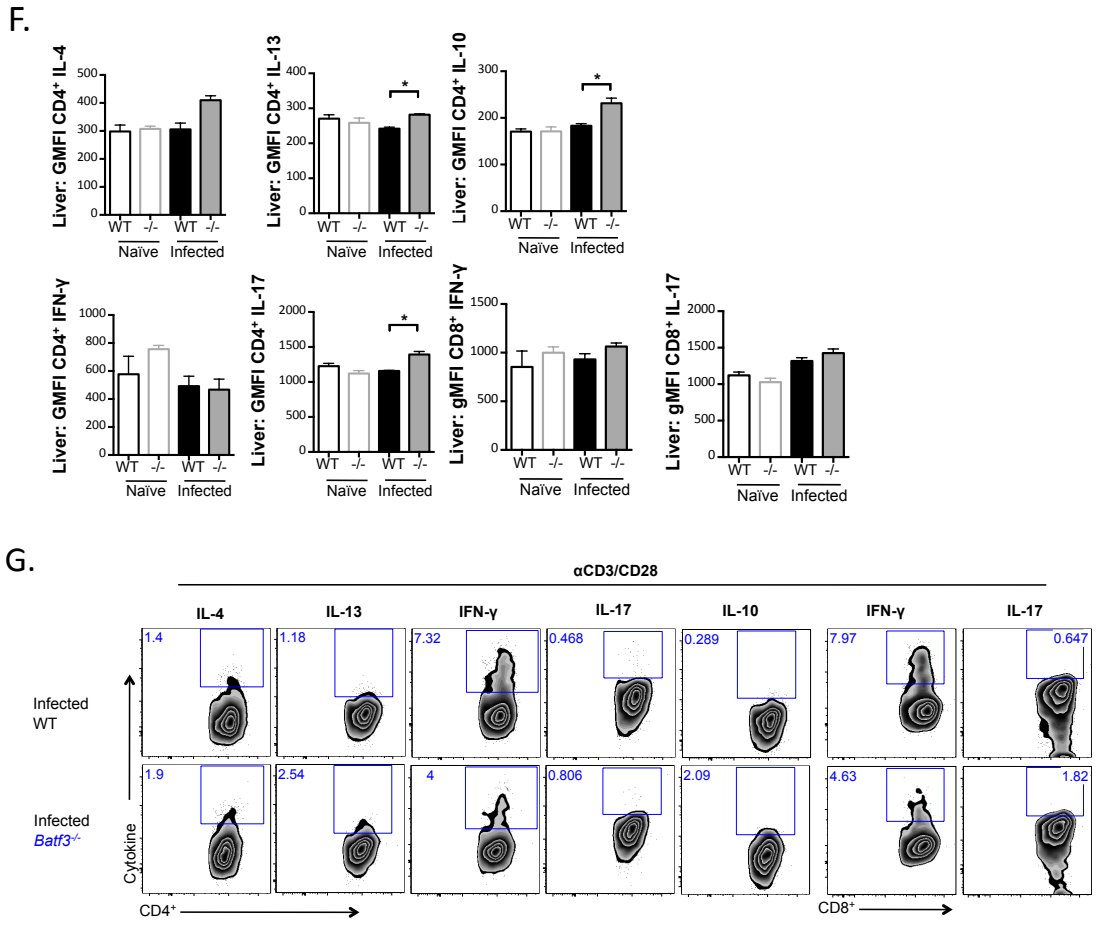

Figure 4.6 Th2 responses are unimpaired in the liver of *Batf3*$^{-/-}$ mice at D42 of *S. mansoni* infection

Livers from naïve or *S. mansoni* infected mice were harvested on D42 of infection. **A.** Trypan blue counts were used to calculate the number of total live leukocytes present in the liver **B-C.** The proportions (B) and absolute numbers (C) of $CD4^+$ and $CD8^+$ T cells in the liver were determined by flow cytometric analysis of naïve or infected WT mice compared with *Batf3*$^{-/-}$ mice. **D.** As done previously for mLNs, liver leukocytes from naïve or infected WT and *Batf3*$^{-/-}$ mice were analysed for cytokine secretion in response to SEA or media alone after 72h of culture (data presented with medium alone background subtracted). **E.** Liver leukocytes were restimulated o/n with αCD3/CD28 and stained by ICC. The proportions of T cells expressing IL-4, IL-13, IL-10, IFN-γ and IL-17 are graphed. **F.** The GMFI of cytokine expression by T cells is shown. **G.** Representative flow plots for $CD4^+$ and $CD8^+$ T cell cytokine production are shown. Gates were set using FMO controls. 1 of 2 experiments (A-C) or 1 of 1 experiment (E-G), two-way ANOVA. Data in (D) are from 2 experiments (from D40 and D42 experiments as described in section 4.4.4) and were analysed by mixed model statistics blocking the day of experiment (*, $P < 0.05$; **, $P < 0.01$; ***, $P < 0.001$, ****, $P < 0.0001$). Error bars are mean values ± SEM of 3-4 samples per group. Each sample was a pool of 2-3 livers (i.e. 8-10 mice per group).

Figure 4.7

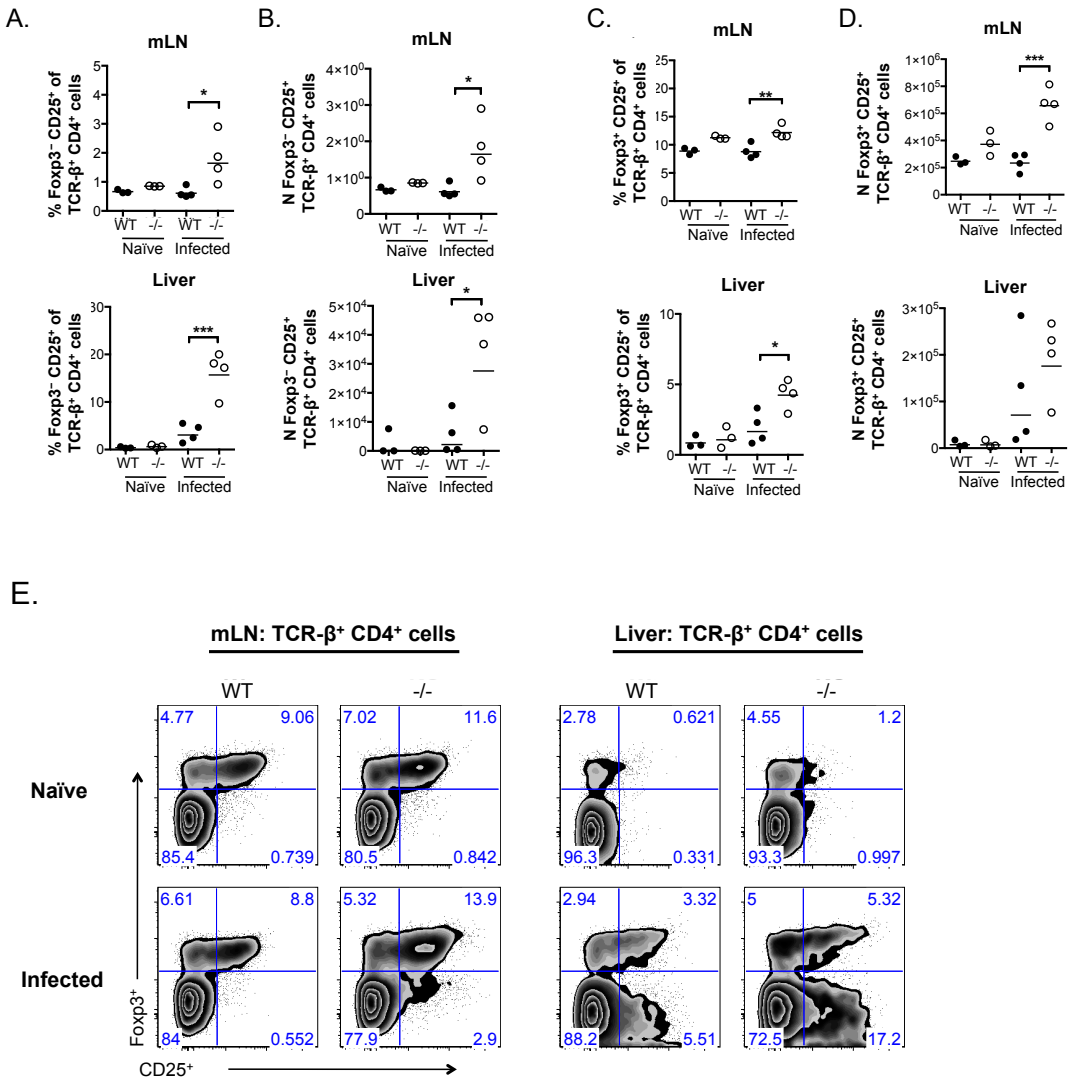

Figure 4.7 Effector CD4$^+$ T cells and Treg populations are increased in *Batf3*$^{-/-}$ mice at D42 of *S. mansoni* infection

mLN and liver leukocytes were isolated from naïve or D42 *S. mansoni* infected WT or *Batf3*$^{-/-}$ mice and examined *ex vivo* by flow cytometry. **A-B.** Proportions and numbers of CD4$^+$ TCR-β$^+$ cells expressing CD25 but not Foxp3 are shown for the mLN (top panel) and the liver (bottom panel). **C-D.** Proportions of CD4$^+$ TCR-β$^+$ cells expressing both CD25 and Foxp3 are presented for the mLN (top panel) and the liver (bottom panel). **E.** Representative flow plots displaying CD25 and Foxp3 expression of CD4$^+$ TCR-β$^+$ T cells are depicted for the mLN (left) and the liver (right). Gates were set using FMO controls. 1 of 1 experiment (A to E). Two-way ANOVA (*, $P < 0.05$; **, $P < 0.01$; ***, $P < 0.001$, ****, $P < 0.0001$). Error bars are mean values ± SEM of 3-4 mice per group (mLN) or 8-10 mice (liver).

Figure 4.8

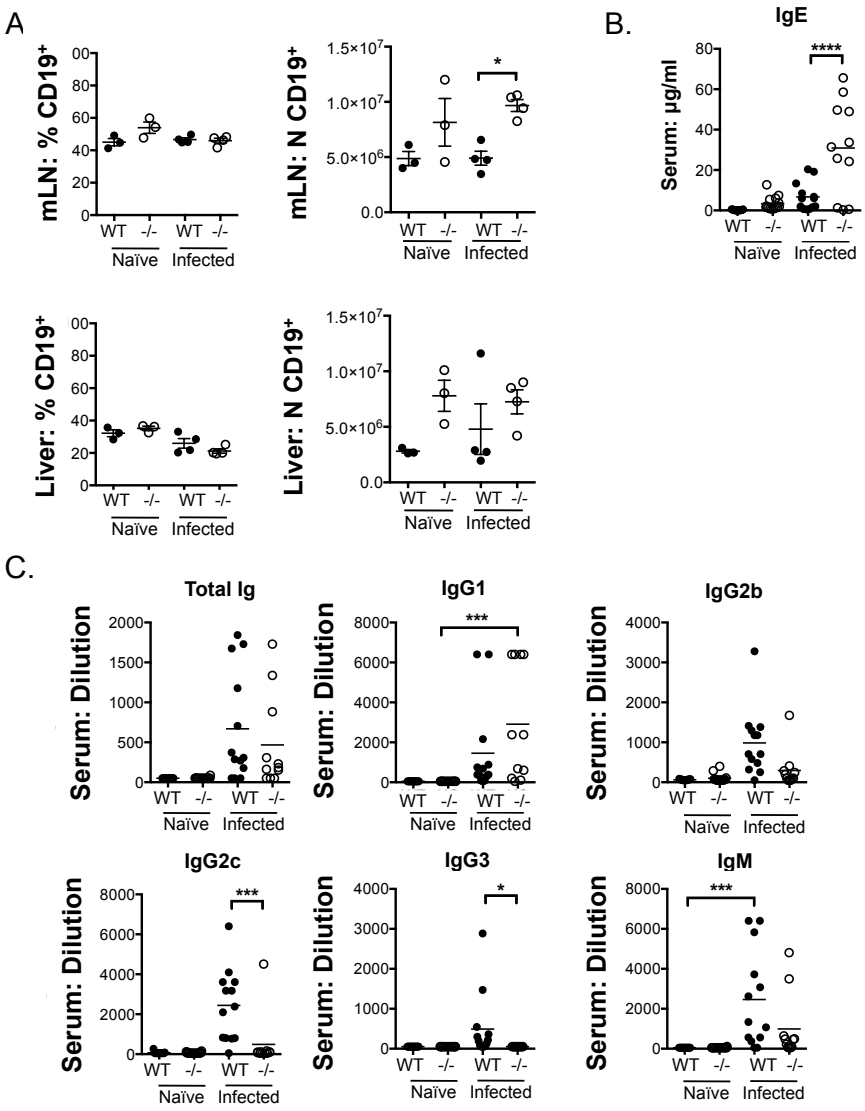

Figure 4.8 Production of antibody isotypes detected in the serum of *S. mansoni* infected *Batf3*$^{-/-}$ mice is altered at D42

A. mLN and liver leukocytes were isolated from naïve or D42 *S. mansoni* infected WT or *Batf3*$^{-/-}$ mice and examined *ex vivo* by flow cytometry. The proportion of live cells and absolute numbers of B cells expressing CD19 are shown for the MLN (top) and the liver (bottom). **B.** Serum was collected from WT or *Batf3*$^{-/-}$ mice 1 day prior to harvest and the total amount of IgE was measured by ELISA. **C.** The dilution of SEA-specific antibody isotypes in the serum was assessed using a serum sample known to contain all of the isotypes measured. The dilution that corresponded to half the OD of the known serum sample was recorded. 1 of 1 experiment, two-way ANOVA (A). Data in (B to C) are from 2 experiments analysed by mixed model statistics blocking the day of experiment (from D40 and D42 experiments as described in section 4.4.4). (*, $P < 0.05$; **, $P < 0.01$; ***, $P < 0.001$, ****, $P < 0.0001$). Bars are SEM of 11-15 mice per group.

Figure 4.9

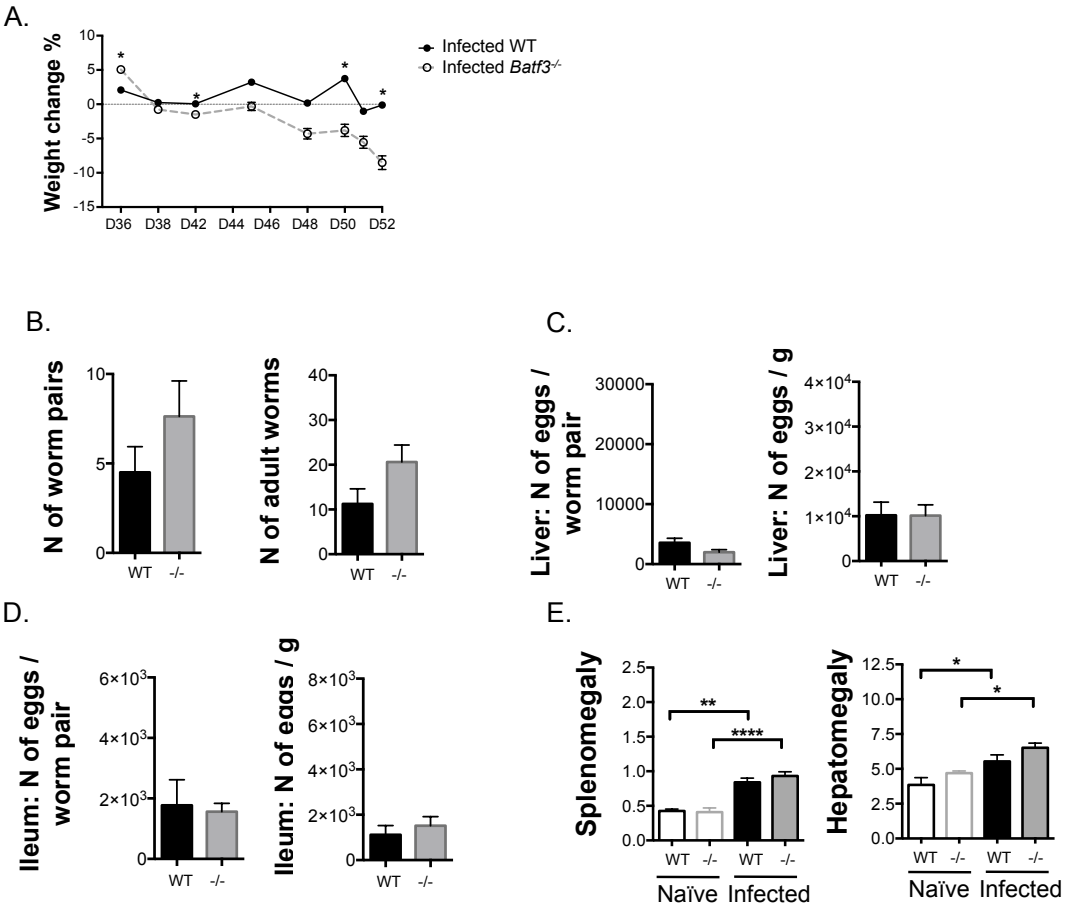

Figure 4.9 Critical weight loss in *Batf3*$^{-/-}$ mice during *S. mansoni* infection.

A. From D36 until D52 of *S. mansoni* infection body weights of both WT and *Batf3*$^{-/-}$ mice were measured, and the percentage weight change was calculated for each mouse. **B.** The worm burden per mouse was assessed by counting the number of adult worms (male and female) and determining the number of worm pairs present in the blood at D42. **C.** The total numbers of eggs in KOH digested liver tissues of D42 infected WT and *Batf3*$^{-/-}$ mice was counted to assess the egg burden in infected WT compared to *Batf3*$^{-/-}$ mice. **D.** The egg burden at D42 was counted in the ileum from WT and *Batf3*$^{-/-}$ mice as in (C). **D**. Splenomegaly and hepatomegaly were calculated as a percentage of body weight in naïve and infected animals at D42. 1 of 1 experiment (A), 1 of 2 experiments (B to E). Two-way ANOVA (*, $P < 0.05$; **, $P < 0.01$; ***, $P < 0.001$, ****, $P < 0.0001$). Error bars are mean values ± SEM for 3 to 7 mice/group.

Figure 4.10

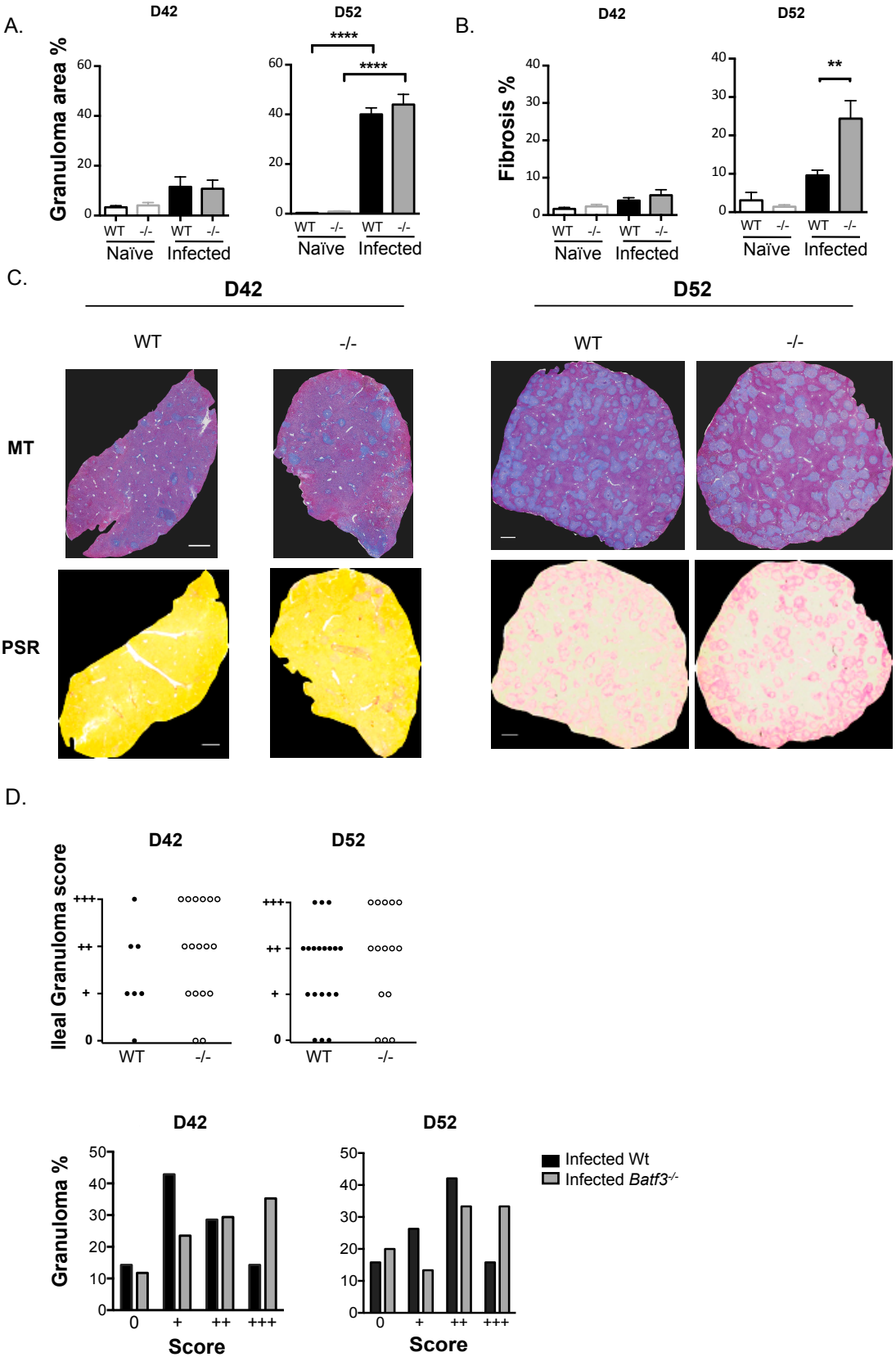
A.
D42
D52
Granuloma area %
****
****
WT -/- WT -/-
Naïve
Infected
B.
D42
D52
Fibrosis %
**
C.
D42
D52
WT
-/-
MT
PSR
D.
D42
D52
Ileal Granuloma score
Granuloma %
Score
Infected Wt
Infected Batf3-/-

Figure 4.10

E.

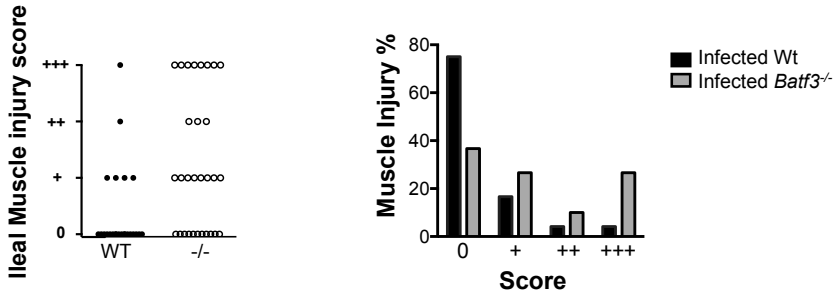

Figure 4.10 Granulomatous pathology is more severe in *Batf3*$^{-/-}$ mice
A-B. Granulomatous inflammation and fibrosis in the median liver lobe was measured using MT or PSR staining slides respectively. Image J software was used to objectively determine the total proportion of granulomas or collagen deposition using a digital slide scanner and an algorithm **C.** Representative BF images are shown of tissue sections from the same liver stained with MT and PSR to compare total granulomatous inflammation staining (blue) with collagen deposition staining (red) respectively. Scale = 1mm. **D.** Single egg granulomas present in the ileum were scored for their intensity and density of immune cells, the amount of collagen deposition, and the severity of damage to the surrounding tissue. Score 0 represents absent granuloma formation around the egg and score $^{+++}$ represents the highest pathological score. The percentage of granulomas per score is plotted graphically. No statistics can be performed on these scores as they are classed as arbitrary. **E.** The number of vacuoles, the size of vacuoles and the structural damage to the circular ileal muscle (termed as muscle injury) at D42 infected WT or *Batf3*$^{-/-}$ mice were scored and graphed in a similar way as granuloma scoring. 1 of 1 experiment (A to E). Two-way ANOVA (*, $P < 0.05$; **, $P < 0.01$; ***, $P < 0.001$, ****, $P < 0.0001$). Bars are SEM of 6 - 8 mice per group.

5 The function of dendritic cells during *S. mansoni* infection

5.1 Abstract

Although DCs can direct $CD4^+$ T cells towards a potent Th2 response and are necessary for this process during *S. mansoni* infection, the exact mechanisms they employ for this process remain elusive. However, the capacity of DCs to induce strong Th2 immune responses during *S. mansoni* infection is not matched by their activation phenotype in response to SEA, which appears muted compared with classical activation in response to viral or bacterial stimuli (MacDonald et al., 2001). Furthermore, the function of distinct DC subsets during *S. mansoni* infection has not yet been addressed. To assess the function of DCs during a dominant Th2 response at D42 in the liver during *S. mansoni* infection, an ovalbumin (OVA) recognition system was used to investigate whether infection alters the ability of DCs to take up, process and present OVA to $CD4^+$ T cells. This approach has shown that cDCs are efficient at inducing and maintaining $CD4^+$ T cell responses during *S. mansoni* infection, but *S. mansoni* infection does not alter the core functions of cDCs. Analysis of cDC subsets revealed that *S. mansoni* infection enhances the ability of $CD8\alpha^-$ cDCs, but not $CD8\alpha^+$, to induce naïve $CD4^+$ T cell proliferation and maintain Th2 cytokine production by activated T cells. Thus, these data further our understanding of the DC subsets required for the induction and maintenance of Th2 responses, and provide new information on the functional characteristics that DCs display during *S. mansoni* infection.

5.2 Introduction

Current understanding of DC function consists mainly of inflammatory Th1/17 responses to bacteria, protozoa or viruses orchestrated by effector T cells, which have become activated by DCs that have recognised PAMPs or DAMPs associated with the pathogen (Janeway, 1989; Kapsenberg, 2003; Matzinger, 2002) (described in section 1.1, chapter 1). PAMPs or DAMPs are bound to PRRs on the surface of DCs, resulting in NFκB activation via the adaptor protein MyD88 (Kawai and Akira, 2010). This leads to conventional activation of DCs hallmarked by stable MHC-II expression and substantial upregulation of co-stimulatory molecules on the surface of DCs, such as CD40, CD80 and CD86, which enables efficient presentation of antigen to T cells (Janeway, 1989; Mogensen, 2009) (section 1.3, chapter 1). In addition, conventionally activated DCs produce significant amounts of inflammatory cytokines including IL-12, TNF-α and IL-6 (Morelli et al., 2001). Yet, how DCs orchestrate the induction of Th2 responses, and which DC subsets are involved in this process, remains less clear compared with the mechanisms that mediate Th1/17 responses.

Helminths including *S. mansoni* commonly fail to conventionally activate DCs (Balic et al., 2004; MacDonald et al., 2001; Whelan et al., 2000), even though BMDCs and *ex vivo* splenic DCs are sufficient to induce dominant Th2 responses against *S. mansoni* eggs or in response to SEA (Jankovic et al., 2004; MacDonald et al., 2001). Due to the rarity of DCs in the body most published research on DC function and activation during *S. mansoni* infection has focused on BMDCs (Jenkins et al., 2007; Kane et al., 2004; MacDonald et al., 2001; MacDonald and Pearce, 2002), *ex vivo* splenic DCs (Jankovic et al., 2004; Steinfelder et al., 2009; Straw et al., 2003) or human peripheral blood DCs (Agrawal et al., 2003; de Jong et al., 2002) (section 1.9.1, chapter 1). This research has elevated our understanding of DC components that are essential for the induction of Th2 responses, such as surface CD40-CD154 (MacDonald et al., 2002a; 2002b), OX40-OX40-L (Jenkins et al., 2007) and MHC-II (MacDonald et al., 2001) interactions, as well as intracellular NFκB signalling (Artis et al., 2005). In contrast to Th1 responses, MyD88 signalling

is not required for the induction of Th2 responses *in vivo* (Layland et al., 2005). Notably, the role of DC subsets in the liver during Th2 induction in murine *S. mansoni* infection has yet to be described, even though this is a crucial effector site where the majority of eggs are deposited (Cheever et al., 1987).

5.2.1 Functions of hepatic dendritic cell subsets in the steady state and in response to antigen

Functions of DCs in liver homeostasis, fibrosis, immune tolerance and pathogenesis are all areas of active research. Human liver biopsies have revealed that although DCs are distributed sparsely throughout the parenchyma, they are mainly found in portal regions (Bosma et al., 2006). This places DCs in an ideal location to monitor the portal circulation (Rahman and Aloman, 2013). The liver has many functions, including the metabolism of carbohydrates, proteins and lipids as well as the clearance of pathogens and toxins that arrive from the intestines to the liver from the blood (Protzer et al., 2012). Constant exposure to harmless dietary and commensal antigens requires a tolerogenic environment in the liver to avoid unnecessary organ tissue damage caused by inflammatory immune responses (Protzer et al., 2012). Liver DCs can broadly be grouped into cDCs and pDCs, similar to lymphoid and other peripheral tissues (Rahman and Aloman, 2013). Both cDCs and pDCs contribute to the tolerogenic environment within the liver by producing IL-10 (Bamboat et al., 2010; 2009; Goddard et al., 2004; Tokita et al., 2008). Thus, the unique environment in the liver makes the comparison of DC functions with other tissues problematic and highlights the necessity for research on hepatic DC function specifically.

pDCs are generally poor presenters of endocytosed antigen in any tissue due to the lack of cellular machinery that is required for the efficient uptake, processing and presentation of antigen to T cells (Villadangos and Young, 2008) (section 1.2.2, chapter 1). Instead, pDCs produce high levels of type I IFNs against viral infections, which leads to activation of numerous immune cells, including NK cells and $CD8^+$ T cells (Pinto et al., 2011; Swiecki et al., 2010). Interestingly, the frequency of pDCs in the naïve liver is higher than in secondary lymphoid organs (Pillarisetty et al., 2004),

yet they are generally less immunogenic (Pillarisetty et al., 2004; Tokita et al., 2008). As such, hepatic pDCs produce reduced levels of IFN-α in comparison with splenic pDCs (Kingham et al., 2007) and are less efficient at activating $CD4^+$ T cell responses (Castellaneta et al., 2009). In contrast to pDCs, cDCs generally display an enhanced ability in the capture, processing and presentation of antigen to T cells compared with pDCs (Merad et al., 2013), but steady state cDC immunogenicity is also lower in the liver compared with the spleen (Abe et al., 2006; Pillarisetty et al., 2004). Pillarisetty *et al.,* (2004) showed that *ex vivo* isolated liver cDCs express lower levels of activation markers including MHC-II and CD40, and are less efficient at taking up FITC labelled dextran or OVA compared with splenic counterparts. Furthermore, the same study reported that freshly isolated liver cDCs are less proficient at inducing T cell proliferation and cytokine production compared with splenic cDCs. This renders hepatic cDCs in the steady state less responsive to danger signals in portal blood, compared with their splenic counterparts, a phenotype that is crucial for maintaining immunological tolerance against antigen in an environment that is continuously exposed to harmless bacterial products from the intestines (Protzer et al., 2012).

The function and activation of DCs in the liver in response to antigen and infection remains understudied, with only a few reports having addressed this. It is thought that activation and immunogenicity of hepatic cDCs requires higher doses of antigen compared with their splenic counterparts (Crispe, 2011). For example, the T cell stimulatory capacity of *ex vivo* liver cDCs is reduced compared with splenic cDCs following activation with low doses of LPS, as T cell proliferation and production of IFN-γ or IL-4 is decreased (De Creus et al., 2005). However, liver and splenic cDCs activated with high doses of LPS induce comparable T cell responses (De Creus et al., 2005). This result can be replicated *in vivo,* when *ex vivo* hepatic or splenic cDCs are stimulated with LPS and adoptively transferred s.c. into allogeneic naïve mice (De Creus et al., 2005). Thus, liver cDCs likely display a comparatively high threshold for activation by LPS, which may be in part due to lower expression levels of TLR4 compared with splenic counterparts (De Creus et al., 2005).

In comparison with splenic cDCs, little is known about the function and T cell stimulatory capacity of distinct hepatic cDC subsets. Pillarisetty *et al.,* (2004) investigated the phenotype and function of different types of cDCs in the liver and showed that hepatic $CD8\alpha^+$ and $CD11b^+$ cDCs display similar T cell activation capacities compared with their splenic counterparts (Pillarisetty et al., 2004). Therefore, hepatic and splenic $CD8\alpha^-$ cDCs induce marginally higher levels of T cell proliferation and cytokine production compared with $CD8\alpha^+$ cDCs (Pillarisetty et al., 2004; Rizzitelli et al., 2005). Pillarisetty *et al.,* (2004) proposed that the liver contains a larger number of phenotypically less mature cDC subsets in comparison with the spleen, including $CD8\alpha^{low/-}$ and $CD11b^{low/-}$ cDCs, which may explain the overall weaker stimulatory phenotype of "bulk" liver cDCs in the steady state. De Creus *et al.,* (2005) compared the function of liver $CD8\alpha^+$ and $CD8\alpha^-$ cDC subsets in response to antigen with their splenic counterparts, and found that the stimulatory capacity of each hepatic subset increased to levels similar in comparison with their splenic counterparts at high doses of LPS. However, both studies outlined above did not differentiate between $CD4^+$ and $CD8^+$ T cells (De Creus et al., 2005; Pillarisetty et al., 2004), which complicates the interpretation of the results, as $CD8\alpha^+$ cDCs and $CD11b^+$ cDCs are thought to preferentially interact with $CD8^+$ and $CD4^+$ T cells respectively (Merad et al., 2013) (section 1.2.2, chapter 1).

It is clear that various open questions remain about the function of hepatic DC subsets in infectious disease, including the relative ability of different types of DCs in the liver to induce or maintain $CD4^+$ T cell responses, particularly in Th2 settings such as *S. mansoni* infection. This chapter aims to improve our understanding of the function of DCs in the liver during infection with *S. mansoni,* by systematically assessing their ability to take up, process and present antigen to naïve or activated $CD4^+$ T cells *ex vivo* using an OT-II co-culture system (Schnorrer et al., 2006; Wilson et al., 2003; Young et al., 2007). Although there is evidence that hepatic DCs can prime naïve T cells in the PALT (Yoneyama et al., 2001) (section 3.2.1.1, chapter 3), $CD4^+$ T cell activation and priming generally occurs in dLNs following DC migration from an effector site, such as the liver (Banchereau and Steinman, 1998). We hypothesised that examining the capacity of hepatic DCs to induce $CD4^+$

T cell responses *ex vivo* would provide an insight into the function of recently activated DCs in the liver that would normally migrate to the dLN to interact with naïve $CD4^+$ T cells. On the other hand, investigating the ability of hepatic DCs to present antigen to effector/memory $CD4^+$ T cells enables the assessment of local DC mediated maintenance of $CD4^+$ T cell responses in the liver/granuloma. In fact, the consistent delivery of new eggs into the liver indicates that DCs may play a dual role during the course of infection: inducing Th2 responses in the dLN as well as maintaining established effector/memory $CD4^+$ T cell responses in the liver during granuloma development (Pearce and MacDonald, 2002). Thus, this chapter investigates the function of hepatic DC subsets isolated from *S. mansoni* infection in terms of their ability to induce or maintain $CD4^+$ T cell responses *ex vivo*.

5.3 Study Rationale

To assess whether *S. mansoni* infection changes the ability of hepatic DCs to take up, process and present exogenous antigen, cDCs and pDCs were isolated from livers of infected mice and cultured with $CD4^+$ T cells *ex vivo*. DCs were isolated at D42, a time-point during infection, which is critical for the induction of Th2 immune responses to *S. mansoni* eggs (Pearce and MacDonald, 2002) (Fig. 3.3, chapter 3). To address the capacity of hepatic DCs to induce or maintain $CD4^+$ T cell responses, we used an OVA-recognition assay with OT-II transgenic $CD4^+$ T cells as described in Cook *et al.,* (2012), since transgenic mice that develop SEA-specific T cells are not available. OT-II $CD4^+$ T cells express a TCR that is specific for class II OVA peptide (323-339) (pOVA) (Barnden et al., 1998), and culturing OT-II T cells with OVA-pulsed DCs provides a measurement of the potential of DCs to present peptide to $CD4^+$ T cells (Wilson et al., 2004). To investigate the capacity of *ex vivo* sorted hepatic DC subsets to induce and maintain $CD4^+$ T cell responses, pOVA-pulsed DC subsets were co-cultured with naïve or *in vitro* activated $CD4^+$ T cells respectively. In a complementary assay, soluble OVA protein (OVA) was added to the co-cultures to examine the ability of DCs to take up, process and present antigen. $CD4^+$ T cell proliferation and cytokine production were measured as readouts of DC APC function. This *ex vivo* OT-II co-culture system approach is well documented in the literature (Schnorrer et al., 2006; Wilson et al., 2003; Young et al., 2007), and enabled controlled investigation of core hepatic DCs functions following *S. mansoni* infection.

Although specific subsets display distinct functions, cDCs are described mainly as superior APCs, whereas pDCs specialise in the secretions of type I IFNs (Merad et al., 2013). Therefore, hepatic cDCs ($CD11c^{high}$ PDCA-1^-) were sorted separately from pDCs ($CD11c^{low}$ PDCA-1^+) to unravel functional differences between these two major subsets during *S. mansoni* infection (Rahman and Aloman, 2013) (see table 1.1). While focusing on the function of cDCs and pDCs, the capacity of hepatic $CD8\alpha^+$ and $CD8\alpha^-$ cDC subsets to induce or maintain $CD4^+$ T cell responses was

also investigated (Pillarisetty et al., 2004). The markers used for these subsets were CD8α and CD205, as conducted in chapter 4 (Fig. 4.1 & 4.4) (Hildner et al., 2008; Pillarisetty et al., 2004).

5.4 Results

5.4.1 The activation phenotype of cDCs and pDCs is marginally increased during *S. mansoni* infection at D42

To investigate the function of hepatic cDCs and pDCs during *S. mansoni* infection at a time-point when Th2 responses are induced, WT mice were infected with *S. mansoni* and livers were harvested at D42 of infection, when a switch from a mixed Th1/Th2 to a dominant Th2 response occurs (Pearce and MacDonald, 2002). Liver leukocytes were isolated and enriched for DCs by using magnetic Dynabeads that removed lineage negative cells from the cell population including T cells, IgM^+ B cells, NK cells, erythrocytes and most granulocytes (section 2.8.3, chapter 2). Enriched hepatic DCs were then sorted by FACS to obtain pure cell populations of live cDCs and pDCs for use in the co-culture assay with $CD4^+$ T cells (Fig. 5.1A-B). Examining F4/80 expression revealed that a $F4/80^+$ $PDCA\text{-}1^+$ $CD11c^{int}$ population was present in both naïve and infection derived enriched liver DC populations (Fig. 5.1A-B). This cell population may represent MΦs (Nobumoto et al., 2009), and so would contaminate sorted DC populations if not excluded during the sort procedure. Thus, enriched hepatic $F4/80^-$ DCs from both naïve and *S. mansoni* infected mice were FACS sorted into live cDCs ($CD11c^{high}$ $PDCA\text{-}1^-$) and pDCs ($CD11c^{int}$ $PDCA\text{-}1^+$) that were >95% pure (Fig. 5.1A-B) (Rahman and Aloman, 2013) (Table 1.1). The proportion of cDCs in the liver (M = 14.4, SEM = 2.434) in naïve mice was unchanged compared with cDCs from *S. mansoni* infected mice (M = 18.47, SEM = 2.325), t(1)=1.208, p=0.2935. Similarly, the proportion of pDCs from naïve mice (M = 7.43, SEM = 0.4010) was not significantly different compared with hepatic pDCs in infected mice (M= 5.543, SEM = 1.461), t(1)=1.245, p=0.2809.

To examine whether *S. mansoni* infection alters hepatic DC activation phenotype, the expression of cell surface activation markers CD40, MHC-II and CD80 by cDCs and pDCs was assessed by flow cytometry (Fig. 5.1C-D). CD86 could not be investigated as an αCD86 antibody with the appropriate fluorochrome for addition to

the flow panel was not available at the time of the experiment. There were no significant changes in the proportion of infection derived cDCs expressing CD40, MHC-II or CD80 compared with cDCs from naïve mice (Fig. 5.1C). Due to the rarity of pDCs in the liver, insufficient cells were present for accurate flow cytometric analysis (6,000-9,000 per liver from naïve and 10,000-20,000 per liver from infected mice). Nevertheless, an increase in hepatic pDC populations expressing MHC-II was found in pDCs isolated from infected compared with naïve animals, although this result was not significant. Analysis of the GMFI revealed that the expression level of MHC-II and CD40 on all infection derived sorted cDCs increased marginally compared with hepatic cDCs from naïve mice, whereas the level of CD80 expression decreased (Fig. 5.1D). The staining on available hepatic pDCs showed subtle increases in the level of CD40, CD80 and MHC-II expressed during infection, but overall expression of these markers was markedly lower compared with cDCs (Fig. 5.1D).

For naïve $CD4^+$ T cell isolation, splenic and LN $CD4^+$ T cells expressing a TCR specific for class II pOVA (323-339) (Barnden et al., 1998) were enriched from OT-IIxLy5.1 mice by negative selection using Dynabeads. This method depleted $CD8^+$ T cells, B cells, monocytes, MΦs, NK cells, DCs, erythrocytes and granulocytes. Freshly isolated class II OVA specific $CD4^+$ T cells were then assessed for purity and activation status by flow cytometry (Fig. 5.1E). Surface markers Vα2 and CD4 were used to determine the purity of OT-II T cells following Dynal negative selection (Barnden et al., 1998), which revealed approximately 80% purity for mixed splenic and lymphoid $CD4^+$ T cells. To assess the activation status of isolated $CD4^+$ T cells, the expression of CD44 and CD69 was examined and showed that approximately >95% of $CD4^+$ T cells were $CD44^-$ $CD69^-$ indicating a naïve phenotype (Sprent and Surh, 2011) (Fig. 5.1E).

To obtain a population of effector/memory $CD4^+$ T cells, splenocytes were isolated from OT-IIxLy5.1 mice and cultured *in vitro* for 7 days in the presence of endotoxin-free soluble OVA protein as well as IL-2, IL-7 and IL-15 to promote effector/memory $CD4^+$ T cell differentiation and proliferation (section 1.4, chapter)

(Caserta et al., 2010; Van Belle et al., 2012). After 7 days, splenocytes were assessed by flow cytometry for $CD4^+$ T cell purity and activation status prior to culture with DCs. The proportion of $CD4^+$ $V\alpha2^+$ cells was approximately 90-95%, and 65-70% of $CD4^+$ $V\alpha2^+$ T cells were $CD44^+$ and $CD69^+$ (Fig. 5.1E). The presence of APCs was assessed by analysing the proportion of MHC-II^+ cells in naïve or activated $CD4^+$ T cell populations, which showed that <1% of cells in samples containing naïve or activated $CD4^+$ T cell populations expressed MHC-II (Fig. 5.1E).

5.4.2 cDCs and pDCs display a differential capacity for antigen presentation to naïve $CD4^+$ T cells

To assess whether *S. mansoni* infection alters the ability of DC subsets to present antigen to naïve $CD4^+$ T cells, sorted cDCs and pDCs from naïve or D42 infected mice were pulsed with pOVA for 45min and washed to remove unbound peptide (Fig. 2.4, chapter 2). To investigate $CD4^+$ T cell proliferation in response to pOVA-pulsed cDCs, naïve OT-II $CD4^+$ T cells were labelled with CFSE before culture. 5000 pOVA-pulsed cDCs or pDCs were then co-cultured with 50,000 freshly isolated naïve CFSE-labelled pOVA specific $CD4^+$ T cells for 72h (Fig. 5.2 & Fig. 5.3) (this OT-II co-culture system is described in detail in section 2.8.7, chapter 2) (Schnorrer et al., 2006; Wilson et al., 2003; Young et al., 2007). The dose of pOVA was titrated from 10 μM down to 0.01 μM to ensure that responses observed were dose dependent, and to provide a measure of whether the dose of antigen impacts DC function. In addition, naïve $CD4^+$ T cells were co-cultured with sorted cDCs or pDCs that were not pulsed with pOVA to control for antigen-specific $CD4^+$ T cell responses. Proliferation of naïve $CD4^+$ T cells was determined by analysing CFSE staining after culture by flow cytometry; the level of CFSE detected decreased by half with every round of $CD4^+$ T cell division (Lyons and Parish, 1994). When pOVA-pulsed cDCs from naïve mice were cultured with naïve $CD4^+$ T cells, the proportion of proliferating $CD4^+$ T cells was highest (approximately 83%) when they were cultured with cDCs pulsed with 10 μM compared with cDCs pulsed with 1 or 0.01 μM pOVA (Fig. 5.2A-B). cDCs from *S. mansoni* infected mice pulsed with 10 μM pOVA induced a similar proportion of $CD4^+$ T cells to proliferate compared with naïve cDCs (Fig. 5.2A). However, when sorted cDCs from infection were pulsed

with 1 μM pOVA a marginal, but significant, increase in $CD4^+$ T cell proliferation was found compared with cDCs from naïve mice.

In contrast to cDCs, both naïve and *S. mansoni* infection derived pOVA-pulsed pDCs induced less than 10% naïve $CD4^+$ T cells to proliferate at every concentration of pOVA tested (Fig. 5.2C-D). This suggests that cDCs are more efficient at inducing $CD4^+$ T cell proliferation than pDCs irrespective of whether the DCs were isolated from naïve or infected mice, and this will be discussed in more detail later.

To examine the average number of divisions performed by dividing $CD4^+$ T cells, the proliferation index was calculated using the proliferation tool in Flowjo (Fig. 5.2E). This function could be used for samples where distinct proliferation peaks were recorded, whereas samples with no apparent proliferation (i.e. low peptide doses or pDC cultures) were not recognised by the software for analysis. These data showed that the average number of divisions by proliferating $CD4^+$ T cells was marginally albeit significantly increased in culture with 1 μM pOVA-pulsed cDCs from infected compared with naïve mice, whereas the number of $CD4^+$ T cell divisions was unchanged in culture with naïve or infection derived cDCs pulsed with 10 μM pOVA (Fig. 5.2E).

To assess the ability of cDCs and pDCs to influence $CD4^+$ T cell polarisation, cytokines present in co-culture supernatants were measured by ELISA (Fig. 5.3). Cytokine production by naïve $CD4^+$ T cells in culture with cDCs was minimal in every condition, such that the amounts of IL-4, IL-5, IL-10 and IFN-γ were below the optimal detection limit of the ELISA assay (shown by a dotted line) (Fig. 5.3A). Although the amounts of IL-13, IFN-γ and TNF-α were above the detection limit for the ELISA, no significant difference was seen when comparing the amount of these cytokines in culture with naïve or infection derived cDCs. In culture with pOVA-pulsed naïve or infection derived pDCs, the amount of every cytokine measured was not significantly above the detection limit of the ELISA (Fig. 5.3B).

5.4.3 cDCs, but not pDCs, take up, process and present antigen to naïve CD4$^+$ T cells

To determine whether the ability of DCs to take up and process antigen in addition to mere peptide presentation is altered at D42 of *S. mansoni* infection, DC subsets and naïve CD4$^+$ T cells were cultured for 72h in the presence of soluble OVA protein (OVA). The amount of OVA used in the assay was titrated from 500 μg/ml to 0.5 μg/ml to control for antigen dependent stimulation (Schnorrer et al., 2006; Young et al., 2007). CFSE analysis showed that cDCs from naïve mice induced approximately 40% and 75% naïve CD4$^+$ T cells to proliferate when either 50 μg/ml or 500 μg/ml OVA was present in culture (Fig. 5.4A-B). Fewer that 5% of CD4$^+$ T cells proliferated in culture with naïve or infection derived cDCs with 0.5 μg/ml OVA protein. Infection derived cDCs induced similar levels of T cell proliferation compared with naïve cDCs at all OVA concentrations tested.

When in culture with either naïve or infection derived pDCs in the presence of OVA, the proportion of proliferating CD4$^+$ T cells was less than 5% in every sample, and no defined division peaks were detected (Fig. 5.4C-D). Thus, analysis of the proliferation index could once again not be performed with pDC cultures.

Assessment of the proliferation index for cDC cultures in the presence of 50 μg/ml or 500 μg/ml OVA protein showed no significant differences in the average number of divisions by proliferating CD4$^+$ T cells in culture with naïve or infection derived cDCs (Fig. 5.4E).

Cytokine production in the cDC:CD4$^+$ T cell co-culture with OVA was minimal, as levels of IL-4, IL-5, IL-13 and IL-10 were below the detection limits of the assay (Fig. 5.5A). Although the amount of TNF-α, IFN-γ and IL-17 was above the detection limit of the assay when cDCs were cultured with naïve CD4$^+$ T cells in the presence of 500 μg/ml OVA protein, no significant differences between *S. mansoni* infection derived and cDCs from naïve mice were detected for every cytokine measured (Fig. 5.5A). The amount of cytokine detected in cultures with pDCs was not above the ELISA detection limit for each cytokine analysed (Fig. 5.5B). These

data, in addition to the cytokine data from figure 5.3A-B, indicate that the amount of cytokine production in cultures with naïve $CD4^+$ T cells was not sufficient for optimal analysis of T cell priming.

5.4.4 Differential ability of cDCs and pDCs to maintain $CD4^+$ T cell responses

Given that the majority of T cells in the liver during *S. mansoni* infection are effector/memory $CD4^+$ T cells (Hogan et al., 2002; Rumbley et al., 1999), we next examined the ability of DCs to maintain effector/memory $CD4^+$ T cell responses. Hepatic cDCs or pDCs isolated from naïve or infected mice were co-cultured *ex vivo* with previously activated CFSE-labelled $CD4^+$ T cells from OT-II mice. No major differences in the proportion of proliferating effector/memory $CD4^+$ T cells were seen in culture with *S. mansoni* infection derived cDCs compared with naïve cDCs pulsed with 1 or 10 μM pOVA (Fig. 5.6A). However, a significant subtle decrease in the ability of cDCs from infection compared with naïve cDCs to induce effector/memory $CD4^+$ T cell proliferation was apparent at the lowest pOVA dose (0.01μM). In contrast to naïve $CD4^+$ T cell proliferation, CFSE staining of activated $CD4^+$ T cells did not produce defined peaks for each division, as all $CD4^+$ T cells were already proliferating prior to culture with DCs (Fig. 5.6B). Therefore, the whole population of CFSE stained $CD4^+$ T cells was observed as one fairly broad peak, which expressed less CFSE as $CD4^+$ T cell proliferation of the whole population increased. Thus, analysis of the proliferation index of dividing $CD4^+$ T cells was not possible with this assay due to the absence of defined proliferation peaks.

In contrast to cDCs, the level of proliferation observed was minimal when *in vitro* activated $CD4^+$ T cells were cultured with pOVA-pulsed pDCs, and culture with both 10 μM pOVA-pulsed naïve or infection derived pDCs induced approximately 20% of effector/memory $CD4^+$ T cells to proliferate (Fig. 5.6C-D). Further, no significant differences were evident when comparing culture with naïve or *S. mansoni* infection derived pDCs.

To assess the capacity of cDCs and pDCs from *S. mansoni* infection to maintain $CD4^+$ T cell cytokine production, the amount of cytokine present in co-cultures was measured by ELISA. Unlike co-cultures with naïve $CD4^+$ T cells, the levels of cytokine produced in cultures with *in vitro* activated $CD4^+$ T cells was above the detection limit of the assay, with the exception of IL-5 and IL-17. An increase in trend for the amount of IL-4, IL-13 as well as IL-17 produced in culture with effector/memory $CD4^+$ T cells was seen with infection derived cDCs compared with naïve cDCs, but no significant differences were found for any of the cytokines measured (Fig. 5.7A).

Overall, levels of all cytokines assessed were substantially lower in cultures of effector/memory $CD4^+$ T cells with pDCs compared with cDCs, with the amounts of IL-5, IL-10, IL-13 and IL-17 being below the detection limit of the ELISAs (Fig 5.7B). Although marginally increased TNF-α was found after co-culture of effector/memory $CD4^+$ T cells with pOVA-pulsed pDCs from infection compared with pDCs from naïve mice (Fig. 5.7B), this was not above the amount of TNF-α produced by effector/memory $CD4^+$ T cells in the absence of DCs (Appendix Fig. 7.6). No significant differences were seen in the levels of IL-4 or IFN-γ produced in culture with effector/memory $CD4^+$ T cells and pDCs from naïve or infected mice. Thus, overall pDCs were inefficient in presenting pOVA to effector/memory $CD4^+$ T cells.

5.4.5 cDCs, but not pDCs can take up, process and present antigen to maintain $CD4^+$ T cell responses

To assess antigen uptake and processing, as well as presentation, to *in vitro* activated $CD4^+$ T cells, cDCs and pDCs from D42 *S. mansoni* infected or naïve mice were FACS sorted and co-cultured for 72h with *in vitro* activated OT-II $CD4^+$ T cells in the presence of endotoxin-free soluble OVA protein. CFSE staining assessed by flow cytometry showed that, in the presence of 500 μg/ml OVA, *S. mansoni* infection derived cDCs induced comparable levels of $CD4^+$ T cell proliferation compared with naïve cDCs (approximately 75-78%; Fig. 5.8A-B). Further, there were no significant differences in $CD4^+$ T cell proliferation in culture with naïve cDCs compared with

infection derived cDCs in the presence of 500, 50 or 0.5 μg/ml OVA. Unlike cDCs, both naïve and infection derived pDCs once again failed to maintain substantial proliferation of effector/memory $CD4^+$ T cells on addition of OVA, as the proportion of proliferating $CD4^+$ T cells was <15% at every concentration of OVA tested (Fig. 5.8C-D).

ELISA analysis of cytokines present in culture supernatants showed that the amount of TNF-α produced by effector/memory $CD4^+$ T cells and 500 μg/ml OVA was significantly increased in the presence of infection derived cDCs compared with naïve cDCs (Fig. 5.9A). Yet, the amount of IL-4, IL-10, IL-13 and IFN-γ produced in culture in the presence of 500 μg/ml OVA with infection derived cDCs was unchanged compared with naïve cDCs. As with previous cultures, levels of IL-5 and IL-17 were below the detection limit of the ELISA.

The production of all cytokines in co-cultures with pDCs in the presence of OVA protein was minimal, such that the amounts detected by the ELISA for each cytokine (with the exception of IL-4) were below the limits of the assay. Although the amount of IL-4 in cultures with pDCs and effector/memory $CD4^+$ T cells in the presence of 500 μg/ml OVA was above the detection limit of the ELISA, no significant difference was found when comparing *S. mansoni* infection derived pDCs with naïve pDCs (Fig. 5.9B). In summary, *ex vivo* hepatic pDCs from naïve or *S. mansoni* infected mice did not maintain substantial $CD4^+$ T cell proliferation or cytokine production.

To assess whether poorer antigen presentation capacity observed with pDCs compared with cDCs was due to increased pDC cell death in culture, the proportion of cDCs and pDCs present after 1 day of culture was examined. These data revealed that both subsets were present in equal proportions (approximately 50%) after 1 day of culture (Appendix Fig. 7.5), and it is unlikely that increased death of pDCs *ex vivo* is the main cause for decreased $CD4^+$ T cell proliferation and cytokine production compared with cDCs. In summary, *S. mansoni* infection at D42 did not significantly

alter the ability of cDCs and pDCs to take up, process and present antigen to naïve or effector/memory $CD4^+$ T cells.

5.4.6 *S. mansoni* infection derived cDC subsets display distinct functional differences in inducing $CD4^+$ T cell responses

Although *S. mansoni* infection at D42 did not significantly alter the ability of cDCs to take up, process and present antigen to naïve or effector/memory $CD4^+$ T cells, it was hypothesised that distinct subsets belonging to this group of DCs may exhibit differential interaction with $CD4^+$ T cells. In support of this, $CD8\alpha^+$ cDCs are important for the induction of Th1 and CTL responses during bacterial and viral infections (Hildner et al., 2008; Mashayekhi et al., 2011), whereas $CD8\alpha^-$ cDCs (i.e. $CD11b^+$ cDCs) preferentially interact with $CD4^+$ T cells and are thought to induce Th2 responses (Gao et al., 2013; Kumamoto et al., 2013; Plantinga et al., 2013; Williams et al., 2013). To investigate the function of liver cDC subsets at D42 of *S. mansoni* infection, isolated liver leukocytes were enriched for DCs as before, and sorted by FACS into $CD8\alpha^+$ and $CD8\alpha^-$ cDC subsets for culture with CFSE-labelled naïve or *in vitro* activated $CD4^+$ T cells. Surface markers CD8α and CD205 were used to sort $CD8\alpha^+$ $CD205^+$ and $CD8\alpha^-$ $CD205^-$ liver cDC populations that were 95.3% and 90.2% pure respectively (Hildner et al., 2008; Pillarisetty et al., 2004) (Fig. 5.10A-B). For the purpose of clarity, these subsets will be referred to as $CD8\alpha^+$ and $CD8\alpha^-$ cDCs from here on. The proportion of $CD8\alpha^+$ cDCs did not change substantially following *S. mansoni* infection compared with naïve animals (Fig. 5.10A-B). This experiment was conducted once, and so statistical analysis of the proportion of cDC subsets in naïve or infection derived livers was not possible.

The ability of isolated hepatic $CD8\alpha^+$ and $CD8\alpha^-$ cDC subsets to present antigen to naïve $CD4^+$ T cells was tested in the same assay that was used to compare the function of cDCs and pDCs previously. In culture with naïve $CD4^+$ T cells, $CD8\alpha^+$ cDCs and $CD8\alpha^-$ cDCs from naïve mice pulsed with 10 μM pOVA induced approximately 70% of naïve $CD4^+$ T cells to proliferate after 72h of culture (Fig. 5.11A-B). Culture with additional concentrations of pOVA or with soluble OVA

protein was not possible due to insufficient $CD8\alpha^+$ and $CD8\alpha^-$ cDC yields from the livers after FACS sorting. When compared with *S. mansoni* infection derived $CD8^+$ cDCs, the proportion of $CD4^+$ T cells that proliferated in culture with $CD8\alpha^-$ cDCs was significantly increased. Moreover, the proliferation index showed a significant increase in the average number of divisions that dividing $CD4^+$ T cells underwent during culture with infection derived $CD8\alpha^-$ cDCs compared with naïve $CD8\alpha^-$ cDCs, but there was no significant difference in the proliferation index when comparing co-cultures with infection derived $CD8\alpha^+$ to $CD8\alpha^-$ cDCs (Fig. 5.11C).

Analysis of cytokines produced in the co-culture assay with naïve $CD4^+$ T cells showed that the amounts of IL-4, IL-5, IL-10, IL-13, IL-17 and IFN-γ stimulated by 10 or 0.01 μM pOVA-pulsed naïve $CD8\alpha^+$ or $CD8\alpha^-$ cDCs were similar to or below the detection limit of the ELISA (Fig. 5.11D). This is in line with previous co-cultures investigating cDC and pDC function when naïve $CD4^+$ T cells were used (Fig. 5.4). Notably, the amount of IL-13 in culture with 10 μM pOVA-pulsed $CD8\alpha^-$ cDCs from infection was significantly increased to levels above the detection limit compared with naïve $CD8\alpha^+$ cDCs (Fig. 5.11D). In contrast, the amount of TNF-α measured in the co-culture was significantly higher in the presence of *S. mansoni* infection derived $CD8\alpha^+$ cDCs, in comparison with $CD8\alpha^-$ cDCs.

To determine whether the capacity of cDC subsets to maintain $CD4^+$ T cell responses is altered during *S. mansoni* infection, $CD8\alpha^+$ or $CD8\alpha^-$ cDCs were pulsed with pOVA and co-cultured with *in vitro* activated OT-II $CD4^+$ T cells that had been labelled with CFSE. Analysis of CFSE dilution by flow cytometry revealed that approximately 50-55% of $CD4^+$ T cells proliferated in culture with either $CD8\alpha^+$ or $CD8\alpha^-$ cDCs derived from infected mice pulsed with 10 μM pOVA (Fig. 5.12A-B). $CD8\alpha^+$ and $CD8\alpha^-$ cDCs pulsed with 0.01 μM pOVA induced <5% of $CD4^+$ T cells to proliferate. Thus, there were no significant differences in the proportion of $CD4^+$ T cells that proliferated in culture with infection derived $CD8\alpha^+$ compared with $CD8\alpha^-$ cDCs. Insufficient numbers of cDC subsets isolated from naïve mice were available for comparison with infection derived $CD8\alpha^+$ and $CD8\alpha^-$ cDCs in this assay, due to low yields of these subsets from naïve livers.

The amount of cytokine detected in the assay with effector/memory $CD4^+$ T cells was substantially higher compared with co-cultures with naïve $CD4^+$ T cells (see Fig. 5.11). The amount of IL-4, IL-13 and IFN-γ in culture with $CD8\alpha^-$ cDCs pulsed with 10 μM pOVA was significantly higher compared with $CD8\alpha^+$ cDCs from *S. mansoni* infected mice (Fig. 5.12C). Levels of IL-5, IL-10 and TNF-α were unchanged in cultures with infection derived $CD8\alpha^-$ cDCs pulsed with 10 μM pOVA compared with $CD8\alpha^+$ cDCs. At a concentration of 0.01 μM pOVA, a significant increase in TNF-α and IFN-γ production was observed in cultures with $CD8\alpha^-$ cDCs compared with $CD8\alpha^+$ cDCs from infection (Fig. 5.12C).

Together, these co-culture experiments using *ex vivo* isolated cDCs and naïve and effector/memory $CD4^+$ T cells strongly suggest that $CD8\alpha^-$ cDCs from *S. mansoni* infection have increased ability to present peptide to $CD4^+$ T cells compared with $CD8\alpha^+$ cDCs, which results in increased induction of naïve $CD4^+$ T cell proliferation and IL-13 production, and maintenance of Th2 cytokine production.

5.5 Summary of Results

- *S. mansoni* infection subtly increased the activation phenotype of cDCs and pDCs isolated from the liver (Fig. 5.1).
- *S. mansoni* infection did not alter the core functions of hepatic cDCs and pDCs to take up, process and present antigen at D42, and cDCs were competent in inducing and maintaining $CD4^+$ T cell responses (Fig. 5.2-5.9)
- $CD8\alpha^-$ cDCs displayed enhanced abilities to induce $CD4^+$ T cell proliferation and IL-13 production compared with $CD8\alpha^+$ cDCs at D42 of *S. mansoni* infection (Fig. 5.11).
- $CD8\alpha^+$ cDCs were more efficient at inducing TNF-α production by naïve $CD4^+$ T cells compared with $CD8\alpha^-$ cDCs (Fig. 5.11).
- $CD8\alpha^-$ cDCs, but not $CD8\alpha^+$ cDCs, maintained Th2 cytokine production by effector/memory $CD4^+$ T cells (Fig. 5.12).
- Both $CD8\alpha^-$ and $CD8\alpha^+$ cDCs maintained IFN-γ and TNF-α production by effector/memory $CD4^+$ T cells (Fig. 5.12).

5.6 Discussion

To investigate the function of DCs in the liver during *S. mansoni* infection, we asked whether the capacity of DC subsets to take up, process and present antigen to naïve or effector/memory $CD4^+$ T cells was altered at a time-point when Th2 immune responses against the eggs are induced (Pearce and MacDonald, 2002). To address this we used an *ex vivo* co-culture system utilising soluble OVA or pOVA as an antigen and OVA specific $CD4^+$ T cells (Schnorrer et al., 2006; Wilson et al., 2003; Young et al., 2007). Functional analysis of *ex vivo* isolated cDCs and pDCs from livers of *S. mansoni* infected mice showed that cDCs were superior in antigen uptake, processing and presentation to naïve or effector/memory $CD4^+$ T cells relative to pDCs, but there was no significant difference in the core functions exhibited by infection derived cDCs compared with those from naïve mice. These data provide an indication that hepatic cDCs, but not pDCs, competently activate naïve $CD4^+$ T cells during *S. mansoni* infection, which would typically occur following migration of DCs in the liver to the dLNs *in vivo* (Bonasio and Andrian, 2006). Furthermore, cDCs maintained effector/memory Th2 cytokine responses, which lends further support to the hypothesis first outlined in chapter 3 that cDCs reactivate Th2 responses in the liver/granuloma (section 3.6.6). Analysis of cDC subsets extended our understanding of which cDC subsets are involved in the induction or maintenance of Th2 responses during *S. mansoni* infection. These results revealed that $CD8\alpha^-$ cDCs, but not $CD8\alpha^+$ cDCs, from infection exhibited an enhanced ability to induce $CD4^+$ T cell proliferation and IL-13 production compared with their counterparts from naïve mice. In addition, hepatic $CD8\alpha^-$ cDCs from infection were proficient in the maintenance of Th2 cytokine production by effector/memory $CD4^+$ T cells. Thus, *S. mansoni* infection improved the capacity of a distinct cDC subset to interact with both naïve and effector/memory $CD4^+$ T cells.

5.6.1 Activation phenotype of cDCs and pDCs following *S. mansoni* infection

To isolate pure hepatic DC populations, liver leukocytes were enriched for DCs and sorted by FACS using various surface markers to distinguish DC subsets. Analysis of F4/80 and NK1.1 expression by liver leukocytes enriched for DCs from naïve and *S. mansoni* infected mice revealed that a population of $F4/80^{+}$ $PDCA\text{-}1^{+}$ cells that was also $CD11c^{low}$ was apparent in the cDC and pDC gates prior to FACS sorting (Fig. 5.1A-B). These $F4/80^{+}$ $PDCA\text{-}1^{+}$ $CD11c^{int}$ cells are likely MΦs similar to those previously identified in peritoneal exudate cells isolated from the peritoneal cavity that display a pDC-like phenotype, and are induced *in vivo* by galectin-9 (a lectin that inhibits metastasis of tumour cells) (Nobumoto et al., 2009). This highlights the necessity for using F4/80 during FACS sorting of DC subsets in order to prevent contamination with pDC-like MΦs in DC populations used for subsequent culture with $CD4^{+}$ T cells in this assay.

It has been shown that the expression level of activation markers including CD40, CD80, CD86 and MHC-II by BMDCs is marginally increased after stimulation with SEA *in vitro*, but this activation phenotype is subtle compared with BMDC activation with bacterial antigens such as *P. acnes* (MacDonald et al., 2001). As expected from the previous literature, the expression of activation markers by *ex vivo* FACS sorted liver cDCs or pDCs in this chapter was increased to a low level at D42 of *S. mansoni* infection compared with those isolated from naïve mice (Fig. 5.1). Furthermore, the expression of CD80 by infection derived cDCs was marginally decreased at this time-point compared with naïve cDCs. Thus, we have shown that *S. mansoni* infection does not substantially enhance hepatic cDC expression of MHC-II and co-stimulatory molecules that are thought to be critical for efficient interaction with, and activation of, T cells (Banchereau et al., 2000), and this extends previous literature that has reported similar activation marker expression profiles by *ex vivo* splenic DCs or BMDCs in response to SEA (Jankovic et al., 2004; MacDonald et al., 2001).

5.6.2 cDCs induce and maintain CD4$^+$ T cell responses during *S. mansoni* infection

To address the capacity of hepatic DCs to induce naïve CD4$^+$ T cell proliferation and cytokine production, we co-cultured *ex vivo* hepatic cDCs from naïve or *S. mansoni* infected mice with freshly isolated naïve or *in vitro* activated OT-II CD4$^+$ T cells. We reasoned that culture with naïve CD4$^+$ T cells would provide an indication of the function of recently activated hepatic DCs in the liver that would migrate to dLNs to prime CD4$^+$ T cells *in vivo* at a time-point when Th2 responses are induced (Pearce and MacDonald, 2002). Although D42 is relatively early in relation to the Th2 immune response induced to *S. mansoni* eggs (Pearce and MacDonald, 2002), cross-reactive effector/memory CD4$^+$ Th2 cell responses against larval antigens are well established at this time-point (Lukacs and Boros, 1991). Thus, culture with effector/memory CD4$^+$ T cells provided a measurement of the ability of cDCs to maintain Th2 responses locally in the liver. The data from the OT-II co-culture assays revealed that proliferation and cytokine production by naïve or effector/memory CD4$^+$ T cells was largely unchanged in co-culture with pOVA-pulsed cDCs from naïve compared with infected mice. This shows that the capacity of hepatic cDCs to present processed antigen to naïve or effector/memory CD4$^+$ T cells is not altered during *S. mansoni* infection at this time-point.

A subtle change in the function of *S. mansoni* derived cDCs was apparent when low concentrations of pOVA were used to pulse cDCs; *S. mansoni* infection derived cDCs appeared more efficient at presenting peptide and inducing proliferation of naïve CD4$^+$ T cells (Fig. 5.2), but less efficient at maintaining effector/memory CD4$^+$ T cell division (Fig 5.6). It is plausible that a subtle functional enhancement to activate naïve CD4$^+$ T cells reflects marginal increases in MHC-II and CD40 expression on infection derived cDCs compared with cDCs from naïve mice. Enhanced MHC:TCR interaction and CD40 co-stimulation mediated by DCs may lead to more effective interaction with and activation of naïve CD4$^+$ T cells, or could increase the number of CD4$^+$ T cells that receive an activatory signal (Banchereau et al., 2000). Indeed, CD40 stimulation has been shown to be required for the induction of intact Th2 responses to *S. mansoni* eggs *in vivo* (MacDonald and Pearce, 2002).

On the other hand, reduced effector/memory $CD4^+$ T cell maintenance by infection derived cDCs may be in part due to decreased expression of CD80 (Fig. 5.1D), as the combined effect of reduced peptide concentration and CD28 stimulation may negatively impact $CD4^+$ T cell proliferation (Chang et al., 1999). In support of this, studies using CD80/CD86 deficient mice have shown that CD28 stimulation is critical for naïve and effector T cell responses during experimental autoimmune encephalomyelitis (Chang et al., 1999). However, the biological significance of these effects during *S. mansoni* infection *in vivo* is negligible, as on-going egg production by worm pairs in the mesentery provides a continuous source of a large amount of antigen (Pearce and MacDonald, 2002). Therefore, it is more conceivable that antigen is in excess in the liver, and both cDCs from naïve mice and antigen-experienced cDCs present antigen peptide to naïve and effector/memory $CD4^+$ T cells efficiently.

Although peptide presentation is a central DC function during $CD4^+$ T cell activation, the uptake and processing of antigen *in vivo* by DCs is critical prior to presentation on MHC molecules (Mellman and Steinman, 2001). Pulsing DCs with pOVA bypasses the need for antigen uptake and processing, and so peptide assays do not enable the examination of such additional core DC functions. To address this cDCs were cultured with soluble OVA that requires the generation of peptides that can be presented to $CD4^+$ T cells via MHC-II (Guermonprez et al., 2002). Results from the co-culture with soluble OVA revealed that sorted liver cDCs from *S. mansoni* infection competently took up, processed and presented antigen to responding $CD4^+$ T cells, but this ability was not altered significantly compared with cDCs from naïve mice (Fig. 5.4 & Fig. 5.8). In addition, infection did not substantially change the capacity of cDCs to induce or maintain cytokine production by $CD4^+$ T cells in the presence of OVA, with the exception of enhanced TNF-α in culture with effector/memory $CD4^+$ T cells and infection derived cDCs (Fig. 5.9). In support of this, elevated levels of TNF-α in the serum of *S. mansoni* infected mice have been previously reported (Haseeb et al., 2001), and possible roles of TNF-α during *S. mansoni* infection will be discussed in more detail later. Yet, overall the

functions of hepatic cDCs to take up, process and present antigen to induce or maintain Th2 responses were not substantially altered at D42 of infection.

In summary, *S. mansoni* infection induced a muted activation state of hepatic cDCs (Fig. 5.1), but their ability to either initiate or maintain $CD4^+$ T cells responses *ex vivo* was not markedly altered compared with cDCs from naïve mice. This suggests that a significant functional enhancement in antigen uptake, processing and presentation by cDCs is not required for the induction or maintenance of Th2 responses against *S. mansoni* infection. Indeed, the subtle differences observed in cDC function described above (e.g. TNF-α production by effector/memory $CD4^+$ T cells) seem insignificant in relation to the strong Th2 immune response that is induced during *S. mansoni* infection (MacDonald and Pearce, 2002) (Fig. 3.3, Chapter 3). Nevertheless the data indicate that cDCs are functional during infection at this time-point, and display a capacity to induce Th2 responses as well as maintain effector/memory Th2 responses. In support of the latter, we have shown in chapter 3 that $CD11c^+$ cells and T cells are found in similar locations throughout hepatic granuloma development (Fig. 3.5). Furthermore, $CD11c^+$ cells are necessary for T cell recruitment/retention at D42 (Fig. 3.9) and the "normal" T cell location at D52 in every region of the granuloma (Fig. 3.10). Thus, analysis of DC location and function during *S. mansoni* infection in this thesis together provide evidence that points towards direct interaction between $CD11c^+$ DCs and T cells in the liver, particularly in the granuloma.

5.6.3 Liver pDCs fail to induce efficient T cell responses during *S. mansoni* infection

In contrast to cDCs, pOVA-pulsed pDCs from naïve or *S. mansoni* infected mice did not initiate marked $CD4^+$ T cell proliferation or cytokine production, indicating that pDCs present exogenous antigen less efficiently to naïve or effector/memory $CD4^+$ T cells (Fig. 5.2 & Fig. 5.6). Furthermore, culture of pDCs in the presence of OVA showed that both naïve and *S. mansoni* infection derived pDCs were incapable of taking up and processing antigen for presentation to naïve or effector/memory $CD4^+$ T cell responses (Fig. 5.4 & Fig. 5.8). The amount of cytokines measured in co-

cultures with pDCs was generally below the detection limit of the assay and cytokines produced by effector/memory $CD4^+$ T cells in the absence of DCs (Appendix Fig. 7.6), which argues that pDCs fail to prime or maintain $CD4^+$ T cell cytokine production. These findings suggest that pDCs are not principal players in the induction of Th2 responses during *S. mansoni* infection, and that cDCs are the main group of DCs that are proficient in the initiation of this process. In line with this finding, it has been reported previously that depletion of lung pDCs has no impact on the priming of naïve $CD4^+$ T cells in an allergic Th2 model of mouse asthma (de Heer et al., 2004). Moreover, we have shown that pDCs are not capable of maintaining established Th2 responses and this function is not improved following *S. mansoni* infection.

It is likely that inefficiency in inducing and maintaining $CD4^+$ T cell responses is due to ineffective interaction between pDCs and $CD4^+$ T cells (Villadangos and Young, 2008). Both naïve and *S. mansoni* infection derived pDCs expressed lower levels of MHC-II, CD40 and CD80 compared with cDCs (Fig. 5.1C-D), which likely results in reduced TCR stimulation (signal 1) and co-activatory signals (signal 2) (Banchereau et al., 2000). Fonteneau *et al.,* (2003) have shown that pDCs exhibit a substantial increase in activation markers including CD86 in response to influenza antigen, and only activated pDCs can initiate or restimulate influenza specific CTL and Th1 responses. Thus, poor antigen presentation by pDCs in our assays may be due to insufficient activation marker expression following *S. mansoni* infection compared with viral infection (Fonteneau et al., 2003). In addition to inefficient interaction with $CD4^+$ T cells, ineffective uptake, processing and presentation of antigen by pDCs is likely due to suboptimal cellular machinery within the cells as introduced in section 1.2.2 (Asselin-Paturel et al., 2001; Boonstra et al., 2002; de Heer et al., 2004; Young et al., 2008). Taken together, the data are in line with the current literature that pDCs do not competently take up, process or present exogenous antigen, and that pDCs are not capable of effective interaction with T cells (Villadangos and Young, 2008).

Interestingly, naïve and effector/memory $CD4^+$ T cell proliferation was increased in culture with cDCs compared with pDCs even in the absence of antigen, which indicates that cDC mediated T cell activation is at least partly independent of antigen-specific stimulation. IL-7 has been shown to increase $CD4^+$ T cell expansion during infection with LCMV, and IL-7 is required continuously for the persistence of the effector $CD4^+$ T cell population (Sun et al., 2006). Thus, cDCs may produce increased amounts of survival cytokines including IL-7, IL-2 and IL-15 compared with pDCs, and this would maintain the balance of pro- and anti-apoptotic factors in the $CD4^+$ T cell in favour of survival (Marrack and Kappler, 2004). The expression of survival cytokines by DCs in our system could be tested in future by ICC, the use of reporter mice or by examining the gene expression of *ex vivo* isolated cDCs and pDCs for IL-7, IL-15 or IL-2 by PCR. To investigate the contribution of survival cytokines to T cell responses in DC:T cell co-cultures, recombinant cytokine could be added into culture. If reduced production of IL-2, IL-7 or IL-15 leads to decreased $CD4^+$ T cell proliferation and cytokine production in culture with pDCs, we would expect the addition of recombinant cytokine to increase the $CD4^+$ T cell responses in the assay. Conversely, the addition of anti-cytokine antibodies (i.e. αIL-7) to the co-culture should reduce the induction or maintenance of $CD4^+$ T cell responses in culture with cDCs. Although the production of survival cytokines by DCs has not yet been addressed during *S. mansoni* infection, this provides a potential mechanism by which naïve and *S. mansoni* infection derived cDCs induce and maintain $CD4^+$ T cell proliferation more efficiently than pDCs even in the absence of antigen.

One potential drawback of the *ex vivo* sorting OT-II culture system used in this chapter is that cDCs and pDCs may die at different rates during the culture, which could impact the interaction with $CD4^+$ T cells. However, we have shown that equal proportions of cDCs and pDCs are present after one day of culture (Appendix Fig. 7.5), which suggests that both types of DCs die at similar rates *ex vivo.* In support of this, Young *et al.,* (2008) isolated cDCs and pDCs from mice expressing a transgene that encodes the anti-apoptosis factor Bcl-2 under the control of the Vav promoter, which ensured equal survival of pDCs and cDCs in culture. This assay revealed that pDCs remain inefficient in antigen presentation to $CD4^+$ T cells in culture compared

with cDCs even when the survival rate is unchanged (Young et al., 2008). Nevertheless, it remains to be established whether this is true for *S. mansoni* infection derived DCs.

Although we have shown that pDCs are incapable of efficient $CD4^+$ T cell response induction and maintenance, it is possible that pDCs may contribute to these processes *in vivo*. It has previously been proposed that DC derived peptide loaded MHC complexes can be transferred from one DC to another, or indeed other cells such as LN stromal cells (Dubrot et al., 2014; Qu et al., 2009; Smyth et al., 2008). In addition, exosomes containing MHC-II/antigen complex can be transferred to DCs which are unable to perform antigen processing function and are devoid of MHC-II (Théry et al., 2002). Whether DC derived exosomes exist during *S. mansoni* infection remains unknown. However, if cDC derived exosomes are generated during *S. mansoni* infection and/or exosome independent transfer of peptide loaded MHC complexes occurs, these represent possible routes used by pDCs to present processed antigen (i.e. from *S. mansoni* eggs) to $CD4^+$ T cells *in vivo*. Nevertheless, the data presented in this chapter argue that induction of $CD4^+$ T cell responses and their maintenance during *S. mansoni* infection is dominantly orchestrated by cDCs rather than pDCs, which raised the question whether distinct subsets that belong to the cDC group are important for this process.

5.6.4 A predominant role for *S. mansoni* infection derived $CD8\alpha^-$ cDCs in antigen presentation to $CD4^+$ T cells

The overall observation that *S. mansoni* infection did not alter core cDC function was somewhat intriguing given the importance of $CD11c^+$ DCs for Th2 induction during *S. mansoni* infection (Phythian-Adams et al., 2010). To extend our understanding of the function of cDCs in the liver during *S. mansoni* infection, hepatic $CD8\alpha^+$ $CD205^+$ and $CD8\alpha^-$ $CD205^-$ cDC subsets were sorted for culture in the same assay as above. $CD8\alpha^+$ and $CD8\alpha^-$ cDCs have been described to exhibit distinct capabilities to interact with T cell subsets (section 1.2.2) (Merad et al., 2013), and we hypothesised that infection with *S. mansoni* may differentially impact the ability of these subsets to interact with $CD4^+$ T cells. Such differences in the function of $CD8\alpha^+$ and $CD8\alpha^-$

cDCs may not be detected in culture with "bulk" cDCs, and this will be discussed in more detail in section 5.6.5. The data from co-cultures with cDC subsets with naïve or effector/memory $CD4^+$ T cells showed that hepatic $CD8\alpha^+$ cDCs induced similar levels of $CD4^+$ T cell proliferation compared with $CD8\alpha^-$ cDCs from naïve mice (Fig. 5.11). This suggests that the capacity of these types of cDCs in the liver to present exogenous antigen to naïve $CD4^+$ T cells is comparable in the steady state. These results differ from previous reports that have shown *ex vivo* splenic $CD8\alpha^+$ cDCs from naïve mice to induce less $CD4^+$ T cell proliferation compared with $CD8\alpha^-$ cDCs (Rizzitelli et al., 2005; Süss and Shortman, 1996). In addition, it has been shown that *ex vivo* hepatic $CD8\alpha^+$ $CD11b^-$ cDCs are marginally less efficient at inducing T cell proliferation and cytokine production compared with $CD8\alpha^-$ $CD11b^+$ cDCs in the steady state (Pillarisetty et al., 2004). Following the hypothesis proposed by Pillarisetty *et al.,* (2004) that the liver may contain increased proportions of immature $CD8\alpha^{-/low}$ $CD11b^{-/low}$ cDCs compared with the spleen, the $CD8\alpha^-$ ($CD205^-$) cDC population in our study may include a population of $CD8\alpha^-$ $CD11b^-$ cDCs that are poor APCs. In chapter 4, we have shown that liver $CD8\alpha^+$ $CD205^+$ cDCs expressed high levels of CD103 and CD24, but not CD11b, whilst $CD8\alpha^-$ $CD205^-$ cDCs expressed CD11b, but not CD103 or CD24 (Fig. 4.4). This result justified the use of CD8α and CD205 for the distinction of cDC subsets in our experiments, but additional markers could be used in future during the DC sorting procedure: an antibody against CD11b could be utilised to further distinguish $CD8\alpha^-$ cDCs in this assay, and CD103, CD24 or XCR1 would better distinguish CD8α lineage cDCs in the liver (Table 1.1). However, Pillarisetty *et al.,* (2004) did not investigate $CD4^+$ T cell responses specifically (i.e. both $CD4^+$ and $CD8^+$ T cells were present in their assay) or use OVA as an antigen, and these are further possible reasons for the discrepancy observed between the results. Clearly additional work is required to fully understand the capacity of different cDC subsets in the naïve liver to interact with naïve and effector/memory $CD4^+$ T cells, the latter of which could not be addressed in this chapter due to a lack of DCs available for the assay. Yet, our data so far suggest that core functions of cDC subsets are similar prior to infection with *S. mansoni.*

Following investigation of the ability of cDC subsets from naïve mice to induce $CD4^+$ T cell responses, we have shown for the first time that the function of hepatic $CD8\alpha^-$ cDCs, but not $CD8\alpha^+$ cDCs, is enhanced after infection with *S. mansoni* leading to increased induction of $CD4^+$ T cell proliferation and IL-13 production (Fig 5.11). Moreover, the amount of IL-4, IL-13 and IFN-γ produced by effector/memory $CD4^+$ T cells was significantly increased in culture with $CD8\alpha^-$ compared with $CD8\alpha^+$ cDCs from infection, even though the proliferation of effector/memory $CD4^+$ T cells was similar in both cultures (Fig. 5.12). In this case, the most striking differences between the cultures were observed for Th2 cytokines, whereas the amount of TNF-α and IFN-γ was more comparable with levels produced in culture with $CD8\alpha^+$ cDCs. Together these data suggest that $CD8\alpha^-$ cDCs, but not $CD8\alpha^+$ cDCs, are proficient in the induction and maintenance of Th2 responses following *S. mansoni* infection, which is in agreement with recent studies that have shown IRF4 dependent $CD11b^+$ cDCs to be important for the induction of Th2 responses in various disease settings including allergic inflammation and infection with *N. brasiliensis* (Gao et al., 2013; Kumamoto et al., 2013; Plantinga et al., 2013; Williams et al., 2013).

An enhanced ability to induce $CD4^+$ T cell proliferation indicates that *S. mansoni* infection increased the effectiveness of the interaction between $CD8\alpha^-$ cDCs, but not $CD8\alpha^+$ cDCs, with naïve $CD4^+$ T cells. Increased expression of surface markers involved in the provision of signal 1 and 2 to $CD4^+$ T cells may improve $CD8\alpha^-$ cDC mediated activation of $CD4^+$ T cells as mentioned previously (Banchereau et al., 2000). In support of this, Dudziak *et al.* (2007) showed that naïve $CD4^+$ $CD11b^+$ splenic cDCs express higher levels of genes coding for proteins involved in the MHC-II pathway compared with $CD8\alpha^+$ cDCs. This suggests that $CD4^+$ $CD11b^+$ cDCs are superior antigen presenters to $CD4^+$ T cells compared with $CD8\alpha^+$ cDCs, resulting in increased $CD4^+$ T cell proliferation in our system.

One additional possible mechanism that would enable $CD8\alpha^-$ cDCs to induce $CD4^+$ T cell proliferation more efficiently than $CD8\alpha^+$ cDCs is via the enhanced production of growth factors and survival signals, including IL-2, IL-7 and IL-15 (Boyman et

al., 2009). This has also been proposed in previous reports in the literature, as naïve splenic CD8α$^+$ cDCs that have been transferred into naïve mice stimulate less IL-2 by D011.10 CD4$^+$ transgenic T cells *in vivo* (De Smedt et al., 2001). Further, it has been shown that insufficient IL-2 reduces CD8$^+$ and CD4$^+$ T cell proliferation *ex vivo* (Kronin et al., 2000; 1996). Upon activation CD4$^+$ T cells become more responsive to IL-2 as its receptor, CD25, is upregulated (Boyman and Sprent, 2012). IL-2 signals through both autocrine and paracrine pathways (Boyman and Sprent, 2012), which suggests two possible mechanisms by which CD8α$^-$ cDCs from infection may augment the amount of IL-2 in the environment. First, infection derived hepatic CD8α$^-$ cDCs may produce higher levels of IL-2 compared with their naïve counterparts and CD8α$^+$ cDCs, which supports CD4$^+$ T cell metabolism and proliferation once activated (Boyman and Sprent, 2012). Second, CD8α$^-$ cDCs might provide increased or more frequent peptide/MHC:TCR interaction and CD28 co-stimulation via CD80/CD86 compared with naïve CD8α$^+$ cDCs, which together stimulate IL-2 production by CD4$^+$ T cells for autocrine signalling (Fathman and Lineberry, 2007). In fact, enhanced expression levels of MHC and co-stimulatory molecules may also promote CD8α$^-$ cDC mediated induction and maintenance of Th2 cytokine production, as King *et al.,* (1995) have shown that the production of IL-4 and IL-5, but not IFN-γ, by CD4$^+$ T cells previously activated *in vitro* with CD3 and PMA/I is promoted by continuous stimulation via CD28. Furthermore, administration of CTLA4-Ig, which blocks CD28 stimulation, decreases Th2 responses induced during allergic responses in the lung (Keane-Myers et al., 1997) or after infection with *S. mansoni* (King et al., 1996) or *H. polygyrus* (Gause et al., 1996). Thus, enhanced expression of IL-2, MHC-II and co-stimulatory molecules may all contribute to increased induction and maintenance of Th2 responses by CD8α$^-$ cDCs. To test this hypothesis, the activatory capacity of *ex vivo* hepatic CD8α$^+$ and CD8α$^-$ cDCs could be assessed by flow cytometric analysis of the expression levels of MHC-II, CD80 and CD86 as well as other activation markers such as CD40 and OX40-L, which may improve direct interaction with CD4$^+$ T cells (Banchereau et al., 2000). The production of IL-2 (and other survival cytokines including IL-7 and IL-15) by CD8α$^+$ cDCs, CD8α$^-$ cDCs and CD4$^+$ T cells during culture could be measured either by PCR, the use of reporter mice or by intracellular

flow cytometry as mentioned previously for cDCs. Such investigation will provide additional insight into the mechanisms that CD8α$^-$ cDCs employ to induce and maintain Th2 responses. Yet it remains likely that the provision of signal 3 is key for this process, and the identification of this signal in future is critical to progress understanding on the mechanisms that orchestrate Th2 induction and maintenance.

By investigating the importance of CD8α$^+$ cDCs *in vivo* in chapter 4 and examining the function of this subset *ex vivo* in this chapter we have shown that unlike CD8α$^-$ cDCs, CD8α$^+$ cDCs are not required or sufficient for the induction or maintenance of Th2 responses during *S. mansoni* infection. However, the amount of TNF-α was significantly higher in culture with *S. mansoni* infection derived CD8α$^+$ cDCs compared with CD8α$^-$ cDCs (Fig. 5.11). These data are in line with levels of TNF-α measured in the mLN of *S. mansoni* infected CD8α$^+$ cDC deficient *Batf3*$^{-/-}$ mice (Fig. 4.5); *Batf3*$^{-/-}$ mice displayed reduced levels of TNF-α compared with WT mice at D42 of infection. Thus, we have shown both *in vivo* and *ex vivo* data that support the hypothesis that CD8α$^+$ cDCs play a role in priming CD4$^+$ T cells to produce TNF-α during *S. mansoni* infection at D42. These findings suggest that CD8α$^+$ cDCs are the main subset responsible for increased amounts of TNF-α measured in the co-culture with infection derived cDCs compared with cDCs from naïve mice, as described earlier (Fig. 5.9).

Numerous studies have suggested that TNF-α may affect the fecundity of *S. mansoni* worms (Amiri et al., 1992; Haseeb et al., 1996), and a recent study reported that schistosomula cultured with human TNF-α *in vitro* exhibit a complex pattern of gene regulation related to egg laying when the parasite gene expression profile was analysed (Oliveira et al., 2009). In chapter 4, analysis of parasitemia in *Batf3*$^{-/-}$ mice did not suggest a difference in the number of eggs produced per worm pair when TNF-α is reduced compared with WT mice, which argues that a reduction in TNF-α did not alter the fecundity of *S. mansoni* in our model (Fig. 4.9). In addition, it is unlikely that TNF-α plays a role in the formation of granulomas, as TNF-α has been shown to be dispensable for granuloma formation at D42 of *S. mansoni* infection (Davies et al., 2004). Instead, TNF-α may promote the expansion of inflammatory

Th1 responses including IFN-γ production *in vivo* (Chatzidakis and Mamalaki, 2010). Thus, the induction of TNF-α production by $CD4^+$ T cells during *S. mansoni* infection may represent a process that is predominantly orchestrated by $CD8\alpha^+$ cDCs, which contributes to the induction of balanced or mixed Th1/Th2 responses.

In chapter 4 we proposed that $CD8\alpha^+$ cDCs regulate effector/memory Th2 responses during *S. mansoni* infection. One of the possible mechanisms for Th2 regulation by $CD8\alpha^+$ cDCs is that the production of IL-12 induces Th1 responses, which then indirectly inhibit IL-4 production and Th2 cell proliferation (Paludan, 1998) (section 4.6.3.2). Yet, the data in figure 5.12 suggests that regulation of Th2 cytokine production is not solely mediated by IFN-γ, as this cytokine was present in substantial amounts in addition to IL-4 and IL-13 when in culture with $CD8\alpha^-$ cDCs. In line with this finding, IFN-$\gamma^{-/-}$ animals do not exhibit markedly increased Th2 responses during *S. mansoni* infection (Yap et al., 1997). This indicates that additional or alternative mechanisms than the induction of IFN-γ production by $CD4^+$ T cells are important for effective regulation of Th2 responses by $CD8\alpha^+$ cDCs.

If IFN-γ is not the crucial element in Th2 regulation, perhaps downstream signalling events after $CD4^+$ T cell binding of IL-12 represent the principal mechanisms that mediate this process. It remains likely that the production of IL-12 by cDC subsets is key for the suppression of effector/memory Th2 responses, as IL-12 mediated mechanisms are the most potent inhibitors of Th2 induction and maintenance known to date (Murphy and Stockinger, 2010). IL-12 induces STAT4 signalling and T-bet expression in naïve $CD4^+$ T cells (Lazarevic et al., 2013; Thierfelder et al., 1996), which leads to Th1 differentiation and IFN-γ production (Szabo et al., 2000). Therefore, IL-12 may also induce T-bet expression and IFN-γ production by effector/memory Th2 cells, possibly via T-bet mediated suppression of GATA3 expression (Lazarevic et al., 2013). Indeed, competition between GATA3 and T-bet may be crucial for $CD4^+$ T cell differentiation as well as the maintenance of Th1/Th2 cells in *S. mansoni* infection described in chapter 4 (Murphy and Stockinger, 2010).

It has been shown IL-12 can restore IL-12 responsiveness by upregulating the expression of the IL-12 receptor (IL-12Rβ2) on established human Th2 cells, which results in increased T-bet expression and IFN-γ production and GATA3 downregulation (Smits et al., 2001b). This and other reports on human $CD4^+$ Th2 cells suggest that overall responsiveness to IL-12 by effector/memory $CD4^+$ T cells may be crucial in regulating Th2 immune responses (Hilkens et al., 1996; Rogge et al., 1999; Smits et al., 2001b), and this provides a potential mechanism for IL-12 produced by $CD8\alpha^+$ cDCs to regulate Th2 responses *in vivo*. Yet, IL-12 does not directly restore IL-12 responsiveness by murine Th2 cells (Heath et al., 2000; Nishikomori et al., 2000), and this is thought to be due to rigorous inhibition of T-bet by IL-4 in murine systems, which is not yet apparent in human cells (Mullen et al., 2001; Varga et al., 2000). However, overexpression of T-bet in committed murine Th2 cells leads to dampened GATA3 expression and Th2 cytokine production (Usui et al., 2006). Thus, it is possible that other cytokines produced by $CD8\alpha^+$ cDCs in addition to IL-12, such as IFN-α, may be required to modulate GATA3 and T-bet expression in established murine Th2 cells (Smits et al., 2001a). Overall, understanding the regulation of the expression of transcription factors involved in $CD4^+$ T cell polarization events may be essential to elevate our understanding of how $CD8\alpha^+$ cDCs regulate Th2 responses.

To further delineate the distinct polarisation events towards Th1 or Th2 immune responses respectively in cultured $CD4^+$ T cells in our system, the expression of transcription factors T-bet and GATA3 by could be measured in future by intracellular staining and flow cytometry. Analysis of IL-12 production (i.e. IL-12p40) in culture with isolated $CD8\alpha^+$ and $CD8\alpha^-$ cDCs from *S. mansoni* infection by ELISA would clarify whether these cDC subsets produce different amounts of IL-12 *ex vivo*. Indeed, $CD8\alpha^-$ cDCs may induce IFN-γ independent of IL-12 enabling the promotion of Th2 cytokine production, as $CD8\alpha^+$ cDCs are thought to be the main producers of IL-12 in certain infectious disease settings (Martínez-López et al., 2014; Mashayekhi et al., 2011). In agreement with this, IL-12 independent IFN-γ production *in vitro* by SEA restimulated splenocytes isolated from *S. mansoni* infection at D47 has been reported (Patton et al., 2001), and such pathways may

involve IL-18 (Schroder, 2003) or Notch dependent signalling (Skokos and Nussenzweig, 2007) mediated induction of IFN-γ production by $CD4^+$ T cells *in vivo*. Taken together, $CD8\alpha^+$ cDCs may be important for regulating the expression of transcription factors in both naïve and effector/memory $CD4^+$ T cells, and this process likely involves the production of IL-12 (Murphy and Stockinger, 2010).

Finally, it is possible that the direct interplay between different cDC subsets during the induction and maintenance of Th2 responses in *S. mansoni* infection is critical *in vivo*, and understanding the impact of one DC subset on the function of another is important to unravel the mechanisms for these processes. For example, TGF-β production by steady state $CD8\alpha^+$ cDCs may increase the induction of Tregs by $CD8\alpha^-$ cDCs, as it has been shown that exogenous TGF-β substantially enhances the capacity of $CD8\alpha^-$ cDCs to induce Tregs *in vitro* (Yamazaki et al., 2008). The impact of $CD8\alpha^+$ cDC derived cytokines on the function of $CD8\alpha^-$ cDCs during the induction and maintenance of Th2 responses has not yet been described. In future, experimental co-cultures containing mixtures of DC subsets at different ratios as suggested in chapter 4 could be used to examine whether the function of one DC subset impacts other DCs during interaction with $CD4^+$ T cells (section 4.6.3.2).

In summary, we can conclude that hepatic cDCs, but not pDCs, are proficient in the induction and maintenance of $CD4^+$ T cell responses during *S. mansoni* infection. More detailed analysis of distinct cDC subsets revealed that hepatic $CD8\alpha^-$ cDCs are likely candidates involved in the initiation and maintenance of $CD4^+$ Th2 immune responses, which extends our understanding of DC function during *S. mansoni* infection considerably. On the other hand, the data from $CD8\alpha^+$ cDC co-cultures support the concept that this subset is involved in the regulation of Th2 immune responses, which may involve the production of cytokines including IL-12 and the induction of Th1 immune responses. Future studies will aim to pinpoint which specific cytokines are important in Th2 regulation by $CD8\alpha^+$ cDCs and whether they directly interfere with $CD8\alpha^-$ cDC function during the induction of Th2 responses.

5.6.5 Limitations and future directions

In this chapter, we have used an *ex vivo* OT-II co-culture system to assess whether infection with *S. mansoni* alters the function of DC subsets in the liver. Although this approach enabled controlled analysis of the ability of DCs to interact with $CD4^+$ T cells, there are various limitations that should be considered when using the OT-II co-culture assay. For example, low level cytokine production by naïve $CD4^+$ T cells in our OT-II co-culture system complicates the analysis of the function of $CD4^+$ T cells following activation by DCs in the culture. In fact, only IFN-γ and TNF-α in cultures with naïve $CD4^+$ T cells and the highest dose of pOVA pulsed cDCs was consistently measured above the detection limit of the assay (Fig. 5.3 and 5.5). Naïve $CD4^+$ T cells must become activated and undergo differentiation into effector T cells to produce substantial amounts of cytokines (Jelley-Gibbs et al., 2000) (section 1.3, chapter 1), and it has previously been reported that upon $CD4^+$ T cell activation *in vitro* the number of cell divisions required for cytokine production varies depending on the cytokine measured (Bird et al., 1998). For example, production of IL-5 and IL-10 is initiated only after 8^+ divisions in culture (Gett and Hodgkin, 1998). Furthermore, peak levels of IL-4 are produced by $CD4^+$ T cells at D5 in culture with pOVA and APCs (irradiated spleen cells), whereas substantial levels of TNF-α and IFN-γ are apparent at D3 of culture (Richter, 1999). In the assays performed in this chapter, naïve $CD4^+$ T cells underwent approximately 5 divisions during culture with cDCs, hence providing insufficient time for optimal cytokine production (particularly for IL-4, IL-5 and IL-10). Therefore, increasing the time of culture in future work would be advantageous for the analysis of cytokine production by naïve $CD4^+$ T cells in this type of assay.

A further limitation associated with our OT-II co-culture system is the possibility that cytokine production by cDCs was detected in the assay. In particular, TNF-α and IL-10 are cytokines known to be produced abundantly by hepatic cDCs (Bamboat et al., 2010; Pillarisetty et al., 2004) and pDCs (Bamboat et al., 2010; Jiang et al., 2002; Kingham et al., 2007; Merad et al., 2013) (as described in section 5.2.1). Indeed, BMDC derived TNF-α is important for IL-10 production by $CD4^+$ T cells *in vitro*, as TNF-$\alpha^{-/-}$ DCs fail to induce IL-10 production (Hirata et al., 2010). In addition, DC

pre-cursors that do not yet express CD8α have been reported to produce low levels of IFN-γ, but this feature is lost when the DCs mature and express CD8α (Vremec et al., 2007). Although SEA does not induce substantial production of IL-4 by DCs indicating that IL-4 is mainly T cell derived (MacDonald et al., 2001; MacDonald and Pearce, 2002), DC IL-4 production has been reported in response to fungal infection (d'Ostiani et al., 2000). Thus, performing ICC on $CD4^+$ T cells in the assay or using cytokine reporter mice could help uncover the definite source of cytokines detected in the assay. However, DC survival rate in the assay is low; 50% of DCs die in the first day of culture (Appendix Fig. 7.5). Therefore, it is likely that the majority of cytokines detected after 3 days are in fact $CD4^+$ T cell derived.

Our cultures containing *ex vivo* hepatic DCs and naïve $CD4^+$ T cells provide important insight into the capacity of hepatic DCs to interact with naïve $CD4^+$ T cells once DCs have migrated to the LN during *S. mansoni* infection, which is an aspect of DC biology that has not previously been addressed. Isolation of cDCs from the liver draining celiac LN in this type of assay would provide more accurate information in future about the function of antigen-experienced cDCs that have migrated from the liver (as well as LN resident DCs) during the induction and priming of $CD4^+$ T cell responses against *S. mansoni* infection. In addition, the Th2 immune response to *S. mansoni* eggs peaks at D56 (Pearce and MacDonald, 2002), making this later time-point an interesting one for future investigation of DC maintenance of effector/memory Th2 cells more accurately. Moreover, the function of DC subsets may change during the course of *S. mansoni* infection, and analysis DC capacity for antigen uptake, processing and presentation at different time-points of infection would be beneficial to determine whether this is the case.

Having established that *S. mansoni* infection derived cDCs are the dominant DC subset for antigen presentation to $CD4^+$ T cells at D42, it would be advantageous to transfer OVA pulsed isolated cDCs or pDCs from infected mice into OT-II mice for investigation of the $CD4^+$ T cell response *in vivo* in future. Given the results in this chapter, we would expect $CD4^+$ T cell responses to be enhanced in mice injected with OVA pulsed cDCs compared with pDCs. In addition, it would be important to

test the impact of naïve or infection derived DCs on *ex vivo* sorted liver $CD4^+$ T cells from *S. mansoni* infection, as this would provide a scenario that resembles DC:T cell interaction during *S. mansoni* infection more accurately. For this type of assay, a MHC-II tetramer specific to immunodominant peptides from SEA would be useful, as this would enable the characterisation of SEA-specific $CD4^+$ T cells from *S. mansoni* infection (Cecconi et al., 2008). Unfortunately, a MHC-II tetramer specific to SEA is not yet available, which prevents sorting of SEA-specific $CD4^+$ T cells. Alternatively, polyclonal $CD4^+$ T cells could be isolated from *S. mansoni* mice and co-cultured with *ex vivo* DCs in the presence of αCD3/CD28. To more selectively sort effector/memory "Th2" cells, IL-4^+ $CD4^+$ T cells could be isolated from IL-4 reporter mice (4get) (León et al., 2012). Thus, future studies would aim to more accurately assess interaction between hepatic DC subsets with *S. mansoni* experienced $CD4^+$ T cells. Nevertheless, the OT-II co-culture system used in this chapter enabled controlled functional analysis of core DC functions in the livers of *S. mansoni* infected mice, and has provided a valuable insight into the distinct roles of different DC subsets during infection.

The functional differences found comparing cultures with $CD8\alpha^+$ and $CD8\alpha^-$ cDCs were not detected in cultures with "bulk" cDCs, which underlines the importance of investigating the role of distinct DC subsets during immune responses and further stipulates that examination of these processes *in vivo* would be beneficial. $CD8\alpha^+$ cDC mediated regulation of Th2 responses that are primed by $CD8\alpha^-$ cDCs, possibly via the secretion of cytokines such as IL-12 and the induction of Th1 responses, may result in overall unchanged $CD4^+$ T cell responses in the assay with all cDCs. Such regulation may appear more pronounced in *ex vivo* culture systems than *in vivo*, as DCs, $CD4^+$ T cells and the cytokines they produce are in close proximity and perhaps more concentrated in an *ex vivo* culture compared with *in vivo* microenvironments. Thus, it is plausible that persistent and potent stimulation by *S. mansoni* egg derived antigens *in vivo* drive a strong Th2 response mediated by $CD8\alpha^-$ cDCs, which is regulated to a certain extent by $CD8\alpha^+$ cDCs to prevent exaggerated Th2 responses. Culturing cDC subsets *ex vivo* at different ratios with $CD4^+$ T cells in the kind of experiment described in the previous section would

address whether CD8α^{+} cDCs are dampening the induction and maintenance of Th2 responses by CD8α^{-} cDCs in “bulk” cDC co-cultures.

5.7 Conclusion

The data in this chapter showed that cDCs were more efficient at antigen uptake, processing and presentation to naïve or activated $CD4^+$ T cells compared with pDCs, as the latter generally failed to induce $CD4^+$ T cell proliferation and cytokine production. Furthermore, infection with the helminth *S. mansoni* did not alter the core functions of "bulk" cDCs and pDCs. Analysis of individual cDC subsets revealed that $CD8\alpha^-$ cDCs displayed an enhanced capacity to induce $CD4^+$ T cell proliferation and maintain Th2 cytokine production during *S. mansoni* infection, when compared with $CD8\alpha^+$ cDCs. Nevertheless, $CD8\alpha^+$ cDCs were functional during infection and capable of inducing and maintaining effector $CD4^+$ T cell responses, in particular the production of TNF-α and IFN-γ. Our data are the first to show this kind of functional difference in cDC subsets following infection with *S. mansoni* infection.

In conclusion, the data in this chapter lend further support to our overall hypothesis and current thinking in the literature that $CD11b^+$ cDCs are the most likely candidates for inducing Th2 responses (Plantinga et al., 2013; Gao et al., 2013; Kumamoto et al., 2013; Williams et al., 2013), whereas $CD8\alpha^+$ cDCs may play an important role in the regulation of Th2 immunity during this infection. The interplay and functional balance between these subsets may be crucial for the induction of appropriate immune responses against *S. mansoni* infection, which is key to promote the survival of the host.

5.8 Figures

Figure 5.1

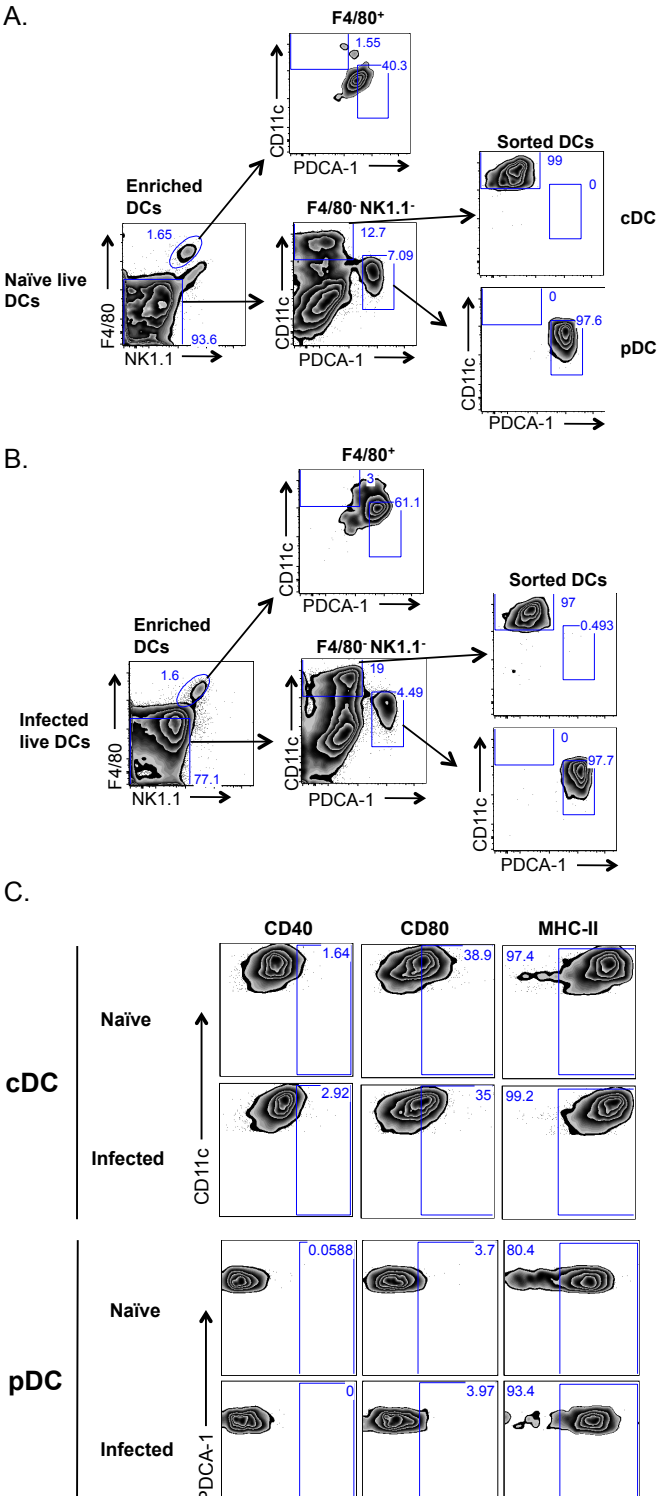

Figure 5.1

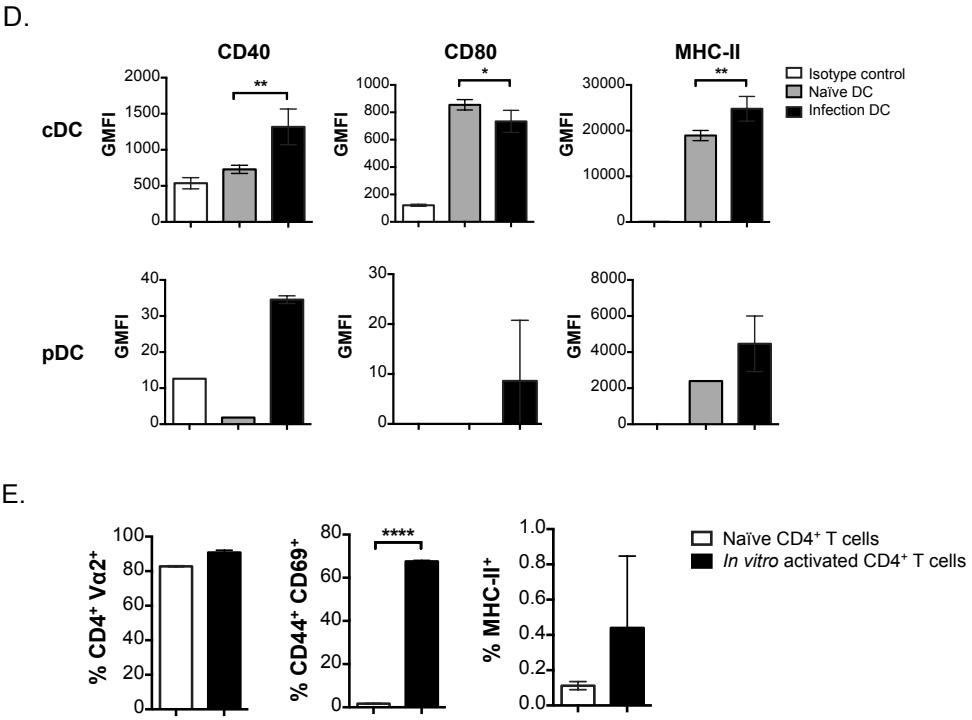

Figure 5.1 Assessing the purity and activation phenotype of cells for *ex vivo* OT-II DC:T cell co-cultures

WT mice were infected with *S. mansoni* and livers were harvested at D42 of infection. Liver leukocytes were isolated and enriched for DCs by negative selection. **A-B.** Enriched hepatic DCs were FACS sorted into pure cDC ($CD11c^+$ $PDCA\text{-}1^-$) and pDC ($CD11c^{low}$ $PDCA\text{-}1^+$) populations that were $F4/80^-$ and $NK1.1^-$. Flow plots are shown for enriched and post FACS sorted DCs from naïve (A) or infected (B) animals. **C.** Sorted cDCs and pDCs were assessed by flow cytometry for the expression of activation markers CD40, CD80 and MHC-II, and representative flow plots of this analysis are shown. **D.** The GMFI of CD40, CD80 and MHC-II expression by cDCs and pDCs is shown graphically. **E.** To purify naïve $CD4^+$ T cells, spleen and LNs were harvested from a naïve OT-IIxLy5.1 mouse. Fresh naïve $CD4^+$ T cells were isolated from spleen/LN cell populations by negative selection using Dynabeads. To obtain an effector/memory $CD4^+$ T cell population, splenocytes from an OT-IIxLy5.1 mouse were isolated 7 days prior to the co-culture set up and DC FACS sorting, and cultured *in vitro* with 1 mg/ml endotoxin-free soluble OVA. Freshly isolated naïve $CD4^+$ T cells and *in vitro* activated $CD4^+$ T cells were assessed by flow cytometry for their purity ($CD4^+$ $V\alpha2^+$) and activation status (CD44 and CD69 expression) prior to culture with DCs. Gates were set using FMO controls. 1 of 2 (cDCs) or 1 of 1 (pDCs) experiments (A to D), and 1 of 3 experiments (E). One-way ANOVA (* $P \leq 0.05$, ** $P \leq 0.01$, *** $P \leq 0.001$, ****$P \leq 0.0001$). Error bars are SEM. N=1-2.

Figure 5.2

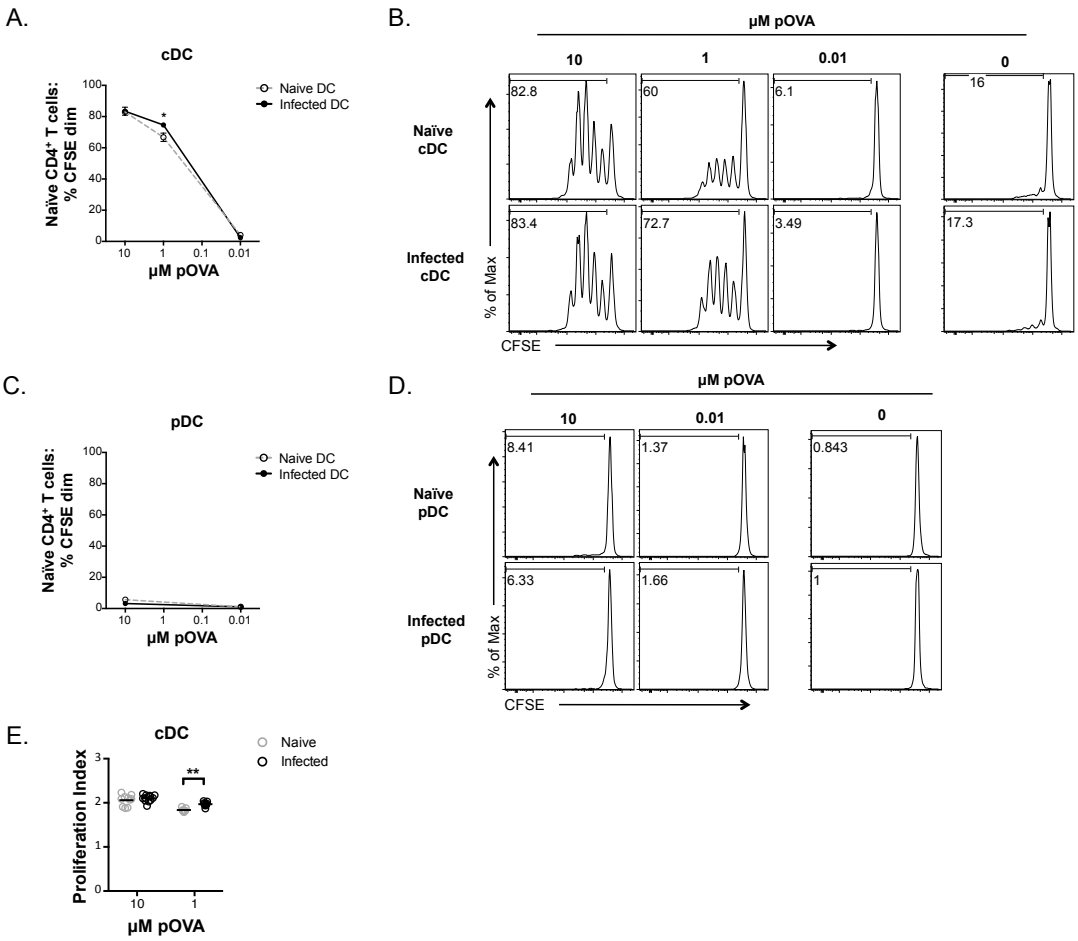

Figure 5.2 Hepatic cDC, but not pDCs, derived from *S. mansoni* infected mice efficiently present pOVA and induce CD4$^+$ T cell proliferation

FACS sorted naïve or *S. mansoni* infection derived liver cDCs or pDCs were pulsed with pOVA (323-339) before culture. 5000 pOVA-pulsed naïve or infection DCs were cultured with 50,000 naïve CFSE-labelled CD4$^+$ T cells for 72h. **A-D.** Naïve or infection derived pOVA-pulsed cDCs (A – B) or pDCs (C – D) were cultured with naïve CD4$^+$ T cells. CD4$^+$ T cells were assessed for their expression of CFSE by flow cytometry after culture, which is shown graphically (A & C)**.** Representative flow plots are shown for CFSE expression by CD4$^+$ T cells in culture with cDCs (B) or pDCs (D). **E.** To determine the average number of divisions by dividing cells, the proliferation index was calculated for CD4$^+$ T cells in culture with pOVA-pulsed cDCs. The gate for proliferating cells was set using controls where no antigen was added to the well. Data are from 3 experiments (A to E). Mixed model analysis (blocking day of experiment), Tukey's HSD (* $P \leq 0.05$, ** $P \leq 0.01$, *** $P \leq 0.001$, ****$P \leq 0.0001$). Bars are SEM. N= 7-10.

Figure 5.3

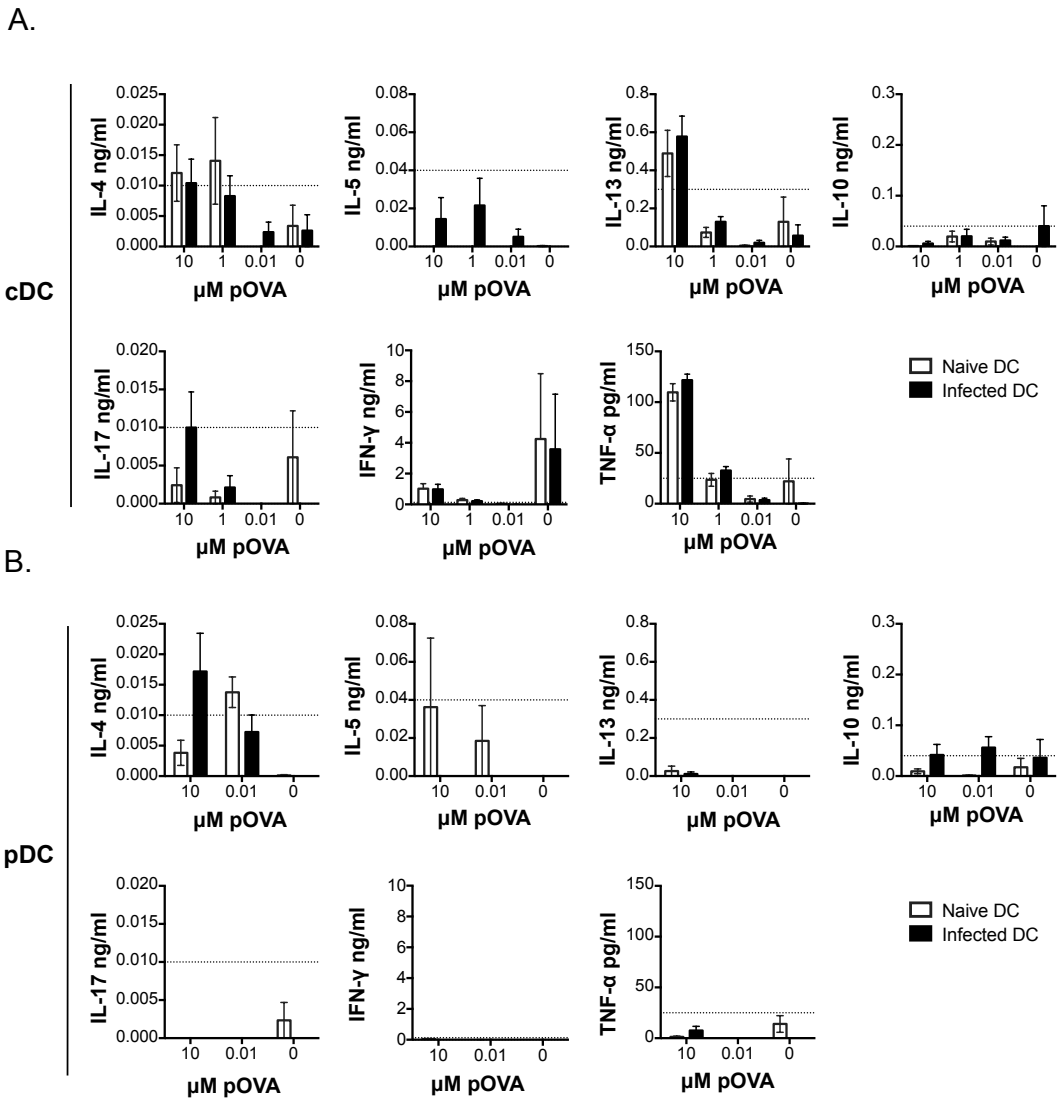

Figure 5.3 cDC, but not pDCs, derived from *S. mansoni* infected mice efficiently present OVA peptide to induce CD4$^+$ T cell cytokine production

FACS sorted naïve or D42 *S. mansoni* infection derived liver cDCs or pDCs were pulsed with pOVA (323-339) before culture. pOVA-pulsed naïve or infection DCs were cultured with naïve CFSE-labelled CD4$^+$ T cells for 72h as in Fig. 5.2. **A-B.** Supernatants from co-cultures with cDCs (A) or pDCs (B) were harvested and analysed by ELISA for cytokine production. The detection limit of the ELISA is shown with a dotted line. Data are from 3 experiments (A to B). Mixed model analysis (blocking day of experiment), Tukey's HSD (* $P \leq 0.05$, ** $P \leq 0.01$, *** $P \leq 0.001$, ****$P \leq 0.0001$). Bars are SEM. N= 7-10.

Figure 5.4

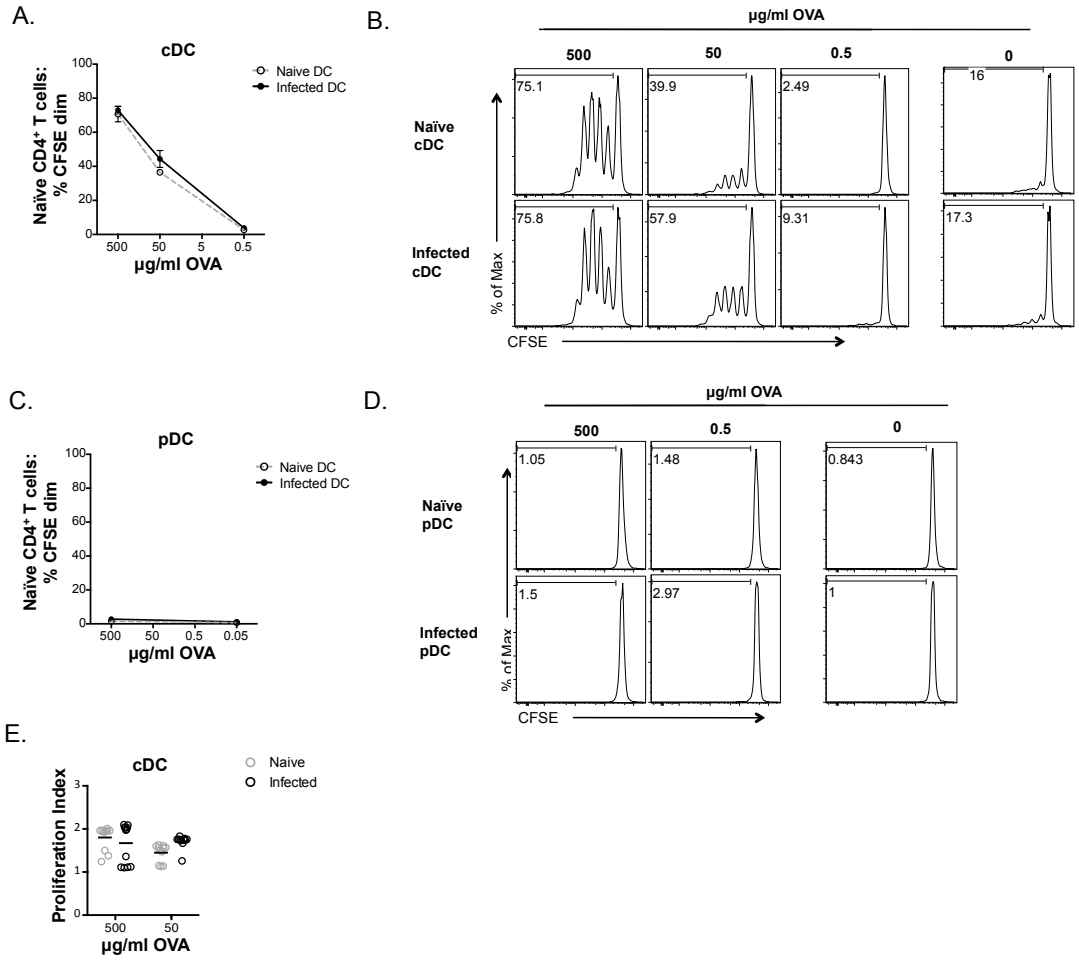

Figure 5.4 cDC, but not pDCs, derived from *S. mansoni* infected mice efficiently take up and process soluble OVA to induce CD4$^+$ T cell proliferation

FACS sorted naïve or D42 *S. mansoni* infection derived liver cDCs or pDCs were cultured with naïve CFSE-labelled CD4$^+$ T cells in the presence of endotoxin-free soluble OVA protein for 72h. **A-D.** Naïve or infection derived cDCs (A – B) or pDCs (C – D) were cultured with naïve CD4$^+$ T cells in the presence of OVA protein. CD4$^+$ T cells were assessed for their expression of CFSE by flow cytometry (A & C)**.** Representative flow plots are shown for CFSE expression by CD4$^+$ T cells in culture with cDCs (B) or pDCs (D) and OVA. **E.** To determine the average number of divisions by dividing cells, the proliferation index was calculated for CD4$^+$ T cells in culture with naïve or infection cDCs. Data are from 3 experiments (A to E). The gate for proliferating cells was set using controls where no antigen was added to the well. Mixed model analysis (blocking day of experiment), Tukey's HSD (* $P \leq 0.05$, ** $P \leq 0.01$, *** $P \leq 0.001$, ****$P \leq 0.0001$). Bars are SEM. N= 7-10.

Figure 5.5

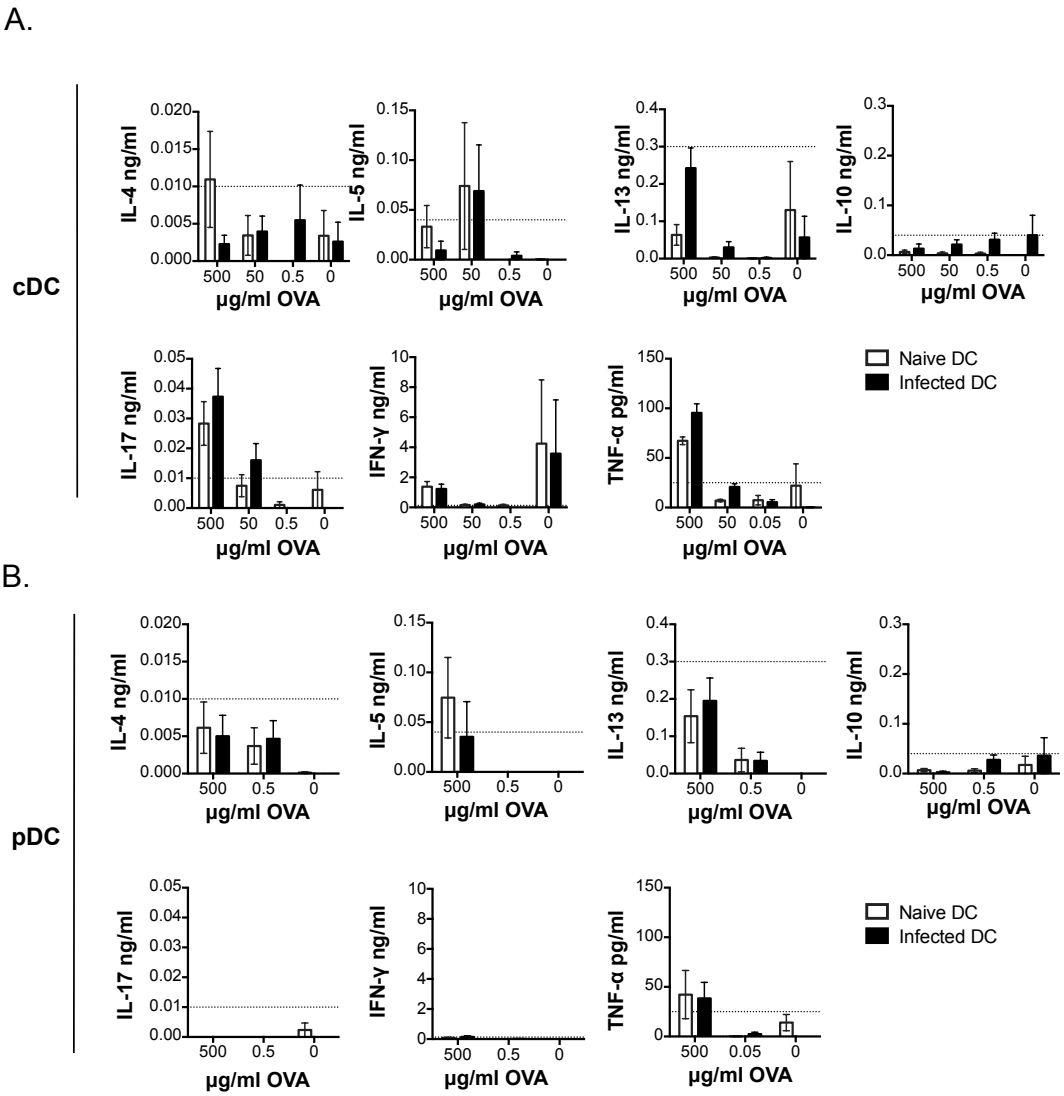

Figure 5.5 cDC, but not pDCs, derived from *S. mansoni* infected mice efficiently take up and process soluble OVA to induce CD4$^+$ T cell cytokine production

FACS sorted naïve or D42 *S. mansoni* infection derived liver cDCs or pDCs were cultured with naïve CD4$^+$ T cells in the presence of endotoxin-free soluble OVA protein for 72h. **A-B.** Supernatants from co-cultures with cDCs (A) or pDCs (B) were harvested and analysed by ELISA for cytokine production. The detection limit of the ELISA is shown with a dotted line. Data are from 3 experiments (A to B). Mixed model analysis (blocking day of experiment), Tukey's HSD (* $P \leq 0.05$, ** $P \leq 0.01$, *** $P \leq 0.001$, ****$P \leq 0.0001$). Bars are SEM. N= 7-10.

Figure 5.6

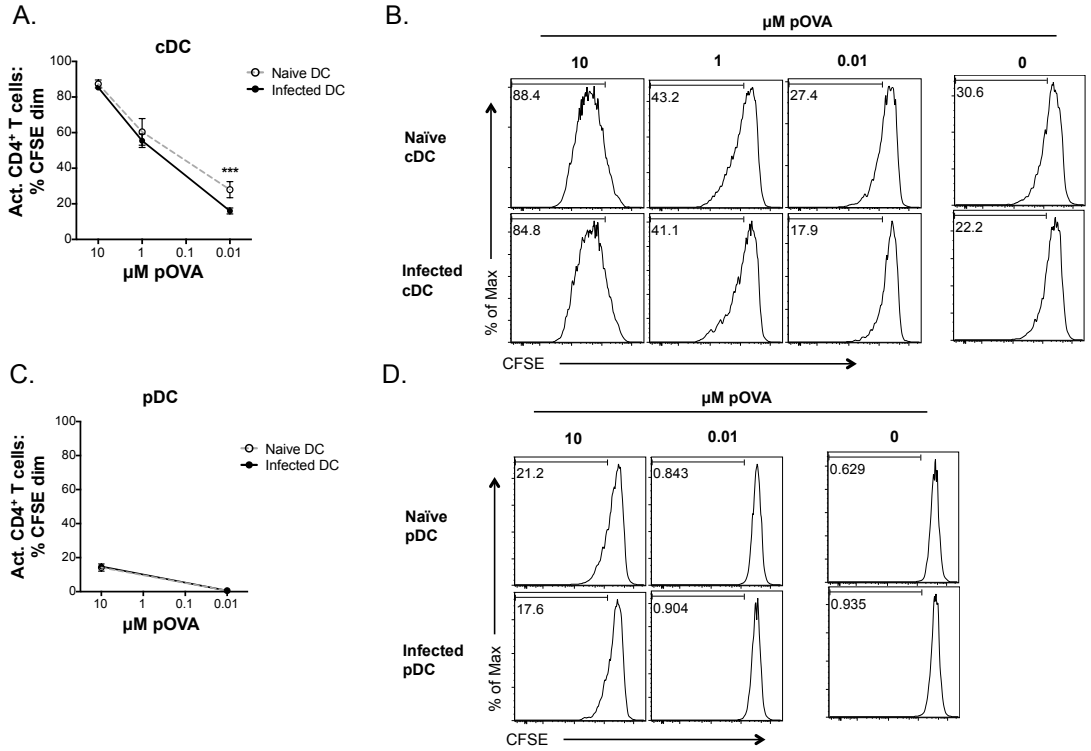

Figure 5.6 cDC, but not pDCs, derived from *S. mansoni* infected mice efficiently present pOVA to maintain CD4$^+$ T cell proliferation

FACS sorted naïve or D42 *S. mansoni* infection derived liver cDCs or pDCs were pulsed with pOVA (323-339) before culture. **A-D.** Naïve or infection derived pOVA-pulsed cDCs (A – B) or pDCs (C – D) were cultured with effector/memory CD4$^+$ T cells for 72h, and CD4$^+$ T cells were assessed for their expression of CFSE by flow cytometry (A & C)**.** Representative flow plots are shown for CFSE expression by effector/memory CD4$^+$ T cells in culture with cDCs (B) or pDCs (D). The gate for proliferating cells was set using controls where no DCs were added to the well. Data are from 3 experiments (A to D). Mixed model analysis (blocking day of experiment), Tukey's HSD (* $P \leq 0.05$, ** $P \leq 0.01$, *** $P \leq 0.001$, ****$P \leq 0.0001$). Bars are SEM. N= 7-10.

Figure 5.7

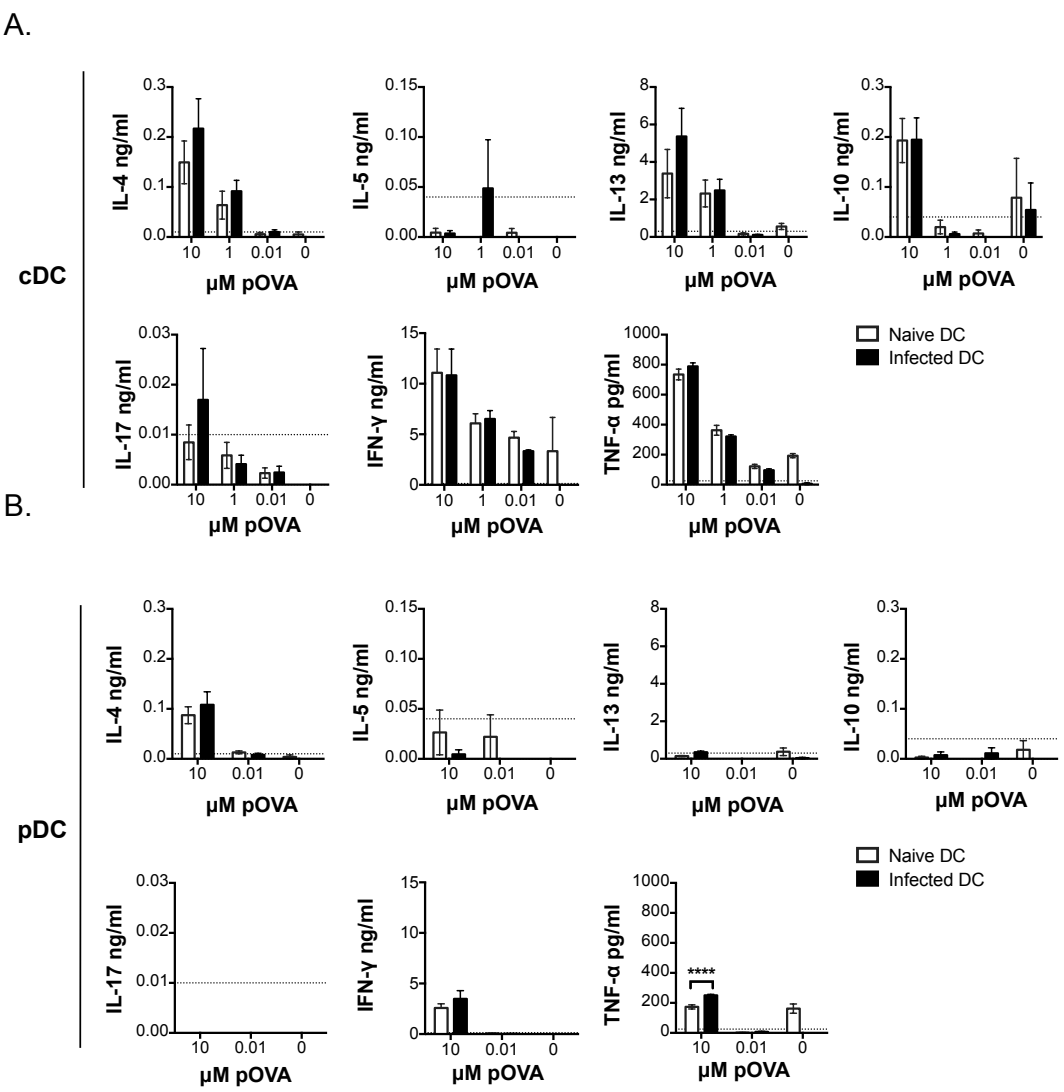

Figure 5.7 Hepatic cDCs from *S. mansoni* infection efficiently present pOVA to maintain CD4$^+$ T cell cytokine production

FACS sorted hepatic cDCs or pDCs from D42 *S. mansoni* infected or naïve mice were pulsed with pOVA before culture. pOVA-pulsed naïve or infection DCs were co-cultured with *in vitro* activated CFSE-labelled CD4$^+$ T cells for 72h. **A-B**. Supernatants from co-cultures were harvested and analysed by ELISA for cytokines present. The detection limit of the ELISA is shown with a dotted line. Data are from 3 experiments (A to B). Mixed model analysis (blocking day of experiment), Tukey's HSD (* $P \leq 0.05$, ** $P \leq 0.01$, *** $P \leq 0.001$, ****$P \leq 0.0001$). Bars are SEM. N= 7-10.

Figure 5.8

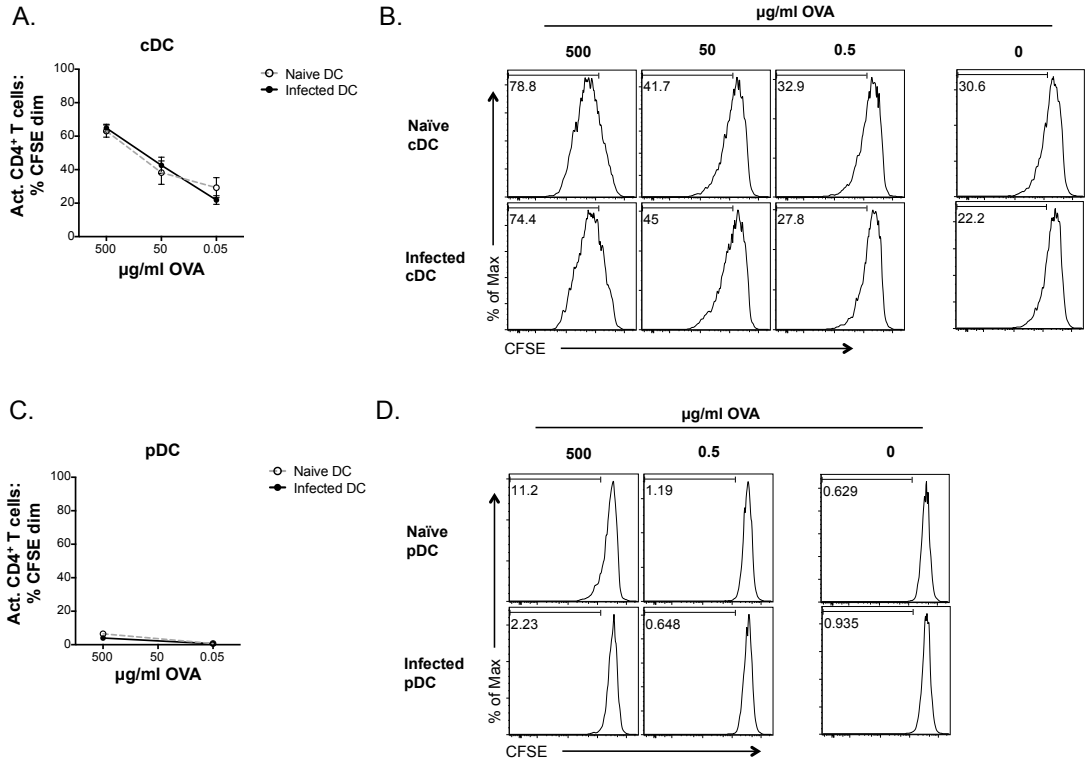

Figure 5.8 cDCs, but not pDCs, derived from *S. mansoni* infected mice take up, process and present OVA efficiently to maintain $CD4^+$ T cell proliferation

Naïve or *S. mansoni* infection derived liver cDCs or pDCs were FACS sorted for *ex vivo* DC:T cell co-cultures. **A-D.** Sorted naïve or infection derived cDCs (A – B) or pDCs (C – D) were cultured with CFSE-labelled effector/memory $CD4^+$ T cells in the presence of OVA protein for 72h. $CD4^+$ T cells were assessed for their expression of CFSE by flow cytometry, which is shown graphically (A & C)**.** Representative flow plots are shown for CFSE expression by $CD4^+$ T cells in culture with cDCs (B) or pDCs (D) and OVA. Data are from 3 experiments (A to D). Mixed model analysis (blocking day of experiment), Tukey's HSD (* $P \leq 0.05$, ** $P \leq 0.01$, *** $P \leq 0.001$, ****$P \leq 0.0001$). Bars are SEM. N= 7-10.

Figure 5.9

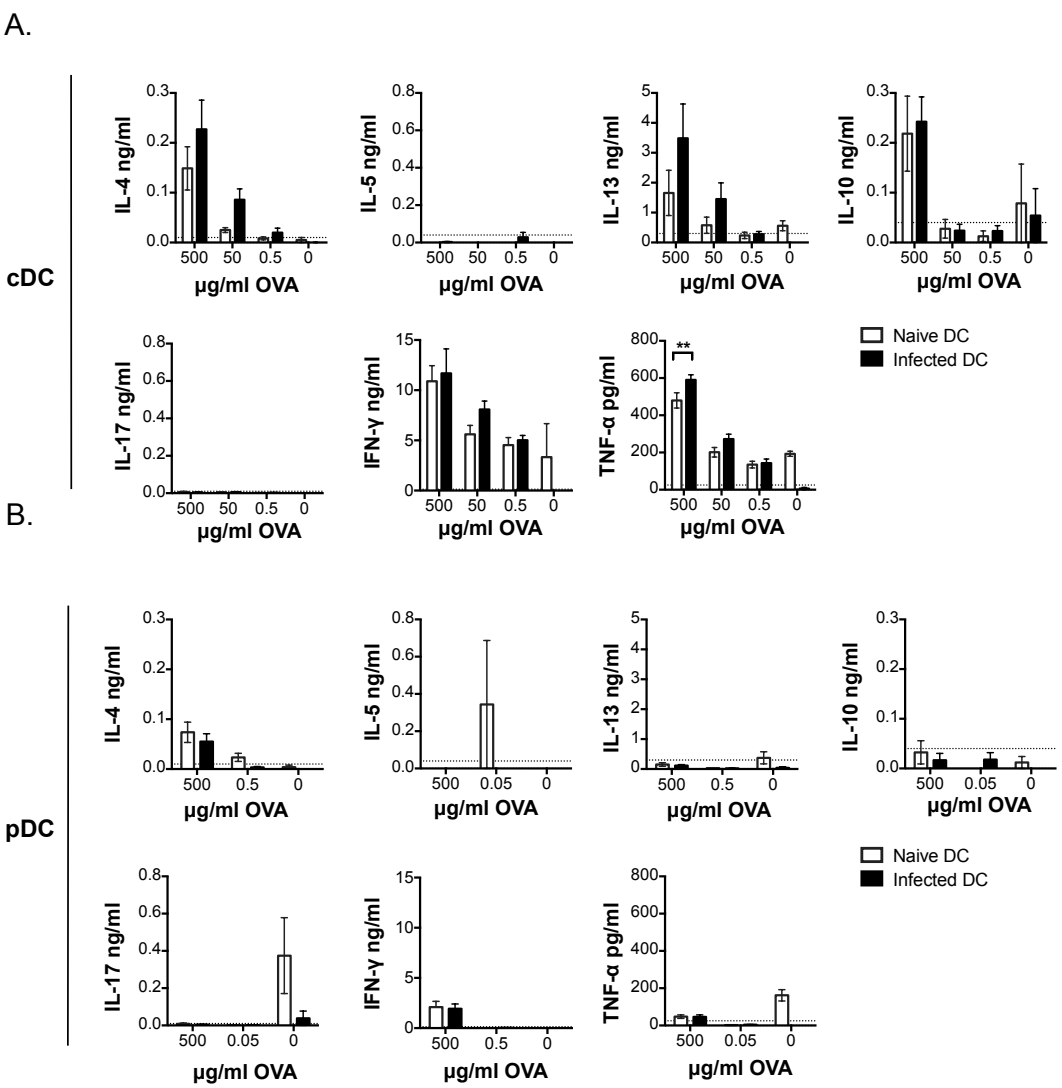

Figure 5.9 cDC, but not pDCs, derived from *S. mansoni* infected mice efficiently take up, process and present OVA to maintain effector/memory CD4$^+$ T cell cytokine production

FACS sorted hepatic cDCs or pDCs from D42 *S. mansoni* infected or naïve mice were cultured with *in vitro* activated CFSE-labelled CD4$^+$ T cells in the presence of endotoxin-free soluble OVA protein for 72h. **A-B**. Supernatants from co-cultures were harvested and analysed by ELISA for cytokine production. The detection limit of the ELISA is shown with a dotted line. Data are from 3 experiments (A to B). Mixed model analysis (blocking day of experiment), Tukey's HSD (* $P \leq 0.05$, ** $P \leq 0.01$, *** $P \leq 0.001$, ****$P \leq 0.0001$). Bars are SEM. N= 7-10.

Figure 5.10

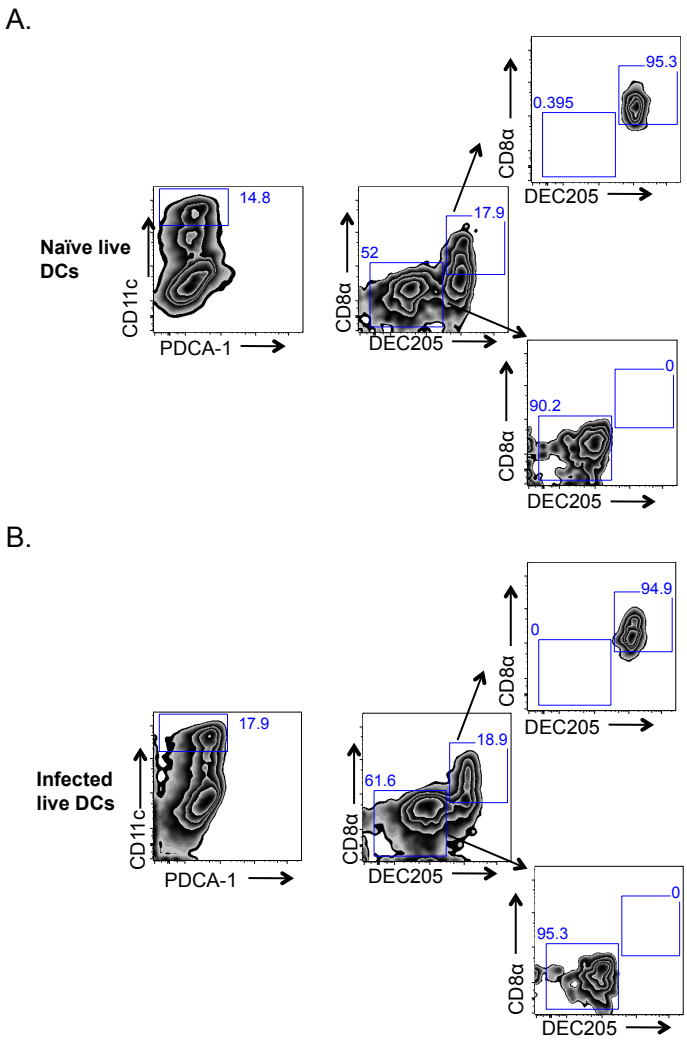

Figure 5.10 Purification and isolation of hepatic CD8α$^+$ and CD8α$^-$ cDC subsets from naïve or *S. mansoni* infected mice

Livers from naïve **(A)** or D42 *S. mansoni* infected mice **(B)** were harvested and liver leukocytes isolated and pooled. Naïve or infection derived pooled leukocytes were enriched for DCs by negative selection using Dynabeads as done previously for cDC vs. pDC cultures. Enriched DCs were then sorted using a FACS cytometer into pure CD8α$^+$ cDC (CD11c$^+$ PDCA-1$^-$ CD8α$^+$ CD205$^+$) and CD8α$^-$ cDC (CD11c$^+$ PDCA-1$^-$ CD8α$^-$ CD205$^-$) populations. Gates were set using FMO controls. 1 of 1 experiment (A to B). N=1.

Figure 5.11

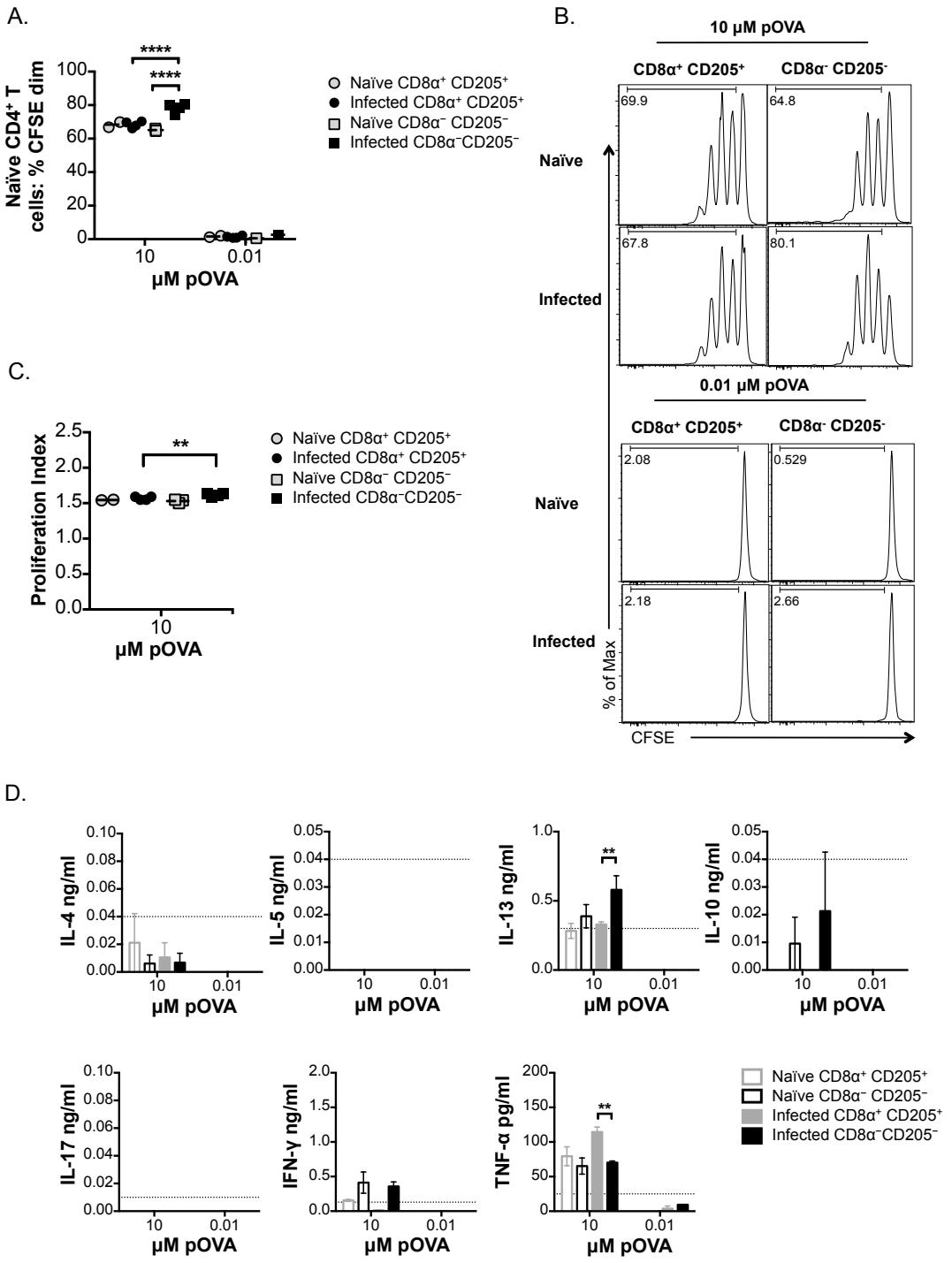

Figure 5.11 CD8α⁻ cDC function is enhanced during *S. mansoni* infection

FACS purified CD8α$^+$ and CD8α$^-$ cDCs from naïve or D42 *S. mansoni* infected mice were pulsed with pOVA and co-cultured with CFSE-labelled naïve CD4$^+$ T cells for 72h. **A.** Cells from the cDC subset co-culture were harvested after 72h and assessed for CFSE dilution by flow cytometry to determine the proportion of CD4$^+$ T cell

proliferation. **B.** Representative flow plots are shown for CFSE-labelled $CD4^+$ T cells in culture with $CD8\alpha^+$ or $CD8\alpha^-$ cDCs. **C.** The proliferation index was determined to assess the average number of divisions that dividing $CD4^+$ T cell in culture with $CD8\alpha^+$ or $CD8\alpha^-$ cDCs underwent. **D.** Supernatants were harvested from the culture after 72h and assessed for cytokine production by ELISA. The detection limit of the ELISA is shown with a dotted line. 1 of 1 experiment (A to D). Two-way ANOVA (* $P \leq 0.05$, ** $P \leq 0.01$, *** $P \leq 0.001$, ****$P \leq 0.0001$). Bars are SEM. N=2-4.

Figure 5.12

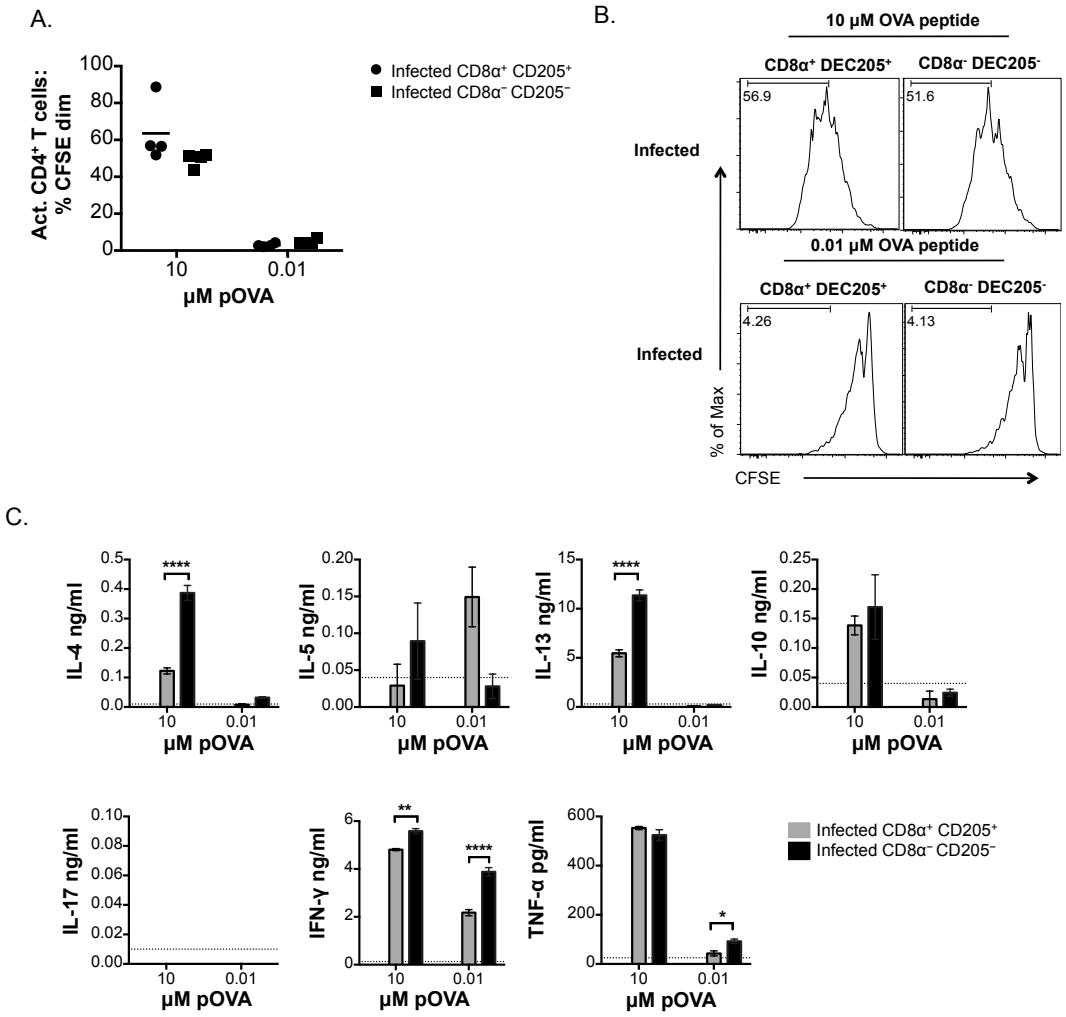

Figure 5.12 CD8α⁻ cDCs, but not CD8α⁺ cDCs, maintain increased Th2 cytokine production by effector/memory CD4⁺ T cells during *S. mansoni* infection.

FACS purified CD8α$^+$ and CD8α$^-$ cDCs from naïve or D42 *S. mansoni* infected mice were pulsed with pOVA and co-cultured with CFSE-labelled *in vitro* activated CD4$^+$ T cells for 72h. **A.** Effector/memory CD4$^+$ T cells were assessed for CFSE dilution by flow cytometry after culture to determine the proportion of CD4$^+$ proliferation. **B.** Representative flow plots are shown for CFSE-labelled CD4$^+$ T cells in culture with the cDC subsets. **C.** Supernatants were harvested from the culture after 72h and assessed for cytokine production by ELISA. The detection limit of the ELISA is shown with a dotted line. 1 of 1 experiment (A to C). Two-way ANOVA (* $P \leq 0.05$, ** $P \leq 0.01$, *** $P \leq 0.001$, ****$P \leq 0.0001$). Bars are SEM. N=3-4.

6 General discussion

At the beginning of the work detailed in this thesis there was a limited understanding of the requirement for DCs in the induction of Th2 responses during helminth infection. In particular, much remained unexplained about the complexity of distinct DC subsets involved in the Th2 process. By assessing the location, importance and function of different types of DCs in the context of Th2 responses and *S. mansoni* infection, with a focus on $CD8\alpha^+$ cDCs, we have elevated our understanding of a number of key roles assumed by DCs in the orchestration of Th2 immunity. Furthermore, we have provided a platform for future work building on our core discoveries, which will address the mechanisms that $CD8\alpha^+$ cDCs may employ to regulate Th2 responses.

6.1 The presence and location of DCs in granulomas during *S. mansoni* infection

The development of granulomatous inflammation during *S. mansoni* infection is dependent on the induction of $CD4^+$ Th2 cells (Amiri et al., 1992; Boros, 1989; Byram and Lichtenberg, 1977; Cheever et al., 1993; 1999; Doenhoff et al., 1981; Dunne and Doenhoff, 1983; Mathew and Boros, 1986). The formation of hepatic granulomas is a key feature of *S. mansoni* infection, and is thought to represent a double-edged sword; although granulomas are necessary to protect surrounding hepatocytes efficiently from toxins released by *S. mansoni* eggs, they are also responsible for the majority of fibrotic and inflammatory pathology associated with the disease (Wilson et al., 2007). To accurately assess the formation of granulomas throughout infection, I have developed a novel technique for efficient and objective quantification of the total proportion of granulomatous inflammation in the liver, which encompasses immune cell aggregation and collagen deposition. Moreover, confocal microscopy allowed for the investigation of the location of immune cells (including DCs) within granulomas, and their quantification, during *S. mansoni* infection. Together these techniques enabled detailed examination of the generation and kinetics of granulomatous inflammation during infection, and the role of DCs in this process.

In chapter 3, I have shown that $CD11c^+$ cells are present in granulomas throughout the course of *S. mansoni* infection, including primary formation of granulomas against newly arrived parasite eggs in the liver. Notably, CD11c is not a specific marker for DCs by confocal microscopy, as $CD11c^{high}$ MΦs are likely also detected. Nevertheless, close proximity to T cells raises interesting questions about the importance of interaction between DCs and $CD4^+$ T cells locally in the granuloma. This pattern of $CD11c^+$ and T cell staining in the granuloma is evident throughout infection (D28-D105), indicating that interaction between these cell types occurs when Th2 responses against *S. mansoni* eggs are induced and continues, as Th2 responses are downmodulated (Pearce and MacDonald, 2002). Thus, the location of T cells in relation to $CD11c^+$ cells provided reason to speculate that their interaction is important for the maintenance of Th2 responses against the *S. mansoni* egg in the granuloma.

6.2 The role of DCs in granuloma formation and development during *S. mansoni* infection

Following the working hypothesis that $CD11c^+$ DCs are interacting with T cells in early granuloma formation, we asked whether this process was important for the formation of granulomas at the onset of egg production. Using the $CD11c^+$ DC depletion model (CD11c.DOG mice) we were able to show that DCs (or $CD11c^{high}$ MΦs) in the liver may play a crucial role in the recruitment or retention of effector/memory T cells during the initial formation of granulomas. This discovery extends our understanding of the function of DCs during *S. mansoni* infection, as it strongly suggests that they are interacting with effector/memory Th2 cells in hepatic granulomas, in addition to their more expected role in Th2 priming in secondary lymphoid organs (Phythian-Adams et al., 2010). When analysing the impact of CD11c deficiency on established granulomas during more chronic stages of infection 2-3 weeks after the onset of egg production, we found that T cells were located primarily in the periphery of granulomas instead of also locating to more central regions as found in non-depleted mice. This indicates that $CD11c^+$ cells are needed

to retain T cells throughout the granuloma rather than just in the periphery and/or recruit effector/memory T cells to more central areas.

Taken together, we propose that DCs may recruit antigen-specific $CD4^+$ T cells to the granuloma during early stages of formation, and thereafter retain $CD4^+$ T cells in the "appropriate" location throughout every region of the granuloma. The localization of T cells with $CD11c^+$ cells in the centre of the granuloma might reflect a functional interaction that could be important for the reactivation of effector/memory Th2 responses locally. Further studies are required to understand the mechanisms that are involved in the recruitment, retention and reactivation of effector/memory $CD4^+$ T cells in the granulomas. It is plausible that DCs mediate the recruitment and retention of $CD4^+$ T cells via the expression and secretions of chemokines such as CCL17 and CCL22 that have previously been shown to be important for the recruitment of Th2 cells to airways during human allergic asthma (Perros et al., 2009; Yoshie and Matsushima, 2015). On the other hand, persistent peptide loaded MHC:TCR stimulation, co-stimulation (i.e. CD28, OX40 or ICOS) or the provision of survival cytokines (IL-2, IL-7 and IL-15) by DCs could be key for promotion of the reactivation and maintenance of effector/memory Th2 responses in the liver (Boyman et al., 2009). Th2 cytokines, in particular IL-13, induce collagen production by fibroblasts (Chiaramonte et al., 1999; Fallon et al., 2000a; Hesse et al., 2001), and so reduced DC:T cell interactions within the granuloma could conceivably decrease granuloma integrity.

Previous studies in the MacDonald laboratory using CD11c.DOG mice to deplete $CD11c^+$ DCs during S. mansoni infection have shown that these cells are not only important for the induction of Th2 responses (Phythian-Adams et al., 2010), but that they are also required for the maintenance of established effector/memory Th2 cells and the survival of the host (unpublished data, Phythian-Adams *et al.*,). It was hypothesised that an impaired Th2 response may lead to a failure to maintain alternative activation of MΦs, resulting in a breakdown of wound healing responses and granuloma integrity in the liver (Herbert et al., 2004). This likely causes leakage of egg derived toxins from granulomas into the surrounding liver parenchyma

causing hepatocyte death, ultimately leading to liver failure (Wilson et al., 2007). Thus, additional work in the MacDonald laboratory lends further support to the hypothesis raised by work in this thesis that close positioning of DCs and T cells may promote the reactivation of effector/memory $CD4^+$ Th2 cells, which may be important to ensure that granulomas remain an impermeable structure for egg derived toxins.

Given that there is increasing evidence in the literature that suggests the induction of Th2 responses is attributed to distinct DC subsets (Tjota and Sperling, 2014), we hypothesised that Th2 dependent granuloma formation during *S. mansoni* infection may also rely on the function of specific DC types. In the final section of chapter 3 we have demonstrated for the first time that at the onset of egg production T cell presence in the *S. mansoni* granuloma is not altered in *Batf3*$^{-/-}$ mice, which are specifically deficient in $CD8\alpha^+$ cDCs and migratory $CD103^+$ cDCs (Hildner et al., 2008). This extends our understanding of which subsets of DCs are important in orchestrating T cell responses and granuloma development in the liver, and points to a more important role for $CD11b^+$ cDCs and pDCs in this process. Nevertheless, the requirement for $CD8\alpha^+$ cDCs during the induction of Th1 immune responses against *T. gondii* (Mashayekhi et al., 2011) and *L. major* (Ashok et al., 2014) infection previously reported in the literature provided reason to speculate that *Batf3* deficiency may impact the development and character of immune responses against *S. mansoni* infection. This raised numerous questions: are $CD8\alpha^+$ cDCs important during the immune response activation against Th2 inducing pathogens such as *S. mansoni,* and if so, are $CD8\alpha^+$ cDCs involved in the induction, regulation or inhibition of Th2 responses during *S. mansoni* infection?

6.3 The importance of $CD8\alpha^+$ cDCs during *S. mansoni* infection

In answer to our original question, we have shown for the first time that $CD8\alpha^+$ cDCs are not a fundamental requirement for the induction of Th2 responses during *S. mansoni* infection. This carries broad implications for Th2 mediated diseases in general such as infection with other Th2 inducing pathogens, atopy and allergic

inflammation, as CD8α$^+$ cDCs are likely not required for the initiation of Th2 responses independent of the antigen. More than this, we have discovered a key and perhaps unexpected regulatory role for CD8α$^+$ cDCs in type 2 settings, as Th2 cytokine production was dramatically elevated in *Batf3*$^{-/-}$ mice injected with *S. mansoni* eggs.

Whilst we have shown that CD8α$^+$ cDCs are not required for the induction of Th2 responses, the clear emergence of dysregulated Th1 and Th2 responses in *Batf3*$^{-/-}$ mice injected with *S. mansoni* eggs and during natural infection indicated that CD8α$^+$ cDCs play an important role in the regulation of Th2 immunity, preventing exaggerated Th2 responses during infection. Whether CD8α$^+$ cDCs are important for the regulation of Th2 responses in other helminth, or indeed non-helminthic Th2 settings including allergy and atopy, remains to be established. Recent findings in the literature suggest this may be the case, as *Batf3* dependent DCs modulate allergic airway inflammation via the production of IL-10 (Engler et al., 2014), and Th2 responses are enhanced in *Batf3*$^{-/-}$ mice infected with the predominantly Th1 inducing parasite *L. major* (Ashok et al., 2014). Thus, our data are in line with the current literature suggesting that CD8α$^+$ cDCs are important for the induction of Th1 responses, and that they may play a role in the regulation of Th2 responses.

At the moment we have a number of different candidate pathways that may mediate Th2 regulation by CD8α$^+$ cDCs, which will be subject to further research in future (Diagram 6.1) (Section 4.6.3.2). Perhaps the most likely mechanism for Th2 regulation is initiated by the production of IL-12 by CD8α$^+$ cDCs, as there are several previous observations in the literature that point to an important role for this cytokine in such a process. First, CD8α$^+$ cDCs are known to be the main producers of IL-12 in several infection settings, which suggests that this cytokine is a central player in the interaction between CD8α$^+$ cDCs and CD4$^+$ T cells (Martínez-López et al., 2014; Mashayekhi et al., 2011). Second, IL-12 is the most potent inhibitor of Th2 responses known to date (Murphy and Stockinger, 2010), which makes this an attractive molecule in the regulation of dominant Th2 responses against *S. mansoni* infection. An important question to answer when examining the role of IL-12 in Th2

regulation is whether this inflammatory cytokine acts directly on newly primed or effector/memory Th2 cells possibly through downstream signalling events in the cell (Murphy and Stockinger, 2010), or if the induction of Th1 responses mediated by IL-12 forms an indirect pathway for Th2 regulation via IFN-γ (Paludan, 1998). There is evidence to suggest that responsiveness to IL-12 by $CD4^+$ T cells may be crucial for understanding Th2 polarisation or maintenance (Hilkens et al., 1996; Murphy and Stockinger, 2010; Smits et al., 2001b). For example, IL-12 can re-establish IL-12 responsiveness in human Th2 committed cells, resulting in a suppression of GATA3 expression and an induction of T-bet in $CD4^+$ T cells (Smits et al., 2001b). This suggests that lowering $CD4^+$ T cell IL-12 responsiveness perhaps by degrading or blocking the IL-12 receptor is a critical requirement during the induction and maintenance of Th2 responses (Hilkens et al., 1996; Murphy and Stockinger, 2010). Therefore, the key to unravelling the mechanisms underlying Th2 responses may likely be to establish a greater understanding of the interplay or crossregulation between transcription factors in Th2 populations, including T-bet and GATA3, and to investigate how DC subsets influence this process. We intend to address this in future by assessing the expression of T-bet and GATA3 by $CD4^+$ T cells *ex vivo* (either OT-II T cells as in chapter 5 or $CD4^+$ T cells isolated from *S. mansoni* infection) in culture with varying ratios of different DC subsets.

Overall, we have shown that $CD8\alpha^+$ cDCs are important for the induction of mixed/balanced Th1 and Th2 responses during *S. mansoni* infection, which may be crucial for the subsequent development of Th2 responses in the host. It is possible that the kinetics of the immune response against *S. mansoni* infection are shifted in *Batf3*$^{-/-}$ mice, with the enhanced Th2 responses evident following the onset of egg production reflecting an earlier peak in type 2 effector responses, compared with WT mice. This could ultimately also result in early $CD4^+$ T cell hyporesponsiveness in the liver effector site in infected *Batf3*$^{-/-}$ mice (Taylor et al., 2009). Taylor *et al.,* (2009) described cell intrinsic $CD4^+$ T cell hyporesponsiveness during chronic stages of *S. mansoni* infection, suggesting that this occurs due to persistent antigen stimulation, which results in the upregulation of expression of molecules such as GRAIL (an E3 ubiquitin ligase that is associated with anergy) (Taylor et al., 2009).

We have some preliminary support for this altered kinetic hypothesis, as Th2 responses against *S. mansoni* eggs following s.c. injection were substantially enhanced in *Batf3*$^{-/-}$ mice at a time-point prior to notable increases in Th2 cytokine production in WT mice. This scenario could be further interrogated in future by conducting time-course experiments, including early stages of infection (i.e. D0 to D42) or following egg injection (i.e. D0 to D5).

Previous studies have outlined the importance of mixed/balanced Th1 and Th2 immune responses during *S. mansoni* infection to prevent excessive Th2 or Th1 driven pathology, which can, in some cases, result in the death of the host (Hoffmann et al., 2000; Wynn, 2004). In chapter 4 we have shown that *Batf3*$^{-/-}$ mice lose a critical amount of weight in later stages of infection and, therefore, do not survive acute infection. This discovery resembles the weight loss phenotype displayed by CD11c.DOG mice when CD11c^{+} DCs are depleted between weeks 6-8 of *S. mansoni* infection (Dr. Alexander Phythian-Adams, unpublished data), and by IL-4 deficient mice lacking an intact Th2 immune response (Brunet et al., 1997). In the case of IL-4 deficiency, it is thought that TNF-α mediated cachexia is responsible for death in IL-4$^{-/-}$ animals (Brunet et al., 1997). This scenario is unlikely in *Batf3*$^{-/-}$ mice, where we have identified that Th2 immune responses were predominantly increased, while levels of TNF-α were reduced, compared with WT mice (Fig. 4.5). This suggests that the processes responsible for the death of *Batf3*$^{-/-}$ mice during *S. mansoni* infection are mechanistically distinct from those mediated by TNF-α or Th2 impairment.

Fibrosis, predominantly driven by Th2 cytokines, is one of the major factors contributing to severe pathology during schistosomiasis (Wynn et al., 2004). Fibrotic legions and scarring in the liver can lead to portal hypertension and shunting of blood vessels to the extent that the blood supply bypasses the liver, which can cause organ failure (Fallon, 2000; Hams et al., 2013). Thus, given their elevated Th2 profile, one possible explanation for premature death of *Batf3*$^{-/-}$ mice during *S. mansoni* infection may be increased fibrotic pathology, which was indicated by more severe fibrosis in the liver in more chronic stages of infection in *Batf3*$^{-/-}$ mice. Moreover, intestinal granulomatous inflammation following the onset of egg production and type I and

type III collagen in hepatic granulomas was more severe during infection in *Batf3* deficient animals. A novel and surprising finding was the accumulation of vacuoles in the circular intestinal muscle during *S. mansoni* infection, which was exacerbated in *Batf3*$^{-/-}$ mice and may indicate increased muscle injury. Taken together, severe intestinal and hepatic granulomatous pathology may lead to increased fibrotic scarring of the tissue when CD8α^{+} cDCs are reduced, ultimately resulting in organ failure and death of the animal (Wilson et al., 2007). It is somewhat intriguing that the lack of a rare DC subset such as CD8α^{+} cDCs, which is not required for the induction of Th2 responses, leads to fatal consequences for the host. This highlights the importance of diverse DC subsets during the generation of immune responses against *S. mansoni* infection.

Numerous studies have previously investigated how exploiting the functions of CD8α^{+} cDCs in inducing CTL and Th1 responses *in vivo* could contribute to the development of vaccines and therapeutics in various disease settings, where these immune responses are beneficial (Shortman et al., 2009). For example, it has been proposed that targeting tumour antigens to CD8α^{+} cDCs may aid the induction of protective anti-tumour responses mediated by CD8^{+} T cells (Sancho et al., 2008). The data in this thesis additionally suggest that targeting CD8α^{+} cDCs could be used in future to promote regulation of Th2 mediated disease such as atopy, allergic inflammation or indeed severe pathology associated with helminth infection. Alternatively, cytokines produced by CD8α^{+} cDCs that may be important for the regulation of Th2 responses could be administered to alleviate excessive Th2 inflammation. In fact, early work that investigated the role of IL-12 during *S. mansoni* infection focused on the potential of IL-12 as a therapeutic against severe pathology associated with *S. mansoni* infection, through downregulation of Th2 responses (Oswald et al., 1994; Wynn et al., 1995). However, administration of IL-12 was ultimately rendered infeasible, particularly during human *S. mansoni* infection, due to deleterious pathology associated with elevated Th1 responses (Wynn and Hoffmann, 2000). Irrespective, the work in this thesis presents multiple reasons to revisit the impact of IL-12 and Th1 responses during Th2 inflammatory

disease including *S. mansoni* in the context of Th2 regulation and the induction of "appropriate" immune responses, particularly in effector sites such as the liver.

6.4 Defining the function of hepatic DC subsets during *S. mansoni* infection

cDCs are thought to be superior APCs in comparison with pDCs in various different settings, including allergic responses (de Heer et al., 2004), and this is largely due to a lack of cellular machinery for efficient uptake, processing and presentation of antigen by pDCs (Villadangos and Young, 2008). We have demonstrated in chapter 5 that *S. mansoni* infection does not dramatically alter the core APC function of hepatic cDCs and pDCs, and that only cDCs can induce and maintain $CD4^+$ T cells responses *ex vivo*. By assessing the function of DC subsets following *S. mansoni* infection we have shown that hepatic $CD8\alpha^-$ cDCs, but not $CD8\alpha^+$ cDCs, exhibit an enhanced ability to induce $CD4^+$ T cell proliferation and maintain Th2 cytokine production. This data and our conclusion that $CD8\alpha^+$ cDCs are dispensable for Th2 response induction in chapter 4 lend further support to our main hypothesis that $CD8\alpha^-$ cDCs are key players in this process. In conjunction with recent literature, it is tempting to suggest that IRF4 dependent $CD11b^+$ cDCs will be critical for the development of Th2 responses during *S. mansoni* infection (Gao et al., 2013; Kumamoto et al., 2013; Plantinga et al., 2013; Williams et al., 2013). Thus, future work will aim to assess the importance of $CD11b^+$ cDCs in the induction and development of Th2 responses during *S. mansoni* infection, and this could be addressed by using transgenic mouse models such as $CD11c^{cre}IRF4^{flox}$ that are deficient in this DC subset (Vander Lugt et al., 2014).

In contrast to $CD8\alpha^-$ cDCs, $CD8\alpha^+$ cDCs did not induce or maintain Th2 cytokine production. However, the induction of TNF-α production by $CD4^+$ T cells was predominantly orchestrated by $CD8\alpha^+$ cDCs (Fig. 5.11). These exciting preliminary findings outline the differential roles of DC subsets in the induction of $CD4^+$ T cell responses and the maintenance of effector/memory $CD4^+$ T cells in the effector site. To improve our understanding of DC function in the granuloma specifically, DCs could be isolated from purified granulomas in future and compared with the

functions of DCs in the surrounding parenchyma. Comparison of the function of lymphoid derived DC subsets with those isolated from the effector site would be beneficial for more accurate analysis of the capacity of DCs to induce Th2 responses in priming sites. In addition, investigating the function of DC subsets at different time-points of *S. mansoni* infection from priming vs. effector tissue sites will clarify whether the capacity to prime or maintain $CD4^+$ T cell responses changes with chronicity. Finally, a more global overview of the APC potential exhibited by DCs during *S. mansoni* infection gene expression could be explored by conducting RNA sequencing (RNA-seq) analysis on *ex vivo* FACS sorted DC subsets.

Many questions remain about how Th2 responses are induced or maintained. Which specific mechanisms do $CD8\alpha^-$ cDCs employ during the Th2 induction and maintenance process? Why do only $CD8\alpha^-$ cDCs appear to possess an increased capacity to induce and maintain $CD4^+$ T cell responses against *S. mansoni* egg antigen? Mechanistically, how do $CD8\alpha^+$ cDCs regulate Th2 responses, either directly or indirectly? Yet, by systematically investigating the location, importance and function of different DC subsets during *S. mansoni* infection, work in this thesis has significantly elevated our understanding of the role of DC subsets in Th2 immune responses. As such, we can conclude that $CD8\alpha^+$ cDCs are not important for the induction of Th2 responses in priming sites, and are not required for the recruitment/retention/reactivation of effector/memory Th2 cells in effector sites during *S. mansoni* infection. This provides further evidence, in addition to that already published in the literature, that $CD8\alpha^-$ cDCs are involved in the induction and promotion of type 2 immunity (Tjota and Sperling, 2014). On the other hand, $CD8\alpha^+$ cDCs conceivably play a crucial role in regulating Th2 immune responses, which provides a platform for novel therapeutics aimed at reducing deleterious type 2 inflammation.

Diagram 6.1

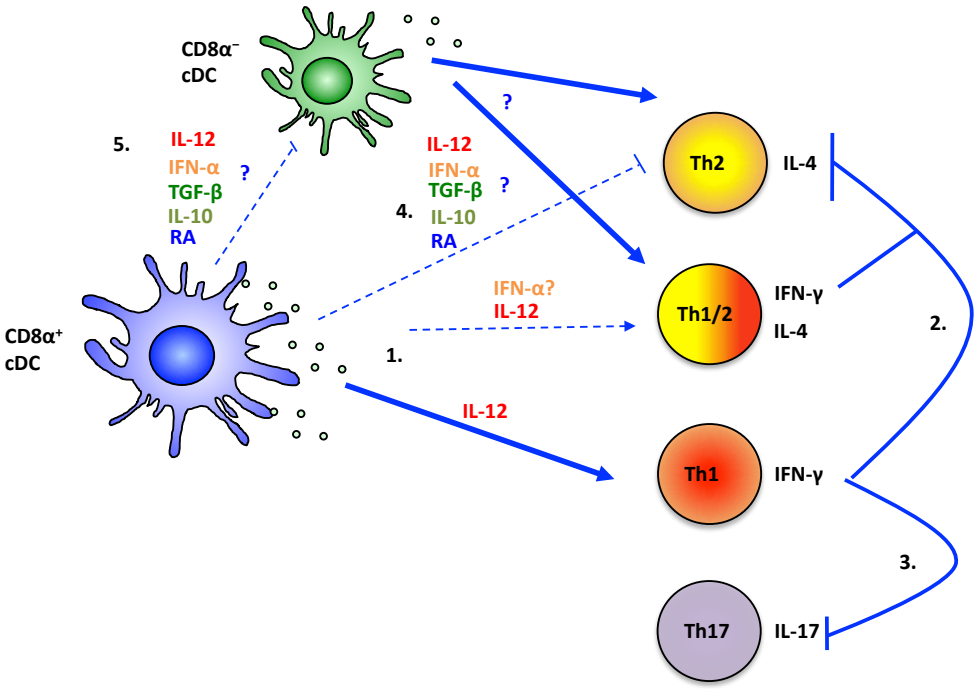

Diagram 6.1 Possible mechanisms employed by CD8α$^+$ cDCs during *S. mansoni* infection.

1. CD8α$^+$ cDCs produce IL-12 (Ashok et al., 2014; Mashayekhi et al., 2011), which induces Th1 and IFN-γ production by Th1 cells (Szabo et al., 2000) and Th1/Th2 double positive cells. IFN-α may promote the induction of Th1 responses (Wenner et al., 1996) and IFN-γ production by Th2 cells (Hegazy et al., 2010). **2.** IFN-γ produced by primed CD4$^+$ T cells inhibits Th2 proliferation and IL-4 production by Th2 cells and Th1/2 cells (Paludan, 1998). **3.** IFN-γ production inhibits IL-17 production by CD4$^+$ T cells (Hochrein et al., 2001). **4.** CD8α$^+$ cDCs produce soluble factors including IL-12, TGF-β, INF-α, IL-10 and/or RA, which may inhibit / regulate Th2 responses directly. **5.** CD8α$^+$ cDC derived cytokines may regulate or inhibit the function of other cDC subsets (i.e. CD11b$^+$ cDCs), which prime Th2 responses in secondary lymphoid organs. Known pathways are shown by continuous lines, whereas hypothetical pathways are depicted by dashed lines.

7 Appendix

Figure 7.1

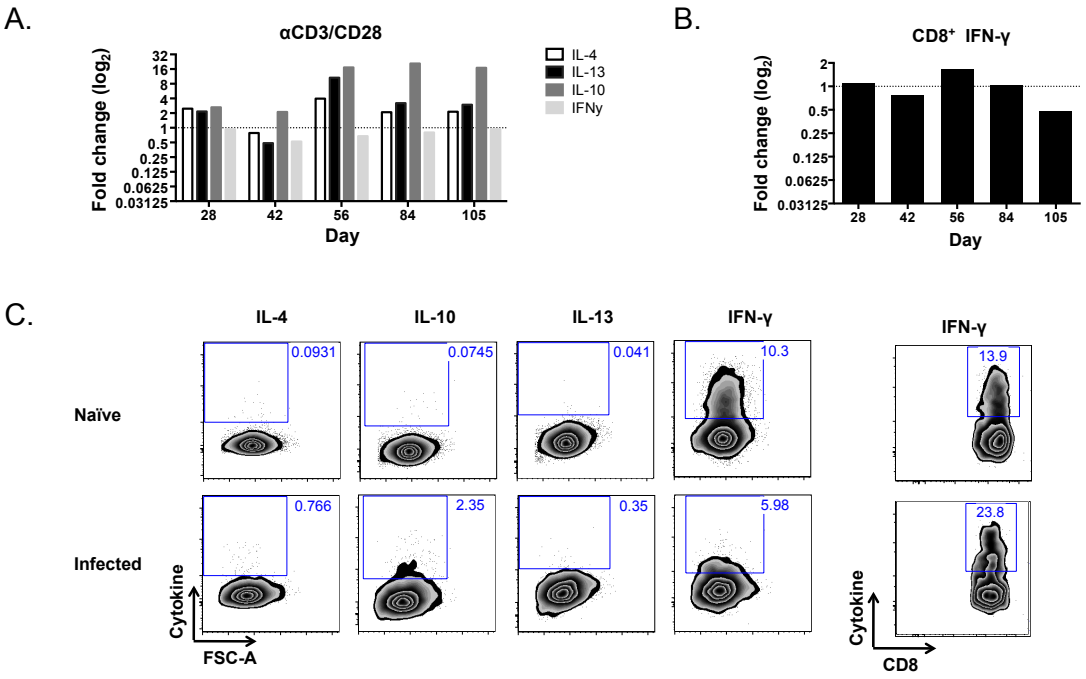

Figure 7.1 Non CD4$^+$ T cell intracellular cytokine production.
Liver leukocytes from naïve or *S. mansoni* infected WT mice were isolated. **A.** Liver leukocytes were restimulated with αCD3/CD28 *in vitro* for 72h before supernatant harvest and ELISA analysis of cytokines. Non T cell cytokine production is shown as fold change compared with naïve controls (dotted baseline). **B.** Intracellular hepatic CD8$^+$ T cell IFN-γ production during infection after restimulation with αCD3/CD28. No other cytokines produced by CD8$^+$ T cells were detected. **C.** Representative flow plots for non CD4$^+$ T cell cytokine production from D56 are shown. Gates were set using FMOs. These plots show that cells other than T cells are producing some IL-10 and IFN-γ but at lower levels. Gates were set using FMO controls. 1 of 1 (A to C) experiments. Bars are SEM of 3-4 samples per group. Cells from 2-3 mice were pooled per sample.

Figure 7.2

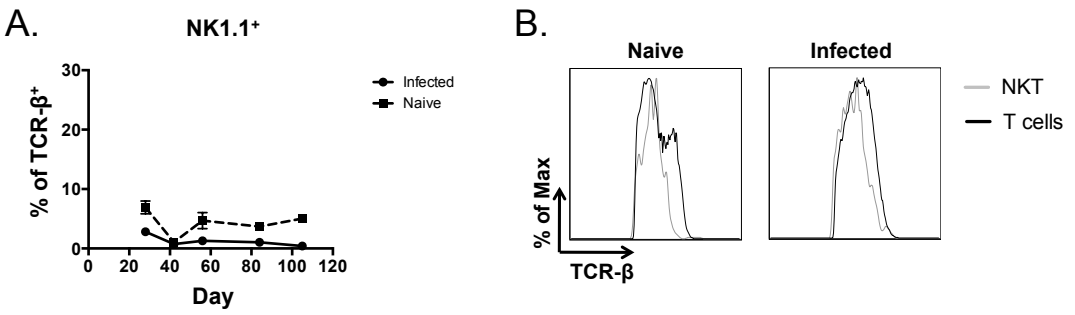

Figure 7.2 Expression of TCR-β by NKT cells

Liver leukocytes from naïve or *S. mansoni* infected WT mice were isolated and assessed by flow cytometry. **A.** Proportions of NKT cells that express TCR-β were determined, which revealed that NKT cell levels are below 10% at every time-point measured. **B.** The level of expression of TCR-β is similar on T cells compared with NKT cells at D56. Gates were set using FMO controls. 1 of 1 (A to B) experiments. Two-way ANOVA (* $P \leq 0.05$, ** $P \leq 0.01$, *** $P \leq 0.001$, ****$P \leq 0.0001$). Bars are SEM of 3-4 samples per group. Cells from 2-3 mice were pooled per sample.

Figure 7.3

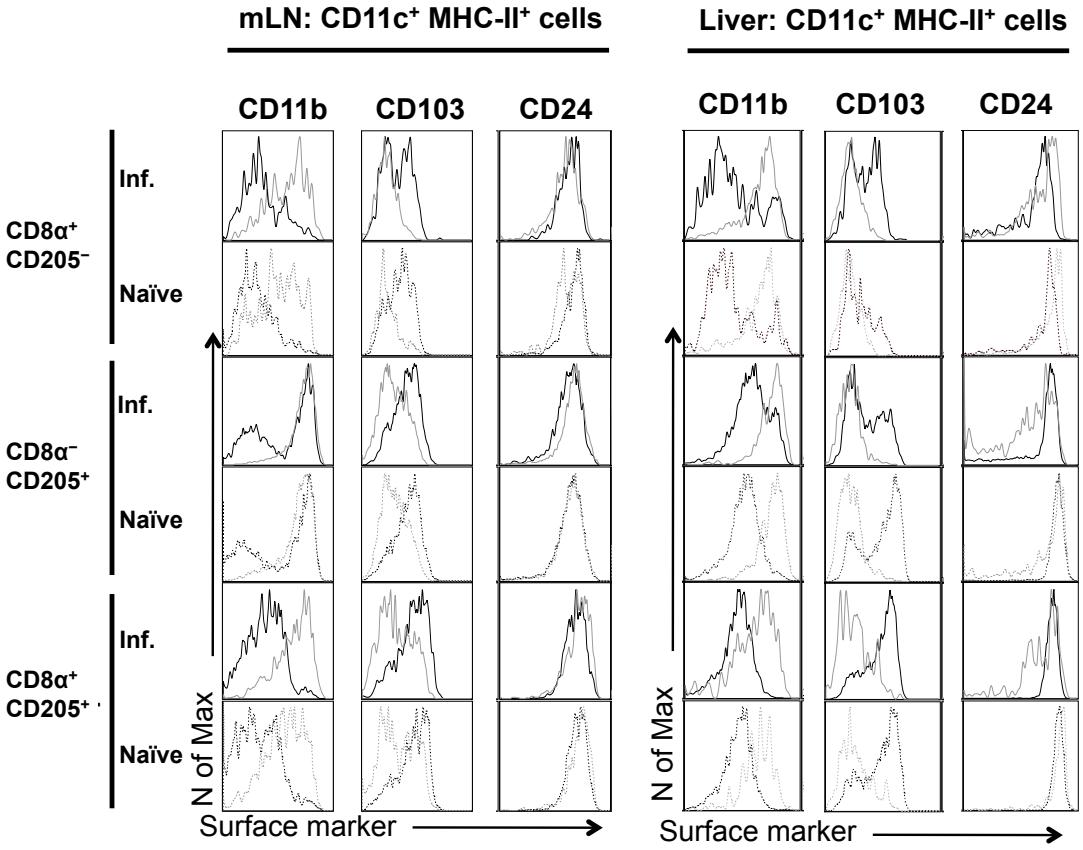

Figure 7.3 Surface marker expression of residual CD8α$^+$ cDCs and possible pre-cursors in the mLN and the liver of *Batf3*$^{-/-}$ mice during *S. mansoni* infection

mLN cells or liver leukocytes were isolated at D42 of *S. mansoni* infection and CD11c$^+$ MHC-II$^+$ cDCs were analysed *ex vivo* by flow cytometry. CD8α$^+$ CD205$^+$, CD8α$^+$ CD205$^-$ and CD8α$^-$ CD205$^+$ cDCs were analysed for their expression of CD11b, CD103 and CD24. Representative histograms are shown for naïve WT (black, dotted), infected WT (black), naïve *Batf3*$^{-/-}$ mice (grey, dotted) and infected *Batf3*$^{-/-}$ mice (grey). Gates were set using FMO controls. 1 of 2 experiments. 3-4 mice per group.

Figure 7.4

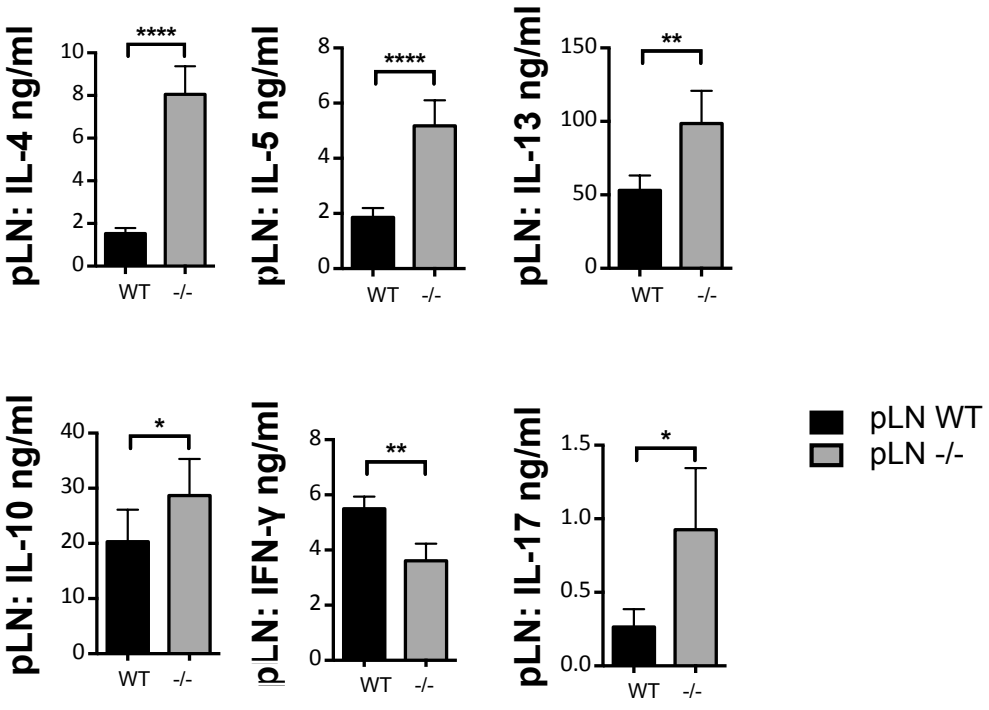

Figure 7.4 Th2 induction is enhanced in *Batf3*$^{-/-}$ mice at D7 post *S. mansoni* egg injection

S. mansoni eggs were injected into WT or *Batf3*$^{-/-}$ mice. 7 days later pLNs were harvested for cytokine production and flow cytometry analysis. Cells from pLNs of WT or *Batf3*$^{-/-}$ mice were cultured for 72h with 15 μg/ml SEA or media alone. Supernatants were collected to assess cytokine production by ELISA (data presented SEA restimulated samples with medium alone background subtracted). Data are from 3 experiments. Mixed model analysis (blocking day of experiment), Tukey's HSD (* $P \leq 0.05$, ** $P \leq 0.01$, *** $P \leq 0.001$, ****$P \leq 0.0001$). Error bars are mean values ± SEM of 13-14 mice per group.

Figure 7.5

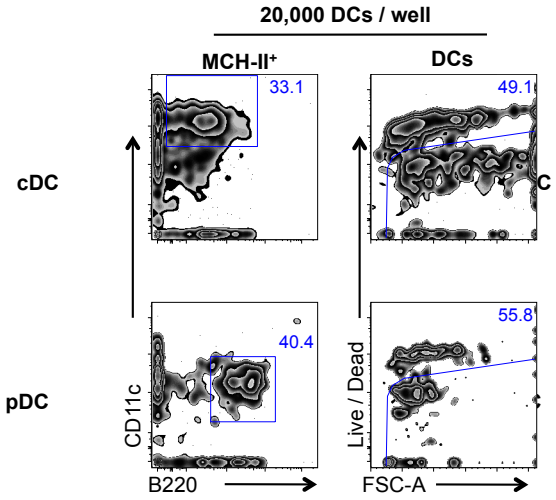

Figure 7.5 The proportion of cDCs and pDCs present in the OT-II co-culture assay after 1 day

Livers leukocytes from naïve WT mice were enriched for DCs by negative selection using Dynabeads. Pure cDC and pDC populations were FACS sorted from enriched DC populations. 20,000 naïve cDCs or pDCs were then pulsed with 10 μM pOVA and co-cultured with 200,000 naïve $CD4^+$ T cells for 24h. The number of cells used in this experiment was increased proportionally from co-cultures shown in chapter 5 (5,000 DCs and 50,000 $CD4^+$ T cells, DC:T cell ration 1:10) to enable efficient detection of DCs by flow cytometry. cDC and pDC populations were analysed for live/dead staining, and the proportion of live cDCs was compared with live pDCs. Gates were set using FMO controls. 1 of 1 experiment. N=2.

Figure 7.6

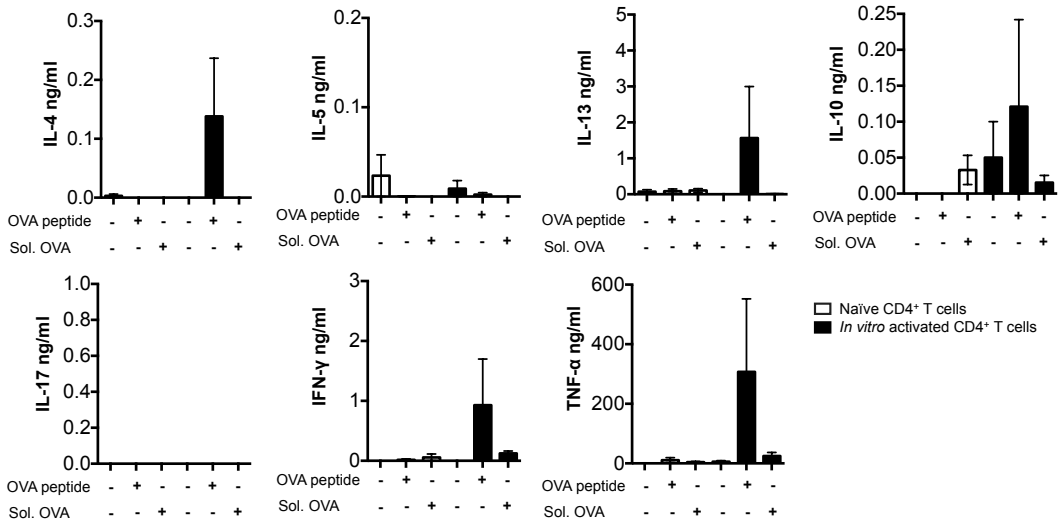

Figure 7.6 Cytokine production by naïve or effector/memory CD4$^+$ T cells in the absence of DCs

To control for cytokine production in the presence of DCs, freshly isolated naïve or *in vitro* activated CD4$^+$ T cells isolated from OT-IIxLy5.1 mice were either pulsed with 10 μM pOVA or cultured with 500 μg/ml soluble OVA in the absence of DCs. Additionally, naïve or activated CD4$^+$ T cells were cultured without antigen or DCs. After 72h, the supernatant was harvested and assessed for cytokine production by ELISA. Data are from 3 experiments. Two-Way ANOVA (* $P \leq 0.05$, ** $P \leq 0.01$, *** $P \leq 0.001$, ****$P \leq 0.0001$). Bars are SEM. N=4-6.

8 Bibliography

Abdulla, M.-H., Lim, K.-C., McKerrow, J.H., and Caffrey, C.R. (2011). Proteomic identification of IPSE/alpha-1 as a major hepatotoxin secreted by Schistosoma mansoni eggs. PLoS Negl. Trop. Dis. *5*, e1368.

Abe, M., Tokita, D., Raimondi, G., and Thomson, A.W. (2006). Endotoxin modulates the capacity of CpG-activated liver myeloid DC to direct Th1-type responses. Eur. J. Immunol. *36*, 2483–2493.

Adnani, Al, M.S. (1985). Concomitant immunohistochemical localization of fibronectin and collagen in schistosome granulomata. J. Pathol. *147*, 77–85.

Agrawal, S., Agrawal, A., Doughty, B., Gerwitz, A., Blenis, J., Van Dyke, T., and Pulendran, B. (2003). Cutting edge: different Toll-like receptor agonists instruct dendritic cells to induce distinct Th responses via differential modulation of extracellular signal-regulated kinase-mitogen-activated protein kinase and c-Fos. J. Immunol. *171*, 4984–4989.

Allen, J.E., and Sutherland, T.E. (2014). Host protective roles of type 2 immunity: parasite killing and tissue repair, flip sides of the same coin. Semin. Immunol. *26*, 329–340.

Allen, J.E., and Wynn, T.A. (2011). Evolution of Th2 immunity: a rapid repair response to tissue destructive pathogens. PLoS Pathog. *7*, e1002003.

Almadi, M.A., Aljebreen, A.M., Sanai, F.M., Marcus, V., Almeghaiseeb, E.S., and Ghosh, S. (2011). New insights into gastrointestinal and hepatic granulomatous disorders. Nat. Rev. Gastroenterol. Hepatol. *8*, 455–466.

Aman, M.J., Tretter, T., Eisenbeis, I., Bug, G., Decker, T., Aulitzky, W.E., Tilg, H., Huber, C., and Peschel, C. (1996). Interferon-alpha stimulates production of interleukin-10 in activated CD4+ T cells and monocytes. Blood *87*, 4731–4736.

Amin, A., and Mahmoud-Ghoneim, D. (2011). Texture analysis of liver fibrosis microscopic images: a study on the effect of biomarkers. Acta Biochim. Biophys. Sinica *43*, 193–203.

Amiri, P., Locksley, R.M., Parslow, T.G., Sadick, M., Rector, E., Ritter, D., and McKerrow, J.H. (1992). Tumour necrosis factor alpha restores granulomas and induces parasite egg-laying in schistosome-infected SCID mice. Nature *356*, 604–607.

Anandasabapathy, N., Ford, G.S., Bloom, D., Holness, C., Paragas, V., Seroogy, C., Skrenta, H., Hollenhorst, M., Fathman, C.G., and Soares, L. (2003). GRAIL: an E3 ubiquitin ligase that inhibits cytokine gene transcription is expressed in anergic CD4+ T cells. Immunity *18*, 535–547.

Anderson, D.M., Maraskovsky, E., Billingsley, W.L., Dougall, W.C., Tometsko, M.E., Roux, E.R., Teepe, M.C., DuBose, R.F., Cosman, D., and Galibert, L. (1997). A homologue of the TNF receptor and its ligand enhance T-cell growth and dendritic-cell function. Nature *390*, 175–179.

Andrian, von, U.H., and Mempel, T.R. (2003). Homing and cellular traffic in lymph nodes. Nat. Rev. Immunol. *3*, 867–878.

Bachem, A., Hartung, E., Güttler, S., Mora, A., Zhou, X., Hegemann, A., Plantinga, M., Mazzini, E., Stoitzner, P., Gurka, S., Henn, V., Mages, H.W., and Kroczek, R.A. (2012). Expression of XCR1 Characterizes the Batf3-Dependent Lineage of Dendritic Cells Capable of Antigen Cross-Presentation. Front. Immunol *3*, 1-12.

Anthony, R.M., Rutitzky, L.I., Urban, J.F., Stadecker, M.J., and Gause, W.C. (2007). Protective immune mechanisms in helminth infection. Nat. Rev. Immunol. *7*, 975–987.

Arora, P., Baena, A., Yu, K.O.A., Saini, N.K., Kharkwal, S.S., Goldberg, M.F., Kunnath-Velayudhan, S., Carreño, L.J., Venkataswamy, M.M., Kim, J., et al. (2014). A Single Subset of Dendritic Cells Controls the Cytokine Bias of Natural Killer T Cell Responses to Diverse Glycolipid Antigens. Immunity *40*, 105–116.

Arram, E.O., Hassan, R., and Saleh, M. (2014). Increased frequency of CD4+CD25+FoxP3+ circulating regulatory T cells (Treg) in tuberculous patients. Egypt. J. Chest Dis. Tubercul. *63*, 167–172.

Artis, D., Kane, C.M., Fiore, J., Zaph, C., Shapira, S., Joyce, K., Macdonald, A., Hunter, C., Scott, P., and Pearce, E.J. (2005). Dendritic cell-intrinsic expression of NF-kappa B1 is required to promote optimal Th2 cell differentiation. J. Immunol. *174*, 7154–7159.

Ashok, D., Schuster, S., Ronet, C., Rosa, M., Mack, V., Lavanchy, C., Marraco, S.F., Fasel, N., Murphy, K.M., Tacchini-Cottier, F., et al. (2014). Cross-presenting dendritic cells are required for control of Leishmania major infection. Eur. J. Immunol. *44*, 1422–1432.

Askew, D., and Harding, C.V. (2008). Antigen processing and CD24 expression determine antigen presentation by splenic CD4+ and CD8+ dendritic cells. Immunology *123*, 447–455.

Asselin-Paturel, C., Boonstra, A., Dalod, M., Durand, I., Yessaad, N., Dezutter-Dambuyant, C., Vicari, A., O'Garra, A., Biron, C., Brière, F., et al. (2001). Mouse type I IFN-producing cells are immature APCs with plasmacytoid morphology. Nat. Immunol. *2*, 1144–1150.

Auffray, C., Fogg, D., Garfa, M., Elain, G., Join-Lambert, O., Kayal, S., Sarnacki, S., Cumano, A., Lauvau, G., and Geissmann, F. (2007). Monitoring of blood vessels and tissues by a population of monocytes with patrolling behavior. Science *317*, 666–670.

Baldwin, T., Henri, S., Curtis, J., O'Keeffe, M., Vremec, D., Shortman, K., and Handman, E. (2004). Dendritic cell populations in Leishmania major-infected skin and draining lymph nodes. Infect. Immun. *72*, 1991–2001.

Balic, A., Harcus, Y., Holland, M.J., and Maizels, R.M. (2004). Selective maturation of dendritic cells by Nippostrongylus brasiliensis-secreted proteins drives Th2 immune responses. Eur. J. Immunol. *34*, 3047–3059.

Bamboat, Z.M., Ocuin, L.M., Balachandran, V.P., Obaid, H., Plitas, G., and Dematteo, R.P. (2010). Conventional DCs reduce liver ischemia/reperfusion injury in mice via IL-10 secretion. J. Clin. Invest. *120*, 559–569.

Bamboat, Z.M., Stableford, J.A., Plitas, G., Burt, B.M., Nguyen, H.M., Welles, A.P., Gonen, M., Young, J.W., and Dematteo, R.P. (2009). Human liver dendritic cells promote T cell hyporesponsiveness. J. Immunol. *182*, 1901–1911.

Banchereau, J., and Steinman, R.M. (1998). Dendritic cells and the control of immunity. Nature *392*, 245–252.

Banchereau, J., Brière, F., Caux, C., Davoust, J., Lebecque, S., Liu, Y.J., Pulendran, B., and Palucka, K. (2000). Immunobiology of dendritic cells. Annu. Rev. Immunol. *18*, 767–811.

Bancroft, A.J., Else, K.J., Sypek, J.P., and Grencis, R.K. (1997). Interleukin-12 promotes a chronic intestinal nematode infection. Eur. J. Immunol. *27*, 866–870.

Bar-On, L., and Jung, S. (2010). Defining dendritic cells by conditional and constitutive cell ablation. Immunol. Rev. *234*, 76–89.

Bar-On, L., Birnberg, T., Lewis, K.L., Edelson, B.T., Bruder, D., Hildner, K., Buer, J., Murphy, K.M., Reizis, B., and Jung, S. (2010). CX3CR1+ CD8alpha+ dendritic cells are a steady-state population related to plasmacytoid dendritic cells. Proc. Natl. Acad. Sci. U.S.A. *107*, 14745–14750.

Barber, D.L., Wherry, E.J., Masopust, D., Zhu, B., Allison, J.P., Sharpe, A.H., Freeman, G.J., and Ahmed, R. (2006). Restoring function in exhausted CD8 T cells during chronic viral infection. Nature *439*, 682–687.

Barnden, M.J., Allison, J., Heath, W.R., and Carbone, F.R. (1998). Defective TCR expression in transgenic mice constructed using cDNA-based alpha- and beta-chain genes under the control of heterologous regulatory elements. Immunol. Cell Biol. *76*, 34–40.

Barr, T.A., Brown, S., Mastroeni, P., and Gray, D. (2009). B cell intrinsic MyD88 signals drive IFN-gamma production from T cells and control switching to IgG2c. J. Immunol. *183*, 1005–1012.

Barron, L., and Wynn, T.A. (2011). Macrophage activation governs schistosomiasis-induced inflammation and fibrosis. Eur. J. Immunol. *41*, 2509–2514.

Baumgart, M., Tompkins, F., Leng, J., and Hesse, M. (2006). Naturally occurring CD4+Foxp3+ regulatory T cells are an essential, IL-10-independent part of the immunoregulatory network in Schistosoma mansoni egg-induced inflammation. J. Immunol. *176*, 5374–5387.

Becker, A.M., Michael, D.G., Satpathy, A.T., Sciammas, R., Singh, H., and Bhattacharya, D. (2012). IRF-8 extinguishes neutrophil production and promotes dendritic cell lineage commitment in both myeloid and lymphoid mouse progenitors. Blood *119*, 2003–2012.

Bedoui, S., Whitney, P.G., Waithman, J., Eidsmo, L., Wakim, L., Caminschi, I., Allan, R.S., Wojtasiak, M., Shortman, K., Carbone, F.R., et al. (2009). Cross-presentation of viral and self antigens by skin-derived CD103+ dendritic cells. Nature Publishing Group *10*, 488–495.

Belperio, J.A., Dy, M., Murray, L., Burdick, M.D., Xue, Y.Y., Strieter, R.M., and Keane, M.P. (2004). The Role of the Th2 CC Chemokine Ligand CCL17 in Pulmonary Fibrosis. J. Immunol. *173*, 4692–4698.

Belvin, M.P., and Anderson, K.V. (1996). A conserved signaling pathway: the Drosophila toll-dorsal pathway. Annu. Rev. Cell Dev. Biol. *12*, 393–416.

Bentley, A.G., Doughty, B.L., and Phillips, S.M. (1982). Ultrastructural analysis of the cellular response to Schistosoma mansoni. III. The in vitro granuloma. Am. J. Trop. Med. Hyg. *31*, 1168–1180.

Berg, M., and Zavazava, N. (2008). Regulation of CD28 expression on CD8+ T cells by CTLA-4. J. Leukoc. Biol. *83*, 853–863.

Bertho, N. (2005). Efficient migration of dendritic cells toward lymph node chemokines and induction of TH1 responses require maturation stimulus and apoptotic cell interaction. Blood *106*, 1734–1741.

Bianchi, M.E. (2007). DAMPs, PAMPs and alarmins: all we need to know about danger. J. Leukoc. Biol. *81*, 1–5.

Bird, J.J., Brown, D.R., Mullen, A.C., Moskowitz, N.H., Mahowald, M.A., Sider, J.R., Gajewski, T.F., Wang, C.R., and Reiner, S.L. (1998). Helper T cell differentiation is controlled by the cell cycle. Immunity *9*, 229–237.

Bluestone, J.A., Mackay, C.R., O'Shea, J.J., and Stockinger, B. (2009). The functional plasticity of T cell subsets. Nat. Rev. Immunol. *9*, 811–816.

Boehm, U., Klamp, T., Groot, M., and Howard, J.C. (1997). Cellular responses to interferon-gamma. Annu. Rev. Immunol. *15*, 749–795.

Bonasio, R., and Andrian, von, U.H. (2006). Generation, migration and function of circulating dendritic cells. Curr. Opin. Immunol. *18*, 503–511.

Bonecchi, R., Bianchi, G., Bordignon, P.P., D'Ambrosio, D., Lang, R., Borsatti, A.,

Sozzani, S., Allavena, P., Gray, P.A., Mantovani, A., et al. (1998). Differential expression of chemokine receptors and chemotactic responsiveness of type 1 T helper cells (Th1s) and Th2s. J. Exp. Med. *187*, 129–134.

Boonstra, A., Asselin-Paturel, C., Gilliet, M., Crain, C., Trinchieri, G., Liu, Y.J., and O'Garra, A. (2002). Flexibility of Mouse Classical and Plasmacytoid-derived Dendritic Cells in Directing T Helper Type 1 and 2 Cell Development: Dependency on Antigen Dose and Differential Toll-like Receptor Ligation. J. Exp. Med. *197*, 101–109.

Boros, D.L. (1989). Immunopathology of Schistosoma mansoni infection. Clin. Microbiol. Rev. *2*, 250–269.

Boros, D.L. (1994). The role of cytokines in the formation of the schistosome egg granuloma. Immunobiology *191*, 441–450.

Boros, D.L., and Whitfield, J.R. (2006). Endogenous IL-10 regulates IFN-gamma and IL-5 cytokine production and the granulomatous response in Schistosomiasis mansoni-infected mice. Immunology *94*, 481–487.

Boros, D.L., Pelley, R.P., and Warren, K.S. (1975). Spontaneous modulation of granulomatous hypersensitivity in schistosomiasis mansoni. J. Immunol. *114*, 1437–1441.

Bosma, B.M., Metselaar, H.J., Mancham, S., Boor, P.P.C., Kusters, J.G., Kazemier, G., Tilanus, H.W., Kuipers, E.J., and Kwekkeboom, J. (2006). Characterization of human liver dendritic cells in liver grafts and perfusates. Liver Transpl. *12*, 384–393.

Bour-Jordan, H., and Bluestone, J.A. (2009). How suppressor cells led to anergy, costimulation, and beyond. J. Immunol. *183*, 4147–4149.

Boyle, M.C., Crabbs, T.A., Wyde, M.E., Painter, J.T., Hill, G.D., Malarkey, D.E., Lieuallen, W.G., and Nyska, A. (2012). Intestinal lymphangiectasis and lipidosis in rats following subchronic exposure to indole-3-carbinol via oral gavage. Toxicol. Pathol. *40*, 561–576.

Boyman, O., and Sprent, J. (2012). nri3156. Nature Publishing Group *12*, 180–190.

Boyman, O., Létourneau, S., Krieg, C., and Sprent, J. (2009). Homeostatic proliferation and survival of naïve and memory T cells. Eur. J. Immunol. *39*, 2088–2094.

Breitfeld, D., Ohl, L., Kremmer, E., Ellwart, J., Sallusto, F., Lipp, M., and Förster, R. (2000). Follicular B helper T cells express CXC chemokine receptor 5, localize to B cell follicles, and support immunoglobulin production. J. Exp. Med. *192*, 1545–1552.

Broere, F., Apasov, S.G., Sitkovsky, M.V., and van Eden, W. (2011). A2 T cell subsets and T cell-mediated immunity. Principles of Immunopharmacol., pp. 15–27.

Brunet, L.R., Finkelman, F.D., Cheever, A.W., Kopf, M.A., and Pearce, E.J. (1997).

IL-4 protects against TNF-alpha-mediated cachexia and death during acute schistosomiasis. J. Immunol. *159*, 777–785.

Bursch, L.S., Wang, L., Igyarto, B., Kissenpfennig, A., Malissen, B., Kaplan, D.H., and Hogquist, K.A. (2007). Identification of a novel population of Langerin+ dendritic cells. J. Exp. Med. *204*, 3147–3156.

Byram, J.E., and Lichtenberg, von, F. (1977). Altered schistosome granuloma formation in nude mice. Am. J. Trop. Med. Hyg. *26*, 944–956.

Byrne, S.N., Limon-Flores, A.Y., and Ullrich, S.E. (2008). Mast Cell Migration from the Skin to the Draining Lymph Nodes upon Ultraviolet Irradiation Represents a Key Step in the Induction of Immune Suppression. J. Immunol. *180*, 4648–4655.

Calvi, E.N. de C., Nahas, F.X., Barbosa, M.V., Calil, J.A., Ihara, S.S.M., Silva, M. de S., Franco, M.F. de, and Ferreira, L.M. (2012). An experimental model for the study of collagen fibers in skeletal muscle. Acta Cir. Bras. *27*, 681–686.

Caminschi, I., Vremec, D., Ahmet, F., Lahoud, M.H., Villadangos, J.A., Murphy, K.M., Heath, W.R., and Shortman, K. (2012). Antibody responses initiated by Clec9A-bearing dendritic cells in normal and Batf3(-/-) mice. Mol. Immunol. *50*, 9–17.

Caserta, S., Alessi, P., Basso, V., and Mondino, A. (2010). IL-7 is superior to IL-2 for ex vivoexpansion of tumour-specific CD4 +T cells. Eur. J. Immunol. *40*, 470–479.

Caserta, S., Nausch, N., Sawtell, A., Drummond, R., Barr, T., MacDonald, A.S., Mutapi, F., and Zamoyska, R. (2012). Chronic infection drives expression of the inhibitory receptor CD200R, and its ligand CD200, by mouse and human CD4 T cells. PLoS ONE *7*, e35466.

Castellaneta, A., Sumpter, T.L., Chen, L., Tokita, D., and Thomson, A.W. (2009). NOD2 ligation subverts IFN-alpha production by liver plasmacytoid dendritic cells and inhibits their T cell allostimulatory activity via B7-H1 up-regulation. J. Immunol. *183*, 6922–6932.

Caux, C., Massacrier, C., Vanbervliet, B., Dubois, B., Van Kooten, C., Durand, I., and Banchereau, J. (1994). Activation of human dendritic cells through CD40 cross-linking. J. Exp. Med. *180*, 1263–1272.

Cecconi, V., Moro, M., Del Mare, S., Dellabona, P., and Casorati, G. (2008). Use of MHC class II tetramers to investigate CD4 +T cell responses: Problems and solutions. Cytometry *73A*, 1010–1018.

Cella, M., Jarrossay, D., Facchetti, F., Alebardi, O., Nakajima, H., Lanzavecchia, A., and Colonna, M. (1999). Plasmacytoid monocytes migrate to inflamed lymph nodes and produce large amounts of type I interferon. Nat. Med. *5*, 919–923.

Cerutti, A., Puga, I., and Cols, M. (2012). New helping friends for B cells. Eur. J.

Immunol. *42*, 1956–1968.

Cervi, L., MacDonald, A.S., Kane, C., Dzierszinski, F., and Pearce, E.J. (2004). Cutting edge: dendritic cells copulsed with microbial and helminth antigens undergo modified maturation, segregate the antigens to distinct intracellular compartments, and concurrently induce microbe-specific Th1 and helminth-specific Th2 responses. J. Immunol. *172*, 2016–2020.

Chang, T.T., Jabs, C., Sobel, R.A., Kuchroo, V.K., and Sharpe, A.H. (1999). Studies in B7-deficient mice reveal a critical role for B7 costimulation in both induction and effector phases of experimental autoimmune encephalomyelitis. J. Exp. Med. *190*, 733–740.

Chatzidakis, I., and Mamalaki, C. (2010). T cells as sources and targets of TNF: implications for immunity and autoimmunity. Curr. Dir. Autoimmun. *11*, 105–118.

Cheever, A.W. (1987). Comparison of pathologic changes in mammalian hosts infected with Schistosoma mansoni, S. japonicum and S. haematobium. Mem. Inst. Oswaldo Cruz *82 Suppl 4*, 39–45.

Cheever, A.W., Duvall, R.H., and Hallack, T.A. (1984). Differences in hepatic fibrosis and granuloma size in several strains of mice infected with Schistosoma japonicum. Am. J. Trop. Med. Hyg. *33*, 602–607.

Cheever, A.W., Duvall, R.H., Hallack, T.A., Minker, R.G., Malley, J.D., and Malley, K.G. (1987). Variation of hepatic fibrosis and granuloma size among mouse strains infected with Schistosoma mansoni. Am. J. Trop. Med. Hyg. *37*, 85–97.

Cheever, A.W., Eltoum, I.A., ANDRADE, Z.A., and Cox, T.M. (1993). Biology and pathology of Schistosoma mansoni and Schistosoma japonicum infections in several strains of nude mice. Am. J. Trop. Med. Hyg. *48*, 496–503.

Cheever, A.W., Poindexter, R.W., and Wynn, T.A. (1999). Egg laying is delayed but worm fecundity is normal in SCID mice infected with Schistosoma japonicum and S. mansoni with or without recombinant tumor necrosis factor alpha treatment. Infect. Immun. *67*, 2201–2208.

Cheever, A.W., Lenzi, J.A., Lenzi, H.L., and Andrade, Z.A. (2002). Experimental models of Schistosoma mansoni infection. Mem. Inst. Oswaldo Cruz *97*, 917–940.

Chen, H., Huang, H., and Paul, W.E. (1997). NK1.1+ CD4+ T cells lose NK1.1 expression upon in vitro activation. J. Immunol. *158*, 5112–5119.

Chen, L., and Flies, D.B. (2013). Molecular mechanisms of T cell co-stimulation and co-inhibition. Nat. Rev. Immunol. *13*, 227–242.

Chen, W. (2003). Conversion of Peripheral CD4+CD25- Naive T Cells to CD4+CD25+ Regulatory T Cells by TGF- Induction of Transcription Factor Foxp3. J. Exp. Med. *198*, 1875–1886.

Chensue, S.W., Otterness, I.G., Higashi, G.I., Forsch, C.S., and Kunkel, S.L. (1989). Monokine production by hypersensitivity (Schistosoma mansoni egg) and foreign body (Sephadex bead)-type granuloma macrophages. Evidence for sequential production of IL-1 and tumor necrosis factor. J. Immunol. *142*, 1281–1286.

Chensue, S.W., Terebuh, P.D., Warmington, K.S., Hershey, S.D., Evanoff, H.L., Kunkel, S.L., and Higashi, G.I. (1992). Role of IL-4 and IFN-gamma in Schistosoma mansoni egg-induced hypersensitivity granuloma formation. Orchestration, relative contribution, and relationship to macrophage function. J. Immunol. *148*, 900–906.

Chensue, S.W., Warmington, K.S., Hershey, S.D., Terebuh, P.D., Othman, M., and Kunkel, S.L. (1993). Evolving T cell responses in murine schistosomiasis. Th2 cells mediate secondary granulomatous hypersensitivity and are regulated by CD8+ T cells in vivo. J. Immunol. *151*, 1391–1400.

Chensue, S.W., Warmington, K.S.,Ruth, J., Lincoln, P.M., Kunkel, S.L. (1994). Cross-regulatory role of interferon-gamma (IFN-gamma), IL-4 and IL-10 in schistosome egg granuloma formation: in vivo regulation of Th activity and inflammation. Clin. Exp. Immunol. *98*, 395.

Chensue, S.W., Wellhausen, S.R., and Boros, D.L. (1981). Modulation of granulomatous hypersensitivity. II. Participation of Ly 1+ and Ly 2+ T lymphocytes in the suppression of granuloma formation and lymphokine production in Schistosoma mansoni-infected mice. J. Immunol. *127*, 363–367.

Chiaramonte, M.G., Donaldson, D.D., Cheever, A.W., and Wynn, T.A. (1999). An IL-13 inhibitor blocks the development of hepatic fibrosis during a T-helper type 2-dominated inflammatory response. J. Clin. Invest. *104*, 777–785.

Chikuma, S., Terawaki, S., Hayashi, T., Nabeshima, R., Yoshida, T., Shibayama, S., Okazaki, T., and Honjo, T. (2009). PD-1-mediated suppression of IL-2 production induces CD8+ T cell anergy in vivo. J. Immunol. *182*, 6682–6689.

Chiodetti, L., Choi, S., Barber, D.L., and Schwartz, R.H. (2006). Adaptive tolerance and clonal anergy are distinct biochemical states. J. Immunol. *176*, 2279–2291.

Choi, Y.S., Kageyama, R., Eto, D., Escobar, T.C., Johnston, R.J., Monticelli, L., Lao, C., and Crotty, S. (2011). ICOS receptor instructs T follicular helper cell versus effector cell differentiation via induction of the transcriptional repressor Bcl6. Immunity *34*, 932–946.

Chuah, C., Jones, M.K., Burke, M.L., McManus, D.P., and Gobert, G.N. (2014). Cellular and chemokine-mediated regulation in schistosome-induced hepatic pathology. Trends Parasitol. *30*, 141–150.

Cisse, B., Caton, M.L., Lehner, M., Maeda, T., Scheu, S., Locksley, R., Holmberg, D., Zweier, C., Hollander, den, N.S., Kant, S.G., et al. (2008). Transcription factor E2-2 is an essential and specific regulator of plasmacytoid dendritic cell development. Cell *135*, 37–48.

Cobbold, S.P., Castejon, R., Adams, E., Zelenika, D., Graca, L., Humm, S., and Waldmann, H. (2004). Induction of foxP3+ regulatory T cells in the periphery of T cell receptor transgenic mice tolerized to transplants. J. Immunol. *172*, 6003–6010.

Colley, D.G. (1975). Immune responses to a soluble schistosomal egg antigen preparation during chronic primary infection with Schistosoma mansoni. J. Immunol. *115*, 150–156.

Collin, M., Bigley, V., Haniffa, M., and Hambleton, S. (2011). Human dendritic cell deficiency: the missing ID? Nat. Rev. Immunol. *11*, 575–583.

Collin, M., McGovern, N., and Haniffa, M. (2013). Human dendritic cell subsets. Immunology *140*, 22–30.

Cook, P.C., Jones, L.H., Jenkins, S.J., Wynn, T.A., Allen, J.E., and MacDonald, A.S. (2012). Alternatively activated dendritic cells regulate CD4+ T-cell polarization in vitro and in vivo. Proc. Natl. Acad. Sci. U.S.A. *109*, 9977–9982.

Coombes, J.L., Siddiqui, K.R.R., Arancibia-Cárcamo, C.V., Hall, J., Sun, C.-M., Belkaid, Y., and Powrie, F. (2007). A functionally specialized population of mucosal CD103+ DCs induces Foxp3+ regulatory T cells via a TGF-beta and retinoic acid-dependent mechanism. J. Exp. Med. *204*, 1757–1764.

Cosmi, L., Liotta, F., Maggi, E., Romagnani, S., and Annunziato, F. (2011). Th17 cells: new players in asthma pathogenesis. Allergy *66*, 989–998.

Cote-Sierra, J., Foucras, G., Guo, L., Chiodetti, L., Young, H.A., Hu-Li, J., Zhu, J., and Paul, W.E. (2004). Interleukin 2 plays a central role in Th2 differentiation. Proc. Natl. Acad. Sci. U.S.A. *101*, 3880–3885.

Couper, K.N., Blount, D.G., and Riley, E.M. (2008). IL-10: The Master Regulator of Immunity to Infection. J. Immunol. *180*, 5771–5777.

Crispe, I.N. (2009). The liver as a lymphoid organ. Annu. Rev. Immunol. *27*, 147–163.

Crispe, I.N. (2011). Liver antigen-presenting cells. J. Hepatol. *54*, 357–365.

Croft, M., Bradley, L.M., and Swain, S.L. (1994). Naive versus memory CD4 T cell response to antigen. Memory cells are less dependent on accessory cell costimulation and can respond to many antigen-presenting cell types including resting B cells. J. Immunol. *152*, 2675–2685.

Crotty, S. (2011). Follicular helper CD4 T cells (TFH). Annu. Rev. Immunol. *29*, 621–663.

Czaja, M.J., Weiner, F.R., Takahashi, S., Giambrone, M.A., van der Meide, P.H., Schellekens, H., Biempica, L., and Zern, M.A. (1989). Gamma-interferon treatment inhibits collagen deposition in murine schistosomiasis. Hepatology *10*, 795–800.

D'Ambrosio, D., Iellem, A., Bonecchi, R., Mazzeo, D., Sozzani, S., Mantovani, A., and Sinigaglia, F. (1998). Selective up-regulation of chemokine receptors CCR4 and CCR8 upon activation of polarized human type 2 Th cells. J. Immunol. *161*, 5111–5115.

d'Ostiani, C.F., Del Sero, G., Bacci, A., Montagnoli, C., Spreca, A., Mencacci, A., Ricciardi-Castagnoli, P., and Romani, L. (2000). Dendritic cells discriminate between yeasts and hyphae of the fungus Candida albicans. Implications for initiation of T helper cell immunity in vitro and in vivo. J. Exp. Med. *191*, 1661–1674.

Daley, J.M., Thomay, A.A., Connolly, M.D., Reichner, J.S., and Albina, J.E. (2007). Use of Ly6G-specific monoclonal antibody to deplete neutrophils in mice. J. Leukoc. Biol. *83*, 64–70.

Davies, L.C., Jenkins, S.J., Allen, J.E., and Taylor, P.R. (2013). Tissue-resident macrophages. Nature Publishing Group *14*, 986–995.

Davies, S.J., Lim, K.C., Blank, R.B., Kim, J.-H., Lucas, K.D., Hernandez, D.C., Sedgwick, J.D., and McKerrow, J.H. (2004). Involvement of TNF in limiting liver pathology and promoting parasite survival during schistosome infection. Int. J. Parasitol. *34*, 27–36.

De Creus, A., Abe, M., Lau, A.H., Hackstein, H., Raimondi, G., and Thomson, A.W. (2005). Low TLR4 expression by liver dendritic cells correlates with reduced capacity to activate allogeneic T cells in response to endotoxin. J. Immunol. *174*, 2037–2045.

de Heer, H.J., Hammad, H., Soullié, T., Hijdra, D., Vos, N., Willart, M.A.M., Hoogsteden, H.C., and Lambrecht, B.N. (2004). Essential role of lung plasmacytoid dendritic cells in preventing asthmatic reactions to harmless inhaled antigen. J. Exp. Med. *200*, 89–98.

de Jesus, A.R., Magalhães, A., Miranda, D.G., Miranda, R.G., Araujo, M.I., de Jesus, A.A., Silva, A., Santana, L.B., Pearce, E., and Carvalho, E.M. (2004). Association of type 2 cytokines with hepatic fibrosis in human Schistosoma mansoni infection. Infect. Immun. *72*, 3391–3397.

de Jong, E.C., Vieira, P.L., Kalinski, P., Schuitemaker, J.H.N., Tanaka, Y., Wierenga, E.A., Yazdanbakhsh, M., and Kapsenberg, M.L. (2002). Microbial compounds selectively induce Th1 cell-promoting or Th2 cell-promoting dendritic cells in vitro with diverse th cell-polarizing signals. J. Immunol. *168*, 1704–1709.

De Smedt, T., Butz, E., Smith, J., Maldonado-López, R., Pajak, B., Moser, M., and Maliszewski, C. (2001). CD8alpha(-) and CD8alpha(+) subclasses of dendritic cells undergo phenotypic and functional maturation in vitro and in vivo. J. Leukoc. Biol. *69*, 951–958.

Deaton, A.M., Cook, P.C., De Sousa, D., Phythian-Adams, A.T., Bird, A., and

MacDonald, A.S. (2014). A unique DNA methylation signature defines a population of IFN-γ/IL-4 double-positive T cells during helminth infection. Eur. J. Immunol. *44*, 1835–1841.

Denning, T.L., Norris, B.A., Medina-Contreras, O., Manicassamy, S., Geem, D., Madan, R., Karp, C.L., and Pulendran, B. (2011). Functional specializations of intestinal dendritic cell and macrophage subsets that control Th17 and regulatory T cell responses are dependent on the T cell/APC ratio, source of mouse strain, and regional localization. J. Immunol. *187*, 733–747.

Dewals, B., Hoving, J.C., Horsnell, W.G.C., and Brombacher, F. (2010). Control of Schistosoma mansoni egg-induced inflammation by IL-4-responsive CD4(+)CD25(-)CD103(+)Foxp3(-) cells is IL-10-dependent. Eur. J. Immunol. *40*, 2837–2847.

Diaz Encarnacion, M.M., Griffin, M.D., Slezak, J.M., Bergstralh, E.J., Stegall, M.D., Velosa, J.A., and Grande, J.P. (2004). Correlation of quantitative digital image analysis with the glomerular filtration rate in chronic allograft nephropathy. Am. J. Transplant. *4*, 248–256.

Dickinson, R.E., Griffin, H., Bigley, V., Reynard, L.N., Hussain, R., Haniffa, M., Lakey, J.H., Rahman, T., Wang, X.-N., McGovern, N., et al. (2011). Exome sequencing identifies GATA-2 mutation as the cause of dendritic cell, monocyte, B and NK lymphoid deficiency. Blood *118*, 2656–2658.

Doenhoff, M.J. (1998). A role for granulomatous inflammation in the transmission of infectious disease: schistosomiasis and tuberculosis *115*. 113–125.

Doenhoff, M.J., Hagan, P., Cioli, D., Southgate, V., Pica-Mattoccia, L., Botros, S., Coles, G., Tchuem Tchuenté, L.A., Mbaye, A., and Engels, D. (2009). Praziquantel: its use in control of schistosomiasis in sub-Saharan Africa and current research needs. Parasitology *136*, 1825–1835.

Doenhoff, M.J., Pearson, S., Dunne, D.W., Bickle, Q., Lucas, S., Bain, J., Musallam, R., and Hassounah, O. (1981). Immunological control of hepatotoxicity and parasite egg excretion in Schistosoma mansoni infections: stage specificity of the reactivity of immune serum in T-cell deprived mice. Trans. R. Soc. Trop. Med. Hyg. *75*, 41–53.

Domingo, E.O., and Warren, K.S. (1968). Endogenous desensitization: changing host granulomatou response to schistosome eggs at different stages of infection with schistosoma mansoni. Am. J. Pathol. *52*, 369–379.

Domínguez, P.M., and Ardavín, C. (2010). Differentiation and function of mouse monocyte-derived dendritic cells in steady state and inflammation. Immunol. Rev. *234*, 90–104.

Donnelly, S., Stack, C.M., O'Neill, S.M., Sayed, A.A., Williams, D.L., and Dalton, J.P. (2008). Helminth 2-Cys peroxiredoxin drives Th2 responses through a mechanism involving alternatively activated macrophages. FASEB J. *22*, 4022–

4032.

Doughty, B.L., and Phillips, S.M. (1982). Delayed hypersensitivity granuloma formation and modulation around Schistosoma mansoni eggs in vitro. II. Regulatory T cell subsets. J. Immunol. *128*, 37–42.

Dubrot, J., Duraes, F.V., Potin, L., Capotosti, F., Brighouse, D., Suter, T., LeibundGut-Landmann, S., Garbi, N., Reith, W., Swartz, M.A., et al. (2014). Lymph node stromal cells acquire peptide-MHCII complexes from dendritic cells and induce antigen-specific CD4$^+$ T cell tolerance. J. Exp. Med. *211*, 1153–1166.

Dudziak, D., Kamphorst, A.O., Heidkamp, G.F., Buchholz, V.R., Trumpfheller, C., Yamazaki, S., Cheong, C., Liu, K., Lee, H.-W., Park, C.G., et al. (2007). Differential antigen processing by dendritic cell subsets in vivo. Science *315*, 107–111.

Duffield, J.S., Forbes, S.J., Constandinou, C.M., Clay, S., Partolina, M., Vuthoori, S., Wu, S., Lang, R., and Iredale, J.P. (2005). Selective depletion of macrophages reveals distinct, opposing roles during liver injury and repair. J. Clin. Invest. *115*, 56–65.

Dunne, D.W., and Doenhoff, M.J. (1983). Schistosoma mansoni egg antigens and hepatocyte damage in infected T cell-deprived mice. Contrib. Microbiol. Immunol. *7*, 22–29.

Dunne, D.W., Jones, F.M., and Doenhoff, M.J. (1991). The purification, characterization, serological activity and hepatotoxic properties of two cationic glycoproteins (alpha 1 and omega 1) from Schistosoma mansoni eggs. Parasitology *103 Pt 2*, 225–236.

Dutton, R.W., Bradley, L.M., and Swain, S.L. (1998). T cell memory. Annu. Rev. Immunol. *16*, 201–223.

Edelson, B.T., Bradstreet, T.R., Wumesh, K.C., Hildner, K., Herzog, J.W., Sim, J., Russell, J.H., Murphy, T.L., Unanue, E.R., and Murphy, K.M. (2011). Batf3-Dependent CD11blow/− Peripheral Dendritic Cells Are GM-CSF-Independent and Are Not Required for Th Cell Priming after Subcutaneous Immunization. PLoS ONE *6*, e25660.

Edelson, B.T., KC, W., Juang, R., Kohyama, M., Benoit, L.A., Klekotka, P.A., Moon, C., Albring, J.C., Ise, W., Michael, D.G., et al. (2010). Peripheral CD103+ dendritic cells form a unified subset developmentally related to CD8alpha+ conventional dendritic cells. J. Exp. Med. *207*, 823–836.

Edungbola, L.D., and Schiller, E.L. (1979). Histopathology of hepatic and pulmonary granulomata experimentally induced with eggs of Schistosoma mansoni. J. Parasitol. *65*, 253–261.

Egen, J.G., and Allison, J.P. (2002). Cytotoxic T lymphocyte antigen-4 accumulation in the immunological synapse is regulated by TCR signal strength. Immunity *16*, 23–35.

Egwuagu, C.E. (2009). STAT3 in CD4+ T helper cell differentiation and inflammatory diseases. Cytokine *47*, 149–156.

el-Shoura, S.M. (1994). Human bilharzial ureters: IV. Ultrastructural interaction between multinucleate giant cells and the parasite eggs. Appl. Parasitol. *35*, 257–265.

Elser, B., Lohoff, M., Kock, S., Giaisi, M., Kirchhoff, S., Krammer, P.H., and Li-Weber, M. (2002). IFN-gamma represses IL-4 expression via IRF-1 and IRF-2. Immunity *17*, 703–712.

Eltoum, I.A., Wynn, T.A., Poindexter, R.W., Finkelman, F.D., Lewis, F.A., Sher, A., and Cheever, A.W. (1995). Suppressive effect of interleukin-4 neutralization differs for granulomas around Schistosoma mansoni eggs injected into mice compared with those around eggs laid in infected mice. Infect. Immun. *63*, 2532–2536.

Engler, D.B., Reuter, S., van Wijck, Y., Urban, S., Kyburz, A., Maxeiner, J., Martin, H., Yogev, N., Waisman, A., Gerhard, M., et al. (2014). Effective treatment of allergic airway inflammation with Helicobacter pylori immunomodulators requires BATF3-dependent dendritic cells and IL-10. Proc. Natl Acad Sci. U.S.A *111,* 1-6.

Eto, D., Lao, C., DiToro, D., Barnett, B., Escobar, T.C., Kageyama, R., Yusuf, I., and Crotty, S. (2011). IL-21 and IL-6 are critical for different aspects of B cell immunity and redundantly induce optimal follicular helper CD4 T cell (Tfh) differentiation. PLoS ONE *6*, e17739.

Everts, B., Hussaarts, L., Driessen, N.N., Meevissen, M.H.J., Schramm, G., van der Ham, A.J., van der Hoeven, B., Scholzen, T., Burgdorf, S., Mohrs, M., et al. (2012). Schistosome-derived omega-1 drives Th2 polarization by suppressing protein synthesis following internalization by the mannose receptor. J. Exp. Med. *209*, 1753–67–S1.

Everts, B., Perona-Wright, G., Smits, H.H., Hokke, C.H., van der Ham, A.J., Fitzsimmons, C.M., Doenhoff, M.J., van der Bosch, J., Mohrs, K., Haas, H., et al. (2009). Omega-1, a glycoprotein secreted by Schistosoma mansoni eggs, drives Th2 responses. J. Exp. Med. *206*, 1673–1680.

Fallon, P.G. (2000). Immunopathology of schistosomiasis: a cautionary tale of mice and men. Immunol. Today *21*, 29–35.

Fallon, P.G., and Doenhoff, M.J. (1994). Drug-resistant schistosomiasis: resistance to praziquantel and oxamniquine induced in Schistosoma mansoni in mice is drug specific. Am. J. Trop. Med. Hyg. *51*, 83–88.

Fallon, P.G., and Dunne, D.W. (1999). Tolerization of mice to Schistosoma mansoni egg antigens causes elevated type 1 and diminished type 2 cytokine responses and increased mortality in acute infection. J. Immunol. *162*, 4122–4132.

Fallon, P.G., Richardson, E.J., McKenzie, G.J., and McKenzie, A.N. (2000a). Schistosome infection of transgenic mice defines distinct and contrasting pathogenic roles for IL-4 and IL-13: IL-13 is a profibrotic agent. J. Immunol. *164*, 2585–2591.

Fallon, P.G., Richardson, E.J., Smith, P., and Dunne, D.W. (2000b). Elevated type 1, diminished type 2 cytokines and impaired antibody response are associated with hepatotoxicity and mortalities during Schistosoma mansoni infection of CD4-depleted mice. Eur. J. Immunol. *30*, 470–480.

Fallon, P.G., Ballantyne, S.J., Mangan, N.E., Barlow, J.L., Dasvarma, A., Hewett, D.R., McIlgorm, A., Jolin, H.E., and McKenzie, A.N.J. (2006). Identification of an interleukin (IL)-25-dependent cell population that provides IL-4, IL-5, and IL-13 at the onset of helminth expulsion. J. Exp. Med. *203*, 1105–1116.

Fathman, C.G., and Lineberry, N.B. (2007). Molecular mechanisms of CD4+ T-cell anergy. Nature Publishing Group *7*, 599–609.

Faveeuw, C., Angeli, V., Fontaine, J., Maliszewski, C., Capron, A., Van Kaer, L., Moser, M., Capron, M., and Trottein, F. (2002). Antigen presentation by CD1d contributes to the amplification of Th2 responses to Schistosoma mansoni glycoconjugates in mice. J. Immunol. *169*, 906–912.

Feng, C.G., Jankovic, D., Kullberg, M., Cheever, A., Scanga, C.A., Hieny, S., Caspar, P., Yap, G.S., and Sher, A. (2005). Maintenance of Pulmonary Th1 Effector Function in Chronic Tuberculosis Requires Persistent IL-12 Production. J. Immunol. *174*, 4185–4192.

Fenwick, A., Savioli, L., Engels, D., Robert Bergquist, N., and Todd, M.H. (2003). Drugs for the control of parasitic diseases: current status and development in schistosomiasis. Trends Parasitol. *19*, 509–515.

Fiebig, T., Boll, H., Figueiredo, G., Kerl, H.U., Nittka, S., Groden, C., Kramer, M., and Brockmann, M.A. (2012). Three-Dimensional In Vivo Imaging of the Murine Liver: A Micro-Computed Tomography-Based Anatomical Study. PLoS ONE *7*, e31179.

Fillatreau, S., and Gray, D. (2003). T cell accumulation in B cell follicles is regulated by dendritic cells and is independent of B cell activation. J. Exp. Med. *197*, 195–206.

Fitzsimmons, C.M., Schramm, G., Jones, F.M., Chalmers, I.W., Hoffmann, K.F., Grevelding, C.G., Wuhrer, M., Hokke, C.H., Haas, H., Doenhoff, M.J., et al. (2005). Molecular characterization of omega-1: a hepatotoxic ribonuclease from Schistosoma mansoni eggs. Mol. Biochem. Parasitol. *144*, 123–127.

Fonteneau, J.-F., Gilliet, M., Larsson, M., Dasilva, I., Münz, C., Liu, Y.-J., and Bhardwaj, N. (2003). Activation of influenza virus-specific CD4+ and CD8+ T cells: a new role for plasmacytoid dendritic cells in adaptive immunity. Blood *101*, 3520–3526.

Fontenot, D., He, H., Hanabuchi, S., Nehete, P.N., Zhang, M., Chang, M., Nehete, B., Wang, Y.-H., Wang, Y.-H., Ma, Z.-M., et al. (2009). TSLP production by epithelial cells exposed to immunodeficiency virus triggers DC-mediated mucosal infection of CD4+ T cells. Proc. Natl Acad. Sci. U.S.A. *106*, 16776–16781.

Fontenot, J.D., Gavin, M.A., and Rudensky, A.Y. (2003). Foxp3 programs the development and function of CD4+CD25+ regulatory T cells. Nat. Immunol. *4*, 330–336.

Förster, R., Schubel, A., Breitfeld, D., Kremmer, E., Renner-Müller, I., Wolf, E., and Lipp, M. (1999). CCR7 coordinates the primary immune response by establishing functional microenvironments in secondary lymphoid organs. Cell *99*, 23–33.

Förster, R., Braun, A., and Worbs, T. (2012). Lymph node homing of T cells and dendritic cells via afferent lymphatics. Trends Immunol. *33*, 271–280.

Frucht, D.M., Fukao, T., Bogdan, C., Schindler, H., O'Shea, J.J., and Koyasu, S. (2001). IFN-gamma production by antigen-presenting cells: mechanisms emerge. Trends Immunol. *22*, 556–560.

Fuchs, A., Vermi, W., Lee, J.S., Lonardi, S., and Gilfillan, S. (2013). Intraepithelial Type 1 Innate Lymphoid Cells Are a Unique Subset of IL-12- and IL-15-Responsive IFN-γ-Producing Cells. Immunity *38,* 769-781.

Fuertes, M.B., Kacha, A.K., Kline, J., Woo, S.R., Kranz, D.M., Murphy, K.M., and Gajewski, T.F. (2011). Host type I IFN signals are required for antitumor CD8+ T cell responses through CD8 + dendritic cells. J. Exp. Med. *208*, 2005–2016.

Fukaya, T., Murakami, R., Takagi, H., Sato, K., Sato, Y., Otsuka, H., Ohno, M., Hijikata, A., Ohara, O., Hikida, M., et al. (2012). Conditional ablation of CD205+ conventional dendritic cells impacts the regulation of T-cell immunity and homeostasis in vivo. Proc. Natl. Acad. Sci. U.S.A. *109*, 11288–11293.

Gajewski, T.F., Goldwasser, E., and Fitch, F.W. (1988). Anti-proliferative effect of IFN-gamma in immune regulation. II. IFN-gamma inhibits the proliferation of murine bone marrow cells stimulated with IL-3, IL-4, or granulocyte-macrophage colony-stimulating factor. J. Immunol. *141*, 2635–2642.

Gao, Y., Nish, S.A., Jiang, R., Hou, L., Licona-Limón, P., Weinstein, J.S., Zhao, H., and Medzhitov, R. (2013). Control of T helper 2 responses by transcription factor IRF4-dependent dendritic cells. Immunity *39*, 722–732.

Garbi, N., Hämmerling, G.J., Probst, H.C., and van den Broek, M. (2010). Tonic T cell signalling and T cell tolerance as opposite effects of self-recognition on dendritic cells. Curr. Opin. Immunol. *22*, 601–608.

Gause, W.C., Lu, P., Zhou, X.D., Chen, S.J., Madden, K.B., Morris, S.C., Linsley, P.S., Finkelman, F.D., and Urban, J.F. (1996). H. polygyrus: B7-independence of the secondary type 2 response. Exp. Parasitol. *84*, 264–273.

Gazzinelli, R.T., Oswald, I.P., James, S.L., and Sher, A. (1992). IL-10 inhibits parasite killing and nitrogen oxide production by IFN-gamma-activated macrophages. J. Immunol. *148*, 1792–1796.

Geissmann, F., Auffray, C., Palframan, R., Wirrig, C., Ciocca, A., Campisi, L.,

Narni-Mancinelli, E., and Lauvau, G. (2008). Blood monocytes: distinct subsets, how they relate to dendritic cells, and their possible roles in the regulation of T-cell responses. Immunol. Cell Biol. *86*, 398–408.

Geissmann, F., Jung, S., and Littman, D.R. (2003). Blood monocytes consist of two principal subsets with distinct migratory properties. Immunity *19*, 71–82.

Geissmann, F., Manz, M.G., Jung, S., Sieweke, M.H., Merad, M., and Ley, K. (2010). Development of monocytes, macrophages, and dendritic cells. Science *327*, 656–661.

Gett, A.V., and Hodgkin, P.D. (1998). Cell division regulates the T cell cytokine repertoire, revealing a mechanism underlying immune class regulation. Proc. Natl. Acad. Sci. U.S.A. *95*, 9488–9493.

Geuskens, M., Borojevic, R., and Van Gansen, P. (1991). Eosinophil granulocytopoiesis in hepatic periovular granulomas during the chronic phase of experimental murine Schistosomiasis mansoni. Biol. Cell *71*, 89–96.

Ghosh, H.S., Cisse, B., Bunin, A., Lewis, K.L., and Reizis, B. (2010). Continuous expression of the transcription factor e2-2 maintains the cell fate of mature plasmacytoid dendritic cells. Immunity *33*, 905–916.

Giblin, P.A., Hwang, S.T., Katsumoto, T.R., and Rosen, S.D. (1997). Ligation of L-selectin on T lymphocytes activates beta1 integrins and promotes adhesion to fibronectin. J. Immunol. *159*, 3498–3507.

Ginhoux, F., and Jung, S. (2014). Monocytes and macrophages: developmental pathways and tissue homeostasis. Nature Publishing Group *14*, 392–404.

Ginhoux, F., Collin, M.P., Bogunovic, M., Abel, M., Leboeuf, M., Helft, J., Ochando, J., Kissenpfennig, A., Malissen, B., Grisotto, M., et al. (2007). Blood-derived dermal langerin+ dendritic cells survey the skin in the steady state. J. Exp. Med. *204*, 3133–3146.

Ginhoux, F., Liu, K., Helft, J., Bogunovic, M., Greter, M., Hashimoto, D., Price, J., Yin, N., Bromberg, J., Lira, S.A., et al. (2009). The origin and development of nonlymphoid tissue CD103+ DCs. J. Exp. Med. *206*, 3115–3130.

Girard, J.-P., Moussion, C., and Förster, R. (2012). HEVs, lymphatics and homeostatic immune cell trafficking in lymph nodes. Nature Publishing Group *12*, 762–773.

Girgis, N.M., Gundra, U.M., Ward, L.N., Cabrera, M., Frevert, U., and Loke, P. (2014). Ly6Chigh monocytes become alternatively activated macrophages in schistosome granulomas with help from CD4+ cells. PLoS Pathog. *10*, e1004080.

Girvin, A.M., Dal Canto, M.C., Rhee, L., Salomon, B., Sharpe, A., Bluestone, J.A., and Miller, S.D. (2000). A critical role for B7/CD28 costimulation in experimental autoimmune encephalomyelitis: a comparative study using costimulatory molecule-

deficient mice and monoclonal antibody blockade. J. Immunol. *164*, 136–143.

Glatman Zaretsky, A., Taylor, J.J., King, I.L., Marshall, F.A., Mohrs, M., and Pearce, E.J. (2009). T follicular helper cells differentiate from Th2 cells in response to helminth antigens. J. Exp. Med. *206*, 991–999.

Goddard, S., Youster, J., Morgan, E., and Adams, D.H. (2004). Interleukin-10 secretion differentiates dendritic cells from human liver and skin. Am. J. Pathol. *164*, 511–519.

Gold, M.J., Antignano, F., Halim, T.Y.F., Hirota, J.A., Blanchet, M.-R., Zaph, C., Takei, F., and McNagny, K.M. (2014). Group 2 innate lymphoid cells facilitate sensitization to local, but not systemic, TH2-inducing allergen exposures. J. Allergy Clin. Immunol. *133*, 1142–1148.

Gorczynski, R.M. (2012). CD200:CD200R-Mediated Regulation of Immunity. Immunology *2012*, 1–18.

Gordon, J.R., Li, F., Nayyar, A., Xiang, J., and Zhang, X. (2005). CD8 alpha+, but not CD8 alpha-, dendritic cells tolerize Th2 responses via contact-dependent and -independent mechanisms, and reverse airway hyperresponsiveness, Th2, and eosinophil responses in a mouse model of asthma. J. Immunol. *175*, 1516–1522.

Gorelik, L., and Flavell, R.A. (2002). Transforming growth factor-beta in T-cell biology. Nat. Rev. Immunol. *2*, 46–53.

Granucci, F., Ferrero, E., Foti, M., Aggujaro, D., Vettoretto, K., and Ricciardi-Castagnoli, P. (1999). Early events in dendritic cell maturation induced by LPS. Microbes Infect. *1*, 1079–1084.

Greenwald, R.J., Freeman, G.J., and Sharpe, A.H. (2005). The B7 family revisited. Annu. Rev. Immunol. *23*, 515–548.

Grimaud, J.A., Boros, D.L., Takiya, C., Mathew, R.C., and Emonard, H. (1987). Collagen isotypes, laminin, and fibronectin in granulomas of the liver and intestines of Schistosoma mansoni-infected mice. Am. J. Trop. Med. Hyg. *37*, 335–344.

Gryseels, B., Polman, K., Clerinx, J., and Kestens, L. (2006). Human schistosomiasis. Lancet *368*, 1106–1118.

Grzych, J.M., Pearce, E., Cheever, A., Caulada, Z.A., Caspar, P., Heiny, S., Lewis, F., and Sher, A. (1991). Egg deposition is the major stimulus for the production of Th2 cytokines in murine schistosomiasis mansoni. J. Immunol. *146*, 1322–1327.

Guermonprez, P., Valladeau, J., Zitvogel, L., Théry, C., and Amigorena, S. (2002). Antigen presentation and T cell stimulation by dendritic cells. Annu. Rev. Immunol. *20*, 621–667.

Guimond, M., Veenstra, R.G., Grindler, D.J., Zhang, H., Cui, Y., Murphy, R.D., Kim, S.Y., Na, R., Hennighausen, L., Kurtulus, S., et al. (2009). Interleukin 7

signaling in dendritic cells regulates the homeostatic proliferation and niche size of CD4+ T cells. Nat. Immunol. *10*, 149–157.

Gunn, M.D., Tangemann, K., Tam, C., Cyster, J.G., Rosen, S.D., and Williams, L.T. (1998). A chemokine expressed in lymphoid high endothelial venules promotes the adhesion and chemotaxis of naive T lymphocytes. Proc. Natl. Acad. Sci. U.S.A. *95*, 258–263.

Haan, den, J.M., Lehar, S.M., and Bevan, M.J. (2000). CD8(+) but not CD8(-) dendritic cells cross-prime cytotoxic T cells in vivo. J. Exp. Med. *192*, 1685–1696.

Halim, T.Y.F., Krauss, R.H., Sun, A.C., and Takei, F. (2012). Lung natural helper cells are a critical source of Th2 cell-type cytokines in protease allergen-induced airway inflammation. Immunity *36*, 451–463.

Halim, T.Y.F., Steer, C.A., Mathä, L., Gold, M.J., Martinez-Gonzalez, I., McNagny, K.M., McKenzie, A.N.J., and Takei, F. (2014). Group 2 innate lymphoid cells are critical for the initiation of adaptive T helper 2 cell-mediated allergic lung inflammation. Immunity *40*, 425–435.

Hambleton, S., Salem, S., Bustamante, J., Bigley, V., Boisson-Dupuis, S., Azevedo, J., Fortin, A., Haniffa, M., Ceron-Gutierrez, L., Bacon, C.M., et al. (2011). IRF8 mutations and human dendritic-cell immunodeficiency. N. Engl. J. Med. *365*, 127–138.

Hammad, H., Plantinga, M., Deswarte, K., Pouliot, P., Willart, M.A.M., Kool, M., Muskens, F., and Lambrecht, B.N. (2010). Inflammatory dendritic cells--not basophils--are necessary and sufficient for induction of Th2 immunity to inhaled house dust mite allergen. J. Exp. Med. *207*, 2097–2111.

Hams, E., Aviello, G., and Fallon, P.G. (2013). The schistosoma granuloma: friend or foe? Front. Immunol. *4*, 89.

Haniffa, M., Shin, A., Bigley, V., McGovern, N., Teo, P., See, P., Wasan, P.S., Wang, X.-N., Malinarich, F., Malleret, B., et al. (2012). Human Tissues Contain CD141hi Cross-Presenting Dendritic Cells with Functional Homology to Mouse CD103+ Nonlymphoid Dendritic Cells. Immunity *37*, 60–73.

Harrell, M.I., Iritani, B.M., and Ruddell, A. (2008). Lymph node mapping in the mouse. J. Immunol. Methods *332*, 170–174.

Harrington, L.E., Hatton, R.D., Mangan, P.R., Turner, H., Murphy, T.L., Murphy, K.M., and Weaver, C.T. (2005). Interleukin 17-producing CD4+ effector T cells develop via a lineage distinct from the T helper type 1 and 2 lineages. Nat. Immunol. *6*, 1123–1132.

Harris, N.L., and Ronchese, F. (1999). The role of B7 costimulation in T-cell immunity. Immunol. Cell Biol. *77*, 304–311.

Hasbold, J., Hong, J.S., Kehry, M.R., and Hodgkin, P.D. (1999). Integrating signals

from IFN-gamma and IL-4 by B cells: positive and negative effects on CD40 ligand-induced proliferation, survival, and division-linked isotype switching to IgG1, IgE, and IgG2a. J. Immunol. *163*, 4175–4181.

Haseeb, M.A., Shirazian, D.J., and Preis, J. (2001). Elevated serum levels of TNF-alpha, sTNF-RI and sTNF-RII in murine schistosomiasis correlate with schistosome oviposition and circumoval granuloma formation. Cytokine *15*, 266–269.

Haseeb, M.A., Solomon, W.B., and Palma, J.F. (1996). Schistosoma mansoni: effect of recombinant tumor necrosis factor alpha on fecundity and [14C]-tyrosine uptake in females maintained in vitro. Comp. Biochem. Physiol. C, Pharmacol. Toxicol. Endocrinol. *115*, 265–269.

Heath, V.L., Showe, L., Crain, C., Barrat, F.J., Trinchieri, G., and O'Garra, A. (2000). Cutting edge: ectopic expression of the IL-12 receptor-beta 2 in developing and committed Th2 cells does not affect the production of IL-4 or induce the production of IFN-gamma. J. Immunol. *164*, 2861–2865.

Heath, W.R., Belz, G.T., Behrens, G.M.N., Smith, C.M., Forehan, S.P., Parish, I.A., Davey, G.M., Wilson, N.S., Carbone, F.R., and Villadangos, J.A. (2004). Cross-presentation, dendritic cell subsets, and the generation of immunity to cellular antigens. Immunol. Rev. *199*, 9–26.

Hebel, R., and Stromberg, M.W. (1976). Anatomy of the laboratory rat.

Hegazy, A.N., Peine, M., Helmstetter, C., Panse, I., Fröhlich, A., Bergthaler, A., Flatz, L., Pinschewer, D.D., Radbruch, A., and Löhning, M. (2010). Interferons direct Th2 cell reprogramming to generate a stable GATA-3(+)T-bet(+) cell subset with combined Th2 and Th1 cell functions. Immunity *32*, 116–128.

Helming, L., and Gordon, S. (2007). Macrophage fusion induced by IL-4 alternative activation is a multistage process involving multiple target molecules. Eur. J. Immunol. *37*, 33–42.

Henderson, G.S., Lu, X., McCurley, T.L., and Colley, D.G. (1992). In vivo molecular analysis of lymphokines involved in the murine immune response during Schistosoma mansoni infection. II. Quantification of IL-4 mRNA, IFN-gamma mRNA, and IL-2 mRNA levels in the granulomatous livers, mesenteric lymph nodes, and spleens during the course of modulation. J. Immunol. *148*, 2261–2269.

Henri, S., Vremec, D., Kamath, A., Waithman, J., Williams, S., Benoist, C., Burnham, K., Saeland, S., Handman, E., and Shortman, K. (2001). The dendritic cell populations of mouse lymph nodes. J. Immunol. *167*, 741–748.

Herbert, D.R., Hölscher, C., Mohrs, M., Arendse, B., Schwegmann, A., Radwanska, M., Leeto, M., Kirsch, R., Hall, P., Mossmann, H., et al. (2004). Alternative macrophage activation is essential for survival during schistosomiasis and downmodulates T helper 1 responses and immunopathology. Immunity *20*, 623–635.

Hernandez, H.J., Wang, Y., Tzellas, N., and Stadecker, M.J. (1997). Expression of

class II, but not class I, major histocompatibility complex molecules is required for granuloma formation in infection with Schistosoma mansoni. Eur. J. Immunol. *27*, 1170–1176.

Hesse, M., Modolell, M., La Flamme, A.C., Schito, M., Fuentes, J.M., Cheever, A.W., Pearce, E.J., and Wynn, T.A. (2001). Differential regulation of nitric oxide synthase-2 and arginase-1 by type 1/type 2 cytokines in vivo: granulomatous pathology is shaped by the pattern of L-arginine metabolism. J. Immunol. *167*, 6533–6544.

Hesse, M., Piccirillo, C.A., Belkaid, Y., Prufer, J., Mentink-Kane, M., Leusink, M., Cheever, A.W., Shevach, E.M., and Wynn, T.A. (2004). The pathogenesis of schistosomiasis is controlled by cooperating IL-10-producing innate effector and regulatory T cells. J. Immunol. *172*, 3157–3166.

Hildner, K., Edelson, B.T., Purtha, W.E., Diamond, M., Matsushita, H., Kohyama, M., Calderon, B., Schraml, B.U., Unanue, E.R., Diamond, M.S., et al. (2008). Batf3 Deficiency Reveals a Critical Role for CD8 + Dendritic Cells in Cytotoxic T Cell Immunity. Science *322*, 1092–1097.

Hilkens, C.M., Kaliński, P., de Boer, M., and Kapsenberg, M.L. (1997). Human dendritic cells require exogenous interleukin-12-inducing factors to direct the development of naive T-helper cells toward the Th1 phenotype. Blood *90*, 1920–1926.

Hilkens, C.M., Messer, G., Tesselaar, K., van Rietschoten, A.G., Kapsenberg, M.L., and Wierenga, E.A. (1996). Lack of IL-12 signaling in human allergen-specific Th2 cells. J. Immunol. *157*, 4316–4321.

Hirata, M., Hara, T., Kage, M., Fukuma, T., and Sendo, F. (2002). Neutropenia augments experimentally induced Schistosoma japonicum egg granuloma formation in CBA mice, but not in C57BL/6 mice. Parasite Immunol. *24*, 479–488.

Hirata, N., Yanagawa, Y., Satoh, M., Ogura, H., Ebihara, T., Noguchi, M., Matsumoto, M., Togashi, H., Seya, T., Onoé, K., et al. (2010). Dendritic cell-derived TNF-alpha is responsible for development of IL-10-producing CD4+ T cells. Cell. Immunol. *261*, 37–41.

Hochrein, H., Shortman, K., Vremec, D., Scott, B., Hertzog, P., and O'Keeffe, M. (2001). Differential production of IL-12, IFN-alpha, and IFN-gamma by mouse dendritic cell subsets. J. Immunol. *166*, 5448–5455.

Hochweller, K., Striegler, J., Hämmerling, G.J., and Garbi, N. (2008). A novel CD11c.DTR transgenic mouse for depletion of dendritic cells reveals their requirement for homeostatic proliferation of natural killer cells. Eur. J. Immunol. *38*, 2776–2783.

Hoeve, M.A., Savage, N.D.L., de Boer, T., Langenberg, D.M.L., de Waal Malefyt, R., Ottenhoff, T.H.M., and Verreck, F.A.W. (2006). Divergent effects of IL-12 and

IL-23 on the production of IL-17 by human T cells. Eur. J. Immunol. *36*, 661–670.

Hoffmann, K.F., Caspar, P., Cheever, A.W., and Wynn, T.A. (1998). IFN-gamma, IL-12, and TNF-alpha are required to maintain reduced liver pathology in mice vaccinated with Schistosoma mansoni eggs and IL-12. J. Immunol. *161*, 4201–4210.

Hoffmann, K.F., Cheever, A.W., and Wynn, T.A. (2000). IL-10 and the dangers of immune polarization: excessive type 1 and type 2 cytokine responses induce distinct forms of lethal immunopathology in murine schistosomiasis. J. Immunol. *164*, 6406–6416.

Hoffmann, K.F., James, S.L., Cheever, A.W., and Wynn, T.A. (1999). Studies with double cytokine-deficient mice reveal that highly polarized Th1- and Th2-type cytokine and antibody responses contribute equally to vaccine-induced immunity to Schistosoma mansoni. J. Immunol. *163*, 927–938.

Hoffmann, K.F., McCarty, T.C., Segal, D.H., Chiaramonte, M., Hesse, M., Davis, E.M., Cheever, A.W., Meltzer, P.S., Morse, H.C., and Wynn, T.A. (2001). Disease fingerprinting with cDNA microarrays reveals distinct gene expression profiles in lethal type 1 and type 2 cytokine-mediated inflammatory reactions. FASEB J. *15*, 2545–2547.

Hogan, L.H., Wang, M., Suresh, M., Co, D.O., Weinstock, J.V., and Sandor, M. (2002). CD4+ TCR repertoire heterogeneity in Schistosoma mansoni-induced granulomas. J. Immunol. *169*, 6386–6393.

Hokke, C.H., and Yazdanbakhsh, M. (2005). Schistosome glycans and innate immunity. Parasite Immunol. *27*, 257–264.

Hori, S., Nomura, T., and Sakaguchi, S. (2003). Control of regulatory T cell development by the transcription factor Foxp3. Science *299*, 1057–1061.

Horino, J., Fujimoto, M., Terabe, F., Serada, S., Takahashi, T., Soma, Y., Tanaka, K., Chinen, T., Yoshimura, A., Nomura, S., et al. (2008). Suppressor of cytokine signaling-1 ameliorates dextran sulfate sodium-induced colitis in mice. Int. Immunol. *20*, 753–762.

Horwitz, D.A., Zheng, S.G., and Gray, J.D. (2008). Natural and TGF-beta-induced Foxp3(+)CD4(+) CD25(+) regulatory T cells are not mirror images of each other. Trends Immunol. *29*, 429–435.

Hsü, S.Y., Hsü, H.F., Davis, J.R., and Lust, G.L. (1972). Comparative studies on the lesions caused by eggs of Schistosoma japonicum and Schistosoma mansoni in livers of albino mice and rhesus monkeys. Ann. Trop. Med. Parasitol. *66*, 89–97.

Huh, J.-W., Shibata, T., Hwang, M., Kwon, E.-H., Jang, M.S., Fukui, R., Kanno, A., Jung, D.-J., Jang, M.H., Miyake, K., et al. (2014). UNC93B1 is essential for the plasma membrane localization and signaling of Toll-like receptor 5. Proc. Natl. Acad. Sci. U.S.A. *111*, 7072–7077.

Hussaarts, L., Smits, H.H., Schramm, G., van der Ham, A.J., van der Zon, G.C., Haas, H., Guigas, B., and Yazdanbakhsh, M. (2013). Rapamycin and omega-1: mTOR-dependent and -independent Th2 skewing by human dendritic cells. Immunol. Cell Biol. *91,* 486-489.

Hutchison, S., Choo-Kang, B.S.W., Gibson, V.B., Bundick, R.V., Leishman, A.J., Brewer, J.M., McInnes, I.B., and Garside, P. (2009). An investigation of the impact of the location and timing of antigen-specific T cell division on airways inflammation. Clin. Exp. Immunol. *155*, 107–116.

Hutloff, A., Dittrich, A.M., Beier, K.C., Eljaschewitsch, B., Kraft, R., Anagnostopoulos, I., and Kroczek, R.A. (1999). ICOS is an inducible T-cell co-stimulator structurally and functionally related to CD28. Nature *397*, 263–266.

Iacobelli, M., Wachsman, W., and McGuire, K.L. (2000). Repression of IL-2 promoter activity by the novel basic leucine zipper p21SNFT protein. J. Immunol. *165*, 860–868.

Iacomini, J., Ricklan, D.E., and Stadecker, M.J. (1995). T cells expressing the gamma delta T cell receptor are not required for egg granuloma formation in schistosomiasis. Eur. J. Immunol. *25*, 884–888.

Ikeda, S., Saijo, S., Murayama, M.A., Shimizu, K., Akitsu, A., and Iwakura, Y. (2014). Excess IL-1 signaling enhances the development of Th17 cells by downregulating TGF-β-induced Foxp3 expression. J. Immunol. *192*, 1449–1458.

Isaksson, M., Lundgren, B.A., Ahlgren, K.M., Kämpe, O., and Lobell, A. (2012). Conditional DC depletion does not affect priming of encephalitogenic Th cells in EAE. Eur. J. Immunol. *42*, 2555–2563.

Ishida, Y., Agata, Y., Shibahara, K., and Honjo, T. (1992). Induced expression of PD-1, a novel member of the immunoglobulin gene superfamily, upon programmed cell death. Embo J. *11*, 3887–3895.

Ito, T., Wang, Y.-H., Duramad, O., Hori, T., Delespesse, G.J., Watanabe, N., Qin, F.X.-F., Yao, Z., Cao, W., and Liu, Y.-J. (2005). TSLP-activated dendritic cells induce an inflammatory T helper type 2 cell response through OX40 ligand. J. Exp. Med. *202*, 1213–1223.

Ivanov, I.I., McKenzie, B.S., Zhou, L., Tadokoro, C.E., Lepelley, A., Lafaille, J.J., Cua, D.J., and Littman, D.R. (2006). The orphan nuclear receptor RORgammat directs the differentiation program of proinflammatory IL-17+ T helper cells. Cell *126*, 1121–1133.

Iwata, M., Hirakiyama, A., Eshima, Y., Kagechika, H., Kato, C., and Song, S.-Y. (2004). Retinoic acid imprints gut-homing specificity on T cells. Immunity *21*, 527–538.

Jackson, J.T., Hu, Y., Liu, R., Masson, F., D'Amico, A., Carotta, S., Xin, A., Camilleri, M.J., Mount, A.M., Kallies, A., et al. (2011). Id2 expression delineates

differential checkpoints in the genetic program of CD8α+ and CD103+ dendritic cell lineages. Embo J. *30*, 2690–2704.

Jacobs, W., Bogers, J., and Van Marck, E. (1999). Distinct B-cell populations are present in hepatic and intestinal Schistosoma mansoni granulomas. Acta Gastroenterol. Belg. *62*, 178–181.

Jakubzick, C., Wen, H., Matsukawa, A., Keller, M., Kunkel, S.L., and Hogaboam, C.M. (2004). Role of CCR4 ligands, CCL17 and CCL22, during *Schistosoma mansoni* egg-induced pulmonary granuloma formation in mice. Am. J. Pathol. *165*, 1211-1221.

Jaensson, E., Uronen-Hansson, H., Pabst, O., Eksteen, B., Tian, J., Coombes, J.L., Berg, P.-L., Davidsson, T., Powrie, F., Johansson-Lindbom, B., et al. (2008). Small intestinal CD103+ dendritic cells display unique functional properties that are conserved between mice and humans. J. Exp. Med. *205*, 2139–2149.

Jakubzick, C., Tacke, F., Llodra, J., Van Rooijen, N., and Randolph, G.J. (2006). Modulation of dendritic cell trafficking to and from the airways. J. Immunol. *176*, 3578–3584.

James, S.L., and Colley, D.G. (1978). Eosinophi-mediated destruction of Schistosoma mansoni eggs in vitro. II. The role of cytophilic antibody. Cell. Immunol. *38*, 35–47.

Janeway, C.A. (1989). Approaching the asymptote? Evolution and revolution in immunology. Cold Spring Harb. Symp. Quant. Biol. *54 Pt 1*, 1–13.

Janeway, C.A. (1992). The immune system evolved to discriminate infectious nonself from noninfectious self. Immunol. Today *13*, 11–16.

Janeway, C.A., and Medzhitov, R. (2002). Innate immune recognition. Annu. Rev. Immunol. *20*, 197–216.

Jankovic, D., Cheever, A.W., Kullberg, M.C., Wynn, T.A., Yap, G., Caspar, P., Lewis, F.A., Clynes, R., Ravetch, J.V., and Sher, A. (1998). CD4+ T cell-mediated granulomatous pathology in schistosomiasis is downregulated by a B cell-dependent mechanism requiring Fc receptor signaling. J. Exp. Med. *187*, 619–629.

Jankovic, D., Kullberg, M.C., Noben-Trauth, N., Caspar, P., Paul, W.E., and Sher, A. (2000). Single cell analysis reveals that IL-4 receptor/Stat6 signaling is not required for the in vivo or in vitro development of CD4+ lymphocytes with a Th2 cytokine profile. J. Immunol. *164*, 3047–3055.

Jankovic, D., Kullberg, M.C., Noben-Trauth, N., Caspar, P., Ward, J.M., Cheever, A.W., Paul, W.E., and Sher, A. (1999a). Schistosome-infected IL-4 receptor knockout (KO) mice, in contrast to IL-4 KO mice, fail to develop granulomatous pathology while maintaining the same lymphokine expression profile. J. Immunol. *163*, 337–342.

Jankovic, D., Wynn, T.A., Kullberg, M.C., Hieny, S., Caspar, P., James, S., Cheever, A.W., and Sher, A. (1999b). Optimal vaccination against Schistosoma mansoni requires the induction of both B cell- and IFN-gamma-dependent effector mechanisms. J. Immunol. *162*, 345–351.

Jankovic, D., Kullberg, M.C., Caspar, P., and Sher, A. (2004). Parasite-induced Th2 polarization is associated with down-regulated dendritic cell responsiveness to Th1 stimuli and a transient delay in T lymphocyte cycling. J. Immunol. *173*, 2419–2427.

Jelley-Gibbs, D.M., Lepak, N.M., Yen, M., and Swain, S.L. (2000). Two Distinct Stages in the Transition from Naive CD4 T Cells to Effectors, Early Antigen-Dependent and Late Cytokine-Driven Expansion and Differentiation. J. Immunol. *165*, 5017–5026.

Jenkins, J.K., Suwannaroj, S., Elbourne, K.B., Ndebele, K., and McMurray, R.W. (2001). 17-beta-estradiol alters Jurkat lymphocyte cell cycling and induces apoptosis through suppression of Bcl-2 and cyclin A. Int. Immunopharmacol. *1*, 1897–1911.

Jenkins, S.J., Perona-Wright, G., Worsley, A.G.F., Ishii, N., and MacDonald, A.S. (2007). Dendritic cell expression of OX40 ligand acts as a costimulatory, not polarizing, signal for optimal Th2 priming and memory induction in vivo. J. Immunol. *179*, 3515–3523.

Jiang, H.-R., Muckersie, E., Robertson, M., Xu, H., Liversidge, J., and Forrester, J.V. (2002). Secretion of interleukin-10 or interleukin-12 by LPS-activated dendritic cells is critically dependent on time of stimulus relative to initiation of purified DC culture. J. Leukoc. Biol. *72*, 978–985.

Jiang, W., Swiggard, W.J., Heufler, C., Peng, M., Mirza, A., Steinman, R.M., and Nussenzweig, M.C. (1995). The receptor DEC-205 expressed by dendritic cells and thymic epithelial cells is involved in antigen processing. Nature *375*, 151–155.

Jiao, J., Dragomir, A.-C., Kocabayoglu, P., Rahman, A.H., Chow, A., Hashimoto, D., Leboeuf, M., Kraus, T., Moran, T., Carrasco-Avino, G., et al. (2014). Central role of conventional dendritic cells in regulation of bone marrow release and survival of neutrophils. J. Immunol. *192*, 3374–3382.

Jiao, J., Sastre, D., Fiel, M.I., Lee, U.E., Ghiassi-Nejad, Z., Ginhoux, F., Vivier, E., Friedman, S.L., Merad, M., and Aloman, C. (2012). Dendritic cell regulation of carbon tetrachloride-induced murine liver fibrosis regression. Hepatology *55*, 244–255.

Joffre, O.P., Segura, E., Savina, A., and Amigorena, S. (2012). Cross-presentation by dendritic cells. Nat. Rev. Immunol. *12*, 557–569.

Johansson-Lindbom, B., Svensson, M., Pabst, O., Palmqvist, C., Marquez, G., Förster, R., and Agace, W.W. (2005). Functional specialization of gut CD103+ dendritic cells in the regulation of tissue-selective T cell homing. J. Exp. Med. *202*, 1063–1073.

Jongbloed, S.L., Kassianos, A.J., McDonald, K.J., Clark, G.J., Ju, X., Angel, C.E., Chen, C.-J.J., Dunbar, P.R., Wadley, R.B., Jeet, V., et al. (2010). Human CD141+ (BDCA-3)+ dendritic cells (DCs) represent a unique myeloid DC subset that cross-presents necrotic cell antigens. J. Exp. Med. *207*, 1247–1260.

Joseph, A.L., and Boros, D.L. (1993). Tumor necrosis factor plays a role in Schistosoma mansoni egg-induced granulomatous inflammation. J. Immunol. *151*, 5461–5471.

Jung, S., Unutmaz, D., Wong, P., Sano, G.-I., De los Santos, K., Sparwasser, T., Wu, S., Vuthoori, S., Ko, K., Zavala, F., et al. (2002). In vivo depletion of CD11c+ dendritic cells abrogates priming of CD8+ T cells by exogenous cell-associated antigens. Immunity *17*, 211–220.

Junqueira, L.C., Cossermelli, W., and Brentani, R. (1978). Differential staining of collagens type I, II and III by Sirius Red and polarization microscopy. Arch. Histol. Jpn. *41*, 267–274.

Kaliński, P., Hilkens, C.M., Wierenga, E.A., and Kapsenberg, M.L. (1999). T-cell priming by type-1 and type-2 polarized dendritic cells: the concept of a third signal. Immunol. Today *20*, 561–567.

Kaliński, P., Smits, H.H., Schuitemaker, J.H., Vieira, P.L., van Eijk, M., de Jong, E.C., Wierenga, E.A., and Kapsenberg, M.L. (2000). IL-4 is a mediator of IL-12p70 induction by human Th2 cells: reversal of polarized Th2 phenotype by dendritic cells. J. Immunol. *165*, 1877–1881.

Kane, C.M., Cervi, L., Sun, J., McKee, A.S., Masek, K.S., Shapira, S., Hunter, C.A., and Pearce, E.J. (2004). Helminth antigens modulate TLR-initiated dendritic cell activation. J. Immunol. *173*, 7454–7461.

Kaplan, M.H., Whitfield, J.R., Boros, D.L., and Grusby, M.J. (1998). Th2 cells are required for the Schistosoma mansoni egg-induced granulomatous response. J. Immunol. *160*, 1850–1856.

Kapsenberg, M.L. (2003). Dendritic-cell control of pathogen-driven T-cell polarization. Nat. Rev. Immunol. *3*, 984–993.

Karanja, D.M., Colley, D.G., Nahlen, B.L., Ouma, J.H., and Secor, W.E. (1997). Studies on schistosomiasis in western Kenya: I. Evidence for immune-facilitated excretion of schistosome eggs from patients with Schistosoma mansoni and human immunodeficiency virus coinfections. Am. J. Trop. Med. Hyg. *56*, 515–521.

Kashiwada, M., Levy, D.M., McKeag, L., Murray, K., Schroder, A.J., Canfield, S.M., Traver, G., and Rothman, P.B. (2010). IL-4-induced transcription factor NFIL3/E4BP4 controls IgE class switching. Proc. Natl. Acad. Sci. U.S.A. *107*, 821–826.

Kawai, T., and Akira, S. (2010). The role of pattern-recognition receptors in innate immunity: update on Toll-like receptors. Nature Publishing Group *11*, 373–384.

Keane-Myers, A., Gause, W.C., Linsley, P.S., Chen, S.J., and Wills-Karp, M. (1997). B7-CD28/CTLA-4 costimulatory pathways are required for the development of T helper cell 2-mediated allergic airway responses to inhaled antigens. J. Immunol. *158*, 2042–2049.

Kephart, G.M., ANDRADE, Z.A., and Gleich, G.J. (1988). Localization of eosinophil major basic protein onto eggs of Schistosoma mansoni in human pathologic tissue. Am. J. Pathol. *133*, 389–396.

Khader, S.A., Gaffen, S.L., and Kolls, J.K. (2009). Th17 cells at the crossroads of innate and adaptive immunity against infectious diseases at the mucosa. Mucosal Immunol. *2*, 403–411.

Khan, S.A., Joyce, J., and Tsuda, T. (2012). Quantification of active and total transforming growth factor-β levels in serum and solid organ tissues by bioassay. BMC Res. Notes *5*, 636.

Kim, P.S., and Ahmed, R. (2010). Features of responding T cells in cancer and chronic infection. Curr. Opin. Immunol. *22*, 223–230.

Kim, T.S., and Braciale, T.J. (2009). Respiratory dendritic cell subsets differ in their capacity to support the induction of virus-specific cytotoxic CD8+ T cell responses. PLoS ONE *4*, e4204.

King, C.L., Xianli, J., June, C.H., Abe, R., and Lee, K.P. (1996). CD28-deficient mice generate an impaired Th2 response to Schistosoma mansoni infection. Eur. J. Immunol. *26*, 2448–2455.

Kingham, T.P., Chaudhry, U.I., Plitas, G., Katz, S.C., Raab, J., and Dematteo, R.P. (2007). Murine liver plasmacytoid dendritic cells become potent immunostimulatory cells after Flt-3 ligand expansion. Hepatology *45*, 445–454.

Kissenpfennig, A., Aït-Yahia, S., Clair-Moninot, V., Stössel, H., Badell, E., Bordat, Y., Pooley, J.L., Lang, T., Prina, E., Coste, I., et al. (2005). Disruption of the langerin/CD207 gene abolishes Birbeck granules without a marked loss of Langerhans cell function. Mol. Cell. Biol. *25*, 88–99.

Kobayashi, T., Walsh, M.C., and Choi, Y. (2004). The role of TRAF6 in signal transduction and the immune response. Microbes Infect. *6*, 1333–1338.

Koo, G.C., and Peppard, J.R. (1984). Establishment of monoclonal anti-Nk-1.1 antibody. Hybridoma *3*, 301–303.

Kool, M., Hammad, H., and Lambrecht, B.N. (2012). Cellular networks controlling Th2 polarization in allergy and immunity. F1000 Biol. Rep. *4*, 6.

Kool, M., Soullié, T., van Nimwegen, M., Willart, M.A.M., Muskens, F., Jung, S., Hoogsteden, H.C., Hammad, H., and Lambrecht, B.N. (2008). Alum adjuvant boosts adaptive immunity by inducing uric acid and activating inflammatory dendritic cells. J. Exp. Med. *205*, 869–882.

Korn, T., Bettelli, E., Gao, W., Awasthi, A., Jäger, A., Strom, T.B., Oukka, M., and Kuchroo, V.K. (2007). IL-21 initiates an alternative pathway to induce proinflammatory T(H)17 cells. Nature *448*, 484–487.

Kriehuber, E., Breiteneder-Geleff, S., Groeger, M., Soleiman, A., Schoppmann, S.F., Stingl, G., Kerjaschki, D., and Maurer, D. (2001). Isolation and characterization of dermal lymphatic and blood endothelial cells reveal stable and functionally specialized cell lineages. J. Exp. Med. *194*, 797–808.

Krishna, M. (2013). Role of special stains in diagnostic liver pathology. Clin. Liver Dis. *2*, S8–S10.

Kronin, V., Hochrein, H., Shortman, K., and Kelso, A. (2000). Regulation of T cell cytokine production by dendritic cells. Immunol. Cell Biol. *78*, 214–223.

Kronin, V., Winkel, K., Süss, G., Kelso, A., Heath, W., Kirberg, J., Boehmer, von, H., and Shortman, K. (1996). A subclass of dendritic cells regulates the response of naive CD8 T cells by limiting their IL-2 production. J. Immunol. *157*, 3819–3827.

Kudo, S., Matsuno, K., Ezaki, T., and Ogawa, M. (1997). A novel migration pathway for rat dendritic cells from the blood: hepatic sinusoids-lymph translocation. J. Exp. Med. *185*, 777–784.

Kuklina, E.M. (2013). Molecular mechanisms of T-cell anergy. Biochemistry Mosc. *78*, 144–156.

Kumamoto, Y., Linehan, M., Weinstein, J.S., Laidlaw, B.J., Craft, J.E., and Iwasaki, A. (2013). CD301b+ Dermal Dendritic Cells Drive T Helper 2 Cell-Mediated Immunity. Immunity 1–11.

Lacy, P., and Stow, J.L. (2011). Cytokine release from innate immune cells: association with diverse membrane trafficking pathways. Blood *118*, 9–18.

Lahoud, M.H., Proietto, A.I., Gartlan, K.H., Kitsoulis, S., Curtis, J., Wettenhall, J., Sofi, M., Daunt, C., O'Keeffe, M., Caminschi, I., et al. (2006). Signal regulatory protein molecules are differentially expressed by CD8- dendritic cells. J. Immunol. *177*, 372–382.

Lamb, E.W., Walls, C.D., Pesce, J.T., Riner, D.K., Maynard, S.K., Crow, E.T., Wynn, T.A., Schaefer, B.C., and Davies, S.J. (2010). Blood Fluke Exploitation of Non-Cognate CD4+ T Cell Help to Facilitate Parasite Development. PLoS Pathog. *6*, e1000892.

Lambrecht, B.N., Kool, M., Willart, M.A.M., and Hammad, H. (2009). Mechanism of action of clinically approved adjuvants. Curr. Opin. Immunol. *21*, 23–29.

Langrish, C.L., Chen, Y., Blumenschein, W.M., Mattson, J., Basham, B., Sedgwick, J.D., McClanahan, T., Kastelein, R.A., and Cua, D.J. (2005). IL-23 drives a pathogenic T cell population that induces autoimmune inflammation. J. Exp. Med. *201*, 233–240.

Larkin, J., III., Ahmed, C.M., Wilson, T.D., and Johnson H.M. (2013). Regulation of interferon gamma signaling by suppressors of cytokine signaling and regulatory T cells. Front. Immunol. *4* 1–8.

Laroui, H., Ingersoll, S.A., Liu, H.C., Baker, M.T., Ayyadurai, S., Charania, M.A., Laroui, F., Yan, Y., Sitaraman, S.V., and Merlin, D. (2012). Dextran sodium sulfate (DSS) induces colitis in mice by forming nano-lipocomplexes with medium-chain-length fatty acids in the colon. PLoS ONE *7*, e32084.

Layland, L.E., Rad, R., Wagner, H., and da Costa, C.U.P. (2007). Immunopathology in schistosomiasis is controlled by antigen-specific regulatory T cells primed in the presence of TLR2. Eur. J. Immunol. *37*, 2174–2184.

Layland, L.E., Wagner, H., and da Costa, C.U.P. (2005). Lack of antigen-specific Th1 response alters granuloma formation and composition in Schistosoma mansoni-infected MyD88-/- mice. Eur. J. Immunol. *35*, 3248–3257.

Lazarevic, V., Glimcher, L.H., and Lord, G.M. (2013). nri3536. 1–13.

Lee, D.U., and Rao, A. (2004). Molecular analysis of a locus control region in the T helper 2 cytokine gene cluster: a target for STAT6 but not GATA3. Proc. Natl. Acad. Sci. U.S.A. *101*, 16010–16015.

Lenzi, H.L., Kimmel, E., Schechtman, H., Pelajo-Machado, M., Romanha, W.S., Pacheco, R.G., Mariano, M., and Lenzi, J.A. (1998). Histoarchitecture of schistosomal granuloma development and involution: morphogenetic and biomechanical approaches. Mem. Inst. Oswaldo Cruz *93 Suppl 1*, 141–151.

Lenzi, H.L., Kimmel, E., Schechtman, H., Pelajo-Machado, M., Vale, B.S., Panasco, M.S., and Lenzi, J.A. (1999). Collagen arrangement in hepatic granuloma in mice infected with Schistosoma mansoni: dependence on fiber radiation centers. Braz. J. Med. Biol. Res. *32*, 639–643.

Lenzi, H.L., Romanha, W. de S., Santos, R.M.Z.D., Rosas, A., Mota, E.M., Manso, P.P.A., Caputo, L.F.G., and Pelajo-Machado, M. (2006). Four whole-istic aspects of schistosome granuloma biology: fractal arrangement, internal regulation, autopoietic component and closure. Mem. Inst. Oswaldo Cruz *101 Suppl 1*, 219–231.

León, B., Ballesteros-Tato, A., Browning, J.L., Dunn, R., Randall, T.D., and Lund, F.E. (2012). Regulation of T(H)2 development by CXCR5+ dendritic cells and lymphotoxin-expressing B cells. Nat. Immunol. *13*, 681–690.

Lewis, K.L., Caton, M.L., Bogunovic, M., Greter, M., Grajkowska, L.T., Ng, D., Klinakis, A., Charo, I.F., Jung, S., Gommerman, J.L., et al. (2011). Notch2 receptor signaling controls functional differentiation of dendritic cells in the spleen and intestine. Immunity *35*, 780–791.

Liang, H.-E., Reinhardt, R.L., Bando, J.K., Sullivan, B.M., Ho, I.-C., and Locksley, R.M. (2011). Divergent expression patterns of IL-4 and IL-13 define unique functions in allergic immunity. Nature Publishing Group *13*, 58–66.

Lichtenberg, von (1962). Host response to eggs of S. mansoni. I. Granuloma formation in the unsensitized laboratory mouse. Am. J. Pathol. *41*, 711–731.

Lichtenberg, von, F., Erickson, D.G., and Sadun, E.H. (1973). Comparative histopathology of schistosome granulomas in the hamster. Am. J. Pathol. *72*, 149–178.

Licona-Limón, P., Kim, L.K., Palm, N.W., and Flavell, R.A. (2013). TH2, allergy and group 2 innate lymphoid cells. Nat. Immunol. *14*, 536–542.

Link, A., Vogt, T.K., Favre, S., Britschgi, M.R., Acha-Orbea, H., Hinz, B., Cyster, J.G., and Luther, S.A. (2007). Fibroblastic reticular cells in lymph nodes regulate the homeostasis of naive T cells. Nat. Immunol. *8*, 1255–1265.

Linsley, P.S., and Ledbetter, J.A. (1993). The role of the CD28 receptor during T cell responses to antigen. Annu. Rev. Immunol. *11*, 191–212.

Linsley, P.S., Bradshaw, J., Greene, J., Peach, R., Bennett, K.L., and Mittler, R.S. (1996). Intracellular trafficking of CTLA-4 and focal localization towards sites of TCR engagement. Immunity *4*, 535–543.

Liu, X., Chen, X., Zhong, B., Wang, A., Wang, X., Chu, F., Nurieva, R.I., Yan, X., Chen, P., van der Flier, L.G., et al. (2014). Transcription factor achaete-scute homologue 2 initiates follicular T-helper-cell development. Nature *507*, 513–518.

Lloyd, C.M., Phillips, A.R.J., Cooper, G.J.S., and Dunbar, P.R. (2008). Three-colour fluorescence immunohistochemistry reveals the diversity of cells staining for macrophage markers in murine spleen and liver. J. Immunol. Methods *334*, 70–81.

Loebermann, M., Sombetzki, M., Langner, C., Fuchsbichler, A., Gumhold, J., Silbert, D., Riebold, D., Holtfreter, M., Fickert, P., Nizze, H., et al. (2009). Imbalance of pro- and antifibrogenic genes and bile duct injury in murine Schistosoma mansoniinfection-induced liver fibrosis. Trop. Med. Int. Health *14*, 1418–1425.

Loke, P., and Allison, J.P. (2003). PD-L1 and PD-L2 are differentially regulated by Th1 and Th2 cells. Proc. Natl. Acad. Sci. U.S.A. *100*, 5336–5341.

Lugo-Villarino, G., Balla, K.M., Stachura, D.L., Banuelos, K., Werneck, M.B.F., and Traver, D. (2010). Identification of dendritic antigen-presenting cells in the zebrafish. Proc. Natl Acad. Sci. U.S.A. *107*, 15850–15855.

Lukacs, N.W., and Boros, D.L. (1991). Identification of larval cross-reactive and egg-specific antigens involved in granuloma formation in murine schistosomiasis mansoni. Infect. Immun. *59*, 3237–3242.

Lukacs, N.W., and Boros, D.L. (1993). Lymphokine regulation of granuloma formation in murine schistosomiasis mansoni. Clin. Immunol. Immunopathol. *68*, 57–63.

Lundy, S.K., and Lukacs, N.W. (2013). Chronic schistosome infection leads to modulation of granuloma formation and systemic immune suppression. Front. Immunol *4*, 1–18.

Lyons, A., and Parish, C.R. (1994). Determination of lymphocyte division by flow cytometry. J. Immunol. Methods *171*, 131–137.

Macatonia, S.E., Hosken, N.A., Litton, M., Vieira, P., Hsieh, C.S., Culpepper, J.A., Wysocka, M., Trinchieri, G., Murphy, K.M., and O'Garra, A. (1995). Dendritic cells produce IL-12 and direct the development of Th1 cells from naive CD4+ T cells. J. Immunol. *154*, 5071–5079.

MacDonald, A.S., and Maizels, R.M. (2008). Alarming dendritic cells for Th2 induction. J. Exp. Med. *205*, 13–17.

MacDonald, A.S., Straw, A.D., Bauman, B., and Pearce, E.J. (2001). CD8- dendritic cell activation status plays an integral role in influencing Th2 response development. J. Immunol. *167*, 1982–1988.

MacDonald, A.S., and Pearce, E.J. (2002). Cutting edge: polarized Th cell response induction by transferred antigen-pulsed dendritic cells is dependent on IL-4 or IL-12 production by recipient cells. J. Immunol. *168*, 3127–3130.

MacDonald, A.S., Patton, E.A., La Flamme, A.C., Araujo, M.I., Huxtable, C.R., Bauman, B., and Pearce, E.J. (2002a). Impaired Th2 development and increased mortality during Schistosoma mansoni infection in the absence of CD40/CD154 interaction. J. Immunol. *168*, 4643–4649.

MacDonald, A.S., Straw, A.D., Dalton, N.M., and Pearce, E.J. (2002b). Cutting edge: Th2 response induction by dendritic cells: a role for CD40. J. Immunol. *168*, 537–540.

MacDonald, H.R. (1995). NK1.1+ T cell receptor-alpha/beta+ cells: new clues to their origin, specificity, and function. J. Exp. Med. *182*, 633–638.

Mack, C.L., and Sokol, R.J. (2005). Unraveling the pathogenesis and etiology of biliary atresia. Pediatr. Res. *57*, 87R–94R.

Malarkey, D., Johnson, K., Ryan, L., Boorman, G., and Maronpot, R. (2005). New Insights into Functional Aspects of Liver Morphology. Toxicol. Pathol. *33*, 27–34.

Maldonado-López, R., De Smedt, T., Michel, P., Godfroid, J., Pajak, B., Heirman, C., Thielemans, K., Leo, O., Urbain, J., and Moser, M. (1999). CD8alpha+ and CD8alpha- subclasses of dendritic cells direct the development of distinct T helper cells in vivo. J. Exp. Med. *189*, 587–592.

Mansy, S.S. (1998). Cellular constituent and intercellular adhesion in Schistosoma mansoni granuloma: an ultrastructural study. J. Egypt. Soc. Parasitol. *28*, 169–181.

Marelli-Berg, F.M., Cannella, L., Dazzi, F., and Mirenda, V. (2008). The highway

code of T cell trafficking. J. Pathol. *214*, 179–189.

Marrack, P., and Kappler, J. (2004). Control of T cell viability. Annu. Rev. Immunol. *22*, 765–787.

MartIn-Fontecha, A., Sebastiani, S., Höpken, U.E., Uguccioni, M., Lipp, M., Lanzavecchia, A., and Sallusto, F. (2003). Regulation of dendritic cell migration to the draining lymph node: impact on T lymphocyte traffic and priming. J. Exp. Med. *198*, 615–621.

Martínez-López, M., Iborra, S., Conde-Garrosa, R., and Sancho, D. (2014). Batf3-dependent CD103(+) dendritic cells are major producers of IL-12 that drive local Th1 immunity against Leishmania major infection in mice. Eur. J. Immunol. *45,* 199-129.

Mascher, B., Schlenke, P., and Seyfarth, M. (1999). Expression and kinetics of cytokines determined by intracellular staining using flow cytometry. J. Immunol. Methods *223*, 115–121.

Mashayekhi, M., Sandau, M.M., Dunay, I.R., Frickel, E.M., Khan, A., Goldszmid, R.S., Sher, A., Ploegh, H.L., Murphy, T.L., Sibley, L.D., et al. (2011). CD8α(+) dendritic cells are the critical source of interleukin-12 that controls acute infection by Toxoplasma gondii tachyzoites. Immunity *35*, 249–259.

Massacand, J.C., Stettler, R.C., Meier, R., Humphreys, N.E., Grencis, R.K., Marsland, B.J., and Harris, N.L. (2009). Helminth products bypass the need for TSLP in Th2 immune responses by directly modulating dendritic cell function. Proc. Natl. Acad. Sci. U.S.A. *106*, 13968–13973.

Mathew, R.C., and Boros, D.L. (1986). Anti-L3T4 antibody treatment suppresses hepatic granuloma formation and abrogates antigen-induced interleukin-2 production in Schistosoma mansoni infection. Infect. Immun. *54*, 820–826.

Mathew, R.C., Ragheb, S., and Boros, D.L. (1990). Recombinant IL-2 therapy reverses diminished granulomatous responsiveness in anti-L3T4-treated, Schistosoma mansoni-infected mice. J. Immunol. *144*, 4356–4361.

Mathieson, W., and Wilson, R.A. (2010). A comparative proteomic study of the undeveloped and developed Schistosoma mansoni egg and its contents: the miracidium, hatch fluid and secretions. Int. J. Parasitol. *40*, 617–628.

Matzinger, P. (1994). Tolerance, danger, and the extended family. Annu. Rev. Immunol. *12*, 991–1045.

Matzinger, P. (2002). An innate sense of danger. Ann. N. Y. Acad. Sci. *961*, 341–342.

McKee, A.S., and Pearce, E.J. (2004). CD25+CD4+ cells contribute to Th2 polarization during helminth infection by suppressing Th1 response development. J. Immunol. *173*, 1224–1231.

McKenna, H.J., Stocking, K.L., Miller, R.E., Brasel, K., De Smedt, T., Maraskovsky, E., Maliszewski, C.R., Lynch, D.H., Smith, J., Pulendran, B., et al. (2000). Mice lacking flt3 ligand have deficient hematopoiesis affecting hematopoietic progenitor cells, dendritic cells, and natural killer cells. Blood *95*, 3489–3497.

McKenzie, G.J., Fallon, P.G., Emson, C.L., Grencis, R.K., and McKenzie, A.N. (1999). Simultaneous disruption of interleukin (IL)-4 and IL-13 defines individual roles in T helper cell type 2-mediated responses. J. Exp. Med. *189*, 1565–1572.

McKinstry, K.K., Strutt, T.M., and Swain, S.L. (2010a). Regulation of CD4+ T-cell contraction during pathogen challenge. Immunol. Rev. *236*, 110–124.

McKinstry, K.K., Strutt, T.M., and Swain, S.L. (2010b). The potential of CD4 T-cell memory. Immunology *130*, 1–9.

Medoff, B.D., Seung, E., Hong, S., Thomas, S.Y., Sandall, B.P., Duffield, J.S., Kuperman, D.A., Erle, D.J., and Luster, A.D. (2009). CD11b+ Myeloid cells are the key mediators of TH2 cell homing into the airway in allergic inflammation. J. Immunol. *182*, 623-635.

Meevissen, M.H.J., Balog, C.I.A., Koeleman, C.A.M., Doenhoff, M.J., Schramm, G., Haas, H., Deelder, A.M., Wuhrer, M., and Hokke, C.H. (2011). Targeted glycoproteomic analysis reveals that kappa-5 is a major, uniquely glycosylated component of Schistosoma mansoni egg antigens. Mol. Cell Proteomics *10*, M110.005710.

Mellman, I., and Steinman, R.M. (2001). Dendritic cells: specialized and regulated antigen processing machines. Cell *106*, 255–258.

Merad, M., and Manz, M.G. (2009). Dendritic cell homeostasis. Blood *113*, 3418–3427.

Merad, M., Sathe, P., Helft, J., Miller, J., and Mortha, A. (2013). The dendritic cell lineage: ontogeny and function of dendritic cells and their subsets in the steady state and the inflamed setting. Annu. Rev. Immunol. *31*, 563–604.

Meredith, M.M., Liu, K., Darrasse-Jeze, G., Kamphorst, A.O., Schreiber, H.A., Guermonprez, P., Idoyaga, J., Cheong, C., Yao, K.-H., Niec, R.E., et al. (2012a). Expression of the zinc finger transcription factor zDC (Zbtb46, Btbd4) defines the classical dendritic cell lineage. J. Exp. Med. *209*, 1153–1165.

Meredith, M.M., Liu, K., Kamphorst, A.O., Idoyaga, J., Yamane, A., Guermonprez, P., Rihn, S., Yao, K.-H., Silva, I.T., Oliveira, T.Y., et al. (2012b). Zinc finger transcription factor zDC is a negative regulator required to prevent activation of classical dendritic cells in the steady state. J. Exp. Med. *209*, 1583–1593.

Metlay, J.P., Witmer-Pack, M.D., Agger, R., Crowley, M.T., Lawless, D., and Steinman, R.M. (1990). The distinct leukocyte integrins of mouse spleen dendritic cells as identified with new hamster monoclonal antibodies. J. Exp. Med. *171*, 1753–1771.

Metwali, A., Elliott, D., Blum, A.M., and Weinstock, J.V. (1993). Granuloma eosinophils enhance IL-5 production by lymphocytes from mice infected with Schistosoma mansoni. J. Immunol. *151*, 7048–7056.

Metwali, A., Elliott, D., Blum, A.M., Li, J., Sandor, M., Lynch, R., Noben-Trauth, N., and Weinstock, J.V. (1996). The granulomatous response in murine Schistosomiasis mansoni does not switch to Th1 in IL-4-deficient C57BL/6 mice. J. Immunol. *157*, 4546–4553.

Mildner, A., and Jung, S. (2014). Development and function of dendritic cell subsets. Immunity *40*, 642–656.

Mills, C.D. (2001). Macrophage arginine metabolism to ornithine/urea or nitric oxide/citrulline: a life or death issue. Crit. Rev. Immunol. *21*, 399–425.

Miyasaka, M., and Tanaka, T. (2004). Lymphocyte trafficking across high endothelial venules: dogmas and enigmas. Nat. Rev. Immunol. *4*, 360–370.

Mizoguchi, C., Uehara, S., Akira, S., and Takatsu, K. (1999). IL-5 induces IgG1 isotype switch recombination in mouse CD38-activated sIgD-positive B lymphocytes. J. Immunol. *162*, 2812–2819.

Mogensen, T.H. (2009). Pathogen Recognition and Inflammatory Signaling in Innate Immune Defenses. Clin. Microbiol. Rev. *22*, 240–273.

Mollenhauer, H.H., Morré, D.J., and Rowe, L.D. (1990). Alteration of intracellular traffic by monensin; mechanism, specificity and relationship to toxicity. Biochim. Biophys. Acta *1031*, 225–246.

Moore, D.L., Grove, D.I., and Warren, K.S. (1977). The Schistosoma mansoni egg granuloma: quantitation of cell populations. J. Pathol. *121*, 41–50.

Morelli, A.E., Zahorchak, A.F., Larregina, A.T., Colvin, B.L., Logar, A.J., Takayama, T., Falo, L.D., and Thomson, A.W. (2001). Cytokine production by mouse myeloid dendritic cells in relation to differentiation and terminal maturation induced by lipopolysaccharide or CD40 ligation. Blood *98*, 1512–1523.

Moriggl, R., Kristofic, C., Kinzel, B., Volarevic, S., Groner, B., and Brinkmann, V. (1998). Activation of STAT proteins and cytokine genes in human Th1 and Th2 cells generated in the absence of IL-12 and IL-4. J. Immunol. *160*, 3385–3392.

Morou, A., Palmer, B.E., and Kaufmann, D.E. (2014). Distinctive features of CD4+ T cell dysfunction in chronic viral infections. Curr. Opin. HIV AIDS *9*, 446–451.

Mosmann, T.R., Cherwinski, H., Bond, M.W., Giedlin, M.A., and Coffman, R.L. (1986). Two types of murine helper T cell clone. I. Definition according to profiles of lymphokine activities and secreted proteins. J. Immunol. *136*, 2348–2357.

Mullen, A.C., High, F.A., Hutchins, A.S., Lee, H.W., Villarino, A.V., Livingston, D.M., Kung, A.L., Cereb, N., Yao, T.P., Yang, S.Y., et al. (2001). Role of T-bet in

commitment of TH1 cells before IL-12-dependent selection. Science *292*, 1907–1910.

Murphy, E., Shibuya, K., Hosken, N., Openshaw, P., Maino, V., Davis, K., Murphy, K., and O'Garra, A. (1996). Reversibility of T helper 1 and 2 populations is lost after long-term stimulation. J. Exp. Med. *183*, 901–913.

Murphy, K.M., and Stockinger, B. (2010). Effector T cell plasticity: flexibility in the face of changing circumstances. Nature Publishing Group *11*, 674–680.

Murphy, K., Mowat, A., and Weaver, C. (2014). Janeway's Immunobiology. Garland Science.

Murphy, T.L., Tussiwand, R., and Murphy, K.M. (2013). Specificity through cooperation: BATF-IRF interactions control immune-regulatory networks. Nat. Rev. Immunol. *13*, 499–509.

Murray, P.J., and Wynn, T.A. (2011). Protective and pathogenic functions of macrophage subsets. Nat. Rev. Immunol. *11*, 723–737.

Mwatha, J.K., Kimani, G., Kamau, T., Mbugua, G.G., Ouma, J.H., Mumo, J., Fulford, A.J., Jones, F.M., Butterworth, A.E., Roberts, M.B., et al. (1998). High levels of TNF, soluble TNF receptors, soluble ICAM-1, and IFN-gamma, but low levels of IL-5, are associated with hepatosplenic disease in human schistosomiasis mansoni. J. Immunol. *160*, 1992–1999.

Nabors, G.S., Afonso, L.C., Farrell, J.P., and Scott, P. (1995). Switch from a type 2 to a type 1 T helper cell response and cure of established Leishmania major infection in mice is induced by combined therapy with interleukin 12 and Pentostam. Proc. Natl. Acad. Sci. U.S.A. *92*, 3142–3146.

Naik, S.H., Metcalf, D., van Nieuwenhuijze, A., Wicks, I., Wu, L., O'Keeffe, M., and Shortman, K. (2006). Intrasplenic steady-state dendritic cell precursors that are distinct from monocytes. Nat. Immunol. *7*, 663–671.

Naik, S.H., Proietto, A.I., Wilson, N.S., Dakic, A., Schnorrer, P., Fuchsberger, M., Lahoud, M.H., O'Keeffe, M., Shao, Q.-X., Chen, W.-F., et al. (2005). Cutting edge: generation of splenic CD8+ and CD8- dendritic cell equivalents in Fms-like tyrosine kinase 3 ligand bone marrow cultures. J. Immunol. *174*, 6592–6597.

Naik, S.H., Sathe, P., Park, H.-Y., Metcalf, D., Proietto, A.I., Dakic, A., Carotta, S., O'Keeffe, M., Bahlo, M., Papenfuss, A., et al. (2007). Development of plasmacytoid and conventional dendritic cell subtypes from single precursor cells derived in vitro and in vivo. Nat. Immunol. *8*, 1217–1226.

Nakazawa, M., Fantappie, M.R., Freeman, G.L., Eloi-Santos, S., Olsen, N.J., Kovacs, W.J., Secor, W.E., and Colley, D.G. (1997). Schistosoma mansoni: susceptibility differences between male and female mice can be mediated by testosterone during early infection. Exp. Parasitol. *85*, 233–240.

Nascimento, M., Huang, S.C., Smith, A., Everts, B., Lam, W., Bassity, E., Gautier, E.L., Randolph, G.J., and Pearce, E.J. (2014). Ly6Chi monocyte recruitment is responsible for Th2 associated host-protective macrophage accumulation in liver inflammation due to schistosomiasis. PLoS Pathog. *10*, e1004282.

Neefjes, J., Jongsma, M.L.M., Paul, P., and Bakke, O. (2011). Towards a systems understanding of MHC class I and MHC class II antigen presentation. Nat. Rev. Immunol. *11*, 823–836.

Neill, D.R., Wong, S.H., Bellosi, A., Flynn, R.J., Daly, M., Langford, T.K.A., Bucks, C., Kane, C.M., Fallon, P.G., Pannell, R., et al. (2010). Nuocytes represent a new innate effector leukocyte that mediates type-2 immunity. Nature *464*, 1367–1370.

Ngo, V.N., Tang, H.L., and Cyster, J.G. (1998). Epstein-Barr virus-induced molecule 1 ligand chemokine is expressed by dendritic cells in lymphoid tissues and strongly attracts naive T cells and activated B cells. J. Exp. Med. *188*, 181–191.

Niess, J.H., Brand, S., Gu, X., Landsman, L., Jung, S., McCormick, B.A., Vyas, J.M., Boes, M., Ploegh, H.L., Fox, J.G., et al. (2005). CX3CR1-mediated dendritic cell access to the intestinal lumen and bacterial clearance. Science *307*, 254–258.

Nishikomori, R., Ehrhardt, R.O., and Strober, W. (2000). T helper type 2 cell differentiation occurs in the presence of interleukin 12 receptor beta2 chain expression and signaling. J. Exp. Med. *191*, 847–858.

Nobumoto, A., Oomizu, S., Arikawa, T., Katoh, S., Nagahara, K., Miyake, M., Nishi, N., Takeshita, K., Niki, T., Yamauchi, A., et al. (2009). Galectin-9 expands unique macrophages exhibiting plasmacytoid dendritic cell-like phenotypes that activate NK cells in tumor-bearing mice. Clin. Immunol. *130*, 322–330.

Nurieva, R., Yang, X.O., Martinez, G., Zhang, Y., Panopoulos, A.D., Ma, L., Schluns, K., Tian, Q., Watowich, S.S., Jetten, A.M., et al. (2007). Essential autocrine regulation by IL-21 in the generation of inflammatory T cells. Nature *448*, 480–483.

O'Brien, R.L., Roark, C.L., and Born, W.K. (2009). IL-17-producing gammadelta T cells. Eur. J. Immunol. *39*, 662–666.

Ohnmacht, C., Schwartz, C., Panzer, M., Schiedewitz, I., Naumann, R., and Voehringer, D. (2010). Basophils orchestrate chronic allergic dermatitis and protective immunity against helminths. Immunity *33*, 364–374.

Ohshima, Y., Tanaka, Y., Tozawa, H., Takahashi, Y., Maliszewski, C., and Delespesse, G. (1997). Expression and function of OX40 ligand on human dendritic cells. J. Immunol. *159*, 3838–3848.

Okano, M., Satoskar, A.R., Nishizaki, K., Abe, M., and Harn, D.A. (1999). Induction of Th2 responses and IgE is largely due to carbohydrates functioning as adjuvants on Schistosoma mansoni egg antigens. J. Immunol. *163*, 6712–6717.

Okano, M., Satoskar, A.R., Nishizaki, K., and Harn, D.A. (2001). Lacto-N-

fucopentaose III found on Schistosoma mansoni egg antigens functions as adjuvant for proteins by inducing Th2-type response. J. Immunol. *167*, 442–450.

Okoye, I.S., and Wilson, M.S. (2011). CD4+ T helper 2 cells--microbial triggers, differentiation requirements and effector functions. Immunology *134*, 368–377.

Olds, G.R., and Mahmoud, A.A. (1980). Role of host granulomatous response in murine schistosomiasis mansoni. eosinophil-mediated destruction of eggs. J. Clin. Invest. *66*, 1191–1199.

Oliphant, C.J., Hwang, Y.Y., Walker, J.A., Salimi, M., Wong, S.H., Brewer, J.M., Englezakis, A., Barlow, J.L., Hams, E., Scanlon, S.T., et al. (2014). MHCII-Mediated Dialog between Group 2 Innate Lymphoid Cells and CD4+ T Cells Potentiates Type 2 Immunity and Promotes Parasitic Helminth Expulsion. Immunity *41,* 1–13.

Oliveira, K.C., Carvalho, M.L.P., Venancio, T.M., Miyasato, P.A., Kawano, T., DeMarco, R., and Verjovski-Almeida, S. (2009). Identification of the Schistosoma mansoni TNF-alpha receptor gene and the effect of human TNF-alpha on the parasite gene expression profile. PLoS Negl. Trop. Dis. *3*, e556.

Olsen, I., and Sollid, L.M. (2013). Pitfalls in determining the cytokine profile of human T cells. J. Immunol. Methods *390*, 106–112.

Oswald, I.P., Caspar, P., Jankovic, D., Wynn, T.A., Pearce, E.J., and Sher, A. (1994). IL-12 inhibits Th2 cytokine responses induced by eggs of Schistosoma mansoni. J. Immunol. *153*, 1707–1713.

Oswald, I.P., Gazzinelli, R.T., Sher, A., and James, S.L. (1992). IL-10 synergizes with IL-4 and transforming growth factor-beta to inhibit macrophage cytotoxic activity. J. Immunol. *148*, 3578–3582.

Otsuka, A., Nakajima, S., Kubo, M., Egawa, G., Honda, T., Kitoh, A., Nomura, T., Hanakawa, S., Sagita Moniaga, C., Kim, B., et al. (2013). Basophils are required for the induction of Th2 immunity to haptens and peptide antigens. Nat. Commun. *4*, 1739.

Ouyang, W., Ranganath, S.H., Weindel, K., Bhattacharya, D., Murphy, T.L., Sha, W.C., and Murphy, K.M. (1998). Inhibition of Th1 development mediated by GATA-3 through an IL-4-independent mechanism. Immunity *9*, 745–755.

Paludan, S.R. (1998). Interleukin-4 and interferon-gamma: the quintessence of a mutual antagonistic relationship. Scand. J. Immunol. *48*, 459–468.

Park, H., Li, Z., Yang, X.O., Chang, S.H., Nurieva, R., Wang, Y.-H., Wang, Y., Hood, L., Zhu, Z., Tian, Q., et al. (2005). A distinct lineage of CD4 T cells regulates tissue inflammation by producing interleukin 17. Nat. Immunol. *6*, 1133–1141.

Parker, D.C. (1993). The functions of antigen recognition in T cell-dependent B cell activation. Semin. Immunol. *5*, 413–420.

Patton, E.A., Brunet, L.R., La Flamme, A.C., Pedras-Vasconcelos, J., Kopf, M., and Pearce, E.J. (2001). Severe schistosomiasis in the absence of interleukin-4 (IL-4) is IL-12 independent. Infect. Immun. *69*, 589–592.

Paul, W.E., and Zhu, J. (2010). How are TH2-type immune responses initiated and amplified? Nat. Rev. Immunol. *10*, 225–235.

Pauschinger, M., Knopf, D., Petschauer, S., Doerner, A., Poller, W., Schwimmbeck, P.L., Kühl, U., and Schultheiss, H.P. (1999). Dilated cardiomyopathy is associated with significant changes in collagen type I/III ratio. Circulation *99*, 2750–2756.

Pearce, E.J., Caspar, P., Grzych, J.M., Lewis, F.A., and Sher, A. (1991). Downregulation of Th1 cytokine production accompanies induction of Th2 responses by a parasitic helminth, Schistosoma mansoni. J. Exp. Med. *173*, 159–166.

Pearce, E.J., La Flamme, A., Sabin, E., and Brunet, L.R. (1998). The initiation and function of Th2 responses during infection with Schistosoma mansoni. Adv. Exp. Med. Biol. *452*, 265–270.

Pearce, E.J., and MacDonald, A.S. (2002). The immunobiology of schistosomiasis. Nat. Rev. Immunol. *2*, 499–511.

Pedras-Vasconcelos, J.A., and Pearce, E.J. (1996). Type 1 CD8+ T cell responses during infection with the helminth Schistosoma mansoni. J. Immunol. *157*, 3046–3053.

Peine, M., Rausch, S., Helmstetter, C., Fröhlich, A., Hegazy, A.N., Kühl, A.A., Grevelding, C.G., Höfer, T., Hartmann, S., and Löhning, M. (2013). Stable T-bet(+)GATA-3(+) Th1/Th2 hybrid cells arise in vivo, can develop directly from naive precursors, and limit immunopathologic inflammation. PLoS Biol. *11*, e1001633.

Pene, J., Rousset, F., Brière, F., Chrétien, I., Bonnefoy, J.Y., Spits, H., Yokota, T., Arai, N., Arai, K., and Banchereau, J. (1988). IgE production by normal human lymphocytes is induced by interleukin 4 and suppressed by interferons gamma and alpha and prostaglandin E2. Proc. Natl. Acad. Sci. U.S.A. *85*, 6880–6884.

Perona-Wright, G., Jenkins, S.J., and MacDonald, A.S. (2006). Dendritic cell activation and function in response to Schistosoma mansoni. Int. J. Parasitol. *36*, 711–721.

Perona-Wright, G., Jenkins, S.J., O'Connor, R.A., Zienkiewicz, D., McSorley, H.J., Maizels, R.M., Anderton, S.M., and MacDonald, A.S. (2009). A pivotal role for CD40-mediated IL-6 production by dendritic cells during IL-17 induction in vivo. J. Immunol. *182*, 2808–2815.

Perona-Wright, G., Lundie, R.J., Jenkins, S.J., Webb, L.M., Grencis, R.K., and MacDonald, A.S. (2012). Concurrent bacterial stimulation alters the function of helminth-activated dendritic cells, resulting in IL-17 induction. J. Immunol. *188*, 2350–2358.

Perrigoue, J.G., Saenz, S.A., Siracusa, M.C., Allenspach, E.J., Taylor, B.C., Giacomin, P.R., Nair, M.G., Du, Y., Zaph, C., Van Rooijen, N., et al. (2009). MHC class II-dependent basophil-CD4+ T cell interactions promote T(H)2 cytokine-dependent immunity. Nature Publishing Group *10*, 697–705.

Perros, F., Hoogsteden, H.C., Coyle, A.J., Lambrecht, B.N., and Hammad, H. (2009). Blockade of CCR4 in a humanized model of asthma reveals a critical role for DC-derived CCL17 and CCL22 in attracting Th2 cells and inducing airway inflammation. Allergy *64*, 995–1002.

Persson, E.K., Uronen-Hansson, H., Semmrich, M., Rivollier, A., Hägerbrand, K., Marsal, J., Gudjonsson, S., Håkansson, U., Reizis, B., Kotarsky, K., et al. (2013). IRF4 transcription-factor-dependent CD103(+)CD11b(+) dendritic cells drive mucosal T helper 17 cell differentiation. Immunity *38*, 958–969.

Perše, M., and Cerar, A. (2012). Dextran sodium sulphate colitis mouse model: traps and tricks. J. Biomed. Biotechnol. *2012*, 718617.

Pesce, J.T., Ramalingam, T.R., Mentink-Kane, M.M., Wilson, M.S., Kasmi, El, K.C., Smith, A.M., Thompson, R.W., Cheever, A.W., Murray, P.J., and Wynn, T.A. (2009). Arginase-1-expressing macrophages suppress Th2 cytokine-driven inflammation and fibrosis. PLoS Pathog. *5*, e1000371.

Phythian-Adams, A.T., Cook, P.C., Lundie, R.J., Jones, L.H., Smith, K.A., Barr, T.A., Hochweller, K., Anderton, S.M., Hammerling, G.J., Maizels, R.M., et al. (2010). CD11c depletion severely disrupts Th2 induction and development in vivo. J. Exp. Med. *207*, 2089–2096.

Pillai, S., and Cariappa, A. (2009). The follicular versus marginal zone B lymphocyte cell fate decision. Nature Publishing Group *9*, 767–777.

Pillarisetty, V.G., Shah, A.B., Miller, G., Bleier, J.I., and Dematteo, R.P. (2004). Liver dendritic cells are less immunogenic than spleen dendritic cells because of differences in subtype composition. J. Immunol. *172*, 1009–1017.

Pinto, A.K., Daffis, S., Brien, J.D., Gainey, M.D., Yokoyama, W.M., Sheehan, K.C.F., Murphy, K.M., Schreiber, R.D., and Diamond, M.S. (2011). A temporal role of type I interferon signaling in CD8+ T cell maturation during acute West Nile virus infection. PLoS Pathog. *7*, e1002407.

Piva, L., Tetlak, P., Claser, C., Karjalainen, K., Renia, L., and Ruedl, C. (2012). Cutting edge: Clec9A+ dendritic cells mediate the development of experimental cerebral malaria. J. Immunol. *189*, 1128–1132.

Plantinga, M., Guilliams, M., Vanheerswynghels, M., Deswarte, K., Branco-Madeira, F., Toussaint, W., Vanhoutte, L., Neyt, K., Killeen, N., Malissen, B., et al. (2013). Conventional and monocyte-derived CD11b(+) dendritic cells initiate and maintain T helper 2 cell-mediated immunity to house dust mite allergen. Immunity *38*, 322–335.

Poltorak, A., He, X., Smirnova, I., Liu, M.Y., Van Huffel, C., Du, X., Birdwell, D., Alejos, E., Silva, M., Galanos, C., et al. (1998). Defective LPS signaling in C3H/HeJ and C57BL/10ScCr mice: mutations in Tlr4 gene. Science *282*, 2085–2088.

Poulin, L.F., Henri, S., de Bovis, B., Devilard, E., Kissenpfennig, A., and Malissen, B. (2007). The dermis contains langerin+ dendritic cells that develop and function independently of epidermal Langerhans cells. J. Exp. Med. *204*, 3119–3131.

Poulin, L.F., Salio, M., Griessinger, E., Anjos-Afonso, F., Craciun, L., Chen, J.-L., Keller, A.M., Joffre, O., Zelenay, S., Nye, E., et al. (2010). Characterization of human DNGR-1+ BDCA3+ leukocytes as putative equivalents of mouse CD8alpha+ dendritic cells. J. Exp. Med. *207*, 1261–1271.

Pradere, J.-P., Kluwe, J., De Minicis, S., Jiao, J.-J., Gwak, G.-Y., Dapito, D.H., Jang, M.-K., Guenther, N.D., Mederacke, I., Friedman, R., et al. (2013). Hepatic macrophages but not dendritic cells contribute to liver fibrosis by promoting the survival of activated hepatic stellate cells in mice. Hepatology *58*, 1461–1473.

Protzer, U., Maini, M.K., and Knolle, P.A. (2012). Living in the liver: hepatic infections. Nat. Rev. Immunol. *12*, 201–213.

Pulendran, B., Smith, J.L., Caspary, G., Brasel, K., Pettit, D., Maraskovsky, E., and Maliszewski, C.R. (1999). Distinct dendritic cell subsets differentially regulate the class of immune response in vivo. Proc. Natl. Acad. Sci. U.S.A. *96*, 1036–1041.

Pulendran, B., and Artis, D. (2012). New paradigms in type 2 immunity. Science *337*, 431–435.

Qu, C., Nguyen, V.A., Merad, M., and Randolph, G.J. (2009). MHC class I/peptide transfer between dendritic cells overcomes poor cross-presentation by monocyte-derived APCs that engulf dying cells. J. Immunol. *182*, 3650–3659.

Qureshi, O.S., Zheng, Y., Nakamura, K., Attridge, K., Manzotti, C., Schmidt, E.M., Baker, J., Jeffery, L.E., Kaur, S., Briggs, Z., et al. (2011). Trans-endocytosis of CD80 and CD86: a molecular basis for the cell-extrinsic function of CTLA-4. Science *332*, 600–603.

Racoosin, E.L., and Swanson, J.A. (1989). Macrophage colony-stimulating factor (rM-CSF) stimulates pinocytosis in bone marrow-derived macrophages. J. Exp. Med. *170*, 1635–1648.

Racoosin, E.L., and Swanson, J.A. (1992). M-CSF-induced macropinocytosis increases solute endocytosis but not receptor-mediated endocytosis in mouse macrophages. J. Cell Sci. *102 (Pt 4)*, 867–880.

Rahman, A.H., and Aloman, C. (2013). Dendritic cells and liver fibrosis. Biochim. Biophys. Acta *1832*, 998–1004.

Rahman, H., Qasim, M., Schultze, F.C., Oellerich, M., and R Asif, A. (2011). Fetal calf serum heat inactivation and lipopolysaccharide contamination influence the

human T lymphoblast proteome and phosphoproteome. Proteome Sci. *9*, 71.

Redmond, W.L., Ruby, C.E., and Weinberg, A.D. (2009). The role of OX40-mediated co-stimulation in T-cell activation and survival. Crit. Rev. Immunol. *29*, 187–201.

Reiman, R.M., Thompson, R.W., Feng, C.G., Hari, D., Knight, R., Cheever, A.W., Rosenberg, H.F., and Wynn, T.A. (2006). Interleukin-5 (IL-5) augments the progression of liver fibrosis by regulating IL-13 activity. Infect. Immun. *74*, 1471–1479.

Reis e Sousa, C., Hieny, S., Scharton-Kersten, T., Jankovic, D., Charest, H., Germain, R.N., and Sher, A. (1997). In vivo microbial stimulation induces rapid CD40 ligand-independent production of interleukin 12 by dendritic cells and their redistribution to T cell areas. J. Exp. Med. *186*, 1819–1829.

Reizis, B. (2010). Regulation of plasmacytoid dendritic cell development. Curr. Opin. Immunol. *22*, 206–211.

Reizis, B., Bunin, A., Ghosh, H.S., Lewis, K.L., and Sisirak, V. (2011). Plasmacytoid Dendritic Cells: Recent Progress and Open Questions. Annu. Rev. Immunol. *29*, 163–183.

Richter, A. (1999). Instruction for Cytokine Expression in T Helper Lymphocytes in Relation to Proliferation and Cell Cycle Progression. J. Exp. Med. *190*, 1439–1450.

Rizzitelli, A., Vremec, D., Villadangos, J.A., Mavaddat, N., Wright, M.D., and Shortman, K. (2005). Switching from a restricted to an effective CD4 T cell response by activating CD8+ murine dendritic cells with a Toll-like receptor 9 ligand. Eur. J. Immunol. *35*, 3209–3220.

Robays, L.J., Maes, T., Lebecque, S., Lira, S.A., Kuziel, W.A., Brusselle, G.G., Joos, G.F., and Vermaelen, K.V. (2007). Chemokine receptor CCR2 but not CCR5 or CCR6 mediates the increase in pulmonary dendritic cells during allergic airway inflammation. J. Immunol. *178*, 5305–5311.

Rodriguez, P.C., Quiceno, D.G., and Ochoa, A.C. (2007). L-arginine availability regulates T-lymphocyte cell-cycle progression. Blood *109*, 1568–1573.

Rogge, L., Papi, A., Presky, D.H., Biffi, M., Minetti, L.J., Miotto, D., Agostini, C., Semenzato, G., Fabbri, L.M., and Sinigaglia, F. (1999). Antibodies to the IL-12 receptor beta 2 chain mark human Th1 but not Th2 cells in vitro and in vivo. J. Immunol. *162*, 3926–3932.

Ross, A.G.P., Bartley, P.B., Sleigh, A.C., Olds, G.R., Li, Y., Williams, G.M., and McManus, D.P. (2002). Schistosomiasis. N. Engl. J. Med. *346*, 1212–1220.

Rothenberg, M.E., and Hogan, S.P. (2006). The Eosinophil. Annu. Rev. Immunol. *24*, 147–174.

Rousset, F., Malefijt, R.W., Slierendregt, B., Aubry, J.P., Bonnefoy, J.Y., Defrance, T., Banchereau, J., and de Vries, J.E. (1988). Regulation of Fc receptor for IgE (CD23) and class II MHC antigen expression on Burkitt's lymphoma cell lines by human IL-4 and IFN-gamma. J. Immunol. *140*, 2625–2632.

Rulifson, I.C., Sperling, A.I., Fields, P.E., Fitch, F.W., and Bluestone, J.A. (1997). CD28 costimulation promotes the production of Th2 cytokines. J. Immunol. *158*, 658–665.

Rumbley, C.A., and Phillips, S.M. (1999). The schistosome granuloma: an immunoregulatory organelle. Microbes Infect. *1*, 499–504.

Rumbley, C.A., Sugaya, H., Zekavat, S.A., Refaei, El, M., Perrin, P.J., and Phillips, S.M. (1999). Activated eosinophils are the major source of Th2-associated cytokines in the schistosome granuloma. J. Immunol. *162*, 1003–1009.

Rutitzky, L.I., and Stadecker, M.J. (2006). CD4 T cells producing pro-inflammatory interleukin-17 mediate high pathology in schistosomiasis. Mem. Inst. Oswaldo Cruz *101 Suppl 1*, 327–330.

Rutitzky, L.I., and Stadecker, M.J. (2011). Exacerbated egg-induced immunopathology in murine Schistosoma mansoni infection is primarily mediated by IL-17 and restrained by IFN-γ. Eur. J. Immunol. *41*, 2677–2687.

Sabin, E.A., Kopf, M.A., and Pearce, E.J. (1996). Schistosoma mansoni egg-induced early IL-4 production is dependent upon IL-5 and eosinophils. J. Exp. Med. *184*, 1871–1878.

Sadler, C.H., Rutitzky, L.I., Stadecker, M.J., and Wilson, R.A. (2003). IL-10 is crucial for the transition from acute to chronic disease state during infection of mice with Schistosoma mansoni. Eur. J. Immunol. *33*, 880–888.

Saeki, H., Moore, A.M., Brown, M.J., and Hwang, S.T. (1999). Cutting edge: secondary lymphoid-tissue chemokine (SLC) and CC chemokine receptor 7 (CCR7) participate in the emigration pathway of mature dendritic cells from the skin to regional lymph nodes. J. Immunol. *162*, 2472–2475.

Saenz, S.A., Siracusa, M.C., Perrigoue, J.G., Spencer, S.P., Urban, J.F., Tocker, J.E., Budelsky, A.L., Kleinschek, M.A., Kastelein, R.A., Kambayashi, T., et al. (2010). IL25 elicits a multipotent progenitor cell population that promotes T(H)2 cytokine responses. Nature *464*, 1362–1366.

Saito, T., Yokosuka, T., and Hashimoto-Tane, A. (2010). Dynamic regulation of T cell activation and co-stimulation through TCR-microclusters. FEBS Lett. *584*, 4865–4871.

Sakaguchi, S., Wing, K., Onishi, Y., Prieto-Martin, P., and Yamaguchi, T. (2009). Regulatory T cells: how do they suppress immune responses? Int. Immunol. *21*, 1105–1111.

Sallusto, F., Cella, M., Danieli, C., and Lanzavecchia, A. (1995). Dendritic cells use macropinocytosis and the mannose receptor to concentrate macromolecules in the major histocompatibility complex class II compartment: downregulation by cytokines and bacterial products. J. Exp. Med. *182*, 389–400.

Sallusto, F., Lenig, D., Mackay, C.R., and Lanzavecchia, A. (1998). Flexible programs of chemokine receptor expression on human polarized T helper 1 and 2 lymphocytes. J. Exp. Med. *187*, 875–883.

Salmond, R.J., and Zamoyska, R. (2011). The influence of mTOR on T helper cell differentiation and dendritic cell function. Eur. J. Immunol. *41*, 2137–2141.

Sancho, D., Mourão-Sá, D., Joffre, O.P., Schulz, O., Rogers, N.C., Pennington, D.J., Carlyle, J.R., and Reis E Sousa, C. (2008). Tumor therapy in mice via antigen targeting to a novel, DC-restricted C-type lectin. J. Clin. Invest. *118*, 2098–2110.

Sandler, N.G., Mentink-Kane, M.M., Cheever, A.W., and Wynn, T.A. (2003). Global gene expression profiles during acute pathogen-induced pulmonary inflammation reveal divergent roles for Th1 and Th2 responses in tissue repair. J. Immunol. *171*, 3655–3667.

Sapoznikov, A., Fischer, J.A.A., Zaft, T., Krauthgamer, R., Dzionek, A., and Jung, S. (2007). Organ-dependent in vivo priming of naive CD4+, but not CD8+, T cells by plasmacytoid dendritic cells. J. Exp. Med. *204*, 1923–1933.

Sarris, M., Andersen, K.G., Randow, F., Mayr, L., and Betz, A.G. (2008). Neuropilin-1 expression on regulatory T cells enhances their interactions with dendritic cells during antigen recognition. Immunity *28*, 402–413.

Sathe, P., Pooley, J., Vremec, D., Mintern, J., Jin, J.-O., Wu, L., Kwak, J.-Y., Villadangos, J.A., and Shortman, K. (2011). The acquisition of antigen cross-presentation function by newly formed dendritic cells. J. Immunol. *186*, 5184–5192.

Satpathy, A.T., Briseño, C.G., Lee, J.S., Ng, D., Manieri, N.A., KC, W., Wu, X., Thomas, S.R., Lee, W.-L., Turkoz, M., et al. (2013). Notch2-dependent classical dendritic cells orchestrate intestinal immunity to attaching-and-effacing bacterial pathogens. Nature Publishing Group *14*, 937–948.

Satpathy, A.T., KC, W., Albring, J.C., Edelson, B.T., Kretzer, N.M., Bhattacharya, D., Murphy, T.L., and Murphy, K.M. (2012a). Zbtb46 expression distinguishes classical dendritic cells and their committed progenitors from other immune lineages. J. Exp. Med. *209*, 1135–1152.

Satpathy, A.T., Wu, X., Albring, J.C., and Murphy, K.M. (2012b). Re(de)fining the dendritic cell lineage. Nature Publishing Group *13*, 1145–1154.

Savina, A., Jancic, C., Hugues, S., Guermonprez, P., Vargas, P., Moura, I.C., Lennon-Duménil, A.-M., Seabra, M.C., Raposo, G., and Amigorena, S. (2006). NOX2 controls phagosomal pH to regulate antigen processing during crosspresentation by dendritic cells. Cell *126*, 205–218.

Schaerli, P., Willimann, K., Lang, A.B., Lipp, M., Loetscher, P., and Moser, B. (2000). CXC chemokine receptor 5 expression defines follicular homing T cells with B cell helper function. J. Exp. Med. *192*, 1553–1562.

Schiavoni, G., Mattei, F., Sestili, P., Borghi, P., Venditti, M., Morse, H.C., Belardelli, F., and Gabriele, L. (2002). ICSBP is essential for the development of mouse type I interferon-producing cells and for the generation and activation of CD8alpha(+) dendritic cells. J. Exp. Med. *196*, 1415–1425.

Schindler, H., Lutz, M.B., Röllinghoff, M., and Bogdan, C. (2001). The production of IFN-gamma by IL-12/IL-18-activated macrophages requires STAT4 signaling and is inhibited by IL-4. J. Immunol. *166*, 3075–3082.

Schnorrer, P., Behrens, G.M.N., Wilson, N.S., Pooley, J.L., Smith, C.M., El-Sukkari, D., Davey, G., Kupresanin, F., Li, M., Maraskovsky, E., et al. (2006). The dominant role of CD8+ dendritic cells in cross-presentation is not dictated by antigen capture. Proc. Natl. Acad. Sci. U.S.A. *103*, 10729–10734.

Schraml, B.U., Hildner, K., Ise, W., Lee, W.-L., Smith, W.A.-E., Solomon, B., Sahota, G., Sim, J., Mukasa, R., Cemerski, S., et al. (2009). The AP-1 transcription factor Batf controls T(H)17 differentiation. Nature *460*, 405–409.

Schraml, B.U., van Blijswijk, J., Zelenay, S., Whitney, P.G., Filby, A., Acton, S.E., Rogers, N.C., Moncaut, N., Carvajal, J.J., and Sousa, C.R.E. (2013). Genetic Tracing via DNGR-1 Expression History Defines Dendritic Cells as a Hematopoietic Lineage. Cell *154*, 843–858.

Schramm, G., Gronow, A., Knobloch, J., Wippersteg, V., Grevelding, C.G., Galle, J., Fuller, H., Stanley, R.G., Chiodini, P.L., Haas, H., et al. (2006). IPSE/alpha-1: a major immunogenic component secreted from Schistosoma mansoni eggs. Mol. Biochem. Parasitol. *147*, 9–19.

Schramm, G., Falcone, F.H., Gronow, A., Haisch, K., Mamat, U., Doenhoff, M.J., Oliveira, G., Galle, J., Dahinden, C.A., and Haas, H. (2003). Molecular characterization of an interleukin-4-inducing factor from Schistosoma mansoni eggs. J. Biol. Chem. *278*, 18384–18392.

Schramm, G., Mohrs, K., Wodrich, M., Doenhoff, M.J., Pearce, E.J., Haas, H., and Mohrs, M. (2007). Cutting edge: IPSE/alpha-1, a glycoprotein from Schistosoma mansoni eggs, induces IgE-dependent, antigen-independent IL-4 production by murine basophils in vivo. J. Immunol. *178*, 6023–6027.

Schroder, K. (2003). Interferon- : an overview of signals, mechanisms and functions. J. Leukoc. Biol. *75*, 163–189.

Schuh, J.M., Power, C.A., Proudfoot, A.E., Kunkel, S.L., Lukacs, N.W., and Hogaboam, C.M. (2002). Airway hyperresponsiveness, but not airway remodeling, is attenuated during chronic pulmonary allergic responses to Aspergillus in CCR4-/- mice. FASEB J. *16*, 1313–1315.

Schwartz, R.H. (2003). T cell anergy. Annu. Rev. Immunol. *21*, 305–334.

Schwickert, T.A., Lindquist, R.L., Shakhar, G., Livshits, G., Skokos, D., Kosco-Vilbois, M.H., Dustin, M.L., and Nussenzweig, M.C. (2007). In vivo imaging of germinal centres reveals a dynamic open structure. Nature *446*, 83–87.

Scott, C.L., Aumeunier, A.M., and Mowat, A.M. (2011). Intestinal CD103+ dendritic cells: master regulators of tolerance? Trends Immunol. *32*, 412–419.

Scott, F.W. (2011). Flow cytometric analysis of intracellular IFN-g, IL-4 and IL-10 in CD3141 T-cells from rat spleen. J. Immunol. Methods 1–12.

Seder, R.A., Gazzinelli, R., Sher, A., and Paul, W.E. (1993). Interleukin 12 acts directly on CD4+ T cells to enhance priming for interferon gamma production and diminishes interleukin 4 inhibition of such priming. Proc. Natl. Acad. Sci. U.S.A. *90*, 10188–10192.

Serbina, N.V., Salazar-Mather, T.P., Biron, C.A., Kuziel, W.A., and Pamer, E.G. (2003). TNF/iNOS-producing dendritic cells mediate innate immune defense against bacterial infection. Immunity *19*, 59–70.

Seroogy, C.M., Soares, L., Ranheim, E.A., Su, L., Holness, C., Bloom, D., and Fathman, C.G. (2004). The gene related to anergy in lymphocytes, an E3 ubiquitin ligase, is necessary for anergy induction in CD4 T cells. J. Immunol. *173*, 79–85.

Shafiani, S., Dinh, C., Ertelt, J.M., Moguche, A.O., Siddiqui, I., Smigiel, K.S., Sharma, P., Campbell, D.J., Way, S.S., and Urdahl, K.B. (2013). Pathogen-Specific Treg Cells Expand Early during Mycobacterium tuberculosis Infection but Are Later Eliminated in Response to Interleukin-12. Immunity *38*, 1261–1270.

Shang, X., Qiu, B., Frait, K.A., Hu, J.S., Sonstein, J., Curtis, J.L., Lu, B., Gerard, C., and Chensue, S.W. (2000). Chemokine receptor 1 knockout abrogates natural killer cell recruitment and impairs type-1 cytokines in lymphoid tissue during pulmonary granuloma formation. Am. J. Pathol. *157*, 2055–2063.

Sher, A., Coffman, R.L., Hieny, S., Scott, P., and Cheever, A.W. (1990). Interleukin 5 is required for the blood and tissue eosinophilia but not granuloma formation induced by infection with Schistosoma mansoni. Proc. Natl. Acad. Sci. U.S.A. *87*, 61–65.

Sher, A., Fiorentino, D., Caspar, P., Pearce, E., and Mosmann, T. (1991). Production of IL-10 by CD4+ T lymphocytes correlates with down-regulation of Th1 cytokine synthesis in helminth infection. J. Immunol. *147*, 2713–2716.

Shin, H., and Wherry, E.J. (2007). CD8 T cell dysfunction during chronic viral infection. Curr. Opin. Immunol *19,* 408–415.

Shortman, K., and Heath, W.R. (2010). The CD8+ dendritic cell subset. Immunol. Rev. *234*, 18–31.

Shortman, K., Lahoud, M.H., and Caminschi, I. (2009). Improving vaccines by targeting antigens to dendritic cells. Exp. Mol. Med. *41*, 61–66.

Sica, A., Invernizzi, P., and Mantovani, A. (2014). Macrophage plasticity and polarization in liver homeostasis and pathology. Hepatology *59*, 2034–2042.

Siebenkotten, G., Esser, C., Wabl, M., and Radbruch, A. (1992). The murine IgG1/IgE class switch program. Eur. J. Immunol. *22*, 1827–1834.

Silva, L.M., Fernandes, A.L., Barbosa, A., Oliveira, I.R., and ANDRADE, Z.A. (2000). Significance of schistosomal granuloma modulation. Mem. Inst. Oswaldo Cruz *95*, 353–361.

Simpson, T.R., Quezada, S.A., and Allison, J.P. (2010). Regulation of CD4 T cell activation and effector function by inducible costimulator (ICOS). Curr. Opin. Immunol. *22*, 326–332.

Singh, K.P., Gerard, H.C., Hudson, A.P., Reddy, T.R., and Boros, D.L. (2005). Retroviral Foxp3 gene transfer ameliorates liver granuloma pathology in Schistosoma mansoni infected mice. Immunology *114*, 410–417.

Singh, R.P., Hasan, S., Sharma, S., Nagra, S., Yamaguchi, D.T., Wong, D., Bh, H., and Hossain, A. (2014). Th17 cells in inflammation and autoimmunity. Autoimmun Rev. *13,* 1174-1181.

Skokos, D., and Nussenzweig, M.C. (2007) CD8- DCs induce IL-12-independent Th1 differentiation through Delta 4 Notch-like ligand in response to bacterial LPS. J. Exp. Med. *204,* 1525-1531.

Smit, J.J., Rudd, B.D., and Lukacs, N.W. (2006). Plasmacytoid dendritic cells inhibit pulmonary immunopathology and promote clearance of respiratory syncytial virus. J. Exp. Med. *203*, 1153–1159.

Smith, K.A., Harcus, Y., Garbi, N., Hämmerling, G.J., MacDonald, A.S., and Maizels, R.M. (2012). Type 2 innate immunity in helminth infection is induced redundantly and acts autonomously following CD11c(+) cell depletion. Infect. Immun. *80*, 3481–3489.

Smith, P., Walsh, C.M., Mangan, N.E., Fallon, R.E., Sayers, J.R., McKenzie, A.N.J., and Fallon, P.G. (2004). Schistosoma mansoni worms induce anergy of T cells via selective up-regulation of programmed death ligand 1 on macrophages. J. Immunol. *173*, 1240–1248.

Smits, H.H., Hilkens, C.M., Kaliński, P., Kapsenberg, M.L., and Wierenga, E.A. (2001a). How to deal with polarized Th2 cells: exploring the Achilles' heel. Int. Arch. Allergy Immunol. *126*, 102–110.

Smits, H.H., van Rietschoten, J.G., Hilkens, C.M., Sayilir, R., Stiekema, F., Kapsenberg, M.L., and Wierenga, E.A. (2001b). IL-12-induced reversal of human Th2 cells is accompanied by full restoration of IL-12 responsiveness and loss of

GATA-3 expression. Eur. J. Immunol. *31*, 1055–1065.

Smyth, L.A., Harker, N., Turnbull, W., El-Doueik, H., Klavinskis, L., Kioussis, D., Lombardi, G., and Lechler, R. (2008). The relative efficiency of acquisition of MHC:peptide complexes and cross-presentation depends on dendritic cell type. J. Immunol. *181*, 3212–3220.

Snapper, C.M., Finkelman, F.D., and Paul, W.E. (1988). Differential regulation of IgG1 and IgE synthesis by interleukin 4. J. Exp. Med. *167*, 183–196.

Snapper, C.M., McIntyre, T.M., Mandler, R., Pecanha, L.M., Finkelman, F.D., Lees, A., and Mond, J.J. (1992). Induction of IgG3 secretion by interferon gamma: a model for T cell-independent class switching in response to T cell-independent type 2 antigens. J. Exp. Med. *175*, 1367–1371.

Soehnlein, O., and Lindbom, L. (2010). Phagocyte partnership during the onset and resolution of inflammation. Nat. Rev. Immunol. *10*, 427–439.

Sokol, C.L., Barton, G.M., Farr, A.G., and Medzhitov, R. (2008). A mechanism for the initiation of allergen-induced T helper type 2 responses. Nature Publishing Group *9*, 310–318.

Sokol, C.L., Chu, N.-Q., Yu, S., Nish, S.A., Laufer, T.M., and Medzhitov, R. (2009). Basophils function as antigen-presenting cells for an allergen-induced T helper type 2 response. Nature Publishing Group *10*, 713–721.

Solomon, B.D., Mueller, C., Chae, W.-J., Alabanza, L.M., and Bynoe, M.S. (2011). Neuropilin-1 attenuates autoreactivity in experimental autoimmune encephalomyelitis. Proc. Natl Acad. Sci. U.S.A. *108*, 2040–2045.

Sornasse, T., Larenas, P.V., Davis, K.A., de Vries, J.E., and Yssel, H. (1996). Differentiation and stability of T helper 1 and 2 cells derived from naive human neonatal CD4+ T cells, analyzed at the single-cell level. J. Exp. Med. *184*, 473–483.

Souza, A.L.S., Souza, P.R.S., Pereira, C.A., Fernandes, A., Guabiraba, R., Russo, R.C., Vieira, L.Q., Correa, A., Teixeira, M.M., and Negrao-Correa, D. (2011). Experimental Infection with Schistosoma mansoni in CCR5-Deficient Mice Is Associated with Increased Disease Severity, as CCR5 Plays a Role in Controlling Granulomatous Inflammation. Infect. Immun. *79*, 1741–1749.

Sprent, J., and Surh, C.D. (2011). Normal T cell homeostasis: the conversion of naive cells into memory-phenotype cells. Nature Publishing Group *12*, 478–484.

Stadecker, M.J. (1999). The regulatory role of the antigen-presenting cell in the development of hepatic immunopathology during infection with Schistosoma mansoni. Pathobiology *67*, 269–272.

Steinberg, M.S. (1996). Adhesion in development: an historical overview. Dev. Biol. *180*, 377–388.

Steinfelder, S., Andersen, J.F., Cannons, J.L., Feng, C.G., Joshi, M., Dwyer, D., Caspar, P., Schwartzberg, P.L., Sher, A., and Jankovic, D. (2009). The major component in schistosome eggs responsible for conditioning dendritic cells for Th2 polarization is a T2 ribonuclease (omega-1). J. Exp. Med. *206*, 1681–1690.

Steinman, R.M., and Cohn, Z.A. (1973). Identification of a novel cell type in peripheral lymphoid organs of mice. I. Morphology, quantitation, tissue distribution. J. Exp. Med. *137*, 1142–1162.

Steinman, R.M., Kaplan, G., Witmer, M.D., and Cohn, Z.A. (1979). Identification of a novel cell type in peripheral lymphoid organs of mice. V. Purification of spleen dendritic cells, new surface markers, and maintenance in vitro. J. Exp. Med. *149*, 1–16.

Steinman, R.M. (2012). Decisions about dendritic cells: past, present, and future. Annu. Rev. Immunol. *30*, 1–22.

Stevens, T.L., Bossie, A., Sanders, V.M., Fernandez-Botran, R., Coffman, R.L., Mosmann, T.R., and Vitetta, E.S. (1988). Regulation of antibody isotype secretion by subsets of antigen-specific helper T cells. Nature *334*, 255–258.

Strauch, U.G., Mueller, R.C., Li, X.Y., Cernadas, M., Higgins, J.M., Binion, D.G., and Parker, C.M. (2001). Integrin alpha E(CD103)beta 7 mediates adhesion to intestinal microvascular endothelial cell lines via an E-cadherin-independent interaction. J. Immunol. *166*, 3506–3514.

Straw, A.D., MacDonald, A.S., Denkers, E.Y., and Pearce, E.J. (2003). CD154 plays a central role in regulating dendritic cell activation during infections that induce Th1 or Th2 responses. J. Immunol. *170*, 727–734.

Sullivan, B.M., Liang, H.-E., Bando, J.K., Wu, D., Cheng, L.E., McKerrow, J.K., Allen, C.D.C., and Locksley, R.M. (2011). Genetic analysis of basophil function in vivo. Nature Publishing Group *12*, 527–535.

Sun, J.C., Lehar, S.M., and Bevan, M.J. (2006). Augmented IL-7 signaling during viral infection drives greater expansion of effector T cells but does not enhance memory. J. Immunol. *177*, 4458–4463.

Surh, C.D., and Sprent, J. (2008). Homeostasis of naive and memory T cells. Immunity *29*, 848–862.

Suzuki, S., Honma, K., Matsuyama, T., Suzuki, K., Toriyama, K., Akitoyo, I., Yamamoto, K., Suematsu, T., Nakamura, M., Yui, K., et al. (2004). Critical roles of interferon regulatory factor 4 in CD11bhighCD8alpha- dendritic cell development. Proc. Natl. Acad. Sci. U.S.A. *101*, 8981–8986.

Süss, G., and Shortman, K. (1996). A subclass of dendritic cells kills CD4 T cells via Fas/Fas-ligand-induced apoptosis. J. Exp. Med. *183*, 1789–1796.

Swartz, J.M., Dyer, K.D., Cheever, A.W., Ramalingam, T., Pesnicak, L.,

Domachowske, J.B., Lee, J.J., Lee, N.A., Foster, P.S., Wynn, T.A., et al. (2006). Schistosoma mansoni infection in eosinophil lineage-ablated mice. Blood *108*, 2420–2427.

Swiecki, M., Gilfillan, S., Vermi, W., Wang, Y., and Colonna, M. (2010). Plasmacytoid dendritic cell ablation impacts early interferon responses and antiviral NK and CD8(+) T cell accrual. Immunity *33*, 955–966.

Szabo, S.J., Jacobson, N.G., Dighe, A.S., Gubler, U., and Murphy, K.M. (1995). Developmental commitment to the Th2 lineage by extinction of IL-12 signaling. Immunity *2*, 665–675.

Szabo, S.J., Kim, S.T., Costa, G.L., Zhang, X., Fathman, C.G., and Glimcher, L.H. (2000). A novel transcription factor, T-bet, directs Th1 lineage commitment. Cell *100*, 655–669.

Takada, K., and Jameson, S.C. (2009). Naive T cell homeostasis: from awareness of space to a sense of place. Nat. Rev. Immunol. *9*, 823–832.

Takatsu, K., and Nakajima, H. (2008). IL-5 and eosinophilia. Curr. Opin. Immunol. *20*, 288–294.

Takeuchi, O., and Akira, S. (2010). Pattern recognition receptors and inflammation. Cell *140*, 805–820.

Tang, Q., Adams, J.Y., Tooley, A.J., Bi, M., Fife, B.T., Serra, P., Santamaria, P., Locksley, R.M., Krummel, M.F., and Bluestone, J.A. (2006). Visualizing regulatory T cell control of autoimmune responses in nonobese diabetic mice. Nat. Immunol. *7*, 83–92.

Tangye, S.G., Ma, C.S., Brink, R., and Deenick, E.K. (2013). The good, the bad and the ugly - TFH cells in human health and disease. Nat. Rev. Immunol. *13*, 412–426.

Taylor, J.J., Krawczyk, C.M., Mohrs, M., and Pearce, E.J. (2009). Th2 cell hyporesponsiveness during chronic murine schistosomiasis is cell intrinsic and linked to GRAIL expression. J. Clin. Invest. *119*, 1019–1028.

Taylor, J.J., Mohrs, M., and Pearce, E.J. (2006). Regulatory T cell responses develop in parallel to Th responses and control the magnitude and phenotype of the Th effector population. J. Immunol. *176*, 5839–5847.

Tesseur, I., Zou, K., Berber, E., Zhang, H., and Wyss-Coray, T. (2006). Highly sensitive and specific bioassay for measuring bioactive TGF-beta. BMC Cell Biol. *7*, 15.

Théry, C., Duban, L., Segura, E., Véron, P., Lantz, O., and Amigorena, S. (2002). Indirect activation of naïve CD4+ T cells by dendritic cell-derived exosomes. Nat. Immunol. *3*, 1156–1162.

Thierfelder, W.E., van Deursen, J.M., Yamamoto, K., Tripp, R.A., Sarawar, S.R.,

Carson, R.T., Sangster, M.Y., Vignali, D.A., Doherty, P.C., Grosveld, G.C., et al. (1996). Requirement for Stat4 in interleukin-12-mediated responses of natural killer and T cells. Nature *382*, 171–174.

Thomas, P.G., Carter, M.R., Atochina, O., Da'Dara, A.A., Piskorska, D., McGuire, E., and Harn, D.A. (2003). Maturation of dendritic cell 2 phenotype by a helminth glycan uses a Toll-like receptor 4-dependent mechanism. J. Immunol. *171*, 5837–5841.

Thomas, P.G., Carter, M.R., Da'Dara, A.A., DeSimone, T.M., and Harn, D.A. (2005). A helminth glycan induces APC maturation via alternative NF-kappa B activation independent of I kappa B alpha degradation. J. Immunol. *175*, 2082–2090.

Throsby, M., Herbelin, A., Pléau, J.M., and Dardenne, M. (2000). CD11c+ eosinophils in the murine thymus: developmental regulation and recruitment upon MHC class I-restricted thymocyte deletion. J. Immunol. *165*, 1965–1975.

Tilney, N.L. (1971). Patterns of lymphatic drainage in the adult laboratory rat. J. Anat. *109*, 369–383.

Tjota, M.Y., and Sperling, A.I. (2014). Distinct dendritic cell subsets actively induce Th2 polarization. Curr. Opin. Immunol. *31C*, 44–50.

Tokita, D., Sumpter, T.L., Raimondi, G., Zahorchak, A.F., Wang, Z., Nakao, A., Mazariegos, G.V., Abe, M., and Thomson, A.W. (2008). Poor allostimulatory function of liver plasmacytoid DC is associated with pro-apoptotic activity, dependent on regulatory T cells. J. Hepatol. *49*, 1008–1018.

Torti, N., Walton, S.M., Murphy, K.M., and Oxenius, A. (2011). Batf3 transcription factor-dependent DC subsets in murine CMV infection: differential impact on T-cell priming and memory inflation. Eur. J. Immunol. *41*, 2612–2618.

Trickett, A., and Kwan, Y.L. (2003). T cell stimulation and expansion using anti-CD3/CD28 beads. J. Immunol. Methods *275*, 251–255.

Trinchieri, G. (2003). Interleukin-12 and the regulation of innate resistance and adaptive immunity. Nat. Rev. Immunol. *3*, 133–146.

Trombetta, E.S., Ebersold, M., Garrett, W., Pypaert, M., and Mellman, I. (2003). Activation of lysosomal function during dendritic cell maturation. Science *299*, 1400–1403.

Tsujimura, H., Tamura, T., and Ozato, K. (2003). Cutting edge: IFN consensus sequence binding protein/IFN regulatory factor 8 drives the development of type I IFN-producing plasmacytoid dendritic cells. J. Immunol. *170*, 1131–1135.

Tsushima, F., Yao, S., Shin, T., Flies, A., Flies, S., Xu, H., Tamada, K., Pardoll, D.M., and Chen, L. (2007). Interaction between B7-H1 and PD-1 determines initiation and reversal of T-cell anergy. Blood *110*, 180–185.

Turner, J.D., Jenkins, G.R., Hogg, K.G., Aynsley, S.A., Paveley, R.A., Cook, P.C., Coles, M.C., and Mountford, A.P. (2011). CD4+CD25+ regulatory cells contribute to the regulation of colonic Th2 granulomatous pathology caused by schistosome infection. PLoS Negl. Trop. Dis. *5*, e1269.

Tussiwand, R., Lee, W.-L., Murphy, T.L., Mashayekhi, M., Wumesh, K.C., Albring, J.C., Satpathy, A.T., Rotondo, J.A., Edelson, B.T., Kretzer, N.M., et al. (2012). Compensatory dendritic cell development mediated by BATF-IRF interactions. Nature *490*, 502–507.

Usui, T., Preiss, J.C., Kanno, Y., Yao, Z.J., Bream, J.H., O'Shea, J.J., and Strober, W. (2006). T-bet regulates Th1 responses through essential effects on GATA-3 function rather than on IFNG gene acetylation and transcription. J. Exp. Med. *203*, 755–766.

Van Belle, T.L., Dooms, H., Boonefaes, T., Wei, X.-Q., Leclercq, G., and Grooten, J. (2012). IL-15 augments TCR-induced CD4+ T cell expansion in vitro by inhibiting the suppressive function of CD25 High CD4+ T cells. PLoS ONE *7*, e45299.

van Blijswijk, J., Schraml, B.U., and Reis E Sousa, C. (2013). Advantages and limitations of mouse models to deplete dendritic cells. Eur. J. Immunol. *43*, 22–26.

van Blijswijk, J., Schraml, B.U., Rogers, N.C., Whitney, P.G., Zelenay, S., Acton, S.E., and Reis E Sousa, C. (2014). Altered Lymph Node Composition in Diphtheria Toxin Receptor-Based Mouse Models To Ablate Dendritic Cells. J. Immunol. *194,* 307-315.

van der Werf, M.J., de Vlas, S.J., Brooker, S., Looman, C.W.N., Nagelkerke, N.J.D., Habbema, J.D.F., and Engels, D. (2003). Quantification of clinical morbidity associated with schistosome infection in sub-Saharan Africa. Acta Trop. *86*, 125–139.

van Liempt, E., van Vliet, S.J., Engering, A., García Vallejo, J.J., Bank, C.M.C., Sanchez-Hernandez, M., van Kooyk, Y., and van Die, I. (2007). Schistosoma mansoni soluble egg antigens are internalized by human dendritic cells through multiple C-type lectins and suppress TLR-induced dendritic cell activation. Mol. Immunol. *44*, 2605–2615.

van Rijt, L.S., Jung, S., Kleinjan, A., Vos, N., Willart, M., Duez, C., Hoogsteden, H.C., and Lambrecht, B.N. (2005). In vivo depletion of lung CD11c+ dendritic cells during allergen challenge abrogates the characteristic features of asthma. J. Exp. Med. *201*, 981–991.

van Rijt, L.S., Prins, J.-B., Leenen, P.J.M., Thielemans, K., de Vries, V.C., Hoogsteden, H.C., and Lambrecht, B.N. (2002). Allergen-induced accumulation of airway dendritic cells is supported by an increase in CD31(hi)Ly-6C(neg) bone marrow precursors in a mouse model of asthma. Blood *100*, 3663–3671.

Vander Lugt, B., Khan, A.A., Hackney, J.A., Agrawal, S., Lesch, J., Zhou, M., Lee,

W.P., Park, S., Xu, M., DeVoss, J., et al. (2014). Transcriptional programming of dendritic cells for enhanced MHC class II antigen presentation. Nat. Immunol. *15*, 161–167.

Vanhoutte, F., Paget, C., Breuilh, L., Fontaine, J., Vendeville, C., Goriely, S., Ryffel, B., Faveeuw, C., and Trottein, F. (2008). Toll-like receptor (TLR)2 and TLR3 synergy and cross-inhibition in murine myeloid dendritic cells. Immunol. Lett. *116*, 86–94.

Varga, E.M., Wachholz, P., Nouri-Aria, K.T., Verhoef, A., Corrigan, C.J., Till, S.J., and Durham, S.R. (2000). T cells from human allergen-induced late asthmatic responses express IL-12 receptor beta 2 subunit mRNA and respond to IL-12 in vitro. J. Immunol. *165*, 2877–2885.

Veldhoen, M., Hocking, R.J., Atkins, C.J., Locksley, R.M., and Stockinger, B. (2006). TGFbeta in the context of an inflammatory cytokine milieu supports de novo differentiation of IL-17-producing T cells. Immunity *24*, 179–189.

Vella, A.T., and Pearce, E.J. (1992). CD4+ Th2 response induced by Schistosoma mansoni eggs develops rapidly, through an early, transient, Th0-like stage. J. Immunol. *148*, 2283–2290.

Villadangos, J.A., and Shortman, K. (2010). Found in translation: the human equivalent of mouse CD8+ dendritic cells. J. Exp. Med. *207*, 1131–1134.

Villadangos, J.A., and Schnorrer, P. (2007). Intrinsic and cooperative antigen-presenting functions of dendritic-cell subsets in vivo. Nat. Rev. Immunol. *7*, 543–555.

Villadangos, J.A., and Young, L. (2008). Antigen-Presentation Properties of Plasmacytoid Dendritic Cells. Immunity *29*, 352–361.

Vinuesa, C.G., Tangye, S.G., Moser, B., and Mackay, C.R. (2005). Follicular B helper T cells in antibody responses and autoimmunity. Nat. Rev. Immunol. *5*, 853–865.

Voehringer, D. (2009). The role of basophils in helminth infection. Trends Parasitol. *25*, 551–556.

Vremec, D., Pooley, J., Hochrein, H., Wu, L., and Shortman, K. (2000). CD4 and CD8 expression by dendritic cell subtypes in mouse thymus and spleen. J. Immunol. *164*, 2978–2986.

Vremec, D., O'Keeffe, M., Hochrein, H., Fuchsberger, M., Caminschi, I., Lahoud, M., and Shortman, K. (2007). Production of interferons by dendritic cells, plasmacytoid cells, natural killer cells, and interferon-producing killer dendritic cells. Blood *109*, 1165–1173.

Wagner, E.F., and Eferl, R. (2005). Fos/AP-1 proteins in bone and the immune system. Immunol. Rev. *208*, 126–140.

Waithman, J., Zanker, D., Xiao, K., Oveissi, S., Wylie, B., Ng, R., Tögel, L., and Chen, W. (2013). Resident CD8(+) and Migratory CD103(+) Dendritic Cells Control CD8 T Cell Immunity during Acute Influenza Infection. PLoS ONE *8*, e66136.

Walsh, K.P., and Mills, K.H.G. (2013). Dendritic cells and other innate determinants of T helper cell polarisation. Trends Immunol. *34*, 521–530.

Wang, H., Peters, N., and Schwarze, J. (2006). Plasmacytoid Dendritic Cells Limit Viral Replication, Pulmonary Inflammation, and Airway Hyperresponsiveness in Respiratory Syncytial Virus Infection. J. Immunol. *177*, 6263–6270.

Wang, Z., Wang, C., Yin, J., Li, T., Song, M., Lu, M., and Wang, H. (2008). Focusing and stabilization of bis-intercalating dye-DNA complexes for high-sensitive CE-LIF DNA analysis. Electrophoresis *29*, 4454–4462.

Warren, K.S., and Domingo, E.O. (1970). Granuloma formation around Schistosoma mansoni, S. HAEMATOBIUM, AND S. japonicum eggs. Size and rate of development, cellular composition, cross-sensitivity, and rate of egg destruction. Am. J. Trop. Med. Hyg. *19*, 292–304.

Waskow, C., Liu, K., Darrasse-Jeze, G., Guermonprez, P., Ginhoux, F., Merad, M., Shengelia, T., Yao, K., and Nussenzweig, M. (2008). The receptor tyrosine kinase Flt3 is required for dendritic cell development in peripheral lymphoid tissues. Nat. Immunol. *9*, 676–683.

Weaver, C.T., Elson, C.O., Fouser, L.A., and Kolls, J.K. (2013). The Th17 pathway and inflammatory diseases of the intestines, lungs, and skin. Annu. Rev. Pathol. *8*, 477–512.

Weinstock, J.V., and Boros, D.L. (1983). Organ-dependent differences in composition and function observed in hepatic and intestinal granulomas isolated from mice with Schistosomiasis mansoni. J. Immunol. *130*, 418–422.

Weinstock, J.V., Elliott, D., Metwali, A., Blum, A., Li, J., Qadir, K., and Sandor, M. (1999). Immunoregulation within the granulomas of murine schistosomiasis mansoni. Microbes Infect. *1*, 491–498.

Wenner, C.A., Güler, M.L., Macatonia, S.E., O'Garra, A., and Murphy, K.M. (1996). Roles of IFN-gamma and IFN-alpha in IL-12-induced T helper cell-1 development. J. Immunol. *156*, 1442–1447.

West, M.A., Bretscher, M.S., and Watts, C. (1989). Distinct endocytotic pathways in epidermal growth factor-stimulated human carcinoma A431 cells. J. Cell Biol. *109*, 2731–2739.

Whelan, M., Harnett, M.M., Houston, K.M., Patel, V., Harnett, W., and Rigley, K.P. (2000). A filarial nematode-secreted product signals dendritic cells to acquire a phenotype that drives development of Th2 cells. J. Immunol. *164*, 6453–6460.

Wherry, E.J., Ha, S.-J., Kaech, S.M., Haining, W.N., Sarkar, S., Kalia, V.,

Subramaniam, S., Blattman, J.N., Barber, D.L., and Ahmed, R. (2007). Molecular signature of CD8+ T cell exhaustion during chronic viral infection. Immunity *27*, 670–684.

Whittaker, P., Kloner, R.A., Boughner, D.R., and Pickering, J.G. (1994). Quantitative assessment of myocardial collagen with picrosirius red staining and circularly polarized light. Basic Res. Cardiol. *89*, 397–410.

Williams, D.L., Asahi, H., Oke, T.T., Lopes da Rosa, J., and Stadecker, M.J. (2005). Murine immune responses to a novel schistosome egg antigen, SmEP25. Int. J. Parasitol. *35*, 875–882.

Williams, J.W., Tjota, M.Y., Clay, B.S., Vander Lugt, B., Bandukwala, H.S., Hrusch, C.L., Decker, D.C., Blaine, K.M., Fixsen, B.R., Singh, H., et al. (2013). Transcription factor IRF4 drives dendritic cells to promote Th2 differentiation. Nat. Commun. *4*, 2990.

Willimann, K., Legler, D.F., Loetscher, M., Roos, R.S., Delgado, M.B., Clark-Lewis, I., Baggiolini, M., and Moser, B. (1998). The chemokine SLC is expressed in T cell areas of lymph nodes and mucosal lymphoid tissues and attracts activated T cells via CCR7. Eur. J. Immunol. *28*, 2025–2034.

Wilson, M.S., Mentink-Kane, M.M., Pesce, J.T., Ramalingam, T.R., Thompson, R., and Wynn, T.A. (2007). Immunopathology of schistosomiasis. Immunol. Cell Biol. *85*, 148–154.

Wilson, N.S., El-Sukkari, D., and Villadangos, J.A. (2004). Dendritic cells constitutively present self antigens in their immature state in vivo and regulate antigen presentation by controlling the rates of MHC class II synthesis and endocytosis. Blood *103*, 2187–2195.

Wilson, N.S., El-Sukkari, D., Belz, G.T., Smith, C.M., Steptoe, R.J., Heath, W.R., Shortman, K., and Villadangos, J.A. (2003). Most lymphoid organ dendritic cell types are phenotypically and functionally immature. Blood *102*, 2187–2194.

Wu, M., Fang, H., and Hwang, S.T. (2001). Cutting edge: CCR4 mediates antigen-primed T cell binding to activated dendritic cells. J. Immunol. *167*, 4791–4795.

Wykes, M. (2003). Why do B cells produce CD40 ligand? Immunol. Cell Biol. *81*, 328–331.

Wynn, T.A. (2008). Cellular and molecular mechanisms of fibrosis. J. Pathol. *214*, 199–210.

Wynn, T.A., and Hoffmann, K.F. (2000). Defining a schistosomiasis vaccination strategy - is it really Th1 versus Th2? Parasitol. Today *16*, 497–501.

Wynn, T.A., Cheever, A.W., Jankovic, D., Poindexter, R.W., Caspar, P., Lewis, F.A., and Sher, A. (1995). An IL-12-based vaccination method for preventing fibrosis induced by schistosome infection. Nature *376*, 594–596.

Wynn, T.A., Eltoum, I., Oswald, I.P., Cheever, A.W., and Sher, A. (1994). Endogenous interleukin 12 (IL-12) regulates granuloma formation induced by eggs of Schistosoma mansoni and exogenous IL-12 both inhibits and prophylactically immunizes against egg pathology. J. Exp. Med. *179*, 1551–1561.

Wynn, T.A., Morawetz, R., Scharton-Kersten, T., Hieny, S., Morse, H.C., Kühn, R., Müller, W., Cheever, A.W., and Sher, A. (1997). Analysis of granuloma formation in double cytokine-deficient mice reveals a central role for IL-10 in polarizing both T helper cell 1- and T helper cell 2-type cytokine responses in vivo. J. Immunol. *159*, 5014–5023.

Wynn, T.A. (2004). Fibrotic disease and the TH1/TH2 paradigm. Nat. Rev. Immunol. *4*, 583–594.

Wynn, T.A., and Barron, L. (2010). Macrophages: master regulators of inflammation and fibrosis. Semin. Liver Dis. *30*, 245–257.

Wynn, T.A., Thompson, R.W., Cheever, A.W., and Mentink-Kane, M.M. (2004). Immunopathogenesis of schistosomiasis. Immunol. Rev. *201*, 156–167.

Yamane, H., Zhu, J., and Paul, W.E. (2005). Independent roles for IL-2 and GATA-3 in stimulating naive CD4+ T cells to generate a Th2-inducing cytokine environment. J. Exp. Med. *202*, 793–804.

Yamashita, T., and Boros, D.L. (1992). IL-4 influences IL-2 production and granulomatous inflammation in murine schistosomiasis mansoni. J. Immunol. *149*, 3659–3664.

Yamazaki, S., Dudziak, D., Heidkamp, G.F., Fiorese, C., Bonito, A.J., Inaba, K., Nussenzweig, M.C., and Steinman, R.M. (2008). CD8+ CD205+ splenic dendritic cells are specialized to induce Foxp3+ regulatory T cells. The J. Immunol. *181*, 6923–6933.

Yap, G., Cheever, A., Caspar, P., Jankovic, D., and Sher, A. (1997). Unimpaired down-modulation of the hepatic granulomatous response in CD8 T-cell- and gamma interferon-deficient mice chronically infected with Schistosoma mansoni. Infect. Immun. *65*, 2583–2586.

Yeh, M.M., and Brunt, E.M. (2014). Pathological features of fatty liver disease. Gastroenterology *147*, 754–764.

Yi, J.S., Cox, M.A., and Zajac, A.J. (2010). T-cell exhaustion: characteristics, causes and conversion. Immunology *129*, 474–481.

Yogev, N., Frommer, F., Lukas, D., Kautz-Neu, K., Karram, K., Ielo, D., Stebut, von, E., Probst, H.C., van den Broek, M., Riethmacher, D., et al. (2012). Dendritic cells ameliorate autoimmunity in the CNS by controlling the homeostasis of PD-1 receptor(+) regulatory T cells. Immunity *37*, 264–275.

Yoneyama, H., Matsuno, K., Zhang, Y., Murai, M., Itakura, M., Ishikawa, S.,

Hasegawa, G., Naito, M., Asakura, H., and Matsushima, K. (2001). Regulation by chemokines of circulating dendritic cell precursors, and the formation of portal tract-associated lymphoid tissue, in a granulomatous liver disease. J. Exp. Med. *193*, 35–49.

Yoshie, O., and Matsushima, K. (2015). CCR4 and its ligands: from bench to bedside. Int. Immunol. *27*, 11–20.

Yoshimoto, T., Yasuda, K., Tanaka, H., Nakahira, M., Imai, Y., Fujimori, Y., and Nakanishi, K. (2009). Basophils contribute to T(H)2-IgE responses in vivo via IL-4 production and presentation of peptide-MHC class II complexes to CD4+ T cells. Nature Publishing Group *10*, 706–712.

Young, H.A., and Hardy, K.J. (1995). Role of interferon-gamma in immune cell regulation. J. Leukoc. Biol. *58*, 373–381.

Young, L.J., Wilson, N.S., Schnorrer, P., Mount, A., Lundie, R.J., La Gruta, N.L., Crabb, B.S., Belz, G.T., Heath, W.R., and Villadangos, J.A. (2007). Dendritic cell preactivation impairs MHC class II presentation of vaccines and endogenous viral antigens. Proc. Natl. Acad. Sci. U.S.A. *104*, 17753–17758.

Young, L.J., Wilson, N.S., Schnorrer, P., Proietto, A., Broeke, ten, T., Matsuki, Y., Mount, A.M., Belz, G.T., O'Keeffe, M., Ohmura-Hoshino, M., et al. (2008). Differential MHC class II synthesis and ubiquitination confers distinct antigen-presenting properties on conventional and plasmacytoid dendritic cells. Nat. Immunol. *9*, 1244–1252.

Zhang, J.Q., Biedermann, B., Nitschke, L., and Crocker, P.R. (2004). The murine inhibitory receptor mSiglec-E is expressed broadly on cells of the innate immune system whereas mSiglec-F is restricted to eosinophils. Eur. J. Immunol. *34*, 1175–1184.

Zheng, S.G., Wang, J., and Horwitz, D.A. (2008). Cutting edge: Foxp3+CD4+CD25+ regulatory T cells induced by IL-2 and TGF-beta are resistant to Th17 conversion by IL-6. J. Immunol. *180*, 7112–7116.

Zheng, S.G., Wang, J., Wang, P., Gray, J.D., and Horwitz, D.A. (2007). IL-2 is essential for TGF-beta to convert naive CD4+CD25- cells to CD25+Foxp3+ regulatory T cells and for expansion of these cells. J. Immunol. *178*, 2018–2027.